Zinc and copper behaviour during stormwater aquifer storage and recovery in sandy aquifers

Anke Wendelborn
Dipl. Geol. (Johannes-Gutenberg University, Mainz, Germany)

Submitted to the Faculty of Engineering
In fulfilment of the requirement for the
Degree of Doctor of Philosophy

Faculty of Engineering, Department of Civil Engineering
Institute for Sustainable Water Resources (ISWR)

MONASH UNIVERSITY

Nov 2008

For a sustainable way of living

"*Water should not be judged by its history, but by its quality.*"

Dr Lucas Van Vuuren
National Institute of Water Research, South Africa

Declaration

I, Anke Wendelborn, hereby declare that this thesis contains no material which has been accepted for the award of any degree or diploma in any university and that, to the best of my knowledge and belief, contains no material previously published or written by another person, except where due reference is made.

Signed……

Date: ……..

Contents

Contents i
List of figures vii
List of tables xiv
Abbreviations and acronyms xvii
Abstract xviii
Acknowledgements xix

Chapter I: Introduction 1
I.1 Overview 1
I.2 Structure of thesis 3

Chapter II: Background and scope 5
II.1 Introduction 5
II.2 The technique – ASR in theory and case studies 7
II.2.1 The ASR cycle 7
II.2.2 Water quantity considerations 8
II.2.2.1 Suitable aquifer 8
II.2.2.2 Recovery efficiency 9
II.2.2.3 Clogging 9
II.2.3 Water quality considerations 10
II.2.3.1 Disinfection byproducts 11
II.2.3.2 Trace organic contaminants 12
II.2.3.3 Microbial pathogens 12
II.2.3.4 NOM and associated redox reactions 13
II.2.3.5 Ion exchange 15
II.2.3.6 Dissolution/precipitation 15
II.2.4 ASR in use 16
II.2.4.1 Bolivar, South Australia 16
II.2.4.2 Andrews Farm, South Australia 17
II.2.4.3 Parafield, South Australia 18
II.2.4.4 The Netherlands 19
II.2.4.5 Other studies 20
II.2.4.6 Melbourne trials and investigations 20
II.2.5 Guidelines and practice 21

II.2.5.1 Current regulatory framework and guidelines 21
II.2.5.2 Best practice and risk assessment 22
II.2.5.3 Implementation 23
II.3 The injectant – urban stormwater pollutants 24
II.3.1 Total suspended solids 24
II.3.2 Nutrients and oxygen 25
II.3.3 Organic carbon 25
II.3.4 Trace organic contaminants 25
II.3.5 Heavy metals 25
II.4 Metal speciation: mechanisms and factors 27
II.4.1 Sorption 27
II.4.1.1 Theory and mechanisms 27
II.4.1.2 The matrix 31
II.4.1.3 The natural system 33
II.4.2 Complexation with organic matter 34
II.4.3 Dissolution/precipitation 35
II.4.4 Colloidal transport 36
II.4.5 Influencing factors 38
II.4.6 Metal behaviour during the ASR cycle 41
II.4.6.1 Pretreatment 41
II.4.6.2 Injection 42
II.4.6.3 Storage 43
II.4.6.4 Recovery 43
II.4.7 Conclusions 43
II.5 Summary 44
II.6 Scope 45
II.6.1 Scientific problem 45
II.6.2. Objectives of this study 46

Chapter III: Stormwater and groundwater quality 47
III.1 Introduction 47
III.2 Stormwater investigation 49
III.2.1 Introduction to the Melbourne catchments 49
III.2.2 Stormwater sampling and analysis 50
III.2.3 Results and discussion of stormwater investigation 51
III.2.4 Stormwater for further experiments 57

III.3 Hydrogeology 58
III.3.1 Introduction to Melbourne's hydrogeology 58
III.3.2 Bore selection, groundwater sampling and analysis 63
III.3.3 Results and discussion of groundwater investigation 64
III.3.4 Groundwater for further experiments 67
III.3.5 Sediments for further experiments 68
III.4 Summary and conclusions 70

Chapter IV: Batch experiments 72
IV.1 Introduction 72
IV.2 Material and methods 72
IV.2.1 Materials 73
IV.2.2 Batch experiments and analysis 73
IV.3 Results and discussion 76
IV.3.1 Adsorption series 76
IV.3.1.1 Adsorption isotherms at natural pH 76
IV.3.1.2 Organic matter influence 79
IV.3.1.3 Influence of solid-solution ratio 81
IV.3.1.4 Influence of pH 83
IV.3.1.5 Influence of solution salinity 85
IV.3.1.6 Influence of pre-equilibration with groundwater 86
IV.3.2 Desorption series 87
IV.3.2.1 Desorption kinetics overview 87
IV.3.2.2 Influence of solid-solution ratio 88
IV.3.2.3 Influence of solution salinity 89
IV.3.2.4 Influence of oxygen concentration of desorption solution 89
IV.3.2.5 Influence of pH of desorption solution 91
IV.4 Conclusions 92

Chapter V: Column experiments 94
V.1 Introduction 94
V.2 Material and methods 95
V.2.1 Sediment materials and solutions 95
V.2.2 Column set up 95
V.2.3 Experimental design 97
V.2.4 Water sampling and analysis 99

V.2.5 Sediment analysis 100
V.2.6 Data analysis 100
V.3 Results and discussion 102
V.3.1 Major cations – ion exchange 102
V.3.2 Physico-chemical parameters 106
V.3.2.1 pH 106
V.3.2.2 Organic carbon 108
V.3.2.3 Turbidity 109
V.3.3 Zn and Cu behaviour 109
V.3.3.1 Stormwater injection (phase 2) – adsorption 110
V.3.3.1.1 Influence of pH 113
V.3.3.1.2 Influence of cation exchange capacity (CEC) 114
V.3.3.1.3 Influence of organic carbon 115
V.3.3.1.4 Influence of flow velocity 116
V.3.3.1.5 Influence of inflow concentration 116
V.3.3.1.6 Influence of non-equilibrium 117
V.3.3.1.7 Comparison with other studies 118
V.3.3.1.8 Comparison with batch results 120
V.3.3.2 Storage (phase 3 and shorter stages during phase 4) 126
V.3.3.3 Recovery (phase 4) – desorption 129
V.3.3.3.1 Ionic strength effects 130
V.3.3.3.2 pH decrease effect (exp. 2) 132
V.3.3.3.3 Organic carbon and redox effects (exp. 3) 132
V.3.3.3.4 Mass balance 134
V.3.4 Arsenic behaviour 135
V.3.5 Metals retained in the sediment 136
V.4 Summary of key processes and conclusions 142

Chapter VI: Modelling 146
VI.1 Introduction 146
VI.2 Background to reactive transport modelling in PHT3D 147
VI.2.1 Solute transport modelling 147
VI.2.2 Geochemical modelling 148
VI.2.2.1 Equilibrium reactions 148
VI.2.2.2 Kinetic reactions 150
VI.2.3 Coupling and numerical effects 150

VI.2.4 Model development 152
VI.3 Modelling setup 155
VI.3.1 Non-reactive solute transport model 156
VI.3.2 Output 157
VI.4 Simple approaches 158
VI.4.1 Modelling of simple approaches 158
VI.4.1.1 Linear equilibrium sorption 158
VI.4.1.2 Ion exchange 159
VI.4.1.3 Mineral phases 160
VI.4.1.4 Generalised composite (GC) approach 161
VI.4.2 Results of simple approaches 162
VI.4.2.1 Linear equilibrium sorption 162
VI.4.2.2 Ion exchange 163
VI.4.2.3 Mineral phases 166
VI.4.2.4 Generalised composite (GC) approach 170
VI.4.3 Summary of simple approaches 171
VI.5. Component additivity (CA) surface complexation modelling 171
VI.5.1 Conceptual model for interactions of metals, organic phases and matrix 171
VI.5.1.1 Surface complexation onto minerals 172
VI.5.1.2 Organic complexation 175
VI.5.1.3 Surface complexation onto organic matter 178
VI.5.1.4 Sorption of organic matter onto minerals 180
VI.5.1.5 Ternary complexes 181
VI.5.1.6 Dual domain 186
VI.5.1.7 Kinetic biodegradation 186
VI.5.2 Sensitivity analysis of conceptual model features 188
VI.5.2.1 Goethite surface sites 189
VI.5.2.2 Strong HA surface sites 192
VI.5.2.3 Weak HA surface sites 195
VI.5.2.4 Combination of surface sites 197
VI.5.2.5 Organic complexes 201
VI.5.2.6 Sorption of organic matter onto goethite 203
VI.5.2.7 Ternary complexes 206
VI.5.2.8 Summary of conceptual CA model 208
VI.5.3 CA model performance for column experiments 211

VI.5.3.1 BR experiment 2 211
VI.5.3.2 WS experiment 2 212
VI.5.3.3 BL experiment 2 212
VI.5.3.4 Experiment 3 214
VI.5.3.5 Dual domain 215
VI.5.3.6 Kinetic biodegradation 216
VI.6 Model evaluation and discussion 218
VI.6.1 Objective functions 218
VI.6.2 Uncertainties 221
VI.6.3 Further improvements 222
VI.7 Conclusions 225

Chapter VII: Conclusions and assessment 226
VII.1 Summary or results 226
VII.1.1 Characterisation of solutions and sediments 226
VII.1.2 Influence of single factors during batch experiments 227
VII.1.3 Influence of multiple factors during column experiments 228
VII.1.4 Implementation of results into reactive geochemical transport modelling 230
VII.2. Implications for stormwater ASR in sandy aquifers 230
VII.3 Critical evaluation and outlook 235

Bibliography 237

Appendix A: Publications and Conferences 268
Appendix B: 269

List of figures

Figure II-1:	Schematic aquifer storage and recovery system (modified after Dillon, 2004)	8
Figure II-2:	Typical concentrations of worldwide stormwater samples for total suspended solids (TSS) and total organic carbon (TOC) (modified after Duncan, 2006).	24
Figure II-3	Typical concentrations of worldwide stormwater samples for Zn and Cu in stormwater (modified after Duncan, 2006).	26
Figure II-4:	Schematic sorption of cations and anions at an oxide or clay mineral surface (modified after Selim and Iskandar, 1999) s: layer of hydroxyl groups of the solid, i: layer for inner-sphere complexes, o: layer for outer-sphere complexes, d: start of diffuse ion layer.	28
Figure II-5:	Schematics of the main four types of isotherms (Limousin et al., 2007); C: concentration in solution at equilibrium; Q: concentration in solid at equilibrium.	30
Figure II-6:	Schematic contaminant facilitated transport in a porous media showing possible interactions like particle mobilisation, deposition, coagulation, and sorption of contaminant between mobile particle or immobile matrix and solution (modified after Buffle and Leppard, 1995).	37
Figure II-7:	Metal adsorption vs. pH on (a) hematite and (b) goethite (McKenzie, 1980)	39
Figure II-8:	Stability fields of (a) Zn species in the system Zn (10-5 mol/L) + CO2 (10-3 mol/L) + S (10-3 mol/L) + H20 at 25°C at 1 atm pressure (after Hem, 1972) and (b) Cu species in the system Cu + H2O + O2 + S + CO2 (PCO2 10-1) at 25°C and 1 atm total pressure in relation to Eh and pH (after Garrels and Christ, 1965).	40
Figure II-9:	Conceptual model of stormwater ASR with relevant processes influencing metals.	46
Figure III-1:	Stormwater sampling sites in Melbourne showing location and insets of close ups (individual pictures courtesy to ISWR).	50
Figure III-2:	µEMC fractionation of Cu and Zn in three Melbourne catchments: MR: Monash Roof, GR: Gilby Rd and RI: Richmond.	54
Figure III-3:	Correlation between (a) pH, (b) total suspended solids (TSS) and (c) dissolved organic carbon (DOC) to dissolved fraction of Cu and Zn for all events (MR, GR, RI) and (d) linear correlation coefficient R^2.	55
Figure III-4:	Simplified geological map of greater Melbourne. Dashed line showing cross-section of Figure III-5 (modified after O'Rourke and Shugg, 1998)	59
Figure III-5:	Geological cross-section of SE Melbourne, from north of Caulfield (A) to east of Frankston about 5-2 km inland from the bay, see A-B in Figure III-4 (after Leonard, 1983).	60
Figure III-6:	Isosalines of the Fyansford Formation - Brighton Group aquifer system (Leonard, 1983).	62

Figure III-7:	Piper diagram displaying main ion groundwater chemistry types.	64
Figure III-8:	Surface geology and groundwater types sampled in the SE of Melbourne (modified after DPI, 2008d).	65
Figure IV-1:	Schematic adsorption edge of (a) Zn and (b)Cu in stormwater to different siliceous aquifer materials (BL – black Tertiary Brighton Group sediment, BR- brown Tertiary Brighton Group sediment, WS – Quaternary Werribee Delta sediment) with no and 30 mg-C/L addition of fulvic acid.	80
Figure IV-2:	Effect of solid-solution ratio [g/mL] on adsorption amounts [mg/kg] of Zn (a) and Cu (b) in stormwater to different siliceous aquifer materials. Normalised amounts of Zn(c) and Cu(d) in solution and sediment showing solid-solution ratio effect was most pronounced for WS, but only limited for BR and BL. (BL – black Tertiary Brighton Group sediment, BR- brown Tertiary Brighton Group sediment, WS – Quaternary Werribee Delta sediment) with 0 or 30 mg-C/L addition of fulvic acid.	82
Figure IV-3:	pH dependency of adsorption behaviour of Zn (left) and Cu (right) in stormwater to different siliceous aquifer materials (BL – black Tertiary Brighton Group sediment (a+b), BR- brown Tertiary Brighton Group sediment (c+d), WS – Quaternary Werribee Delta sediment (e+f)) with no addition of fulvic acid.	84
Figure IV-4:	Dissolved concentration of Fe and organic carbon during pH adjusted (NaOH) batch experiments, showing a significant increase for BL and a slight increase for BR in both parameters with increasing pH	85
Figure IV-5:	Influence of desorption solid-solution ratio on desorption. Normalised amounts of (a) Zn and (b) Cu in solution and sediment of different siliceous aquifer materials (BL – black Tertiary Brighton Group sediment, BR- brown Tertiary Brighton Group sediment, WS – Quaternary Werribee Delta sediment) previously adsorbed with Zn or Cu and 0 or 30 mg-C/L addition of fulvic acid.	89
Figure IV-6:	Influence of desorption solution pH on desorption [%] of previously adsorbed amount for (a) Zn and (b) Cu in different siliceous aquifer materials (BL – black Tertiary Brighton Group sediment, BR- brown Tertiary Brighton Group sediment, WS – Quaternary Werribee Delta sediment). Lines are indicative trends only.	91
Figure V-1:	(a) Experimental set up of column experiments (not to scale) and (b) packed column.	96
Figure V-2:	Blank graph concentration versus sample. X-axis labels indicate the start of a new phase (stw, storage, gw). Samples after shorter storages in phase 4 are indicated by st and their length is given in days [d]. pH of inflow solution dropped to pH 5 in experiment 2 at sample pH5 (2). stw: stormwater; gw: groundwater; (2): in experiment 2; (3): in experiment 3. See also Table VI-2.	101
Figure V-3:	EC versus samples taken for all three experiments showing the influence of EC meter volume on breakthrough in exp. 1+2 compared to exp. 3 with no EC meters; especially visible at the beginning of the stormwater injection phase (arrow). See Figure VI-2 for sample labels.	103

Figure V-4:	Behaviour of major ions (a) sodium, (b) magnesium and (c) calcium, normalised to inflow concentration for all three experiments (negative concentration: retardation via adsorption, positive values: release via desorption). Inserts(‘) show the cation concentrations in the stormwater injection phase versus no of PV. See Figure VI-2 for sample labels.	104
Figure V-5:	Outflow and inflow values of (a) pH, (b) TOC and (c) turbidity for exp. 2 and 3. See Figure VI-2 for sample labels.	107
Figure V-6:	Outflow and inflow concentrations of (a) Zn and (b) Cu for exp. 2 and 3. See Figure VI-2 for sample labels.	110
Figure V-7:	Analysis of Zn (left) and Cu (right) of exp. 2+3 during stormwater injection (phase 2). (a + b): breakthrough curves with adsorbed percentage of inflow concentration versus number of pore volumes (PV) (negative values = adsorption; positive values = desorption); (c+d): adsorption isotherms with accumulated adsorbed concentration versus dissolved concentration; (e+f): adsorption isotherms in log-log scale as in c+d for data of exp. 3 only.	112
Figure V-8:	Breakthrough curves of calcium and zinc for stormwater injection phase of exp. 3 (no mixing in EC meter involved).	115
Figure V-9:	Column study retardation factors (Rf) for Zn and solid-solution ratio show a significant first order law dependency with increasing Rf value for increasing solid-solution ratio, as has been reported for batch studies. Linear regression of “other studies” data (see Table VI-4) gave a linear coefficient of determination R^2=0.9866. See text below for explanation of lines.	122
Figure V-10:	Outflow and inflow concentrations [mg/L] of Fe and Mn for exp. 3. The grey bar indicates the 2-week storage phase at the end of the stormwater injection.	127
Figure V-11:	Desorption of metals during recovery phase. Percentage of accumulated sorbed concentration of recovery (phase 4) in relation to accumulated sorbed concentration of stormwater infiltration (phase 2) for (a) Zn and (b) Cu without storage samples. Insets (‘) show the first two stages in more detail. Negative values = desorption, positive values = adsorption. See Figure V-2 for sample labels.	130
Figure V-12:	Total arsenic outflow concentrations for BR and BL. Inflow, BR exp. 1 and 2 and WS outflow concentrations were <10 µg/L. 95% level of protection trigger value for freshwater aquatic ecosystems is 13 µg/L As(V) (ANZECC and ARMCANZ, 2000). See Figure VI-2 for sample labels.	135
Figure V-13:	Extracted metal concentrations for (a) Zn and (b) Cu for three steps: non-specifically adsorbed (exchangeable), specifically adsorbed (reducible) and very strongly bound (oxidisable).	138
Figure V-14:	Extracted (a) Al, (b) Fe and (c) Mn from column sediments for three steps: non-specifically adsorbed (exchangeable), specifically adsorbed (reducible) and very strongly bound (oxidisable).	140
Figure VI-1:	Data flow in a MODFLOW based PHT3D simulation (modified after Prommer et al., 2003)	151

Figure VI-2:	Flow model set up for (a) injection and (b) recovery. A: injection well, B: recovery well, C: constant head flow boundary, mS: medium filter sand, fS: fine filter sand, sed: sediment.	156
Figure VI-3:	Blank graph concentration versus time indicating changes in phases and stages for (a) experiment 2 and (b) experiment 3. Shaded areas indicate shorter storages during recovery (phase 4) (compare to Figure VI-2).	158
Figure VI-4:	Simulated and observed concentrations of (a) Zn and (b) Cu using the linear K_d sorption approach for BR2 with K_dZn = 5 L/kg; K_dCu = 37 L/kg.	163
Figure VI-5:	Simulated and observed (a) pH and concentrations of (b) Ca, (c) Zn and (d) Cu using the ion exchange approach for BR2 with standard database values (dataset a) (Table VII-1) with insets (‘) for pH and Ca of breakthrough at start of stormwater injection.	164
Figure VI-6:	Simulated and observed concentrations of (a) Ca breakthrough at start of stormwater injection and (b) Ca release at start of recovery phase using adjusted Ca selectivity values (dataset b, Table VII-1).	165
Figure VI-7	Simulated and observed concentrations of (a) Ca at start of stormwater injection, (b) Ca at start of recovery phase, (c) pH, (d) Zn and (e) Cu using the ion exchange approach with dataset c (Table VII-1) (compare to Figure VII-11).	166
Figure VI-8:	Simulated pattern of mineral precipitation and dissolution for BR2 in first (cell 12) and last cell (cell 23) of the aquifer sediment. (a) quartz, initial 30 mol, (b) goethite, initial 0.093 mol, (c) gibbsite, initial 0.173 mol, (d) malachite ($Cu_2(OH)_2CO_3$), initial 0 mol, without cupric ferrite, (e) goethite, initial 0.093mol, with cupric ferrite, initial 0 mol, (f) cupric ferrite ($CuFe_2O_4$), initial 0 mol with goethite, initial 0.093 mol (g) cupric ferrite, initial 0.0 mol with goethite, initial 0.0 mol.	168
Figure VI-9	Simulated and observed concentrations of (a) Zn and (b) Cu for BR2 using a single GC-site with 0.014 mol (solid line) and 0.07 mol (dashed line) surface sites.	170
Figure VI-10:	Conceptual model of metal – surface – organic acids interactions. Solid lines: simple implemented model, dashed lines: species and transformations are not implemented yet. HA: humic acid, FA: fulvic acid, Me: metal ion.	172
Figure VI-11:	Surface complexation of 1 mg/L Zn/Cu vs. pH onto 0.01 mol Goethite in 0.01 M Ca-HCO_3 solution.	175
Figure VI-12:	Aqueous speciation of metals (Me) vs. pH in 0.01 M Ca-HCO_3 solution with 10 mg/L Srfa: (a) Zn, total 1 mg/L and (b) Cu, total 1 mg/L.	177
Figure VI-13:	Surface complexation of 1 mg/L Zn/Cu versus pH onto $5*10^{-3}$ mol goethite, $5*10^{-4}$ mol Haw, $5*10^{-6}$ mol Has sites in 0.01 M Ca-HCO_3 solution.	180
Figure VI-14:	Speciation of Srfa (total 10 mg/L) vs. pH in 0.01M Ca-HCO_3 solution onto (a) 0.01, (b) 0.007, (c) 0.004, (d) 0.001 mol goethite surface site.	181

Figure VI-15:	Sorbed metal speciation vs. pH with 1 mg/L Zn/Cu in 0.01 M Ca-HCO_3 solution and 10 mg/L Srfa onto 0.01 mol goethite surface site with decreasing affinity constants for ternary complexes Goe_SrfaMe$^-$ (a) log k 12.7, (b) log k 10.7, (c) log k 8.7 and (d) log k 6.7.	184
Figure VI-16:	Simulated and observed concentrations for BR2 of (a) Zn, (b) Cu and (c) pH with 0.054 mol/kgw exchanger site, no surface sites and no organic complexation.	189
Figure VI-17:	Simulated and observed Zn concentrations when adding the goethite surface site with (a) 0.01 mol (solid line) and 0.03 mol (dashed line) and (b) 0.05 mol (solid line) and 0.07 mol (dashed line).	190
Figure VI-18:	Simulated and observed Cu concentrations when adding the goethite surface site with (a) 0.01 mol (solid line) and 0.03 mol (dashed line) and (b) 0.05 mol (solid line) and 0.07 mol (dashed line).	191
Figure VI-19:	Simulated adsorbed species of Zn and Cu to 0.03 mol goethite surface site as (a) inner-sphere sorbed Zn, (b) outer-sphere sorbed Zn, (c) inner-sphere sorbed Cu and (d) outer-sphere sorbed Cu.	191
Figure VI-20:	Simulated and observed pH when adding the goethite surface site with (a) 0.01 mol (solid line) and 0.03 mol (dashed line) and (b) 0.05 mol (solid line) and 0.07 mol (dashed line). Insets (‘) show pH at start of stormwater injection in detail.	192
Figure VI-21:	Simulated and observed Zn concentrations when adding the strong humic acid (Has) surface site with (a) 0.01 mol (solid line) and 0.02 mol (dashed line) and (b) 0.03 mol (solid line) and 0.04 mol (dashed line).	193
Figure VI-22:	Simulated and observed Cu concentrations when adding the strong humic acid (Has) surface site with (a) 0.01 mol (solid line) and 0.02 mol (dashed line) and (b) 0.03 mol (solid line) and 0.04 mol (dashed line).	194
Figure VI-23:	Simulated adsorbed species of Zn and Cu to 0.03 mol Has as (a) inner-sphere sorbed Zn and (b) inner-sphere sorbed Cu.	194
Figure VI-24:	Simulated and observed pH when adding the strong humic acid (Has) surface site with (a) 0.01 mol (solid line) and 0.02 mol (dashed line) and (b) 0.03 mol (solid line) and 0.04 mol (dashed line). Insets (‘) show pH at start of stormwater injection in detail.	195
Figure VI-25:	Simulated and observed (a) Zn concentrations, (b) Cu concentration and (c) pH when adding increasing numbers of weak humic acid (Haw) surface site. Solid line: 0.05 mol, dashed line: 0.4 mol of weak humic acid (Haw) site. Inset (c‘) shows pH at start of stormwater injection in detail.	196
Figure VI-26:	Simulated adsorbed species of Zn and Cu onto 0.02 mol Haw surface site as (a) inner-sphere sorbed Zn and (b) inner-sphere sorbed Cu.	197

Figure VI-27:	Simulated and observed (a) Zn concentrations, (b) Cu concentration and (c) pH when adding 0.02 mol goethite surface sites to 0.02 mol Has surface sites. Inset (c‘) shows pH at start of stormwater injection in detail.	198
Figure VI-28:	Simulated and observed (a) Zn concentrations, (b) Cu concentration and (c) pH when adding 0.1 mol Haw surface site to 0.02 mol Has surface site. Inset (c‘) shows pH at start of stormwater injection in detail.	199
Figure VI-29:	Simulated and observed (a) Zn concentrations, (b) Cu concentration and (c) pH when adding 0.1 mol Haw surface site to 0.02 mol goethite surface site. Inset (c‘) shows pH at start of stormwater injection in detail.	200
Figure VI-30:	Simulated and observed (a) Zn concentrations, (b) Cu concentration and (c) pH when adding 0.1 mol Haw surface site to 0.02 mol goethite and Has surface sites. Inset (c‘) shows pH at start of stormwater injection in detail.	201
Figure VI-31:	Simulated and observed concentrations of (a) total (solid line) and organically complexed (dashed line) Zn and (b) total (solid line) and organically complexed (dashed line) Cu when adding organic complexation to 0.03 mol goethite surface site.	202
Figure VI-32:	Simulated and observed concentrations of Cu when adding organic complexation to 0.03 mol goethite surface site.	202
Figure VI-33:	Simulated sorbed concentrations of (a) Goe_OSrfa-5 species and (b) Goe_HSrfa^{-2} species onto 0.03 mol goethite surface site.	203
Figure VI-34:	Simulated and observed concentrations of TOC without DOC sorption (solid line) and with DOC sorption (dashed line) onto 0.03 mol goethite surface site. Inset (a‘) shows TOC at start of stormwater injection in detail.	204
Figure VI-35:	Simulated and observed (a) Zn concentration, (b) Cu concentration and (c) pH when adding DOC sorption to 0.03 mol goethite surface site. Inset (c‘) shows pH at start of stormwater injection in detail.	205
Figure VI-36:	Simulated adsorbed species of Zn and Cu onto 0.03 mol goethite surface site without DOC sorption (black line) and with DOC sorption (grey lines) as (a) inner-sphere sorbed Zn, (b) outer-sphere sorbed Zn (c) inner-sphere sorbed Cu and (d) outer-sphere sorbed Cu.	206
Figure VI-37:	Simulated and observed concentrations of (a) Zn concentration, (b) cu concentration and (c) pH with no ternary complexes (solid line), ternary complexes with lower log_k values (dashed line) and ternary complexes with higher log_k values (dash-dotted line) onto 0.03 mol goethite surface sites. See Table VII-6 for log_k values. Inset (c’) shows pH at start of stormwater injection in detail.	207
Figure VI-38:	Simulated adsorbed species of Zn and Cu onto 0.03 mol goethite surface site without ternary complexation (black line) and with ternary complexation (grey lines) as (a) inner-sphere sorbed Zn, (b) outer-sphere sorbed Zn (c) inner-sphere sorbed Cu, (d) outer-sphere sorbed Cu, (e) ternary Zn complex and (f) ternary Cu complex.	208

Figure VI-39:	Simulated adsorbed species of Zn and Cu to 0.02 mol Has, 0.1 mol Haw and 0.02 mol goethite surface sites with ternary complexation (8.7/6.7) as (a) Zn sorbed on Haw, (b) Cu sorbed to Haw, (c) Zn sorbed to Has, (d) Cu sorbed to Has, (e) inner-sphere sorbed Zn on goethite, (f) outer-sphere sorbed Zn on goethite, (g) inner-sphere sorbed Cu, (h) outer-sphere sorbed Cu on goethite, (i) ternary Zn complex and (j) ternary Cu complex.	210
Figure VI-40:	Simulated and observed concentrations of (a) Zn concentration, (b) Cu concentration and (c) pH for BR2 (solid line) and WS2 (dashed line). See TableVII-8 for used amounts of surface sites.	212
Figure VI-41:	Simulated and observed concentrations of (a) Zn concentration, (b) Cu concentration and (c) pH for BL2. See TableVII-8 for used amounts of surface sites.	213
Figure VI-42:	Simulated and observed concentrations of (a) Zn concentration, (b) Cu concentration and (c) pH for WS3. See TableVII-8 for used amounts of surface sites.	215
Figure VI-43:	Simulated and observed concentrations of (a) Zn concentration, (b) Cu concentration and (c) pH onto 0.012 mol goethite and 0.016 mol Has with kinetic biodegradation (dashed line) using values after Parkhurst and Appelo (1999), see Table VII-7, and increased maximum degradation rate for aerobic degradation of $1.57*10^{-8}$ mol/L/s (dash-dotted line).	217
Figure VI-44:	Correlation between different objective functions for model runs listed in Table VII-8. MAE: mean absolute error, RMSE: root mean squared error, R: linear correlation function, E: coefficient of efficiency; E': modified coefficient of efficiency, see VII.2.4 for equations.	219

List of tables

Table II-1:	Selected average properties of FA and HA (compiled after Stevenson, 1982; Sparks, 2003)	13
Table III-1:	Stormwater monitoring sites in Melbourne	49
Table III-2:	Summary of mean EMC (µEMC), minimum (min), maximum (max) and standard deviation (std dev) for measured event parameters including storm event characteristics, physico-chemical parameters, major ion and metal concentrations (Cd, Cr and Ni were below or close to detection limits and were excluded in the statistical analysis; Cu and Zn see Table III-3). Individual results for all events incl. Values for all events including SR and ER see Table A-1 in appendix.	52
Table III-3:	Mean EMC (µEMC), site mean concentration (SMC), minimum (min), maximum (max) and standard deviation (std dev) for Cu and Zn divided in three size categories and added up for each event sample to total concentrations.	53
Table III-4:	Comparison of main stormwater characteristics of this study with freshwater guidelines, other roof runoff studies, studies from Europe/USA and other Australian literature data (empty fields indicate not reported parameters).	56
Table III-5:	Selected parameters of samples used for batch and column experiments, inlet biofilter (IBF) mean and standard deviation (14 events) (Hatt et al., in press) and ASR injectant (21 events) at Andrews Farm, Adelaide (Barry et al., 2002) for comparison.	58
Table III-6:	Principal aquifer properties and groundwater quality average (range) of selected unconsolidated sedimentary aquifers in Melbourne (compiled after Leonard, 1992; AGT et al., 2002).	60
Table III-7:	Lithology and main groundwater quality parameters of bores sampled.	65
Table III-8:	Selected groundwater quality of the Fyansford Formation-Brighton Group aquifer systems*.	67
Table III-9:	Sampling bore 125273 for further use in batch and column experiments.	68
Table III-10:	Characterisation of used aquifer materials (air-dried, <2 mm).	69
Table III-11:	Analysis of sediment particles <0.45 µm.	70
Table IV-1:	K_d values for linear adsorption isotherms at natural pH (series A1), corresponding linear coefficient of determination (R^2), % sorbed of initial metal concentration for highest initial concentration and % sorption of added OC (BR- brown Tertiary Brighton Group sediment, BL – black Tertiary Brighton Group sediment, WS – Quaternary Werribee Delta sediment with no and 30 mg-C/L addition of fulvic acid.	77
Table IV-2:	Experimental conditions and distribution coefficients of selected similar studies.	78

Table IV-3:	Desorption behaviour of Zn and Cu from different siliceous aquifer materials (BL – black Tertiary Brighton Group sediment, BR- brown Tertiary Brighton Group sediment, WS – Quaternary Werribee Delta sediment) previously adsorbed with Zn or Cu and 0 or 30 mg-C/L addition of fulvic acid without pH adjustments. Desorption solution groundwater at pH 7.	87
Table IV-4:	Influence of desorption solution oxygen concentration on desorption amounts for Zn and Cu in different siliceous aquifer materials.	90
Table V-1:	Mean packing parameters of duplicate columns for aquifer material (excluding the filter sand), while hydraulic parameters are for whole column (including filter sand).	97
Table V-2:	Variations of inflow solutions for experiments 1-3 (see also Figure VI-2).	99
Table V-3:	Chemical reagents and analytical conditions in the modified three-step sequential extraction procedure after Sahuquillo et al. (1999). All pH adjustments were done with conc. HNO_3.	100
Table V-4:	Retardation factor and calculated linear K_d of Zn from exp. 3 and from selected other column experiments including additional important experimental parameters.	120
Table V-5:	Retardation factor (Rf), calculated linear Kd (after equation (VI-1)) of Zn from column experiments compared to batch Kd values around pH 7, corresponding solid-solution ratios (SSR) and normalised Kd SS values [dimensionless] after Fehse (2004). See text for further explanations.	123
Table V-6:	Comparison of Zn loading in column test at 50% breakthrough (= Rf) and batch test.	124
Table V-7:	Linear regression for desorption (=negative) distribution coefficient (K_d) from (phase 4) storage stage samples obtained from dissolved versus sorbed concentration plot and corresponding linear coefficient of determination (R^2).	129
Table V-8:	Summary on accumulated Zn and Cu onto column aquifer sediments. Adsorption (positive) during stormwater injection (phase 2) and desorption (negative) during all combined storage samples (phases 3 + 4) and during recovery (phase 4).	134
Table V-9:	Mass balance [mg/kg] of introduced (inflow) Zn and Cu versus released (outflow) and retained amount (extracted from sediments) and percent accounted for (recovered).	142
Table VI-1:	Selected log_k values for reactions: $cation^{n+} + n\ X^- = cationX_n$ for BR2 with 0.054 mol/kgw exchanger sites.	159
Table VI-2:	Derivation of complexation constants for Cu and Zn onto the three sediments used in this study after Wang et al. (1997).	162
Table VI-3:	Selected surface complexation values showing a range of values for goethite, HFO and HAO.	173
Table VI-4:	Selected literature values for organic complexation constants of various metals with organic acids.	177
Table VI-5:	Selected stability constants for the formation of ternary complexes from reaction 1.	183

Table VI-6:	Added mass action equations and stability constants (log_k). Srfa (Suwannee River Fulvic Acid); Goe_OH: goethite surface site; HasOH: strong humic acid surface site; HawOH: weak humic acid surface site.	185
Table VI-7:	Kinetically modelled redox reactions with half stauration constants (after Parkhurst and Appelo, 1999) and various maximum degradation rates reported in the literature.	187
Table VI-8:	Modified coefficient of efficiency (E') (see equation VII-6) values for Zn, Cu and pH for simulations shown in graphs. All simulations are for BR2 if not indicated otherwise.	220
Table A-1:	Full analysis of all stormwater samples. See Table IV-1 for catchment parameters	269
Table A-2:	Analysis of mean values for column samples of experiment 2: flow parameters, physico-chemical parameters and anions.	273
Table A-2a	K_d values for adsorption experiments (series A4) with varying salinity of adsorption solution (BR- brown Tertiary Brighton Group sediment, BL – black Tertiary Brighton Group sediment, WS – Quaternary Werribee Delta sediment with no and 30 mg-C/L addition of fulvic acid.	277
Table A-2b	% metal sorbed for adsorption experiments (series A5) with varying pre-equilibration condition (BR- brown Tertiary Brighton Group sediment, BL – black Tertiary Brighton Group sediment, WS – Quaternary Werribee Delta sediment with no and 30 mg-C/L addition of fulvic acid.	277
Table A-2c	% metal desorbed for desorption experiments of series D3 with varying salinity of desorption solution (BR- brown Tertiary Brighton Group sediment, BL – black Tertiary Brighton Group sediment, WS – Quaternary Werribee Delta sediment with no and 30 mg-C/L addition of fulvic acid. Negative values indicate adsorption.	277
Table A-3:	Analysis of mean values for column samples of experiment 2, cations and metals.	278
Table A-4:	Analysis of mean values for column samples of experiment 3: flow parameters, physico-chemical parameters and anions.	282
Table A-5:	Analysis of mean values for column samples of experiment 3, cations and metals.	285
Table A-6:	Equations used by PHREEQC. For more details see Parkhurst and Appelo (1999	289
Table A-7:	PHREEQC database used for PHT3D simulations in Chapter VI.	290

Abbreviations and acronyms

0 or 30 in front of sediment ID	amount of added organic carbon [mg-C/L]
ASR	aquifer storage and recovery
ASTR	Aquifer storage, transport and recovery
BL	Tertiary black sandy sediment (see III.3.5)
BR	Tertiary brown sandy sediment (see III.3.5)
CA	component additivity
CEC	cation exchange capacity
DOC	dissolved organic carbon
EC	electrical conductivity
FA	fulvic acids
GC	generalised composite
HA	humic acids
K_d	distribution coefficient
NOM	natural organic matter
OC	organic carbon
Oxides	surrogate for oxides, hydroxides and oxyhydroxides
POC	particulate organic carbon
PZC	point of zero charge
SCM	surface complexation modelling
SOM	solid organic matter
TDS	total dissolved solids
TOC	total organic carbon
TSS	total suspended solids
WS	Quaternary sandy sediment (see III.3.5)

Abstract

In the light of increasing demand and diminishing supplies a sustainable urban water management for Melbourne and other cities will need to include water recycling and reuse of reclaimed water and stormwater. One key issue in stormwater reuse is the need for storage between times of collection until times of demand. Aquifer storage and recovery (ASR) would be a valuable option as it has limited space requirements and restricts loss from evaporation. However, stormwater commonly contains elevated levels of heavy metals, of which Zn and Cu are the most mobile. Stormwater also contains suspended solids, organic carbon, oxygen and nutrients, which influence the behaviour of injected metals and induce geochemical changes in the aquifer. While stormwater ASR has been practiced in limestone aquifers in South Australia, field data for sandy aquifers, which are more prevalent around Melbourne, are very limited. Risk assessment regarding the potential impact of stormwater ASR on the quality of the aquifer and groundwater resources in sandy aquifer is therefore necessary.

After a characterisation of stormwater from different Melbourne catchments confirmed comparatively high concentrations of Zn and Cu in stormwater, three siliceous aquifer sediments were used in a series of batch sorption experiments as well as column experiments imitating one ASR cycle to assess the impact of different parameters on Zn and Cu behaviour. The reactive geochemical transport model PHT3D was then modified to simulate experimental results with the outlook that it could be used as a predictive tool for long term evaluation.

The study showed that Zn adsorption was limited and desorption of large fractions occurred, indicating that injected amounts of Zn are mobile and would mainly be recovered. In contrast, Cu adsorption was higher and desorption was limited, indicating that injected amounts of Cu would mainly accumulate in the aquifer. The release of metals was triggered by reduction in pH, increase in ionic strength and particle mobilisation. Metal concentrations were also increased after storage phases, while minor sediment constituents, especially organic matter, significantly reduce metal mobility. The different role of dissolved and solid organic carbon is critical in understanding Cu behaviour during stormwater ASR.

Pretreatment of stormwater to reduce the injection of colloids, organic carbon and metals are recommended to limit metal accumulation in the subsurface. Monitoring of water quality throughout the ASR cycle would be encouraged to validate the current findings with field data. Special attention should be paid to backflushed water quality to ensure correct disposal.

Acknowledgements

I am profoundly indebted to my supervisors Dr. Gavin Mudd and A/Prof. Ana Deletic for their guidance, encouragement and financial support and my co-supervisor Dr. Peter Dillon, CSIRO Land and Water, Urrbrae, for professional advice and discussions.
I also owe immense gratitude to Dr. Henning Prommer, CSIRO Land and Water, Floreat, for sacrificing his personal time to show me the pleasures of modelling and without whom and the access to the CSIRO servers Chapter VI would not have been possible.
Special thanks go to Paul Pavelic, CSIRO Land and Water, Urrbrae, for funding my second trip to Perth courtesy of the Aquifer storage transport and recovery (ASTR) research project (see http://www.megalomedia.com.au/astr for details).

I would also like to acknowledge in no particular order the help of a number of people during my field trips and laboratory experiments:

- Justin Lewis and Peter Poelsma for the collection of stormwater samples
- Belinda Hatt for the supply of data from the biofilter and partial analysis of stormwater samples
- Bradley Pedler, Coffey Geosciences, and Dr. Chris Haberfield, Golder Associates, for the acquisition of aquifer sediments
- Sinclair Knight Merz (SKM) and private bore owners for access to groundwater bores
- Dr. Ian Cartwright (Geosciences) for the provision of laboratory facilities for batch experiments and metal extractions, as well as the use of the ion chromatograph.
- Deirdre Griepsma and Judy Beamish, Australian Sustainable Industry Research Centre (ASIRC), for assistance with the ICP-OES and TOC-analyser
- Tina Hines (Water Studies Centre) for access to the laboratory and the conduction of parts of the stormwater analysis
- Simon Roberts (Water Studies Centre) for the access to the nitrogen glove box in the wet laboratory and advice on oxygen analysis
- Prof. Peter Scales and Dr. Felix Meiser (Melbourne University) for the kind provision and assistance with the Malvern Nanosizer
- John Barnard (Chemical Engineering) for instruction to the Malvern Mastersizer and the supply with chemicals and utensils
- Frank Winston, Alan Taylor and Derek George for building and supplying my column set up
- Kevin Nievaart for setting up the datataker program

I would like to thank my fellow postgraduate students from Monash University for good company and sharing the joy and pain of a PhD research.

I also wish to extent my gratitude to my parents for their unconditional love combined with continuous financial and moral support.
Finally, I would like to announce my thankfulness to my partner, Martin Steinel, who has not only directly contributed to this work through academic discussions and proof reading, but to whom I owe my sanity. Thanks for your love and the wonderful years.

Chapter I: Introduction

"Anyone who can solve the problems of water will be worthy of two Nobel prizes - one for peace and one for science."
John F. Kennedy

I.1 Overview

Water is vital to the survival and growth of all life and all economic and environmental processes, but the world's supplies of freshwater are under increasing threat from overexploitation, pollution and climate change (Miller, 2005). Australia has experienced a severe drought over the last ten years and in Melbourne water supply reservoirs are at an all time low. 2007 had the lowest storage levels on record with below 30% at the end of June (Melbourne Water, 2008). A climate change study for Melbourne predicts higher temperatures and reduced rainfall for the future, which would increase demand and decrease supply (Howe et al., 2005). A sustainable water management is therefore vital for Melbourne and other cities around the world facing a similar challenge.

Decision makers have largely opted for desalination as the main solution to the problem. The high energy needs and the problems associated with disposal of highly saline brine make it an environmentally challenging option (Lattemann and Höpner, 2008). On the other hand, urban areas produce stormwater and treated effluent streams in volumes matching the demand (Mitchell et al., 2002; Radcliffe, 2004) and dispose of them into urban water ways and adjacent coastal areas leading to degradation of these ecosystems (Harris et al., 1996; Walsh et al., 2005). It is therefore of twofold benefit to recycle stormwater and reclaimed water and this has been identified as an important strategy in maintaining a sustainable water supply for Melbourne (Victorian Government, 2004).

The progress in this direction is often hindered, not by technical or economical reasons, but due to perceived health concerns by the public and decision makers (Po et al., 2003; Dolničar and Schäfer, 2006) and by institutional structures that are not suitable for non-centralised system. While water treatment is capable of rendering wastewater to superior quality than potable water (Cheremisinoff, 2002; Qin et al., 2005; Hammer, 2008), there is great potential to use recycled water for non-potable uses, which constitutes more than 70% of urban water demand (Mitchell et al., 2002). Public confidence is also increased when the water has been put back into the natural system before reuse (Dillon et al., 2006). This is the first benefit of aquifer storage and recovery (ASR), which is defined as well injection of

source water into a suitable aquifer for later recovery: it increases water quality, e.g. through the removal of pathogens and nutrients, in actual and perceived terms (Toze, 2006).

The biggest constraint to water recycling is the seasonal fluctuation in supply and demand, i.e. high demand in summer and in years with lower than average rainfall. The problem of water storage in an urban environment with limited space is serious for projects greater than household scale (Hatt et al., 2006). ASR could provide capacity for inter-seasonal or inter-year storage, especially in aquifers of higher salinity that are of limited beneficial use (Pyne, 1995; Maliva et al., 2006). It has the additional advantage over surface storage of limited space requirements, limited loss of water due to evaporation and other surface water related problems like algal blooms (Pyne, 1995; Dillon et al., 2006).

Despite these benefits, uptake of ASR in Melbourne has been limited by

- insufficient legislation and guidelines for water recycling including water ownership issues (Hatt et al., 2006).
- lack of experience and knowledge in the water industry and relevant authorities (Dillon, 2005; Hatt et al., 2006)
- lack of detailed hydrogeological knowledge (Dudding et al., 2006)
- limited well designed and monitored field project (see II.2.4) with long-term performance data
- limited hydrogeological knowledge on contaminant attenuation processes and contaminant mobility (Dillon, 2005; Maliva et al., 2006)

As policies on water recycling and guidelines for ASR in Victoria are currently under review (see II.2.5), there is increased requirement to prove the long-term sustainability of ASR systems using resources of non-potable water quality. Before field trials commence, laboratory studies and geochemical modelling are therefore needed to assess potential risks to help establish management measures and pretreatment targets.

Reclaimed wastewater and stormwater are two rather different sources. Treated effluent contains much higher amounts of nutrients, organic matter and dissolved solids, while stormwater has generally better water quality with the common exception of metals concentrations (Mitchell et al., 2002). This study focuses on stormwater reuse and is therefore mainly concerned with non-degradable heavy metals. The metals of main interest in stormwater in general and in Melbourne specifically have been found to be zinc and copper (see III.2.3; Duncan, 2006) and were hence selected to be the main focus.

ASR scheme feasibility depends largely on the storage capacity of the aquifer and they are preferably implemented in transmissive sandy or limestone aquifers (Pyne, 1995). Limestone aquifers have been used successfully for stormwater ASR in South Australia (see II.2.4) and provide a high retention capacity for metals due to the alkaline pH (see II.4.5). The hydrogeological setting of Melbourne (see III.3) is quite different and potential ASR sites are situated in sandy alluvial aquifers (AGT et al., 2002; Dudding et al., 2006), which have lower pH and might have limited sorption capacity for heavy metals. A clear gap in ASR experience in alluvial sands has been recognised (AGT et al., 2002) and further confined the focus of this thesis.

The general aim of this study was the assessment of injected metals derived from stormwater during stormwater ASR in sandy aquifers. As no field sites fulfilling these criteria are in operation in Melbourne or anywhere else in Australia, this study was limited largely to laboratory experiments. Common empirical methods to investigate metal solid-solution interactions are batch (OECD/OCDE, 2000) and column tests (Schweich and Sardin, 1981; Bürgisser et al., 1993) and were hence employed. Currently available hydrogeochemical models (Prommer et al., 2003) were adapted and enlarged to help interpret the empirical results.

I.2 Structure of this thesis

The approach of this thesis is to use three different sandy sediments, metal-spiked stormwater and native groundwater from Melbourne to investigate important aspects of metal behaviour during stormwater ASR.

- Chapter II presents the background to the ASR technology, related quantitative and qualitative issues and current use and guidelines. A brief introduction to priority pollutants in stormwater are given along with the main processes and factors influencing metal speciation in the subsurface environment. It also states the aim and objective of this work as identified by the literature review.
- Chapter III gives a characterisation of Melbourne's stormwater contaminants and hydrogeological setting and presents the materials used for the following laboratory work.
- Chapter IV illustrate the results from a number of batch test series for adsorption and desorption of Zn and Cu.
- Chapter V shows the results from three column test series simulating one complete ASR cycle.
- Chapter VI develops an approach to simulating the column results with a geochemical reactive transport model.

- Chapter VII summarises the thesis with a review of key findings and their implication on future ASR implementation in the field. It also evaluates the strengths and weaknesses of the thesis and concludes with recommendations for further research.

Chapter II: Background and scope

"The Romans realized, as have every civilized people since, that living in cities is impossible if the water supply is not reliably clean and fresh."
Frank and Francis Chapelle, The Hidden Sea: Ground Water, Springs and Wells, 1997

This chapter will identify and review the main issues related to stormwater ASR. It will start with an introduction to the general aspects of stormwater reuse and especially of injection ASR and will then highlight research undertaken at already established ASR systems and how to establish new systems. A look at the source of water will identify priority pollutants in stormwater. The interactions of metals with solids and solutions will be introduced and followed through an ASR cycle. The lessons learned and conclusions drawn from this background analysis will then lead to the objectives for this study outlined in chapter III.

II.1 Introduction

Urbanisation and population growth are two dominant demographic trends that lead to greater localised demand on freshwater resources on the one hand and decreasing supply from natural surface water and groundwater sources due to increasing pollution and land use changes (Miller, 2005). Australia has the second highest per capita domestic water use (320 L/day/person) in the world (Radcliffe, 2004) and is generally a dry continent with climate change forecasts predicting even lower rainfall over wide areas for the future (CSIRO and BOM, 2008). The annual volumes of urban stormwater and treated wastewater commonly exceed the average urban demand in Australian cities (Mitchell et al., 2002), and are degrading urban streams and adjacent coastal areas under current urban water cycle management (Walsh et al., 2005). However, recycling of these water resources has been very limited in Australia and only about 4% of rain- and stormwater and 1% of reclaimed wastewater was reused in 2004 (Dillon and Ellis, 2004). It has therefore been recognised that the reuse of urban treated effluent and stormwater, especially for non-potable use, must be a greater part of a future sustainable urban water management (DSE, 2004).

Compared to treated effluent, stormwater has the advantage of lower concentrations in nutrients, organic matter and total dissolved solids (Mitchell et al., 2002) and is perceived more acceptable for reuse by the public (Po et al., 2003). On the other hand, treated effluent streams are a relatively constant and continuous source, while stormwater is generated in single events of different magnitudes and often occurs seasonally confined. A vital part of stormwater reuse is therefore the collection and storage of the spatial and temporal variable

source for later access. The most common form of small scale stormwater reuse is the collection of roof runoff in rainwater tanks. It has been widely employed in rural areas and is increasingly implemented in urban households for domestic use (Coombes and Kuczera, 2001; Mitchell, 2004; Zwar, 2004). For larger catchments, detention ponds, retarding basins and reservoirs are needed (Hatt et al., 2006) requiring increasingly more space, which is a limited and costly asset in the urban environment and poses a mayor problem. Recharge of stormwater to underlying aquifers has therefore a range of advantages over surface impoundments (Asano, 1985; Pyne, 1995; Dillon et al., 2006):

- overcome storage issue by potentially providing high capacity for inter-seasonal and inter-year storage
- limited space requirements above ground
- reduced evaporation losses
- reduced algal blooms or mosquito breading spaces
- attenuation of pathogens and organic stormwater contaminants

The artificial recharge of groundwater can occur via three main techniques (Dillon, 2005):

(a) Infiltration of stormwater can occur via infiltration basins, seepage trenches or vadose zone wells and requires the availability or construction of an adequate permeable soil and unconfined aquifer (Bouwer, 2002). The main problem with these infiltration systems are low infiltration rates, decreasing with increasing clogging. A major advantage is the water quality improvement, e.g. nutrient removal, during the passage of the vadose zone (Pitt et al., 1999; Fischer et al., 2003). Soil Aquifer Treatment (SAT) utilises the geopurification qualities of the soil as a natural filter and involves cyclic infiltration with wet and dry stages (Bouwer, 1996; Kopchynski et al., 1996).

(b) Indirect recharge of groundwater can be achieved via bank filtration where recovery wells are placed close to rivers or artificial stormwater basins to draw the surface water through a passage of shallow groundwater aquifer (Tufenkji et al., 2002; Grünheid et al., 2005, Hubbs, 2006).

(c) Injection of water into the aquifer can involve one well for injection and recovery and is defined as aquifer storage and recovery (ASR), while the use of one well for injection and one well for recovery is defined as aquifer storage, transport and recovery (ASTR). It requires a suitable aquifer (see II.2.2.1) and more infrastructure, but injection rates are usually higher than infiltration rates (Bouwer, 2002).

II.2 The technique – ASR in theory and case studies

ASR (see II.2.1) has been practiced for a number of decades worldwide, most prominently in the USA (Pyne, 1995), mainly for long-term and emergency storage. It is becoming more popular in the Middle East together with desalination plants (e.g. Almulla et al., 2005). Most of these schemes have been performed with high quality water in order to enhance drinking water supplies and are therefore mainly concerned with quantitative aspects of the operation (see II.2.2). In Australia (see II.2.4) the focus has been mainly on using lower quality water to enhance non-potable water resources. For these schemes qualitative aspects of injected, recovered water, groundwater and the aquifer (see II.2.3) are paramount and will be the main focus of the following sections.

II.2.1 The ASR cycle

In general, managed underground storage involves the following elements (Figure II-1):

1. Collection or harvesting: the water sources can include potable water, surface water, groundwater, treated effluent, and stormwater. This study will be concerned with urban stormwater runoff.
2. Pretreatment: As a result of atmospheric deposition and urban surfaces wash off, runoff waters are contaminated by various compounds including suspended solids, heavy metals, organic compounds, nutrients and pathogens (Mikkelsen et al., 1997; Pitt et al., 1999). Pretreatment options can include standard stormwater pollution control design practices (US EPA, 1999; Victoria Stormwater Committee, 1999; Ellis, 2000) like litter and sediment traps, wetlands and ponds, advanced treatment and disinfection (Hatt et al., 2006).
3. Injection: Aquifers can be recharged via direct recharge wells into a wide spectrum of confined or unconfined aquifer types, from unconsolidated sands and gravels to limestones and fractured sedimentary or volcanic rocks.
4. Storage: The water is stored in the aquifer surrounded by a buffer zone which separates the native groundwater from the injected stormwater.
5. Recovery: Recovery is typically achieved through dual-purpose recharge and recovery wells (ASR) or extraction wells (ASTR) in a number of recovery stages depending on demand.
6. End use: Recovered water can be used for drinking water, irrigation, fire fighting, environmental flows, toilet flushing, industrial cooling, and other purposes and might be subjected to post treatment.

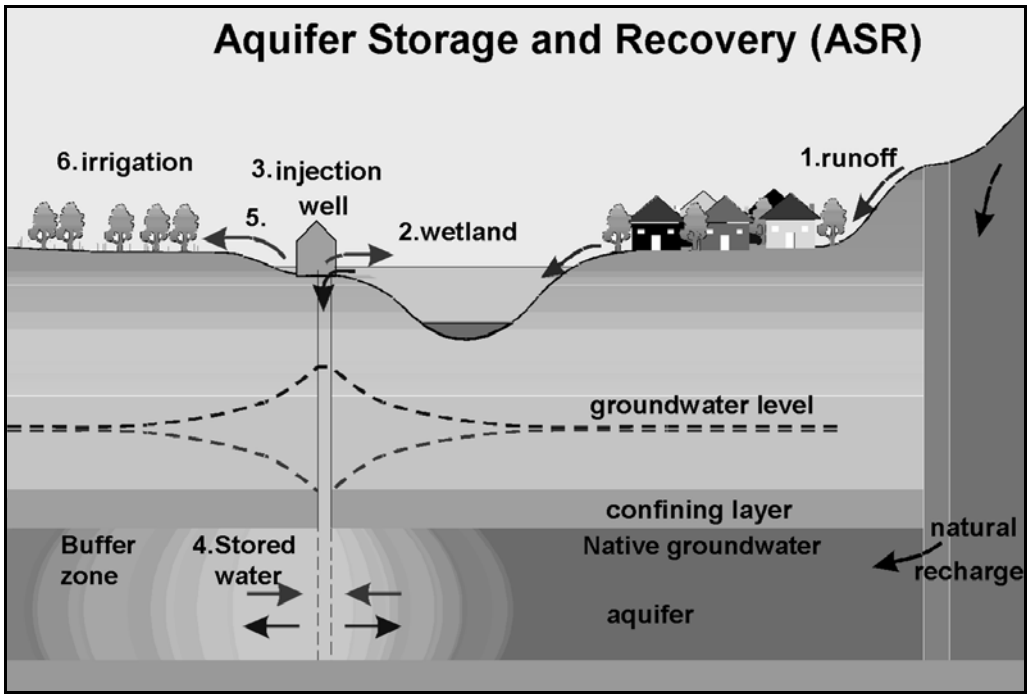

Figure II-1: Schematic aquifer storage and recovery system (modified after Dillon, 2004)

II.2.2 Water quantity considerations

The site selection for an ASR scheme will depend on a range of factors. Firstly a suitable water source and a local demand together with the availability of same space for stormwater collection and pretreatment are needed. Secondly, administrative, economic and operational constraints have to be met and finally a suitable aquifer must be available (Pyne, 1995).

II.2.2.1 Suitable aquifer

The suitability of the aquifer is mainly defined by (Pyne, 1995; AGT et al., 2002; NRC, 2007):

- Storage capacity: Both fractured and unconsolidated rock systems could be used for ASR systems. While storage capacity in fractured rock can be quite high, their recovery efficiency is often lower due to the usually not well known heterogeneous characteristics of the fractures (Parsons and Evans, 2002; NRC, 2007) Dual porosity limestone aquifers have been favoured in many regions due to their potential for increasing the storage volume by calcite dissolution and water quality improvements even with low recovery efficiency in karstic regions (Gerges et al., 2002a) Unconsolidated porous aquifer systems have potentially the highest storage capacity. Predictions about the hydraulic performance of the system are much more reliable than for fractured rocks. In general, the aquifer should be sufficiently transmissive to avoid excessive build-up of groundwater mounds, preferably homogeneous and of sufficient extent for the scale of the ASR scheme.
- Groundwater quality: Areas with drinking water quality groundwater are unfavourable for stormwater ASR, as interference with other values are highly likely. It is commonly advisable to have a lower quality groundwater, so beneficial use will not be impaired by

the injection of non-potable water. Very high salinity levels on the other hand will increase the buffer zone of an ASR scheme substantially or will limit the recovery efficiency. Contaminated aquifers need to be avoided, as this would compromise the quality of the recovered water.

- Confinement: Implementation of ASR systems is technically feasible in either confined or unconfined aquifer systems. Unconfined aquifer use is generally cheaper as they are shallower, but there are constraints on the recharge volume as groundwater levels have be kept low enough not to cause any impact on building foundations, tunnels or natural surface recharge area or create unwanted surface discharge. Unconfined aquifers are also more prone to contamination deriving from surface land use. Confined aquifers have very limited impact on surface features, but caution must be taken not to over pressurise the aquifer and cause rupture of the confining layer. Proximity to recharge areas should be avoided.

II.2.2.2 Recovery efficiency

The recovery efficiency is defined as the percentage of water volume injected compared to the water volume that can be recovered within the target water quality criteria. Theoretically in the case of fresh stormwater injection (e.g. 100 mg/L) into brackish groundwater (e.g. TDS 3000 mg/L) recovered for irrigational use (TDS <1500 mg/L) it means that recovery efficiency could be higher than 100% as a certain amount of groundwater could be recovered in addition to the injected stormwater before the target value of 1500 mg/L TDS is met. Usually though, a buffer zone of injectant is created either at the start of the ASR scheme or over a number of first cycles (with increasing recovery efficiency) to build a barrier between the native groundwater and the injectant (Pyne, 1995).

Recovery efficiency can be reduced due to

- high regional hydraulic gradient leading to advective loss of injectant
- highly saline aquifers with either density stratification occurring or high transmissivity leading to breakthrough of more saline waters at the well
- highly inhomogeneous, e.g. fractured or karstic, aquifers
- leaky aquifers resulting in loss to over- or underlying aquifers

Most of these problems could be overcome with using ASTR schemes rather than single well schemes or trickle flow during storage to compensate for density stratification.

II.2.2.3 Clogging

One problem not only experienced with infiltration but also associated with injection ASR is clogging. This reduction in porosity mainly around the injection well leads to a decrease in injection rate and an increase in hydraulic head. It can be caused by various mechanisms

like physical clogging by suspended solids, mechanical clogging by gas binding (esp. with increase in temperature), chemical clogging due to precipitation, clay swelling or dispersion and biological clogging due to microbial growth (Pyne, 1995; Rinck-Pfeiffer, 2000; AGT et al., 2002; Bouwer, 2002). Clogging is a process that will usually occur, but in most cases can be managed with pretreatment and redevelopment (Dillon et al., 1997; Brown et al., 2006). The pretreatment can include filtration/coagulation of suspended particle and microorganisms, addition of pH elevating substances to reduce iron precipitation and disinfection to avoid microbial growth (Pyne, 1995; Stuyfzand et al., 2006; Dillon et al., 2007). Periodical redevelopment by purging the well will nevertheless be undertaken in more or less regular intervals at all sites. The disposal of these backflushed waters that are usually of low quality have to be accounted for in the planning stage of ASR schemes (Dillon, 2004). Limestone aquifers are likely to compensate for loss in porosity by dissolution of carbonic matrix and addition of acidic agents has been used to enhance this process and decrease the effect of clogging (Gerges et al., 2002b).

II.2.3 Water quality considerations

The uncertainty regarding the possible impacts of recharge water on the beneficial use of the native groundwater resources, the potential for increased discharge into streams and wetlands and the quality of the recovered water is the motivation for an understanding of the fate of contaminants present in the recharge water and the interactions taking place in the disturbed groundwater system. A better understanding of these processes will also help with guideline development and is of crucial importance for protecting environmental values and beneficial uses of the groundwater as required by statutory authorities such as the Environmental Protection Agency (EPA Victoria, 2003).

Temporally, water quality changes are maximal during the initial ASR operating cycles. During consecutive cycles the groundwater in the storage zone will be completely exchanged and geochemical reactions will have adjusted to the new equilibrium of the stored water, especially if not all injected water is recovered. However, in very heterogeneous aquifers lenses and layers of low hydraulic conductivity diffusion processes might require several cycles to flush the residual native groundwater (Pavelic et al., 2006b).

Spatially, water quality changes are at a maximum around the injection well, where the number of pore flushes, geochemical variations and the hydraulic gradient are highest. In the main storage zone the number of pore flushes is reduced and water quality changes are less pronounced as the water has been pre-equilibrated around the well. Depending on the differences between injectant and native groundwater, the differences in water quality in the buffer zone furthest away from the well could nevertheless still be significant. Ideally this

buffer zone will not be recovered but changes in injection and recovery volume might significantly shift the buffer zone and will require re-equilibration of waters (Dillon et al., 2005).

Depending on the source water and the end use different aspects of water quality will be of importance. A good compilation of water quality improvements that can be achieved during ASR has been presented by Dillon et al. (2005) based on experimental research and monitoring from 10 ASR sites implemented in limestone, alluvium or sandstone using potable water, stormwater or reclaimed water as injectant. When using potable water as injectant or recovering water for potable use, micropollutants like disinfection byproducts (II.2.3.1) and endocrine disruptors (II.2.3.2) are of concern. When using lower quality water as recharge the removal of pathogens (II.2.3.3), natural organic matter (NOM) and nutrients and associated redox reactions (II.2.3.4) are of more importance. For all schemes biogeochemical interactions with the aquifer matrix like ion-exchange (II.2.3.5) and dissolution/precipitation (II.2.3.6) will have an impact on the recovered water quality though. As the use of stormwater as injectant is a relatively new development and has only been monitored in limestone aquifers (see II.2.4.2+3) the fate of injected metals has not been addressed so far. Hence no critique of previous studies can be given. Pollutants associated with stormwater will be discussed in section II.3 and processes influencing metal behaviour are presented in section II.4.

II.2.3.1 Disinfection byproducts

The formation of carcinogenic disinfection byproducts (DBPs) like trihalomethanes (THMs) and haloacetic acids (HAAs) can occur during chlorination of waters containing natural organics acids and bromide or can form in situ when residual chlorine comes in contact with dissolved organic matter in the aquifer (Pyne, 1995; McQuarrie and Carlson, 2003). It has been shown that HAAs are highly degradable under aerobic conditions (Thomas et al., 2000) found near the injection well and are usually eliminated in a few days and were not found in the recovered water of any monitored site (Dillon et al., 2005; Pyne, 2006). THMs on the other hand are degraded under anaerobic conditions and elimination rates are highly variable depending on the redox state of the aquifer system (McQuarrie and Carlson, 2003; Dillon et al., 2005). They are typically attenuated in a few weeks of storage due to anaerobic microbial activity, but might be very persistent in aerobic unconfined ASR systems (Nicholson et al., 2002; Pyne, 2006). As DBPs degradation is enhanced by microbial activity, very low organic carbon concentration (<1 mg/L) in the recharge water can increase their half-life significantly (Pyne, 2006).

The formation of DBPs could be avoided when disinfection of injectant is undertaken with UV or is used in post-treatment rather than pretreatment, as ASR provides the opportunity for natural pathogen removal (Pyne, 2006).

II.2.3.2 Trace organic contaminants

Endocrine disrupting components (EDCs) and pharmaceutically active compounds (PhACs) have been detected in treated effluents at concentrations usually in ng/L range (Toze, 2006) and are spreading into a wide range of aquatic environments and might also be present in stormwater (Heberer, 2002). They comprise a range of complex organic contaminants with varying chemical properties leading to rather diverse behaviour (Boethling and Mackay, 2000). Experiments with five different EDCs showed that some degraded at different rates under aerobic conditions, while all of them were persistent under anaerobic conditions (Ying et al., 2003). Field experiments with six different PhACs showed that while four of them were retarded, two of them were very mobile (Oppel et al., 2004). It is likely that the more persistent components would be attenuated by sorption to the matrix, which would increase their residence time and hence increase the chances of degradation (Boethling and Mackay, 2000). While redox zonation varies spatially in the aquifer, microbial reactions are also temperature dependent and hence temporal variation of redox zones might increase or decrease degradation, depending on the component under investigation (Howard, 2000; Greskowiak et al., 2006).

Overall, generalisation of degradation rates for organic micropollutants are not possible (Howard, 2000), but estimations about their potential for biodegradation might be obtained from their chemical structure and functional groups (e.g. Boethling et al., 1994; Hiromatsu et al., 2000; Raymond et al., 2001).

II.2.3.3 Microbial pathogens

Pathogens comprise a diverse group of microorganisms, most commonly enteric viruses, bacteria and protozoa (Pitt et al., 1999; Toze, 2006). Bacteria (e.g. E. coli, Salmonella, Streptococci, Legionella, Shigella) are the most common but usually least infectious microbial pathogens. Pathogens have been found in high concentrations (e.g. total coliforms average 100 000 to 200 000 cfu/100mL) in wet weather urban runoff originating from animal faeces and sewer overflow (Duncan, 2006). Protozoa (e.g. Giardia) can persist as dormant stages (cysts or oocysts) outside of their host. While suspended in the stormwater flow, they are subject to degradation by UV or can attach to suspended solids. The fraction of organisms associated with settleable particles varies by type of microbe, and the partitioning behaviour of each organism generally changes between dry weather and storm conditions (Characklis et al., 2005; Haydon and Deletic, 2006).

Once injected, their inactivation in the subsurface can be achieved by adsorption, filtration, oxidation, degradation by native groundwater microorganisms and die-off (Pitt et al., 1999; Schijven et al., 2000; Vega et al., 2003; Foppen and Schijven, 2006). The main factors favouring long-term survival of pathogens in the ground are small size (reduced straining esp. for viruses (Powelson et al., 1993)), soluble organics (reduced adsorption), low oxygen levels (reduced oxidation), low temperature, high pH and low salinity (prolonged life span) and the native microbiota (John and Rose, 2005). Monitored ASR sites achieved complete removal of pathogens (Dillon et al., 2005) and storage times longer than 90 days can be assumed to be long enough for pathogen levels to drop sufficiently (Pyne, 2006).

II.2.3.4 NOM and associated redox reactions

Natural organic matter (NOM), usually measured as total organic carbon (TOC), consists of both particulate (POC) and dissolved (DOC) organic carbon and comprises a complex mixture of low to high molecular weight organic molecules usually classified into simple organic compounds (e.g. amino acids, carbohydrates, hydrocarbons, carboxylic acids, proteins) and humic substances (e.g. fulvic acids (FA), humic acids (HA) and humin). The bulk of NOM found in stormwater are fulvic and humic acids (Sekaly et al., 1999; Li and Dai, 2006). The degradation rate of NOM varies widely, depending on molecular weight and chemical structure, especially functional groups (Table II-1). In general, smaller molecules with carboxylic and phenolic groups are favourable for biodegradation while large aromatic and branched molecules with nitrogen containing functional groups are more stable (e.g. Thurman, 1985; Howard, 2000).

Table II-1: Selected average properties of FA and HA (compiled after Stevenson, 1982; Sparks, 2003)

	Fulvic acids	Humic acids
molecular weight [kDa]	0.3-2	2-1000
size of aggregates [µm]*	<0.1-1.2	0.2-5
solubility [pH]	1-14	>5.5
carboxyl groups [cmol/kg]	400	310
phenolic hydroxyl groups [cmol/kg]	460	420
alcoholic hydroxyl groups [cmol/kg]	80	130
total acidity [cmol/kg]	860	720

* depending on pH, complexing cation and salinity of solution; configurations can be globular, sheet or thread like.

FA are soluble over the whole pH range, while HA are insoluble at lower pH. Coagulation of HA starts at pH lower than 4.5 (Greenland, 1971) - 6.5 (Kerndorff and Schnitzer, 1980). Depending on type and amount of cations, amount of NOM in solution and pH humic substances change their configuration. They are most elongated and flexible at high pH, low salinity and low NOM concentration (e.g. stormwater), while they form spheres at higher salinity (>0.05 M), in the presence of trivalent cations and at high NOM concentrations (Ghosh and Schnitzer, 1980). This weak-acidic polyelectrolyte behaviour is due to their acidic

functional groups, which play an important role for cation and metal binding and pH buffering. Acid-base titrations are commonly employed to characterise the amount and type of functional acidic groups (Stevenson, 1982).

NOM can adsorb to clay minerals and oxides via a range of mechanisms, e.g. physical bonding (van der Waals' forces), electrostatic bonding (ion exchange), hydrogen bonding, depending on the properties of the organic molecule, pH (maximal at pH 4.5 (Jardine et al., 1989) and surface properties of the clay or oxide (Stevenson, 1982). The usually positive surface charge of the underlying clay or oxide thus changes to negative surface charge and thereby influences the cation exchange capacity, sorption of other organic molecules and colloidal stability of the particles (e.g. Stevenson, 1982; Kaplan et al., 1993; Kretzschmar and Sticher, 1997). A complete reversal of surface charge and complete coating of matrix with NOM can be achieved with as little as 0.5 mg-C/L TOC (Day et al., 1994). Mono-layer coverage of organic matter may impede further sorption of NOM (Jardine et al., 1989; Day et al., 1994), but competitive exchange of more hydrophobic macromolecules with less hydrophobic molecules has been observed (Gu et al., 1996a, b; Knabner et al., 1996), resulting in higher mobility of smaller organic molecules.

NOM in the injectant is the major driving force for microbial growth. Its oxidation acts as an energy source for microorganisms and controls the redox status especially near the injection well. In the theoretical sequence of subsurface reduction reactions from a highly oxidizing to highly reducing condition the dominant redox sensitive species are oxygen, nitrate, manganese (IV), iron (III), sulfate and methane (Stumm and Morgan, 1996). If the electron acceptor is an aqueous species like O_2, protons are consumed, while reactions involving reduced minerals (e.g. sulfides, ferrous oxides) can release protons (Appelo and Postma, 1999a). In the natural subsurface environment these processes will be partly taking place simultaneously due to heterogeneities of the matrix, distribution of reactants and microorganisms, meaning that there is usually no equilibrium between all redox couples in the groundwater (Lindberg and Runnels, 1984). Meaningful Eh or pe values are therefore very difficult to obtain (Chapelle et al., 1995).

Typically groundwaters are low in both particulate and dissolved organic carbon (<0.5 mg-C/L) (Malard and Hervant, 1999; Pabich et al., 2001). The recharge with organic, oxygen and nutrient enriched injectant therefore is a major disturbance to the system (Bahr et al., 2002). Around the well (<10 m) where particulates are entrained (Skjemstad et al., 2002; Greskowiak et al., 2005), a so called "treatment" or "proximal" zone with highly elevated microbial activity develops. Here dissolved oxygen is eliminated in a few days, followed by

nitrate reduction lowering the redox potential from +300 to +400 mV to -200 to -400mV (Vanderzalm et al., 2006b) triggering further geochemical reactions like degradation of organic contaminants, mineral dissolution/precipitation, sorption and pH changes that influence the quality of the recovered water (Dillon et al., 2005).

II.2.3.5 Ion exchange

The aquifer matrix provides a number of cation exchange sites on clay minerals, oxides and organic matter (Appelo and Postma, 1999a, see II.4.1.2). The injection of low salinity, mostly Ca dominated recharge water, into brackish mostly Na-Mg dominated groundwater, firstly decreases the salinity, which might cause swelling of clays and a decrease in permeability (Johnson et al., 1999; Konikow et al., 2001). Secondly, it will lead to simultaneous homo- and heterovalent ternary cation exchange. While exchange coefficients are not constant but vary with ionic strength and type of ions in solution, as well as exchanger phase composition and pH (McBride, 1994; Sparks, 2003), the selectivity sequence would usually favour Ca, which would replace Mg, which in turn replaces Na, leading to a high loading of Ca on the exchanger and increased concentrations of Na and Mg in the solution (Appelo et al., 1990; Appelo et al., 1993). This usually helps to restore the permeability (Beekman et al., 1990). During the establishment of an ASR scheme these ion exchanges will be moved outwards into the buffer zone and not play a major role for later ASR cycles (Bahr et al., 2002).

II.2.3.6 Dissolution/precipitation

The chemical stability of minerals depends on redox and pH conditions as well as the activity of ions in solution (Appelo and Postma, 1999a). As stormwater is usually neutral, the change in redox state is the main driver for mineral dissolution and precipitation reactions, which are therefore mainly taking place near the injection well. Minerals of high reactivity and main importance in ASR are carbonates, hydr-/oxides and sulfides. Dissolution of minerals, especially carbonates, is induced by undersaturation with low ion activity in the recharge waters, especially by highly treated injectants (Johnson et al., 1999). The decrease of pH due to release of CO_2 during organic matter degradation also accelerates dissolution of carbonates (Herczeg et al., 2004). In limestone aquifers this relieves the effect of clogging but might lead to collapse of the aquifer matrix structure (Pavelic et al., 2006b).

The interplay between oxidative/reductive changes induced by ASR and dissolution/ precipitation reactions with minerals can be complex. The injection of oxygen into an anoxic aquifer with dissolved Fe and Mn will lead to the precipitation of amorphous hydroxides, while reductive dissolution of Mn- and Fe-oxides starts after oxygen is completely depleted and nitrate is in the progress of reduction (von Gunten and Zobrist, 1993; Stumm and Morgan, 1996; Grybos et al., 2007). Both reactions occur in ASR operations close to the

injection well, where the injected organic matter induces redox and pH changes (Vanderzalm et al., 2002; Greskowiak et al., 2005). While the precipitation of minerals will lead to co-precipitation and adsorption of trace metals, the dissolution will in turn mobilise previously incorporated or adsorbed trace metals (Bahr et al., 2002). Pyrite oxidation is of special importance as it releases mobile oxyanions like arsenate and selenate and mobile cations like nickel and zinc. It also significantly reduces the pH due to the formation of sulphuric acid in solution, which can mobilise other adsorbed metals (see II.4.5). Multiple ASR sites (see II.2.4) have experienced a reduction in recovered water quality due to geogenic metal release related to pyrite oxidation (Brown et al., 2006). Over a number of ASR cycles these effects seem to be decreasing and shifting towards the buffer zone of the ASR scheme (Pyne, 2006).

II.2.4 ASR in use

Research on potable injection and infiltration ASR has been going on for some decades (Dillon et al., 1994), with most emphasise on quantitative aspects like clogging and recovery efficiency. Australia appears to be at the forefront of non-potable water recycling and as one of the driest countries in the world has focused on water reuse in urban areas. Adelaide, South Australia, has taken on a leading role in ASR research and has operational, trial and proposed sites, which are more or less well studied (Gerges et al., 2002b) and findings will be introduced here in more detail. As these sites are all situated in limestone, they will be complemented by other sites situated in sandy aquifers, before potential sites in Melbourne will be introduced.

Generally, performance results are somewhat limited, partly because some projects are still relatively new, partly because water quality monitoring has only been carried out infrequently or documented. This is partly due to the fact that currently in Australia no specific guidelines for stormwater recycling are in place and that existing (usually treated wastewater recycling) guidelines are not enforceable standards (Hatt et al., 2006).

II.2.4.1 Bolivar, South Australia

By far the best monitored ASR site in Australia is Bolivar, where treated effluent has been injected into a confined Tertiary limestone aquifer in the Northern Adelaide plains since 1999. 17 monitoring bores positioned at a radius of 4, 50, 75, 120, 300 and 700 metres from the main injection well with various screened intervals (Dillon et al., 2005) allowed research on clogging (Rinck-Pfeiffer, 2000; Dillon et al., 2001; Pavelic et al., 2007), biogeochemical processes (Skjemstad et al., 2002; Vanderzalm et al., 2002; Vanderzalm et al., 2006b), pathogen survival (Toze , 2004), fate of organic compounds like DBPs and EDCs (Toze et al., 2001; Nicholson et al., 2002), hydraulic characterisation (Le Gal La Salle et al., 2002,

Pavelic et al., 2006a), metal behaviour (Vanderzalm et al., 2006a; Vanderzalm et al., 2007) and modelling of fate of organic matter (Greskowiak et al., 2005). Of main interest for this study are the results on the fate of organic matter and geogenic release of metals.

Treated effluent is higher in salinity (~1300 mg/L), nutrients and NOM than stormwater (Mitchell et al., 2002). TOC levels in the reclaimed wastewater are on average 15-20 mg-C/L with high amounts of small organic molecules and only little aromatic material (average molecular weight < 0.2 kDa) (Skjemstad et al., 2002). While POC (~ 8% of TOC) was intercepted close to the well resulting in a continuous localised source of DOC (Greskowiak et al., 2005), only a reduction by about 14-18% of DOC was observed over 4 m from the injection bore due to mineralisation by oxygen and nitrate. The drop in DOC further away from the bore (50-75 m) to about 5 mg-C/L was mainly due to mixing, as the total reduction of DOC was 20-24% over a complete cycle (Vanderzalm et al., 2006b). Further away from the injection bore (50 m) mainly higher molecular weight organic matter was missing due to sorption onto the matrix (Skjemstad et al., 2002). Denitrifying conditions were prevalent throughout the storage zone. Only around the well lower redox conditions were developed during the storage phase (Vanderzalm et al., 2006b). It can be speculated that once the sorption capacity of the aquifer matrix has been reached a higher percentage of the injected DOC will be mobile and transported further into the aquifer. As microbiological activity is less significant further away from the injection bore, its degradation will also be limited (Dillon et al., 2005) and DOC concentration might increase in the storage zone over time.

The injectant had higher dissolved Ni concentration than the native groundwater, while Zn and As were comparable in both. The high pH of the limestone aquifer generally favoured the sorption and precipitation of these metals as carbonates (Vanderzalm et al., 2006a). The low redox values that developed during storage in the vicinity of the injection bore resulted in reductive dissolution of minerals and release of previously adsorbed/precipitated and geogenic metals, but metal concentrations dropped rapidly after the start of recovery and also over consecutive cycles (Vanderzalm et al., 2007). As this zone of low redox value was spatially limited, the effect on the overall water quality of the recovered water was minimal. Nevertheless, the water recovered initially after storage should be disposed of accordingly as arsenic concentrations reached a maximum of 186 µg/L (Vanderzalm et al., 2007).

II.2.4.2 Andrews Farm, South Australia

The most intensively investigated stormwater injection scheme is Andrews Farm, where stormwater from a detention pond was injected into a brackish confined Tertiary limestone aquifer and monitored at three observation bores (25, 65 and 325 m) from 1993-1998. Geochemical processes characterisation (Rattray, 1999; Herczeg et al., 2004), hydraulic

characterisation (Herczeg et al., 2004; Pavelic et al., 2006b), batch and column tests on attenuation of contaminants (Oliver et al., 1996), pathogen fate (Pavelic et al., 1998) and water quality changes (Dillon and Pavelic, 1996) have since been investigated.

The geochemical reactions found were similar to Bolivar but to a lesser degree as the source water had much lower values in nutrients and NOM. Carbon isotopes indicated that a substantial fraction of the occurring dissolved inorganic carbon (DIC) resulted from oxidation of fresh organic material (Herczeg et al., 2004). In addition the sulphur isotopes in combination with the sulphate mass balance suggests that sulfide oxidation and sulphate reduction occur simultaneously in different zones in the aquifer due to heterogeneities or may be attributed to a non-steady state (Herczeg et al., 2004). Breakthrough of injectant was observed fastest along high permeability flow paths and heterogeneity in the aquifer was visible from temperature and chloride data. Mixing between injectant and native groundwater occurred during the main storage periods with decreasing magnitude over a number of cycles, when dual-porosity characteristics were overcome (Pavelic et al., 2006b).

One interesting aspect of this study was the mass balance of sediments injected and recovered during air-lifting. Injectant had suspended solid concentration of 100-200 mg/L. More than the injected sediment mass was recovered during redevelopment, but particle analysis showed that it comprised only 1% of injected stormwater sediments, while 99% was aquifer sediment mass, which was partially mobilised due to dissolution of cementing carbonates (Pavelic et al., 2006b). This implies that nearly all injected particles are retained within the aquifer and colloidal transport of contaminants could be a major pathway for metals to enter the aquifer. Injected dissolved metal concentration were low (see Table III-5) and metals were retained due to the high pH of the limestone as observed for Bolivar.

Overall, this site showed that a brackish limestone aquifer can be used to create water suitable for irrigation using lower quality source water without the need for major pre- or post-treatment (Dillon et al., 1997).

II.2.4.3 Parafield, South Australia

The Parafield Airport scheme is a fully operational stormwater ASR scheme since 2003 with stormwater harvesting from a 1600 ha catchment and pretreatment in sedimentation basin and reed bed that is either reused directly or stored in a confined Tertiary limestone aquifer (Marks et al., 2005). Water quality monitoring of stormwater inflow and outflow showed a reduction of nutrient, metal and organic pollutant loads of up to 90%, resulting in high standard injectant water quality with Zn and Cu concentrations of ~30 and 8 µg/L, respectively (Rinck-Pfeiffer et al., 2006). Recovered water quality usually meets Australian

Freshwater Aquatic Ecosystem Guidelines (ANZECC and ARMCANZ, 2000). Due to the high pretreatment and the implementation in limestone this project cannot be compared to potential sites in Melbourne.

While there are other small scale stormwater reuse projects around Adelaide, funding is often too limited to allow for adequate water quality monitoring, even when concerns for groundwater contamination are raised (J. Argue, personal communication).

II.2.4.4 The Netherlands

Deep well injection trials of highly pretreated surface water into a sandy anoxic aquifer and recovery from a second well after 85 m (ASTR) for drinking water purposes was undertaken from 1996-1999 at Dizon with emphasis on clogging, pathogen transport and water quality changes (de Ruiter and Stuyfzand, 1998). This trial showed in detail the processes of displacement, mixing, ion-exchange, sorption, organic matter oxidation and redox zonation, mineral dissolution and precipitation during injection, storage and recovery (Stuyfzand et al., 2002). Suboxic conditions only occurred for a short period after injection and a short distance from injection and anoxic conditions were re-established. A major problem at this site was the oxidation of pyrite with increased As concentrations in the recovered water. This showed the mobility of arsenic as an oxyanion, compared to other metals like Ni and Zn, which were readsorbed along the flowpath, most likely on newly formed iron hydroxides (Stuyfzand et al., 2002).

Another ASR trial in Herten from 2000-2003 into a similar deep anoxic sandy aquifer with emphasis on pretreatment testing showed that the main water quality changes were caused by oxidation of sedimentary organic matter, pyrite oxidation and dissolution of calcite and manganous siderite (Stuyfzand et al., 2006). Strong mobilisation of Fe and Mn around the injection well during storage was recorded. All processes decreased in intensity over time, as reactive components in the aquifer are gradually diminished (Stuyfzand et al., 2006). The addition of oxidising, disinfecting and pH raising chemicals were found to be useful for buffering of acidifying pyrite oxidation and reduction in bacterial growth, which decreased reductive dissolution of oxides, but also increased the cost of the scheme (Stuyfzand et al., 2006).

The Langerak deep-well recharge site (ASTR) investigated clogging effects, water quality changes and the development of trace metal concentrations during passage through the aquifer since 1994 (Timmer and Stuyfzand, 1998). Redox reactions and the presence of calcite and pyrite dominated the water quality changes and resulted in release of Ni, As, Cd and Zn (Brun et al., 1998; Saaltink et al., 1998; Saaltink et al., 2003).

All sites are insightful for the complex reactions taking place in anoxic sandy aquifers, but were not done with stormwater but with highly treated water and therefore did not investigate the fate of injected metals.

II.2.4.5 Other studies

Many ASR schemes are operational in the USA in different aquifer settings. All schemes need to comply with the ASCE (2001) standards, which do not allow the injection of poor quality water (Brown et al., 2006). Therefore the only metal related water quality problems in these schemes are geogenic metal mobilisation, mainly concerned with As (Mirecki, 2004; Jones and Pichler, 2007).

II.2.4.6 Melbourne trials and investigations

As wide areas of Melbourne's groundwater are brackish, which would be advantageous for ASR schemes, there is currently limited groundwater use and also limited detailed hydrogeological knowledge. A broad scale mapping for potential ASR sites has been undertaken in Melbourne and recommendations for treated effluent ASR schemes at the Western and Eastern Treatment Plants have been made, but none of these have been implemented at this stage (AGT et al., 2002; Dudding et al., 2006). Smaller scale investigation into stormwater ASR have been undertaken for new housing estate developments as part of a more holistic approach to water reuse (McLean, 2004; Parson and Sibenaler, 2004). At Mernda, Epping North, a successful trial injection has been undertaken into a localised gravely alluvium and further injections are planned (N. Gerges, personal communication). As well as economic considerations concerns about impacts on building foundations and discharge into surface waters due to the highly heterogenous nature of the proposed fractured basalt aquifer at the Aurora site, Epping North, were raised (J. McLean, personal communication) and this scheme has not been implemented.

To the best of my knowledge only one stormwater ASR field trial (Rossdale golf course, Aspendale) is currently in progress in Melbourne. It is envisaged to inject stormwater treated to potable standards into dual-porosity bedrock (mainly siltstone) at 0.5 L/s (Dillon et al., 2007). Mains water injection trials have been finished, but no stormwater injection has been taken place as yet. Another golf course in the area is also investigating ASR (T. Ford, personal communication) possibly into the overlying porous Werribee Formation or Fyansford Formation-Brighton Group aquifer system (see III.3.1).

II.2.5 Guidelines and practice

Apart from purely research based ASR schemes, operational schemes are primarily concerned with economical viability and operational feasibility. The main considerations are usually of quantitative nature (e.g. clogging and recovery efficiency) and that the recovered water is fit for its intended purpose. Hence, pretreatment is mainly applied to reduce biological and mechanical clogging potential of injectant, aquifer selection is based on storage capacity and recovery efficiency and monitoring is often confined to recovered water quality. However, ASR schemes have to take into account the protection of the aquifer and groundwater to reduce the impact on downstream environments and be sustainable in the long-term.

II.2.5.1 Current regulatory framework and guidelines

In Australia, State governments are responsible for water management, while national guidelines are non-binding but should encourage nation wide consistency. In Victoria, the Water Act 1989 (Victorian Government, 2004) provides the legal framework for allocating surface- and groundwater, but does not include aquifer recharge; policies on quantitative aspects are developed by the Department for Sustainability and Environment (DSE) and water licenses are distributed by regional water authorities.

The protection of water quality values are enshrined in law under the Environment Protection Act 1970 (Victorian Government, 2007) and supported by the statutory framework of the State Environmental Protection Policy (SEPP) (EPA Victoria, 2003). The SEPP “Waters of Victoria“ outlines beneficial and principal uses, sets environmental quality objectives and details protection programs and is managed by the Environmental Protection Agency (EPA). The beneficial use categories for groundwater are segmented by total dissolved solids (TDS) and incorporate as principal uses potable water (desirable <500 mg/L, acceptable <1000 mg/L), mineral water and irrigation (<3500 mg/L), and stock water (<13 000 mg/L). Industry, structures/buildings and ecosystem needs are protected for all salinity levels.

Currently Victoria does not have an integrated legislative framework to facilitate managed aquifer recharge schemes and no specific regulatory guidance is currently available (Victorian Government, 2006), but guidelines for water recycling and managed aquifer recharge are currently under development (NWQMS, 2007). The Victorian Government initiated guidelines for alternative water supplies in “Securing our water future together” (DSE, 2004). They should implement the recently released “National Guidelines for Water Recycling: Managing Health and Environmental Risk” (NWQMS, 2006), which apply a hazard analysis and critical control point (HACCP) system. While South Australia has

adopted a Code of Practice for ASR (EPA SA, 2004), Victoria is still developing a code of practice based on a technical guidance to ASR (Dillon and Molloy, 2006).

II.2.5.2 Best practice and risk assessment

The best practice guiding principles to be considered for ASR are (Dillon and Molloy, 2006):

1. Adopting a risk management approach
2. Preventing irreparable damage
3. Demonstrations and continuous learning
4. Adopting a precautionary principle
5. Establishing water quality requirements
6. Rights of water bankers and recoverable volume
7. Finite storage capacity of aquifers and interference effects between sites
8. Community and other stakeholder consultation
9. Highest valued use of resources

These principles should be implemented into a risk base management plan, e.g. HACCP, and could include the following barriers (EPA SA, 2004; Dillon and Molloy, 2006):

- Knowledge of pollutant sources in catchment see II.3 and III.2
- Source selection: e.g. diversion from drain, diversion of low flow or first flush, monitoring of source water quality, control to shut down stormwater harvesting
- Aquifer selection: e.g. brackish aquifers, other users, see II.2.2
- Pretreatment of injectant: see II.4.6.1
- Injection shutdown system: e.g. continuous monitoring of injectant quality, pressure head, water level, volumes
- Maintenance and contingency plans: e.g. protection of injectant water quality with nets, no use of pesticides/herbicides in area, flood protection, spill structure for detention pond, monitoring well, regular inspection of monitoring and shut down equipment, replacement of filters, well redevelopment, establish monitoring intervals
- Recovered water post-treatment: e.g. monitoring of recovered water quality, filtration, disinfection
- Discharge of well re-/development water: e.g. monitoring of water quality to discharge into sewer, detention pond or irrigational use
- Management of pond sediments: e.g. regular removal of sediments and appropriate disposal

An ASR scheme should therefore involve a number of infrastructure components. To ensure the protection of the environment monitoring of water quantity and quality should ideally be implemented (a) at the stormwater drain to divert highly polluted parts of the flow, (b) before injection to control the effectiveness of the pretreatment, (c) in the injection bore for hydraulic

heads to avoid over pressuring, (d) in observation bores in increasing distance from the injection bores to monitor the breakthrough of the injectant and (e) of the recovered water to ensure the water quality meets the end use requirements. Control systems that are able to shut down the operation if requirements are not fulfilled at any stage are needed (Dillon, 2004). This involves expertise during the implementation of the scheme and skilled operators during use.

II.2.5.3 Implementation

An ASR installation program can be divided in three main phases (Pyne et al., 1995):

a) site selection:

The site selection and feasibility assessment starts with determining the quality and quantity of water supply and demand. Then hydrogeological data has to be gathered (aquifer thickness, depth, transmissivity, hydraulic conductivity, flow velocity, confining layers, catchment boundaries, head level, groundwater quality etc.). The site selection is also based on available land for installation of storage and pretreatment facilities and disposal of unwanted water. A conceptual design of the ASR system and risk assessment can then be proposed to the authorities for approval.

b) investigation:

Once a site is selected and economic, environmental and operational feasibility has been assessed, drilling of injection and monitoring wells can be undertaken. This will allow site specific characterisation of the aquifer (hydraulic and geochemistry) and groundwater quality. Laboratory experiments like batch and column tests are advisable to test clogging potential and the compatibility of the proposed injectant with the aquifer matrix and groundwater to help determine the injectant water quality requirements. Hydrogeo-chemical modelling based on the preliminary data will allow further insights into the viability of the ASR scheme.

c) trials and expansion:

Mains water injection trials are the next step and if the investigation and trials outcomes are positive first stormwater injection can be started. The rule is to start small and expand stepwise (Bouwer, 2002). Intensive monitoring and regular assessments should be undertaken during the early years of operation to confirm that the scheme works within the set limits.

From the review so far it can be stated that ASR offers a valuable solution to the storage problem associated with stormwater reuse in urban areas, but implementation has been slow due to administrative hurdles and a previous lack of political will. In addition, the interactions between microbial, geochemical and hydraulic processes during ASR are complex. They are dependent on injectant, aquifer and groundwater site specifics and have not yet been fully understood. Current ASR scheme are mostly conducted with high quality water or in

limestone areas, where injected metals concentrations are low. To the best of my knowledge there has been no quality monitored stormwater ASR scheme into sandy aquifers in operation worldwide.

II.3 The injectant – urban stormwater pollutants

Urban stormwater is a valuable water resource that needs to be integrated into an urban water conservation management to meet future water demands. Nevertheless, urban stormwater contains a range of pollutants that have negative impacts on receiving ecosystems and potentially need to be treated before reuse (Pitt et al., 1999). In general, stormwater contamination is highly variable both spatially and temporally, but commonly occurring priority pollutants have been identified (Eriksson et al., 2007).

II.3.1 Total suspended solids

Total suspended solids (TSS) comprise organic and inorganic particulates (>0.45 µm) deriving from natural and anthropogenic sources (Droppo, 2001). Concentration in stormwater range typically from 50-450 mg/L with lower concentrations found in roof runoff and highest concentrations found in urban road runoff (Figure II-2). Apart from their clogging potential during infiltration or injection, their importance arises from the attachment of other pollutants (e.g. nutrients, hydrophilic organics, heavy metals) mainly with the finer fraction of particulates (e.g. Dempsey et al., 1993; Mikkelsen et al., 1994; Deletic and Orr, 2005). While the coarser particles are likely to be settling out before use in ASR schemes, the finer, more contaminated proportion is likely to be injected into the aquifer and not to be recovered, as observed at Andrews Farm (see II.2.4.2). Particulate facilitated transport (see II.4.4) is therefore a potential pathway for contaminants to be distributed in the aquifer and should not be neglected (McCarthy and Zachara, 1989).

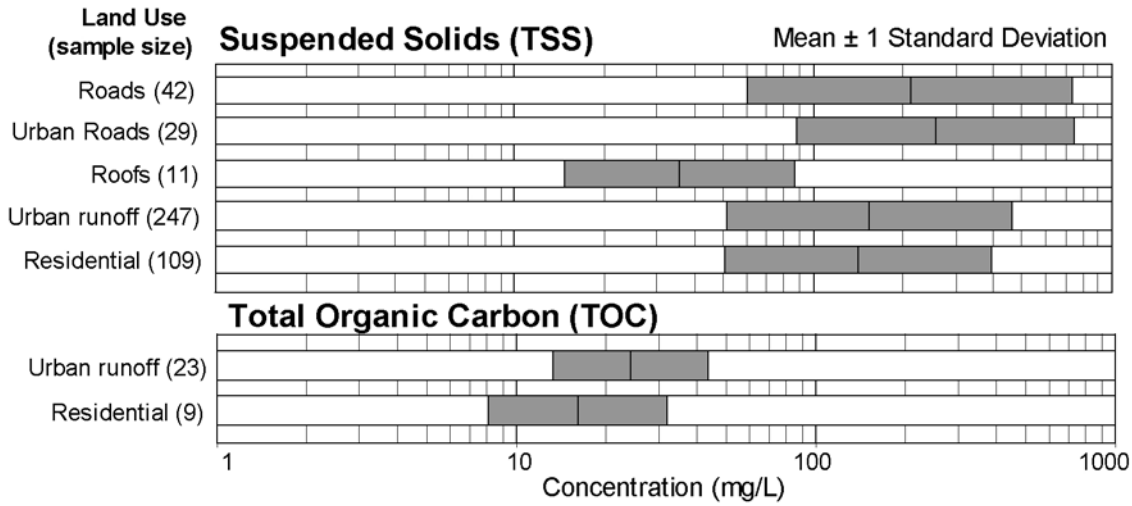

Figure II-2: Typical concentrations of worldwide stormwater samples for total suspended solids (TSS) and total organic carbon (TOC) (modified after Duncan, 2006).

II.3.2 Nutrients and oxygen

Nitrogen and phosphorus in stormwater derive from fertilisers, faecal matter, plant debris and combustion processes. While they are essential nutrients for plant growth, increased levels may lead to eutrophication and toxic algal blooms (Murray and Parslow, 1999; Anderson et al., 2002). While phosphorus attaches readily to particulates, nitrate is highly soluble and very likely to be injected during ASR. Dissolved oxygen and nitrate are the major electron donors injected into the aquifer stimulating microbial activity, significantly altering the aquatic ecosystem community (Datry et al., 2004). Their fate in the subsurface is closely linked with the availability of organic matter and can result in suboxic and denitrifying conditions limiting aerobic degradation of pathogens and trace organics and indirectly affecting metal speciation (Stumm and Morgan, 1996; Appelo and Postma, 1999a).

II.3.3 Organic carbon

Organic carbon found in stormwater is a mixture of natural organic matter (NOM), hydrocarbons, microorganisms etc. derived from degraded plant material, animal faeces, organic urban contaminants like oil, polycyclic aromatic hydrocarbon (PAH), pesticides etc. (Pitt et al., 1999). Fulvic acids are the major colloidal and dissolved constituent in natural organic matter (see II.2.3.4) (Sekaly et al., 1999; Li and Dai, 2006). Concentrations typically range from 8-35 mg/L (Figure II-2). Interactions between DOC, dissolved constituents and solid matter are numerous. DOC stimulates the growth of biofilms, biological production and subterranean ecosystem metabolism and redox reactions (Stumm and Morgan, 1996; Baker et al., 2000). Its presence influences the speciation of heavy metals and can increase their solubility through complexation (see II.4.2).

II.3.4 Trace organic contaminants

Trace organic contaminants include pesticides, aliphatic hydrocarbons (HC), polycyclic aromatic hydrocarbon (PAH), volatile organic compounds (VOC), phthalate esters, benzene-toluene-ethylbenzene-xylene (BTEX), pharmaceutically active compounds (PhACs) and endocrine disrupting chemicals (EDC). They can undergo various degradation mechanisms (physical, chemical and biological) and are often attached to solids (Fetter, 1993; Kretzschmar et al., 1999). Their concentrations and attenuation processes in the subsurface are the subject of a broad range of research (see also II.2.3.2) (e.g. Bouwer et al., 1984; Fetter, 1993; Sinke et al., 1998; Barry, D.A et al., 2002; Mulligan and Yong, 2004; Dillon et al., 2005), but are not the focus of this study.

II.3.5 Heavy metals

Heavy metals in stormwater derive from natural sources as well as from different anthropogenic sources like hydrocarbon combustion, vehicle exhaust, brake and tyre wear,

roof materials, corrosion of metal objects etc. (Makepeace et al., 1995; Duncan, 2006). They are often significantly toxic at low concentrations and are therefore considered priority pollutants in stormwater (Scholze et al., 1993; Eriksson et al., 2007). Their importance stems from the fact that they (in contrast to organic contaminants) cannot be degraded, but are persistent and tend to bioaccumulate (Alloway, 1990).

Metal concentration in stormwater are highly variable depending on a number of factors like land use, climate and rain event characteristics with reported levels of 0.3-37 µg/L Cd, 0.6-300 µg/Cr, 3-1800 µg/L Cu, 0.3-425 µg/L Ni, 0.2-2745 µg/L Pb, and 1-3560 µg/L Zn (Fuchs et al., 2004). According to their prevalence in stormwater and toxicity most interest has therefore been devoted to Pb, Zn, Cu and Cd (e.g. Barbosa and Hvitved-Jacobsen, 1999; Legret and Pagotto, 1999; Pitt et al., 1999; Zimmermann et al., 2005). Zn and Cu concentrations are highest from urban road runoff and Zn concentrations are increased through runoff from Zn roofs (Figure II-3).

Particle size distributions (PSD) analysis of Australian surface runoff showed that higher fractions of smaller particles are generated compared to Europe or the USA with a mean particle size of about ~50 µm (Walker and Wong, 1999). This finding is of importance when knowing that finer particles account for a much higher proportion of metal load due to their favourable surface area to mass ratio allowing for increasing metal attachment (Dempsey et al., 1993; Mikkelsen et al., 1997; Liebens, 2001).

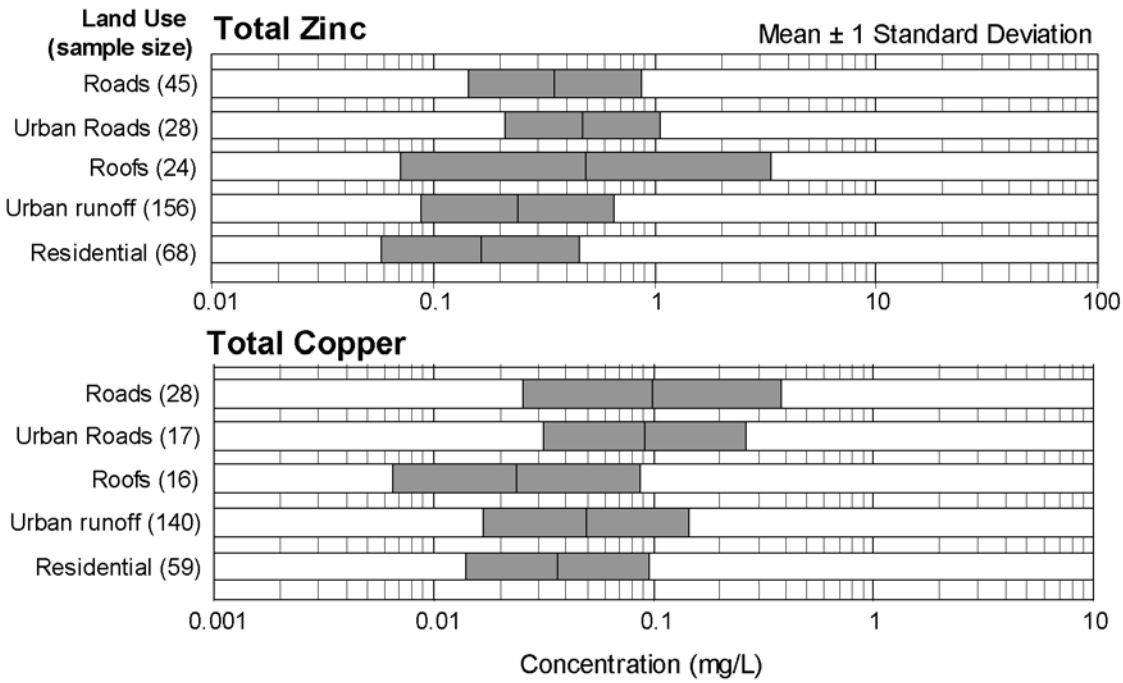

Figure II-3: Typical concentrations of worldwide stormwater samples for Zn and Cu in stormwater (modified after Duncan, 2006)

This speciation of metals is vital to assess their potential for injection during stormwater ASR, as larger particulates will be settling out in the detention ponds before injection, while fine

particulates and dissolved metals would not (Wong, 2006). While Pb has been found to be nearly completely attached to particulates Zn, Cu and Cd are more associated with dissolved solids and colloidal material (Sansalone and Buchberger, 1997; Legret and Pagotto, 1999; Tuccillo, 2006). As Cd is frequently below detection limit in Melbourne's stormwater (see III.2.3) and non-settleable fractions of Pb are also low, the main focus of this study is Zn and Cu. Their speciation, distribution and behaviour in the environment is discussed in further detail below.

II.4 Metal speciation: mechanisms and factors

The mobility, toxicity and bioavailability of metals are controlled by their speciation and partitioning. The speciation of a metal in solid and solution is the particular chemical form in which it exists. In solution metal ions can be present as free ion, inorganic complex or organic complex/molecule. In the sediment the metal can be part of a mineral phase or adsorbed to a phase, both of which could be mobile or immobile (Stumm and Morgan, 1996). Changes in speciation can occur due to sorption (II.4.1), complexation with organic matter (II.4.2) and dissolution/ precipitation (II.4.3) reactions (McBride, 1994). While metal mobility is mainly accomplished in their dissolved form, colloidal transport is another mode of transport, which can be important under special circumstances (II.4.4). All of these reactions are influenced by factors like pH, redox and other constituents in solution (II.4.5) (Bradl, 2004). The interplay between these processes and factors during ASR are then discussed (II.4.6).

II.4.1 Sorption

Sorption is probably the most important mechanism for metal speciation in the natural aquatic environment. It is defined as the mass transfer of a chemical from solution to solid (adsorption) or from solid to solution (desorption). It can include only one chemical, which can be described with distribution coefficients (sorption), or can involve the replacement of another chemical, which can be described with selectivity coefficients (exchange) (II.4.1.1). In either case it is limited by the sorption or exchange capacity of the solid (II.4.1.2).

II.4.1.1 Theory and mechanisms

The sorption interactions between a molecule or ion in solution and a solid take place at the exchanger surface and are described with diffuse layer models (DLM), where an electrical potential changes gradually over a distance from the solid surface extending into the solution. Diffuse double layer (DDL) models after Gouy and Chapman (Lyklema, 1991) or triple layer models (TLM) including an extra internal "Stern" layer (Lyklema, 1991), as well as constant capacitance models (CCM) are currently employed to describe binding (Davis and Kent, 1990). They are mathematically based on the Poisson-Boltzmann differential equations that describe the electrostatic interactions between the molecules in solution. The thickness

of the diffuse layer depends on ionic strength of the solution and can be calculated with the Debye-Hückel law and is important for the stability of particles in solution (see II.4.4).

Metals can be adsorbed by two mechanisms (Figure II-4). The non-specific adsorption is a physical, electrostatic sorption or ion-exchange due to weak outer-sphere complex formation, where at least one water molecule is between the surface and the complex. It occurs fast and is mostly reversible (Jenne, 1968; Tiller et al., 1984a; McBride, 1989). The specific adsorption is a chemical sorption with strong inner-sphere (covalent) binding, which shows high selectivity and can take up to years and is therefore often considered irreversible (Barrow, 1986a; McBride, 1989). The number of high energy, specific sorption sites is usually much smaller than the number of low energy, non-specific sorption sites (Benjamin and Leckie, 1981a), as the latter can occur at values below the zero-point of charge of minerals (Murray et al., 1968; Kuo and Baker, 1980).

As the actual binding reactions and changes in potential are quite complex and still not completely understood, sorption has been described conceptually by different approaches in the literature.

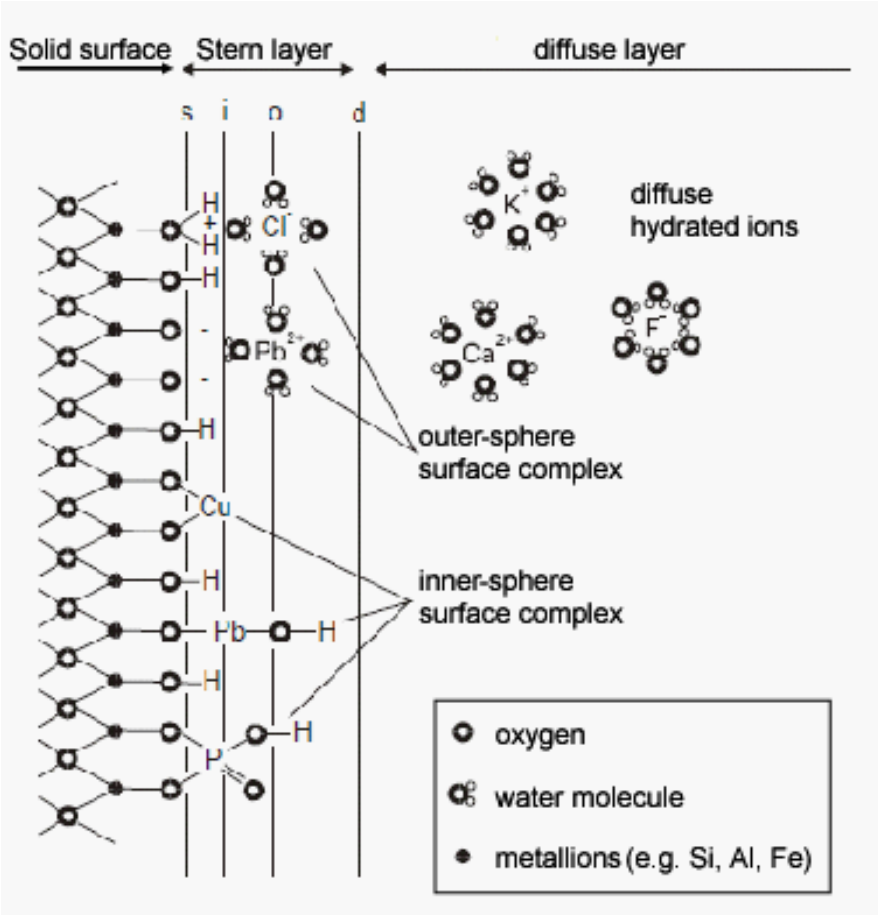

Figure II-4: Schematic sorption of cations and anions at an oxide or clay mineral surface (modified after Selim and Iskandar, 1999) s: layer of hydroxyl groups of the solid, i: layer for inner-sphere complexes, o: layer for outer-sphere complexes, d: start of diffuse ion layer.

Empirical adsorption isotherms

The sorption isotherm is an empirical approach relating the concentration of one chemical in solution to its concentration in the solid at equilibrium and is usually derived from batch tests. This is only a descriptive approach and does not prove a reaction mechanism and can even include precipitation (Sparks, 2003). The distribution between solid and solution of the component can commonly be described by either of four types of isotherm (Figure II-5; Giles et al., 1974a; Sposito, 1984; Hinz, 2001):

- The “C” isotherm is linear, the slope is called K_d or distribution coefficient [L/kg] and often fits adsorption data at low concentrations, when there is no limitation in sorption sites (Thiele and Leinweber, 2001; Covelo et al., 2007).
- The “L” isotherm is concave with decreasing slope with increasing concentration leading towards (Freundlich-isotherm) or reaching a saturation limit of the solid (Langmuir-isotherm) and is the most common isotherm (Elzinga et al., 1999). The lowering in distribution coefficient with increasing metal can be interpreted as a shift from specific to non-specific sorption sites (Tiller et al., 1979; Arias et al., 2005; Singh et al., 2006). It implies that K_d values derived from high surface coverage experiments are likely to underestimate specific adsorption behaviour at low metal loadings (Lehmann and Harter, 1984; Mesquita and Vieira e Silva, 1996; Sastre et al., 2007).
- The “H” isotherm is similar to the “L” isotherm, but has two distinct segments with a very steep initial slope and results from limited very high affinity sites (Sparks, 2003).
- The “S” isotherm is sigmoidal with a point of inflection and can be observed where organic ligands influence metal sorption (Sposito, 1984). The initial segment would be dominated by complexation and the following segment by metal adsorption.

These isotherms are not constant though, but vary depending on the experimental conditions, e.g. pH, ionic strength, metal loading, other components in solution, and are therefore not necessarily applicable beyond these conditions (Elzinga et al., 1999; Koretsky, 2000; Goldberg et al., 2007).

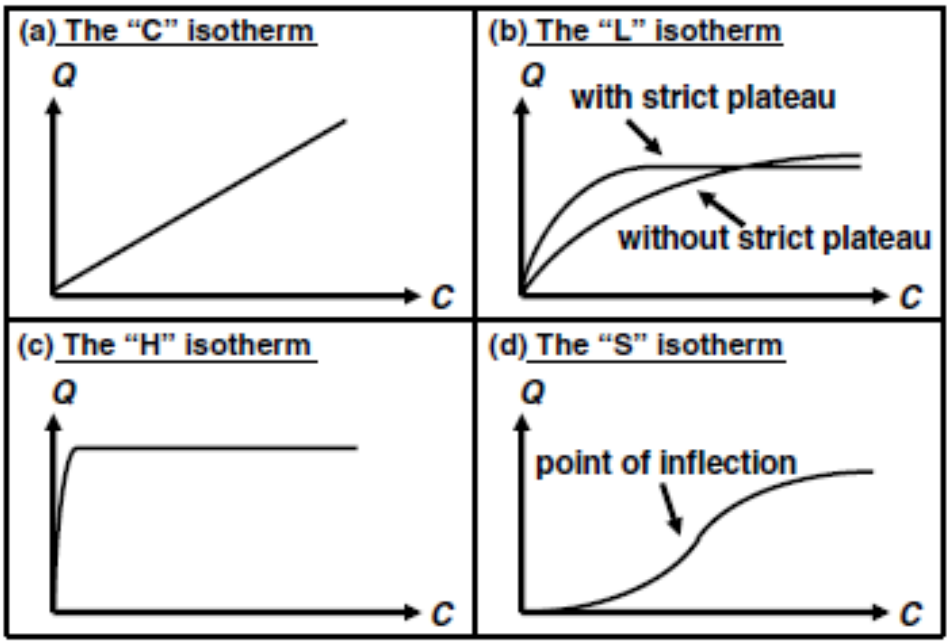

Figure II-5: Schematics of the main four types of isotherms (Limousin et al., 2007), C: concentration in solution at equilibrium, Q: concentration in solid at equilibrium.

Ion exchange

While the above described isotherms present an empirical approach to observable sorption phenomena, simple types of non-specific outer-sphere complexation, i.e. ion exchange favoured by major cations (e.g. H^+, Na^+, K^+, Ca^{2+}, Mg^{2+}), can be explained on the basis of chemical principles (Rubin and James, 1973; Grove and Stollenwerk, 1987). Ion-exchange takes into account the fact that surface charge at the surface of exchangers will already be counteracted by ions in solutions, when changes in the activity of ions in the solution occur, which will be reflected by a change of ions at the exchanger. The equilibrium exchange constants are calculated from ion activity ratios in water, using the Debye-Hückel law, and the number of exchangeable sites using either the Gapon (Gapon, 1933), Vanselow (Vanselow, 1932) or the Gaines-Thomas (Gaines and Thomas, 1953) convention (Appelo and Postma, 1999a). As the valence of the cation becomes the exponent in the mass action equation, divalent cations are preferred over monovalent ions, but selectivity coefficients can vary depending mainly on the type of exchanger and the normality of the solution (Appelo and Postma, 1999a).

Surface complexation models

These more thermodynamically based models use mass action laws analogous to aqueous phase equilibrium reactions, which can account for changes in pH, solution speciation and competing components in solution and are therefore more applicable over a wide range of geochemical conditions (Davis and Kent, 1990). Intrinsic stability constants for these mass reactions include the electrostatic interactions at the solid-solution interface using the Coulombic correction factor (Sposito, 1983; Koretsky, 2000), but the structural representation

of the surface might vary from model to model, e.g. 2pK models like CCM, DLM, TLM (Davis and Kent, 1990; Hayes et al., 1991; Wen et al., 1998) or 1pK model (Weerasooriya et al., 2000). All of them use the surface functional hydroxy group (S-OH). In the 2pK-models this group can be protonated ($S\text{-}OH_2^+$) or deprotonated ($S\text{-}O^-$), while in the 1pK only one protonation step is assumed ($S\text{-}OH_2^{+1/2}$) (Goldberg, 2005). In the CCM and DLM all surface complexes are inner-sphere complexes located in a single plane, while in the TLM inner- and outer-sphere complexes at two different planes are assumed (Goldberg et al., 2007). These thermodynamic considerations are underpinned by direct measurements of formed complex at the matrix (e.g. X-ray absorption spectroscopy (XAS), X-ray standing wave spectroscopy, infrared (IR) spectroscopy, nuclear magnetic resonance (NMR) spectroscopy) and indirect (e.g. point of zero charge shifts, ionic strength dependence, calorimetry) experiments that provide information about the actual adsorbed complex formation (Goldberg et al., 2007).

II.4.1.2 The matrix

Natural sediments comprise a variety of different sorption sites of permanent or variable charge.

While the bulk of the aquifer is comprised of quartz, it provides only limited sorption for trace metals (Sansalone, 1999; Genç-Fuhrmann et al., 2007). The primary reason for this low sorption capacity (CEC values 2-4 cmol/kg) is the low surface area, e.g. 0.08 m²/g (Borkovec et al., 1996), low number of surface sites and mostly non-specific electrostatic interaction with ions in solution (McBride, 1989).

The phases of main interest for metal sorption are clay minerals, oxides and organic matter as they have a much higher surface area and sorption site density. Even though these phases account only for a small percentage of the bulk material, their importance is increased as they often occur as surface coatings (Davis et al., 1998).

Clay minerals

Clay minerals have permanently negatively charged sites independent of pH due to isomorphous substitution in the mineral structure and variable, pH-dependent charge sites on the edges of clay minerals due to de-/protonation (McBride, 1994). The pH at which the charge of the mineral is zero is called point of zero charge (PZC) or point of zero net proton charge if only non-permanent charge is expressed (Sposito, 1998) and can be obtained from acid-base titration. Commonly this PZC lies below pH in natural aquatic systems, and these minerals behave as cation exchanger (Sposito, 1984). The permanent charge sites retain cations by non-specific electrostatic sorption, while variable charged sites are also capable of specific sorption (McBride, 1989).

The sum of charged sites accessible for cation exchange is commonly expressed as cation exchange capacity (CEC). Due to their structure two-layer clay minerals (e.g. kaolinite 2-15 cmol/kg) have much lower cation exchange capacity than three layer clay minerals (e.g. montmorillonite 80-150 cmol/kg). While variable charged sites are pH dependent, permanent charge sites are strongly ionic strength dependent (Baeyens and Bradbury, 1997; Voegelin et al., 2001). Gillman (1981) showed that one magnitude of ionic strength increase resulted in 2 to 4 fold increase in CEC for different soils, meaning that CEC values measured at standard pH and ionic strengths are not necessarily the CEC values that can be obtained under different natural conditions. In some studies the cation exchange capacity was correlated to metal sorption behaviour (Schulte and Beese, 1994; Warwick et al., 1998; Elzinga et al., 1999; Arias et al., 2005). This would clearly be the case for higher metal loadings, when specific sites are saturated and metals start binding to low affinity sites or for less selected metals. CEC is not a good measure for specific sorption capacity though (Ziper et al., 1988; Zehetner, 2000).

Oxides

Si-, Al-, Fe- and Mn-oxides (including hydroxides and oxyhydroxides) contain variably charged surface sites due to protonation/deprotonation of surface oxygens. In contrast to clay minerals their PZC is often higher than naturally occurring pH and they are therefore positively charged, behaving as anion exchanger (Appelo and Postma, 1999a). The exchange capacity decreases with increasing crystallinity of the oxide (McBride, 1989) and generally decreases from Mn > Fe > Al oxides (McKenzie, 1980; Brümmer et al., 1986). Nevertheless, specific, covalent sorption occurs below the PZC and is the main retention mechanism for metal ions (Dzombak and Morel, 1990). Indirect evidence for specific binding is given by changes in surface charge properties after adsorption, the limited influence of ionic strengths, the release of protons during adsorption and the high selectivity for certain metals (McBride, 1989). While the particular selectivity order varies with the mineral phase (see also Figure II-5), in general, Cr, Pb and Cu are highly retained, while Zn, Ni and Cd are less preferred (e.g. McKenzie, 1980; McBride, 1982; Gomes et al., 2001; Covelo et al., 2007). This selectivity has been related to the hydrolysis constants of metals (e.g. James and Healy, 1972; Davis et al., 1978; Herms and Brümmer, 1984; Elliot et al., 1986). The amount of specific surface sites of oxides and organic matter is commonly measured with titration, e.g. acid/base, potentiometric or backtitration (e.g. Hayes et al., 1991; Baeyens and Bradbury, 1997; Papini et al., 1999; Tournassat et al., 2004).

Organic matter

Natural organic matter contains a range of different pH dependent, variable charge functional surface groups, of which the carboxylic and phenolic hydroxyl groups are the most abundant

(see Table II-1). Different functional groups deprotonate/protonate at different pH values, but the overall PZC is commonly low (about pH 4.5) and humic substances are negatively charged in natural waters (Sparks, 2003). Depending on pH, the cation exchange capacity of organic matter is often much higher than of clay minerals (Stevenson, 1982). Due to the negative charge they behave like oxyanions in solution and are able to coat positively charged oxides (Day et al., 1994; Evanko and Dzombak, 1999). Due to the high amount of specific sorption sites they have a high retention for metals.

II.4.1.3 The natural system

To explain adsorption behaviour from a macroscopic point of view one has to consider that whole sediments and soils are not pure phases but a complicated mixture of clay minerals, amorphous hydrous and crystalline Al-, Fe- and Mn-oxides as well as organic matter. The situation is even more complicated by the fact that these phases are often mixed by coatings of oxides and humic material on the mineral particles (Davis and Leckie, 1978; Tiller et al., 1984b; Buffle et al., 1990). It has been postulated (Jenne et al., 1968; Dzombak and Morel, 1990) that hydrous manganese and iron oxides are the principal control on fixation of trace metals in soils due to their ubiquitous nature as coatings, which exposes a much higher surface area to the contact solution than its measured amount would indicate. The same argument applies to coatings of organic matter which can dominate the surface-solution interactions (Beckett and Le, 1990; Day et al., 1994; Kretzschmar and Sticher, 1997; Mosley et al., 2003).

While ion-exchange is usually a fast process considered to be in equilibrium, inner-sphere surface complexation reactions are often rate limited (Padmanabham, 1983; Bahr and Rubin, 1987; Honeyman and Santschi, 1988). The kinetic behaviour often derives from diffusive processes (i.e. inter- and intraparticle diffusion) of the components to reach surfaces (Sparks, 2003) and can be limited by the activation energy (McBride, 1989) taking up to months and years to reach equilibrium. It is commonly described with rate laws of zeroth, first or second order derived from kinetic sorption experiments (Lasaga and Kirkpatrick, 1981; Arnaut et al., 2006). In addition, natural systems often exhibit other non-equilibrium conditions due to heterogeneities of the matrix (Kookana et al., 1994; Brusseau et al., 1997; Johnson et al., 2003).

To describe the complexity of a natural system that contains a range of different surface sites with different affinities, semi-empirical site-binding models that combine concepts from empirical and surface complexation models are therefore often used (Borkovec et al., 1996; Davis et al., 1998; Koretsky, 2000). These can either use the generalised composite (GC) approach or the component additivity model (CA) approach. The latter predicts adsorption by

combining known surface complexation properties of different pure phases to the complex mineral assemblage of the natural sediment (Wen et al., 1998; Weng et al., 2001), while the former fits experimental field data to a generic set of surface complexation properties that combines all available surfaces (Fuller et al., 1996; Wang et al., 1997; Lofts and Tipping, 1998; Davis et al., 1998). As coatings of sediments often dominate the adsorption of a mineral assemblage the CA approach is often appropriate.

II.4.2 Complexation with organic matter

Organic carbon concentrations are not only important in regulating the pH/Eh system (see II.2.3.4), but they are also critical for metal sorption in a more direct way. The different functional groups like carboxyl, phenolic hydroxyl, alcoholic hydroxyl, carbonyl, phthalic, sulfonic groups, vary in their binding strength from only slightly covalent to highly chelating (Stevenson, 1982; Town and Powell, 1993; Karlsson, 2005; Hay and Myneni, 2007). Surface complexation of free or hydrolysed heavy metals with organic matter can occur as multidentate sorption, chelation with carboxyl and hydroxyl groups or can involve only one functional group (McBride, 1989). In general, the complex stability increases with the number of bonds formed, but varies with ionic strength, metal concentration and pH (Schnitzer and Skinner, 1966; Murphy et al., 1992; Milne et al., 2003). As with oxides, preferential complexation of organic acids with metals has been found, which exhibits a similar preferential order, i.e. Cu complexes are more stable than Zn complexes (Irving and William, 1948; van Dijk, 1971; Milne et al., 2003). Cu is therefore consistently found to be associated with organic matter (Elliot et al., 1986; Mason et al., 1999; Weng et al., 2001; Cances et al., 2003). The strong complexation of Cu is commonly explained with the Jahn-Teller effect, which distorts the normal octaedric configuration (Elzinga et al., 2006; Ponthieu et al. 2006; Carbonara and Di Toro, 2007).

Ternary interactions

When investigating the influence of organic matter presence on metal sorption behaviour to mineral phases contrasting effects have been found (Elliot and Huang, 1979; McBride et al., 1997). This is due to the metal-ligand ratio and to the different interactions that can take place (Davis and Leckie, 1978; Benjamin and Leckie, 1981b):

a) the organic ligand itself can be sorbed strongly by the solid matter, leading either to competition for sorption sites and therefore decreased metal sorption, or adding new sorption sites as coating enhancing metal sorption (Jardine et al., 1989; Yuan et al., 2007);

b) the organic ligand can form stable dissolved complexes with the metal, especially with smaller soluble ligands like fulvic acids (Manning and Ramamoorthy, 1973; Herms and Brümmer, 1984) leading to a higher dissolved metal fraction or

c) the organic ligand-metal complex can be preferably sorbed to the surface increasing the overall metal sorption.

Overall, the long-chain hydrophobic humic acids are preferentially sorbed and therefore often enhance metal sorption while the short-chain fulvic acids often reduce it (Herms and Brümmer, 1984; Zhao et al., 2007b). Furthermore organic complexation and adsorption is strongly pH dependent and it is often difficult to decouple the combined effects (see II.4.5).

II.4.3 Dissolution/precipitation

Fundamentally, precipitation and dissolution reactions in equilibrium are described with mass action laws relating the activity of ions in solution with the solubility constant of a mineral phase. The saturation index (SI) is the logarithmic ion activity product of the participating ions divided by the solubility product and a mineral phase will be supersaturated and precipitate of SI>0 and be undersaturated and dissolve for SI<0, respectively (Appelo and Postma, 1999a). The formation of inorganic or organic complexes in solution reduces the activity of free ions in solution and hence hinders precipitation. In reality, most mineral reactions are kinetic and depend on a number of other factors, e.g. temperature, pH, redox potential, crystallisation seeds. For example precipitation of undersaturated minerals has been observed, when structurally favourable crystal surfaces were available (Stumm and Morgan, 1996) and the transition between adsorption and surface precipitation can be described as continuous (Sparks, 2003). On the other hand, even highly supersaturated solutions might not result in precipitation if the activation energy is too high (McBride and Blasiak, 1979).

With respect to Zn and Cu, precipitation of sulfides, carbonates, hydroxides or oxides could be considered and have been shown to occur under the appropriate redox and pH (see also Figure II-8; Brümmer et al., 1983; Vanderzalm et al., 2006a; Davis et al., 2007). Of even greater importance though are dissolution and precipitation of Mn- and Fe-hydr-/oxides and sulfides (Jenne, 1968; Jacobs et al., 1988; McBride, 1989). The solubility of Fe is probably the most important and is controlled by its redox state. If soluble Fe^{+2} is oxidised to Fe^{+3} it is likely to precipitate as amorphous hydrous ferric oxide (HFO). Cu and Zn can be co-precipitated with these or adsorb to these newly formed sorption sites (Iu et al., 1981b; Tessier et al., 1996; Davranche and Bollinger, 2000). Recrystallisation or dehydrating/aging of iron hydroxides to iron oxyhydroxide (e.g. goethite) and iron oxides (e.g. hematite) has also been shown to occlude other heavy metals and enhance their retention (Thompson et al., 2006). The presence of DOC can hinder the precipitation of HFO as Fe forms strong metal-organic complexes (Schnitzer and Skinner, 1966; van Dijk, 1971; Tipping et al., 2002). DOC also promotes reductive dissolution of iron oxides (Hering and Stumm, 1990; Stumm and Sulzberger, 1992), while sorbed ions may reduce the reductive dissolution rate by blocking oxide surface sites or preventing the release of Fe/Mn into solution (McBride, 1989).

Of special interest in this context is also the oxidation of sulfides, e.g. pyrite. The reaction releases free metal ions as well as protons and sulfate into solution. As pyrite often contains other trace metals like As, Ni and Zn from isomorphous substitution these are released as well. While precipitation of HFO might scavenge Zn and Ni cations, As can remain in solution as oxyanion (Lee and Saunders, 2003).

II.4.4 Colloidal transport

Colloids and organic macromolecules are an important third phase and are ubiquitous in the subsurface environment. Their size range is commonly defined from 1 nm to 1 µm (Buffle and Leppard, 1995a) or up to 10 µm (Hunter, 2001). They have to be considered as important for contaminant-facilitated transport if (a) colloids are available and are mobilised in sufficient amounts (b) colloids are stable and transported (c) the sorption of the contaminant to the colloid must be strong and only slowly reversible (McCarthy and Zachara, 1989; Ryan and Elimelech, 1996) (see Figure II-6).

Sources for colloids can be from in-situ mobilisation due to chemical or physical perturbations (reviewed by Ryan and Elimelich, 1996), from precipitation, e.g. iron oxides (Liang et al., 1993), from dissolution of cementing particles (Ryan and Gschwend, 1990) or introduced from the surface via infiltration or injection (McCarthy and Zachara, 1989). All cases must be considered possible during artificial recharge, as colloids and macromolecules will be injected with the stormwater, and the change in geochemical conditions and flow rates/directions can induce in-situ mobilisation and dissolution/precipitation of mineral phases. The main chemical disturbance is the lowering of ionic strength, which increases the diffuse double layer thickness and hence increases repulsion between colloids and between colloids and matrix (Elimelech and O'Melia, 1990; Kaplan et al., 1993; Grolimund et al., 1996; Ko and Elimelech, 2000). This therefore reduces attachment and aggregation of colloids. The critical ionic strength that induces particle release is also sensitive to the ionic composition of the solution (Khilar and Fogler, 1984; Liu et al., 1995; Roy and Dzombak, 1996; McCarty and McKay, 2004). Monovalent cations increase dispersion, while bivalent cations induce coagulation.

To fulfil the second condition, the colloids must be repulsed, e.g. have the same surface charge as the matrix, and pores must be sufficiently wide and frequent for colloids to pass through the aquifer without interception or filtration (Kretzschmar et al., 1999; Karathanasis and Johnson, 2006; Sen and Khilar, 2006). The former condition is usually achieved by a coating of natural organic matter that masks underlying surface charge heterogeneities (Liang and Morgan, 1990; McCarthy and Degueldre, 1993; Johnson et al., 1996; Elimelech et al., 2000). The latter conditions also leads to size exclusion effects, resulting in an earlier

breakthrough of colloids compared to a non-reactive tracer (Enfield et al., 1989; Grolimund et al., 1996; Kretzschmar and Sticher, 1997). Both conditions would be present during stormwater injection (Nightingale and Bianchi, 1977).

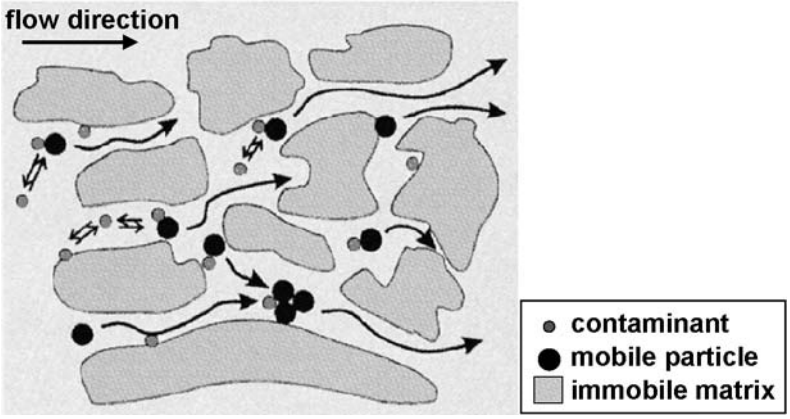

Figure II-6: Schematic contaminant facilitated transport in a porous media showing possible interactions like particle mobilisation, deposition, coagulation, and sorption of contaminant between mobile particle or immobile matrix and solution (modified after Buffle and Leppard, 1995a).

The third condition has been shown to be valid for a range of contaminants like radionuclides, hydrophobic organics and trace metals (Buddemeier and Hunt, 1988; Johnson and Amy, 1995; Karathanasis, 1999). Sorption of metals to colloids underlies the same principles as sorption to immobile solid matter. As colloids have a comparatively higher surface area and consist of organically coated clay mineral and oxides, they offer comparatively more sorption sites than the average siliceous matrix (Mills et al., 1991; Kretzschmar et al., 1999). This means that in general metals would sorb preferentially to colloids and desorption has been shown to be slow esp. for Cu compared to Zn (Lehman and Harter, 1984; McBride, 1989; Hogg et al., 1993). In column studies break-through of metals has been shown to be associated with the colloid peaks (Kaplan et al., 1995; Grolimund et al., 1996; Karathanasis, 1999). Some field studies nevertheless discovered that colloidal associated transport was negligible under the given conditions (Baumann et al., 1998).

As has been shown in the field (see II.2.4.2) injected colloids are only partially recovered and it could be argued that colloid facilitated transport in the subsurface is a major mechanism for migration of stormwater pollutants into groundwater aquifers. However, current models are not sufficient to predict colloid release, aggregation and deposition mechanisms and cope with chemical and physical surface heterogeneities under changing geochemical conditions (Song et al., 1994; Tufenkji and Elimelich, 2004; Tufenkji and Elimelech, 2005; Sen and Khilar, 2006). Therefore colloid-facilitated transport can only be described qualitatively.

II.4.5 Influencing factors

As described above a number of mechanisms influence the speciation of metals in the environment. It has also been mentioned that these processes are influenced by a number of factors like pH, redox potential, ionic strength, competition between ions and presence of organic ligands. The direct influence of any single factor is often hard to decouple from its indirect effects on other factors and processes though.

pH

Without question pH is the most important factor influencing metal sorption behaviour (Elrashidi and O'Connor, 1982; Pulford, 1986; Welp and Brümmer, 1998; Arias et al., 2005) as it not only controls the speciation of metals, but also the state of variable charged mineral and organic matter surface sites (Cavallaro and McBride, 1984; McBride et al., 1997; Christensen and Christensen, 2000) and the solubility of mineral and organic phases (Jenne, 1968; Elliot and Huang, 1979; Stumm and Morgan, 1996; Sparks, 2003). This means that pH has direct and indirect effects on metal sorption through changes in available adsorption sites due to e.g. dissolution of oxides or carbonates (Jenne, 1968) and through competition for sorption sites at low pH (Barrow, 1986b; Warwick et al., 1998; Elzinga et al., 1999).

All adsorption processes are pH dependent as they involve deprotonation of surface OH-groups or the hydrolysis of the metal ions (Barrow, 1986b; McBride, 1989; Bradl, 2004; Singh et al., 2006), which means that pH operates through mass-action effect (Davis et al., 1978; Schindler et al., 1976) and through effects on electrostatic potential (Davis and Leckie, 1978). Benjamin and Leckie (1981a) found that Cu and Zn released 1.9 and 3.2 protons respectively during adsorption onto amorphous iron oxyhydroxide due to bidentate binding and concurrent hydrolysis and shows that Zn sorption is qualitatively different to Cu sorption. As the order of adsorption of metals resembles the order for hydrolysis (see Figure II-7; McKenzie, 1980; Barrow et al., 1981), most authors assume the adsorption of the hydroxy ions rather than the free ions (Forbes et al., 1976; McBride and Blasiak, 1979; Barrow, 1986b; Pardo and Guadalix, 1996; Elzinga et al., 1999) onto materials like clays and iron oxides (Barrow, 1986b; Dzombak and Morel, 1990). Due to the addition of NaOH for pH adjustments the metals will be more hydrolysed and therefore sorb more (Figure II-7). The importance of chemisorption or surface complexation therefore increases with increasing pH (Schindler and Stumm, 1987; Tiller et al., 1984a) in conjunction with increasing hydrolysis.

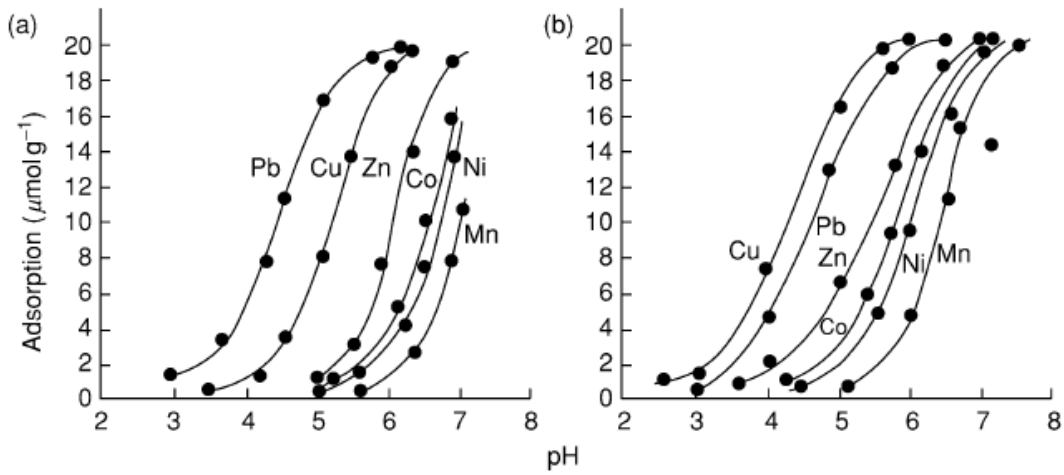

Figure II-7: Metal adsorption vs. pH on (a) hematite and (b) goethite (McKenzie, 1980)

The position and shape of the adsorption edge depends on the metal and sediment concentration, on the type of sorption surface (Figure II-7) and on the presence of ligands. It moves towards higher pH values with increasing metal concentration or decreasing solid concentrations (Benjamin and Leckie, 1981a; Dzombak and Morel, 1990) and can be interpreted as reflecting the various amounts of less and highly reactive surfaces (Tiller et al., 1984a). If adsorption is metal-like, adsorption increases with increasing pH (McBride and Blasiak, 1979; Harter, 1983; Pulford, 1986; Pardo and Guadalix, 1996) and the adsorption edge can move parallel with increasing ligand concentration (Stevenson, 1977; Goodman, 1986; Benjamin and Leckie, 1981b). If the adsorption is ligand like, adsorption decreases with increasing pH, but can also be more trough or dome shaped depending on ligand concentration (Benjamin and Leckie, 1981b). This means ligand-like sorption dominates at low pH and metal-like sorption dominates at high pH (Brümmer et al., 1983; Tiller et al., 1984a; Bradl, 2004). Higher pH promotes also dissolution of soil organic matter and the formation of organic-metal complexes, which are more stable at higher pH (Schnitzer and Skinner, 1966; Murphy et al., 1992; Milne et al., 2003; Mosley et al., 2003).

Redox potential

The redox potential is strongly coupled with the presence of organic matter (II.2.3.4) and its effect on metal solubility is intimately related to pH. Commonly metal solubility is depicted in pH/Eh or pe diagrams (Figure II-8). These diagrams display equilibrium stability fields at the defined conditions of temperature, pressure and concentration of other components. However, metal speciation might vary significantly from the depicted field of stability, as the diagrams do not present kinetically controlled dissolution/precipitation rates, ligand effects or changes in solution composition or activity (Hem, 1961; Jenne, 1968). Despite these limitations it can be stated, that the free Zn^{+2} exhibits a much larger stability field than Cu^{+2}, and that Zn occurs only in one oxidation state, i.e. Zn(II), while Cu can occur as Cu(II) and Cu(I). The redox potential is indirectly affecting the speciation of Zn and Cu due to

reductive/oxidative dissolution/precipitation of other phases, e.g. Fe-/Mn-oxides or sulfides (see II.4.3).

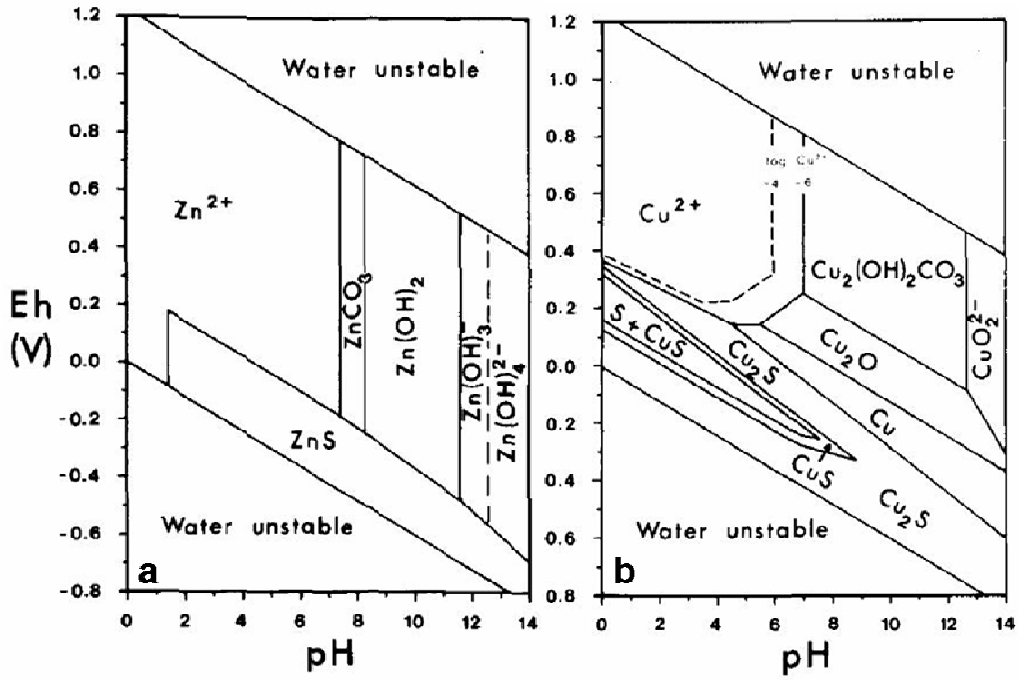

Figure II-8: Stability fields of (a) Zn species in the system Zn (10-5 mol/L) + CO2 (10-3 mol/L) + S (10-3 mol/L) + H20 at 25°C at 1 atm pressure (after Hem, 1972) and (b) Cu species in the system Cu + H2O + O2 + S + CO2 (PCO2 10-1) at 25°C and 1 atm total pressure in relation to Eh and pH (after Garrels and Christ, 1965).

Ionic strength

Ionic strength has four main effects (a) competition of major ions for non-specific sorption sites (Malandrino et al., 2006; Limousin et al., 2007), (b) formation of inorganic complexes with metals (Shuman, 1986; Mesquita and Vieira e Silva, 1996); (c) change in permanent charge sorption sites (Gillmann, 1981; Baeyens and Bradbury, 1997; Voegelin et al., 2001), and (d) effect on mobility of colloids (Khilar and Fogler, 1984; Elimelech and O'Melia, 1990). Increases in ionic strength will expel non-specifically sorbed metals due to the cations higher ion activity, will increase the amount of inorganic complexes and favour coagulation and deposition of mobile colloids. The general trend therefore is a decrease in metal adsorption with increasing ionic strength (McBride, 1978; Herms and Brümmer, 1984).

The type of cation and anion in solution has to be taken into consideration though as it influences the diffuse double layer chemistry (Harter and Naidu, 2001). The monovalent ions generally enhance particle dispersion, while divalent ions enhance aggregation (Pulford, 1986; McBride et al., 1997). Metal adsorption is decreased in nitrate or sulphate solutions, as Cu and Zn can form inorganic nitrate and sulphate complexes, while adsorption is decreased less (or even increased) in chloride solutions (Barrow et al., 1981; Padmanabham, 1983; Pulford, 1986; Shuman, 1986).

Metal competition

In general, Zn and Cu are competing for the same sorption sites in the natural sediment and metals present in higher concentration will be sorbed to a greater extent. Due to the higher selectivity of most surfaces for Cu though, Zn will be more susceptible to competition from Cu than the other way round (Mesquita and Vieira e Silva, 1996; Arias et al., 2006; Tsang and Lo, 2006). In addition, kinetic effects might influence the adjustment to changes in equilibrium, e.g. Cu showing a slow dissociation rate from organic ligands (Fasfous et al., 2004).

Enhanced mobility of Cu or Zn due to competition for complexing sites on organic matter, natural soils and inorganic phases with other cations like Ca, Fe and Al (Warwick et al., 1998; Tipping et al., 2002; Agbenin and Olojo, 2004; Tipping, 2005; Miretzky et al., 2006) or other trace metals (Sonnenberg, 2003; Antoniadis et al., 2007; Covelo et al., 2007) has been reported.

Organic ligands

As has been mentioned before, organic matter is of major influence to metal solubility as it influences the redox potential (see II.2.3.4), is involved in complexation and ternary interactions (see II.4.2), promotes reductive dissolution and can hinder precipitation reactions (see II.4.3) and can also stabilise mobile particles (see II.4.4). The speciation of organic ligands on the other hand is influenced by pH. At low pH coagulation and flocculation of larger humic substances occurs, adsorption of ligands onto other surfaces is favoured (Schnitzer and Kodama, 1966; Greenland, 1971; Li and Dai, 2006) and the stability of dissolved metal complexes is decreased (Schnitzer and Skinner, 1966; Murphy et al., 1992; Milne et al., 2003; Mosley et al., 2003). At high pH the opposite effects lead to a higher solubility of organic ligands and associated metals. Coagulation can also be instigated by an increase in ionic strength.

II.4.6 Metal behaviour during the ASR cycle

Some of the above introduced processes are more or less important for stormwater ASR in general and at different stage of the cycle and will be briefly highlighted below.

II.4.6.1 Pretreatment

In most cases stormwater will not be used for injection straight from the source, but would be collected and pretreated to a degree. Best management practices for urban stormwater (US EPA, 1999; Victoria Stormwater Committee, 1999; Hatt et al., 2006) offer a range of primary treatment methods to reduce contaminant loads, the most common being wetlands and detention ponds, which utilise the effect of sedimentation of suspended solids and attached

contaminants (Yousef et al., 1990; Braskerud, 2000; Walker, 2001). This helps to prevent clogging of bores and also decreases metal loads attached to settlable solids. However, sedimentation does not affect loads from dissolved metals or metals attached to particles about <20 µm (Walker and Hurl, 2002; Lin et al., 2008), and the accumulated metals and organic matter in the sediment have the potential to be remobilised (Kalbitz and Wennrich, 1998; Olivie-Lauquet et al., 2001; Walker and Hurl, 2002; Grybos et al., 2007). Further improvements to the water quality has been achieved by using vegetation, which takes up nutrients and accumulates heavy metals (Maine et al., 2007; Sun and Davis, 2007; Zhao et al., 2007a; Read et al., 2008). A release of metals can be expected during decay of plant material and removal rates in the long-term are uncertain. Release of nutrients and dissolved organic matter from wetlands has also been reported and can be increased by wildlife, e.g. birds (Sharpin and Morison, 1995)

Further treatment with filtration through gravel, sand or roughing filters has been shown to decrease particle concentration and associated metals further (Page et al., 2006; Hatt et al., 2007). Secondary treatment with filter material of different material (e.g. alumina, activated bauxsol-coated sand, bark, bauxsol-coated sand, fly ash, granulated activated carbon, granulated ferric hydroxide, iron oxide-coated sand, natural zeolite (Genç-Fuhrmann et al., 2007), synthetic zeolites (Pitcher et al., 2004), peat (Zhou et al., 2003), activated carbon, oxide-coated sand (Sansalone, 1999), zero-valent iron (Rangsivek and Jekel, 2005)) have been tested with varying degrees of success. Conventional secondary treatment (Kurniawan et al., 2006) with flocculation/coagulation, liming or dissolved air flotation are possible and effective, but require the right dosing of chemicals and the handling of sludge waste that are usually not practicable within the ASR setting (Dillon et al., 2007).

Clearly, the pretreatment step is the most crucial step for metal behaviour as their fate might already be established if no metals are injected into the aquifer. This would be a favourable outcome.

II.4.6.2 Injection

The injection phase is the main disturbance of the groundwater system, as oxic, nutrient and organic matter enriched, low ionic strength water enters a commonly anaerobic, nutrient poor, brackish groundwater. The pH is commonly around neutral for stormwater and free dissolved metals are likely to adsorb to the immobile or mobile groundwater matrix near the injection well. Complexed metals and colloidal metals are more mobile though and are likely to get transported until they reach areas of higher salinity (McDowell-Boyer, 1992; Bunn et al., 2002). Due to the increase in flow velocity (McCarty et al., 1993; Ryan and Gschwend, 1994) and low salinity of the injected water colloids near the well might also be mobilised

(Nightingale and Bianchi, 1977; Johnson et al., 1999; Konikow et al., 2001) carrying attached metals with them. The increase in dissolved organic carbon might also desorb previously adsorbed metals, if complexation is more favourable. If free Fe^{+2} was present in the groundwater this would precipitate and scavenge dissolved metals. Other mineral phases are likely to dissolve due to undersaturation or change in Eh-pH stability conditions in the solution and release metals. Metals leached from the aquifer matrix near the well are then redeposited further away from the well, within the radius defined by the storage bubble.
Mixing along the flow path will diminish the difference between the injectant and the native groundwater, but due to heterogeneities in the aquifer, zones of fast preferential flow will develop next to diffusion dominated areas and local disequilibrium might increase, meaning that the geochemical conditions and hence the dominating process can be quite different depending on the location.

II.4.6.3 Storage

The injection of organic matter and nutrients will have stimulated microbial activity in the vicinity of the injection well. During storage organic matter degradation and associated reduction in redox potential will be the main factor for metal behaviour. Metals that were attached to the organic matter might be released and reductive dissolution of minerals might also release metals. If redox potential drops low enough sulfide precipitation of metals might occur. Changes in pH during this stage might also influence the solubility of metals.
In general, disequilibrium will be lessened due to time for rate limited reactions and diffusive processes. After a number of ASR cycles diffusive processes will have replaced the native groundwater with infiltration water completely (Dillon et al., 1997).

II.4.6.4 Recovery

The extent of geochemical changes during recovery is much lower than during injection and depends also on the change in volume and the extent of the buffer zone. Free metals in solution will be recovered and especially non-specifically adsorbed metals are likely to be desorbed with an increase in ionic strength. In the well vicinity, particles and all attached metals will also be recovered.

II.4.7 Conclusions

Speciation of Cu and Zn depends on range of different processes and factors. Nevertheless, Zn and Cu behaviour is influenced to a different degree by the individual mechanisms and factors. Cu speciation is mostly influenced by the presence of organic matter, in solution it is mainly found as organic complex and sorption is dominated by specific surface complexes, resulting in slow desorption. Zn speciation is mostly influenced by pH, in solution it is mainly

found as free ion and sorption is dominated by non-specific surface complexes, resulting in fast desorption.

Overall, metals are persistent in the environment and mechanisms are reversible, meaning that metals retained in the aquifer could eventually become mobile again with time and change in geochemical conditions. In conclusion, the interactions of metals with solution and solid described in this section are complex and intertwined. At this stage, no single theoretical approach or model is capable of incorporating all processes and factors and empirical approaches are therefore still common. It is therefore critical to undertake site-specific studies and ongoing monitoring to assess key processes and outcomes.

II.5 Summary

Australia has great possibilities and requirements to integrate stormwater treatment and recycling into its water managements plans to reduce water demands on current potable water resources. It could be shown from the literature that:

- Aquifer storage and recovery allows direct injection into deeper aquifer systems, including those containing poor quality groundwater thereby creating freshwater storage where none existed previously and improving injectant water quality via biodegradation.
- Previous monitored stormwater ASR studies have used limestone aquifers, which are rather different in their geochemical properties, and have not been going on for long enough to show long-term effects. No monitored study in sandy aquifers has been undertaken so far
- While research has been undertaken on the release of geogenic metals no study has investigated the fate of injected metals.
- Protecting the environment and preserving water quality is of vital importance and proper risk assessment has to be undertaken.
- Heavy metals are present in stormwater in variable concentrations with Zn and Cu regularly exceeding freshwater guidelines. These metals are a primary concern due to their toxicity and persistence in the environment.
- Zn and Cu occur in colloidal and dissolved form and undergo various reversible speciation processes and transport during an ASR cycle, with injected colloids being retained within the aquifer.
- Major influences on metal speciation are pH, redox potential, ionic strength and organic ligands.

- The behaviour of heavy metals is a complex combination of different processes. They are time and space dependent and zones where one or the other process occurs are likely to shift during ASR cycles. No current model is capable to incorporate all possible interactions.

In conclusion, there is a need for a better understanding of the behaviour of injected heavy metals in different types of aquifer systems to help develop an improved code of practice.

II.6 Scope

II.6.1. Scientific problem

Sustainable reuse of stormwater is an important issue in urban water management and ASR could be one part of the solution. While ASR with potable injectant has been practiced for a number of decades, the use of stormwater is a relatively recent phenomenon. The quality of stormwater runoff is highly variable and can be compromised by heavy metals, esp. Zn and Cu (see II.3.5). The understanding of major processes that control the water quality changes occurring during recharge and recovery is complicated by site specific aquifer characteristics and complex interactions between solid and solution (see Figure II-9 and section II.4). The identification and quantification of these processes from field data is further limited by highly transient conditions of the ASR cycle with change in flow direction, recharged/recovered volumes and storage times, which would involve the costly acquisition of high resolution spatial and temporal data. Adding this to the limited number of existing field sites results in sparse to non-existent field records, meaning there is currently no monitored field site of stormwater ASR in a sandy aquifer (see II.2.4). However, future implementation in sandy aquifers is a likely scenario.

This study is concerned about a weighed balance between sustainable urban water management and environmental protection of groundwater, aquifer and adjacent ecosystems. Therefore the main aim of this study is to investigate the behaviour of heavy metals in stormwater injection ASR based on laboratory experiments.

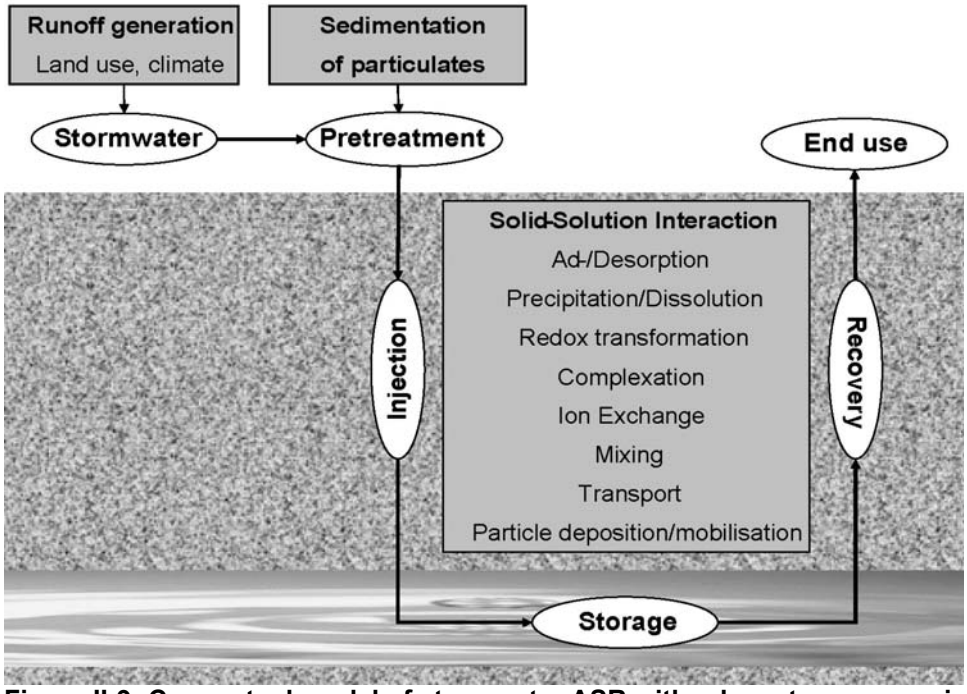

Figure II-9: Conceptual model of stormwater ASR with relevant processes influencing metals.

II.6.2. Objectives of this study

The evaluation of risk to the environment posed by injected metals during stormwater ASR will be addressed by:

- Characterisation of stormwater pollutant concentrations in different Melbourne catchments with special focus on Zn and Cu speciation
- Characterisation of groundwater and aquifer material found at potential ASR sites in Melbourne
- Investigation of single factor influence to sorption behaviour of Zn and Cu in batch tests
- Investigation of multiple factor and hydraulic influence to sorption behaviour of Zn and Cu in specially designed column tests
- Investigation of processes of Zn and Cu behaviour found during column tests by geochemical transport modelling

Chapter III: Stormwater and groundwater quality

"When the well is dry, we know the worth of water."
Benjamin Franklin, Poor Richard's Almanac, 1746

III. 1 Introduction

Urbanisation and population growth has been a dominant demographic trend during the last century with widespread effects for all natural systems (Miller, 2005). The clearing of natural vegetation and sealing of surfaces reduces the amount of infiltration and increases the flux of stormwater. The hydrogeological cycle is further altered through water drainage systems that transport runoff from streets and buildings efficiently to receiving water bodies leading to degradation of urban streams (Walsh et al., 2005).

The urban environment with its traffic, industry and infrastructure also introduces a range of pollutants, e.g. heavy metals, organic contaminants, particulates, nutrients (see II.3, Makepeace et al., 1995; Pitt et al., 1999). Heavy metals are priority pollutants due to their phyto- and cytotoxicity and their persistence in the environment (Eriksson et al. 2007; Kayhanian et al., 2008). Diffuse sources like atmospheric deposition, wear and tear from automobiles and corrosion of metal objects are the main contributors of particulate and dissolved heavy metals (Makepeace et al., 1995; Wong, 2006). As about 70% of all impervious surfaces are related to traffic (Wong, 2006), urban runoff contains about 100 times more heavy metals than non-urban runoff and metals like Zn, Cu and Pb regularly exceed the Australian guidelines for freshwater aquatic ecosystems (see Table III-4; Pettigrove and Hoffmann, 2003; Lawrence and Breen, 2006). Stormwater quality and quantity though is rather variable and depends on a range of parameters, e.g. land use, rainfall intensity, frequency and volume (Vaze and Chiew, 2003a; Wong, 2006). Even in one catchment pollutant concentration can change more than one magnitude (Sansalone et al., 1995) during the hydrograph of one event (e.g. first flush effect (Sansalone and Buchberger, 1997; Bucheli et al., 1998; Barbosa and Hvitved-Jacobsen, 1999)), from one event to the next and over the seasons (e.g. seasonal first flush (Lee et al., 2004)). Both quantity and quality of stormwater are needed to calculate pollutant loadings and various models with increasing complexity have been developed to incorporate site specific parameters with varying success (e.g. Ahyerre et al. 1998; Kanso et al., 2003; Wong et al., 2003; Obropta and Kardos 2007). A number of studies have monitored stormwater quality mainly in the USA and Europe (e.g. Torno et al., 1986; Smullen et al., 1999; Fuchs et al., 2004,), while studies from Australia are less comprehensive, small scale and have mainly been concerned with

suspended solids and nutrients (e.g. Hogan et al., 1995; Emmett et al., 1996; Vaze and Chiew, 2003b). A general trend of decreasing pollution over time has been found (Smullen et al., 1999) and could be related to the overall decreased atmospheric pollution, especially of finer particles (Fitz-Simons et al., 1998). An overall lower population density and hence atmospheric deposition in the southern hemisphere would also result in lower average pollution values in Australia compared to Europe and USA.

As heavy metals are often associated with particulates (e.g. Mikkelsen et al., 1997; Sansalone and Buchberger, 1997; Gromaire-Mertz et al., 1999) especially with the fine fraction (e.g. Liebens, 2001; Muthukaruppan et al., 2002; Deletic and Orr, 2005; Tuccillo, 2006), special attention has been paid to solid build-up, mobilisation and particle size distribution (Sansalone and Buchberger, 1997; Liebens, 2001; Yuan et al., 2001; Deletic and Orr, 2005). Speciation and distribution of heavy metals between the dissolved and particulate phase is crucial to assess their probability of being injected during stormwater ASR. This potential is high for all forms of dissolved metals and those attached to the fine solids and colloids, as coarser solids would have been settled before injection (see II.4.6.1). In this context complexation of metals with organic matter has also to be mentioned, as it can increase their dissolved fraction (e.g. Davis, 1984; Barraud et al., 1999; Mason et al., 1999). Even though organic matter is frequently found in urban stormwater, it is often not monitored. Once injected, organic matter as well as oxygen and nitrate also influence redox reactions in the groundwater which in turn affects metal behaviour (Stumm and Morgan, 1996; Baker et al., 2000).

As it is crucial for every ASR scheme to know the pollutant loads of the injected water, characterisation of Melbourne stormwater was undertaken and is presented in the first part of this chapter. This included the association with particulates as well as correlation with other surrogate variables like pH and organic matter.

The second part of this chapter is concerned with the receiving end of the ASR scheme. Geochemical reactions that occur when recharged water interacts with the ambient groundwater and aquifer matrix are expected to be site-specific. Such information for Melbourne aquifer systems is largely unknown and aquifer geochemical properties are poorly studied. A literature review was conducted on the hydrogeology of Melbourne, mostly from reports of the Geological Survey of Victoria (DPI, 2008b). Relevant data were also gathered from the Borehole database (DPI, 2008a), Victorian Geoscientific Database (DPI, 2008c), Groundwater Database (DSE, 2008a), the Victorian Water Resources Data Warehouse (DSE, 2008c) and from personal communication with senior hydrogeologists. In addition a

small survey of accessible bores in one of the potential ASR target aquifers was conducted and results along with characterisation of sampled aquifer material will be presented.

III. 2. Stormwater investigation

To understand the characteristics of stormwater inflows into possible ASR sites in Melbourne, a brief introduction to the catchments and a review of existing data sets on stormwater characteristics for Melbourne will be presented. More specific results from a new round of stormwater samples are then gathered and the implications of the results are discussed.

III. 2.1 Introduction to the Melbourne catchments

The Port Phillip Region catchment (with 22 sub-catchments) drains about 10,000 km², with mostly low relief, rising to about 1200 m in the NE area. The urban area sprawls around the bay with an area of around 1300 km² (Leonard, 1992), which has increased since then and will be further increasing (Dept. of Infrastructure, 2002). Melbourne enjoys a temperate climate with main rainfall during winter and relatively dry summers. The mean annual rainfall increases from 450 mm west of the city centre to 700 mm in the east and south of the wider metropolitan area (Melbourne Water, 2004; BOM, 2008). Climate change models predict an overall decrease in rainfall in the future (Howe et al., 2005).

The Institute of Sustainable Water Resources (ISWR) funded by Victoria EPA has been monitoring and collecting stormwater quality and quantity around Melbourne at a number of sites, representing different typical land uses (see Table III-1 + Figure III-1). In a first step calculations of pollutant loads and correlation of major pollutants (TSS, TN and TP) with storm characteristics have been undertaken, showing that rainfall intensity was the most important factor for pollutant loading (Francey et al., submitted). In a second step the program was enlarged to incorporate sampling for size-fractionated heavy metals at these sites. To enable a full characterization of Melbourne stormwater for the ASR assessment the project was enlarged by this study to incorporate further analysis of pH, EC, organic carbon and major ions (see III.2.2).

Table III-1: Stormwater monitoring sites in Melbourne

Site	Primary land use	Area (m²)	Imperviousness (%)	Events sampled
Monash Roof (MR)	coated aluminium roof	460	100	17
Gilby Rd (GR)	light industrial	282 000	80	18
Shepherds Rd (SR)	medium density	379 800	45	2 #
Richmond (RI)	high density residential	891 200	74	14
Eley Rd (ER)	residential and commercial	1 860 400	46	3 #

malfunction of sampling apparatus at this site

The Monash Roof (MR) site is a coated aluminium roof above the Civil Engineering Laboratories at Monash University, Clayton. The roof is in close proximity to the exhaust pipes from the surrounding laboratories, e.g. metal working, and atmospheric deposition is the main pollution input.

The Gilby Road (GR) site is part of a light industrial area (e.g. glass manufactures, transport companies) and is surrounded by main roads and highways. Vegetated strips are mainly restricted to roadsides. Main pollutant sources are mainly atmospheric deposition from traffic and industry, as well as other industrial and traffic related inputs.

The Richmond (RI) catchment is located a few km to the east of the Melbourne CBD. The high density residential streets with only small confined gardens are surrounded by a grid of main roads. Stormwater pollution stems mainly from traffic and corrosion of housing and traffic infrastructure.

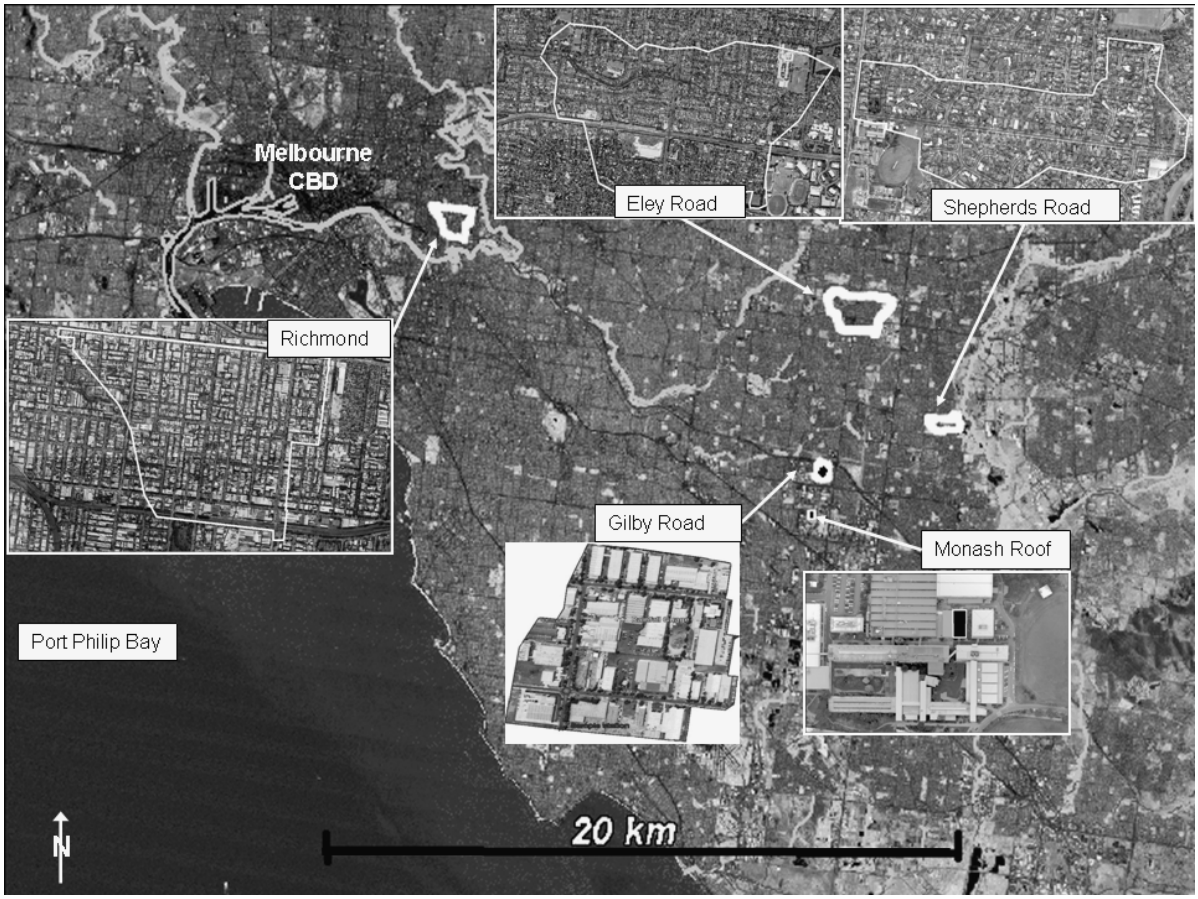

Figure III-1: Stormwater sampling sites in Melbourne showing location and insets of close ups (individual pictures courtesy to ISWR).

III. 2.2 Stormwater sampling and analysis

Close to the centre of the catchment sites 0.2 mm tipping gauges were logging rainfall data every minute. Close to the catchment outlet Doppler-base flow-meters (Sigma 950) recorded flow runoff rates every minute and automated samplers (Sigma 900) were installed. Sampling was triggered at increased flow (based on 3-month average return interval volumes) and subsequent 1 L samples were taken at set times afterwards with high sampling

frequency in the rising limb of the hydrograph and decreased sampling in the hydrograph tail (flow-weighted sampling approach). According to the hydrograph volumes, flow-weighted composite samples for event mean concentration (EMC) measurements were composed. Previously these samples had been analysed for TSS (APHA, 1998), as well as TN and TP (Lachat - QuikChem 8000 Flow Injection Analyser) (Francey et al., submitted). To enable a full characterization of Melbourne stormwater for the ASR assessment the ongoing project was enlarged. From Jan - Nov 2005 incoming individual samples were analysed for pH (Radiometer PHM82), EC (TPS Model 2100) and alkalinity (Gran-plot (Stumm and Morgan, 1996)) as soon as possible and flow-weighted EMC calculated. TOC (Shimadzu TOC-5000 Total Carbon Analyser) analysis was performed on a composite subsample. The composite samples where then sieved through a nylon sieve (63 µm) and further filtered (0.45 µm). Further size differentiation was not possible due to limited amounts of solids. Dissolved samples were analysed for major ions (Na, K, Mg, Ca (AAS) and Cl, SO_4, (Lachat - QuikChem 8000 Flow Injection Analyser)) and DOC (Shimadzu TOC-5000 Total Carbon Analyser) according to standard methods (APHA, 1998). The separated particles and dissolved subsamples were extracted with nitric acid on a hotplate (APHA, 1998) for size fractionated metal analysis (ICP-OES, Varian).

Due to uncertainty inherent in the sampling, storage and analysis of individual samples and a high variability of flow during and between storm events, about 30% uncertainty can be expected for most pollutants (Ahyerre et al., 1998; Bertrand-Krajewski and Bradin, 2002; McCarty et al., 2008). Bootstrapping analysis (Chernick, 2007) of an independent data set showed that 25 events are needed for parameters other than TSS (Francey et al., submitted). Technical problems and unusually dry climate conditions resulted in the number of events sampled falling short of this target number. As Shepherd Rd and Eley Rd had only 2 and 3 events, respectively, no meaningful statistical analysis could be performed for these sites. For the other three sites (MR, GR and RI) simple statistical analysis was undertaken to determine site average EMC (µEMC), its standard deviation, and range. For Zn and Cu the site mean concentration (SMC) was also determined as the sum of all measured event loads divided by the total volume of all measured events.

III. 2.3 Results and discussion of stormwater investigation

The summary of main parameters (Table III-2) showed that all three sites exhibited a wide range for all parameters (with the exception of pH) with standard deviations mostly between 30-100%. This is due to the fact that many parameters e.g. catchment characteristics, antecedent dry-weather period, rainfall volume and rainfall intensity have a bearing on this variation (Wong, 2006).

The roof catchment has the highest relative variability of the three catchments and the lowest values for all parameters, as only atmospheric deposition can reach it. The significantly lower pH measured at MR is in conjunction with pH found in rainwater in equilibrium with atmospheric CO_2 (Appelo and Postma, 1999a) and showed that only limited buffering takes place on the roof. It is an extremely specialised catchment that cannot be compared to GR and RI and is unlikely to be representative for an ASR scheme catchment.

Even though GR is a light industrial catchment, it showed mostly lower pollutant concentration than the residential catchment (RI). While pH was very similar in both catchments, EC values and accordingly all major ions were overall higher in Richmond. Richmond also had higher concentration of TSS, organic matter and nutrients. Only Al and Fe were higher in GR, which could be due to metal related industry. As Richmond is close to the city centre it could be speculated that more traffic passes through this area, compared to the light industrial area that would have limited traffic especially during the weekend, resulting in higher pollutant concentrations for RI.

Table III-2: Summary of mean EMC (µEMC), minimum (min), maximum (max) and standard deviation (std dev) for measured event parameters including storm event characteristics, physico-chemical parameters, major ion and metal concentrations (Cd, Cr and Ni were below or close to detection limits and were excluded in the statistical analysis; Cu and Zn see Table III-3). Individual results for all events incl. Values for all events including SR and ER see Table A-1 in appendix.

	Monash Roof (MR) 17 events				Gilby Road (GR) 18 events				Richmond (RI) 14 events			
	µEMC	**min**	**max**	**std dev**	**µEMC**	**min**	**max**	**std dev**	**µEMC**	**min**	**max**	**std dev**
total rainfall [mm]	**9.2**	2.0	65	15	**7.8**	2.40	20	5.3	**7.8**	0.6	20	5.4
rain intensity [mm/h]*	**1.6**	0.6	4.4	1.1	**1.7**	0.40	4.8	1.0	**2.1**	0.6	8.4	2.1
peak flow rate [L/s]	**1.5**	0.2	4.0	1.1	**468**	115	1156	305	**612**	11	2850	737
total flow volume [ML]	**0.002**	0.001	0.004	0.001	**1.45**	0.31	3.78	1.09	**2.10**	0.58	4.58	1.37
duration [h]	**3.2**	0.3	9.2	2.3	**4.6**	0.27	11	3.2	**4.7**	0.1	15.5	4.1
ADWP [d]	**5**	0	11	4	**6**	1	22	6	**8**	1	22	6
pH	**5.7**	5.0	6.9	0.42	**6.6**	6.2	6.9	0.25	**6.7**	6.4	7.1	0.24
EC [µS/cm]	**17**	4	61	17	**57**	31	95	17	**103**	52	171	38
Ca [mg/L]	**0.8**	0.1	3.8	0.9	**4.9**	3.3	7.4	1.1	**8.2**	4.8	12.0	1.9
Mg [mg/L]	**0.2**	0.0	0.8	0.2	**0.9**	0.6	1.5	0.3	**1.4**	0.7	2.1	0.5
Na [mg/L]	**1.8**	0.2	7.4	1.8	**5.0**	3.2	7.4	1.2	**7.2**	3.8	12.0	2.7
K [mg/L]	**0.2**	0.1	0.5	0.1	**1.1**	0.7	2.7	0.5	**2.5**	1.2	4.4	1.0
HCO_3 [mg/L]	**3.5**	0.4	13	2.8	**14**	10	28	4.4	**27**	15	47	7.9
Cl [mg/L]	**2.4**	0.2	14	3.6	**5.1**	2.5	11	2.3	**8.9**	2.0	20	5.9
SO_4 [mg/L]	**1.5**	0.4	3.6	1.0	**4.3**	1.6	8.6	1.9	**6.4**	3.4	9.9	2.2
TOC [mg-C/L]	**3.1**	1.0	7.0	1.8	**8.7**	3.0	17	4.2	**11.7**	5.0	21	5.8
DOC [mg-C/L]	**2.4**	1.0	4.0	0.9	**5.8**	3.0	11	2.7	**6.9**	3.0	10	2.8
TSS [mg/L]	**34**	2.3	198	55	**75**	17	197	45	**194**	46	525	134
TP [mg-P/L]	**0.1**	0.0	0.2	0.1	**0.2**	0.1	0.7	0.2	**0.7**	0.3	1.8	0.4
TN [mg-N/L]	**1.2**	0.3	5.8	1.3	**1.7**	1.0	4.7	1.2	**3.3**	1.7	7.4	1.6
Al (total) [mg/L]	**0.90**	0.02	4.4	1.2	**7.98**	0.75	52	15	**5.47**	1.1	11	3.0
Fe (total) [mg/L]	**1.12**	0.06	7.3	2.0	**7.40**	0.63	70	16	**6.95**	1.4	13	3.9
Mn (total) [µg/L]	**21**	3.7	111	27	**114**	16	1052	237	**121**	36	228	55
Pb (total) [µg/L]	**5.8**	0.1	21	6.0	**43**	2.1	342	78	**119**	26	243	63

*peak rainfall intensity over 10 mins; ADWP: antecedent dry weather period; TOC/DOC: total/dissolved organic carbon; TSS: total suspended solids; TP: total phosphorus; TN: total nitrogen.

A size fractionated site summary for Cu and Zn (Table III-3) showed that GR and RI lay within comparable ranges, while MR had also considerably lower values for Cu and Zn. The SMC was lower than the µEMC in most cases, which had also been observed for TSS, TN and TP (see Francey et al., submitted). This suggests that events with high volume have a comparatively lower concentration than smaller events and could be attributed to a source limitation. This was underlined by the fact that events with a short antecedent dry weather period (ADWP) and low rainfall intensity resulted in lower pollutant concentrations, as pollutant load is a function of build-up and wash-off (Duncan, 2006).

Table III-3: Mean EMC (µEMC), site mean concentration (SMC), minimum (min), maximum (max) and standard deviation (std dev) for Cu and Zn divided in three size categories and added up for each event sample to total concentrations.

		Cu				Zn			
	[µg/L]	>63µm	0.45-63µm	<0.45 µm	**total**	>63µm	0.45-63µm	<0.45 µm	**total**
Monash Roof (MR) 17 events	µEMC	2.0	1.8	2.6	**6.4**	12	7	97	**116**
	SMC	1.4	1.4	2.5	**5.3**	7.7	2.2	89	**99**
	min	0.1	0.2	0.5	**1.5**	0.1	0.3	39	**40**
	max	15	7.8	5.7	**27**	76	71	267	**343**
	std dev	3.6	2.1	1.7	**6.2**	24	18	53	**71**
Gilby Road (GR) 18 events	µEMC	10	28	7.9	**46**	148	353	448	**950**
	SMC	11	39	6.2	**57**	133	495	356	**985**
	min	0.4	3.7	2.9	**11**	11	19	173	**335**
	max	30	268	19	**273**	503	3630	905	**3814**
	std dev	10	61	4.8	**61**	154	825	239	**794**
Richmond (RI) 14 events	µEMC	32	20	8.8	**61**	631	313	413	**1357**
	SMC	27	16	7.2	**50**	506	274	370	**1150**
	min	5.2	4.7	4.0	**20**	72	8.5	84	**643**
	max	92	48	18	**119**	1626	748	744	**2835**
	std dev	27	14	3.9	**30**	495	250	188	**596**

note: Samples below detection limit (only occurred for the roof catchment) were assigned half the detection limit value. Total min/max concentrations are not the addition of min/max over the three fractions as min/max did not occur in all three fractions simultaneously. Similarly, the total standard deviation was calculated from all total concentrations and not added up over the three fractions.

As mentioned before PSD is an important characteristic of stormwater and has implications for the fate of heavy metals. Monitoring from another site in Melbourne (Hampton Park wetland, Fletcher et al., 2004) showed that median particles sizes decreased from about 150 µm at the inflow to about 20 µm in the open water zone of the wetland. PSD of injectant at Andrews Farm, SA, reported a mean particle size of about 5 µm, with the bulk of particles ranging from 1-20 µm (Barry, K. et al., 2002). Analysis of particle distribution of one storm event at GR indicated that more than 50% of all particles are <20 µm (unpublished data). This leads to the conclusion that particles <20 µm constitute a substantial amount of particles in stormwater runoff and are likely to stay in suspension and are therefore likely to be introduced into the aquifer.

A closer look at the size fractionation of Cu and Zn (Figure III-2) at the three sites showed that both metals had significant portions in the dissolved (<0.45 µm) and fine particle fraction (0.45-63 µm). In contrast, other metals like Al, Fe and Pb were usually <5% dissolved (not shown) in accordance with other studies (e.g. Harrison and Wilson, 1985; Herngren et al., 2005; Béchet et al., 2006), emphasising the importance of Zn and Cu for ASR schemes. It could also be seen that the dissolved fraction decreased for both metals from MR > GR > RI. This order reflected an inverse relationship with the important parameters pH and TSS, which increased in the same order MR < GR < RI.

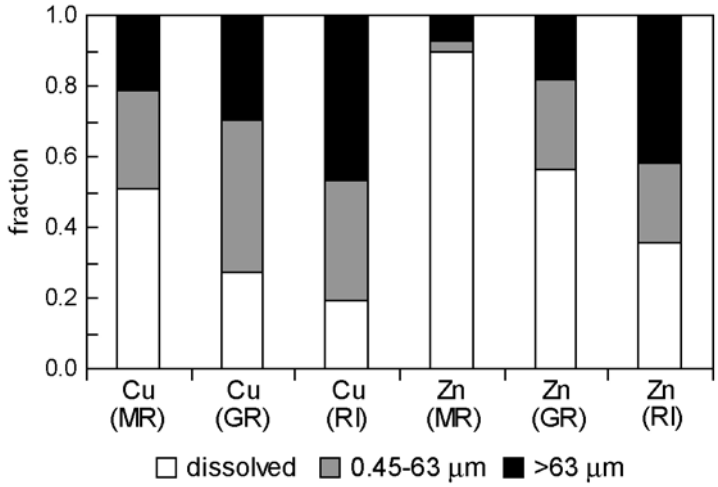

Figure III-2: µEMC fractionation of Cu and Zn in three Melbourne catchments: MR: Monash Roof, GR: Gilby Rd and RI: Richmond.

As seen before (see II.4.5) metal solubility increases significantly over a narrow pH range with the adsorption edge for Zn between pH 5-7 (McBride, 1989; Sparks 2005), which was the range displayed by most samples. Especially samples from MR had pH values favourable for Zn solubility and Zn was found to be on average 90% dissolved (Figure III-2). Similarly low pH and high percentages of dissolved fraction for Zn from roof runoff have been reported in the literature (Duncan, 2006; Göbel et al., 2007). As the Cu adsorption edge lies between pH 4-6, much lower Cu solubility could be observed. Even though linear correlation coefficients are low (Figure III-3d), it could be observed that high dissolved Cu and Zn values correlated with low pH values (Figure III-3a). In correspondence with the difference in adsorption edge, it was observed, that Zn solubility was >75% once pH was <6.2, while Cu solubility dropped below 50% once the pH was >6.5.

Obviously adsorption of metals can only take place when particulate matter with adsorption sites is available. Inverse relationships between the dissolved fraction of Zn and Cu for all sites was visible with TSS <250 mg/L (Figure III-3b) and was highest for RI (Zn: R^2 = 0.58; Cu: R^2 = 0.67). This is in agreement with findings from Herngren et al. (2005) and Hallberg et al. (2007).

The comparatively high solubility of copper is often due to its complexation with dissolved organic matter (see II. 4.2). Surprisingly, the correlation between DOC and Cu was not positive but weakly inverse (Figure III-3c). It could be speculated that the interplay with other parameters like pH, competing cations and the type of DOC were overshadowing a clear correlation.

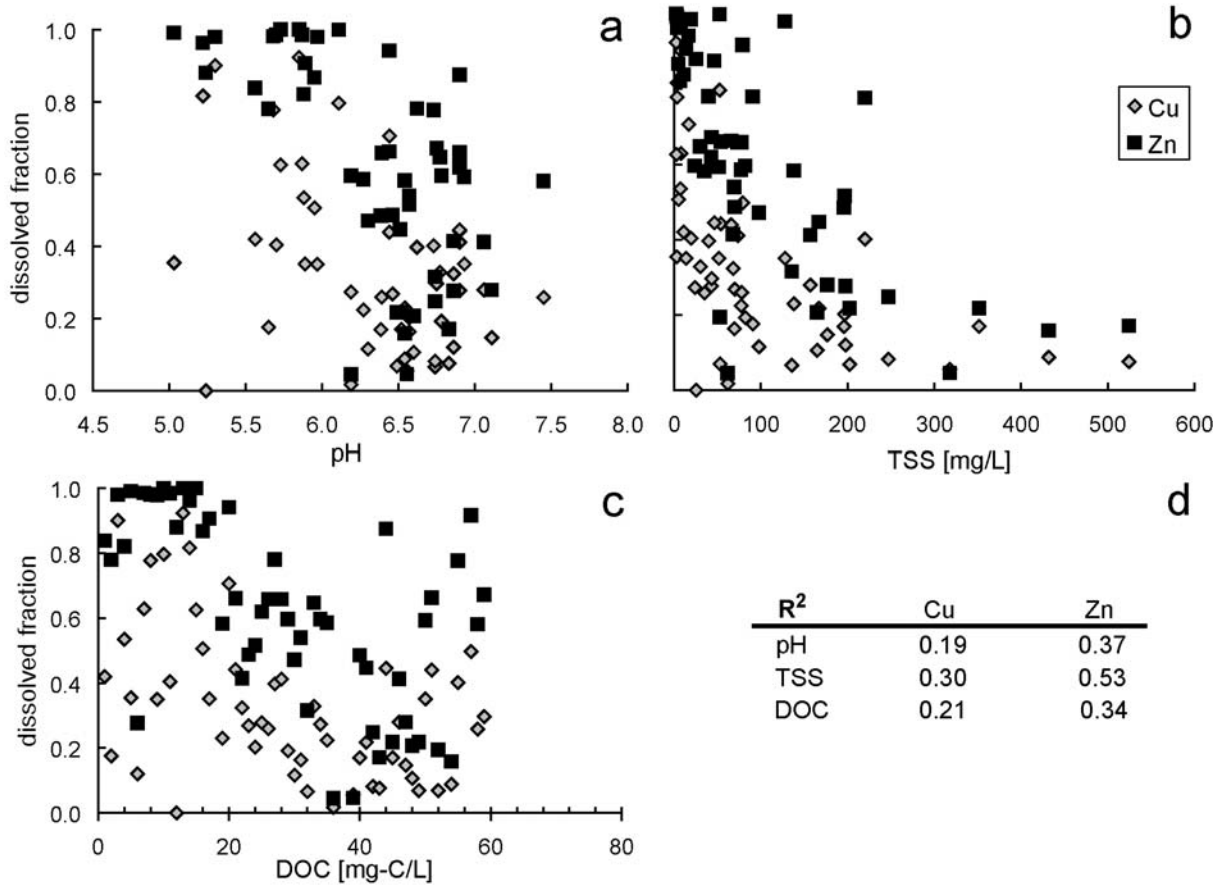

R^2	Cu	Zn
pH	0.19	0.37
TSS	0.30	0.53
DOC	0.21	0.34

Figure III-3: Correlation between (a) pH, (b) total suspended solids (TSS) and (c) dissolved organic carbon (DOC) to dissolved fraction of Cu and Zn for all events (MR, GR, RI) and (d) linear correlation coefficient R^2.

Similarly, the interconnectivity between other storm event parameters like rainfall intensity, peak flow etc and metal concentrations were found to be too complex to yield any strong single correlation. A more vigorous statistical analysis, like multivariate analysis or principal component analysis (e.g. Dechesne et al., 2004; Herngren et al., 2005; Han et al., 2006), might yield more significant results, but was beyond the scope of this study.

Comparison with other studies (Table III-4) showed that MR values for pH, EC and TSS are within the commonly found range for roof runoff, while Zn and Cu are at the lower end of the spectrum, but even these low metal values were above the guidelines for freshwater aquatic ecosystem (ANZECC and ARMCANZ, 2000). For the other catchments EC, TSS and organic matter was at the lower end of the reported values, Cu values were within the reported range, while Zn values are higher than reported mean values from overseas, but similar to

values from Sydney (Hogan et al., 1995) and have stayed in the same range since 1981 (GHD, 1981). This might indicate that Australian buildings and infrastructure use comparatively more Zn galvanised parts. From this assessment it seems reasonable to assume that this study is representative for urban Australian stormwater runoff.

Table III-4: Comparison of main stormwater characteristics of this study with freshwater guidelines, other roof runoff studies, studies from Europe/USA and other Australian literature data (empty fields indicate not reported parameters).

	catchment	sample info	pH	EC [µS/cm]	TSS [mg/L]	TOC [mg-C/L]	DOC [mg-C/L]	Zn tot [µg/L]	Zn diss [µg/L]	Cu tot [µg/L]	Cu diss [µm/L]
Aus. freshwater aquatic system guideline, 95% protection level (ANZECC and ARMCANZ, 2000)			*6.5-9*		*20*	*15*		*8*		*1.4*	
Gromaire-Mertz et al., 1999	France, roof	16 events/ 4 sites			29 (3-304)			3422 (802-38000)		37 (3-247)	
Mason et al., 1999	Swiss roof	one month 3 sites,	7-7.6				6-36		0.4-468		1-56
Davis et al., 2001b	USA, roof	13 events						110-760		7-2100	
Göbel et al., 2007	roof	meta-study	4.7-6.8	25-270	13-120			24-4880		6-3416	
this study	**MR**	**17 events**	**5.7 (5.0-6.9)**	**17 (4-60)**	**34 (2.3-198)**	**3.1 (1-7)**	**2.4 (1-4)**	**116 (40-343)**	**97 (39-267)**	**6.4 (1.5-27)**	**2.6 (0.5-5.7)**
Cole et al., 1984	USA	86 events/ 51 sites						92 (10-2400)	0.4	18 (1-100)	0.4
Horner et al., 1994	USA	meta-study						160 (10-5750)		34 (4-560)	
Gromaire-Mertz et al., 1999	France, street	26 events/ 6 sites			92 (50-500)			550 (246-3840)		61 (27-190)	
Smullen et al., 1999	USA	meta-study			78.4			162		13.50	
Fuchs et al., 2004	Europe, USA	200 sites	7.1 (5.9-8)	390 (74-1810)	281 (2-3093)	24.5 (7.8-58)	22.3 (5-112)	444 (1-3560)		133 (3-1800)	
Duncan, 2006	mainly Europe, USA	30-360 events	6.9 (6.3-7.6)		50-450	25 (12-42)		250 (90-650)		50 (15-150)	
Göbel et al., 2007	roads	meta-study	6.4-7.9	100-2400	66-937			15-2000		21-140	
Han et al., 2006	USA, highway	62 events/ 3 sites			58 (8.8-466)		29 (2.9-850)	268 (83-8880)	178 (42-8150)	56 (16-920)	35 (5.2-735)
GHD, 1981	Melb.	54 events/ 5 sites			162-920	23-61		120-3610		28-353	
Hogan et al., 1995	Sydney	5 events							48-908		9.1-143
Dillon & Pavelic, 1996	mainly Aus.	18 sites	6.7-8.5	197-8740	6 - 476			20-5800		0-480	
Walsh et al., 2004	Melb. urban streams	72 events/ 3 sites						520 (37-14400)		28 (3-127)	
this study	**GR+RI**	**32 events/ 2 sites**	**6.6 (6.2-7.1)**	**76 (30-170)**	**127 (17-525)**	**10 (3-21)**	**6.3 (3-11)**	**1128 (335-3815)**	**432 (84-905)**	**53 (11-273)**	**8.3 (2.9-19.4)**

Melb.: Melbourne, Aus: Australia

III. 2.4 Stormwater for further experiments

Stormwater ASR systems are not using stormwater straight out of the drain, but the stormwater would be harvested and be detained in sedimentation ponds/tanks where stormwater is then sampled from floating devices at the surface to minimise injection of particulate matter (see II.2.1).

Unrelated to the monitoring of stormwater sites reported above, the Facility for Advancing Water Biofiltration at Monash University is investigating the performance of biofilters for treating stormwater runoff. Stormwater runoff from a 100% impervious multi storey carpark (4500 m²) on Monash University campus is collected in two sedimentation tanks. Pipes about 50 cm above the bottom of the tanks allow flow from the first to the second tank and further into a field trial biofilter.

The stormwater used for further batch study was at first collected twice during rain events at GR and filtered with GF-50 before use. As rain events were too unreliable for column experiments, later stormwater samples used for batch and column experiments were collected from the second sedimentation tank (ST) at the biofilter during dry weather. Samples were extracted with a bucket with minimal resuspension of sediment and sieved through 75 µm to retain floating organic matter. Apart from the advantage of having a reliable source of stormwater this would also resemble an ASR injection scheme most closely. The final stormwater sample for column experiment 3 was collected with buckets from a stormwater detention basin (pond) on Monash University Campus, as the sedimentation tank was used for tracer testing the biofilter.

Results of stormwater samples used for batch and column experiments (Table III-5) still showed a high variability in most parameters. As, Cd, Cr, Ni and Pb were close to or below the detection limit, confirming the fact, that these metals are mostly attached to particles and therefore drop to very low values after sedimentation. Similarly TOC, Zn and Cu values were reduced compared to original stormwater values, but still above freshwater ecosystem guidelines (see Table III-4). While Zn and Cu values were similar to inflow values of the biofilter (Table III-5), the latter samples were collected during overflow and contained higher particulate values, which could be seen in higher values for Al and Fe. Values from the Andrews Farm stormwater ASR, Adelaide (Barry, K. et al., 2002, see Table III-5)) reflect the different geology (i.e. limestone) of the catchment with higher pH, EC and major ions values. Due to the higher pH, Zn values are much lower than in Melbourne, emphasising the influence of geology not only on groundwater and aquifer characteristics, but also on stormwater quality.

Table III-5: Selected parameters of samples used for batch and column experiments, inlet biofilter (IBF) mean and standard deviation (14 events) (Hatt et al., in press) and ASR injectant (21 events) at Andrews Farm, Adelaide (Barry, K. et al., 2002) for comparison.

site/date		GR	GR	ST	ST	ST	ST	Pond			IBF 21/01-29/05/07		ASR (1993-96)
	unit	Oct-05	Feb-06	6/03/06	15/06/06	24/07/06	11/01/07	28/02/07	**mean**	std dev [%]	**mean**	std dev [%]	mean (range)
pH		7.2	6.9	6.3	7.0	7.4	6.7	6.9	**6.9**	5.2			7.7-8.2
EC	µS/cm	66	62	102	51	52	145	105	**83**	42			200-400
TOC	mg-C/L			1.4		4.3			**2.9**	72			6.5 (3-9.8)
DOC	mg-C/L	6.0	6.0	1.0	4.2	1.5	6.5		**4.2**	57			5.5 (3-12)
TN	mg-N/L			0.40		0.41			**0.41**	1.7	**1.06**	47	
TSS	mg/L										**39**	159	23-200
Na	mg/L	4.4	4.5	2.9	4.2	3.3	13.3	4.5	**5.3**	68			11-45
K	mg/L	1.0	1.0	0.5	0.7	0.6	1.4	1.4	**0.9**	39			3.1-7.8
Ca	mg/L	5.2	4.5	13.7	4.1	11.6	18.4	1.3	**8.4**	74			20-26
Mg	mg/L	1.1	0.9	0.6	0.9	0.5	1.3	6.3	**1.7**	123			5-12
HCO_3	mg/L	18	13	38		27		32	**26**	39			66-140
Cl	mg/L		3.7	3.9		0.9		8.0	**4.1**	70			12-65
NO_3	mg/L		1.7	0.9		1.1		0.6	**1.1**	43			0.1-0.86
SO_4	mg/L		2.9	2.5		0.2		1.8	**1.8**	64			7-20
Al	µg/L	13	69	31	<10	240	<10	<10	**88**	118	**1426**	151	
Cu	µg/L	14	23	5	10	3	7	16	**11**	63	**16**	13	<5-25
Fe	µg/L	39	47	<20	<20	23	283	47	**88**	125	**1132**	107	625-5430
Mn	µg/L	<10	11	<10	<10	<10	42	13	**22**	79	**27**	66	13-67
Zn	µg/L	693	526	<10	526	15	24	557	**390**	75	**251**	215	<4-40

GR: Gilby Rd; ST: second sedimentation tank; TOC/DOC: total/dissolved organic carbon, TN: total nitrogen, TSS: total suspended solids; empty field: not analysed

III. 3 Hydrogeology

Apart from the availability of possible stormwater harvesting and a local demand, the site selection for an ASR scheme depends largely on hydrogeological characteristics. In this section the hydrogeology of favourable porous aquifers around Melbourne are introduced and the results of a small scale groundwater sampling round will be reported. The results of this groundwater investigation were the basis to choose the groundwater used for laboratory experiments. Characteristics of sediments used in batch and column studies are also presented.

III. 3.1 Introduction to Melbourne's hydrogeology

Information on geology and especially hydrogeology around Melbourne is incomplete and scattered and deep bores are rather limited. The most comprehensive study on the geology and hydrogeology of Port Phillip Region has been compiled by Leonard (1992) and Peck et al. (1992).

The geology is dominated by three main provinces and three main groundwater systems accordingly (see Figure III-4):

- Palaeozoic-Mesozoic basement rocks (mainly fractured): sandstones, mudstones and shales to the northeast and east;

- Cainozoic extrusives (mainly fractured): Older and Newer Volcanics basaltic plains to the north and west ;
- Cainozoic unconsolidated sediments (porous or aquitard): Tertiary to Quaternary sediments along the southeast and in the Yarra and Werribee River deltas

The Cainozoic aquifers, which are of main interest for this study, can be subdivided into four broad age groups (lower (LTA), middle (MTA), upper Tertiary (UTA) and Quaternary). Usually there is only one aquifer present within each age group at any one location (AGT et al., 2002). There is great variability in the properties of the aquifer from location to location but they also fluctuate considerably across one province.

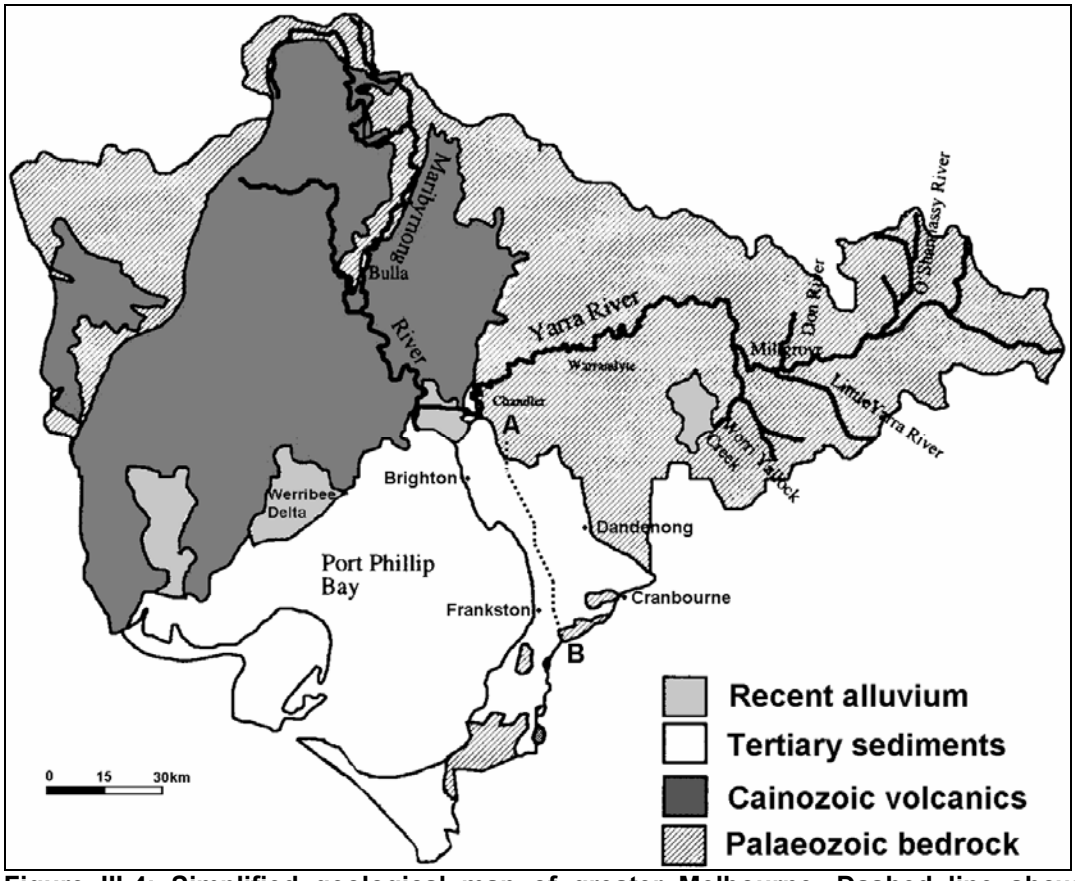

Figure III-4: Simplified geological map of greater Melbourne. Dashed line showing cross-section of Figure III-5 (modified after O'Rourke and Shugg, 1998)

Apart from the Quaternary Werribee Delta, which has great potential for reclaimed water ASR due to the proximity to the Western Treatment Plant, the Tertiary sediments in the SE province have good potential for small scale stormwater ASR and also reclaimed water ASR near the Eastern Treatment Plant (AGT et al., 2002). Sediments from both areas were used in batch and columns experiments (see III.3.5) and will be presented in more detail.

Werribee Formation

The Werribee Formation is a confined Lower Tertiary aquifer, which directly overlies the Silurian bedrock. It forms the largest and deepest formation west of Melbourne, where it is overlain by up to 400 m of Newer Volcanics and the Werribee Delta alluvial, but can also be

found in the SE. In the West it consists predominantly of very dense fine to coarse clean quartz sands and minor gravels, hard silty clays and clayey silts (Hancock, 1992). In the SE triangle (Caulfield (A) -Cranbourne-Frankston in Figure III-4) some ligneous sand and clay are present. There, it is overlain by 40 - 90 m of Older Volcanics, sediments of the Fyansford Formation - Brighton Group and Quaternary deposits (Figure III-5). More details on aquifer and groundwater properties of the SE section are presented in Table III-6.

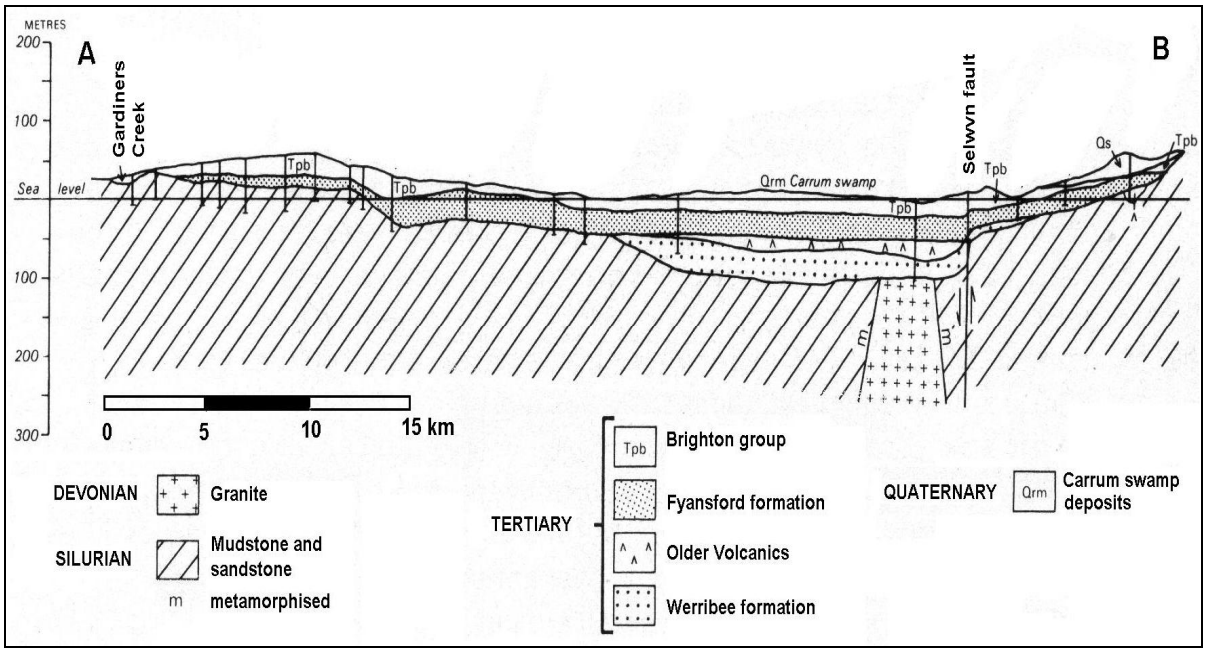

Figure III-5: Geological cross-section of SE Melbourne, from north of Caulfield (A) to east of Frankston about 5-2 km inland from the bay, see A-B in Figure III-4 (after Leonard, 1983).

Table III-6: Principal aquifer properties and groundwater quality average (range) of selected unconsolidated sedimentary aquifers in Melbourne (compiled after Leonard, 1992; AGT et al., 2002).

Aquifer	Werribee Formation (SE)	Fyansford Formation - Brighton Group (SE)	Werribee Delta (W)
Age Group	Lower Tertiary	Middle-Upper Tertiary	Quaternary
Aquifer depth [m]	40-90	0-10	outcropping
Water table [m BGL]	~5-20	~5-20	3-10
Saturated thickness [m]	10-40	50 (15-80)	5-40
Transmissivity [m²/d]	50-200	25 (1-50)	50-500
Effective porosity	0.2 (0.15-0.3)	0.1 (up to 0.3)	0.1 (0.05-0.25)
Hydr. Conductivity [m/d]	5 (0.5-20)	0.4 (0.001-1.7)	5 (1-15)
Bore yields [L/s]	10-20 (up to 50)	2 (up to 18)	5 (up to 15)
Potential aquifer capacity [GL/a]	10-20	1.5-10	2.5-5
pH	7.6 (5.8-8.3)	7.4 (4.4-8.6)	8.3 (7.8-9.5)
TDS [mg/L]	1500 (160-4000)	1570 (100-6800)	3200 (500-6000)
Cl [mg/L]	700 (40-2115)	740 (40-4150)	1400 (360-4470)
SO_4 [mg/L]	45 (3-145)	50 (<0.1-265)	255 (60-745)
HCO_3 [mg/L]	210 (4-510)	185 (<0.1-740)	25 (<0.1-78)
NO_3 [mg/L]	1 (<0.1-10)	18 (<0.1-95)	15 (<0.1-40)
Na [mg/L]	485 (100-1110)	435 (30-1370)	940 (360-2470)
Ca [mg/L]	75 (3-180)	70 (2-360)	45 (7-100)
Mg [mg/L]	40 (1-75)	50 (1-220)	115 (7-400)

BGL: below ground level

Fyansford Formation - Brighton Group aquifer system

The Fyansford Formation-Brighton Group is an unconfined to semi-confined aquifer system that stretches from St. Kilda to the Mornington peninsula and over to the Dandenong-Cranbourne area (Figure III-6). The Fyandford Formation and Brighton Group are regionally hydraulically connected, the boundary ill defined and they have similar properties and are therefore considered to be one aquifer system (see Table III-6). The underlying semi-confined Fyansford Formation is very heterogenous, made up mainly of marine interbedded silty sand and sandy silts with coarse to fine grained sand, gravel and discontinuous sandy limestone bands. The sediments can contain ligneous, carbonaceous and pyritic deposits (Hancock, 1992). Clay minerals are kaolinitic and illitic. The Fyansford Formation is up to 60 m thick with thinning towards the north (Leonard, 1983; Gronvall, 1992), but most of the water bearing strata with transmissivity of 20-30 m²/d are thin (2 - 5 m) and at a depth of 30-50 m (Leonard, 1983; Lane et al., 1992).

The late Tertiary unconsolidated sediments of the Brighton Group are usually fine grained to clayey sands and of low transmissivity (<5 m²/d) but some horizons of higher hydraulic conductivity are present (Hancock, 1992). The marine to fluvio-lacustrine and deltaic sands, silts and silty clays that were deposits during marine regression (Leonard, 1992) overlie unconformably the Fyansford Formation and are in places covered by the Newer Volcanics and the Quaternary Carrum Swamp deposits and have a max thickness of 40 m. Clay minerals are mainly kaolinitic. In areas of shallow water tables a groundwater podsol with organic carbon precipitates and pyritic accumulations has developed (Hancock, 1992). These so called “Black Sands” is one of the sediments used for further batch and column studies (see III.3.5). Downward leakage from the Brighton Group into the Fyansford Formation takes about two months (Leonard, 1983). The recharge areas are found in the Oakleigh - Dingley area to the N and SE of the Carrum Swamp, while discharge occurs in the Carrum Swamp and into Port Phillip Bay. The hydraulic gradient is 0.006 in the northern section and decreases to 0.001 in the central section of the aquifer system. Low hydraulic gradients are favourable for ASR schemes as this increases the recovery efficiency.

Salinity levels vary greatly (~100 -7000 mg/L) for the limited extent of the area (Figure III-6) reflecting the influence of recharge-discharge effects and anthropogenic influences (e.g. waste disposal into sand pits), as there are no evaporates present in the sediments (Leonard, 1983). The groundwater is a hard water of the sodium chloride or calcium chloride type (see Table III-6). The area has historically been used for intensive horticultural use and presently a number of golf courses are operating in the area. The leaching from these diffuse sources to the groundwater is expected to have contributed significant nutrient loads,

especially nitrate (Leonard, 1992). Localised point contamination sources are landfills (Leonard, 1979) and fuel stations. The relatively low velocity of the groundwater within the semi-confined silty clayey sand aquifers provide some time for attenuation processes, so that groundwater is generally not yet degraded beyond ~100 metres from these landfills, but might spread further in the future. The groundwater tends to be weakly acidic (5.5 - 6.2) in the Brighton Group with a low natural sulfate (Hancock, 1992). However, oxidation of sulfidic minerals in the deeper sequences of the Fyansford Formation and the shallower section of the Brighton Group can give rise to acid generation (pH ~4) releasing sulfate, iron (max total iron 175 mg/L), zinc (max 150 µg/L), nickel (e.g. 20 µg/L) and arsenic (max 30 µg/L) (Leonard, 1983; Hancock, 1992).

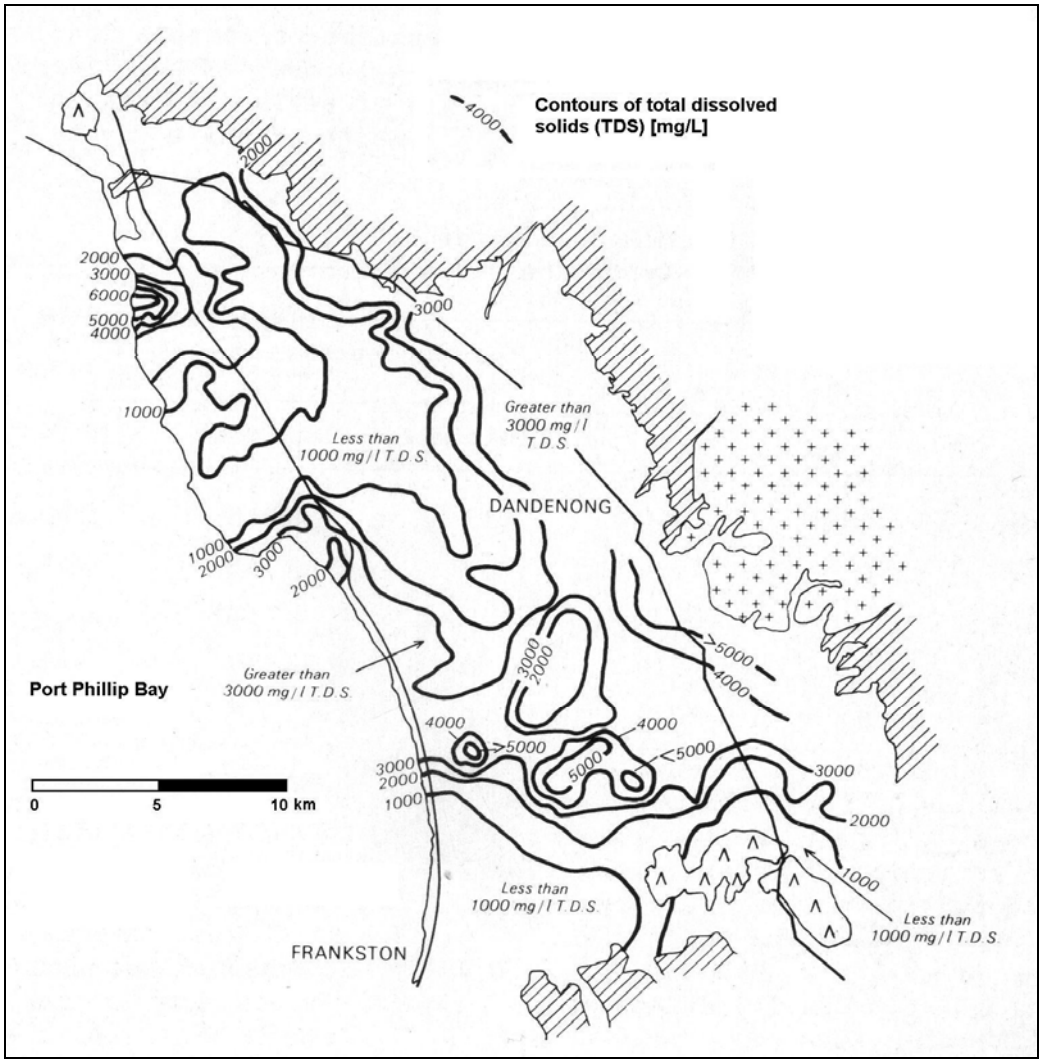

Figure III-6: Isosalines of the Fyansford Formation - Brighton Group aquifer system (Leonard, 1983).

The comparison of available groundwater quality data (DSE, 2008b) revealed the above mentioned great variation even over very short distances underlining the heterogeneity of the aquifer system. Tidal influences were detected in bores close to the bay and would decrease the recovery efficiency significantly and deteriorate the recovered water quality.

Werribee Delta

The Quaternary Werribee Delta is a smaller coastal mainly unconfined aquifer thinning out (maximum 40 m) away from the coast. Due to the alluvial nature the predominantly sand is mixed with gravel, silt and clay deposits (Leonard, 1992). This heterogeneity is reflected in varying groundwater quality and aquifer properties (Table III-6). While large areas of the western section is occupied by the Western Treatment Plant, horticulture is the main use of the area east of the Werribee River, where fresher groundwater occurs naturally in the coarser palaeo-river channel sediments. The intensive irrigation has also freshened up the groundwater closest to the surface and elevated nitrate levels have been found (DSE, 2008b). Overall, published aquifer and groundwater quality data is scarce, even though farmers extensively use groundwater bores to supplement irrigation water, leading to concerns of possible salt water intrusions (AGT et al., 2002; Beddek et al., 2005).

III. 3.2 Bore selection, groundwater sampling and analysis

Initially this study was intended as collaborative research to the implementation of a field trial stormwater ASR in Melbourne undertaken by CSIRO, Adelaide, and SKM, Melbourne, under the Smart Water Fund. The project chose Rossdale Golfcourse, Edithvale, in the SE bay area of Melbourne, targeting the Werribee Formation (SKM and CSIRO, 2005). Due to low yields and high organic matter content in the Werribee Formation the target aquifer was later changed to the dual-porosity mudstone bedrock (Pavelic et al., 2006c), changing it into a non-suitable field site for this study. Further groundwater investigation around the field trial area was hence terminated as well.

A list of bores in a radius of about 10 km to the Rossdale site was compiled from available databases (Borehole Database (DPI, 2008a); Victorian Geoscientific Database (DPI, 2008c); Groundwater Database (DSE, 2008a); Victorian Water Resources Data Warehouse (DSE, 2008b)). This list was then narrowed down mainly by the following criteria:

- still existing (e.g. not refilled, overbuilt or collapsed)
- recorded lithology log (many private bores did not properly record the lithology)
- depth (very shallow bores were excluded)
- access possible (e.g. owners had to be known and permits obtained)
- aquifer characteristic (preferably thicker sandy layers)
- previous analysis of groundwater chemistry (optional)

In total 9 bores could be sampled (23-25.05.2005) from the Fyansford Formation-Brighton Group aquifer, and one from the Werribee Formation later (12.09.2005) at the newly drilled Rossdale Golfcourse (bore BH2). Three of these bores were in use and had pumps with filter

units installed (see + in Table III-7, total values are therefore nearly equivalent to dissolved values), BH2 was sampled 2 h into a pump test with a submersible pump, while the rest of the bores were bailed due to pump failure on the day, which limited purging of the bore. Samples were taken once field parameters had stabilised. In the field measurements of pH, EC, DO and temperature (Horiba Multiprobe), Fe+2 (HACH test kit) and hydrogen sulfide (Microquant Merck test kit) were undertaken. At each bore filtered (0.45 µm) and non-filtered samples in appropriate vials were collected for dissolved and total concentrations and samples for cations/metals were acidified in the field. Analysis for TSS (APHA, 1998), alkalinity (Gran-plot), TOC/DOC (TOC-analyser, Shimadzu), nutrients (FIA), anions (Ion chromatograph, Metrohm), dissolved and total (nitric acid digested) cations and metals (ICP-OES, Varian) was performed after standard methods (APHA, 1998). When particle concentration were high enough, PSD (Malvern Sizer E) were also performed.

III. 3.3 Results and discussion of groundwater investigation

Differences (mostly <10%) in major ion balances suggested that cations were slightly too low. The analysis of the major ions in the Piper diagram classified the groundwaters into three different types (Figure III-7). Three bores in close vicinity to each other were of sodium chloride type (1) with very low pH ~5 and overall higher metal concentrations, while EC encompassed the widest range (640-3520 µS/cm). Most bores, widely spread across the area, fell within a mixed sodium chloride and calcium bicarbonate type (2) with high pH of ~7.3 and also a wide EC range (716-3000 µS/cm). Only one bore within a sandy marl aquifer was of calcium bicarbonate type (3), which unusually low pH for this class of 6.8, high organic carbon concentration and the highest metal concentrations (Table III-7 and Figure III-8).

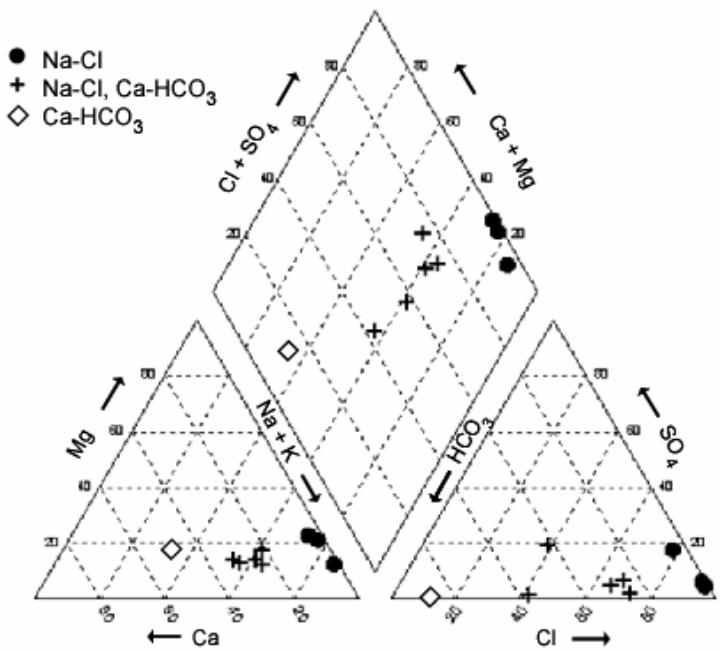

Figure III-7: Piper diagram displaying main ion groundwater chemistry types.

Table III-7: Lithology and main groundwater quality parameters of bores sampled.

Bore ID	detection limit	81756+	125270	125273	76306	81717+	127481	127483	140634+	BH2, Rossdale	127486
Piper type^		1	1	1	2	2	2	2	2	2	3
screen [m BGL]		11-15	16-18	21-23	~6-30	12-16	12-14	12-14	66-69	69-79	27-29
lithology*		sC, S	gS	gS	mS	stG, cS	fS	stC	stS	pS	sM
D_{50} [µm]	1.2	na	108	38	122	na	45	21	na	5.6	105
temperature [C]		17.1	16.8	17	16.3	16.8	17.2	15.8	17.9	17.3	16.6
EC [µS/cm]	1	2520	640	3520	2540	2350	716	2750	850	3000	387
DO [mg/L]	0.1	1	2	3.5	2	2.5	2	0	4	na	3
pH		5.3	4.9	5.0	7.3	7.5	7.1	7.1	7.6	7.5	6.8
TSS [mg/L]	1	<1	37	240	31	2	15	88	<1	246	60
TOC [mg-C/L]	1	13	5	9	6	3	5	7	4	10	25
DOC [mg-C/L]	1	13	3	5	4	3	4	4	3	5	20
Cl [mg/L]	50	634	170	1044	592	592	101	674	137	740	19
HCO_3 [mg/L]	0.5	48	2.4	16	380	290	155	345	260	260	190
SO_4 [mg/L]	1	188	10.3	92	59	21	68	88	6.9	53	0.44
NO_3 [mg/L]	0.01	0.22	1.0	8.3	3.3	0.04	3.0	0.13	0.03	<0.01	1.1
Na [mg/L]	0.1	397	80	510	311	297	91	314	100	356	7.7
K [mg/L]	0.1	1.3	1.4	1.1	8.5	8.1	2.2	5.5	2.9	4.9	36
Ca [mg/L]	0.1	6.6	4.1	12	93	96	32	162	47	94	36
Mg [mg/L]	0.01	30	13	73	47	30	11	43	12	36	8.0
Al (tot) [mg/L]	0.002	0.05	3.6	15	1.8	0.005	1.5	3.6	0.02	2.1	7.5
Fe (tot) [mg/L]	0.001	5.7	23	700	9.5	1.7	5.7	25	0.5	7.8	28
Mn (tot) [µg/L]	0.4	45	283	222	324	102	58	406	18	104	509
Cu (tot) [µg/L]	0.3	70	76	31	32	1	27	21	0	2	73
Zn (tot) [µg/L]	0.5	689	531	178	152	21	110	118	1154	28	7625

+ filter unit on bore; ^ 1: Na-Cl, 2: NaCl-CaHCO3, 3: CaHCO3; *at screen: G: gravel; S: sand, C: clay; M: marl; g: gravely, m: medium, f: fine, st: silty, c: clayey; p: peaty; na: not available, D_{50}: mean particle size

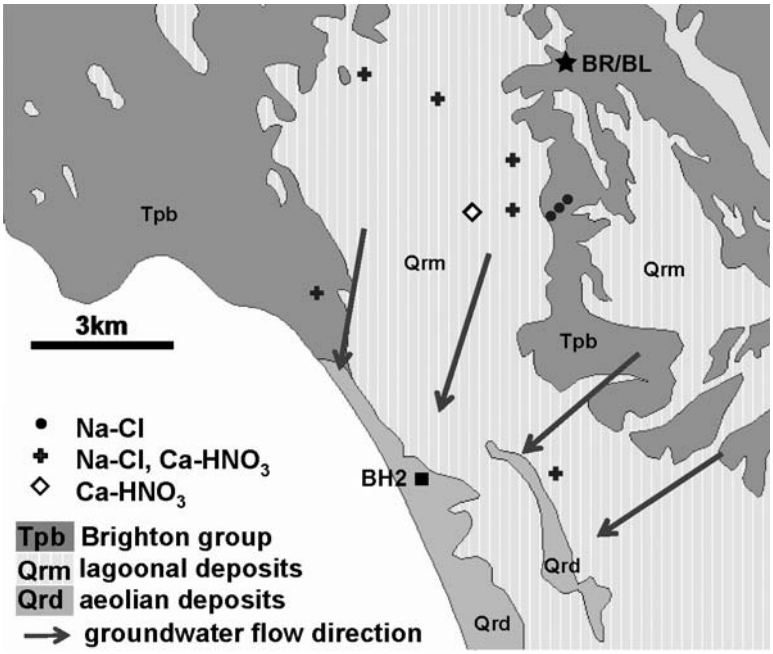

Figure III-8: Surface geology and groundwater types sampled in the SE of Melbourne (modified after DPI, 2008d).

The high TOC and metal concentrations of the type 3 bore (Table III-7) seemed to be due to contamination. A likely explanation for this could be contamination from landfill leachate, as the sampling area has a number of older sand pits that have been reused as landfill sites,

often without proper lining and most state observation bores in the area were drilled for monitoring landfill leachate (A. Shugg, personal communication). Leachate contamination is usually accompanied by high concentration in TOC, alkalinity (from CO_2 gas evolution), salinity and ammonia (Nicholson et al., 1983; Baun and Christensen, 2004). As the bore has rather low levels of salinity and ammonia (1.2 mg-N/L), and high alkalinity can be explained with the carbonates in the aquifer, some other form of anthropogenic contamination is likely to have influenced the values in this bore. It was subsequently excluded from the list of possible groundwater sources.

The results (Table III-7) lay within the indicated range for this region (Table III-6), but showed that heterogeneity is a dominant feature of the aquifers in the region. The EC values vary widely with no apparent correlation to depth of screen, location or lithology. This wide range of parameter values has also been found in previous groundwater samples (Table III-8). This is due to the heterogeneous deposition of the sediments in a coastal region with changing climatic conditions and emphasises the need for site specific measurements. The only bore sampled in this study with previous groundwater quality data (125270) had high variability in data even on two consecutive days (Table III-8), raising questions about the sampling techniques of these samples and on the reliability of other groundwater data. Information on sampling and analysis methods was not available, but bailing is often used (C. Lawrence, personal communication). It could be possible that the bore was not purged enough on the first day and emphasises the need for sampling more reliable groundwater quality data. Sampling a bore once will not necessarily yield representative data. Values for bore 125270 from this study lay mostly between the previous two data sets (Table III-8). Groundwater samples taken from the bedrock mudstone at Rossdale (Table III-8) are comparatively similar to values measured in BH2 above the bedrock (Table III-7).

The results of the particle size analysis (data not shown) showed that the bulk of particles was smaller than 100 µm for most bores. As samples were bailed these particles are not mobilised from increased groundwater velocity as has often been observed when disturbance is induced by pumps (Csuros, 1994). This indicates that colloidal transport might be an important mechanism. Nevertheless these values should be taken with caution, as transport, storage handling and analysis procedures are going to change the particle size distribution (Backhus et al., 1993; Buffle and Leppard 1995b). Precipitation of iron hydroxides would significantly change the particle concentration and size distribution. In addition the Malvern Sizer works on the principle of Fraunhofer diffraction and assumes that particles are spherical, meaning that elongated particles will not be represented correctly. The analysis also introduces shear stress during the mixing which would cause large aggregates to break

apart and small single particles to aggregate due to the increased possibility of collisions (Buffle and Leppard, 1995a). There might be a difference of one magnitude between the median particle size of the primary particle and the effective particle (aggregated particles) size distribution (Walling and Moorehead, 1989).

Table III-8: Selected groundwater quality of the Fyansford Formation-Brighton Group aquifer systems*.

	81421, Clayton South (9.09.1987)	76208, Parish Lyndhurst, (25.11.1991)	57179, Parish Cranbourne, (19.12.1991)	Brighton Group, Mordialloc B 307, (Leonard, 1983)	Fyansford Formation, Mordialloc, B338, (Leonard, 1983)	12570 (22.11.1995)	12570 (23.11.1995)	12570 (this study)	125272 (next to 73), shallower (21.11.1995)	Rossdale (bedrock), (Pavelic et al, 2006c)
EC [µS/cm]	2700	450	1100	1000	230	510	1000	640	1500	2650
TDS [mg/L]	1533	273	495	600	174	235	555	na	732	1560
pH	7.8	6.5	5	6.03	6.7	5.8	5.9	4.85	6	7.4
TOC [mg-C/L]	40	16	180	32	6.7	81	2	5	11	6
Cl [mg/L]	730	81	300	218	47	100	250	170	390	730
HCO_3 [mg/L]	305	111	19.5	100	38	20	75	2.4	22	230
SO_4 [mg/L]	56	3.6	67	30	13.5	15	24	10.3	46	120
NO_x [mg-N/L]	0.15	0.15	0.15	37	1.1	0.02	2.3	1.0	1.5	0.01
Na [mg/L]	380	40	150	129	36	80	150	80	230	555
K [mg/L]	12	3.1	3.4	13	2.6	0.8	1.4	1.4	1.4	6.6
Ca [mg/L]	378	113	67	5.8	4.5	na	na	4.1	na	86
Mg [mg/L]	44	29	18	22	3.4	11	26	13	28	28
Fe (tot) [mg/L]	6.8	24	110	1.6	99	180	2.1	23	21	0.5
Mn (tot) [mg/L]	0.13	0.06	0.13	30	80	1.7	0.12	0.28	0.32	0.07
Cu (tot) [µg/L]	10	30	50	20	10	40	10	76	10	na
Zn (tot) [µg/L]	190	70	140	70	70	950	20	531	160	na

na: not available; *data from Victorian Water Resources Data Warehouse (DSE, 2008b), if not indicated otherwise.

III. 3.4 Groundwater for further experiments

The selection of a bore for further experimental work was mainly based on the following criteria:

- high EC values (ASR should not impair existing groundwater quality)
- not excessively high values of Cu and Zn (not to overshadow the effect of injected metals)
- depth of screen (preferably deep)
- accessibility (preferably state observation bores and no pump filters)

This narrowed the selection down to bore 125273. It was also the preferred choice due to its low pH value that would match the low pH of two of the sediments that were sampled close by (2.5 km north) and used for further study (see III.3.5). Unfortunately the water quality changed significantly when the sampled groundwater was in contact with normal atmosphere

for more than a few hours. An increase in pH to about 7 occurred in conjunction with degassing of CO_2 and precipitation of iron hydroxides.

Further sampling from this bore was undertaken with an electric pump and purging before sampling and continued until EC and pH values were stable. It can be seen that pH, EC and the main ions Na, Mg and Cl are fairly consistent over the 18 months sampling period (Table III-9). The low pH, reasonably high sulfate and metal concentrations are considered to be related to pyrite oxidation. Increases in metal concentrations like As, Zn and Cu were mostly observed during or at the end of summer and might be related to a lower groundwater flow rate during the drier months of the year (Table III-9). TOC, alkalinity and nitrate values also showed variability. This might be related to a commercial waste disposal that is not far away (Note: this bore was drilled for the landfill monitoring, but only water level observations have been undertaken).

Apart from big flocs of iron precipitation, particles were included in further batch experiments, while all particles >20 µm were excluded from the columns test due to a mesh at the inflow (see V.2.2).

Table III-9: Sampling bore 125273 for further use in batch and column experiments.

date	8/12/05	10/02/06	29/03/06	24/07/06	07/09/06	11/01/07	11/04/07	**mean**	std dev [%]
EC [µS/cm]	3300	3300	2940	3130	2830	2550	2990	**3006**	8.9
pH	4.7	4.9	4.7	4.8	4.8	4.7	4.8	**5**	1.6
TOC [mg-C/L]	7	7	7	27	25	10	14	**14**	63.5
Cl [mg/L]	795	724	767	1078	749	na	na	**823**	17.6
HCO_3 [mg/L]	21	21	1.4	7.2	11	na	1.4	**10**	85.5
SO_4 [mg/L]	60	52	54	21	83	na	na	**54**	41.1
NO_3 [mg/L]	12	1.9	3.7	3.2	8.9	na	na	**5.9**	72.6
Na [mg/L]	445	485	486	431	422	514	531	**473**	8.8
K [mg/L]	1.2	3.1	1.0	1.0	1.0	1.0	1.6	**1.4**	55.4
Ca [mg/L]	10	14	10	13	13	10	12	**12**	16.1
Mg [mg/L]	68	55	59	69	68	62	69	**64**	8.7
Fe (tot) [mg/L]	1.2	0.4	1.7	0.9	0.4	0.17	2.2	**1.0**	75.5
Mn (tot) [mg/L]	0.10	0.08	0.08	0.10	0.09	0.09	0.10	**0.1**	9.8
As (tot) [µg/L]	<4	<4	21	<4	<4	13	18	**9**	99.4
Cu (tot) [µg/L]	<1	14	7	<1	<1	11	3	**5**	98.5
Zn (tot) [µg/L]	1.5	110	45	55	54	34	135	**62**	73.5

na: not available

III. 3.5 Sediments for further experiments

Acquisition of deep aquifer sediments was not possible as no drilling in the Fyansford Formation was undertaken at the time. Therefore two samples were excavated in Clayton South (South-East Melbourne), where the Tertiary Brighton Group outcrops (see Figure III-8). The first sediment was found in 3-4 m depth and was of light brown colour ('BR'). The underlying sediment (5-6 m depth) was coloured black ('BL') due to increased organic and pyritic content. The third sediment ('WS') came from the alluvial Quaternary Werribee Delta

(Werribee South, West Melbourne) and was sampled during hollow auger drilling from 14-15 m depth.

All sediments were homogenised, air-dried and sieved (2 mm) (OECD/OCDE, 2000).The following characterisations (Table III-10) of the sediments were performed: Grain size distribution was done via dry sieving and the finer fraction (<75 µm) was mixed with deionised water and analysed with a Malvern Mastersizer E. Sediment-pH and electrical conductivity (EC) were measured on 20 g of sediment mixed (1h) with 100 mL of double deionised water. For acidic sediments pH was also measured in 0.01M $CaCl_2$ and 1M KCl solution. Cation exchange capacity (CEC) and base saturation were analysed at pH 7 with a two step compulsive exchange with $BaCl_2$-triethanolamine and $MgCl_2$ solution (Mehlich, 1948; Krause et al., 1993; DIN ISO 13536, 1997). Major elements and loss of ignition (lithium borate fusion tablet on Philips PW1480) and trace elements (pressed powder tablet on Spectro X-Lab 2000) were obtained from finely grinded sediment (tungsten carbide mill) by X-ray fluorescence at CSIRO, Urrbrae, South Australia. Other major elements not listed in Table III-10 were below 0.3 %wt and other trace metals like Cd, Cr, Ni, Mn, Pb were close to or below the detection limit of 0.3-1.5 ppm. Semi-quantitative analysis for minerals was performed by X-ray diffraction (Philips PW1710) at CSIRO, Urrbrae, South Australia. No sub-dominant (20-60%) or minor (5-20%) minerals were found.

Table III-10: Characterisation of used aquifer materials (air-dried, <2 mm).

	BR	BL	WS
sand (0.05-2 mm) [%wt]	99.1	98.5	98.7
silt (2-50 µm) [%wt]	0.8	1.3	1.2
clay (<2 µm) [%wt]	0.1	0.2	0.1
EC [uS/cm]	330	120	60
pH H_2O	4.5	2.9	8.5
pH $CaCl_2$	4.3	2.8	7.4
pH KCl	4.1	3.3	
Base saturation [%]	83	15	100
mean CEC [cmol/kg]	0.9	8.5	1.3
SiO_2 [%wt]	97.5	94.4	92.2
Al_2O_3 [%wt]	0.7	0.8	3.2
Fe_2O_3 [%wt]	0.3	0.3	1.6
K_2O [%wt]	<0.05	<0.05	0.7
Loss of ignition [%wt]	1.0	4.1	1.4
Chemical index of alteration [%]	100	100	72
As [mg/kg]	9	15	4
Cu [mg/kg]	3	8	5
Zn [mg/kg]	38	76	61
dominant minerals (>60%)	quartz	quartz	quartz
trace minerals (<5%)		pyrite	orthoclase, albite, mica (muscovite)
possible minerals	amorphous Al- and Fe-hydroxides		smectite (montmorillonite)

The two Clayton sediments showed similar characteristics of strongly weathered acidic quartz sands, with a chemical index of alteration (CIA, Nesbitt and Young, 1982) of 100%, while the Werribee sample was slightly less mature and of neutral pH.

During pH adjusted batch series (see V.2.4) it was found that the sediments showed an increased turbidity due to dispersed particles <0.45 µm. These particles were also found to leach out of the columns at the start of stormwater injection (see VI.3.2.3). To investigate the character of these colloids, fresh soil samples were dispersed in sodium hexaphosphate and sodium carbonate solution. The filtered solutions were analysed with ICP-OES (Varian) and TOC (Shimadzu) (Table III-11). It revealed high concentration of Al, Fe and K especially for BL, indicative for inorganic clay particles. BL and to a smaller extent BR and WS also showed increased concentration of organic carbon. Dissolution of organic carbon has been found to be enhanced with high pH (Brigante et al., 2008). It could be seen that about 30-65% of total Zn was found in the small fraction, while only a small fractions of Cu was present. Size analysis (HPPS 5001 Malvern Nanosizer at Melbourne University) showed a mean particle size of about 200 nm for all dispersed sediments.

Table III-11: Analysis of sediment particles <0.45 µm.

mg/kg	K	Ca	Mg	Al	Cu	Fe	Mn	Zn	TOC
BR	210	214	42	663	1.4	331	0.7	25	1076
BL	221	90	104	1182	0.4	718	0.9	24	8537
WS	184	75	97	84	0.3	143	1.5	25	921

III. 4. Summary and conclusions

The presented stormwater data set showed that stormwater quality is highly variable from event to event, which poses a challenge for generalisation about stormwater quality that could be expected at other sites. Nevertheless, it was shown that Zn is rather abundant (~1.1 mg/L) in Melbourne's urban stormwater and compared to other metals are found often in dissolved and the fine particulate form. Cu concentrations were comparable to previously reported values in the literature (~50 µg/L). Both metals were found to be significantly reduced in concentration after sedimentation (by 40-99% for Zn and 65-95% for Cu), but still greatly exceeded the recommended freshwater ecosystem trigger values. It is believed that stormwater samples used for further experiments were representative in their main characteristics and preferred over artificially mixed water as the stormwater samples would contain all ions, molecules and colloids that could interact with metals.

A small scale groundwater sampling round in the Tertiary Fyansford Formation-Brighton Group aquifer showed highly variable groundwater quality within a small area. Groundwater for further experiments was withdrawn from a bore with salinity levels above the beneficial

use for irrigation, which would be a criterion for potential ASR sites. Its low pH stands in contrast to existing ASR schemes in limestone that exhibit alkaline pH and will therefore add a significantly different parameter to this study. The problem of injected metals have largely not been investigated due to low metal concentrations found in limestone areas, but it can be speculated that the low pH of some sandy aquifers will increase metal solubility.

Three sandy aquifer materials from areas with potential for small scale ASR in Melbourne were obtained from the Tertiary Brighton Group aquifer and the Werribee Delta, representing a highly weathered sand with only very minor other components, the same weathered sand with small amounts of organic matter and pyrite and a less weathered sand with higher amount of Al- and Fe oxides. These three different sediments will allow the investigation of the influence of minor components on Zn and Cu behaviour.

In conclusion, heterogeneity and variability is not only a feature of stormwater quality but also of groundwater and aquifer quality. Site specific sampling and monitoring are therefore paramount for every future ASR site. Nevertheless, the solutions and sediments used within this study are representative for Melbourne and conclusions found for these materials will be applicable to similar sediments in other areas.

Chapter IV: Batch experiments

"To understand water is to understand the cosmos, the marvels of nature, and life itself."
Masaru Emoto, The Hidden Messages in Water, 2001

IV.1 Introduction

Batch tests are an established empirical technique to investigate sorption behaviour of various adsorptives (e.g. metals, trace organics, nutrients) onto various adsorbents (soil, clay minerals, oxides, organic matter, filter media). The rate of sorption and the amount sorbed depends mostly on pH, loading of adsorptive, solid-solution ratio, presence of competing or complexing agents, reaction time allowed, temperature, redox potential, and of course surface properties of the adsorbent (e.g. surface area, particle size, surface charge) (OECD/OCDE, 2000; ASTM, 2001; Harter and Naidu, 2001). Due to the complexity of these parameters and their interrelated effects, a generally applicable sorption isotherm or distribution coefficient does not exist, especially not for natural sediments that are a heterogeneous mix of many different adsorbents (sand, clay minerals, oxides, organic matter) (Limousin et al., 2007). Reported values in the literature are often hard to compare as different experimental conditions have been used and not all variables are always reported. Therefore site-specific sorption tests have to be undertaken to obtain realistic values if further transport modelling or field predictions are to be made (Zheng and Bennett, 1995; Elzinga 1999). Desorption data are even rarer to find but clearly vital to model the potential reversibility of contaminant-transport, especially during repeated ASR injection and extraction cycles.

Therefore as a first approach adsorption and desorption batch tests were undertaken to investigate the influence of various parameter on Zn and Cu sorption behaviour onto the three different aquifer materials. Firstly, distribution coefficients (K_d) under natural conditions are presented. The influence of change in pH, salinity, addition of organic acids and solid-solution ratio for adsorption and desorption are shown as well as pre-equilibration for adsorption and reduced oxygen concentrations for desorption.

IV.2 Material and methods

In this study, three urban aquifer sediments with a range of different sediment characteristics (see III.3.5) have been mixed with solutions of urban stormwater (see III.2.4) and groundwater (see III.3.4), and the metal behaviour was observed in a series of controlled batch tests, as explained below.

IV.2.1 Materials

To investigate the sorption isotherm of Zn and Cu on the sediments, initial metal concentrations had to be increased by metal spiking. Analytical grade solid $ZnCl_2$ and $CuSO_4$ were diluted with double deionised water (Milli-Q) and added to the stormwater solution to receive desired metal concentrations. Stormwater was diluted with double deionised water to achieve metal concentrations less than original values in batch tests. The used metal concentrations ranged from the detected lower stormwater concentrations to a worst case scenario of accumulated metals over years of ASR operation. Preliminary studies showed only minimal competitive effects between Zn and Cu at these concentrations.

As organic matter greatly influences metal behaviour, additional DOC was added to simulate a worst case scenario. Commercial liquid fulvic acid (Fulife, Nutrified ©) originating from plant material was used for addition of DOC. It was diluted 1:10 with double deionised water before adding 0.78 mL to 50 mL of stormwater solution resulting in about 30 mg-C/L. No purification was undertaken to simulate natural composition as close as possible, as strongly manipulated DOC might not represent natural complexing capacities (Christensen et al., 1996). Characterisation of the undiluted solution was done for total organic carbon (Shimadzu TOC-5000 Total Carbon Analyser), total nitrogen (TN, Lachat - QuikChem 8000 Flow Injection Analyser), filtered reactive phosphorus (FRP, Lachat - QuikChem 8000 Flow Injection Analyser) and cations (ICP-OES, Varian) and showed H_2O 94wt%, TOC 19 g-C/L, TN 45 mg-N/L, FRP 55 mg-P/L, pH 5, EC 19.5 mS/cm, Na 565 mg/L, Ca 1590 mg/L, Cu <2 µg/L and Zn <5ug/L. On average, fulvic acids are characterised by a high total acidity deriving from high amounts of carboxyl, carbonyl and phenolic hydroxyl groups and contain a higher oxygen to carbon ratio than humic acids (see II.2.3.4; Sparks, 2003). Even though they are soluble over the whole pH range, they are more aggregated at lower pH and at higher ionic strengths (Ghosh and Schnitzer, 1980). As TOC values are not directly related to the amount of active functional groups (Harter, 1983; Thiele and Leinweber, 2001), they do not sufficiently describe the complexity of natural organic matter. Further analysis with NMR (neutron magnetic resonance spectroscopy) and IR (infrared spectroscopy) could complement a detailed description (Deshmukh et al., 2007; Hay and Myneni, 2007), but is beyond the scope of this work.

IV.2.2 Batch experiments and analysis

The experiments were conducted at room temperature under aerobic conditions if not stated otherwise. For the general adsorption experiment, 10 g of sediment and 45 mL of stormwater as well as Zn, Cu and/or fulvic acid solutions were placed into a 50 mL plastic centrifuge vial (Falcon). The recommended solid solution ratio is 1:4 (ASTM, 2001) but a lot of studies use

1:10 or even 1:50 (e.g. Tiller et al., 1984a; Thiele and Leinweber, 2001). We preferred a high solid concentration close to the actual soil-solution ratio of the investigated system. The amount 10 g of sediment was chosen (modified after Oliver et al., 1996), to compensate for the low clay content of the sediment and to guarantee that final concentrations as well as the differences between initial and final concentrations are well above the detection limit to minimise error propagation. Adsorption and desorption samples were shaken for at least 24 h on an overhead shaker (30 rpm) or a platform shaker (130 rpm), then centrifuged (3500-4750 rpm) and the supernatant decanted. In some samples adjusted to high pH settling of particles could not be achieved with centrifugation and these were filtered (<0.45 µm). After measurement of pH and EC (TPS benchtop meters), samples were acidified with 2% concentrated HNO_3 and stored at 4 °C before analysis for metals with ICP-OES (Varian) and in some cases for TOC (Shimadzu). Although various species occur in solution, only total dissolved concentrations were considered in this study, as PHREEQC (Parkhurst and Appelo, 1999) speciation simulations showed that free metal ions and metal-fulvate complexes are likely to comprise >90% of dissolved metals. Adsorbed Cu or Zn concentrations (C_{ads} [mg/kg]) were calculated as the difference between the amount initially present in solution (C_{ini} [mg/L]) and the amount remaining in solution after equilibration (C_{diss} [mg/L]) in relation to solution volume (V [L]) and sediment mass (M [kg]). The linear partition coefficient K_d [L/kg]:

$$K_d = \frac{(C_{ini} - C_{diss})\frac{V}{M}}{C_{diss}} = \frac{C_{ads}}{C_{diss}} \qquad \text{(IV-1)}$$

can therefore be derived by linear regression from the slope of a graph of dissolved versus adsorbed concentration. The linear isotherm is a special case of the Freundlich isotherm (n = 1) and represents the initial part of the Langmuir isotherm, when the effect of site saturation is minimal. At low concentration, the linear isotherm is commonly found to fit adsorption data of heavy metals onto heterogenous surfaces like soils (Limousin et al., 2007). A large K_d value represents a high affinity of the metal to the soil and low mobility. The amount sorbed [%] was calculated from the difference of initial to final dissolved concentration in relation to the initial concentration.

Controls without sediment showed minimal change in Zn and Cu concentrations, possibly due to an influence of the vial or an analytical error. Controls with DI water instead of stormwater resulted in low level desorption of metals from the sediment.

Five series of adsorption experiments (Series A) for each metal and sediment were undertaken to investigate the influence of parameters that are important for metal sorption behaviour and are likely to vary during ASR, e.g. dissolved organic carbon concentration, pH,

solid-solution ratio and salinity (Harter and Naidu, 2001). Apart from Series A3 (see below), all tests were done without addition of any buffer at the natural occurring pH, i.e. around pH 3.5, 5.0, and 7.5 for BL, BR and WS respectively, as would be the case in ASR systems.

- Series A1 - looked at general adsorption isotherms in 8 steps. Initial Zn and Cu concentrations ranged from 50% of original stormwater concentration to a maximum of about 6.5 mg/L Zn and 1.8 mg/L Cu. Cu concentrations were kept lower due to lower concentrations in stormwater. Either no or 30 mg-C/L of fulvic acid (e.g. '0BR' or '30BR') was added to compare the influence of increased organic matter on the adsorption. As the original stormwater already contained organic matter (see Table III-5), no experiments were free of organic matter though.
- Series A2 - As solid-solution ratio could vary greatly in an ASR setting, Series A2 was undertaken with sediment amounts of 0.5, 1, 2, 5 g to evaluate the influence of the solid-solution ratio. No or 30 mg-C/L OC was added.
- Series A3 - Changes in pH are the main driving factor for metal sorption behaviour. In this series, samples were equilibrated over several days with 0.1M HCl or NaOH to four values between pH 3 and 7.5 covering worst case pH values. Then Zn and Cu were added in 6 steps with initial concentrations ranging from 1.1 - 9 mg/L Zn and 0.3 - 2.5 mg/L Cu. No OC was added.
- Series A4 used groundwater diluted with DI water (20, 50, 80% mixtures) to evaluate the influence of salinity on the adsorption process, as stormwater would be injected into saline aquifers. Initial concentrations were 6.5 mg/L Zn or 1.8 mg/L Cu with no or 30 mg-C/L OC addition.
- Series A5 investigates the influence of pre-equilibration with groundwater solution, both under aerobic and oxygen-depleted conditions as it could occur in ASR. The groundwater was either purged with nitrogen gas (leading to an oxygen concentration of 0-0.5 mg/L and a decrease in alkalinity to nearly zero) or exposed to the normal atmosphere (oxygen concentration 7-8 mg/L). In the following description of batch experiments and also for nitrogen-purged solutions in the column experiments the term anaerobic will be used for oxygen-depleted solution, even though they might contain small amounts of oxygen. Both groundwater solutions were adjusted to its natural pH 5 with diluted HCl. Afterwards adsorption with oxic stormwater was carried out as usual. Initial concentrations were 6.5 mg/L Zn or 1.8 mg/L Cu with no or 30 mg-C/L OC added.

Five desorption series (Series D) were undertaken to investigate the potential of metal desorption during the ASR recovery cycle. Immediately after the adsorption test, solution

(usually groundwater) without extra metals was added to the residue of the adsorption tests with the maximum initial metal concentration.

- Series D1 encompassed three desorption steps with 50 mL groundwater each, so kinetic behaviour could be evaluated. Residual concentrations of the entrained solution were incorporated in the initial concentration for the next step.
- Series D2 used 10, 20, 30, 40 mL of groundwater to investigate the influence of the solid-solution ratio on desorption. Residues came from adsorption replicates with similar adsorbed metal concentrations for each sediment.
- Series D3 used 50 mL of solutions of different salinity (20, 50, 80% dilution of groundwater with DI water) to estimate the influence of ionic strength on desorption behaviour.
- Series D4 used residues from Series A5 for three desorption steps with 50 mL of either nitrogen purged or oxic groundwater adjusted to pH 5 with diluted HCl. Low oxygen samples were shaken and handled under nitrogen atmosphere to decrease contamination with oxygen.
- Series D5 used the residues from Series A3 with initial 6 and 9 mg/L Zn and 1.5 and 2.5 mg/L Cu for three desorption steps with 50 mL of groundwater adjusted to pH 5 to evaluate the influence of adsorption pH on desorption.

IV.3 Results and discussion

IV.3.1 Adsorption series

IV.3.1.1 Adsorption isotherms at natural pH

The results for adsorption isotherms for Zn and Cu from series A1 are shown in Table IV-1. In the used metal concentration range, adsorption isotherms of all sediments were mainly linear and saturation limits were not reached (see also Figure VI-3, series BR-pH5, BL-pH4 and WS-pH7.8). This behaviour has been widely observed for low metal concentrations when adsorption sites are in excess (Benjamin and Leckie, 1981a). Application of the Langmuir and Freundlich isotherm yielded poorer fits with higher least square errors than the linear isotherm. Langmuir graphs were curved which could show either competition between species or the existence of more than one type of adsorption site (Limousin et al., 2007). The latter assumption is highly likely as other metal concentrations were too low to cause significant competition effects.

For Zn, adsorption isotherms of the more weathered Tertiary sediments BR and BL were similar with a mean K_d of 2.6 L/kg, while the Quaternary sediment WS showed K_d values approximately two magnitudes higher (Table IV-1). Desorption of Zn occurred in sediments

BR and BL below a maximum initial concentration of about 0.8-1 mg/L. An average of 1.3 mg/kg of Zn was desorbed from these sediments representing 2-3% of the original sediment metal content. Desorption at low initial concentration has been observed by other authors (Schulte and Beese, 1994) and reflected the metal level of the native groundwater. Sorbed Zn [%] reached an equilibrium concentration of about 30% for BR and BL. In contrast, WS showed an adsorption rate for Zn of above 95%, which can be attributed to the much higher pH (see section 3.1.4). The resulting isotherms were so steep that their slopes could only be estimated.

With the exception of 30WS the linear adsorption of Cu was stronger than for Zn and more consistent for all sediments with a percental sorption of around 90% (Table IV-1). At initial Cu concentrations <10 µg/L an average of 0.05 mg/kg Cu were desorbed from BR and WS constituting 1-2 % of their geogenic content.

Table IV-1: "K_d values for linear adsorption isotherms at natural pH (series A1), corresponding linear coefficient of determination (R^2), % sorbed of initial metal concentration for highest initial concentration and % sorption of added OC (BR- brown Tertiary Brighton Group sediment, BL – black Tertiary Brighton Group sediment, WS – Quaternary Werribee Delta sediment with no and 30 mg-C/L addition of fulvic acid.

		Zn				Cu			
	pH	K_d	R^2	Zn sorbed [%]	OC adsorbed [%]	K_d	R^2	Cu sorbed [%]	OC adsorbed [%]
0BR	4.9	2.6	0.920	32		59	0.996	91	
30BR	5.0	2.6	0.953	33	54	41	0.999	88	47
0BL	3.6	2.5	0.997	31		79	0.992	93	
30BL	3.6	2.7	0.979	31	15	75	0.999	93	21
0WS	7.5	~440	0.906	98		~800	0.840	98	
30WS	7.3	~200	0.952	95	43	63	0.868	90	48

Comment: the very high K_d values are only approximates with high standard deviation, as the final concentration values were close to the detection limit.

As mentioned earlier comparison with other batch studies is not without difficulties, as different experimental designs are tailored to each specific problem and experimental conditions may vary greatly. Nevertheless generally higher affinity of soils for Cu than for Zn has been established in the literature (e.g. Sposito, 1984; Mesquita and Vieira e Silva, 1996; Arias et al., 2005) and measured K_d values seem to be within the range found in others studies with similar sediments (Table IV-2). Linear relationships are often found for low metal concentration (e.g McLaren et al., 1983; Thiele and Leinweber, 2001; Covelo et al., 2007), when sorption sites are still in excess, while Freundlich and Langmuir isotherm describe the behaviour at higher metal concentrations, when sorption sites become a limiting factor (see II.4.1.1).

Heavy metals can be retained by two sorption mechanisms (see II.4.1.1). Firstly, specific adsorption is a highly selective chemical sorption requiring high energy. It can take years and

is often considered irreversible (McBride, 1989). Secondly, non-specific adsorption is a low energy physical sorption that occurs fast and is mostly reversible. In general, sediments commonly contain a smaller number of specific than non-specific sorption sites. This means that with increasing loading metal ions are forced to adsorb onto low-energy sites (Benjamin and Leckie, 1981b; Arias et al., 2005; Singh et al., 2006). This shift in sorption behaviour has been observed as a lowering of distribution coefficients with increasing metal loading (Lehmann and Harter, 1984; Arias et al., 2005). K_d values derived from high surface loading experiments are therefore underestimating the specific adsorption behaviour at low metal loadings (Lehmann and Harter, 1984; Mesquita and Vieira e Silva, 1996; Sastre et al., 2007). The generally lower retention of Zn compared to Cu can be explained with the higher specific sorption of Cu.

Table IV-2: Experimental conditions and distribution coefficients of selected similar studies.

K_d Zn [L/kg]	K_d Cu [L/kg]	sediment	solution pH	background electrolytes	soil [g]/ solution [mL]	Zn range [mg/L]	Cu range [mg/L]	reference
0	50	sand	6.5	0.01M NaCl	1 / 50	0.0225-52.3	0.0026-1.82	Genç-Fuhrmann et al. (2007)
0.33	1.75	Spodosol	4.3	0.005M $Ca(NO_3)_2$	1 / 10	0.01-100	0.01-100	Buchter et al. (1989)
2-200	80-500	Oxisol, Podsol, silty soil	4.5-5.5	0.011mol/L $CaNO_3$	1 / 10	6.5-49	6.5-49	Msaky and Calvet (1990)
1.2-22	0.9-330	sandy Fluvisol + Podsol	5.5	$CaCl_2$, $MgNO_3$, NaCl, KCl	1.5 / 30	6.35-635	6.35-635	Sastre et al. (2007)
0.07-83		<2um Palexeralf + Haplohumox	5-7	0.01M $Ca(NO_3)_2$	0.02 / 10	0.064-6.4		Tiller et al. (1984a)
~33	~66	subsoil of Podsol region	4.6	0.005M $CaCl_2$	0.5 / 25	0-17	0-34	Thiele and Leinweber (2001)

Macroscopically, sediments are a complex mix of clays, oxides and organic matter with varying morphology, grain sizes and surface coatings (see II.4.1.2 and II.4.1.3). These aspects as well as parameters like pH and Eh can have direct and indirect effects on sorption processes and must be considered in any investigation (McBride, 1989; Sparks, 2003). As virtually no Mn was detected in any of the used sediments, sorption would mainly be controlled by Al- and Fe-oxides and organic matter. The high pH of WS would have increased the amount of hydrolysed surface metal ions and hence increase adsorption. Clays also offer a variety of different permanent and variable charge surface sites for high to low energy sorption of metal ions and retention is strongly dependent on the type of clay and the level of loading rather than the amount of clay present (Sparks, 2003). However, we consider the influence of clay on the sorption behaviour of all sediments in this study to be

minor due to the weathered state of the sediments and the very low clay contents (0.1-0.2%, Table III-10).

As the low K_d values show, the sorptive capacity for the highly weathered sediments BR and BL is rather limited due to their acidic nature. Adsorption would be mostly onto coatings of oxide and organic matter around the sand grains. The higher sorptive capacity of WS would be mainly due to the higher pH and partially due to higher amounts of oxides and to the potential presence of small amounts of three layer clay minerals like smectites. Near complete adsorption of Cu onto BL at low loading was observed and could stem from the higher organic matter content of BL (see IV.3.1.2).
Some studies have correlated the influence of different soil parameters and metal loading with metal sorption behaviour (e.g. Kinniburgh, 1986; Elzinga et al., 1999; Sauvé et al., 2000). Applying the equations found by Elzinga et al. (1999) or by Sauvé et al. (2000) to the data from series A1, A2 and A3 did not result in any significant relationships for either Cu or Zn sorption. No direct correlation of K_d values to either CEC, pH, organic matter or oxide content could be established between the three sediments.

IV.3.1.2 Organic matter influence

The addition of fulvic acid had variable effects on non-pH adjusted experiments. While Zn adsorption onto BR and BL showed no change, it was significantly reduced in WS. Cu adsorption was also significantly decreased for WS, only slightly for BR and did not significantly change for BL (Table IV-1). In pH-adjusted experiments (Figure IV-1), addition of fulvic acid had no influence on the pH_{50} value of Zn adsorption onto BR, but let to a much gentler adsorption edge. The curve of Cu adsorption on BR and WS had the same shape but was slightly decreased, while for BL it increased at higher pH (Figure IV-1).
The organic matter itself adsorbed to the sediments to different degrees (Table IV-1). While it strongly adsorbed to BR and WS, it only weakly adsorbed to BL, which was initially richer in organic matter. Series without OC addition even showed desorption of organic matter at higher pH especially for BL.

Fulvic acids are the major colloidal and dissolved constituent in stormwater (see II.3.3); Sekaly et al., 1999; Li and Dai, 2006) and interactions between fulvic acids with other dissolved and solid constituents are numerous (see II.2.3.4 and II.4.2). Processes that directly influence metal sorption behaviour are complexation of metals with dissolved organic matter, surface complexation of metals with immobile organic matter and formation of ternary complexes (see II.4.2). Furthermore, both organic complexation and adsorption are strongly pH dependent due to deprotonation of functional groups (McBride, 1989) and it is often difficult to decouple the combined effects (see II.4.5). Depending on the organic matter of

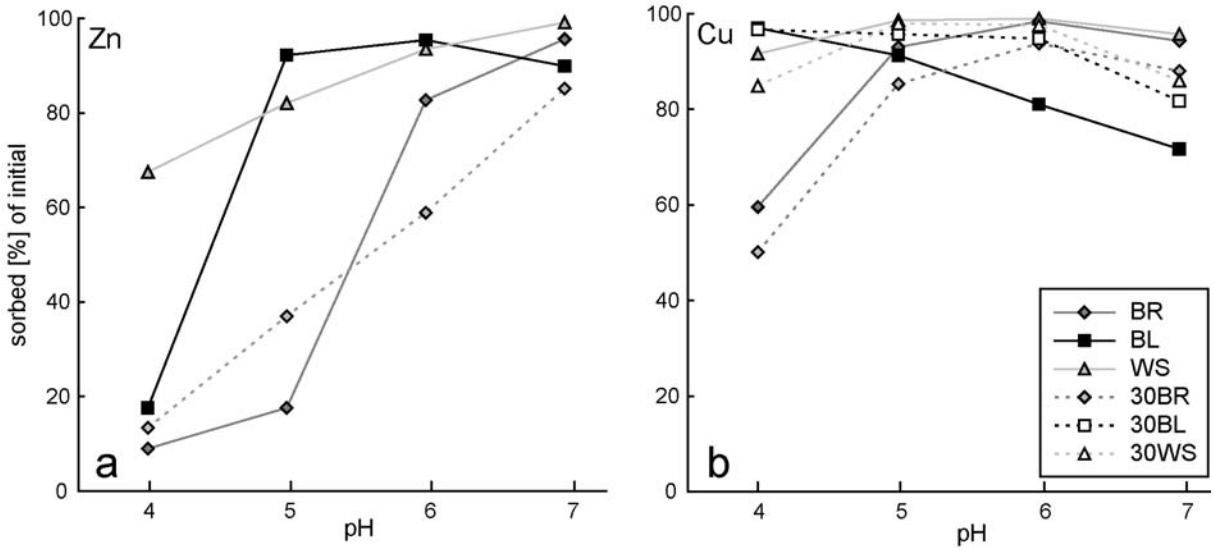

Figure IV-1: Schematic adsorption edge of (a) Zn and (b)Cu in stormwater to different siliceous aquifer materials (BL – black Tertiary Brighton Group sediment, BR- brown Tertiary Brighton Group sediment, WS – Quaternary Werribee Delta sediment) with no and 30 mg-C/L addition of fulvic acid.

investigation, sorption maxima for Cu and Zn have been found at pH 4.5-6 (Schnitzer and Kodama, 1966; Davis, 1984; Jardine et al., 1989). The influence of organic matter on adsorption is usually greatest at low pH, but fulvic acid was found to lower metal adsorption also at higher pH (Brümmer et al., 1983; Davis, 1984; Li and Dai, 2006).

In this study, addition of OC influenced sorption to various degrees. The metal sorption onto the sediment with the highest geogenic organic matter content (BL), presumably containing longer chain humic acids, is not significantly affected by the addition of dissolved fulvic acids. The added OC was mainly still dissolved and it seems that at the natural low pH the sites of the original solid organic matter offered energetically preferred sorption sites, as humic acids are a stronger complexant than fulvic acids (Town and Powell, 1993). However, the formation of dissolved complexes might also lower the presence of free metal ions and hence influence the metal sorption onto the sediment. In contrast, at higher pH, Cu sorption onto BL is decreased (Figure IV-1) and humic acids were found to dissolve from the soil which has been reported in the literature as well (Schnitzer and Kodama, 1966; He et al., 2006). The presence of stabile Cu-organic complexes would therefore increase the measured dissolved Cu amount.

For BR, Zn sorption seemed not to be affected by OC addition at the natural pH (Table IV-1). However, as shown in Figure IV-1, upon OC addition Zn sorption increased with lower pH and decreased with higher pH. A decreased Zn adsorption at high pH was also found for WS (Table IV-1). This behaviour can be explained with a ligand-like adsorption at increased ligand concentration (Benjamin and Leckie, 1981b). In addition, at high pH organic matter disperses and metal complexes would therefore be found in the dissolved phase. However,

mainly suspension of clay particles was observed for WS (compare Table III-11). At low pH values, added OC could aggregate (Sparks, 2003) and thus increases the number of sorption sites.

Cu adsorption onto BR and WS was decreased over the whole pH range, which would be in concordance with the formation of stable complexes between Cu and fulvic acids (see II.4.2). It seems that the formed Cu-complex is sorbed to a lesser extent than free Cu ions. This effect is usually greater at lower than at higher pH values, when the bonding between the ligand and metal is strong (Benjamin and Leckie, 1981b).

IV.3.1.3 Influence of solid-solution ratio

Using a graph of adsorbed metal concentration over solid-solution ratio, Series A2 showed that the adsorption of Zn and Cu increased at low sediment concentrations for all sediments but reached a plateau at the adopted ratio of 0.2 g/ml (Figure IV-2a+b). All sediments had an apparent strong dependency of solid-solution ratio and metal adsorption. The explanation to this phenomenon is that a graph of adsorbed amounts versus solid-solution ratio is essentially a rational function of $(C_{ini}-C_{diss})/(M/V)$ versus (M/V). K_d values are by definition solid-solution ratio dependent, as the solid-solution ratio is incorporated in the value for adsorbed concentration (see equation IV-1). It is therefore necessary to compare the data without this bias. One possible normalisation is to divide the dissolved concentration by the solid-solution ratio as well (Fehse, 2004). This graph (Figure IV-2c+d) then shows the mass of metal per kg solid that is present in the solution vs. the mass of metal per kg solid that is present in the sediment. If values from experiments with the same initial mass of metal but different solid-solution ratios result in a linear relationship, the distribution of the metal between solution and solid is constant and therefore shows no solid concentration effect. In such a graph, WS showed a decrease of slope with decreasing sediment mass for all cases, meaning that metals were found to a greater extent in the dissolved phase when sediment mass was decreased. This could occur when the saturation limit of the sediment has been reached, but this seems unlikely as BR with a similar CEC (Table III-10) did not show such behaviour. BL and BR displayed a linear behaviour for Zn and Cu without OC addition, i.e. they show no solid concentration effect, while with addition of OC (30BR and 30BL) their slope decreased slightly. In other words, a solid concentration effect was only detected for BR and BL with OC addition and for WS in all cases.

When analysing the solid concentration effect, all other parameters have to be stable. This is obviously not the case in our system. The decrease in sediment concentration resulted in a decrease in solution pH by one unit for WS and in an increase in solution pH by one unit for both BR and BL. These changes can be explained with the decreasing influence of the

sediment and the increasing influence of the stormwater solution characteristics. At the very high soil acidity of BR and BL, more sediment will release more protons and therefore decrease the pH of the solution. In contrast, at the high pH of WS, higher soil concentrations will buffer the lower pH solution more effectively. However, while the increased pH for BR and BL could explain the higher sorption at low solid concentrations, the decreased pH for WS can not. Therefore, pH changes alone cannot explain the observed effects for all sediments.

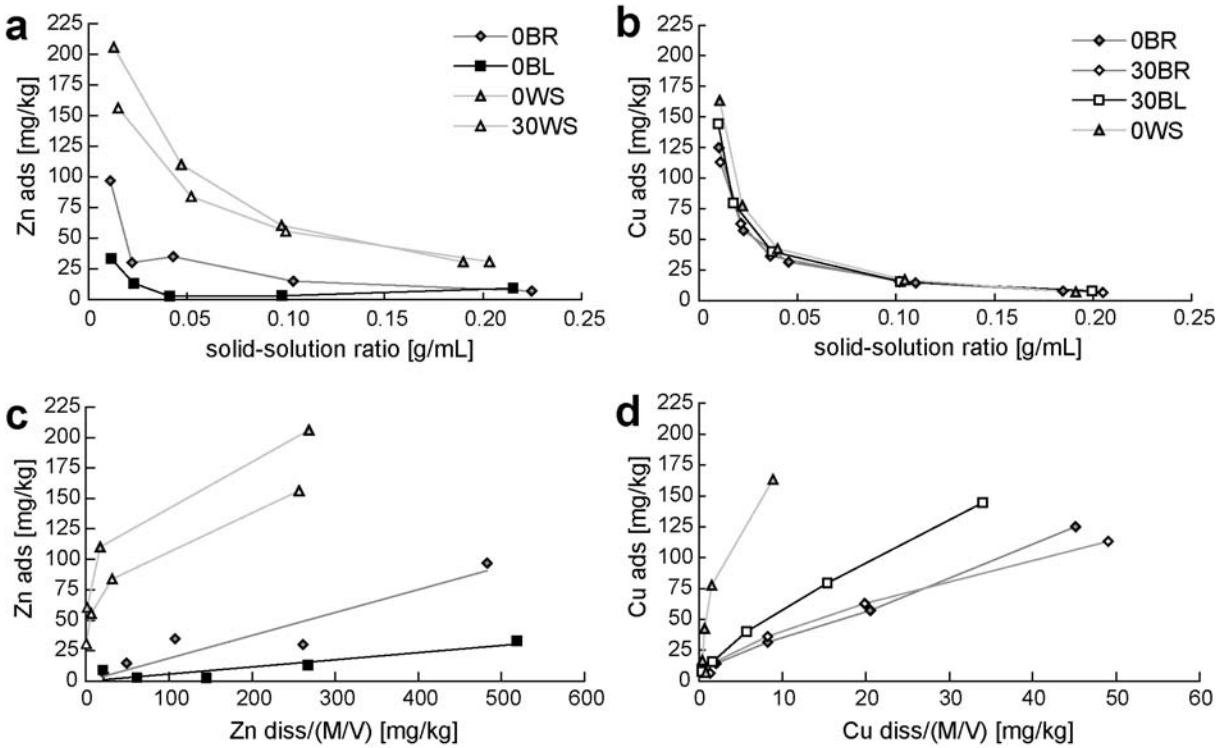

Figure IV-2: Effect of solid-solution ratio [g/mL] on adsorption amounts [mg/kg] of (a) Zn and (b) Cu in stormwater to different siliceous aquifer materials. Normalised amounts of (c) Zn and (d) Cu in solution and sediment showing solid-solution ratio effect was most pronounced for WS, but only limited for BR and BL. (BL – black Tertiary Brighton Group sediment, BR- brown Tertiary Brighton Group sediment, WS – Quaternary Werribee Delta sediment) with 0 or 30 mg-C/L addition of fulvic acid.

The existence or non-existence of the so called “solid concentration effect”, is a matter of debate. It has been found quite frequently for heterogeneous matrices, while it is often not observed for pure phases (O’Connor and Connolly, 1980; McKinley and Jenne, 1991; Fehse, 2004). A range of theories have been developed to explain this phenomenon including a third-phase effect, particle-particle interactions and metastable equilibrium theory (O’Connor and Connolly, 1980; Di Toro et al., 1986; Pan and Liss, 1998; He et al., 2006). Dzombak and Morel (1990) state that non-proportional sorption could be caused by a multipicity of sorption site types. In addition, different sorption kinetics of fast and slow sorption processes influence the distribution coefficient (Griffiths, 2004). The combination of these two effects could be the explanation to the solid effect observed for WS. This sediment is the youngest and contains the most diverse composition with oxides, three-layer clays and organic matter and maybe

even some carbonates. In reverse this could explain the missing solid effect for pure phases that have mostly uniform sorption sites.

As discussed in section IV.3.1.2 added OC is partially sorbed by the sediments. As this adsorption was reduced at low sediment concentrations, the formation of soluble metal complexes could be highest at low sediment concentrations and therefore lead to the observed decrease in slope. We therefore assume that the solid-concentration effect is most likely due to the existence of different adsorption sites and the formation of stable metal-organic complexes. In addition, equilibrium conditions might not have been reached and further adsorption over time is likely especially for Cu (Martínez -Villegas and Martínez, 2008), which might resolved the observed solid-solution effect.

The challenge is to understand the implication of this. When looking at a porous aquifer at any point in time the solid-solution ratio will be quite high, but when looking at the aquifer over a number of ASR cycles the volume of water that will flow passed the same solid will obviously decrease this ratio by magnitudes. This could mean that ASR schemes with high injection volumes would lead to decreased adsorption.

IV.3.1.4 Influence of pH

Stormwater is usually more or less pH neutral, whereas groundwater pH can be much lower. Adsorption behaviour of Zn at different pH values showed a strong influence of this parameter (Figure IV-3). Zn adsorption increased from as low as <10% at pH 3 to as high as 80-100% at pH >7 (Figure IV-1). The Zn sorption edges for BL and BR were very steep with a pH_{50} at about 4.5 and 5.5, respectively. For WS, the sorption edge was quite gentle resulting in an estimated pH_{50} value of about 3 (Figure IV-1). pH-adjusted Zn isotherms were more or less linear for all sediments. BR and BL showed a significant jump in slope at values greater than their natural pH, while WS showed a more gradual increase (Figure IV-3).
Cu adsorption responded differently to changes in pH. It reached a maximum of 97-99% at about pH_{max} 6 and 6.5 for BR and WS respectively and decreased either side of the pH_{max} resulting in a dome shaped graph. pH_{max} was reached at ~4.5 for BL and decreased towards higher pH (Figure IV-1) reminiscent of ligand-like adsorption. All adsorption isotherms were more or less linear with the exception of the one for WS at pH 4, which had a logarithmic form (Figure IV-3).

BL and to a lesser extent BR and WS dispersed considerably at pH values above their natural pH and neither centrifugation nor filtration (0.45 µm) separated the phases sufficiently (see Table III-11). However, subsequent addition of 2% concentrated HNO_3 (for metal analysis) to the supernatant resulted in flocculation of the colloids, interfering with exact

measurements. We, therefore, used only the remaining dissolved phase for metal analyses, as the acidification of the solution would have lead to an at least partial metal release from the flocculated particles. Nonetheless, as some metals might have remained bound to the colloids we undertook some measurements of the unseparated solution to estimate the potential error of these data. They revealed that not all metals desorbed back into solution after acidification and adsorbed metal concentrations shown in Figure IV-3 might be higher than actual values by 1-12% for Cu and 1-2% for Zn.

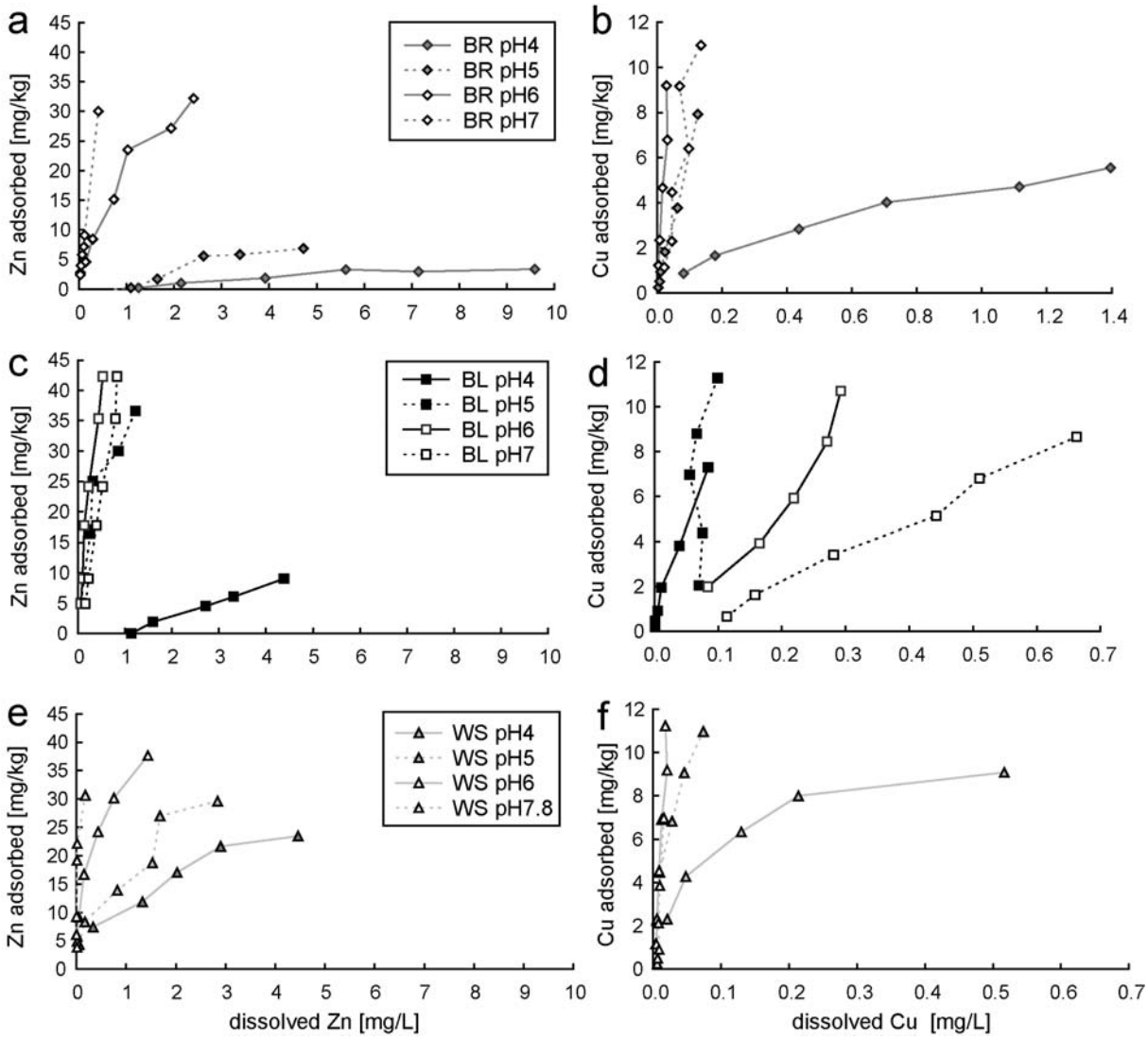

Figure IV-3: pH dependency of adsorption behaviour of Zn (left) and Cu (right) in stormwater to different siliceous aquifer materials (BL – black Tertiary Brighton Group sediment (a+b), BR- brown Tertiary Brighton Group sediment (c+d), WS – Quaternary Werribee Delta sediment (e+f)) with no addition of fulvic acid.

Metal sorption behaviour is affected directly and indirectly by pH, as it controls for example metal speciation, surface charge and organic complexation (see II.4.5). For the more commonly found metal-like adsorption onto soils (e.g. Figure II-7) pH_{50} values are reported around pH 3-5 for Cu and between pH 5-7 for Zn (Jenne, 1968; Benjamin and Leckie, 1981a; Tiller et al., 1984b; McBride, 1989; Stumm and Morgan, 1996). While pH_{50} values for Zn adsorption onto BR were within that range, they were clearly lower for BL and WS (Figure IV-

1). The low pH_{50} value for BL might be due to the comparatively low metal concentration and to a dominance of organic matter in the sediment (Tiller et al., 1984b). The low pH_{50} value for WS might be due to more cation exchange on the permanent charge sites (Baeyens and Bradbury, 1997). The significant jump in Zn adsorption behaviour for BR and BL around pH 5 (Figure IV-3) is reminiscent of results reported for a Podsol (Msaky and Calvet, 1990). The steep adsorption curves at pH values above 5 are indicative for surface complexation. Weakly inclined slopes are characteristic for ion-exchange.

The more complex pH-dependency of Cu sorption can be assigned to ligand-like adsorption behaviour. The adsorption edges for BR and WS were dome shaped with a maximal sorption between pH 5-7 (Figure IV-1). Similar behaviour has been reported in previous studies (McLaren et al., 1983; He et al., 2006). BL, the sediment with the highest organic matter content, shows a clear trend of decreasing sorption with increasing pH (Figure IV-3). This can be explained with an increased desorption of organic matter (Figure IV-4) at high pH that occurred for all sediments but most pronounced for BL. The dispersion of organic matter at pH >6 was also found in other studies (Schnitzer and Kodama, 1966; McBride, 1989). Schnitzer and Kodama (1966) also observed an increase in iron concentration when using NaOH for pH adjustments, which also occurred for BL at high pH (Figure IV-4). The adsorption of metals onto colloids seems to be more pronounced for Cu as all sediments showed a decrease in sorption at high pH, while for Zn only BL showed a minor decrease at high pH (Figure IV-3). This is in accordance with a higher stability of Cu complexes (Irving and William, 1948; van Dijk et al., 1971; Milne et al., 2003).

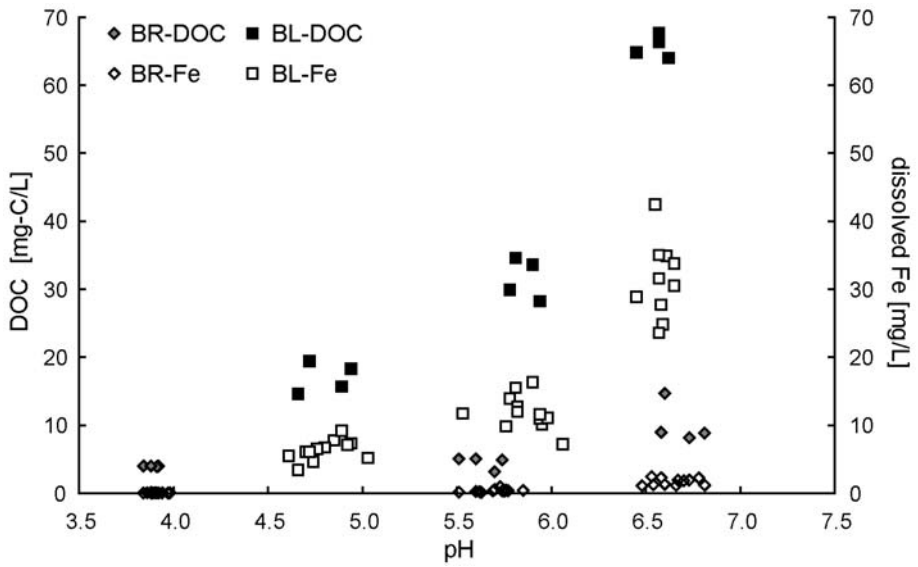

Figure IV-4: Dissolved concentration of Fe and organic carbon during pH adjusted (NaOH) batch experiments, showing a significant increase for BL and a slight increase for BR in both parameters with increasing pH

IV.3.1.5 Influence of solution salinity

Over the range of salinities that could be expected at an ASR site due to mixing of low salinity stormwater with intermediate salinity groundwater in the aquifer (100-3300 µS/cm or

about 0.001-0.02 M) adsorption of Zn and Cu was not significantly different (see appendix Table A-2a) in accordance with other studies (Elrashidi and O'Connor, 1982; Barrow, 1986b). Series with OC addition only had a slight influence on adsorption with a decrease of about 2% for Cu adsorption.

The main effect of increasing ionic strength in the solution (see II.4.5) is the competition for ion-exchange sites on clays (Malandrino et al., 2006; Limousin et al., 2007) and the possible formation of inorganic complexes with metals (Shuman, 1986; Mesquita and Vieira e Silva, 1996). As our sediments contained very low clay content, potential effects on sorption processes from salinity and clays are considered minimal. In addition, at the low metal loading of this study, an increase in ionic strength results in similar changes of free energy of species on the surface (Gouy-Chapman effect) and in bulk solution (Debye-Hückel effect), so that the specific sorption reactions of metals remain constant (Dzombak and Morel, 1990).

IV.3.1.6 Influence of pre-equilibration with groundwater

Adsorption of Cu for all sediments was not changed if the sediments were pre-equilibrated with oxic or anoxic groundwater or no groundwater and ranged from 89 to 99%. On the other hand Zn adsorption for BR and BL varied from 26 to 64% under the different condition, but no clear trend was recognizable for all sediments. BR showed a decrease in adsorption from pre-equilibration with oxic groundwater to pre-equilibration with anoxic groundwater and further to no pre-equilibration. BL had the highest adsorption for pre-equilibration with anoxic groundwater and lowest for no pre-equilibration (see appendix Table A-2b).

The main effects on adsorptive properties of sediments during air-drying are possible oxidation of reduced minerals, dehydration of minerals and organic matter and changes to the microbial community (Schulte, 1995; Kaiser et al., 2001; Akagi et al., 2007). When the sediments are rewetted, microorganisms are reactivated and increased denitrification and CO_2 production have been observed that can last for days (Raveh and Avnimelech, 1978; Bartlett and James, 1980; Jenne, 1995). Microorganisms and their extracellular polymeric substance (EPS) offer sorption sites to metals (Muris et al., 2005; Toner et al., 2005; Guine et al., 2006) and can therefore increase the observed adsorption significantly. This would be expected to be especially important shortly after rewetting.

The dehydration of oxides has been found to significantly lower their isoelectric point, decrease the accessibility to surfaces and to reduce the adsorption rate during rehydration of oxides (Thomson et al., 1980; Jenne, 1995). Schulte (1995) found dried soils had a significantly decreased sorption for Cu but not for Cd and assumed that drying might have blocked specific sorption sites. Organic matter releases labile compounds during drying,

which can be metabolised on rewetting, so more DOC could be released from dried sediments (Kaiser et al., 2001; Akagi et al., 2007). All these latter factors would therefore possibly decrease adsorption. The sum of counter effects is therefore unclear and could equal themselves out. It seems likely that rewetting was not intensive enough in pre-equilibrated experiments to show a considerable difference, as column tests with longer groundwater equilibration showed a marked difference in sorption behaviour (see V.3.3.1).

IV.3.2 Desorption series

IV.3.2.1 Desorption kinetics overview

In all soils at pH 7 the desorption of Zn was overall considerably greater than for Cu, but the three sediments showed marked differences, especially for Zn (Table IV-3). Desorption decreased from BR > BL > WS for both metals. It could be noted that Cu was slightly more desorbed when it had previously been adsorbed with higher amounts of OC. In most cases desorption decreased over the course of the three steps. This phenomenon was significant for BR and less obvious for WS as the values were very small overall.

Table IV-3: Desorption behaviour of Zn and Cu from different siliceous aquifer materials (BL – black Tertiary Brighton Group sediment, BR- brown Tertiary Brighton Group sediment, WS – Quaternary Werribee Delta sediment) previously adsorbed with Zn or Cu and 0 or 30 mg-C/L addition of fulvic acid without pH adjustments. Desorption solution groundwater at pH 7.

	Zn					Cu				
	adsorbed	total %	stepwise [%] of total			adsorbed	total %	stepwise [%] of total		
	[ug]	desorbed	step1	step2	step3	[ug]	desorbed	step1	step2	step3
0BR	288	24	75	18	7	72.2	3.8	58	24	16
30BR	287	23	70	21	9	65.1	5.5	49	31	22
0BL	269	13	63	23	11	74.4	2	50	25	25
30BL	270	13	62	25	12	75	2.1	57	29	19
0WS	304	2.4	38	29	33	70.3	0.8	0	63	37
30WS	292	5.4	46	35	19	73.6	1.6	31	31	38

There are variations on methods for assessing desorption, commonly based around the same principles for adsorption tests – just in the opposite direction. For our purpose the use of native groundwater is the most appropriate solvent. As with adsorption, principal desorption variables of the solution include pH, Eh, ionic strength, ligand type and concentration. The main difference to adsorption is that desorption requires a higher activation energy and hysteresis or irreversibility is therefore often observed (McBride, 1989). Some authors assume that solid-state diffusion of metals into mineral structures is partially responsible for irreversibility (e.g. Sposito, 1984; Scheidegger and Sparks, 1996) and reversing diffusive processes would be very slow. Even though it is unlikely that metal ions are able to penetrate minerals at room temperature, they could penetrate small and dead end pores or inner layers. It is more likely that equilibrium conditions might take very long to

reach rather than being completely irreversible (Hogg et al., 1993), as observed in field studies, where leaching of contaminants continues for decades.

In general, non-specifically sorbed metals are more likely to desorb than specifically bound (Arias et al., 2005; Singh et al., 2006), and symmetric adsorption and desorption has been observed for this fraction (Barrow, 1986a). The amount of non-specifically bound metals will be higher when previous metal loadings were high, the material did not offer many specific sorption sites, and when the pH is low (Singh et al., 2006). It was also found that desorption rates decreased, when time since adsorption increased, which was attributed to a redistribution of metals from low to high energy sites (McLaren et al., 1983; Lehmann and Harter, 1984; Singh et al., 2006). Low rates of desorption due to high binding strength between the metal and the material has been observed for various metals onto oxides (McLaren et al., 1983; Yang et al., 2006) and also for Cu onto organic matter (He et al., 2006; Yang et al., 2006).

In accordance with its less specific sorption, Zn was found to desorb more than Cu in this study under otherwise similar conditions. Similar results with 12-30% desorption of Zn and <6% desorption for Cu was found by Arias et al. (2005) for acidic soils and 2.4-8% desorption for Cu was observed by Hogg et al. (1993). The amount Zn desorbed was in correlation with the lower K_d values for Zn and was reported in other studies (Yang et al., 2006; Sastre et al., 2007). The first desorption step was usually the most efficient and is in agreement with the literature (Tiller et al., 1984a). The fact that hysteresis for Cu was higher than for Zn is in contrast to results from Pan et al. (1999) on goethite and might indicate that this mineral is not the main sorbent in our sediments, as mineral surfaces are likely to be coated with organic matter.

The influence of ligands as discussed for adsorption (see section 3.1.2) is also valid for desorption (Lehman and Harter, 1984; He et al., 2006; Yang et al., 2006). The formation of Cu-ligand complexes increased their solubility and therefore Cu release. When metals are extracted with organic ligands desorption rates increases to as high as 80-90% (Harter, 1983; Yang et al., 2006; Yuan et al., 2007). In conclusion Zn is more mobile due to its lower specific sorption, but Cu might be increasingly mobile with addition of dissolved organic matter.

IV.3.2.2 Influence of solid-solution ratio

For this series adsorbed metal concentrations were similar in each replicate, while the solution volume for desorption was varied. A solid-solution ratio normalised graph of desorbed amounts of metal, as discussed in IV. 3.1.3, showed linear correlation (Figure IV-

5). This means that desorption was not influenced by the different extraction volumes. This seems a reasonable finding, as for this short term desorption experiment groundwater would only be able to desorb the nearly constant amount of non-specific metals from each sediment. However, it seems a realistic assumption that in the long term with more leaching more metals would desorb, as it reflects a chemical reaction that would drive the equilibrium towards dissolved ions with increasing dilution. This means that higher volumes pumped in and out of ASR settings will increase desorption for both metals.

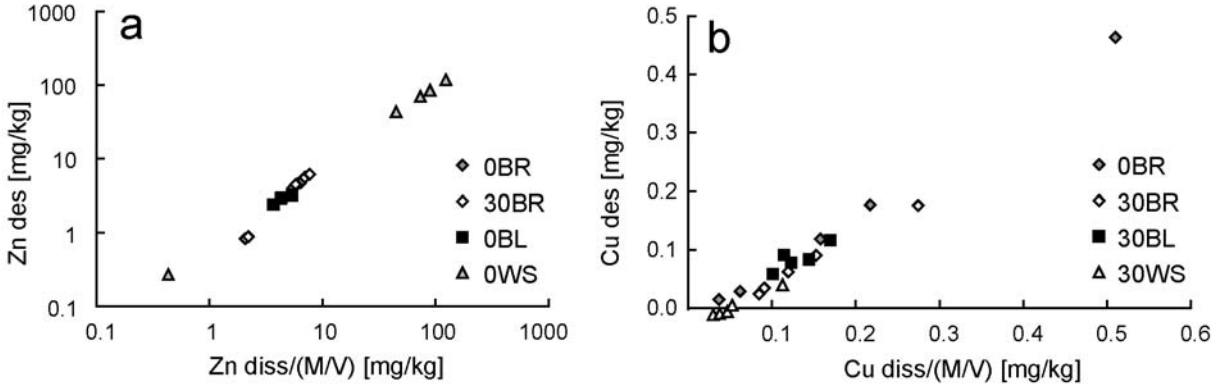

Figure IV-5: Influence of desorption solid-solution ratio on desorption. Normalised amounts of (a) Zn and (b) Cu in solution and sediment of different siliceous aquifer materials (BL – black Tertiary Brighton Group sediment, BR- brown Tertiary Brighton Group sediment, WS – Quaternary Werribee Delta sediment) previously adsorbed with Zn or Cu and 0 or 30 mg-C/L addition of fulvic acid.

IV.3.2.3 Influence of solution salinity

As mixing between groundwater and injected stormwater are expected, lower salinity solutions have been tested for desorption. The influence of desorption solution salinity was inconsistent. If at all there was a slight tendency for increased desorption at higher salinity. At low ionic strength even some additional adsorption could occur for both metals (see appendix Table A-2c).

As with adsorption, it has been observed that more metals are in solution at higher ionic strength, i.e. that desorption increased with increasing ionic strength due to ion competition and the formation of inorganic metal complexes (Shuman, 1986; Yuan et al., 2007) in agreement with our trend. Nevertheless, the formation of inorganic complexes is usually small for Zn at used molarities (Miretzky et al., 2006). Similar to adsorption results, the salinity effect seems not to be significant at ranges used in this study. This would mean that the mixing of groundwater and stormwater in terms of salinity changes would not impact greatly on sorption behaviour.

IV.3.2.4 Influence of oxygen concentration of desorption solution

During storage in an ASR cycle, the oxygenated stormwater would become oxygen depleted due to microbial reduction processes. Therefore desorption was tested with nitrogen purged

groundwater. The influence of oxygen concentration in the desorption solution was not uniform. It did not show a significant effect on Zn desorption for the series without additional DOC, but increased desorption for 30BL, while it decreased desorption for 30WS (Table IV-4). Cu desorption was consistently decreased with anoxic groundwater and even resulted in more adsorption (negative values Table IV-4). This was also found to occur in column studies (see V.3.3.3).

Table IV-4: Influence of desorption solution oxygen concentration on desorption amounts for Zn and Cu in different siliceous aquifer materials.

	Zn		Cu	
% desorbed	oxic	anoxic	oxic	anoxic
0BR	71	74	23	16
30BR	71	77	13	12
0BL	76	74	13	5
30BL	87	127	6	5
0WS	16	21	0.9	-0.2
30WS	20	5	1.5	-1.6

Note: oxic = oxygenated, oxygen 7-8 mg/L; anoxic = purged with nitrogen gas, oxygen 0-0.5 mg/L; BL – black Tertiary Brighton Group sediment, BR- brown Tertiary Brighton Group sediment, WS – Quaternary Werribee Delta sediment previously adsorbed with Zn or Cu and 0 or 30 mg-C/L addition of fulvic acid. Desorption solution groundwater, pH 5 adjusted, accumulated values of three desorption steps

Both pH and redox potential play an important role in metal solubility, as illustrated in Eh-pH diagrams (see II.4.5). Theoretically the dissolution of Mn- and Fe-oxides at low Eh values releases desorbed and incorporated metals (Davranche and Bollinger, 2001) and precipitation of oxides due to oxidation should decrease the amount of metals in solution (see II.2.3.6; Chuan et al., 1996; Charlatchka and Cambier, 2000). Increased amounts of organic matter present in the soil usually speed up reduction processes as it donates the electrons (see II.2.3.4), but can also hinder adsorption onto newly formed oxides due to coating. Some organic metal complexes seem to be bound stronger under anoxic conditions (Kashem and Singh, 2001).

Contradictory results regarding metal solubility under different redox conditions have been found in the literature, sometimes because pH and Eh were not decoupled in their effects. Nevertheless, it is often found that metal solubility is decreased under anoxic conditions and increased under oxic conditions. This seems to be due to repeated cycles of oxic and anoxic conditions. Occlusion of metals into newly precipitated minerals and an increase in sorption sites due to partial dissolution as well as increased crystallinity of hydro-/oxides has been postulated (Thompson et al., 2006).

In an ASR setting reduced Eh is often found near the injection well, due to high concentrations of TOC and nutrients close to the well (Vanderzalm et al., 2002; Greskowiak et al., 2005). Our results suggest that Cu desorption could be decreased in this region, which

makes Cu accumulation more likely. As metal behaviour is influenced by injection of oxygen, nutrients and organic matter and the resulting activity of microorganisms, all these factors have to be taken into consideration.

IV.3.2.5 Influence of pH of desorption solution

It was found that the pH of the adsorption and desorption solution had a profound influence on sorption behaviour. Similar to adsorption, Zn desorption showed a generally linear increase in affinity to the sediment with increasing pH and BR and BL slopes were steeper than the desorption slope of WS (Figure IV-6). Zn desorption reached a minimum at pH 5.5, 6 and 7 for BL, BR and WS respectively. BR had a maximum of >100% at low pH values (not shown), meaning desorption of geogenic Zn occurred. Zn desorption behaviour was consistent with its adsorption behaviour, where BL and BR showed a steep adsorption edge with the maximum adsorption reached at about the same values as the minimum of desorption (Figure IV-1). Similarly WS showed a less steep adsorption curve and reached the highest affinity to the sediment later.

Cu showed a more logarithmic decrease of desorption for BR and WS with increasing pH, reaching a minimum around pH 5.5-6. The graph was consistent with adsorption behaviour that showed a steep increase for BR between pH 4-5 and generally lower sediment affinity for WS (Figure IV-1). BL showed only limited desorption at low pH and even adsorption at pH values >4.5 (Figure IV-6), in accordance with ligand like behaviour. Unfortunately it can only be speculated that desorption would go up at higher pH values in concurrence with adsorption behaviour, as no data for this range were generated. The comparison of desorption amounts at pH 7 (Table IV-3) to pH 5 (Table IV-4) showed a clear increase in desorption for both metals for BR and BL and for Zn only for WS.

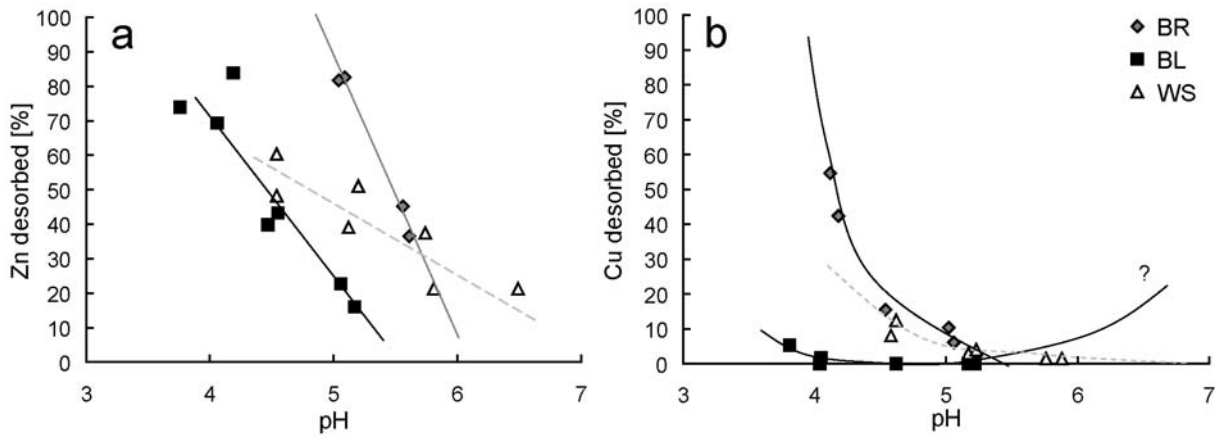

Figure IV-6: Influence of desorption solution pH on desorption [%] of previously adsorbed amount for (a) Zn and (b) Cu in different siliceous aquifer materials (BL – black Tertiary Brighton Group sediment, BR- brown Tertiary Brighton Group sediment, WS – Quaternary Werribee Delta sediment). Lines are indicative trends only.

Zn desorption behaviour is in conjunction with results found by other studies. Desorption values ranged from 5-68% (Cavallaro and McBride, 1984), 10-60% (Tiller et al., 1984a), 50% at pH 3 (Pardo and Guadalix, 1996), 90% for acid extraction (Harter, 1983) and cover most of our found values. Linear behaviour was also found by He et al. (2006). Minimum values were found in the range of pH 7 (Béchet et al., 2004) to pH 6 (Pardo and Guadalix, 1996). The correlation between the decreased extractability with increasing pH can be attributed to the decreasing amount of exchangeable Zn, decreasing competition with protons and increasing amount of specific binding of the hydroxy species (Cavallaro and McBride, 1984; Tiller et al., 1984a; McBride, 1989; He et al., 2006).

Cu desorption behaviour has been found to have a minimum value between pH 5-7 (Hogg et al., 1993; Béchet et al., 2004; He et al., 2006). An increase at higher pH values was attributed to increased organic matter dissolution, which can be speculated to happen for BL. Hysteresis of Cu on soils is common (Hogg et al., 1993), while it did not show large hysteresis onto goethite (Pan et al., 1999). This leads to the assumption that Cu is most strongly bound to solid organic matter and coincides with the low values for BL. Nevertheless if the organic matter is dissolved this will enhance desorption, especially at higher pH as found by Yuan et al. (2007). The much lower overall desorption of Cu is attributed to its more specific adsorption compared to Zn. Reversibility of adsorption is limited due to slow diffusion and the bottle neck effect (McBride, 1989). When looking at ASR schemes that run over extended periods of time diffusion might have enough time to reach a more ideal equilibrium and desorption of Cu is likely to increase in the long run.

IV.4 Conclusions

During a series of adsorption and desorption batch tests with three different siliceous aquifer materials, it was found that the most important parameter was pH.

Zn adsorption increased steeply with increasing pH and desorption in conjunction decreased steeply for the two acidic sediments, while the neutral sediment with the highest amount of clay minerals had a softer sorption edge slope. Changes in solution ionic strength or oxygen concentration had no major influence on sorption. The addition of organic matter showed only minor effects on sorption behaviour due to limited organic complexation of Zn.

Cu sorption behaviour was also strongly influenced by pH, but showed a more dome-like response rather than the classic adsorption edge due to ligand-like sorption. The addition of organic matter therefore had a more pronounced influence on increasing Cu solubility and

confirmed the higher organic complex stability of Cu. The reduction of oxygen concentration significantly increased desorption hysteresis.

At this point it can already be stated that sorption behaviour of Cu and Zn is significantly different. At a natural siliceous aquifer pH of 5, Zn will be mostly mobile due to low adsorption and high desorption values, while Cu is found mostly adsorbed and desorption values are low, but could be increased with an increased amount of organic matter.

When these results are transferred to possible ASR scenarios it seems reasonable to assume that significant amounts of Zn will remain mobile in the aquifer and will therefore be recaptured during the recovery cycle. Conversely, Cu seems to be retained within the sediment and might accumulate in the aquifer in the long term and therefore pose a risk of aquifer contamination. As sorption behaviour is strongly pH dependent the risk of accumulation in the aquifer matrix is also given for Zn in a limestone aquifer. Here precipitation of Zn and Cu would play a significant role and it has been found that metal recovery is low (Vanderzalm et al., 2006a). This is obviously beneficial for the quality of the recovered water, but aquifer remediation is more expensive and difficult to perform than treatment of recovered or injected water. Overall, these results demonstrate the need to consider source term concentrations and aquifer geochemistry. ASR configurations should be combined with sufficient water quality monitoring to minimise potential issues.

Chapter V: Column experiments

"There is nothing softer and weaker than water,
and yet there is nothing better for attacking hard and strong things.
For this reason there is no substitute for it"
Lao-Tzu (B.C. 550)

V.1 Introduction

While batch tests are a useful way to investigate the influence of changes in selected parameters on sorption, column studies provide further useful experimental information and are required to extrapolate to porous media. As batch systems are closed systems, they describe a static equilibrium between adsorption and desorption, while columns are able to reach steady state due to constantly renewed solution (Limousin et al., 2007). Secondly, batch tests do not simulate the dynamic aspects of transport like preferential flow, hydrodynamic dispersion and diffusion, while column tests come much closer to realistic aquifer conditions (Harter and Naidu, 2001). However, inclusion of non-equilibrium conditions and the before mentioned hydrodynamic parameters to the experiment also complicates the interpretation of column results (Limousin et al., 2007).

From the previously performed batch tests (chapter IV), linear adsorption coefficients for Zn and Cu for the three different sediments were derived. It was found though, that these coefficients varied considerably with changes in pH, with addition of dissolved organic carbon (DOC) and slightly with or without the presence of oxygen. This means that retardation is not adequately described with equilibrium equations, when any of the above mentioned parameters change (Goldberg et al., 2007). As stormwater ASR is not a constant system, but rather dynamic and a number of parameters change considerably over the course of one cycle, batch-derived K_d values are insufficient to extrapolate sorption behaviour of Zn and Cu over progressive ASR cycles. Column tests are a commonly used technique to investigate transport behaviour of dissolved and colloidal metals and dynamic biogeochemical reactions (e.g. von Gunten and Zobrist 1993; Seaman et al., 1995; Barna et al., 2007) and were therefore chosen to simulate one cycle of ASR. While a number of studies have investigated the adsorption of stormwater to various media (e.g. Sansalone, 1999; Davis et al., 2001a) and metal breakthrough and elution curves have been produced before (e.g. Voegelin et al., 2001; Delolme et al., 2004), to the author's knowledge this is the first time a column experiment has been undertaken to simulate a full cycle of stormwater ASR in siliceous aquifers. The geochemical transport modelling of the columns is presently being completed.

V.2 Materials and methods

V.2.1 Sediment materials and solutions

The same sediments BR, BL and WS as in the batch experiments were used (see III.3.5). Undisturbed sediment columns would have been preferable, but were not available. This means that the packed columns would be different from the natural sediment in hydraulic conductivity and particle size distribution due to loss of very fine dust and removal of coarse grains (>2 mm). In addition, the disturbance of the material would have disrupted any cementation and preferential flowpaths, as well as larger scale heterogeneities, e.g. lenses, which are commonly found in terrestrial and alluvial aquifers around Melbourne (Kenley, 1992; Leonard, 1992).

Stormwater was collected from a carpark runoff sedimentation tank at Monash University for the first two runs and from a residential area stormwater retarding basin for the third run, as the tank was in use for other testing (see III.2.4). Stormwater was sieved with 75 µm to retain floating organic matter that would normally be filtered before injection. Spiking with metals and fulvic acid was done with the same agents as for the batch experiments (see IV.2.1). Groundwater was obtained from the same bore as for the batch tests (see III.3.4).

V.2.2 Column set up

The experiments were conducted under aerobic conditions (if not stated otherwise) at room temperature (20-23°C), which is only slightly higher than the native groundwater temperature of 17°C. The setup consisted of three 50 L PE tanks for the inflow solution. Each of them had a pump (1-MD, Little Giant) for recirculation the water in the tank to prevent settling of fines. The inflow solution was transported in two outlet tubes (2.5 mm reducing to 1.3 mm ID, PVC) from each tank via a peristaltic pump (Minipuls 3, Gilson) in upflow mode through six threaded glass columns (Chromaflex, Multi-Lambda Scientific) of 2.5 cm diameter and 15 cm lengths. Each outflow solution flowed through an in-line EC meter (HI 7635 with HI8636CL, Hanna Instruments), and a tipping bucket rain gauge (RG 12, Environdata) into collection vials. Small sample volumes would be collected before the rain gauge to prevent any contamination from the rain gauge and weighed for flow measurements. EC values and rain gauge flow counts were logged continuously (DT800, dataTaker) (Figure V-1a).

To spread the inflow solution evenly, the columns contained a 20 µm porosity HDPE bed support, about 2.5-3 cm acid washed medium quartz sand (Unimin, 16/30 FD, ~700 µm) and 2 cm of acid washed fine filter quartz sand (Unimin, 50N, ~100 µm) on either end of the column, which left a height of about 5-6 cm for the aquifer material (Figure V-1b). Column 1

and 2 were packed with BR, column 3 and 4 with BL and column 5 and 6 with WS, corresponding to inflow tanks A (BR), B (BL) and C (WS). All values presented will be the mean value of the two duplicate columns. All used materials were weighed dry during packing, so entrained water could be calculated from weighing the full wet column. Packing with slight compaction was done in 3 mm layers under saturated conditions (water level about 1-2 mm above the material) to prevent air entrapment and preferential flow paths (Oliviera et al., 1996). Columns were wrapped in tin foil to shield them from light and prevent biological growth (Smith and Dillon, 1997). It would have been desirable to have sampling ports along the column to measure the concentration profile along the column, but due to the small size of the column compared to the needed sample size, this would have seriously disrupted the experiment. It was therefore only an inflow-outflow column experiment.

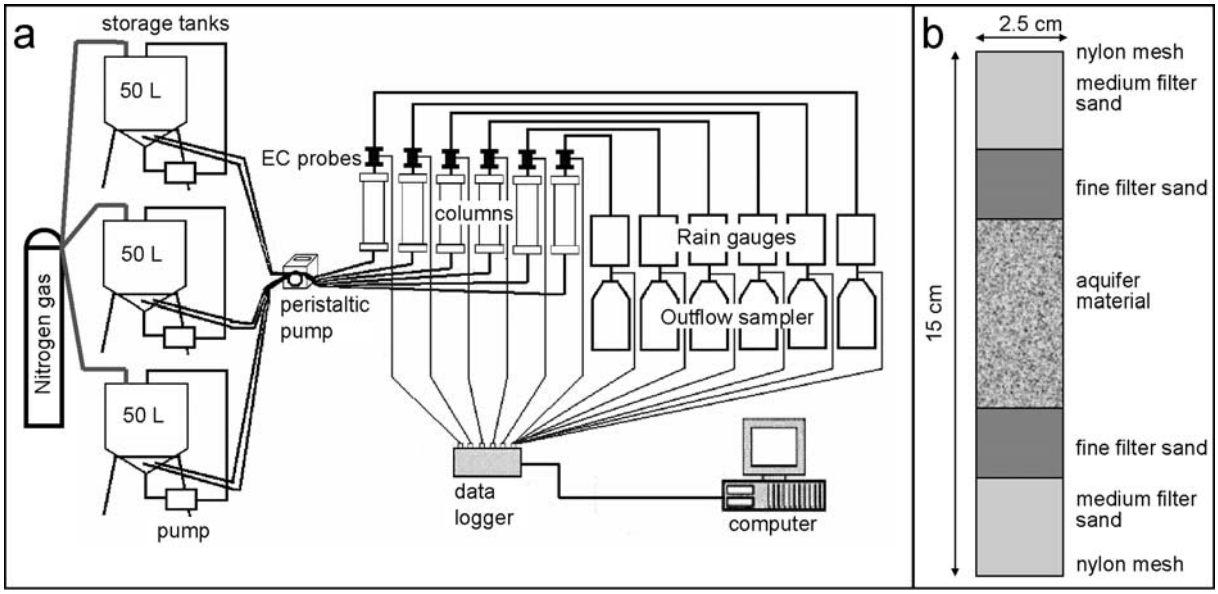

Figure V-1: (a) Experimental set up of column experiments (not to scale) and (b) packed column.

The dispersivity of each column was estimated by using alternating inflow cycles of diluted (EC ~1500 µS/cm) and undiluted (EC ~ 3300 µS/cm) groundwater solutions. The salinity of the used solutions was high enough not to trigger any colloidal release (see section 3.2). EC measurements of the outflow solution were taken and the breakthrough curves analysed (e.g. Fetter, 1993).

The in-line EC meters have an inner volume of 50 mL, which is about twice the total porevolume (PV) of the column. This contributed significantly to mixing of the outflow solution and resulted in retarded breakthrough, especially when lowering the salinity of the solution. To avoid this artificial interference, all in-line EC meters were disconnected for the whole of exp. 3 (see Figure V-3 and Figure V-4), and EC was measured manually (model 2100, TPS). The dispersivity testing cycles varied in flow rate and EC difference. Breakthrough curves done under these different conditions could be superimposed and were symmetrical,

meaning there was no kinetic effect (Bürgisser et al., 1993; Hinz and Selim, 1994; Limousin et al., 2007).

Hydraulic conductivity was measured in triplicate for each column with constant head under gravitational flow (ASTM, 1968). Mean values of the duplicate columns for packing and hydraulic parameters are presented in Table V-1. While hydraulic parameters are measured for the whole column including the filter sand, porevolumes for example were calculated for the aquifer sediment only. Dispersivity was within the expected range of 0.1-1 cm typically found in column experiments (Zheng and Bennett, 1995). The Peclet numbers were mostly between 0.02-6, i.e. the range where transport is governed by advection and also influenced by diffusion (Zheng and Bennett, 1995). Hydraulic conductivity was lower in the first run due to more compaction during packing.

Table V-1: Mean packing parameters of duplicate columns for aquifer material (excluding the filter sand), while hydraulic parameters are for whole column (including filter sand).

	for aquifer sediment only					for complete column			
	aquifer material (M)	pore volume (V)	solid-solution ratio (M/V)	porosity (n)	bulk density (ρ)	longitudinal hydraulic dispersion (D_L)	dispersivity (α)	Peclet number (Pe)	hydraulic conductivity
unit	g	cm³	g/cm³	fraction	g/cm³	cm²/s	cm		10^{-4} cm/s
BR-exp. 1	60.20	7.23	8.32	0.24	2.01	0.0033	0.11	5.1	1.7
BR-exp. 2	53.75	8.69	6.19	0.30	1.85	0.0039	0.10	7.8	8.3
BR-exp. 3	44.75	6.93	6.46	0.29	1.88	0.0111	0.43	1.2	14.1
BL-exp. 1	43.54	8.12	5.36	0.33	1.77	0.0030	0.18	2.3	0.4
BL-exp. 2	41.00	6.81	6.02	0.31	1.83	0.0040	0.11	8.0	4.5
BL-exp. 3	41.75	6.25	6.68	0.28	1.90	0.0060	0.26	1.6	8.1
WS-exp. 1	48.27	8.79	5.49	0.33	1.78	0.0041	0.16	3.0	1.1
WS-exp. 2	44.25	7.61	5.82	0.31	1.82	0.0060	0.18	3.8	8.7
WS-exp. 3	43.50	8.13	5.35	0.33	1.77	0.0169	0.73	0.6	19.3

V.2.3 Experimental design

In general the experiments consisted of four phases that would mimic one complete ASR cycle, and to the author's knowledge this study was the first experiment to do so for stormwater ASR in siliceous aquifers:

- **Phase 1 - equilibration with ground water**: To mimic the equilibrium state that sediment and groundwater are naturally in before any stormwater is injected, columns were injected with groundwater for about 2 weeks alternating flow with no flow. Freshly sampled groundwater was used to inoculate the columns with groundwater-derived bacteria.
- **Phase 2 - stormwater injection:** About 1200-2000 PV of stormwater was injected under continuous flow (1-1.4 mL/min) over one week. The switch to stormwater defined the start of the experiment.

- **Phase 3 - storage:** The following two weeks after stormwater injection the columns were in storage and only disrupted after each week for sampling 6-7 PV using stormwater as inflow solution.
- **Phase 4 - recovery:** To mimic the recovery and mixing in the aquifer, the flow was reversed (i.e. the columns were turned around) and increasing fractions of groundwater were mixed with the previously collected stormwater injection (phase 2) outflow. Fractions and volumes of groundwater during these stages were 0% (~30 PV), 20% (~350 PV), 50% (~350 PV) and 80% (~350-3000 PV), which would equal the limit for irrigation use of about 2500 µS/cm. Flow was varied throughout the last stage (i.e. groundwater 80%) from 0.9 – 3.6 mL/min to mimic variable pumping rates and also included a number of shorter storages (see Figure V-2 for lengths) as recovery would usually take place in a number of stages and to test equilibrium conditions.

After each experiment tanks were rinsed with deionised water and tubing and columns were rinsed with a diluted HCl solution (pH 2) for a couple of hours to avoid cross contamination.

Three experimental runs with increasing complexity were undertaken, outlined in Table V-2. The first experiment (exp. 1) with non-spiked stormwater was done to obtain a baseline for ion-exchange and flow characterisation and to simulate ASR with metal-pretreated water. Column 4 (BL) started to clog up during the injection (phase 2) and the experiment could not be continued to the end for this column. The second experiment (exp. 2) looked at adsorption and desorption behaviour of Zn and Cu enriched in stormwater and the impact of pH change in the groundwater at a later stage (80% groundwater). The third experiment (exp. 3) introduced complexing ligands in the form of added fulvic acid and included a lower groundwater pH throughout the run. It also mimicked anaerobic groundwater conditions by de-oxygenating the groundwater with nitrogen gas aeration before and during inflow (Wisotzky and Cremer, 2003). This also decreased alkalinity of the groundwater to <0.1 mg/L, but did not change the occurrence of iron precipitates. The outflow was nevertheless exposed to the normal atmosphere and therefore re-oxygenated. Acidification of inflow solutions, where needed, was completed with HCl rather than nitric or sulphuric acid, as not to introduce extra nutrients and to avoid inorganic complexation.

After the experiments were finished the column sediments were carefully taken out of the column and air dried. Metal extractions from the sediment were undertaken (see section 2.5) to complete the mass balance and to obtain further insight into the binding form of metals and their potential mobility. The aquifer sediment was divided into 5 equal parts from the top to the bottom, homogenised and subsamples (3 g) taken thereof, as well as from

homogenised top and bottom medium and fine filter sands (5 g). Fresh sediments (3 g) pre-equilibrated with either oxygenated or deoxygenated groundwater were also included for comparison. The mass of sediment per sample was increased, compared to the commonly used 1 g, to counteract the fact that the sediments contained large amounts of inactive quartz.

Table V-2: Variations of inflow solutions for experiments 1-3 (see also Figure V-2).

Exp.	Phase 1 gw equilibration	Phase 2 stw injection	Phase 3 storage	Phase 4 recovery (stages: gw 0%, 20%, 50%, 80%) including shorter storages
1	oxygenated gw, pH7	stw, nothing added		no 0% gw stage, oxygenated gw, pH7, stopped after ~330 PV of gw 80% stage
2	oxygenated gw, pH7	stw with added Zn (2 mg/L) and Cu (0.75 mg/L)		oxygenated groundwater (pH 7), stepwise decrease of pH to 6.5 (~240 PV), pH 6 (~220 PV) and pH 5 during the gw 80% stage
3	N_2 de-oxygenised gw, pH5	stw with added Zn (2 mg/L), Cu (0.75 mg/L) and DOC (30 mg-C/L)		N_2 de-oxygenised groundwater (pH 5), decreasing pH from 7 to 5 over gw 20% stage

gw: groundwater; stw: stormwater; PV: number of porevolumes

After each completed experiment tanks were rinsed with deionised water and tubing and columns were rinsed with a diluted HCl solution (pH 2) for a couple of hours to avoid cross contamination.

V.2.4 Water sampling and analysis

All solution samples were measured for pH (model 1852, TPS), EC (model 2100, TPS), turbidity (2100P, HACH) and in regular intervals for alkalinity by Gran titration and silicon (Microquant, Merck, only exp. 3). For dissolved parameters samples were filtered with 0.45 µm cellulose acetate filters. Samples were acidified with 2% conc. HNO_3 for total and dissolved cation and metal analysis (ICP-OES, Varian), acidified with 2% conc. HCl for TOC/DOC analysis (TOC-analyser, Shimadzu) and unacidified for dissolved anion analysis (Ion chromatograph, Metrohm). If turbidity was >1 NTU, samples were digested on a hotplate with conc. HNO_3 (APHA, 1998). Due to the small sample size, all parameters were analysed only when sufficient volume was available. Only total and dissolved concentrations were considered in this study. As high turbidity was only encountered at the start of the stormwater injection (phase 2) (see later Figure V-2c), most results shown will be of total concentrations. For major ions the difference between total and dissolved concentrations was typically within the analytical error..

Outflow sampling and phase changes occurred for all columns at the same time. Outflow sampling frequency ranged from a minimum of ~6 PV to a maximum of ~550 PV, with higher frequency after a phase change. Inflow samples were obtained from each tank for every change in inflow solution.

V.2.5 Sediment analysis

The method used for the metal recovery from the aquifer material (at the end of each experiment) was carefully designed based on the literature. There are a variety of sequential extraction procedures in the literature (Beckett, 1989), the most common being the five step procedure of Tessier et al. (1979). Due to the low carbonate content in all sediments used and readsorption found for the classical first step for the exchangeable fraction using $MgCl_2$ (Gómez-Ariza et al., 1999), a combined step for exchangeable and carbonate bound metals in acetic acid was regarded as sufficient. The residual fraction was expected to be constant and not to be available for sorption reactions (Martin et al., 1987; Nirel and Morel, 1990) and was thus omitted. A three step metal extraction (e.g. Quevauviller et al., 1994; Sutherland, 2002; Marguí et al., 2004) was therefore adopted for this study (Table V-3), modified after Sahuquillo et al. (1999). All dissolutions and dilutions were performed with double deionised water (Milli-Q). After each step the samples were centrifuged, the supernatant siphoned off for analysis and the residual weighed to calculate the entrained solution. The final volume of added solution in step 3 was also determined by weighing before siphoning off the supernatant. No washing steps between the extraction steps were undertaken to minimise loss of metals in discarded washing solutions. This is especially crucial as washing with distilled water leads to dispersion of colloidal and organic matter, which could not be centrifuged sufficiently (Kheboian and Bauer, 1987). A slight loss of sediment occurred for some BL samples due to the vigorous reaction after the addition of H_2O_2. For total metal analysis (ICP-OES, Varian) step 1 samples were acidified to pH 2 with conc. HNO_3 , while step 2 and 3 samples were already pH<2.

Table V-3: Chemical reagents and analytical conditions in the modified three-step sequential extraction procedure after Sahuquillo et al. (1999). All pH adjustments were done with conc. HNO_3.

step	fraction	procedure
1	acid extractable (exchangeable + bound to carbonates)	25 mL of 0.17M acetic acid (pH 3), shaken for 16 h at 20°C
2	reducible (bound to Fe-/Mn-hydroxides)	40 mL 0.1 M hydroxylamine-hydrochloride solution (pH 1.5); shaken 16 h at 20 °C
3	oxidisable (bound to organic matter)	5 mL of 30 % H_2O_2 (pH 1.5), shaken 1 h at 20°C; heat lightly covered to 85°C for 1h; add 5 mL of 30 % H_2O_2 (pH 1.5) and reduce volume of solution at 85°C over 4-5 h; add 40 mL of 1 M ammonium acetate solution (pH 1.6), shaken 16 h at 20°C

V.2.6 Data analysis

For all outflow samples mean number of PV and mean time of sampling were calculated. Even though the peristaltic pump speed was the same for all columns, the flow rates varied due to different hydraulic conductivity in the columns and number of PV also drifted apart as the actual volume of each PV was not the same for all columns. As samples were taken and phases changed at the same time for all columns, each column had a slightly different

number of PV for the equivalent sample, making graphs of concentration versus PV only possible for time spans that did not involve a phase change. While results are presented as concentration versus time to compare observed values to modelled values for a single column experiment (see Figure VI-3), here the results are presented as concentration versus sample starting from stormwater injection (phase 2) (see Figure V-2). As the number of samples per phase were not always the same for the different experiments some empty fields were inserted to line up phase shifts. This allows the similarity between the columns and between experiments to be depicted clearly. It elongates times with higher sampling frequency, therefore deskewing areas with higher changes in concentration, while it shortens times with low sampling frequency, e.g. cutting out times of storage. Final values presented are mean values of the two duplicate columns including mean PV (see Table A2-5 in appendix for full results), as same sediment columns had generally good agreement.

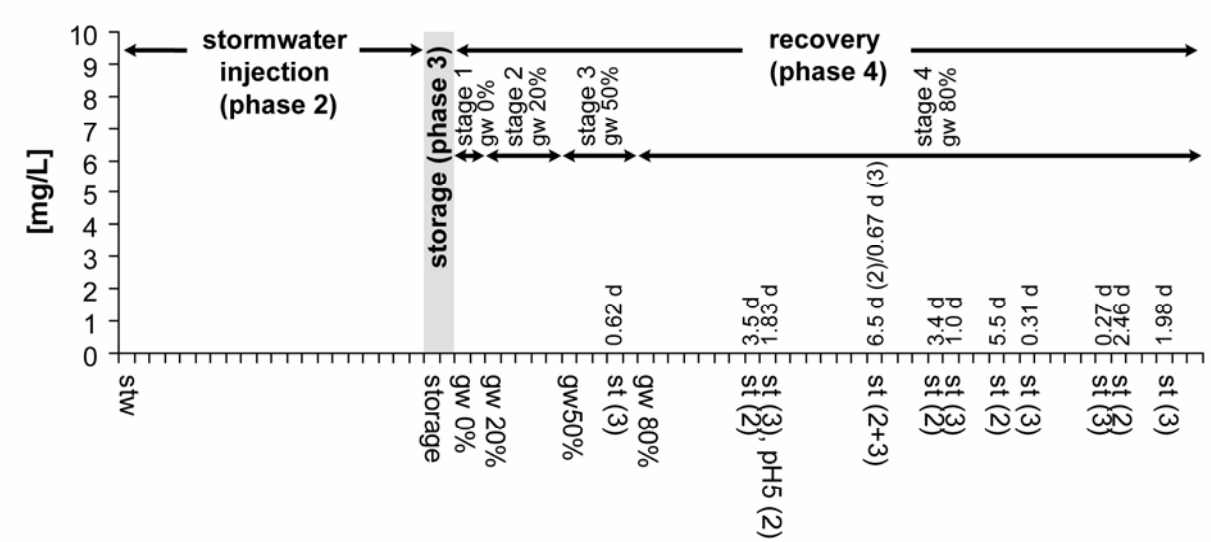

Figure V-2: Blank graph concentration versus sample. X-axis labels indicate the start of a new phase (stw, storage, gw). Samples after shorter storages in phase 4 are indicated by st and their length is given in days [d]. pH of inflow solution dropped to pH 5 in experiment 2 at sample pH5 (2). stw: stormwater; gw: groundwater; (2): in experiment 2; (3): in experiment 3. See also Table V-2.

Slight differences in the used inflow solutions existed. To facilitate the comparison between the experiments this difference was circumnavigated in the results by using relative differences between inflow and outflow rather than absolute values for most graphs. Negative values were created when the inflow solution had a higher value than the outflow solution, meaning the cation was retarded in the column by adsorption and positive values showed a release of the cation due to desorption.

As no systematic differences between the metal concentrations extracted from the five sections of each aquifer material as well as between the column duplicates were found, mean values of the equivalent ten aquifer sediment samples were calculated. Mean values were also calculated for the duplicate metal concentrations of the fresh sediments.

V.3 Results and discussion

In the following sections the behaviour of major cations (V.3.1), pH, TOC and turbidity (V.3.2) and their influence on the behaviour of metals are presented. The quite different adsorption and desorption pattern of Zn and Cu are then shown in more detail (V.3.3), influential parameters are investigated and the results of this study are compared with results from similar column experiments where possible. A brief investigation on potential As release is included for completeness (V.3.4). The results are completed by a mass balance and speciation analysis from the metal extraction (V.3.5).

V.3.1 Major cations - ion exchange

There are two main processes happening for the major cations when the stormwater is injected. Firstly the entrained groundwater solution will be displaced and secondly ion-exchange reactions will occur to establish a new equilibrium.

The former process is not retarded and occurs at pore water velocity and therefore only affects the first couple of porevolumes if hydrodynamic dispersion is not excessive (Valocchi et al., 1981). The change in total normality or ionic strength will therefore form the first, so called “normality front” (Černík et al., 1994). It can be seen as a drop in EC in Figure V-3 and a drop in the concentration of all major cations simultaneously as a result of the dilution (Figure V-4). The EC reached stormwater values in exp. 3 after the first sample. In the other two experiments the EC meter, containing about 6-7 PV of solution itself, retained a significant portion of the groundwater (arrow in Figure V-3). It was discovered during dispersivity tests that this retardation was about 100-120 PV when decreasing the EC, but only about 8 PV when increasing the EC. This phenomenon was likely due to density differences of the solutions, as density differences of only 0.0066 g/cm^3 are sufficient to create layering (Beekman et al., 1990). It is presumed that the heavier salty water sat at the bottom of the tilted EC meters and the fresh water flowed slowly over it, only removing a thin layer of saltier water with the low shear stress of the slow velocity as has been observed in related settings (Western et al., 1998). This process therefore greatly overshadowed the ion-exchange process during the stormwater injection of exp. 1and 2. For all experiments, hydrodynamic dispersion effects, the ~8 PV containing filter material above the sediment and the comparatively large sample size (~6 PV) also obscure, retard and broaden fronts and decrease the amplitude of positive or negative peaks (Schweich and Sardin, 1981). Hydrodynamic dispersion effects are even greater when the total normality drops (Černík et al., 1994). Nevertheless, similar trends could be observed for all three experiments, even though later than in most column experiments found in the literature without the above mentioned retarding influences.

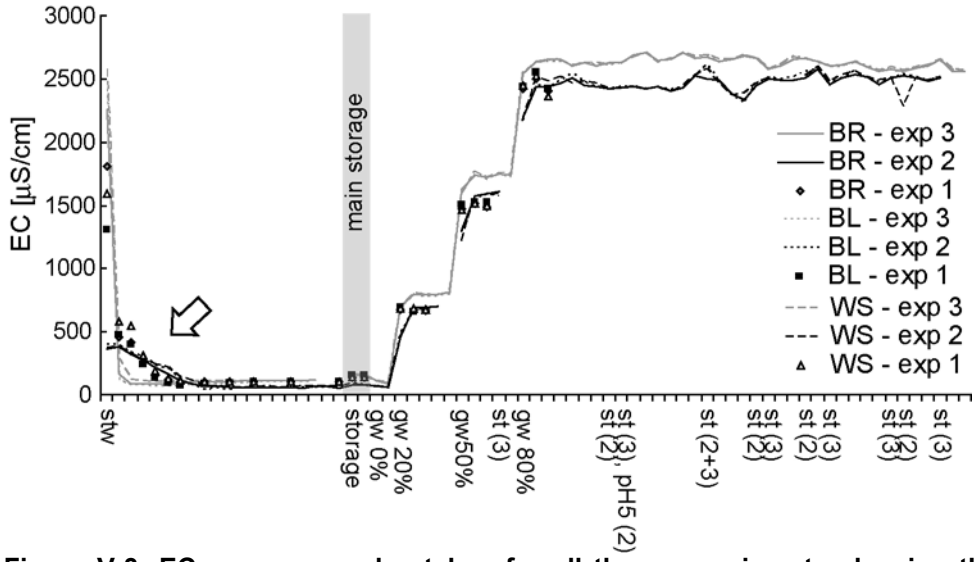

Figure V-3: EC versus samples taken for all three experiments showing the influence of EC meter volume on breakthrough in exp. 1+2 compared to exp. 3 with no EC meters; especially visible at the beginning of the stormwater injection phase (arrow). See Figure V-2 for sample labels.

Once most of the background groundwater had been flushed from open pores, adjustments in the ion concentration and composition occur via ion-exchange (see II.4.1.1) as mass and charge balance have to be maintained at all times. From the measured CEC, porosity and bulk density (Table V-1) an estimation of exchanger sites in the column resulted in a total number of exchanger sites of 0.4, 0.64 and 3.6 mmol for BR, WS and BL, respectively, as BL exhibited a significantly higher CEC due to organic matter. To put this into perspective, the undiluted groundwater had about 21-25 mmol/L and the stormwater 0.45-0.7 mmol/L cations.

During the groundwater equilibration phase the columns were saturated with sodium and magnesium as the major cations. The stormwater on the other hand was dominated by calcium. This means that the exchanger sites would be filled by about 50% with Na, 35% with Mg and 15% Ca before the stormwater injection, while in equilibrium with stormwater nearly all sites would be filled with Ca (Appelo, 1994). Potassium concentrations were minimal in all groundwater and stormwater of exp. 1 and 2 (<2 mg/L). Only stormwater of exp. 3 had a noticeable K concentration (5 mg/L) and breakthrough patterns were similar in shape to Ca, only earlier (data not shown). Due to the selectivity sequence of Ca >>Mg>Na (see II.2.3.5) the exchanger complex would adapt to the stormwater injection by Ca replacing Mg, which in turn replaces Na (Appelo et al., 1990; Appelo et al., 1993). One would therefore expect a normality front followed by three fronts of Na, Mg and Ca, respectively. Sodium is consequently eluted first and reaches stormwater concentration after about 30 PV in exp. 3 (Figure V-4a). This is about three times later than would have been expected (Voegelin et al., 2000) and is due to the large ratio of PV to sample size and the delay due to the filter material on top of the sediment as mentioned above.

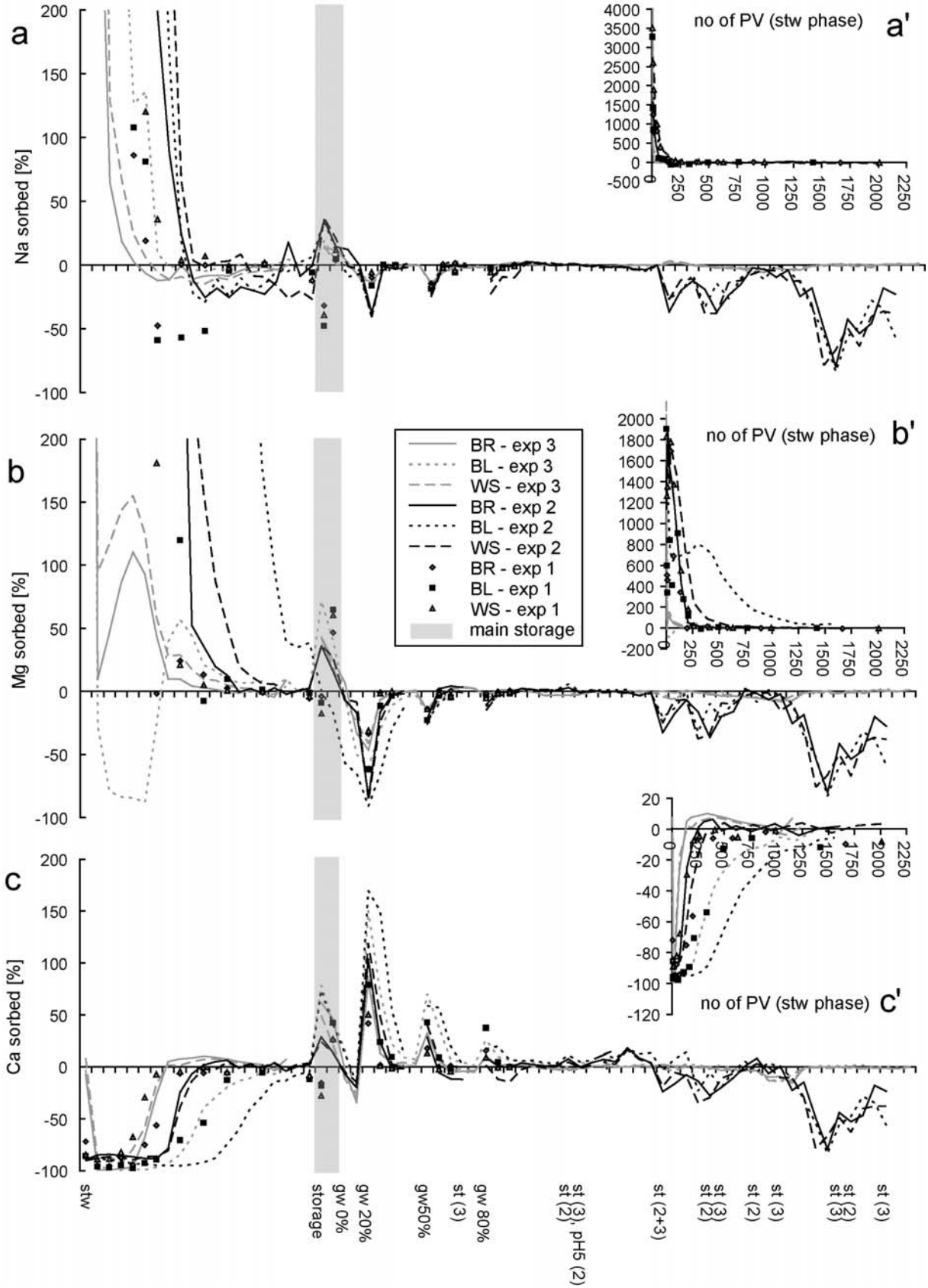

Figure V-4: Behaviour of major ions (a) sodium, (b) magnesium and (c) calcium, normalised to inflow concentration for all three experiments (negative concentration: retardation via adsorption, positive values: release via desorption). Inserts(') show the cation concentrations in the stormwater injection phase versus no of PV. See Figure V-2 for sample labels.

In general, magnesium values dropped with the first normality front, then came back up and then declined again to inflow values (Figure V-4b). This happens at overall higher values in exp. 1+2 due to the EC meter mixing, while the first drop is below injection concentration in exp. 3. All sediments show the same pattern, but BL showed a deeper and longer sink and a later and less pronounced peak due to its higher cation capacity. This pattern agrees with the expected heterovalent exchange of Mg expelling Na (sink) and the consequent homovalent exchange by Ca (peak).

Calcium concentrations dropped to a minimum below inflow concentration the longest, as Ca is being adsorbed preferentially on the exchanger (Figure V-4c). The second decrease in Mg concentration corresponded with an increase in Ca concentrations, underlining their exchange. Again, Ca breakthrough is considerably later for BL. Ca breakthrough was finished at about 131 PV for BR, 145 PV for WS, and at 1350 PV for BL (exp. 3). This elution order corresponds quite well with the differences in CEC. The breakthrough of Ca came earlier than one would expect from estimations based on stormwater cations compared to exchanger site concentrations, but would most likely be due to the fact that a number of exchanger sites were already occupied by Ca and complete equilibrium was not achieved. A very similar elution pattern of Mg and Ca has been observed by Appelo et al. (1990) and Voegelin et al. (2000). Only the expected plateau of Ca concentration during the Mg peak is obscured here.

During the storage phase all cation concentrations were higher than the inflow concentration. This would be due to the fact that stagnant pockets or dead end pores that had not reached equilibrium with the stormwater were releasing trapped groundwater into the stormwater solution via diffusion. High flow velocities and preferential flow could sweep the solution away before homogenisation was completed and would result in a physical non-equilibrium (James and Rubin, 1979; Valocchi, 1985). This phenomenon was also observed for other parameters (see V.3.3.2)

In the last phase where the injected stormwater is mixed with increasing proportions of groundwater the reverse cation exchange reactions occurred, e.g. Ca was released from the exchanger by Mg and Na. This could be seen by simultaneous negative peaks (retainment) for Na and Mg and positive peaks (release) for Ca at each step of increased groundwater (Figure V-4). The amplitude of the peaks decreased for each step, as the degree of change was highest with the first mixing. In the first step mainly Mg would expel Ca as could be seen from the peak height of Mg. The next step would increase the amounts of Mg and Na on the exchanger less drastically. This agreed with an estimation of exchanger occupancy from

Appelo (1994), where the percental increase in Mg was very steep at small seawater fractions, while Na occupancy increase was more gradual. It agreed also with the concentration-charge effect that monovalent ions are preferentially sorbed at higher ionic strength (McBride, 1989). The sample size resolution during this phase was not high enough to show more detailed fronts, but it was still observed that the peaks lasted longest for BL.

Experiment 2 showed a few rather curious simultaneous decreases in all major ions towards the end of the experiment that was not matched by a similar decrease in EC and could not be satisfactorily accounted for by increases in protons, other ions, analytical error or any other cause. Saturation indexes calculated with PHREEQC v. 2.1 (Parkhurst and Appelo, 1999) did not support the precipitation of any minerals containing major ions either. No explanation for this phenomenon can be given, but the results were retained for completeness.

V.3.2. Physico-chemical parameters

Metal sorption behaviour cannot be explained without looking at major influential parameters like pH, organic carbon concentration and colloid mobility. To facilitate later interpretation the behaviour of pH, TOC and turbidity are presented at this point, while the implications for metals are discussed in section V.3.3. Redox potential is another important parameter. Though it could not be measured due to the experimental set up, it can be assumed to be lower during storage and the recovery phase of exp. 3 due to oxygen depletion via nitrogen gas (see Table V-2).

V.3.2.1 pH

pH is of crucial importance as it stimulates a number of direct and indirect consequences (see II.4.5). Its marked influence on Zn and Cu sorption behaviour for the studied sediments was previously shown in batch experiments (see IV.3.1.4 and IV.3.2.5). Stormwater road runoff pH is usually near neutral (Duncan, 2006) and was not changed in either experiment. Groundwater pH on the other hand can vary considerably depending on the aquifer (see III.3.3). Exp. 2 and 3 therefore had varied inflow pH values from pH 5-7 (Table V-2).

pH outflow values corresponded to pH inflow values with some delay (Figure V-5a). An increase in inflow pH was delayed less than a decrease in inflow pH. BL responded more slowly to pH changes compared to the other two sediments, meaning it was generally lower during injection (phase 2) in exp. 3 and generally higher during recovery (phase 4) due to its higher buffer capacity. Outflow pH increased during storage stages and never quite reached the low inflow values in exp. 3. The increase of pH during storage stages could be due to diffusive equilibration as mentioned before, but could also be related to redox reactions due

to organic matter degradation (Stumm and Morgan, 1996). As exp. 3 had oxygen free inflow apart from injection (phase 2), reduction reactions started at a lower Eh already and increased concentrations of Mn and Fe were observed during exp. 3 storages (see also Figure V-10). Other studies have shown that all these post-oxic reductions can occur in the first few cm in soil columns within a few days, especially with addition of easily degradable organic matter (e.g. Iu et al., 1981a; von Gunten and Zobrist, 1993; Schlieker et al., 2001). It seems therefore reasonable to assume redox potential to drop considerably during the main storage (phase 3) and noticeably during shorter storage stages during recovery (phase 4). This could also explain why the pH did not reach inflow values in exp. 3. The constant inflow of oxygen depleted, OC enriched water could promote constant proton consumption by redox reactions.

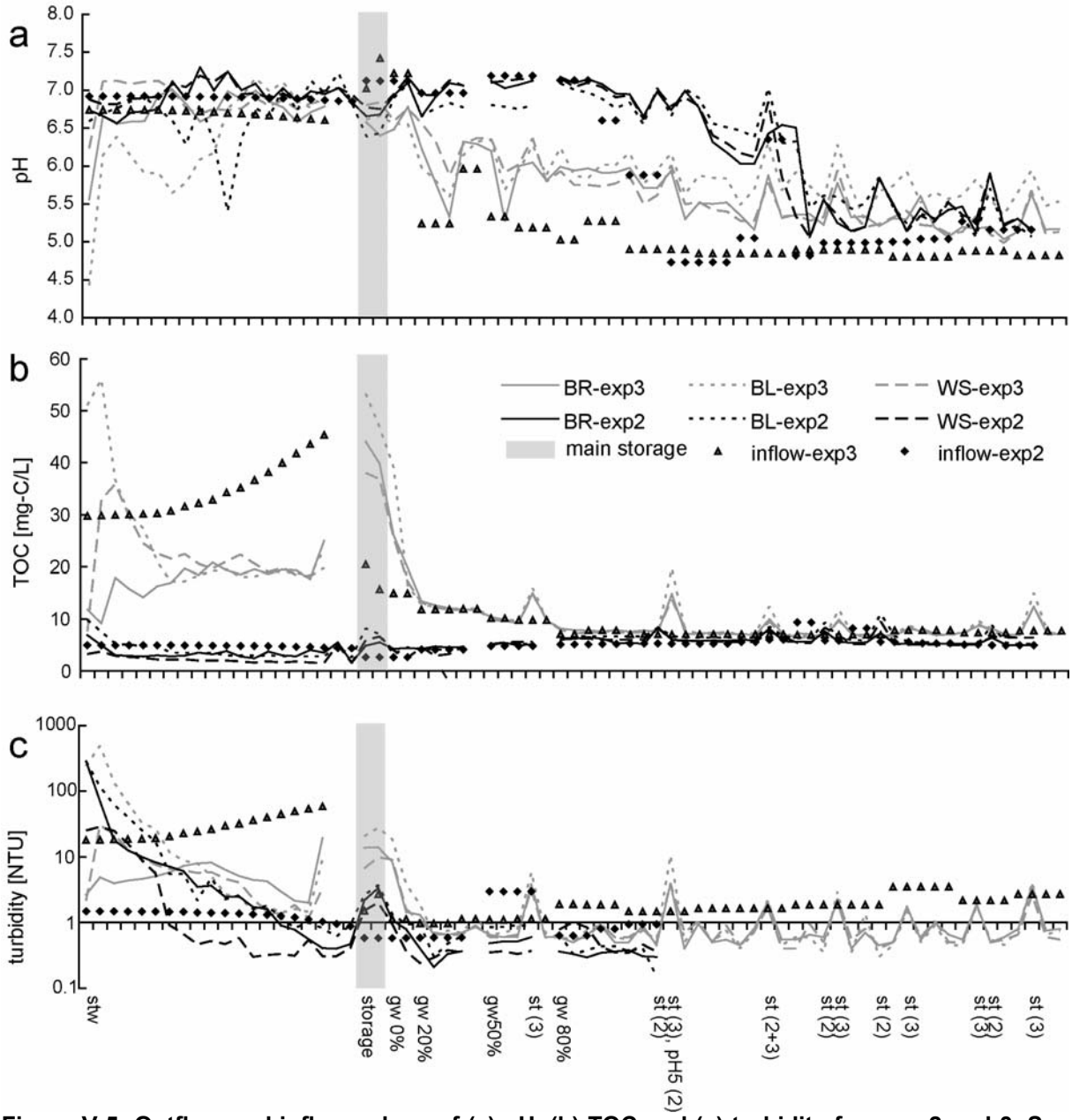

Figure V-5: Outflow and inflow values of (a) pH, (b) TOC and (c) turbidity for exp. 2 and 3. See Figure V-2 for sample labels.

V.3.2.2 Organic carbon

The direct and indirect effects of organic matter for metal behaviour have been emphasized before (see II.2.3.4, II.4.2, II.4.5). In this study two types of organic matter were present, namely the dissolved or colloidal organic matter present in groundwater and stormwater and the solid organic matter (SOM) existing in the sediment matrix, esp. in BL. The former consists of added fulvic acid and natural DOC in stormwater (see II.3.3), while SOM would be derived from peat that is commonly observed in the Brighton Group aquifer (Leonard, 1992). Peat derived humic acids contain a much higher percentage of aromatic structures, are less biodegradable, less water soluble (Thurman, 1985; Sparks, 2003) and are therefore more attached to minerals than the more soluble and smaller fulvic acids (Murphy et al., 1992; Day et al., 1994). The long-chain hydrophobic SOM therefore often enhances metal sorption while the short-chain fulvic acids often reduce it (Herms and Brümmer, 1984; Zhao et al., 2007b).

In exp. 1 (data not shown) and exp. 2 inflow TOC concentration were overall quite low (<2 mg-C/L in exp. 1 and < 5 mg-C/L in exp. 2). In exp. 3 the inflow concentration ranged from 30-45 mg-C/L and increased towards the end of the stormwater injection phase, as the organic matter had started to flocculate and settle at the bottom of the tank and biotic growth had visibly increased the TOC (see Figure V-5b). Outflow concentration were significantly lower than inflow concentrations towards the end of this phase (Figure V-5b), mostly due to deposition of organic aggregates.

Even though outflow concentrations were magnified in exp. 3, a similar pattern between all three experiments was observed (Figure V-5b). While outflow concentrations were mostly below inflow concentrations, a first peak of organic carbon was observed at the start of stormwater injection, esp. for BL sediments. This first peak was a result of the drop in ionic strength. This has been shown to lead to a different repulsive steric configuration of organic macromolecules (Murphy et al., 1992) and to colloidal release (see below). As the presence of >0.1 mg/L TOC is enough (Liang et al., 1993; Kretzschmar and Sticher, 1997) to cover solid surfaces, inducing a surface charge reversal from positive to negative, and this sorption is also rather fast, it could be assumed that surfaces would not remain uncovered for very long and most colloids in this study would be covered with natural organic matter (Day et al., 1994). This means that any particle mobilisation contributes to a release of TOC.

Further peaks in TOC (again highest for BL) were detected for each storage stage, with a positive correlation between concentration and storage time. This correlation confirmed that microbial activities were taking place during storage, converting previously immobile larger

organic molecules into smaller dissolved organic molecules (Gödde et al., 1996; Kalbitz et al., 2000; Rees and Parker, 2005; Kedziorek et al. 2008). This was supported by increased alkalinity (data not shown), which would arise from CO_2 release (Champ et al., 1979; Petrunic et al., 2005; Greskowiak et al., 2005). In addition, the simultaneous pH increase during storage stages could have promoted DOC release due to electrostatic repulsion (Avena and Koopal, 1998; Grybos et al., 2007; Brigante et al., 2008).

V.3.2.3 Turbidity

Colloids and organic macromolecules are an important third phase that is ubiquitous in the subsurface environment and have to be considered for contaminant-facilitated transport mainly during stormwater injection (see II.4.4). A high turbidity reading was observed at the start of the stormwater injection (Figure V-5c), as the lowering of ionic strength increases the diffuse double layer and hence increases repulsion between colloids and between colloids and matrix (Elimelech and O'Melia, 1990; Kaplan et al., 1993; Ko and Elimelech, 2000). Grolimund et al. (1996, 1998) reported that particle peaks arrived with the normality front and disappeared with the arrival of the Ca exchange front (see V.3.1). A similar behaviour can be seen in Figure V-5c as turbidity values were below 10 NTU after the arrival of the Ca front and values are <1NTU once ionic strength had been increased in the recovery phase. The implication of this is that once the colloids reach more saline areas in the aquifer, coagulation and deposition of colloids would occur. During ASR cycles colloids can be remobilised and redeposited. In the end the main body of colloids would be deposited at the critical salt concentration boundary as colloids cannot move much further than the perturbation (McDowell-Boyer, 1992; Bunn et al., 2002). Influenced by the amounts of water injected and withdrawn, this might potentially lead to a reduced local permeability and local increase in metal concentration.

It can also be seen that turbidity levels rise again during storages in conjunction with organic matter peaks (Figure V-5c). Turbidity measures the combined effect of light absorption and light scattering (Treweek and Morgan, 1980; Kretzschmar et al., 1999), which depend on particle size and composition. Organic macromolecules, especially when slightly coloured, will therefore increase the turbidity reading. It is therefore assumed that most of the detected turbidity during storage is due to organic matter.

V.3.3 Zn and Cu behaviour

As the first experiment had no added metals in the stormwater, the outflow concentrations of Zn and Cu were overall very low. The metal concentrations in the groundwater were actually higher than in the stormwater and the only noteworthy concentrations were measured at the start of stormwater injection (phase 2) and during the main storage phase (phase 3) when

release of entrained groundwater solution could be observed. The focus will therefore be on the metal spiked stormwater exp. 2 and 3. In- and outflow concentrations of Zn and Cu for the complete exp. 2 and 3 are shown in Figure V-6. It can be seen that the inflow concentrations are similar in both experiments during the stormwater injection (phase 2), but split for the groundwater recovery (phase 4) as previous stormwater outflow was used. This means that a higher degree of adsorption in phase 2 would result in lower inflow concentration in the following phase and was exhibited by BL in exp. 3 for Zn and Cu and also for Cu in all sediments in exp. 2 compared to exp. 3. The spike concentrations of 2-2.5 mg/L Zn and 0.65-0.85 mg/L Cu were in the middle of the range used in batch tests (see IV.2.2) and could be viewed as cumulative burden over a few small scale ASR cycles or one cycle in a larger scale project. Outflow concentrations and influential parameters will be discussed in detail in the following sections.

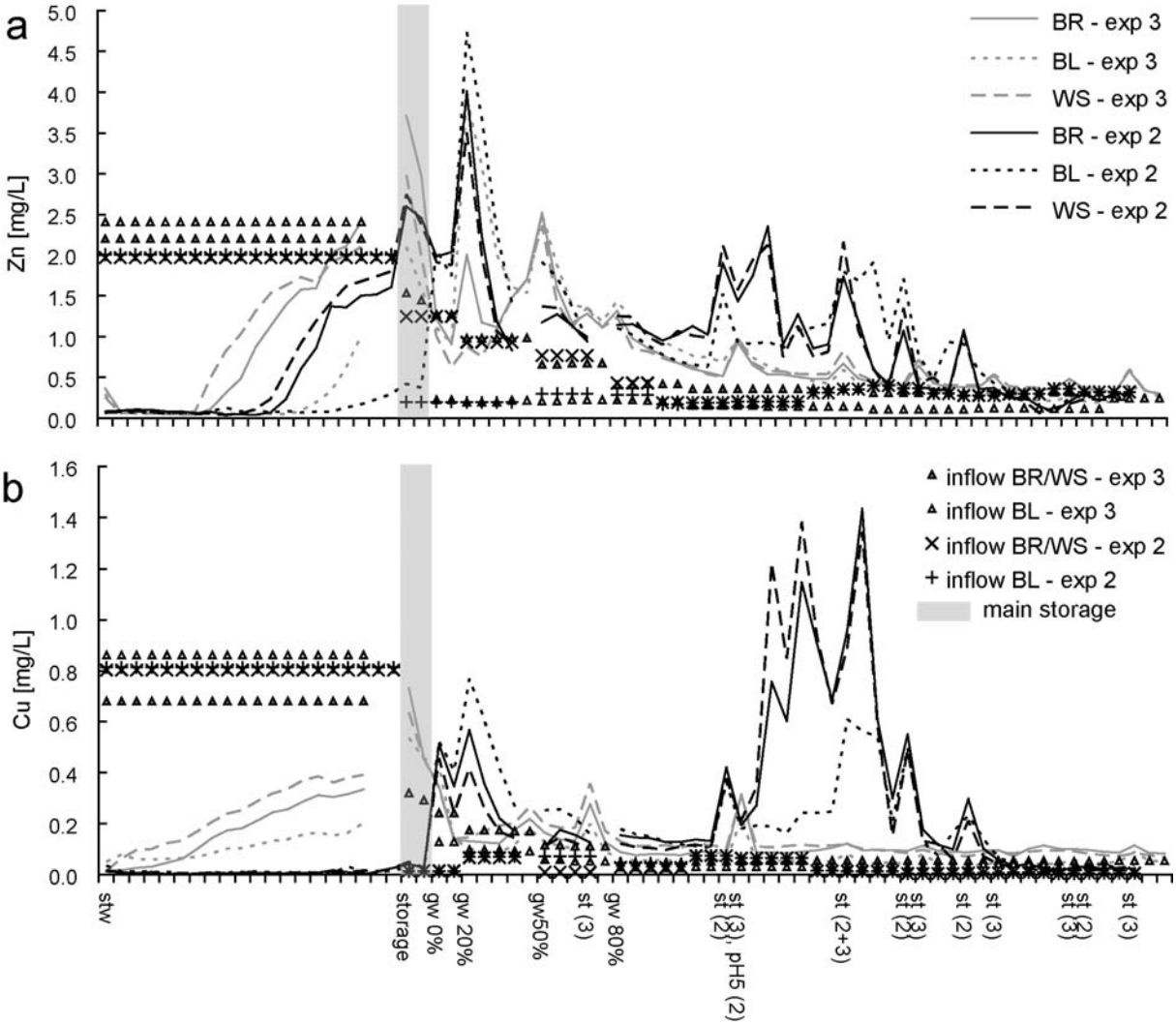

Figure V-6: Outflow and inflow concentrations of (a) Zn and (b) Cu for exp. 2 and 3. See Figure V-2 for sample labels.

V.3.3.1 Stormwater injection (phase 2) – adsorption

Heavy metal sorption at the metal loading used in this study is predominantly a specific sorption process (see II.4.1.1) for Cu (e.g. Sposito, 1984; Mesquita and Vieira e Silva, 1996;

Arias et al., 2005), while Zn sorption shifts from specific to non-specific due to competition with Cu (Arias et al., 2006; Tsang and Lo, 2006). In this study the specific sorption sites would be mainly organic coatings, Fe and Al hydrous oxides and only limited amounts of Mn hydrous oxides for WS (see Table III-10, III-11).

The injection of metal enriched stormwater showed marked differences for the two experiments. It could be observed that the adsorption was stronger for both metals in exp. 2 (Figure V-7a+b) with Cu concentration only around 10-20 µg/L for all three sediments (Figure V-6). Zn breakthrough was nearly complete for WS and BR, with 50% reached after about 650 PV, and pronounced tailing over the last 30 %. BL on the other hand only reached a maximum of 15% inflow concentration. The same order of Zn breakthrough was observed for exp. 3, but significantly earlier with 50% reached after 310 and 395 PV for WS and BR, respectively, and less tailing for BR. BL reached a maximum of 42% of inflow concentration and half the inflow concentration would be expected after about 1430 PV. When analysing this forward shift of the breakthrough curve, one has to consider that exp. 2 was done with EC meters. As observed with cations (see V.3.1), a lag due to mixing in the EC meter volume of about 100 PV could be expected and could explain a shift for Zn. In addition, the slightly different inflow concentration and sediment mass between the experiments (see also Table V-6) had to be taken into consideration and showed that Zn breakthrough in BR-exp. 3 was actually at nearly the same value as BR-exp. 2.

The added organic carbon in exp. 3 had a pronounced effect on Cu breakthrough, after only 8-20 PV the outflow was about 10 % of the inflow concentration and then slowly increased to a plateau of 53, 50 and 25% for WS, BR and BL, respectively, which cannot be explained with the absence of mixing in the EC meter.

Adsorbed concentrations of metals can be calculated for each sample as in batch tests by multiplying the difference between inflow and outflow concentration with the volume of the sample and divide it by the total sediment mass. When plotting dissolved versus accumulated adsorbed concentration like an adsorption isotherm plot (Figure V-7c+d), the same trend as in the breakthrough curves was visible. BL clearly showed the highest adsorption for Zn, with a very steep increase until about 400 mg/kg that started to even off to >500 mg/kg, while BR and WS only showed a steep increase up to about 100 mg/kg and then slowly increased to 210-250 mg/kg. These curves are typically classified as H-isotherms (see Figure II-5), which are a special case of the Langmuir or L-isotherm with a very steep initial slope (Giles et al., 1974a; Sparks, 2003; Limousin et al., 2007). On the log-log scale Zn data were also clearly divided into two segments with initial fast adsorption followed by slow

adsorption closer towards the saturation limit (Figure V-7e), often interpreted as multi-site sorption (Benjamin and Leckie, 1981a; Elrashidi and O'Connor, 1982; Msaky and Calvet, 1990). The first segment would be due to high affinity specific sorption sites. Once these are saturated the slope and adsorption decreases and sorption occurs onto low affinity sites (Tiller et al., 1979; McKinley and Jenne, 1991; Welp and Brümmer, 1998). The amount at which this change occurs could therefore be a measure of the amount of specific sorption sites for Zn, meaning that BL would have about 4 times more specific sorption sites available than BR and WS.

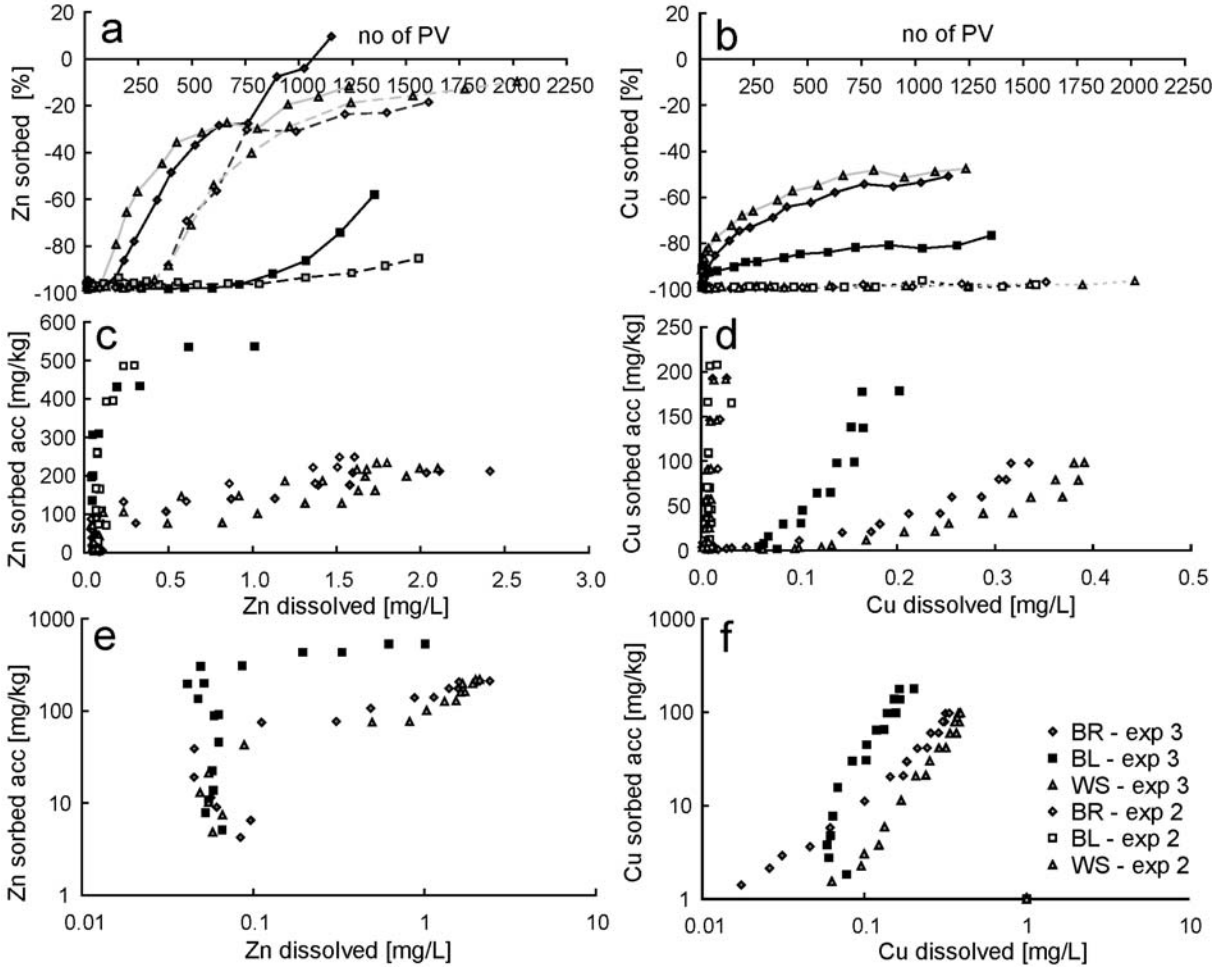

Figure V-7: Analysis of Zn (left) and Cu (right) of exp. 2+3 during stormwater injection (phase 2). (a + b): breakthrough curves with adsorbed percentage of inflow concentration versus number of pore volumes (PV) (negative values = adsorption; positive values = desorption); (c+d): adsorption isotherms with accumulated adsorbed concentration versus dissolved concentration; (e+f): adsorption isotherms in log-log scale as in c+d for data of exp. 3 only.

As would be expected from the Cu breakthrough curve, the adsorption isotherm was extremely steep for all sediments in exp. 2 (Figure V-7d), due to specific sorption (Sparks, 2003). The amount of strong affinity sorption sites was clearly not saturated in exp. 2. In exp. 3 the slope decreased in the order BL, BR, WS, but the shape was more convex than concave and no adsorption maximum was observed (Figure V-7d). This could be the start of an S-isotherm before the point of inflection (see Figure II-5). The S-isotherm occurs due to

the presence of soluble ligands such as DOC (Giles et al., 1974b; Sposito, 1984; Hinz, 2001). The adsorption is limited by the presence of the ligand at low metal concentrations. The point of inflection marks the metal concentration at which the ligand becomes saturated and adsorption can proceed unhindered. These isotherms are also observed in cases where the total metal concentration is measured including complexed species like in the present study, rather than the free metal concentration (Hinz, 2001). This was further supported by PHREEQC speciation simulation, which showed that in exp. 3 nearly all dissolved Cu was complexed to fulvic acid (see chapter VI.5.1.2 for details). On the log-log scale (Figure V-7f) data showed a more or less linear increase over the concentration range with slopes of 1.4, 2.4 and 3.7 for BR, WS and BL, respectively. These values obviously do not fit with the values for the typical Freundlich or Langmuir isotherms, which have a slope of unity at low metal loading or less at higher loadings (Dzombak and Morel, 1990; McKinley and Jenne, 1991; Sonnenberg, 2003).

The results showed nevertheless that the three sediments behaved qualitatively similar for the two metals and the two experiments. The lowest sorption capacity was exhibited by WS, followed closely by BR and was the highest for BL. As the initial Cu concentration was only about a third of the Zn concentration, direct comparison between the two metals is difficult. Note that the Cu data in Figure V-7d would be only a small corner on the same scale as Zn in Figure V-7c. Predictions about the overall shape of the Cu sorption isotherm must therefore be considered with caution. A stronger sorption of Cu compared to Zn in the absence of DOC has been reported in the literature (Calmano et al., 1993; Arias et al., 2005, Tsang and Lo, 2006) as well as a strong complexation of Cu with DOC (e.g. Cabaniss et al. 1988a,b; Benedetti et al., 1995; Christl et al., 2001) and increased transport of Cu-organic complexes (Harter and Naidu, 2001; Weng et al., 2002a; Zhao et al., 2007b). It therefore seems likely that overall sorption was stronger for Cu in exp. 2 and weaker to start with for exp. 3 than for Zn.

Further interpretation of these results requires an examination of the most influential parameters for metal adsorption, e.g. pH, CEC, complexation with inorganic and organic ligands. Breakthrough curves are also influenced by flow velocity, inflow concentrations and nonequilibrium, which will be discussed in the subsequent sections.

V.3.3.1.1 Influence of pH

During stormwater injection the pH value varied between 6.7-7.2 for BR and WS, but did not show any systematic change. It was lower at the start for BL (pH 5.8-7.2), which could be due to the higher adsorption onto BL, as adsorption would result in release of protons and therefore lower the pH (Papini et al., 1999; Sonnenberg, 2003). It was determined in the

batch tests (see IV.3.1.4) that at this neutral pH range Zn adsorption would be favourable in all sediments and changes from pH 6.7 to 7.2 would only have minimal influence. As the adsorption edge in sediment BL was between pH 4 and 5, even the lowest pH of 5.8 would not make a significant difference. For Cu the adsorption behaviour was ligand like and adsorption decreased at neutral pH, but did so for all sediments to a similar degree. As there was no systematic variation, pH seems not a critical explanatory factor for the observed adsorption behaviour.

V.3.3.1.2 Influence of cation exchange capacity (CEC)

CEC is a surrogate value deriving from (a) permanent negative charges in clays and (b) from variable charge sites from clay edges and NOM (see II.4.1.2; Baeyens and Bradbury, 1997; Voegelin et al., 2001). CEC measurements are usually performed at neutral pH in saline solutions. Measurements made at these conditions will overestimate effective CEC at lower pH and lower ionic strength (Gillman, 1981; Rowell, 1994). In the present study CEC was measured in 100 mmol/L solution, while the adsorption was occurring in 1.5 mmol/L solution. This would lead to a significant decrease in CEC due to the lower ionic strength. On the other hand the equilibration with groundwater beforehand, which was not performed for CEC measurements, would ensure coating of organic ligands on the surface as mentioned above (see V.3.2.2). This could considerably change the surface charge on sediment grains and offer more specific sorption sites.

When looking at the elution order, BL with the significantly higher CEC, clearly showed the most retardation. This sediment offers more specific sorption sites for both metals due to its organic matter content and also offers more non-specific exchange sites as seen in section 3.1. The elution order of BR and WS nevertheless is not conforming to their difference in CEC, which might be due to the slightly different amount of sediment used. When comparing Ca breakthrough curves with the Zn breakthrough curves for BR and WS (Figure V-8), it seems that Zn breakthrough starts when Ca breakthrough reaches inflow values for the first time. During the Zn breakthrough, Ca concentrations are overshooting inflow concentration, and reach inflow values for the second time together with Zn concentrations. This could be interpreted as competitive sorption behaviour (Borkovec et al., 1996; Tsang and Lo, 2006; Zhao et al., 2007b), where Ca would be desorbed by increasing amounts of Zn that arrive later due to greater retardation. Competitive adsorption behaviour would mean that specific sorption sites for Zn were exhausted and Zn sorption was shifting to non-specific, low affinity sites instead (Bradl, 2004; Egirani et al. 2005; Miretzky et al., 2006). These are much more easily desorbed than specifically sorbed metals (see V.3.3.3 and V.3.5). A similar phenomenon was not observed for BL breakthrough curves or for Cu in BR and WS. BL offered more complexing sites and Cu adsorption was governed by specific sorption and did

not show competition with Ca in accordance with other studies (Hering and Morel, 1988; Mesquita and Vieira e Silva, 1996; Agbenin and Olojo, 2004).

Overall, CEC is not a dominant factor for Cu, but influences the retardation of Zn breakthrough and increases the amount of Zn release at the first introduction of higher salinity groundwater.

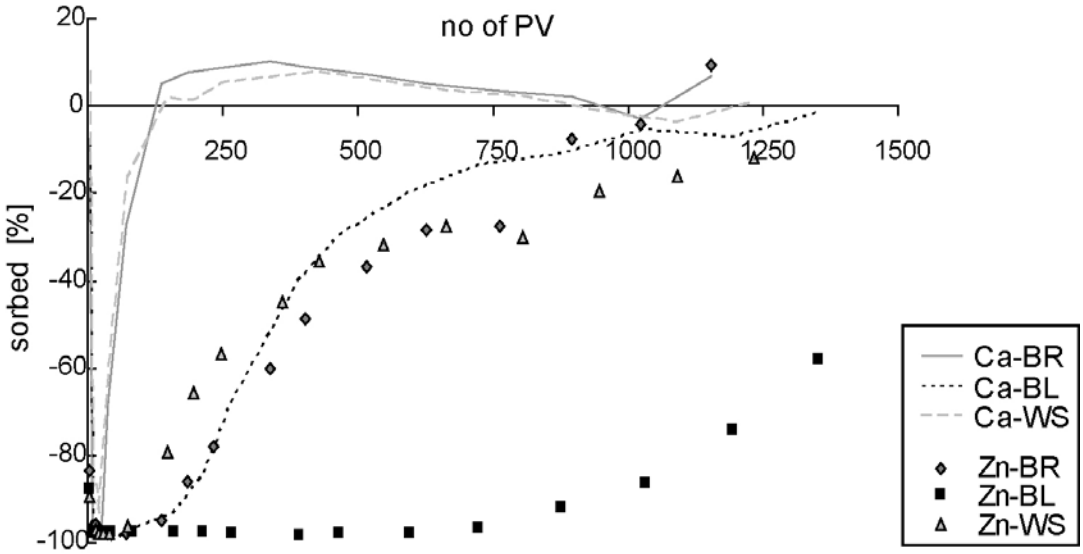

Figure V-8: Breakthrough curves of calcium and zinc for stormwater injection phase of exp. 3 (no mixing in EC meter involved).

V.3.3.1.3 Influence of organic carbon

In the presence of DOC Zn breakthrough was earlier than without, but the influence was not extreme, when accounting for mixing effects in the EC meter. On the other hand Cu breakthrough was significantly enhanced by DOC. This is in conjunction with the higher complexation capacity for Cu compared to Zn by fulvic and humic acids (Laxen, 1985; Weng et al., 2001; Milne et al., 2003). Zn complexation is relatively labile and Zn can re-complex with stronger complexing agents or adsorb onto free minerals surfaces (Schmitt, 2002; Kent et al., 2002). Zhao et al. (2007b) measured that about 98% of Cu would be complexed with DOM, while only 20-40% of Zn was complexed near neutral pH, where complexation stability is highest (Murphy et al., 1992; Milne et al., 2003; Mosley et al., 2003). Similar speciation calculation and measurements have been determined by others (McLaren et al., 1983; McBride et al., 1997; Weng et al., 2001).

The formation of organic complexes, however, is not enough to determine metal transport, as complexes can be mobile or immobile. At the experimental conditions of low ionic strength and neutral pH as present in stormwater, repulsion of organic covered surfaces is strong, as a consequence of a thick electrical double layer and steric repulsive forces (Mosley et al., 2003). This means that injected organic colloids and molecules are comparatively stable and mobile.

In the current study it seems that around 50% of Cu was associated with mobile dissolved organic matter for BR and WS, but only 20 % with BL, even though the same DOC solution was injected. BL seemed to provide more immobile sorption sites for metal-organic complexes than the other two sediments.

V.3.3.1.4 Influence of flow velocity

The flow velocity has two main influences related to relative and absolute velocity.
Firstly, a relative increase or decrease in flow velocity can lead to particle mobilisation or deposition (McCarthy et al., 1993; Ryan and Gschwend, 1994; Kaplan et al., 1995). In the current experiments, flow velocity changed significantly after the storage stages when flow was increased from zero to 0.9-3.6 mL/min to take storage samples. This could be responsible for the observed particle mobilisation (see Figure V-5c). On the other hand, particle mobilisation observed at the start of the stormwater injection phase was not induced by a change in flow velocity but was due to chemical disturbance of lowering the ionic strength significantly.

Secondly the absolute velocity determines if advective or diffusive transport is dominant and influences the adsorption kinetics. A faster flow decreases the thickness of the immobile boundary layer, which ions have to cross via film diffusion to reach the solid surface. In addition the flowing solution carries more ions for adsorption and also carries desorbed ions away. Both mechanisms allow the adsorption rate to speed up (Akratanakul et al., 1983; Kretzschmar et al., 1999). Therefore breakthrough occurs earlier with increasing flow velocity under otherwise same conditions (Puls and Powell, 1992; Miretzky et al., 2006). In the present study the flow rate during the stormwater injection varied by about 30% between the columns. This difference in flow velocity would be too small to influence the breakthrough curve (Fehse, 2004). On the other hand a fast velocity might transport the ions too fast past the surface to attain equilibrium (Appelo et al., 1990). Valocchi (1985) recommended a flow velocity of <75m/year for 1 mm dispersivity. This would be significantly slower than the 1-1.4 mL/min that was used in the current study. This would lead to the assumption that this system was not in equilibrium (see V.3.3.1.6). Overall, flow velocity appears to be a minor factor in interpreting the results.

V.3.3.1.5 Influence of inflow concentration

The adsorption behaviour is sensitive to metal concentrations and over the course of a concave adsorption isotherm it is stronger at low concentrations and decreases with increasing proximity to the saturation limit. When two runs, done with different inflow concentration under otherwise same conditions, do not superimpose, it signifies a non linear sorption isotherm (Delolme et al., 2004; Limousin et al., 2007). In the current study, Zn

sorption is not linear at the applied concentration as seen in Figure V-7c. Therefore different inflow concentration would lead to a different breakthrough curve. Miretzky et al. (2006) detected a threshold concentration above which Zn breakthrough curves superimposed, while at decreasing lower concentrations the breakthrough curves were increasingly retarded. This is in agreement with a strong adsorption at low concentration to strong sorption sites, a less strong adsorption at medium concentrations at weak sorption sites and no further adsorption at concentration above the saturation limit.
During exp. 3 Cu inflow concentrations were slightly lower for BL (Figure V-6) and showed a convex sorption isotherm (Figure V-7d). In analogy to a concave sorption isotherm, there would be limited difference between breakthrough curves at low concentration and increasing difference at higher inflow concentration. As the experiments are still in the low concentration range, where no complete breakthrough occurred, this would indicate a small influence of the inflow concentration in this study. In addition, other parameters between exp. 2 and 3 are too different to evaluate the slight difference in inflow concentration in Zn and Cu between the two runs.

In a column test the inflow concentration is also related to the solid-solution ratio as the same amount of metal will be passed through in a different volume of solution. Even though similar volumes were needed to reach complete breakthrough (Fehse, 2004), the intermediate values before complete breakthrough are not equilibrium values (Seidel-Morgenstern, 2004), but depend on the solid-solution ratio and the inflow concentration. The implication for this study is that all incomplete breakthrough data cannot be compared easily. It also precludes the comparison of Zn with Cu data, as the inflow values for both were different and Cu breakthrough curves were never complete.

V.3.3.1.6 Influence of non-equilibrium

As could be seen for Zn (Figure V-7a), the breakthrough curve exhibited a broad front and extensive tailing before reaching inflow concentration, which is the product of non-equilibrium conditions. They cause an earlier start of the breakthrough than predicted by local equilibrium assumption and a slower approach of complete breakthrough (Brusseau et al., 1989; Kookana et al., 1994). Non-equilibrium conditions can be an outcome of physical, hydraulic and/or chemical origin and can exist inside the column even when inflow and outflow concentration are the same (Barna et al., 2007). The mechanisms of physical and hydraulic non-equilibrium (e.g. hydrodynamic dispersion, diffusion) are closely related and affect both conservative and reactive molecules, while the chemical equilibrium (e.g. rate-limited adsorption, non-linear sorption behaviour, intrasorbent diffusion and/or the heterogeneity of the surface with strong and weak sorption sites) only affects reactive molecules (Appelo et al., 1990; Kookana et al., 1994; Brusseau, 1995). Therefore chemical

non-equilibrium can be differentiated from the other forms by changing the flow rate. Flow interruption eliminates hydraulic factors completely and therefore can be used to exclude physical non-equilibrium. If a non-reactive tracer is not affected by it, this indicates that physical non-equilibrium is not important (Reedy et al., 1996; Brusseau et al., 1997).

As in this study no classical elution test was performed, only the breakthrough curve can be examined. The start of the Cu breakthrough curve was steep for all sediments in exp. 3 and increase occurred within the first 8 PV. The start of the Zn breakthrough on the other hand did not occur before 80 PV in all cases. As hydraulic non-equilibrium like preferential flow would have the same effect on Cu and Zn, it seems unlikely to explain the Cu behaviour. Colloidal transport on the other hand seems highly likely as Cu-organic complexes could travel fast through the column due to size exclusion effects (Enfield et al., 1989; Grolimund et al., 1996; Kretzschmar and Sticher, 1997). This is another indicator that Zn complexation would be considerably smaller (see section 3.3.1.3) than Cu complexation, as Zn would otherwise show the same colloidal breakthrough in exp. 3. Nevertheless, hydraulic effects did definitely exist in exp. 2 due to the use of the EC meter. The tailing of about 100 PV in the elution curve of EC (Figure V-3) suggested that low flow pockets developed in the meter.

The storage (phase 3) following the stormwater injection phase could be interpreted as a flow interruption test. While non-reactive ions like chloride and bromide (data not shown) showed no major difference after the interruption, outflow concentrations of Zn and Cu were drastically higher than inflow concentrations and higher than before the interruption in all cases. Even though kinetic effects cannot be excluded totally (Tsang and Lo, 2006), this behaviour cannot be explained by rate limited sorption, as it would result in the contrary effect, namely a decrease of metal concentration during storage (Brusseau and Rao, 1989). It is therefore obvious that other forms of chemical non-equilibrium would have to be taken into account for Zn and Cu (see V.3.3.2). The existence of strong and weak sorption sites and non-linear sorption for example are both more prominent for BL. Accordingly the start of the Zn breakthrough curves is even broader for BL than for BR and WS.

Overall, physical non-equilibrium was of minor importance for the flow in the column, while chemical non-equilibrium would have been prevalent throughout the stormwater injection phase due to non-linear sorption and surface heterogeneities.

V.3.3.1.7 Comparison with other studies

The retardation factor Rf is defined as the number of pore volumes needed for the outflow concentration to reach 50% of the inflow concentration and would be unity for a non-reactive tracer (van Genuchten and Wierenga, 1986; Tran et al., 1998). The linear distribution

coefficient K_d could be calculated from the retardation factor with the following equation (Fetter, 1993):

(V-1) $Rf = 1 + K_d * (\rho/\theta)$,

where ρ is the bulk density (mean 1.85 g/cm^3 in this study) and θ is the porosity (mean 0.3 in this study) of the column sediment. For a Freundlich adsorption isotherm, however, the retardation is a function of concentration (Kookana et al., 1994). Based on the batch and column tests, it is not considered realistic to estimate Freundlich adsorption isotherms, and retardation and linear K_d values will be estimated and assessed, as was done for batch tests (see IV.3.1.1). Table V-4 and V-5 show the retardation and linear K_d values from the Zn breakthrough curves. Unfortunately the stormwater phase was not long enough to generate sufficient breakthrough for Zn in BL, so only estimates could be used here. The breakthrough of Cu in exp. 2 was too incomplete to even warrant an estimate and the breakthrough curves are too gentle in exp. 3 to give a reliable assessment. Therefore this and the next section will be dealing primarily with Zn.

When comparing the retardation factor for Zn with other values in the literature (Table V-4), parameters discussed above have to be considered. As expected, it could be seen that at lower pH of the solution and/or the soil the Rf values tend to be lower. Also, soils with higher CEC tend to have a higher retardation. It was noted also that apart from Davis et al. (2001a) all inflow concentrations are a magnitude higher than in this study, which would tend to result in lower retardation values. Similarly most studies use about two magnitude higher ionic strengths as background solution, which would principally also lead to smaller retardation factors. When comparing flow velocities in mL/min, one has to take into account the size of PV, so a better indicator would be pore water velocity, which is usually not reported. Therefore PV per min is used as an indicator of pore water velocity in Table V-4. It can be seen that this study had the lowest flow rate and therefore would probably have higher retardation factors compared to other studies. All these factors would therefore increase retardation factors in this study, and the values are accordingly found in the upper range but within a similar magnitude to the literature.

Table V-4: Retardation factor and calculated linear K_d of Zn from exp. 3 and from selected other column experiments including additional important experimental parameters.

Rf	K_d (after equation (V-1))	solution pH	material, pH / CEC [cmol/kg]/ organic carbon* [%]	solid-solution ratio [kg/L]	PV [mL]	flow velocity [PV/min]	inflow conc. [mg/L]	background solution	reference
<20	<4	6.5	silica sand, na / <1 / 0	0.250	243	0.21	10	artificial stw	Sansalone, 1999
26	10	5	sandy loam 4-5 / 2.5 / 0.6	0.099	100	na	100	EC 6.4 mS/cm; 25 mg/L Cu	Smith et al., 1999
30	11	na	kaolinitic soil 5.2 / 2 / 1.7	0.089	~450	0.069	60	0.01 M $CaCl_2$	Liu et al., 2006
~8	~1.8	na	loamy sand 5.3 / 2.0 / 2.0	0.471	132	$3.8 * 10^{-6}$	67	5 mM $Ca(NO_3)_2$	Hinz and Selim, 1994
~40	~10	na	fine silty soil 6.6 / 8.6 / 0.8	0.095		$7.6 * 10^{-6}$			
~100	~40	6.5	loamy soil 4.1 / 0.6 / 0.9	0.020	4	0.13	60	0.01 M $CaCl_2$; competing metals	Voegelin et al., 2002
~400[1]	~125[2]	7	sandy loam, 6.4 / 2.9 / 0.3	0.008	4.7	0.64	0.6	1 mM $CaCl_2$	Davis et al., 2001a
~400	~135	6	sandy loam, 8 / 10 / 0.25	0.0081	0.31	0.28	20	0.1 M $CaCl_2$	Miretzky et al., 2006
445	153			0.0072		0.38	20	0.1 M $NaNO_3$	
500	172			0.0065		0.28	20	0.1 M $NaNO_3$	
~700	~240			0.0046		0.28	20	0.025 M $CaCl_2$	
~800	~275			0.0040		0.28	10	0.1 M $NaNO_3$	
395	60	7	sand BR 4.3 / 0.9 /1	0.010	7.5	0.044	2	stormwater, 1.5 mM	this study, exp. 3
310	58		sand WS 7.4 / 1.3 / 1.4	0.011					
~1430	~210		sand BL 2.8 / 8.5 / 4.1	0.002					

* assumed organic carbon = 0.5 organic matter, na: not available; 1 Davis et al. (2001a) uses bedvolumes of 9.9 mL in graphs, while the PV is only 4.7 ml in text; 2 using porosity of 0.47 and bulk density of 1.5 g/cm^3 as per article

V.3.3.1.8 Comparison with batch results

Comparison of batch and column experiments are not as straight forward as would be desirable due to a number of general differences (Harter and Naidu, 2001). Firstly, batch experiments represent a closed system with static equilibrium between adsorption and desorption, as desorbed molecules stay in contact with the surface and the concentration of metals in solution decreases continuously over the course of the adsorption test. Conversely, column experiments are an open system, where desorbed molecules are transported away and inflow concentrations stay constant, reaching dynamic or steady state equilibrium (Fehse, 2004; Miretzky et al., 2006; Limousin et al., 2007). Compared to a decreasing metal concentration in batch tests, a constantly high metal concentration in column tests would drive the equilibrium towards more metal sorption after the Le Châtelier's principle and as the reverse reaction is prevented, sorption must reach saturation before complete breakthrough

can occur (Harter and Naidu, 20001; Miretzky et al., 2006). Secondly, in batch tests all the surface areas are accessible to the solution and new surfaces might even be created due to disaggregation or rubbing off during the shaking process, while in columns some surface areas are not accessible due to grain-grain contacts and dead end pores that are not in equilibrium with the current solution (Harter and Naidu, 2001). Thirdly, batch results can be solid-solution ratio dependent data (see IV.3.1.3), while in columns the solid concentration is constant and percolated solution volume increases over time until equilibrium is reached. Intermediate values of column breakthrough curves are therefore also solid-solution ratio dependent, but at the equilibrium endpoint adsorption is independent from the solid-solution ratio, as the same ratio would be reached with different solid concentrations (Fehse, 2004). If there is no correction made for the solid-solution ratio then batch data can lie either above (higher solution volume) or below (higher solid amount) column endpoint sorption data. Fourthly, column experiments are flow derived retardation values, meaning that hydrodynamic parameters like preferential flow, hydrodynamic dispersion, immobile regions etc are included in the data (Limousin et al., 2007). This is obviously closer to the actual field situation and column tests are therefore more realistic. In addition, redox conditions might be different in column experiments as, for example, stagnant areas can evolve. As a result of the above mentioned differences, which do not exert their effect in the same direction, batch and column test results are not consistent (e.g. Hinz and Selim, 1994; Bajracharya et al., 1996; Tran et al., 1998; Sonnenberg, 2003).

The importance of solid-solution ratio has been widely discussed for batch tests (see IV.3.1.3), and it is usually stated that the difference in solid-solution ratio between batch and column tests make comparison rather difficult (Harter and Naidu, 2001). Nevertheless, discussions about the solid-solution ratio dependence of column data are rather scarce. For batch tests plots of K_d values versus solid-solution ratio are usually employed and could be transferred to column studies using either the retardation factor or K_d value. When plotting the Zn retardation factors from Table V-4 versus the solid-solution ratio on a log-log scale, a significant linear relationship between the two parameters, with decreasing retardation factor with increasing solid-solution ratio is apparent (Figure V-9). Obviously the retardation factor and the solid-solution ratio (see equation V-5) are not independent to each other as the solid-solution ratio decreases with increasing retardation factor during a column test. Similarly, K_d batch data are not independent of solid-solution ratio, as K_d values include the volume of the solution (see equation IV-1). The consistency over a number of studies is striking and will be resolved below.

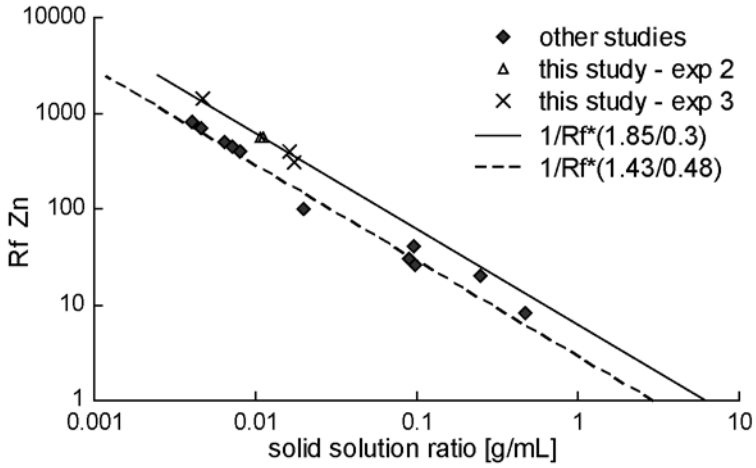

Figure V-9: Column study retardation factors (Rf) for Zn and solid-solution ratio show a significant first order law dependency with increasing Rf value for increasing solid-solution ratio, as has been reported for batch studies. Linear regression of "other studies" data (see Table V-4) gave a linear coefficient of determination R^2=0.9866. See text below for explanation of lines.

Variations between column derived K_d values with batch derived K_d values (Table V-5) showed a rather irregular pattern in this study. BR K_d values were similar for both tests, while WS batch K_d values were significantly higher and BL batch K_d values were considerably lower than the corresponding column K_d values. Although BR and WS values were derived at rather similar solid-solution ratios during either experiment and had similar retardation in the column experiments, interestingly WS showed a much higher sorption capacity during batch test. On the other hand, BL, which had the lowest sorption capacity during batch tests, showed the highest during column tests, even though the solid-solution ratio was so much smaller.

To test, if the difference between column and batch data was only due to of solid-solution ratios, Fehse (2004) proposed to normalise both data by dividing the dissolved concentration by the corresponding solid-solution ratio (see IV.3.1.3). This assigns a relationship between the per g solid adsorbed mass and per g solid dissolved mass rather than concentration. The slope of the corresponding graph of adsorption concentration versus dissolved/SSR would be equivalent to multiplying the K_d values by the solid-solution ratio:

(V-2) $K_{d\,SS}$ = adsorbed conc. / (dissolved conc. / SSR) => $K_{d\,SS} = K_d * SSR$

Fehse (2004) found that a normalised plot of adsorption concentration versus dissolved/SSR of his column and batch data and other studies aligned well with only minor divergence. The latter was assigned to the difference in accessible surface area and preferential flow in column experiments. When applying this normalisation to data of this study, column $K_{d\,SS}$ values are the same for all sediments, but still did not agree with batch $K_{d\,SS}$ values.

A value of unity for column $K_{d\,SS}$ can be easily explained, when looking at the mathematical equations. As

(V-3) $SSR = M / (Rf * PV)$ and

(V-4) $PV = \theta * (M / \rho)$

a substitution of PV from equation (V-4) in equation (V-3) yields

(V-5) $SSR = M / [Rf * \theta * (M / \rho)] = \rho / (Rf * \theta)$

and re-arranging equation (V-1) and substituting this and equation (V-5) into equation (V-2) to arrive at K_{dSS}

(V-6) $K_{dss} = [(Rf-1) / (\rho / \theta)] * [\rho /(Rf * \theta)] = (Rf – 1)/Rf$

Table V-5: Retardation factor (Rf), calculated linear Kd (after equation (V-1)) of Zn from column experiments compared to batch Kd values around pH 7, corresponding solid-solution ratios (SSR) and normalised Kd SS values [dimensionless] after Fehse (2004). See text for further explanations.

Zn	Rf	column K_d [L/kg]	SSR [kg/L]	column $K_{d\ SS}$	batch K_d [L/kg]	SSR [kg/L]	batch $K_{d\ SS}$	$1/K_{d\ SS}$ [%]
BR-exp2	550*	90	0.011	1.00	80	0.22	17.6	5.7
BR-exp3	395	60	0.016	0.99	27	0.22	5.94	17
BL-exp2	-	-			40	0.22	8.8	11
BL-exp3	~1430	~210	~0.005	~0.98	-	-	-	
WS-exp2	550*	94	0.011	0.99	400	0.22	88	1.1
WS-exp3	310	58	0.017	0.99	200	0.22	44	2.3

* values have been decreased by 100 PV to account for the mixing in the EC meter

With a sufficiently high number for Rf, this is equivalent to unity as can be seen in Table V-5 and could also be calculated for all the other studies presented in Table V-4. Equation (V-5) also explains why a plot of Rf versus SSR (Figure V-9) results in a straight line on log-log scale. This rational graph has a constant of bulk density divided by porosity. For the current study with a bulk density of mean 1.85 g/cm³ and a mean porosity of 0.3, this is represented by the solid line in Figure V-9. As the packing density was generally lower in the other studies with a mean bulk density of 1.43 g/cm³ and a mean porosity of 0.48, this results in a lower constant (dashed line, Figure V-9).

When analysing the batch $K_{d\ SS}$, equation (IV-1) and (V-2) can be re-written as:

(V-7) $K_{d\ SS} = [(C_{ini} – C_{diss}) * V/M] / [C_{diss}/ (M/V)] = (C_{ini} - C_{diss}) / C_{diss} = C_{ini} / C_{diss} – 1$

with C_{ini} being the initial metal concentration and C_{diss} being the final metal concentration in a batch test. This is equivalent to the reciprocal value of the sorbed [%] commonly plotted for breakthrough curves. The reciprocal batch K_{dSS} values (last column in Table V-5) are not reaching 50% breakthrough equivalents (=Rf), which means that the metal loading in the batch tests was not in a comparable range to the columns test. The batch tests had a sediment mass of 10 g and received a maximum of about 6.5 mg/L * 0.045 L solution = 0.29 mg Zn, which resulted in a Zn loading of 29 µg/g (Table V-6). In comparison column tests received a much higher loading at the 50% breakthrough point (Table V-6). If batch values

were plotted in Figure V-7c, they would be hardly visible near the origin due to the different scale. A direct comparison of batch and columns results seems therefore not to be feasible.

Table V-6: Comparison of Zn loading in column test at 50% breakthrough (= Rf) and batch test.

experiment	material (M) [g]	PV [mL]	Rf = 50% breakthrough [no of PV]	total solution [L]	Zn conc. [mg/L]	mass of Zn in solution at Rf [mg]	Zn loading at Rf [µg/g]
BR-exp. 2	53.75	8.12	550	4.47	1.97	8.80	164
BR-exp. 3	44.75	8.79	395	3.47	2.20	7.64	171
BL-exp. 3	41.75	7.61	1430	10.9	2.41	26.2	627
WS-exp. 2	44.25	6.25	550	3.44	1.97	6.77	153
WS-exp. 3	43.50	8.13	310	2.52	2.20	5.55	128
batch	10			0.045	6.50	0.29	29

A different aspect that can be taken from Table V-6 is that BR breakthrough was nearly the same for exp. 2 and exp. 3 due to the lower initial mass and the higher inflow concentration in exp. 3. This means that the additional organic matter did not seem to have an influence on Zn sorption onto BR.

Despite the difficulty of quantitatively comparing column and batch data, it can be stated qualitatively, that at pH 7 BR and WS behaved similarly in column tests with a lower sorption capacity than BL, while in batch tests BL and BR had a similar lower retention capacity compared to WS. In other words, BL showed an increase in its sorption capacity from batch to column tests, while WS exhibited a decrease. This finding needs some further explanation and might be explained by chemical differences. WS has a natural pH of >7, while BR (pH 4.3) and BL (pH 2.8) are of increasingly acidic character related to organic acids, exchangeable H^+ and/or Al^{3+} and non-exchangeable forms of acidity on minerals as in functional hydroxyl groups bound to Fe or Al. This pool of reserve acidity gradually releases acidity into the active form when adding a base (McBride, 1994), which corresponds with the slow response of BR and BL observed during pH adjustments in batch tests (see IV.3.1.4). It seems that the fresh sediments have a number of surface sites occupied by difficult to exchange Al and Fe ions. While these would have been released and flushed away in the column equilibration (phase 1), they would be still present in the adsorption solution in batch tests. A main difference in procedure between batch and column experiments was therefore the fact that pre-equilibrium with a few litres of groundwater was undertaken for the columns, while only one washing of 50 mL was undertaken for pH adjusted batch experiments. It was noted that batch K_d values did increase for BR and BL with one washing compared to no washing (see IV.3.1.6). From this it could be concluded that pre-equilibration of sediments significantly altered the character of the surface sites.

In addition, the batch pH adjustments (with 0.1 M NaOH) were done in low ionic strength stormwater solution and not in higher ionic strength groundwater solution like in the columns. Increased turbidity in samples due to colloid dispersion in low ionic strength was observed in BR and BL sediments during batch tests and would be stabilised due to increased electrostatic repulsion when covered with organic matter (Kuo and Baker, 1980; Liang et al., 1993; Karathanasis, 1999). The addition of Na hydroxide might also have lead to precipitation of colloidal hydroxides (McBride, 1994). It could be seen in batch solutions that BL (~7-fold) and BR (~ 3-fold) showed a significant increase of dissolved Fe and dissolved organic carbon with increasing pH (Figure IV-4) in agreement with findings from Schnitzer and Kodama (1966) and Kuo and Baker (1980).

The above means there are a number of processes to take into consideration. (a) dissolution of Fe minerals is highly likely and could even be promoted by organic matter (Liang et al., 1993; Kent et al., 2002; Dries et al., 2005); (b) newly formed hydroxide colloids could be stabilised by DOC, which would hinder their aggregation and sedimentation (Jardine et al., 1989; Liang and Morgan, 1990); (c) DOC could complex free Zn^{2+} (Düker et al., 1995; Warwick et al., 1998; Dries et al. 2005) and even more strongly free Fe^{3+}(Schnitzer, 1969; Liang et al., 1993; Kent et al., 2002), and the complexes are not sorbed strongly at neutral pH (Nowack and Sigg, 1996; Schmitt et al., 2003); (d) any Fe that is not complexed by DOC or precipitated would decrease zinc sorption due to competition, especially when present in concentrations a magnitude higher than Zn (Harter and Naidu, 2001) and (e) dissolved organic matter could compete for sorption sites with Zn (Davis and Leckie, 1978; Elrashidi and O'Connor, 1982; Malandrino et al., 2006). The exact extent and combination of all factors is not known (Tessier et al., 1996), but overall all these mechanisms would lead to a decrease in Zn sorption onto the solids (McBride and Blasiak, 1979; Düker et al., 1995; Dries et al., 2005). This would happen to a greater extent for BL than BR, as BL has more organic material to be dissolved and an even lower pH to start with. It is therefore reasoned that the observed differences between column and batch sorption behaviour is mainly due to the difference in sediment preparation between the two techniques.

Likewise, Grolimund et al. (1995) could show good agreement for Cu in batch, column and flow through reactor experiments after an extensive washing procedure, which was not produced beforehand. The same authors also noticed a substantial decrease in Al and DOC concentration after washing. The flow through reactor is a helpful intermediate technique with recirculation of the solution and a fixed solid-solution ratio similar to batch tests, but with a flow setting similar to groundwater systems. More studies with all three techniques would be

desirable to help quantify factors that are responsible for deviations in sorption parameters derived from different techniques.

V.3.3.2 Storages (phase 3 and shorter stages during phase 4)

Samples taken after storage (labelled st) represent a mixture of the solution that was subject to storage in contact with either the filter material or the aquifer material and about 40% of some fresh inflow to achieve a large enough sample for analysis. In most cases, where the inflow concentration was below the measured outflow concentration, it can be assumed that the actual stored water concentration would be even higher than measured due to the dilution effect during sampling. The main storage (phase 3) resulted in an increase in all parameters compared to the last injection sample and, apart from Cu, also compared to inflow values (Figure V-4 to V-6). A trend of higher storage values in exp. 3 than in exp. 2 was also found for most parameters. During subsequent shorter storages in the final recovery (phase 4), major ions did not show concentration changes, while turbidity, TOC, Zn and Cu were generally increased.

A number of mechanisms have to be considered for the main storage (phase 3) and to a lesser extent for the shorter storages (phase 4): (a) non-equilibrium effects and diffusion in and out of micropores; (b) reductive dissolution of Mn and Fe oxides in combination with (c) organic matter degradation; (d) particle mobilisation due to change in flow velocity when restarting flow for sampling; (e) release of metals from organic matter and oxides and (f) competition for sorption sites in the now closed system.
As mentioned in V.3.3.1.6 non-equilibrium can lead to a change in solution concentration towards the direction of previous inflow values. Apart from the spiked Cu and Zn, all other ions had higher concentration in the previous groundwater compared to the injected stormwater. This means that groundwater diffusing out of micropores or other stagnant area during main storage would lead to increased concentrations for nearly all parameters, but to a decrease in Cu and Zn. This mechanism could therefore explain increased major ion concentration, but obviously not Zn behaviour as those concentrations were higher than injected stormwater. During the later storages (phase 4) though, hysteretic desorption leads to higher concentrations during flow interruption (Brusseau et al., 1997) and is one reason for the observed increased metal concentrations.

Reductive dissolution of Mn and Fe oxides visible as an increase in Fe and Mn concentrations has been observed when waterlogging soils for extended periods (Iu et al., 1981a; Ma and Dong, 2004; Petrunic et al., 2005; Grybos et al., 2007) or in ASR operations close to the injection well, where the injected organic matter has accumulated (Vanderzalm et al., 2003; Greskowiak et al., 2005). The timeframe for this to happen depends on the

amount of oxygen and nitrate available for reduction at the start and the amount of organic matter that can be oxidised in exchange. It has been observed that complete nitrate reduction can be achieved within a few days especially when promoted by organic matter (von Gunten and Zobrist, 1993; Stuyfzand, 1998a; Grybos et al., 2007). Apart from this indirect effect on reductive dissolution due to lowering of the redox potential, organic ligands can also directly promote oxide dissolution (Lovley et al., 1996; Nowack and Sigg, 1997; Davis, J. A. et al., 2001). In agreement, the release of Mn and Fe was much higher in exp. 3, where additional organic matter was available (Figure V-10). Concentrations also decreased with decreasing storage time as the redox values would not have had time to decrease sufficiently over the shorter storage times. Additionally, metals previously bound to organic or inorganic surface sites could be released into solution during organic matter degradation and oxide dissolution (e.g. Calmano et al., 1993).

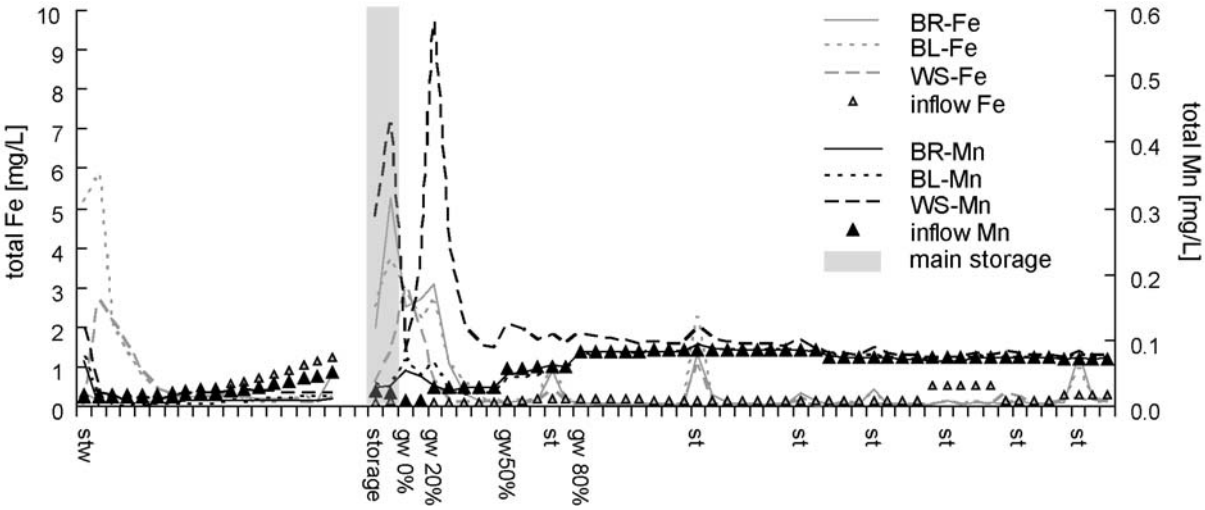

Figure V-10: Outflow and inflow concentrations [mg/L] of Fe and Mn for exp. 3. The grey bar indicates the 2-week storage phase at the end of the stormwater injection.

Turbidity (Figure V-5c) generated during storage could originate from dissolution of inorganic or organic coatings that would release previously cemented particles and from released organic matter (Liang et al., 1993; Seaman et al., 1995; Kretschmar et al., 1999). It is possible that the change in flow velocity after storage was enough to mobilise previously deposited and newly generated colloids (see V.3.3.1.4) thereby carrying attached metals with them (see V.3.2.3) and leading to increased total metal concentrations. The datasets for dissolved metals were incomplete and values were sometimes below detection limit, but on average dissolved Fe was about 40% in both experiments and dissolved Mn 53% and 95% in exp. 3 and 2, respectively. About 50% and 95% of each Zn and Cu were measured in the dissolved phase in exp. 3 and 2, respectively. This suggests a mainly colloidal metal release in exp. 3 compared to a dissolved metal release in exp. 2.

Metals previously bound to organic or inorganic surface sites could be released into solution during organic matter degradation and oxide dissolution (Calmano et al., 1993; Davranche

and Bollinger, 2001; Olivie-Lauquet et al., 2001). Grybos et al. (2007) provides evidence that metal released by OM are often greater than metals released by oxide dissolution and can also happen under aerobic conditions, if DOC release is promoted by high pH (Avena and Koopal, 1998). Nevertheless, dissolution also exposes new surface sites to the solution (Iu et al., 1981b) and readsorption can take place and could lead to a decrease in metal mobility during storage (Iu et al., 1981b; Förstner, 1993; Ma and Dong, 2004). The overall results will therefore be influenced by competition between molecules in solution for complexation with the released dissolved organic matter and sorption sites on the solid.

This highlights another significant issue. During storage the otherwise open column system is closed and resembles a batch test system, where an equilibrium between adsorption and desorption is being established. In addition, the solid-solution ratio in this newly closed system is now much higher than in batch tests. As seen above (Figure V-9), with increasing solid-solution ratio there is a first order decrease in Rf or, in analogy, of the distribution coefficient, resulting in a much lower distribution coefficient (i.e. K_d <1). In addition, there is also competition of ions in the system similar to batch test, which also results in lower sorption capacity (Tran et al., 1998). In combination this would lead to the observed desorption of Zn and Cu during storage periods.

When plotting dissolved versus adsorbed concentration for shorter storages during the groundwater recovery (phase 4), a good linear relationship for desorption (negative K_d) of between 0.6 and 1.1 L/kg (Table V-7) for both Zn and Cu was established, which matches quite well with the above calculated solid-solution ratio related decrease of K_d <1. It can be seen that K_d is most negative for BL in all cases, followed by WS and BR. This means that BR desorbed the most, while BL retained the most. It could also be seen that K_d values were less negative in exp. 3 compared to exp. 2 for both metals. This shows that the addition of DOC increased desorption during storage corresponding to the higher metal concentrations in main storage samples from exp. 3.

In exp. 3, where conditions were more constant, a general decrease in storage peak concentration over time is observed. As the height of the concentration peak in the elution curve during flow interruption is a sign for the deviation from equilibrium (Brusseau et al., 1997), it shows that the system is moving towards equilibrium conditions. In exp. 2 peaks are more erratic due to changes in pH, but the last storage phase also showed only a very small peak.

Table V-7: Linear regression for desorption (=negative) distribution coefficient (Kd) from (phase 4) storage stage samples obtained from dissolved versus sorbed concentration plot and corresponding linear coefficient of determination (R^2).

	Zn		Cu	
	K_d [L/kg]	R^2	K_d [L/kg]	R^2
BR-exp. 2	-1.35	0.8837	-1.66	0.9329
BR-exp. 3	-0.83	0.9155	-0.98	0.9993
BL-exp. 2	-1.68	0.8553	-1.91	0.8567
BL-exp. 3	-1.03	0.9718	-1.08	0.9816
WS-exp. 2	-1.66	0.8822	-1.98	0.9355
WS-exp. 3	-0.75	0.9300	-0.95	0.9979

V.3.3.3 Recovery (phase 4) – desorption

For the recovery (or elution) flow was reversed and four stages can be distinguished, in which the fraction of groundwater in the inflow solution increased stepwise from 0, 20, 50 to 80%. Accordingly, the fraction of stormwater and with it the concentration of Cu and Zn decreased stepwise. Additionally, the inflow pH was decreased from pH 7 to 5 with the 20% inflow in exp. 3 and later in the 80% stage in exp. 2. The lowering in inflow concentration in the first stage resulted only in a slight release of metals, while slight desorption was usually triggered with change in ionic strength (increase in slope in Figure V-11). Some adsorption occurred in the first two stages of exp. 3 for WS (maximum 4.3% for Zn and 2.7% for Cu) and BR (maximum 0.9% for Zn and 2.2% for Cu). Overall, the rate of desorption decreased with each step but concentrations stayed above inflow values for most of the experiment, showing extensive tailing behaviour. In addition, metal release was triggered by the decrease in pH in exp. 2. Zn release showed a small increase at change to pH 6, and both metals showed the biggest increase after the introduction of pH 5 inflow solution. While BL had the highest release upon changes in ionic strength, it showed delayed release of metals upon changes in pH. Desorption seems to have been reached final values for exp. 2, while it was still increasing in exp. 3. Overall, Zn leached to a greater extent than Cu in both experiments and both metals showed less desorption during exp. 3.

As in this study, elution is often observed to have a more pronounced tailing than breakthrough curves (Grolimund et al., 1995; Delolme et al., 2004; Seidel-Morgenstern, 2004). This is due to the fact that desorption requires activation energy to overcome the adsorption energy (McBride, 1989) and also involves reversing diffusive penetration (Barrow, 1986a) and can therefore be several orders of magnitude slower than adsorption (Ainsworth et al., 1994; Limousin et al., 2007). Additionally, desorption of metals with diluted salts mainly desorbs exchangeable or non-specifically adsorbed metals and hysteretic behaviour is therefore commonly observed (McLaren et al., 1986; Fotovat et al., 1997). Column leaching results can therefore only be indicative for short term leaching losses, but do not necessarily reflect long-term losses (He et al., 2006).

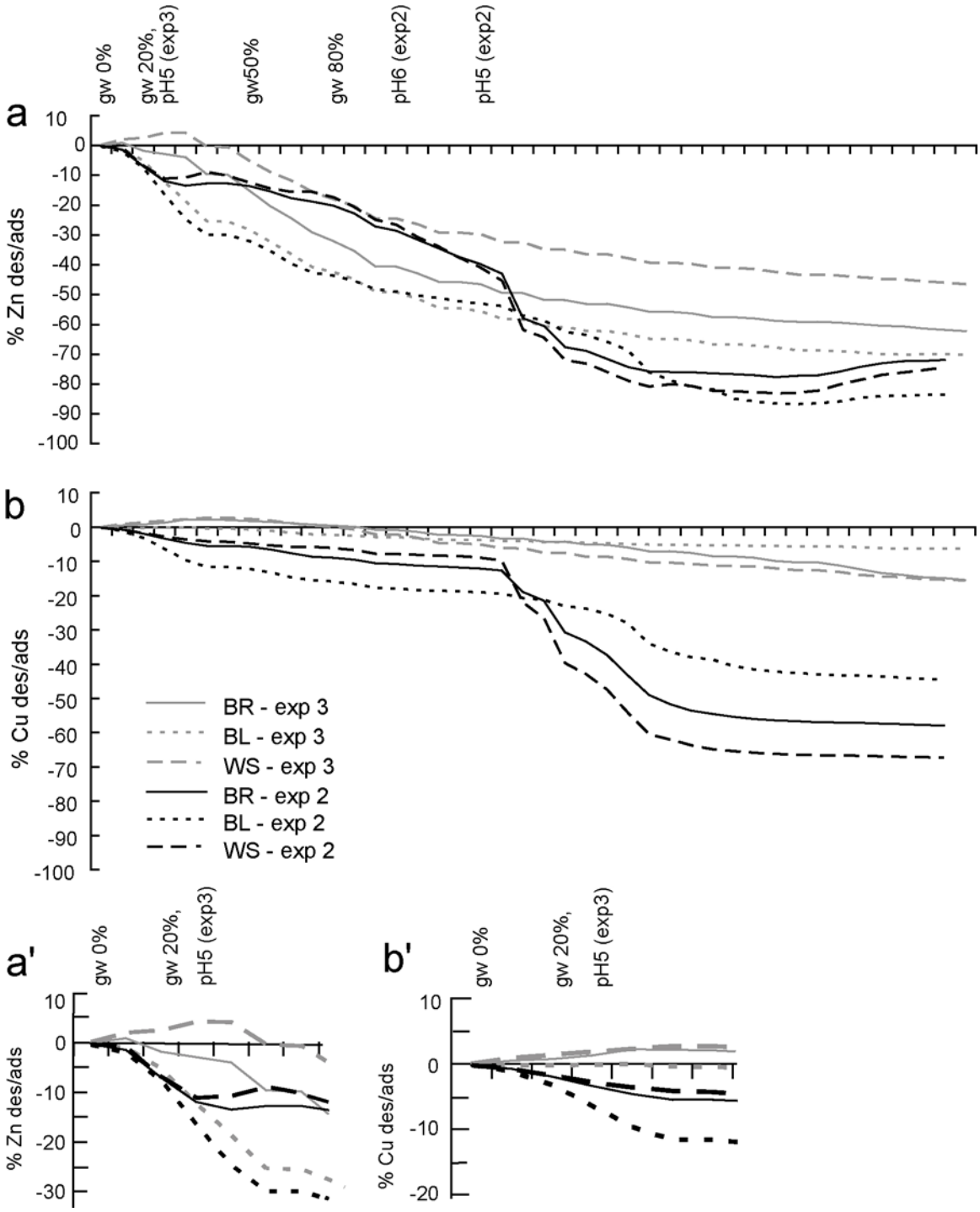

Figure V-11: Desorption of metals during recovery phase. Percentage of accumulated sorbed concentration of recovery (phase 4) in relation to accumulated sorbed concentration of stormwater infiltration (phase 2) for (a) Zn and (b) Cu without storage samples. Insets (') show the first two stages in more detail. Negative values = desorption, positive values = adsorption. See Figure V-2 for sample labels.

V.3.3.3.1 Ionic strength effects

The first stage of the recovery (phase 4, 0% groundwater) did not involve a change in ionic strength, only a decrease in inflow concentration and a reversal of flow direction. While adsorption for both metals in exp. 3 for BR and WS occurred, it resulted in a slight desorption

for both metals in exp. 2 and in exp. 3 for BL. The metal release was accompanied by a release in TOC and increased turbidity (see Figure V-5c).

Flow reversal is not usually performed in column tests, but is obviously occurring in single well ASR techniques. As most particulate matter would be intercepted at the column inlet, these particles are more readily mobilised on flow reversal as they only have a short distance to travel to the outflow. This effect is exploited when backflushing wells (Pyne, 1995) and would explain the increased TOC and turbidity observed in this study due to particle release. It could also be assumed that metal sorption would progress from the inlet towards the outlet during injection with less contaminated sediment near the outlet, if breakthrough was not complete. The above generates two phenomena. After flow reversal, particulate and organic matter bound metals are leached out of the column due to the short distance to the former inlet and newly introduced metals are adsorbed at the less contaminated former outlet. The latter would explain the continued adsorption of Cu. In addition, the concentration of metals is lower in the inflow solution, as it has flown through the column once before, and lower still when it reaches the former inlet, where the bulk of adsorbed metal would be located. This dilution would result in elution of exchangeable adsorbed metals as observed in exp. 2.

In the subsequent stages the ionic strength of the inflow solution increased from 1.5 (stormwater) to 45 mmol/L (80% groundwater), mainly due to an increase in Na (~100 fold) and Mg (~20 fold), while Ca concentrations only increased slightly (1.25 fold). Iron (~4 fold) and Mn (~10 fold) concentration also increased in the inflow. The highest release of Cu and Zn was found at the first increase of salinity and resulted in concentrations much higher than the previous inflow concentration for Zn (Figure V-6). This desorption effect is often called “snow plow effect” (Starr and Parlange, 1979; Dunnivant et al., 1992; Seidel-Morgenstern, 2004) and is due to reversible ion exchange reactions.

An increase in ionic strength leads to desorption due to (a) competition for surface sites (Shuman, 1986; Barrow, 1986a), (b) activity decrease of metals in solution and possible formation of ionic pairs, especially chloro complexes (Herms and Brümmer ,1984; Appelo and Postma, 1999a) as well as (c) compression of the electric double layer (Appelo and Postma, 1999a). The magnitude of the desorption can vary logarithmically with ionic strength (Saiers and Hornberger, 1999) and is more pronounced for Zn when divalent ions are dominant in the solution (Voegelin et al., 2002, 2003). The latter effect is due to an increased competition between Ca and Zn that can both be specifically sorbed on Fe oxides (Herms and Brümmer, 1984; Barrow, 1986a). Exp. 2 showed that the first increase in ionic strength effectively desorbed easily exchangeable metals, and a further salinity increase leached Zn

most likely as chloro complex (Norrström, 2005). Cu leaching on the other hand was not increased significantly after the first salinity increase.

V.3.3.3.2 pH decrease effects (exp. 2)

Analogous to adsorption where protons are released, protons can be re-adsorbed during desorption (Voegelin et al., 2003). This resulted in higher pH outflow values than inflow values as long as desorption was continuing (see Figure V-5a). Nevertheless there was a significant increase in desorption in exp. 2 after the introduction of groundwater adjusted to pH 5 (Figure V-11). Immediate release of metals on pH decrease is a common phenomenon (Barbosa and Hvitved-Jacobsen, 1999; Kent et al., 2002; Voegelin et al., 2003). In agreement with adsorption edges (see II.4.5 and IV.3.1.4) Zn release is usually increased at values pH < 7 and Cu at pH <5 (Herms and Brümmer, 1984; Tiller et al., 1984a). This is due to competition of protons with metal surface complexes (He et al., 2006; Kent et al., 2007), an increase in positive surface charge (Davis and Leckie, 1978) and a decrease in hydrolysed metal species (Sparks, 2003). The retarded response to pH decrease in BL resulted again from its higher buffer capacity as discussed previously. As ionic strength and pH were adjusted in conjunction in exp. 3, the influence of pH was not distinguishable.

V.3.3.3.3 Organic carbon and redox effects (exp. 3)

A major difference between exp. 2 and exp. 3 was the addition of organic carbon during stormwater injection, which also resulted in initially higher DOC values for the recovery water (Figure V-5b). The DOC in the recovery inflow solution would contain mostly non-sorbing DOC, as the solution flowed through the column already and sorbing fractions would have remained in the column (Gu et al., 1996a). Therefore TOC outflow and inflow values were nearly identical during recovery (Figure V-5b). Competitive exchange of stronger sorbing fractions of DOC against weaker sorbing fractions cannot be ruled out though (Gu et al., 1996b). In addition, desorption of NOM is usually low in solutions with pH <7 and high in chloride (Dunnivant et al., 1992; Gu et al., 1996b; Naidu and Harter, 1998). Accordingly, desorption is significantly lower for Cu in exp. 3, as Cu forms strong organic complexes that are less likely to desorb. In addition, Eh values were reduced in exp. 3 due to oxygen free inflow solutions. Biodegradation of organic matter can occur under aerobic, denitrifying, and Mn-reducing conditions, but is usually increased with decreasing Eh (Furrer et al., 1996). It can release previously immobile organic matter and break down larger molecules to smaller ones, which could offer new sorption sites for metals.

Ionic strength and pH also affect organic matter. With increasing ionic strength the diffuse double layer is increasingly compressed. This favours coagulation of organic molecules and colloids (Liang and Morgan, 1990; Kretzschmar et al., 1999; Weng et al., 2002a). This

formational change of organic molecules can lead to more adsorption of organic molecules due to less steric repulsion (Weng et al., 2007). This also has the effect that functional groups are less accessible, meaning adsorbed metals are less likely to desorb (Murphy and Zachara, 1995). This seems to strongly affect sorption behaviour of Cu. Since Cu would mostly occur as metal-organic complex (Weng et al., 2001), some more complexes might have been able to adsorb to the matrix as salinity increased and enclosed Cu was not able to desorb. While it has been shown that organic matter disperses at higher pH and leads to increased metal desorption (Naidu and Harter, 1998), organic matter shows increasing adsorption with decreasing pH. This enhanced the effect of ionic strength increase and yielded desorption minima between pH 5-6 for Cu in batch desorption tests (see IV.3.2.5; He et al., 2006). Cu desorption was therefore only 15% in exp. 3.

The effect on Zn is less dramatic, consistent with its lower stability constant of organic complexes, although considerable proportions of Zn might still exist in complexed forms (Weng et al., 2002b; Milne et al., 2003; Delolme et al., 2004). Final desorption was reduced by 12% for BL and BR and by 28% for WS compared to exp. 2. Interpretations are complicated by the fact that a number of parameters were changed at the same time. Inflow solution was of lower pH, lower oxygen content and higher organic carbon concentration in exp. 3 compared to the first half of recovery phase in exp. 2. This obviously makes distinguishing the effect of any one factor impractical. Nevertheless, it seems that the presence of organic matter dampens the effect of decreased pH. One would expect a higher desorption of Zn during the first half of exp. 3 due to the decreased pH, but desorption behaviour was very similar for BL in both experiments, lower for WS and with more desorption occurring only partially for BR (Figure V-11). The increased solid organic matter in exp. 3 apparently leads to a decreased Zn desorption.

Lower Eh conditions might also be responsible for precipitation/dissolution reactions, especially for the start of the recovery phase, where adsorption was observed for Cu and Zn in BR and WS, even though Zn breakthrough was complete and existing sorption sites should have been saturated. The generation of new sorption sites seems therefore likely. It coincides with increased values of Fe and Mn (see Figure V-10) in solution. Even though Fe and Mn speciation is not confirmed, they are likely to be the result of reductive dissolution and/or release from organic matter degradation (Grybos et al., 2007). The dissolution of these coatings would entail that fresh mineral surfaces could become available for metal adsorption especially for Zn. In addition, Cu^{2+} in solution can be reduced by Fe^{2+} and lead to Fe precipitation, favoured at pH >5.5 (Matocha et al., 2005; Hutchins et al., 2007). This

reaction might decrease over the course of the experiment due to the flushing of dissolved Fe and due to the lowering in pH.

V.3.3.3.4 Mass balance

In accordance with Figure V-11, a mass balance (Table V-8) showed that for all three sediments desorption was more pronounced in exp. 2 compared to exp. 3 for both metals and more pronounced for Zn compared to Cu in both experiments. Even though there is considerable release of metals during storage (see V.3.3.2), the absolute mass released was small due to small sample volumes. In total, significant amounts of Cu were retained in the sediments even after prolonged leaching, while Zn was leached out of the sediments to a greater extent.

Table V-8: Summary on accumulated Zn and Cu onto column aquifer sediments. Adsorption (positive) during stormwater injection (phase 2) and desorption (negative) during all combined storage samples (phases 3 + 4) and during recovery (phase 4).

	Zn					Cu				
mg/kg	stormwater injection	storage phases	recovery	sum	**% retained**	stormwater injection	storage phases	recovery	sum	**% retained**
BR-exp. 2	249	-8	-193	48	19	193	-3	-119	72	37
BR-exp. 3	212	-5	-132	75	35	98	-1	-15	82	84
BL-exp. 2	487	-7	-419	62	13	207	-2	-94	111	54
BL-exp. 3	540	-2	-370	167	31	179	0	-11	168	94
WS-exp. 2	236	-10	-190	37	15	193	-3	-143	48	25
WS-exp. 3	220	-4	-102	114	52	98	-1	-15	82	84

On one hand, some column studies report that elution results in complete desorption of the previously adsorbed metal (e.g. Hogg et al., 1993; Voegelin et al., 2001; Delolme et al., 2004) and increases with addition of DOC (e.g. Dunnivant et al., 1992, Kent et al., 2000; Miretzky et al., 2006). On the other hand, batch studies provide evidence for desorption hysteresis even after a number of desorption steps (e.g. Elrashidi and O'Connor, 1982; Arias et al., 2005) and was found for the used materials in batch desorption studies (see IV.3.2). Batch studies (IV.3.2.5) showed that 20-8 % of Zn and only 1-8% of Cu were desorbed with pH 5 adjusted groundwater without DOC addition after three desorption steps. These values are a bit lower than the column values of exp. 2. However, the same differences between column and batch tests as discussed for adsorption (see V.3.3.1.8) are valid for desorption. This means that desorption would be greater in column studies due to the flushing of desorbed ions and also because of the magnitudes greater volume used during desorption in column experiments.

V.3.4 Arsenic behaviour

A different problem is posed by geogenic metals. A major concern in ASR operation is the dissolution of in-situ and authigenic pyrite during oxidation of previously anoxic aquifers and the concomitant release of heavy metals like arsenic, nickel and zinc (see II.2.3.6, II.4.3; Welch and Stollenwerk, 2003). ASR operations in the USA used for drinking water storage have reported As recovery concentrations greater than the threshold for American drinking water standards of 10 µg/L (e.g. Arthur et al., 2002; Mirecki, 2004; Jones and Pichler, 2007), while Australian drinking water standards are 7 µg/L (NHMRC, 2004). Australian irrigation long term trigger values are 100 µg/L, while freshwater aquatic ecosystem (95% level of protection) trigger values are 13 µg/L for As(V) (ANZECC and ARMCANZ, 2000). As most stormwater ASR schemes would be used for irrigation, drinking water values do not apply, but threshold values for freshwater ecosystems where backflushed waters from ASR systems might be discharged to, would have to be taken into account.

While inflow values were always below 10 µg/L (detection limit 2 µg/L), outflow values from the pyrite containing sediments BL were considerably higher than this (Figure V-12), even ranging close to the irrigation trigger value of 100 µg/L (one sample is higher). Between 60-100% of this As was in dissolved form. The use of anaerobic groundwater during equilibration and the introduction of organic matter in exp. 3 yielded the highest concentrations and even resulted in slightly elevated values for BR. Increased concentrations occurred at the start of the injection phase and during prolonged storage phases (Figure V-12). WS outflow concentration on the other hand never exceeded 4 µg/L.

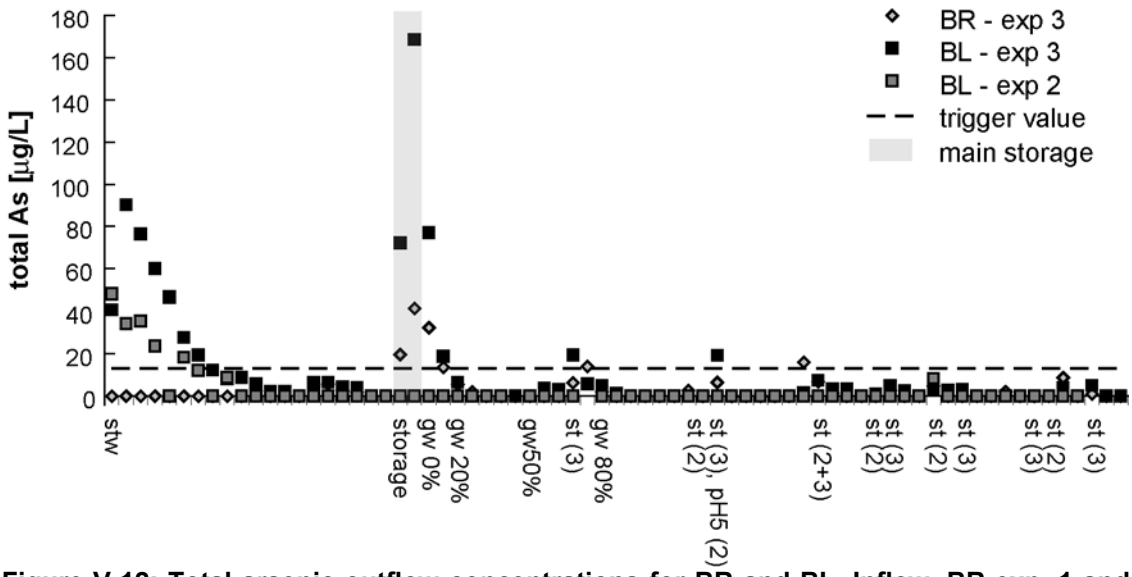

Figure V-12: Total arsenic outflow concentrations for BR and BL. Inflow, BR exp. 1 and 2 and WS outflow concentrations were <10 µg/L. 95% level of protection trigger value for freshwater aquatic ecosystems is 13 µg/L As(V) (ANZECC and ARMCANZ, 2000). See Figure V-2 for sample labels.

When previously anoxic aquifers that contain trace amounts of pyrite or similar minerals are exposed to higher Eh values due to introduction of oxygen and nitrate, pyrite oxidation

releases Fe and heavy metals incorporated in the mineral structure (Bahr et al., 2002). The reaction is favoured at higher pH and by oxygen over nitrate (Cullen and Reimer, 1989; Stuyfzand, 1998a; Smedley and Kinniburgh, 2002). While most metals will be released as cations, As will form oxyanions that show different surface complexation reactions than cations and are subject to competition with other anions esp. phosphate (Smedley and Kinniburgh, 2002; Goh and Lim, 2005; Amirbahman et al., 2006). The released Fe^{3+} is not stable and will result in the precipitation of Fe hydroxides, which are able to scavenge a number of previously released heavy metals by coprecipitation and/or adsorption (Stuyfzand, 1998a; Cappuyns and Swennen, 2005).

The presence of organic matter alters these reactions. Firstly, it increases the rate of oxidation of the kinetically hindered reaction, secondly it can reduce Fe precipitation by complexation with Fe and thirdly it can reduce readsorption of anions by increasing the negative charge on precipitated hydroxides (Kalbitz et al., 1998; Bauer and Blodau, 2006). All three mechanisms would increase the As concentration in solution, which agrees with the finding that As concentration were highest in exp. 3. The use of oxygenated groundwater for equilibration in phase 1 of exp. 2 could have flushed released As out of the column or could have resulted in its scavenging by Fe hydroxide precipitates. During the following storage phases, these newly formed Fe hydroxides could be dissolved again, releasing As once more (Horneman et al., 2004; van Geen et al., 2004; Swartz et al., 2004). Increased As values are therefore also found after storage intervals in this study and at field sites (Vanderzalm et al., 2003, 2007).

The presence of pyrite in any target aquifer is therefore an undesirable feature. Site investigation should always contain mineral analysis for trace metals and monitoring of As in the recovered water is highly recommended. It is especially important that water recovered after some period of storage should not be discarded into streams unless metal analysis and water quality risk assessment confirms otherwise.

V.3.5 Metals retained in the sediment

Following the completion of column experiments, the sediments were subject to sequential metal extractions to distinguish between different sorption sites. The three fractions are commonly described as: first fraction from exchangeable sites, second fraction from dissolutive reduction of Fe and Mn (hydr-)oxides (reducible) and the third fraction from oxidation of organic matter (oxidisable). For comparison, unused sediments (‘fresh’) washed once with groundwater solution were included and showed much lower values. Significant differences between the three sediments and Zn and Cu were found (Figure V-13).

The mass balance of amounts of Zn and Cu (Table V-9) introduced via inflow volume, compared to recovered amounts in solution and sediment showed that Zn mass balances were reasonable, while considerable amounts of Cu, especially for exp. 3 (up to 48%), were not accounted for and retained values were too low when compared to Table V-8. The missing Cu is highly likely to be readsorbed in step 3.

Overall, Zn distribution (Figure V-13a) showed a common pattern across the three sediments with the highest fraction in the exchangeable fraction, the second highest in the reducible fraction and the smallest fraction associated with organic matter. The total amounts retained in the sediments increased from BR < WS < BL reflecting the respective sediments' CEC. While there was no significant difference for BR, the first and second fraction increased for BL and WS from exp. 2 to exp. 3. An increase in the exchangeable fraction could be associated to the longer exposure to lower pH value in exp. 3, which resulted in higher competition with protons on the other fractions.

Cu distribution (Figure V-13b) showed the same order as Zn in BR, while Cu was much higher in the reducible and oxidisable fraction in BL and lower in exchangeable fraction in WS compared to Zn. The total amounts retained increased from WS < BR < BL. General pattern stayed the same in BR and WS when comparing exp. 2 with exp. 3. In contrast, BL had a significant increase in the reducible fraction and a decrease in the oxidisable fraction in exp. 3.

A common feature between Zn and Cu is an overall increase in the magnitude of metals retained from exp. 2 to exp. 3, which agreed with the overall decreased leaching in exp. 3 (Figure V-10). Another congruence was the increase in the reducible fraction. The organic matter fraction also stayed about the same for all cases with the exception of Cu in BL.

From the previous discussions, looking at the above results triggers the following questions:
a) Why are Cu amounts in the exchangeable fraction higher than Zn for BR, when it is usually stated that Cu is specifically sorbed.
b) Why is the reducible fraction increased in all sediments from exp. 2 to exp. 3, when reductive dissolution would have reduced available sorption sites?
c) Why is the organic matter fraction reduced for Cu in BL in exp. 3, when organic matter degradation should be working in all sediments and for both metals?
d) Why are amounts of Zn and Cu in the organic fraction about the same for BR and WS, when Cu has higher complexation stability than Zn?

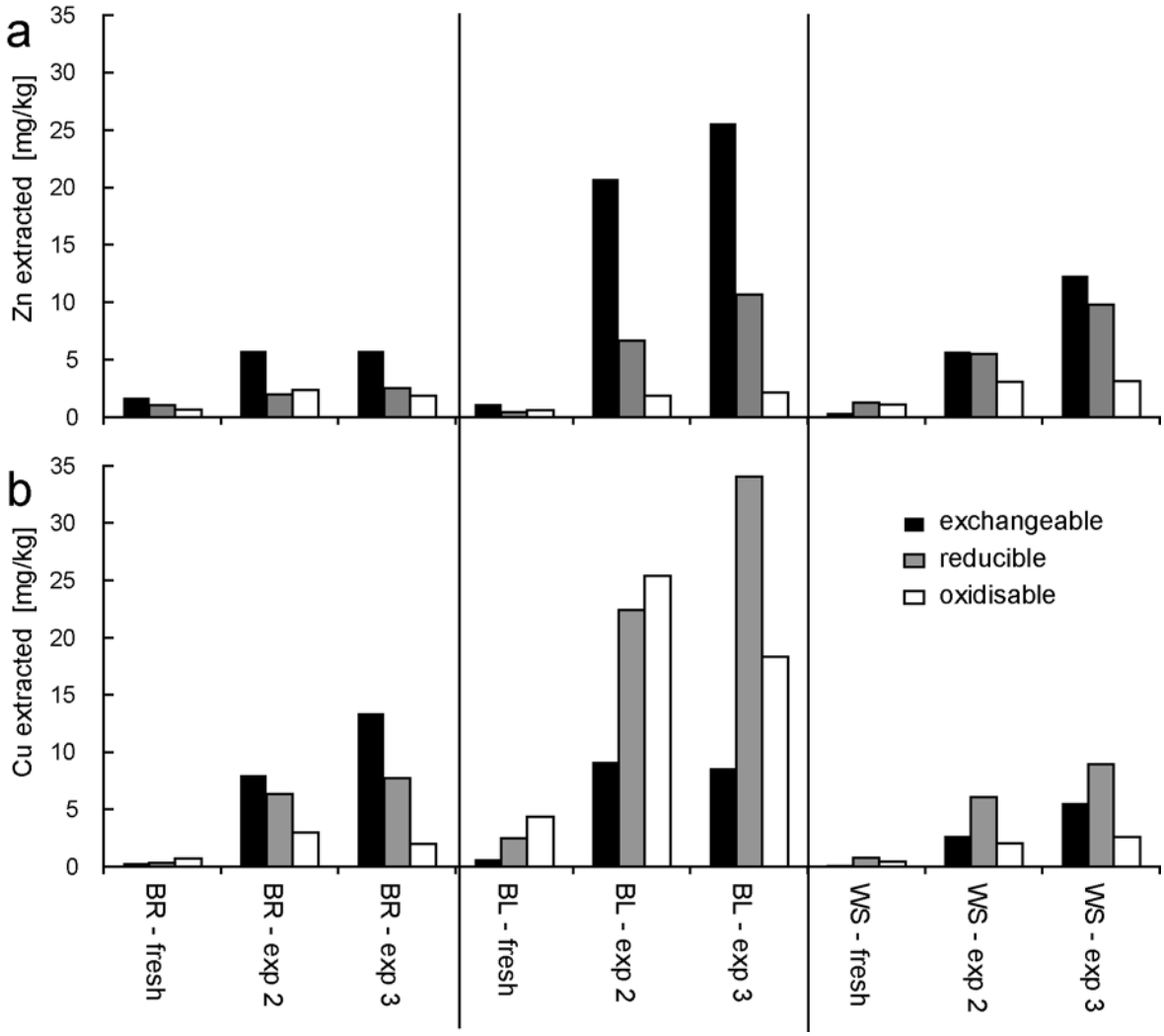

Figure V-13: Extracted metal concentrations for (a) Zn and (b) Cu for three steps: non-specifically adsorbed (exchangeable), specifically adsorbed (reducible) and very strongly bound (oxidisable).

For the interpretation of these questions a closer look at the method is necessary. While sequential metal extractions are commonly used to investigate the binding forms of metals in order to assess potential mobility, bioavailability etc., there are a variety of problems associated with it. As with batch and column tests there are a number of various methods described for metal extraction ranging from single to nine step extractions, variations in extracting agents and molarity, solution pH and extraction time for example, making comparison between different studies a challenging task (e.g. Martin et al., 1987; Sutherland, 2002; Silveira et al., 2006). In addition, samples were air dried before extraction to avoid biological processes during storage, which would especially change speciation of metals from the anaerobic sediments in exp. 3 (Morabito, 1995; Davidson et al., 1999). Upon aeration Cu and Zn could be transferred to the reducible fraction and exchangeable/acetic acid extractable fraction (Miller et al., 1986b; Kersten and Förstner, 1987). Both observations were made in this study to some degree.

Regardless of the exact procedure there are a series of different problems present including low reproducibility, especially when reagents are not strong enough to completely dissolve the target phases or when the reagent is not specific enough to target only one phase (Rendell et al., 1980; Kheboian and Bauer 1987; Kim and Fergusson, 1991) as well as potential for substantial redistribution by readsorption of elements among phases during extractions (Rendell et al., 1980; Kheboian and Bauer, 1987; Ahnstrom and Parker, 1999). A critical problem is also the lack of reference material with known trace metal phase distributions, which hinders the possibility of validation (Kheboian and Bauer, 1987). The defined fractions are therefore more operational than actual (Tessier et al., 1979), which means interpretation of results has to be made with caution (Nirel and Morel, 1990). Kim and Fergusson (1991) suggested therefore a new classification with increasing sorption strength: weakly adsorbed to various phases and/or carbonate bound (step 1), strongly adsorbed to organic matter and/or Mn oxides and amorphous Fe oxides (step 2), and very strongly bound to organic matter and/or other oxidisable species (step 3).

Step 1: non-specifically adsorbed metals

Acetic acid is used to extract weakly adsorbed and carbonate bound trace metals. Compared to other organic acids it is characterised by low complexation (Slavek et al., 1982; Naidu and Harter, 1998), but it has been found to dissolve poorly crystalline hydroxy phases as well as being able to displace covalently bonded trace metals (Miller et al., 1986b). Apart from the postulated ion-exchange it was found to extract recently adsorbed metals from most inorganic and organic phases (Luoma and Jenne, 1976) due to proton competition and chelating properties (Slavek et al., 1982). With respect to question (a) this means that this fraction could contain Cu desorbed from organic matter, explaining higher values. For BR and to an extent for WS, it also seems that the other two fractions are saturated, so Cu would have to switch to less specific sorption sites (Tsang and Lo, 2006). If Cu had precipitated as cupric ferrite during the experiment this phase would dissolve at the lower pH and could have lead to higher concentration of Cu in the first fraction (see VI-4.3).

The high amounts of Zn in the first fraction in BL could be related to competition with Fe and Al (Figure V-14) (Halder and Mandal, 1979). The increased Al and Fe values in fraction 1 for BL and BR are another evidence of the acidic nature of these sediments.

Step 2: specifically adsorbed metals

Hydroxylamine hydrochloride is a mild reducing agent known for its selective dissolution of Mn oxides (Rendell et al., 1980; Kim and Fergusson, 1991), while it affects amorphous Fe oxides only to a small degree (<10%) (Kheboian and Bauer, 1987; Beckett, 1989). It does not

dissolve crystalline Fe oxides, organic matter or sulfides (Tessier et al., 1979; Miller et al., 1986a), but can displace freshly adsorbed metals from oxides and organic matter (Luoma and Jenne, 1976), if there were any left after step 1.

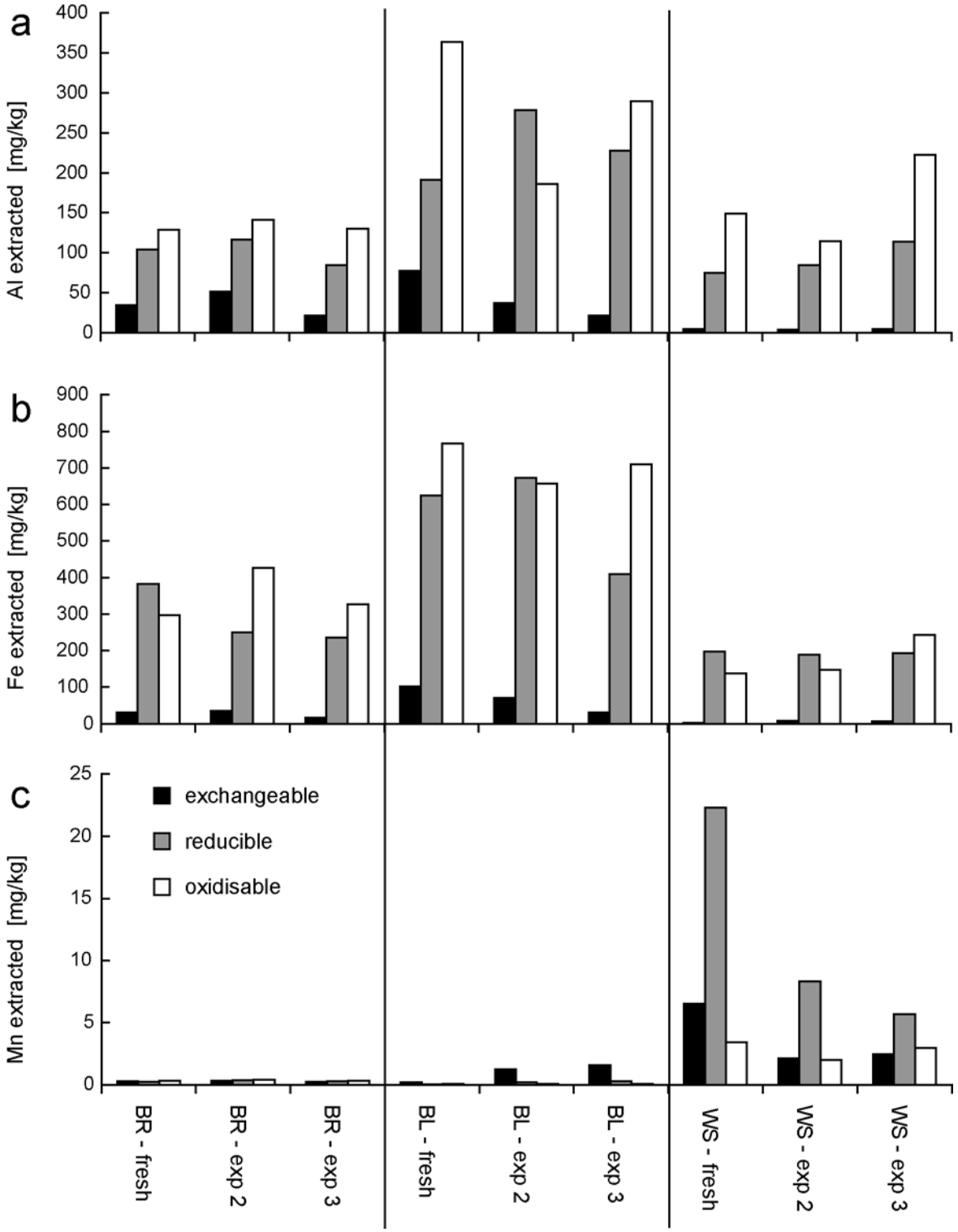

Figure V-14: Extracted (a) Al, (b) Fe and (c) Mn from column sediments for three steps: non-specifically adsorbed (exchangeable), specifically adsorbed (reducible) and very strongly bound (oxidisable).

Based on Figure V-14, it seems that dissolution of some Fe and Al oxides was taking place though. A major difference between the sediments was that only WS contained appreciable

amounts of Mn that were released mainly during step 2 (Figure V-14c), which can be correlated to reasonably high values of Cu and Zn extracted during step 2 in WS.

The main problem with hydroxylamine hydrochloride is readsorption (Rendell et al., 1980; Aualiitia and Pickering, 1988), which would lower the actually extracted amount of metals in this fraction. Sediments are often coated heterogeneously with various layers of organic matter and oxides. The dissolution of hydrous oxides will therefore release adsorbed organic coatings (including metals) and expose new surfaces to the solution. Uncomplexed organic matter might complex metal ions in solution and coagulate again, which would shift metals between fraction 2 and 3, or already complexed metals could stay in solution and shift metals from fraction 3 to fraction 2. This makes interpretation of the results rather ambiguous. Nevertheless, the increase in fraction 2 for all cases in exp. 3 (question b) is a common feature. It would most likely be linked to the fact that exp. 3 ended under anaerobic conditions, but extraction was undertaken on the oxic sediment. The destruction of organic compounds, oxidation of minerals, precipitation of minerals etc. would redistribute metals during storage phases. However, alternating the redox regime a couple of times as in the current experiment could lead to an increase in metals in the first and second fraction and decrease values in the third fraction (Calmano et al., 1993; Contin et al., 2007). Both was mostly observed and could be the answer to question (c) as well.

Step 3: very strongly bound

Acidic hydrogen peroxide is a strong oxidant, that causes oxidation of most organic matter, some oxides, sulfides and partially of clay minerals (Tessier et al., 1979; Martin et al., 1987, Beckett, 1989) with good recoveries of organic bound Zn and Cu during single extraction (Slavek et al., 1982). A by-product of organic matter oxidation is the possibility of formation of oxalates (Miller et al., 1986a), which could be responsible for an increased dissolution of oxides and higher metal recoveries in the organic fraction compared to the use of other reagents (Sonnenberg, 2003). In the adopted method partial evaporation of H_2O_2 solution before final extraction with ammonium acetate was undertaken. This can lead to precipitation of minerals, especially previously dissolved oxides (Jenne, 1968) and the creation of fresh adsorption sites. Ammonium acetate was used due to its capacity to block readsorption of trace metals (Beckett, 1989) and because it can extract metals from organic matter and oxides (Luoma and Jenne, 1976). Readsorption especially of Cu has been observed nevertheless (Rendell et al., 1980). In some BL samples there was also minor loss of sediment material due to vigorous reactions with H_2O_2. As this loss was experienced in fresh BL samples and samples from exp. 2 and exp. 3, it could not be a satisfying answer to question (c). Cu was extracted in high amounts from the third fraction in BL, while it had

rather low values in BR and WS. It seems that the solid organic matter geogenic to BL has a much stronger complexation capacity than the dissolved organic matter added during the experiment. The answer to question (d) could be related to the previously mentioned problems of selectivity and readsorption of Cu (Rendell et al., 1980). It means that Cu would actually be higher in the last fraction than Zn and that Zn in the last fraction might actually result from oxides and clay minerals rather than organic matter. The latter assumption was reinforced by the fact that Al and Fe were found in similar amounts in fraction 2 and fraction 3 in all sediments (Figure V-14).

In this study, although some insights have been obtained from sequential metal extraction tests, a variety of possible competing processes could not be adequately isolated from the tests. More comprehensive test work would be required to isolate and confirm the role of specific processes, such as flow through column extraction techniques (e.g. Wisotzky and Cremer, 2003; Barna et al., 2007; Fedotov et al., 2007). This technique has the advantage of limited readsorption and precipitation as released ions are flushed away and would be recommended for further studies.

Table V-9: Mass balance [mg/kg] of introduced (inflow) Zn and Cu versus released (outflow) and retained amount (extracted from sediments) and percent accounted for (recovered).

	Zn				Cu			
mg/kg	inflow	outflow	extracted	**% recovered**	inflow	outflow	extracted	**% recovered**
BR exp. 2	729	581	12	**81**	206	135	20	**75**
BR exp. 3	815	745	14	**93**	266	118	29	**55**
BL exp. 2	760	768	33	**105**	230	149	64	**93**
BL exp. 3	761	600	23	**82**	240	77	49	**52**
WS exp. 2	865	843	17	**99**	209	168	14	**87**
WS exp. 3	891	762	29	**89**	225	144	21	**73**

V.4 Summary of key processes and conclusions

This column study has shown that there are a number of interconnected reactions taking place during a single cycle of stormwater ASR. The injection of stormwater constitutes a major biogeochemical disturbance to the aquifer and generates three main changes:

(1) changes in ionic strength

Urban stormwater is usually of low salinity (when de-icing salts are not in use), while target aquifers are generally selected to have a salinity above the beneficial use threshold of total dissolved solids >1500 mg/L. The drop in salinity instantly induces particle mobilisation and pushes colloids to the outer edges of the freshwater “bubble”. Apart from operational issues due to the associated change in hydraulic conductivity, it is of importance for metal transport as colloids offer a large number of specific and non-specific sorption sites, and therefore

facilitate the transport of metals. This leads to a faster migration for a fraction of metals than would be accounted for with the standard advection-dispersion-retardation model. Furthermore, ion-exchange reactions are taking place, expelling Na and Mg from the exchanger and replacing it with Ca. Metals are competing with major cations for adsorption sites on the exchanger and also adsorb to more specific surface sites, which are only present in limited amounts. As Cu has a higher affinity for specific sorption sites, it has the potential to expel previously adsorbed Zn and Zn breakthrough therefore occurred in the columns. On a larger field scale this would translate to limited amounts of Zn being retarded by the sediment and the bulk of Zn moving behind the main stormwater injection front. Cu on the other hand was more or less completely retained by the sediment and would saturate the surface sites from the well outwards. However, Cu behaviour changed significantly when the stormwater had increased DOC.

(2) the role of organic carbon

Unless they have naturally organic rich strata aquifers usually have relatively low levels of mainly inert DOC, while stormwater contains biodegradable organic matter in varying amounts. Colloidal or particulate organic matter would be deposited in the aquifer, providing a constant source of DOC during mineralisation and allowing it to penetrate deep into the aquifer. Once injected the organic matter does not only influence redox reactions, but has also implications for metal sorption, especially for Cu. In DOC-rich stormwater, Cu is mainly present in organic complexes as organic matter contains high numbers of specific sorption sites for metals. These organic-metal complexes are usually negatively charged and therefore behave like anions rather than cations, meaning they do not take part in cation exchange reactions. Even though specific sorption of these complexes can occur, higher DOC concentrations during injection increases metal mobility especially of Cu, leading to wider metals distribution throughout the stormwater bubble.

(3) changes in redox potential

While most aquifers are anaerobic in nature, stormwater contains reducible species like oxygen and nitrate which increase the redox potential significantly. A number of redox reactions is therefore started that mineralise the injected organic matter and in addition dissolve Fe- and Mn- minerals usually present in the aquifer. Apart from the possible release of arsenic from the sediment, Fe hydroxides are likely to precipitate. The net balance of loss in sorption sites from dissolved minerals and gain in sorption sites on freshly precipitated minerals is likely to be slightly positive as amorphous minerals have a higher surface area.

After the stormwater injection and also usually during the recovery, ASR systems are subjected to periods of storage. The main process during this time is the adjustment to a new equilibrium after the major change to conditions during the injection. Conceptually, it would be expected that metal adsorption continues, as previously bypassed surfaces can now be reached via diffusion. In contrast the storage phase was followed by a significant release in metals in the column experiments due to changes in redox conditions and induced processes like mineral dissolution.

During recovery the changes induced by stormwater injection are mostly reversed. Ionic strength will be increased due to mixing with ambient groundwater, DOC levels will have dropped due to degradation and redox equilibrium might be closer to the original value again. Metals on the exchanger sites will desorb due to the increase in competing cations from the groundwater. As Zn was mostly retained on non-specific sorption sites, Zn will be easily desorbed and present in outflow. Surges of higher Zn concentration than previously injected can be expected after storage. The mostly specifically adsorbed Cu on the other hand will not be released as easily, with only a low fraction desorbing at best. The desorbed proportion was decreased for both metals with an increase in injected DOC. For a field site this translates to an accumulation of considerable portions of Cu in the aquifer, while Zn will mostly be recovered.

The presented experiments did include only one cycle. However, it can be speculated that during long-term use of sandy aquifers with very low sorption potential Zn would be mobile throughout the cycles with concentrations in the recovered water being in the same range as injected water concentrations. Cu concentrations would be lower in the recovered water than in the injected water for a number of cycles, as it would progressively fill up most of the available sorption sites of the sediment. Thereafter Cu would become mobile as well and be recovered with the extracted water.

The aquifer would slowly become saturated with highly sorbing metals like Cu and Pb, while less sorbing metals like Zn, Cd or Ni would be recovered with the water. These experiments also showed that the choice in target aquifer can exaggerate potential problems. An increased amount of sorption sites due to higher amounts of solid organic matter, oxides or clay minerals as well as high pH would increase the retention of metals, which is beneficial for the recovered water quality in the short term. Nevertheless, it means that the amount of metals that accumulates in the aquifer is increased, potentially compromising the recovered water quality in the longer-term. It is also unclear what the long term consequences of metal accumulation in the aquifer are for adjacent ground- and surface water ecosystems. Once

the ASR system would be out of use and previous groundwater flow is re-established, these metals might over time be released into groundwater receiving ecosystems like streams or wetlands. Further study regarding the long term effect of stormwater ASR is therefore needed. At this stage it might be advisable to reduce the load of metals, especially strongly sorbing metals like Cu and Pb. This could be achieved by running the stormwater through an exchanger or reactive filter before injection, to avoid long-term aquifer contamination.

Overall, the column studies have provided very useful information on Cu and Zn behaviour for a stormwater ASR project in siliceous aquifers. The critical role of minor sediment constituents, especially organic matter, has been demonstrated. These data will be used for reactive transport modelling and will help to predict longer-term and larger scale effects.

Chapter VI: Modelling

Water, thou hast no taste, no colour, no odour; canst not be defined, art relished while ever mysterious. Not necessary to life, but rather life itself, thou fillest us with a gratification that exceeds the delight of the senses.
Antoine de Saint-Exupery, Wind, Sand, and Stars, 1939

VI.1 Introduction

Geochemical modelling can enable a quantitative assessment and an evaluation of geochemical reaction mechanisms of experimental and field data. They can be very helpful in analysing relevant processes and their interactions and have been applied to numerous geochemical problems, especially for modelling of field sites contaminated with organic or inorganic pollutants (e.g. van der Lee and De Windt, 2001; Brun and Engesgaard, 2002; Zhu and Anderson, 2002). To this date a limited number of ASR-specific modelling studies incorporating hydrological transport and geochemical reactions are reported. For example, ASRRI (Miller et al., 2002) concentrated on biodegradation processes with the main focus on pathogen and organic pollutants and used the Kd approach for sorption processes. The 2D-solute transport model SUTRA (Konikow et al., 2001) was mainly concerned with hydrodynamic modelling and the permeability changes during ASR initiated by clay dispersion. Parkhurst and Petkewich (2002) modelled water quality changes during drinking water injection ASR with ion-exchange and mineral dissolution/precipitation. EASY-LEACHER (Stuyfzand, 1998b) incorporated 2D-solute transport in spread sheet format with ion exchange, dissolution of calcite, OM and iron sulfides, filtration of suspended solids and sorption and kinetic degradation of OM and was successfully applied to deep well injection ASTR (see II.2.4.4). The model for this site was extended into a 3D model incorporating temperature dependency of reactions (Prommer and Stuyfzand, 2005). Recently, the fate of organic and inorganic carbon during the injection of reclaimed water into limestone at Bolivar (see II.2.4.1) was modelled (Greskowiak et al., 2005). None of these models though incorporated surface complexation or aqueous complexation with organic matter of metals.

The latter two modelling studies used the freely available PHT3D v.1 (Prommer, 2002; Prommer et al., 2003), which combines the commonly used 3D multicomponent solute transport model MODFLOW/MT3DMS (Zheng and Wang, 1999; Harbaugh et al., 2000; Zheng et al., 2001) with the geochemical speciation model PHREEQC (Parkhurst and Appelo, 1999). PHT3D was chosen for this study for a number of reasons. Previous studies have demonstrated its capability of dealing with complex ASR field settings, which will allow an easy adaptation of the present laboratory scale model for future field sites or scenario

modelling. The use of PHREEQC facilitates an easy integration of new species and reactions and therefore allowed the implementation of a new conceptual model. Finally the code is freely available and couples two well known and tested programs into a new credible model. The following section will be accordingly limited to processes relevant to PHT3D, but will not go into detailed mathematical equations, numerical solution or code specific problems, as these can be found in the respective manuals, but will rather describe important concepts relevant to the research work in this study.

PHT3D has previously been used successfully for organic contaminant degradation (e.g. Barry, D.A. et al., 2002; Prommer et al., 2002; Haerens, 2004) and ion exchange/mineral phases (Medina, 2006; Prommer et al., 2007). While PHREEQC has the capability of incorporation surface complexation and dual domain transport, these features have not yet been confirmed with PHT3D. Metal complexation by organic matter is currently not incorporated into PHREEQC (personal communication D. Parkhurst). Increasing complexity was implemented in the model in cooperation with H. Prommer (CSIRO Land and Water, Perth, Australia) and advice from V. Post (Vrije Universiteit, Amsterdam, Netherlands) and these features were tested to simulate the results of the column tests (Chapter V). The main goal was to integrate surface complexation and metal-organic complexation as new features into the PHT3D model and to investigate the influence of these processes on metal retention and release.

VI.2 Background to reactive transport modelling in PHT3D

Reactive solute transport model consists of two different components, i.e. hydrodynamic solute transport (VI.2.1) and reactive geochemical processes (VI.2.2). The third component of the model is to combine or couple these very different processes (VI.2.3). The efficiency of the model has then to be evaluated (VI.2.4).

VI.2.1 Solute transport modelling

Solute transport is driven by advective flow after Darcy's law and depends on the hydraulic gradient and the hydraulic conductivity of the porous media (Appelo and Postma, 1999a). A solute that is transported with advective flow will experience hydrodynamic dispersion in both longitudinal and transverse direction. Hydrodynamic dispersion combines a number of microscopic and macroscopic heterogeneities in flow velocity into an average bulk value (Zheng and Bennett, 1995). These differences in effective flow velocity result from (a) difference in pore sizes, where faster flow can be achieved in wider pores, while some dead end pores might not take part in the flow at all, (b) friction at the pore walls, where flow will be maximal in the centre of the pore and be essentially zero at the pore wall, (c) different flowpaths around the grains, called tortuosity, where longer flow paths will lead to slower

arrival times, and (d) molecular diffusion, where gradients in solute concentration allow the diffusive movement in and out of slow flow areas after Fick's law (Fetter, 1993). MT3DMS supports the numerical solution to the advective-dispersive transport by finite difference (FD), three different types of method of characterisation (MOC) or a third-order total-variation-diminishing (TVD) scheme (Zheng and Wang, 1999). In addition, macroscopic heterogeneities in hydraulic conductivity, which allow the development of preferential flow paths and nearly stagnant zones, lead to macrodispersivity resulting in dual-domain or two-region development (e.g. Haggerty and Gorelick, 1995; Feehley et al., 2000; Flach et al., 2004).

Coupled reactive solute transport models also include a dimensionless general expression called retardation factor, which delays reactive solutes compared to non-reactive solutes, resulting in the general advection-dispersion-retardation (ADR) equation for species k in 3D (Zheng and Wang, 1999):

(VI-1) $$\frac{\partial\left(\theta C^k\right)}{\partial t} = \frac{\partial}{\partial x_i}\left(\theta D_{ij}\frac{\partial C^k}{\partial x_j}\right) - \frac{\partial}{\partial x_i}\left(\theta v_i C^k\right) + q_s C_s^k + \sum R_n$$

where θ: porosity of medium; C^k: dissolved concentration of species k, t: time, $x_{i,j}$: distance in longitudinal (i) and transverse (j) direction; Di_j: hydrodynamic dispersion coefficient tensor, v_i: pore water velocity, q_s: volumetric flow rate; C_s: concentration of the source or sink flux, $\sum R_n$: chemical reaction term. The retardation factor can include linear or non-linear equilibrium sorption of solutes, first-order irreversible kinetic rate reactions and ion-exchange.

VI.2.2 Geochemical modelling

An alternative approach to the above mentioned complex fully coupled multispecies ADR-transport modelling (equation VI-1) is to use only the advective-dispersive transport equations and solve the chemical reaction term separately (i.e. with PHREEQC) and couple both results in sequential fashion (see VI.2.3), which allows for the incorporation of more geochemical reactions. While PHREEQC is foremost an equilibrium reaction based speciation model (VI.2.2.1), it also enables user-defined non-equilibrium and kinetic reactions (VI.2.2.2) to be incorporated into the model.

VI.2.2.1 Equilibrium reactions

PHREEQC is a chemical speciation model based on ion-association in aqueous solution in contact with gas or solid phases (Parkhurst and Appelo, 1999). System equilibrium is obtained by mole, charge and phase balancing all elements among the aqueous, gas and solid phase species in an optimised iterative Newton-Raphson method (Barrodale and Roberts, 1980; Peitgen, 1989). The charge balance equation is necessary to calculate the

pH and pe and might include charge imbalances of surfaces. The thermodynamic database with heterogeneous mass action equation constants and enthalpy values is derived from various literature sources and should be considered preliminary. The main processes of interest for this study are (see Table A-6 in appendix for main equation used by PHREEQC):

Aqueous speciation

Dissolved species in the solution phase are in thermodynamic equilibrium regarding valence states of redox elements and inorganic complexation reactions. PHREEQC uses the Davies equation to calculate ion activities, which is adequate at ionic strengths below sea water concentration (Stumm and Morgan, 1996). Solution compositions are entered by the user and charge balanced with either the most abundant cation/anion, pH or a user defined dummy ion. PHREEQC does not incorporate organic complexation in the standard database, but organic species can be added by defining a new species with related mass equation reactions and stability constants. For example the MINTEQ database (Allison et al., 1990) includes a range of low molecular weight organic acids and complexation of these with metals. Speciation calculations are then handled analogous to inorganic complexation.

Ion Exchange

The number and amount of exchange sites can be defined by the user and mass action expressions and mole balance equations for exchange sites are included using the Gaines-Thomas convention (Gaines and Thomas, 1953). Commonly the activity of exchanger sites is unity, but optionally Davies or Debye-Hückel activity coefficients can be used. Exchange sites can be specified as fixed or can be linked to the mole of mineral phases or kinetic reactants, e.g. they can decrease with mineral dissolution or kinetic degradation.

Mineral dissolution/precipitation

Amounts of multiple mineral phases in equilibrium with the solution and target saturation indices (SI) (see II.4.3) can be defined by the user. Dissolution or precipitation reactions occur based on the mass action expressions and defined SI values, meaning that some phases can be defined as only precipitating/dissolving.

Surface complexation

A number of surface sites (e.g. on oxides, clays or organic matter) and surface site types (e.g. weak and strong affinity sites (Dzombak and Morel, 1990)) can be defined. Surface complexes can be mono- or multidentate (e.g. Tipping and Hurley, 1988; Ponthieu et al., 2006) and can be formed with single ions or be ternary including other ligands or ion-pairs (Zachara et al., 1995; Nowack and Sigg, 1996). Surface species may be anionic, cationic or neutral. Mass action equations for surface species have to be defined with intrinsic stability

constants including the coulombic term to account for electrostatic interactions (Koretsky, 2000). The user has to define the number of surface sites (either as fixed or linked to a mineral phase/kinetic reactant), the specific area and the mass of the surface species.
The default option for surface complexation in PHREEQC is the diffuse double layer model after Dzombak and Morel (1990) (see II.4.1.1), which relates the charge density on the surface with the potential at the surface, without calculating an explicit diffuse layer. Explicit diffuse layer calculations after Borkovec and Westall (1983) could be used in the earlier versions, assuming a fixed thickness of the double layer. Later versions also include the option to calculate the diffuse double layer with the Donnan model (e.g. Benedetti et al., 1996; Kinniburgh et al., 1996; Dudal and Gerard, 2004). In addition, the CD-MUSIC approach (Hiemstra et al., 1996) can be used by defining capacitance values. The DLM model is preferred though as it requires fewer parameters.

VI.2.2.2 Kinetic reactions

Non-equilibrium and kinetic reactions can be incorporated into PHREEQC by using an embedded Basic program and are integrated with an automatic time-stepping algorithm. The rate expression equations are solved with the Runge-Kutta algorithm (Fehlberg, 1969; Cash and Karp, 1990) or with the more sophisticated numerical integration method CVODE (Cohen and Hindmarsh, 1996). Kinetic reactions of interest are for example rate limited sorption processes, kinetically hindered mineral dissolution/precipitation (e.g. Plummer et al., 1978; Steefel and Lasaga, 1994; Bolton et al., 1999) or mineral reduction/oxidation reactions (e.g. Williamson and Rimstidt, 1994; Walker et al., 2006), filtration of particulates (e.g. Horner et al., 1986; Kim and Corapcioglu, 2002) and biodegradation (e.g. van Cappellen and Wang, 1996; Lensing et al., 1994; Di Chio et al., 1999). Monod rate equations are commonly used for simulating the sequential steps in the oxidation of organic matter where the coefficients are derived from first-order rate equations. Greskowiak et al., (2005) used a range of Monod reactions to describe the complex reaction network of the carbon cycle during ASR at Bolivar. First order rate expressions can also be used to simulate biomass growth/decay and transfer of species from mobile to immobile phase or vice versa.

VI.2.3 Coupling and numerical effects

Coupling of the hydrodynamic advection and dispersion model MODFLOW/MT3DMS with the geochemical reaction model PHREEQC is done via a modified sequential split-operator scheme (Yeh and Tripathi, 1989; Walter et al., 1994). MODFLOW/MT3DMS acts as the main program and PHREEQC is a subroutine (Figure VI-1; Prommer et al., 2003). PHT3D is implemented amongst others into the graphical user interface (GUI) PMWINpro (Chiang and Kinzelbach, 2001; Chiang and Kinzelbach, 2005), which was used in this study. In a first step the transport module of MT3DMS calculates the new concentrations in the cells, then

changes in concentrations in each cell due to geochemical reactions are calculated. Both time steps can have different lengths, so that reactions can be calculated more or less frequently than transport steps to increase numerical accuracy and stability. Reaction steps can be completely omitted for grid cells, when concentration changes are below a user-defined value to save computer time (Prommer et al., 2003). In addition to standard MT3DMS input files, three additional input files are needed for PHT3D v.2:

- definition of equilibrium and kinetic components, minerals and exchanger sites (pht3d_ph.dat)
- PHREEQC database (pht3d_datab.dat)
- PHREEQC input file (postfix.phrq) for surface complexation (not implemented in v.1). This file can also include exchanger sites, minerals or kinetic reactions, but will overwrite values entered before.

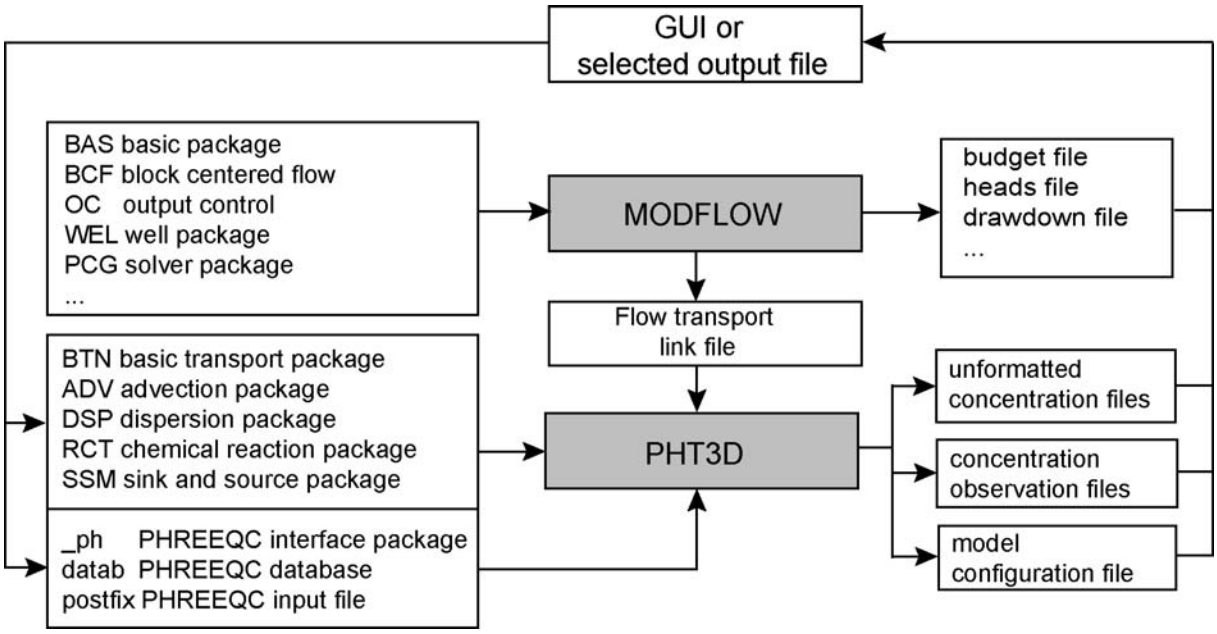

Figure VI-1: Data flow in a MODFLOW based PHT3D simulation (modified after Prommer et al., 2003)

Numerical dispersion effects are an unavoidable side effect of any transport model and are biggest with large time steps and grid cells and where physical dispersion is small. Finer spatial and temporal discretisation can reduce numerical dispersion, but also increases computing time. MT3DMS adjusts transport time step length based on the Courant condition for advective transport (e.g. Press et al., 1992; Zheng and Bennett, 1995). Temporal truncation errors due to the splitting operation also contribute to numerical dispersion (Barry, D. A. et al., 2000; Simpson and Landmann, 2008). Convergence problems either in the transport or reaction step due to the nature of iterative methods have therefore been experienced.

VI.2.4 Model development

The procedure to develop a model can usually be divided in four parts: (1) model construction, e.g. conceptual model, parameterisation, (2) model calibration, including sensitivity analysis, statistical evaluation and uncertainty analysis, (3) model verification and (4) predictive modelling under changed conditions or for the future. All these steps involve some uncertainties and will be discussed below.

Model construction

The conceptual model development is a crucial step and is a source of various errors. Firstly, no matter how sophisticated the model, it will always be a simplification and approximation of the reality (Sun et al., 1998; Rode et al., 2007). Uncertainties are introduced for example due to simplification of existing heterogeneities (e.g. Skaggs and Barry, 1996; Carrera et al., 2005), numerical dispersion and truncation errors (see above), and the simplification of hydrodynamic dispersive transport with Ficks law, which consistently results in scaling problems (e.g. Carrera, 1993; Beckie, 1996). Secondly, even if the model would be able to incorporate all natural processes in specific detail, the existence of knowledge gaps regarding these processes would make it practically impossible to do so (e.g. Tebes-Stevens et al., 2001; Gaganis and Smith, 2006). Thirdly, a lack of data often limits the model accuracy from the outset as the inclusion of a number of processes cannot be supported by data. In other words model uncertainties arise from incomplete understanding of the system being modelled and the inability to accurately reproduce natural processes (Harmel and Smith, 2007). Statistical objective functions are by their nature not able to measure these types of model error (Yeh, 1986; Gaganis and Smith, 2006).

Calibration

Calibration is an iterative process of improving the fit of the simulated data with the observed data. Firstly, a decision has to be made, which input parameters are known with sufficient certainty to be fixed and which parameters will be varied to match the observed data. Secondly, the “closeness of fit” has to be evaluated (see below) and parameters varied to improve it (Boyle et al., 2000). This optimisation can either be automated with inverse modelling subroutines such as PEST (Doherty, 2000) or manual trial-and-error procedures.

Traditionally trial-and-error methods have been employed and manual calibration is still most widely used to calibrate complex hydrogeochemical models (Boyle et al., 2000). This is a tedious process depending largely on the experience and subjective judgement of the modeller and the “optimal” calibration might not be reached (Middlemis, 2000). Automated optimisation has become more widespread with increasing computer capacities and is often used for simpler hydrological models. Nevertheless, its use is restricted when data are too

limited or too many parameters have to be optimised simultaneously (Yeh, 1986; Skaggs and Barry, 1996; Middlemis, 2000). While a number of numerical optimisation algorithms (Nocedal and Wright, 2006) exist, their implementation into PHT3D is beyond the scope of this study. In addition, automated calibration procedures require >1000 repeated model runs, which is an impractical task for a model that operates a few hours for a single run. Parameter errors or uncertainties are introduced in the calibration step for example due to non-uniqueness of a set of parameters, local optima, spatial and temporal heterogeneities of parameters, database inaccuracy and measurement errors (e.g. Zheng and Bennett, 1995; Doherty, 2000; Middlemis, 2000).

A helpful tool for calibration is the sensitivity analysis, which tests the overall responsiveness of one input parameter at a time and quantifies the impact on the model response (Dagan, 1989; Zheng and Bennett, 1995). Calibration can then be prioritised to the most sensible parameters. A full sensitivity analysis is computationally extremely demanding when many model parameters are involved and is therefore often only feasible for physical models, but not for highly complex biogeochemical models (Skaggs and Barry, 1996; Tebes-Stevens et al., 2001; Carrera et al. 2005).

Evaluation

The evaluation of the goodness of fit can be both quantitative (statistical) or qualitative (pattern-matching) (Middlemis, 2000). Many of the common quantitative objective functions used to evaluated calibrations are simple indicators involving the sum of differences between the simulated and the measured data (Zheng and Bennett, 1995; Middlemis, 2000; Harmel and Smith, 2007).

Examples include the mean absolute error (MAE):

(VI-2) $$\mathrm{MAE} = \frac{1}{n}\sum_{i=1}^{n}\left|\mathrm{obs}_i - \mathrm{sim}_i\right|$$

the root mean squared error (RMSE):

(VI-3) $$\mathrm{RMSE} = \sqrt{\frac{1}{n}\sum_{i=1}^{n}\left(\mathrm{obs}_i - \mathrm{sim}_i\right)^2}$$

the coefficient of determination (R^2)

(VI-4) $$R^2 = \left(\frac{\sum_{i=1}^{n}\left(\mathrm{obs}_i - \overline{\mathrm{obs}}\right)\left(\mathrm{sim}_i - \overline{\mathrm{sim}}\right)}{\sqrt{\sum_{i=1}^{n}\left(\mathrm{obs}_i - \overline{\mathrm{obs}}\right)^2}\ \sqrt{\sum_{i=1}^{n}\left(\mathrm{sim}_i - \overline{\mathrm{sim}}\right)^2}}\right)^2$$

and the Nash–Sutcliffe coefficient (Nash and Sutcliffe, 1970) or coefficient of efficiency (E):

(VI-5) $$E = 1 - \frac{\sum_{i=1}^{n}\left(obs_i - sim_i\right)^2}{\sum_{i=1}^{n}\left(obs_i - \overline{obs}\right)^2}$$

with obs_i = measured data, sim_i = modelled data, $\overline{obs}$ = mean of measured data, $\overline{sim}$ = mean of modelled data and n = number of observations. The MAE and RMSE are absolute values describing the difference between the model simulations and observations in the units of the variable. R^2 and E are dimensionless indicators ranging from 0 to 1 and minus infinity to 1, respectively, with values close to unity indicating good agreement. All indicators that do not include the difference between observed and measured values (e.g. r or R^2) cannot detect proportional differences, but only a and those indicators that are based on squared differences (e.g. RMSE, E, index of agreement) are sensitive to extreme values. Legates and McCabe (1999) therefore introduced a modified coefficient of efficiency (E') using absolute differences instead of squared differences:

(VI-6) $$E' = 1 - \frac{\sum_{i=1}^{n}\left|obs_i - sim_i\right|}{\sum_{i=1}^{n}\left|obs_i - \overline{obs}\right|}$$

While performance indicators provide an overall value, they do not provide information on systematic, spatial or temporal distribution of error and they do not necessarily facilitate finding the best parameter set (Gupta et al., 1998; Middlemis, 2000). Debate about the usefulness of single objective functions to characterise the success of a model are therefore frequent and there is growing research on multi-objective calibration procedures (e.g. Gupta et al., 1998; Boyle et al., 2000; Rode et al., 2007). The use of these procedures is beyond the scope of this study though. The above introduced indicators have been chosen as quantitative indicators in this study and have been used for water quality assessment before (e.g. Harmel and Smith, 2007; Rode et al., 2007).

Qualitative assessment of calibration is commonly undertaken by visual comparison of model output and measured data and is frequently the method of choice for highly complex models (Gupta et al., 1998; Boyle et al., 2000) and has been used in the past for evaluation PHT3D results (Barry, D. A. et al., 2002; Haerens, 2004; Prommer et al., 2007).

Verification and Validation

A calibrated model is verified when an independent set of data can be simulated successfully. It is often limited due to the fact that only one set of data is available (Middlemis, 2000). Model validation is defined as the ability of the model to predict future conditions and can only be done by post-audits (Konikow, 1986). In general, both therms

should be avoided as they convey a non-existing sense of accuracy. Models can usually only be invalidated in reality due to the non-uniqueness problem and the inability to predict future physical and chemical stresses (Konikow, 1986; Gupta et al., 1998). Nevertheless a calibrated but unverified model can still be used as an interpretive tool to gain enhanced understanding of the importance of different factors and processes (Walter et al., 1994). It can help to identify parameters that should be investigated in more detail in further studies and by providing probabilistic results, it can also give valuable insights for management decisions (Zhu and Anderson, 2002).

It therefore depends on the amount of data available, the number of processes that can be reliably modelled and also on the purpose of the model, what level of calibration and verification will be possible and necessary.

VI.3 Modelling setup

The model was designed to simulate column experiments described in the previous chapter focussing on correct reproduction of ion-exchange, pH, Zn and Cu results. While the model is effectively 1D at this stage, the aim is to facilitate adaptation for 3D modelling in the future. The model set up started with creating a solute transport model based on measured parameters that was used for all model simulations (VI.3.1). A brief description of the model output and presentation is given (VI.3.2) to help the interpretation of later graphs.

A number of simple approaches (VI.4) were then trialled to simulate metal retention:

1. linear sorption for metals
2. ion exchange for major ions and metals
3. addition of mineral phases in equilibrium
4. generalised composite (GC) surface complexation approach

As these approaches were found to be too simple to represent the results, a more complex conceptual model (VI.5) was then derived from the literature. This component additivity (CA) surface complexation and organic complexation model included:

1. surface complexation of metals onto minerals
2. organic metal complexation in solution
3. surface complexation of metals onto organic surfaces
4. sorption of dissolved organic matter onto minerals
5. formation of ternary complexes

Dual domain behaviour and kinetic biodegradation were investigated last and added to the CA surface complexation model separately.

VI.3.1 Non-reactive solute transport model

The flow model was comprised of one layer with a length of 150 mm, a height of 20 mm and a width of 25 mm to match the surface area of the 25 mm diameter round column. Discretisation into 5 mm thick cells resulted in 30 column cells. In addition, a 5 mm cell representing the injection point and an empty 95 mm cell, together representing the volume of 50 mL of the EC meter, were added on either side to be used during the injection phase or the recovery phase, respectively, resulting in a total of 34 cells (Figure VI-2). As the EC meter was only used during exp. 2 the outflow concentrations were recorded in cell 34 and 1 for exp. 2 and in cell 33 and cell 2 for exp. 3, respectively (see V.2.2 for column set up). The numerical dispersion resulting from this grid size discretisation was within the analytical error.

During groundwater equilibration (phase 1) and stormwater injection (phase 2) well injection was taking place in cell 2 and outflow was through a constant head boundary in cell 34 (Figure VI-2a). During recovery (phase 4), when the column was turned around, an injection well in cell 33 and a recovery well in cell 1 allowed for a reverse flow (Figure VI-2b). During storage periods no inflow through the injection wells occurred (see V.2.3 for experimental design). Injection rates were matched to recovered flow rates during the experiment and adjusted for each experiment. Injection rates and lengths of stress periods were matched to the recorded flow rates and times during the actual experiments and adjusted for each experiment and column. Advective flow was solved with the upstream finite difference scheme with central-in-space weighing, a Courant percentile of 0.75 and the solver GCG (Jacobi) was used. Standard units for spatial dimensions, time and quantity of metre [m], days [d] and [mol], respectively, were consistently used throughout the modelling.

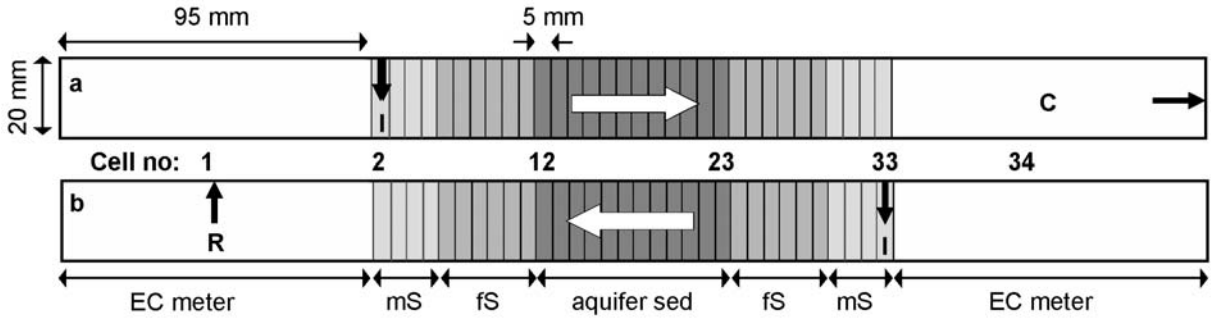

Figure VI-2: Flow model set up for (a) injection and (b) recovery. I: injection well, R: recovery well, C: constant head flow boundary, mS: medium filter sand, fS: fine filter sand, sed: sediment.

Aquifer properties

The aquifer sediments were assumed to be the limiting factor for hydraulic conductivity and measured values (see Table V-1) were assigned to the aquifer sediments only (cell 12-23), while fine filter sand and coarse filter sand/EC meter was assigned 1 and 10 m/d, respectively. Similarly, values for effective porosity from Table V-1 were assigned to the

aquifer sediment cells. Packing tests with only fine or medium sand filter material resulted in effective porosities of 0.36 and 0.39, respectively, while the EC meter was assigned a porosity of 1. Bulk density and longitudinal dispersivity values from Table V-1 were assigned for the whole column. The ratio between horizontal/vertical transverse to longitudinal dispersivity was set to 0.001 and the molecular diffusion coefficient to 10^{-9} m²/d (Fetter, 1993).

Input concentrations

Input concentrations [mol/L] for equilibrium components, i.e all measured major cations (Na, K, Ca, Mg), anions (Cl, alkalinity as C(4), sulfate as S(6), nitrate as N(5), Br), heavy metals (Al, Fe(3), Mn(2), Cu(2), Zn), DOC as Srfa (see VI.5.1.2), pH and estimated values for O(0) and pe were entered for each stress period matching changes in inflow concentrations as analysed. Charge balance was calculated with PHREEQC (for windows, version 2.14). While charge balances for solutions containing fractions of groundwater were <10%, stormwater solutions had higher errors due to the overall low concentrations. The addition of Srfa as negative species decreased ion balance accuracy especially in exp. 3. The missing concentration was entered as dummy cation (D) or dummy anion (A), which do not participate in any reaction.

Database

All speciation calculations were based on the standard database (phreeqc.dat) and used the standard mass action coefficients and enthalpies values unless indicated otherwise. Additions to the database included mineral phases from wateq4f.dat (Ball and Nordstrom, 1991) and minteq.v4.dat (Allison et al., 1990), dummy species A and D and the new species defined in VI.4.1.4 (see Table VI-2) and VI.5.1 (see Table VI-6). For the complete database see Table A-7 in appendix.

VI.3.2 Output

The output was created in the PHREEQC postfix file with the “user_punch” option under “selected_output”. This created a tab delimited spreadsheet output file for each cell at 1000 time steps for the user specified species that was then read by MATLAB v.7.1 (2005). Concentrations were converted from mol/kgw to mg/L for dissolved species and to mg/kg for sorbed species. The graphs show the simulated concentrations as line and observed concentrations as symbols versus time. For dissolved species simulated concentration were read at the model cell that represented the cell where the sample had been taken, i.e. cell 34 (phase 1-3) and cell 1 (phase 4) for experiment 2 and cell 33 and cell 2 for experiment 3, respectively. For sorbed species simulated concentrations are displayed for cell 12 (solid lines) and cell 23 (dashed), which represent the top/bottom of the aquifer material. For

guidance the injection phase has a light grey bar and all storage phases a black bar at the top of the graph and vertical dashed lines indicate the start and end of a phase (Figure VI-3).

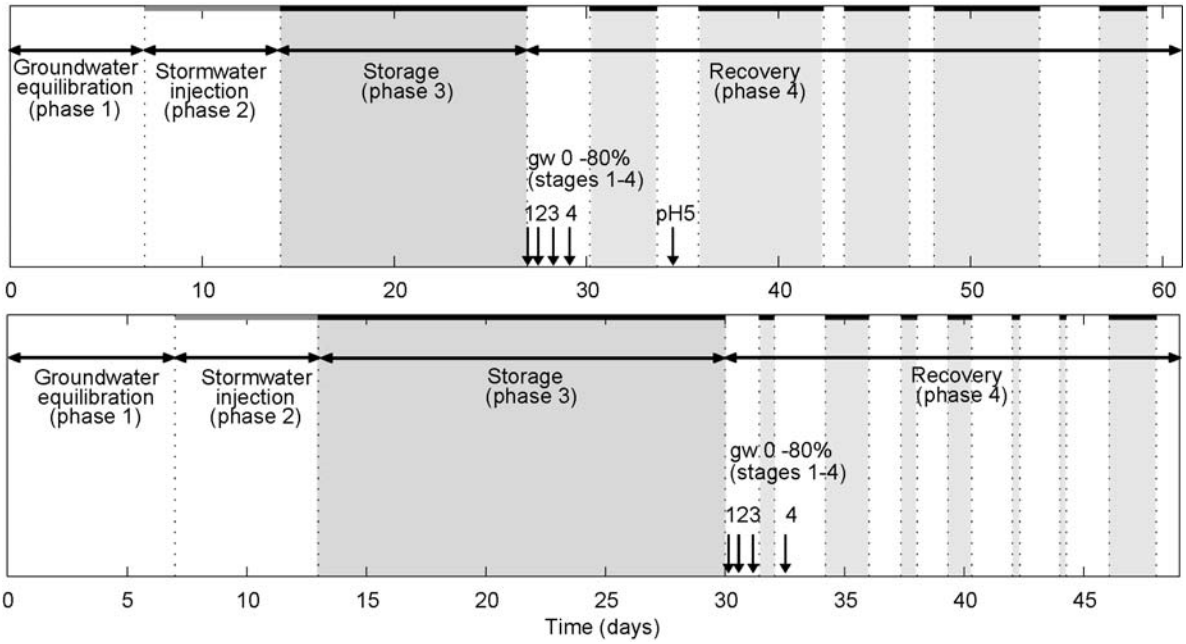

Figure VI-3: Blank graph concentration versus time indicating changes in phases and stages for (a) experiment 2 and (b) experiment 3. Shaded areas indicate shorter storages during recovery (phase 4) (compare to Figure V-2).

VI.4 Simple approaches

Overall 6 models were created for the three different sediments under the two different experimental conditions. This section will show simple approaches to modelling metal retardation in the subsurface. For this the simplest sediment BR and the simpler experiment 2 will be used as example ('BR2'). The next section (VI.5) will show the improvements that can be achieved by using a surface complexation model.

VI.4.1 Modelling of simple approaches

VI.4.1.1 Linear equilibrium sorption

Linear and non-linear (Freundlich/Langmuir isotherm) equilibrium sorption models have long been used for modelling retardation (e.g. Bürgisser et al., 1993; Hinz and Selim, 1994; Antoniadis et al., 2007) and are implemented in MODLFOW/MT3DMS despite the long known shortcomings of this approach (Reardon, 1981; Bethke and Brady, 2000). The main disadvantages are that this retardation approach models one species at a time without any interaction to any other component, meaning that there is neither competition for sorption sites, nor influence in sorption behaviour with changes in geochemical conditions and no complexation with other components (Langmuir, 1997; Goldberg et al., 2007). The K_d approach is therefore not appropriate where geochemical conditions change significantly over space or time or for species that are involved in a number of interactions and reactions

(Reardon, 1981; Koretsky, 2000), as distribution coefficients can change over numbers of magnitude with changing geochemical conditions (Davis et al., 1998; Bethke and Brady, 2000; Kent et al., 2000). Its popularity stems from the fact that it is easy to apply, as only one or two sorption parameters are needed. The K_d approach can lead to acceptable results if geochemical conditions do not vary dramatically (Reardon, 1981; King, 2005; Goldberg et al., 2007). A number of different K_d values were trialled for both Zn and Cu and visual optimisation was undertaken.

VI.4.1.2 Ion exchange

As the K_d approach does not impose mass balance on the sorption sites and therefore does not account for competition nor for reversible sorption reactions (Reardon, 1981), the ion-exchange approach would be a better approach. The ion exchange approach is the main retardation mechanism for major cations and has been used successfully to model their behaviour under changing solution composition (e.g. Valocchi et al., 1981; Appelo et al., 1990). Apart from differences due to different conventions (Appelo and Postma, 1999a), selectivity coefficients vary with CEC, sediment composition, solution composition and ionic strength (Appelo and Postma, 1999a). They are therefore site specific (Bjerg et al., 1993) and are usually calibrated for each model.

In contrast to PHT3D v.1, where specific exchange species, e.g. Ca_ex, Na_ex had to be defined, the PHT3D v.2 requires only undefined exchange species and cation distribution is calculated via the selectivity coefficients. One exchange specie (X_ex) was incorporated to account for ion exchange. The amount of exchanger sites has to be expressed as mol/kg water, meaning that values had to be adjusted to the mass of water in the system via the porosity. Maximum exchanger sites values were calculated using the measured CEC (see Table III-10) and the porosity for each experiment (Table V-1). As CEC does incorporate exchange sites from various solids (see II.4.1.2), the CEC was assumed to be unrealistically high for BL sediments due to the organic content of this sediment (see Table III-10) and BL exchanger sites. Selectivity coefficients were adjusted during calibration (Table VI-1) to match ion-exchange pattern (see VI.4.2.2). Na was used as reference cation and H^+ was included to account for proton buffering. One ion exchange site was with dataset (b) (Table VI-1) was included in all further model runs.

Table VI-1: Selected log_k values for reactions: cation^{n+} + n X^- = cationX_n for BR2 with 0.054 mol/kgw exchanger sites.

cation	Ca^{2+}	Mg^{2+}	K^+	Cu^{2+}	Zn^{2+}	H^+
(a) wateq4f.dat	0.8	0.6	0.7	0.6	0.8	1.0
(b) ion exchange for Ca, Mg	1.4	0.6	0.7	0.6	0.8	1.0
(c) ion exchange for Cu, Zn	0.8	0.6	0.7	4.6	2.5	5.0

VI.4.1.3 Mineral phases

The addition of mineral phases is necessary if dissolution/precipitation reactions are an important mechanism and is not a stand alone approach but an additional mechanism to be investigated. The sediment analysis (see Table III-10) indicated that apart from quartz effectively only Fe- and Al-oxides were likely to be of significance for all sediments. Preliminary PHREEQC calculations with a hypothetical mineral assemblage of amorphous $Al(OH)_3$ and $Fe(OH)_3$, gibbsite, boehmite and goethite showed that amorphous Fe- or Al hydroxides and boehmite were not stable either in contact with groundwater or stormwater solution and were instantly dissolved, and precipitated as goethite and gibbsite, respectively. Traces of calcite were unstable as well and dissolved during the first day of the groundwater equilibrium (phase 1) in a preliminary model run. It was therefore postulated that 7 days of equilibrium would be long enough to allow for any undetected amount of calcite to dissolve.

Pyrite was detected for BL (see Table III-10) and pyrite dissolution would definitely be of interest for BL (see V.3.4), while it does not occur in WS and is only of minor importance for BR. Addition of pyrite as equilibrium phase resulted in a dissolution of pyrite during the first day of equilibrium (phase 1) and resulted in pH <1. Hence by the end of the equilibrium (phase 1) all pyrite was dissolved and addition as equilibrium phase would not result in changes in the column experiment under the current model set up.

For most mineral phases kinetic dissolution is considered to be a more realistic representation than equilibrium controlled dissolution (Appelo and Postma, 1999a). Kinetic dissolution could be implemented in PHREEQC, but choosing a representative dissolution rate is not straight forward. Dissolution rates are slowing when approaching equilibrium, are generally dependent on pH and rate-limiting transport/transfer of electrons/ions to and from the mineral surface, grain size and mineral surface properties and can also be hindered by sorbed ions or enhanced by ligands in solution (e.g. McBride, 1989; Cornell and Schwertman, 1996; Reichard et al., 2007). Pyrite dissolution is rate-limiting by the transfer of electrons from the mineral to the oxidant (Williamsen and Rimstidt, 1994; Walker et al., 2006) and depends on pH, redox potential and ligand concentration (Xu and Gao, 2008). Precipitation of iron hydroxides would have to be considered as well. To represent the effect of this precipitation, surface sites would have to be coupled to mineral phases, which they are currently not. The implementation of this complex interaction into PHT3D with respect to arsenic at the Langerak deep-well recharge site (Brun et al., 1998; Saaltink et al., 2003) is the focus of a different PhD study (I. Wallis, Flinders University, Adelaide, Australia). It would be desirable to implement kinetic arseno-/pyrite oxidation and coupling of surface sites with

mineral phases similar to Postma and Appelo (2000), but at this stage the model was not able to cope with all processes simultaneously.

For this study, mineral equilibria constraints for quartz (30 mol), goethite (0.093 mol) (added to database from minteq.v4.dat) and gibbsite (0.173 mol) were tested. In contrast to exchanger sites, mineral phases have to be entered as mol/dm³ bulk volume. The percentage of Al and Fe from the sediment analysis was hence transformed into mol/dm³ by using gibbsite (for Al) and goethite (for Fe) phases molar weight and the bulk density of the experiment. In addition, a range of possible Cu and Zn minerals (e.g. cupric ferrite, malachite, smithsonite, $Zn(OH)_2$) were allowed to precipitate (added to database from waterq4f.dat).

VI.4.1.4 Generalised composite (GC) approach

Two different approaches can be found in the literature to model surface complexation onto natural heterogeneous sediments: the generalised composite (GC) approach and the component additivity (CA) approach (Davis et al., 1998; Goldberg et al., 2007). The CA approach assumes that a number of different pure inorganic/organic surfaces that do not interact with each other can be used to describe the sediment surface. This will be most applicable when the sediment is dominated by surface coatings or secondary minerals (Cowan et al., 1992; Zachara et al., 1992). This approach requires a comparatively large amount of parameters as site densities, stability constants etc have to be defined for each phase (Koretsky, 2000). In contrast, the GC approach assumes that the mineral assemblage is too complicated to be characterised properly and assumes “generic” surface sites that represent average properties of the sediment and are fitted to the data of the study. While this approach simplifies the adsorption model, the disadvantage of this approach is that values are not transferable and only apply to the specific sediment (Davis et al., 1998; Koretsky, 2000; Goldberg et al. 2007).

In a first attempt of a surface complexation model for this study, the DLM study from Wang et al. (1997) for 11 diverse sediments was used to derive a single surface site for each sediment. They found linear free energy relationships (LFERs) (Carbonara and Di Toro, 2007) between the surface complexation constants (K_s) and first hydrolysis constants (K_1)

$$\log K_s = a * \log K_1 + b$$

and that the slope (a) of this correlation was a function of the sediment composition:

$$a = 0.19 * TOC\,[\%] - 0.09 * Oxides\,[\%] + 1.31$$

where the oxides include reactive Fe-, Al- and Mn-oxides. The intercept (b) can be calculated by weighing pure phase values for the sediment. Using the first hydrolysis constant from Dzombak and Morel (1990), weighing surface area and site densities from the pure phases,

and applying the above relations to the sediments of this study yielded the following results (Table VI-2) and these new species and reactions were implemented in the database.

Table VI-2: Derivation of complexation constants for Cu and Zn onto the three sediments used in this study after Wang et al. (1997).

	BR	**BL**	**WS**	b for pure phases
SiO_2	97.5%	94.4%	92.2%	0.13
Al_2O_3	0.73%	0.83%	3.19%	-0.29
Fe_2O_3	0.32%	0.29%	1.60%	3.97
TOC	0.48%	2.08%	0.67%	13.6
a	1.31	1.60	1.01	a = 0.19*TOC – 0.09 Ox + 1.31
b	0.20	0.42	0.27	weighed from pure phases
log K_s Cu	8.70	10.85	6.81	log K_s = a * 6.5 + b
log K_s Zn	6.74	8.44	5.30	log K_s = a * 5 + b
surface area [m²/g]	1.40	3.56	2.57	weighed from pure phases
surface sites [mol]	0.014	0.06	0.02	assuming 2.31 sites/nm² for all phases

VI.4.2 Results of simple approaches

VI.4.2.1 Linear equilibrium sorption

In the column experiments, conditions are relatively stable during injection once the groundwater is flushed from the column and the linear K_d modelling approach was therefore able to model Cu and Zn breakthrough relatively well (Figure VI-4). However, the optimised values of 5 L/kg (K_dZn) and 37 L/kg (K_dCu) were lower than the values found in the column experiment (K_dZn 90 L/kg, K_dCu >>300) or batch experiment for pH 7 (K_dZn 80 L/kg, K_dCu 82 L/kg), while pH breakthrough could not be modelled with this approach. K_d values vary for example with pH, metal loading, solid-solution ratios, particle composition (see chapter IV.3; Tipping, 1998; Harter and Naidu, 2001), and do not account for changes in pH induced by adsorption of reactive compounds (see II.4.5; McBride, 1989; Scheidegger et al., 1994). Therefore direct translation of measured K_d values could not represent the occurring breakthrough during stormwater injection, as the use of K_d values >40 resulted in no breakthrough.

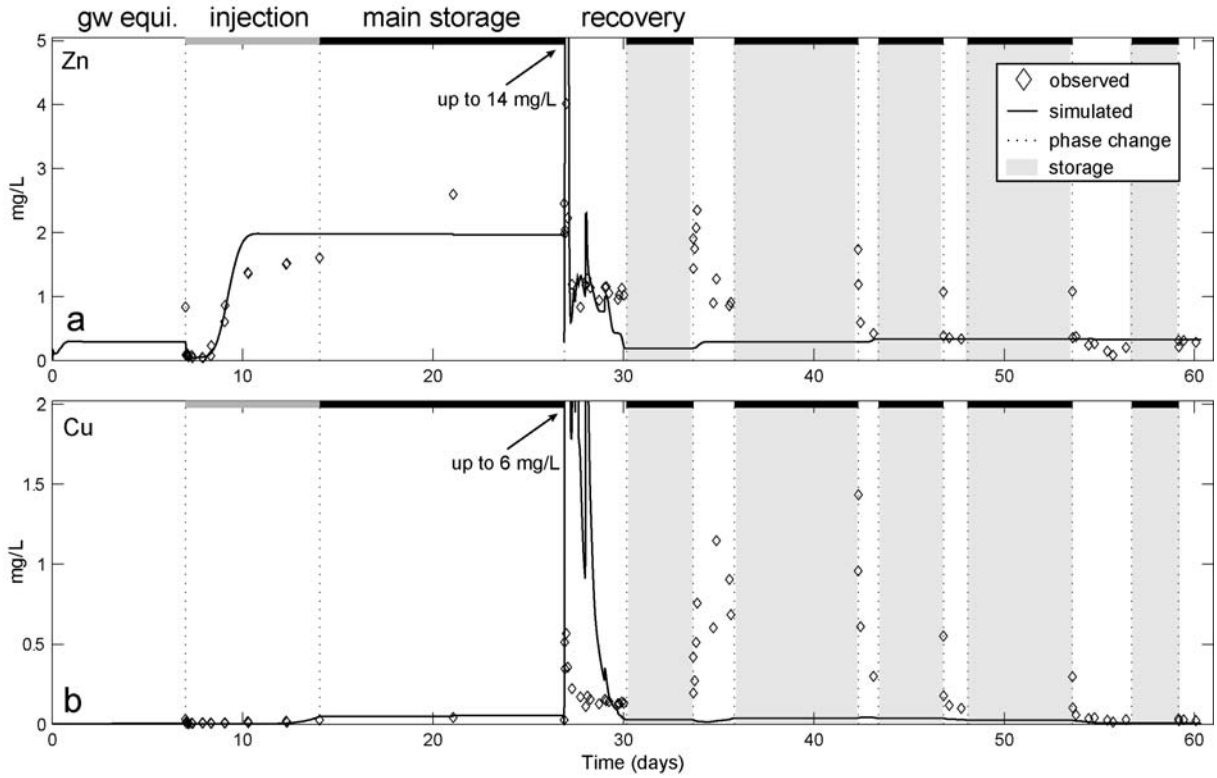

Figure VI-4: Simulated and observed concentrations of (a) Zn and (b) Cu using the linear K_d sorption approach for BR2 with K_dZn = 5 L/kg; K_dCu = 37 L/kg.

While the breakthrough could be modelled, the recovery phase, where the flow direction and geochemical conditions change, could obviously not be modelled with the K_d approach. The first spike was significantly too high and the release was significantly too low during stage 4 of the recovery (>30 d). This misrepresentation of tailing during desorption has been observed in a number of studies and will be most significant for specifically sorbed compounds (Selim et al., 1992; Bethke and Brady, 2000). Overall, the K_d approach was not able to cope with the change in flow direction and change in solution composition as expected (see VI.4.1.1) and was therefore disregarded.

VI.4.2.2 Ion exchange

For BR2 the CEC of 0.87 cmol/kg translated to 0.054 mol/kgw, which was considered to be the upper limit of number of exchanger sites and subsequently used. Starting with the standard database values (dataset a, Table VI-1) showed that the retardation of Ca at the start of stormwater injection (phase 2, inset Figure VI-5) was not strong enough and metal breakthrough was nearly instant (Figure VI-5).

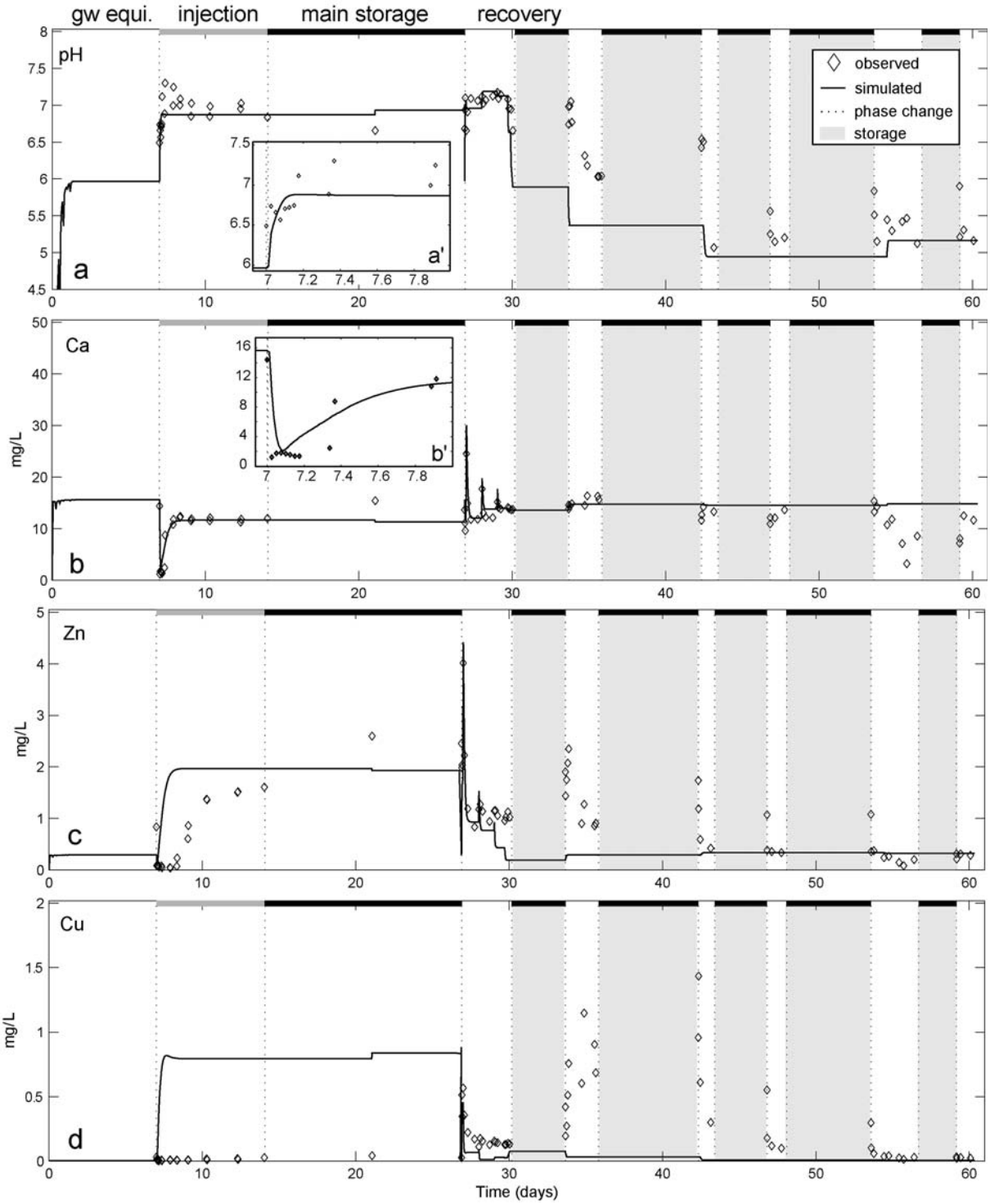

Figure VI-5: Simulated and observed (a) pH and concentrations of (b) Ca, (c) Zn and (d) Cu using the ion exchange approach for BR2 with standard database values (dataset a) (Table VI-1) with insets (') for pH and Ca of breakthrough at start of stormwater injection.

Increasing the selectivity coefficient for Ca from 6.3 to 25 (dataset b, Table VI-1) showed a significant improvement in Ca breakthrough and release behaviour (Figure VI-6). For experiment 3, where no EC meter was used, selectivity constants for Ca could be reduced to the original set, showing that the mixing in the EC meter was stronger than simulated by the extra cell in the model.

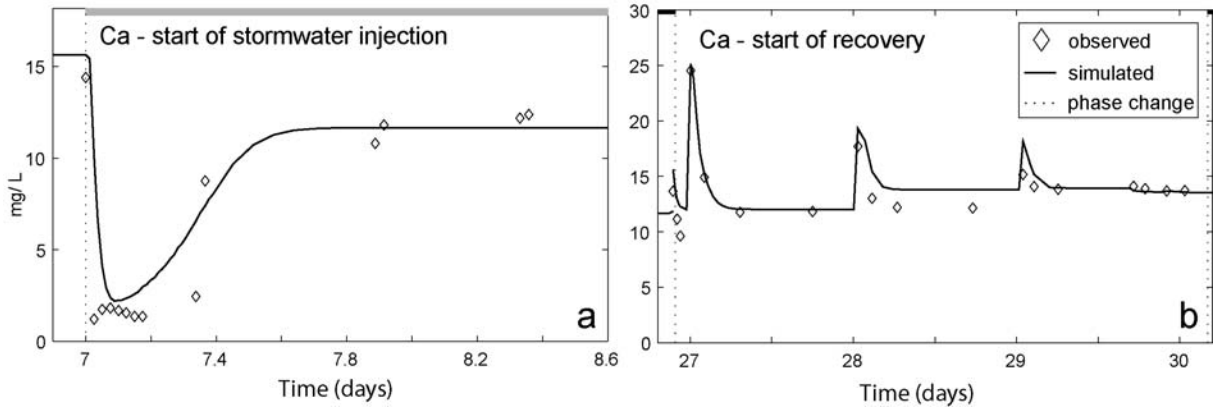

Figure VI-6: Simulated and observed concentrations of (a) Ca breakthrough at start of stormwater injection and (b) Ca release at start of recovery phase using adjusted Ca selectivity values (dataset b, Table VI-1).

To match Cu and Zn breakthrough behaviour, their selectivity values had to be increased by orders of magnitude (dataset c, Table VI-1). To achieve some Cu release during the pH decrease in the recovery phase, the proton selectivity constant had to be increased in conjunction (Prommer et al., 2007). While this improved Cu and Zn curves significantly, it also let to a considerable worsening of Ca, Mg and pH breakthrough at the start of stormwater injection (phase 2) (Figure VI-7). As Ca and Mg were lower in the selectivity order Mg is quickly expelled from the exchanger (not shown) and only limited amounts of Ca are able to adsorb resulting in a less pronounced and shorter dip in Ca concentration (Figure VI-7a). In accordance Ca peaks at the start of the recovery (phase 4) were also significantly too low (Figure VI-7b).

While the calibration of the selectivity coefficients were done manually and a number of variations have been trialled, it is considered unlikely that an optimised combination of values to simultaneously fit all parameters could be found with an automated calibration program (i.e. PEST) due to the limited amount of exchanger sites. If Cu and Zn have high selectivity values, there is just not enough sites for the other major ions. It is also considered highly unlikely that Cu would be retarded strongly due to ion exchange, as numerous studies including this one (see IV.3.2.1; McBride, 1989; Mesquita and Vieira e Silva, 1996; Tsang and Lo, 2006), have shown that Cu is mainly sorbed specifically rather than non-specifically. The dataset (b) (Table VI-1) was hence adopted for further modelling to allow for minor ion-exchange for Cu and Zn.

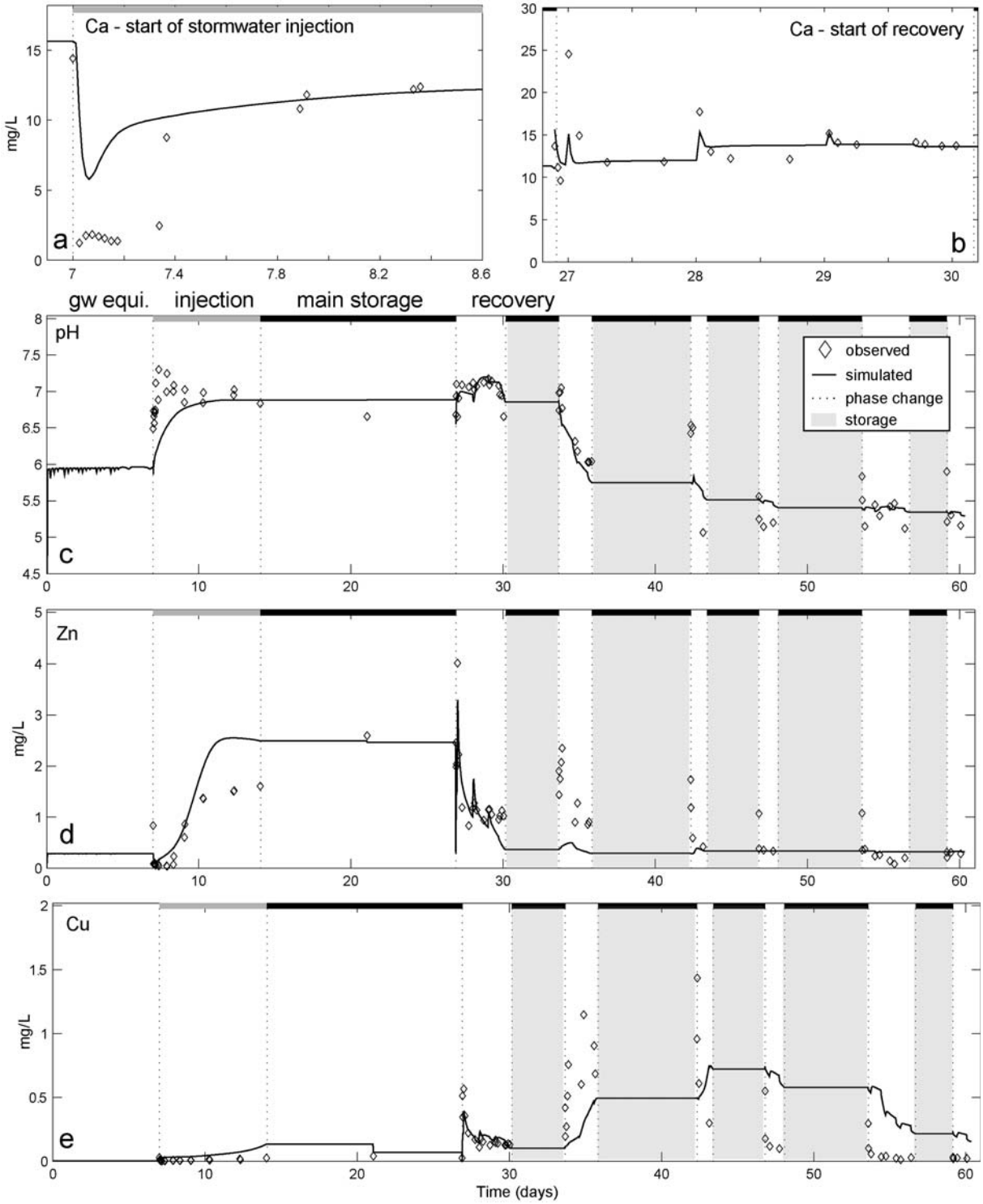

Figure VI-7: Simulated and observed concentrations of (a) Ca at start of stormwater injection, (b) Ca at start of recovery phase, (c) pH, (d) Zn and (e) Cu using the ion exchange approach with dataset c (Table VI-1).

VI.4.2.3 Mineral phases

As discussed in VI.4.1.3 a number of equilibrium mineral phases were added to test their behaviour. As expected a slow dissolution of quartz from 30 to 28.45 mol occurred over the 60 days (Figure VI-8a). This reaction would realistically be much slower due and it does not influence any other species and hence quartz was not included in later models. Goethite precipitated (maximum 0.21 mol) during the recovery phase decreasing from cell 23 (closest

to inflow during recovery) to cell 12 (Figure VI-8b). Gibbsite was stable and showed only slight changes (± 6% from initial concentration) over the whole range of the experiment (Figure VI-8c). Changes in both goethite and gibbsite concentration would change sorption sites for Cu and Zn. At this stage of the model surface sites are not coupled to mineral phases though.

If no cupric ferrite was allowed to precipitate, malachite precipitation (maximum 0.01 mol) was simulated during stormwater injection, followed by fast dissolution around day 35 (Figure VI-8d) when the pH drops below 6.5, resulting in a Cu release spike of 2.5 mg/L (not shown). While Prommer et al. (2007) also found that Cu concentrations were influenced by malachite precipitation, their experiment involved much higher Cu concentrations, calcite dissolution and a higher input of organic carbon. Malachite precipitation was considered unlikely for our experiment and did not occur if cupric ferrite was allowed to precipitate instead.

Adding cupric ferrite as possible mineral phase in conjunction with goethite (case A) did not influence goethite precipitation during recovery, but significantly dissolved goethite (minimum 0.043 mol) during stormwater injection (Figure VI-8e).Cupric ferrite precipitation (maximum 0.028 mol) showed a linear increase during stormwater injection (Figure VI-8f). PHREEQC speciation modelling showed that it dissolved at pH < 5.2, resulting in a slow dissolution during the recovery phase, which is not finished by the end of the experiment.

If no initial goethite phase was available, but cupric ferrite and goethite were allowed to precipitate (case B), cupric ferrite precipitation was more than a magnitude lower (maximum 0.0013 mol) and dissolution was complete by day 35 (Figure VI-8g). This meant that Cu breakthrough during injection was only minimally influenced and the increase in Cu concentration due to this dissolution was less pronounced. In addition, the introduction of surface sites reduced both the amount of cupric ferrite precipitated and the spike in Cu concentration due to dissolution even more.
No other Zn or Cu containing mineral phase precipitated.

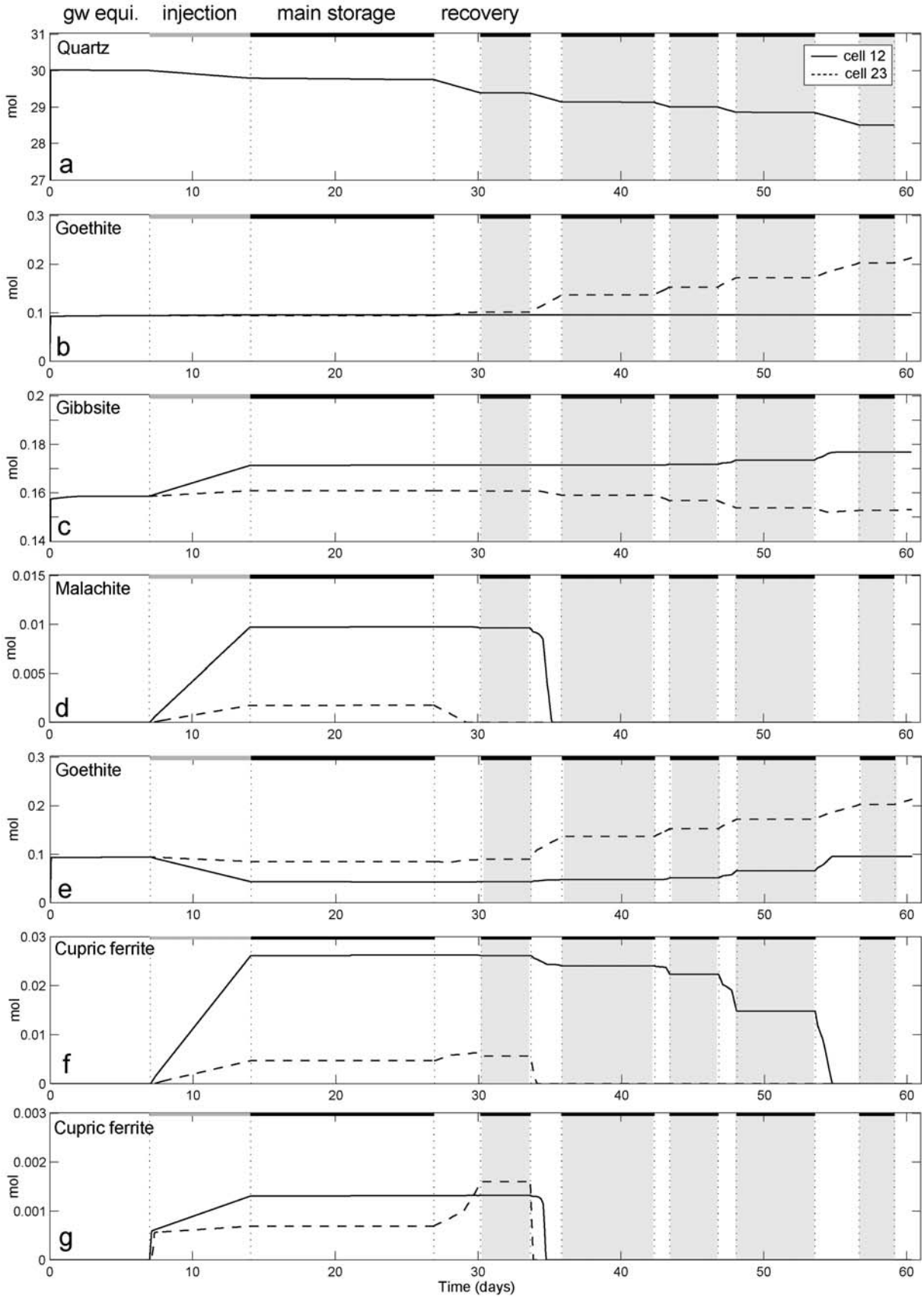

Figure VI-8: Simulated pattern of mineral precipitation and dissolution for BR2 in first (cell 12) and last cell (cell 23) of the aquifer sediment. (a) quartz, initial 30 mol, (b) goethite, initial 0.093 mol, (c) gibbsite, initial 0.173 mol, (d) malachite ($Cu_2(OH)_2CO_3$), initial 0 mol, without cupric ferrite, (e) goethite, initial 0.093mol, with cupric ferrite, initial 0 mol, (f) cupric ferrite ($CuFe_2O_4$), initial 0 mol with goethite, initial 0.093 mol (g) cupric ferrite, initial 0.0 mol with goethite, initial 0.0 mol.

As no direct evidence for the precipitation or dissolution of mineral phases during the column tests was available, arguments for and against including these mineral phases have to be based on indirect evidence and theoretical considerations. The precipitation of cupric ferrite is generally possible at room temperature and pressure (e.g. Shum and Lavkulich, 1999; Agbenin and Felix-Henningsen, 2004; Butler, 2006) and surface precipitation cannot be distinguished from adsorption and might occur even at concentrations below the saturation index (McBride, 1989; Sparks, 2005). Cupric ferrite precipitation in combination with goethite dissolution (case A) resulted in no breakthrough of Cu during stormwater injection matching the found results. Its existence at the end of the experiment could also explain higher than expected values for Cu found in step 1 of the metal extraction (see V.3.5). The simultaneous dissolution of goethite could theoretically be ligand-promoted by organic acids in stormwater (Cornell and Schwertmann, 1996; Reichard et al., 2007). However, goethite dissolution is considered to be rate-limited and its instantaneous dissolution seems unlikely. However, rate-limited reductive dissolution of goethite during prolonged storage times could be a realistic process. Considering the case of no goethite dissolution (case B) showed that the influence of cupric ferrite on Cu concentration was very limited and once enough surface sites were available for Cu sorption, cupric ferrite precipitation was hardly occurring anymore. Hence the addition of mineral phases would not result in significant changes to the model outcome.

The solubility product for goethite is also not a fixed value, but is influenced for example by solution composition, pH, mineral properties or degree of under/oversaturation (Cornell and Schwertmann, 1996), meaning that discrepancies between published values of the solubility product for goethite by orders of magnitude exist. While the above results were generated using minteq.v4.dat values for goethite (log_k 0.49), the use of wateq4f.dat values for goethite (log_k -1) showed that there was no goethite dissolution and no cupric ferrite precipitation occurring in either case A or B. This affirmed the decision not to include mineral phases. The main argument against including mineral phases in equilibrium though would be that equilibrium between mineral phases and solution is not attained instantly, but is rate-limited. Equilibrium approaches therefore cannot represent the dynamics of actual chemical processes (Rose and Waite, 2007) and especially for trace elements solution concentrations can often not be explained by solution isotherms but with sorption processes (Brümmer et al., 1983). As discussed above for pyrite (see VI.4.1.3) the implementation of rate-limited dissolution/precipitation reactions that would also reflect changes in surface sites would be desirable (Postma and Appelo, 2000), but has not been achieved in this study. To keep the model simple and due to missing direct evidence no mineral phases were hence included in further model runs.

VI.4.2.4 Generalised composite (GC) approach

Using the surface site values derived above (see Table VI-2) and the ion exchange site with dataset b (Table VI-1) for BR2 showed that adsorption during stormwater injection was much too low for both Zn and Cu (Figure VI-9, solid line). Zn breakthrough showed the typical snow-plow effect (Starr and Parlange 1979; Seidel-Morgenstern, 2004) during the Cu breakthrough, when Zn is expelled from the surface site by Cu.

As the single surface site created was dominated by the most abundant mineral (i.e. quartz) and hence did not account for surface coatings with the less abundant minerals, the number of sites was increased to account for this effect. As expected, an increase in surface sites delayed the breakthrough of both metals, but could not match simultaneously Zn and Cu breakthrough. A compromise value of 0.07 mol showed that neither the final concentration nor the shape of the Zn breakthrough curve could represent the observed results (Figure VI-9, dashed line), as the modelled breakthrough was linear rather than concave. A further increase in surface sites could lower the final concentration of the modelled Zn breakthrough curve, but at the expense of an even later start (not shown). In addition, the pH curves showed not enough buffering and simulated results were too low overall (not shown).

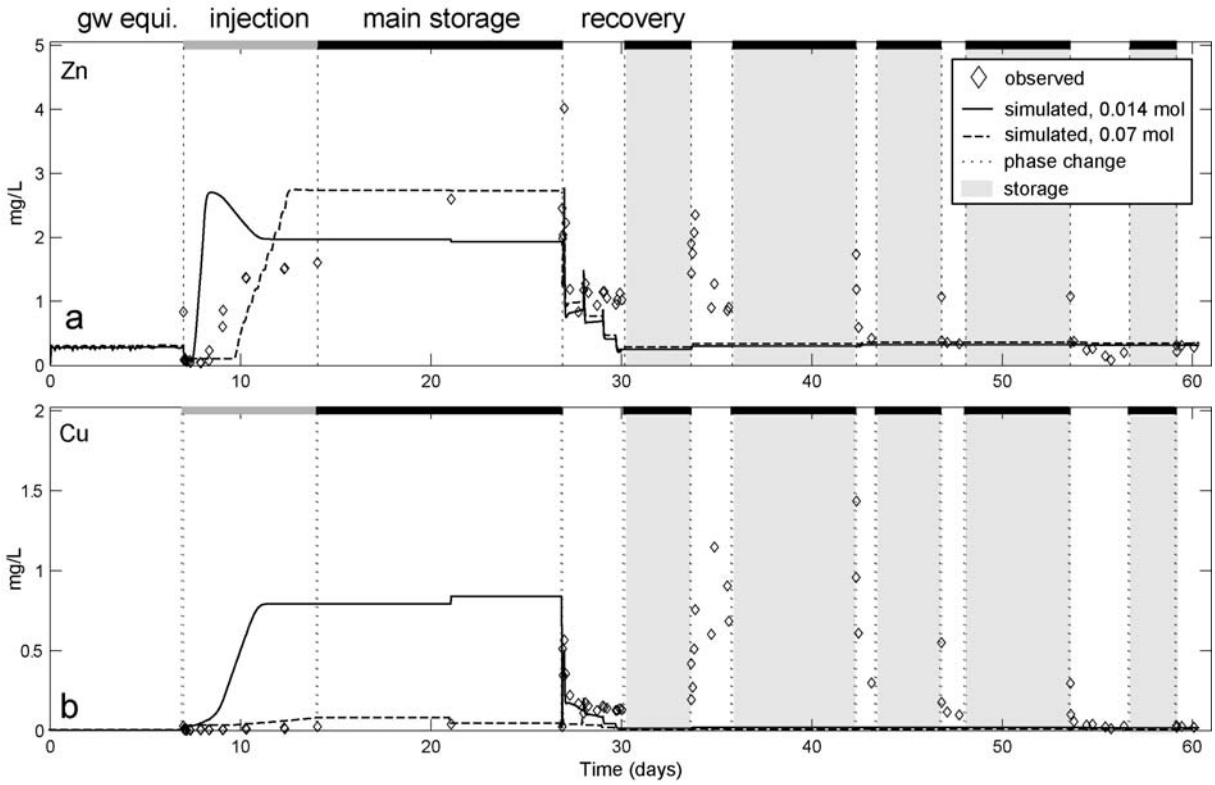

Figure VI-9: Simulated and observed concentrations of (a) Zn and (b) Cu for BR2 using a single GC-site with 0.014 mol (solid line) and 0.07 mol (dashed line) surface sites.

Figure VI-9 also showed that neither Zn nor Cu were desorbed sufficiently during recovery, especially when factoring in that the release observed during day 27-30 was also due to the ion exchange site. The GC approach used (Wang et al., 1997) was derived from adsorption

test, and did not incorporate desorption data, which might explain why it performed poorly for desorption. In addition, using only Cu and Zn surface complexation reactions does not account for competition of ions. While more analysis of the sediment to determine surface area and surface site characteristics might be able to improve the GC approach, it would not be transferable to other sediments.

This approach was therefore abandoned and the CA approach adopted.

VI.4.3 Summary of simple approaches

The above results showed that:

- The Kd approach was not appropriate, as solution composition and flow direction changed significantly.
- The number of measured exchanger sites was not sufficient to account for the observed major cation and metal sorption behaviour simultaneously and hence ion exchange will only be used to account for major cations.
- Some minerals were found to dissolve and precipitate during the column simulation when assuming equilibrium conditions. Nevertheless, it was considered unlikely that equilibrium conditions were achieved during the experiment. It would be desirable to incorporate kinetic mineral dissolution/precipitation coupled with changes in number of surface sites, but could not be achieved at this stage. Further simulations therefore did not include any mineral phases.
- The single site of the GC approach could not account for the observed metal behaviour during injection and recovery simultaneously.

The quantitative evaluation of these simple approaches can be found in VI.6.1.

VI.5 Component additivity (CA) surface complexation modelling

As the simple approaches could not match the observed behaviour, a component additivity approach was undertaken. In the following the used components are presented (VI.5.1) and the basic response of the simulated results to the individual components is shown (VI.5.2) for BR2 as example. Then the combination of all components will be applied to different column experiments (VI.5.3). The effect of adding dual domain (VI.5.3.5) and kinetic biodegradation (VI.5.3.6) are shown for BR2. The evaluation of the model, model uncertainties and further improvements are then presented in VI.6.

VI.5.1 Conceptual model for interactions of metals, organic phases and matrix

As discussed in previous chapters, metal-organic complexation is an important speciation mechanism for Zn and Cu. From the observed results and from theory, a conceptual model (Figure VI-10) would need to allow for:

- surface complexation of metals with the bare mineral surface
- complexation of metals with mobile aqueous organic surfaces
- surface complexation of metals with immobile organic surfaces
- interaction of mobile organic matter with the mineral surface
- formation of ternary surface complexes
- transport of all mobile species

The simple version would consider one mobile (FA) and one immobile organic phase (HA), while a more complex model would also allow for the transition of mobile phase into immobile phase and vice versa (i.e. dissolution/precipitation) with changes in pH and hence the same complexation, sorption and ternary complex formation with HA as seen for FA (Figure VI-10, dashed). At this point only the simpler version has been implemented.

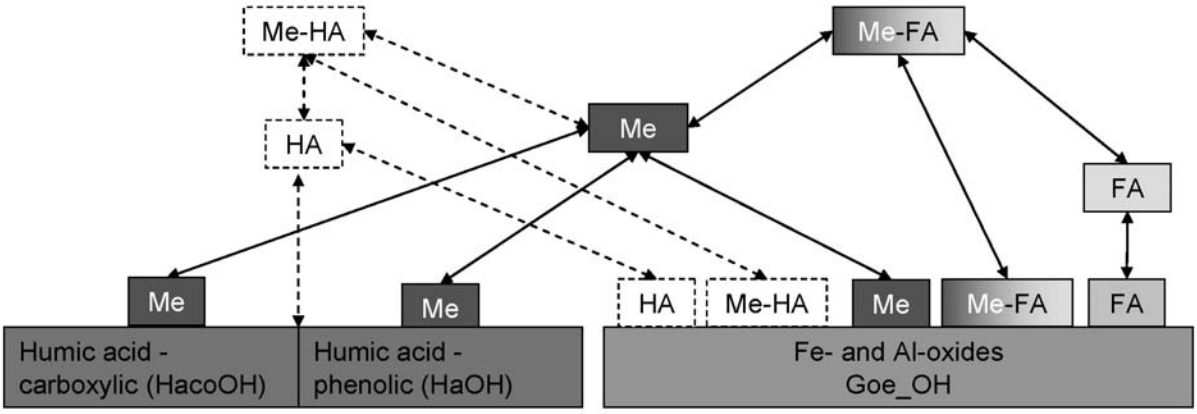

Figure VI-10: Conceptual model of metal – surface – organic acids interactions. Solid lines: simple implemented model, dashed lines: species and transformations are not implemented yet. HA: humic acid, FA: fulvic acid, Me: metal ion.

VI.5.1.1 Surface complexation onto minerals

Surface complexation of metals onto mineral surfaces has been described extensively in the literature (e.g. Sposito, 1983; Davis and Kent, 1990; Koretsky, 2000; Goldberg, 2005). It assumes that mineral surfaces are composed of specific functional groups that react with dissolved solutes to form surface species and that this reaction can be described with equilibrium mass action equations (see II.4.1).

The first decision was what mineral or combination of minerals would be most appropriate for the sediment used and data available. In this study, clay mineral surfaces (mainly kaolinite) would be represented by the exchanger site and have been found to be of less importance for trace metal sorption (Davies-Colley et al., 1984; Lofts and Tipping, 1998; Covelo et al., 2007). This leaves Al- and Fe-oxides and only minimal amounts of Mn-oxides in sediment WS to be considered (see Table III-10 and Figure V-15). It is generally found that SCM values are similar for Al- and Fe-oxides (see Table VI-3; Lofts and Tipping, 1998) and to simplify the model one phase is often chosen as a surrogate to account for all oxides

(Anderson and Benjamin, 1990; Meima and Comans, 1998; Dijkstra et al., 2002). Dzombak and Morel (1990) created a coherent set of parameters for hydrous ferric oxides (HFO) that has been used in many other studies (e.g. Meima and Comans, 1998; Dijkstra et al., 2002) and is incorporated into PHREEQC. But as HFO had been found to be unstable before (see VI.4.2.3) and hydrous aluminous oxides (HAO) and goethite values are also more comparable, goethite was chosen as a surrogate mineral. Mathur and Dzombak (2006) have recently extended the database from Dzombak and Morel (1990) to incorporate goethite and their de-/protonation values were subsequently used (see Table VI-3). They also found that stability constants are similar between goethite and HFO, when surface area and site density are taken into account, supporting the idea that the sorption mechanism is the same in both cases.

Table VI-3: Selected surface complexation values showing a range of values for goethite, HFO and HAO.

mineral	Surface area [m^2/g]	site density [sites/nm²]	site density [mol/mol Fe or Al]	log_k_1	log_k_2	Reference
goethite	60	2	0.018	6.93	-9.65	Mathur and Dzombak, 2006
goethite	21.4	1.3		5.6	-8.9	Buerge-Weirich et al., 2003
goethite	49	2.31	0.188 mmol/g	7.72	-10.09	Robertson and Leckie 1998
goethite	79.4	1.4	0.016	7.68	-8.32	Ali and Dzombak, 1996
goethite	43.1	2.31		7.52	-10.6	Manning and Goldberg, 1996
goethite	21		0.079 mmol/g	5.67	-9.01	Nowack and Sigg, 1996
goethite	48.5	4		6.3	-10.48	RES^3T (DDL)
HFO	327	2.31	0.112	7.18	-8.82	Hanna 2007
HFO	193	27		5.0	-9.4	Anderson and Benjamin, 1990
HFO	600		s: 0.005 w: 0.2	7.29	-8.93	Dzombak and Morel, 1990
HFO	244	4.62		5.87	-10.11	RES^3T (DDL)
HAO	210		s: 0.009 w: 0.25	7.38	-9.09	Karthikeyan and Elliott 1999
HAO	41	8		6.8	-11.0	Anderson and Benjamin, 1990
HAO	101	4.1		6.54	-9.93	RES^3T (DDL)

log_k_1: $S_OH + H^+ = S_OH_2^+$; log_k_2: $SOH = SO^- + H^+$; HFO: hydrous ferric oxide = $Fe(OH)_3$; HAO: hydrous aluminous oxide = $Al(OH)_3$; s: strong sites; w: weak sites; RES^3T: Brendler et al. (2004) median values for DDL (diffuse double layer) model values.

The second decision was the definition of the type of surface sites (i.e. single site or weak and strong sites) and stoichiometry of metal complexes (i.e. monodentate/multidentate). While incorporating a weak and strong site as well as multidentate binding would be a more realistic representation, it however increases the number of parameter values significantly. Mathur and Dzombak (2006) used one surface site and monodentate binding as inner- and outer-sphere complex. Only monodentate complexes are also used by Dzombak and Morel (1990) and Lofts and Tipping (1998). Taking into account that more surface sites would be added for organic matter, one site with monodentate binding was therefore considered to be sufficient for this study and metal complexation constants from Mathur and Dzombak (2006)

for Cu, Zn, Ca and Mg were incorporated in the database as competition between major divalent ions can be important (Davis et al., 1998) (see Table VI-6).

Once the database is enlarged, PHREEQC needs three more parameters:

(a) total number of surface sites (mol) or site density (sites/nm², since version 2.13)

This parameter is the most uncertain and models are usually sensitive to it (Goldberg, 1991). Crystal structure and chemical analysis have been undertaken to measure site density directly (Koretsky, 2000), but for amorphous minerals and varying grain sizes this still involves a number of assumptions. A number of studies have used fixed site densities, e.g. 2.31 sites/nm² (Davis and Kent, 1990), 10 sites/nm² (Hayes et al., 1991), 5 sites/nm² (Lofts and Tipping, 1998) or 0.005/0.2 mol/mol Fe for strong/weak sites (Dzombak and Morel, 1990). As a fixed site density basically shifts the uncertainty to the other two parameters, this parameter is usually adjusted during calibration. A first approximation of this value for pure phases can be obtained from a Langmuir sorption isotherm using the sorption maximum (Dzombak and Morel, 1990). For the natural sediments used in this study total amounts of sites (assuming 1 mol Al equals 1 mol Fe (Meima and Comans, 1998)) were estimated to lie between the total amounts of Al and Fe (see Table III-10) and the extracted amounts (see Figure V-15), assuming 0.018 sites/mol and incorporating total sediment mass per column and bulk density.

(b) specific surface area (m²/g)

Specific surface area is commonly measured with nitrogen gas BET analysis. Values reported in the literature vary from 1.4-186 m²/g for goethite (RES^{3}T, Brendler et al., 2004), but commonly used values range from 20-80 m²/g (see Table VI-3). Values for Al-oxides are slightly higher. As the surface area has been found to be an insensitive parameter (Appelo and Postma, 1999b), 60 m²/g (Mathur and Dzombak, 2006) was considered to be an appropriate value.

(c) mass of surface mineral (g):

The mass of mineral available for surface complexation was estimated from the extractable amounts of Al and Fe (Meima and Comans, 1998; Weng et al., 2001; Dijkstra et al., 2002) incorporating bulk density of each column. Uncertainties in this parameter will be incorporated in the calibrated value for total amount of sites.

Finally the diffuse double layer was calculated using the Donnan option, as this was the most stable setting.

Using the above defined parameters for metal speciation in a generic stormwater solution (0.01M Ca-HCO_3) with 0.01 mol goethite sites showed the typical earlier adsorption edge for Cu compared to Zn and also shows that Cu is mainly sorbed as inner-sphere complex, while Zn is mainly present as outer-sphere complex (Figure VI-11).

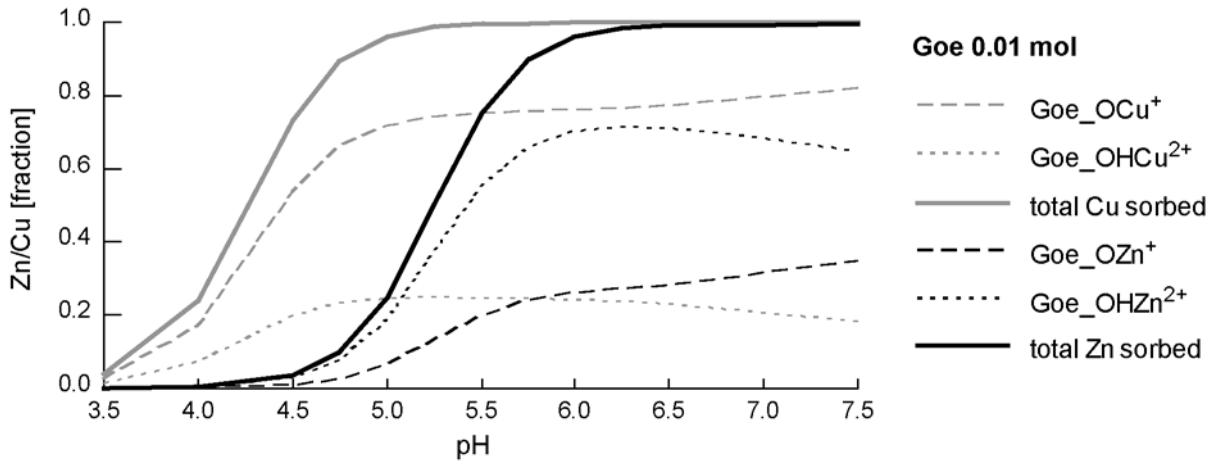

Figure VI-11: Surface complexation of 1 mg/L Zn/Cu vs. pH onto 0.01 mol Goethite in 0.01 M Ca-HCO_3 solution.

VI.5.1.2 Organic complexation

Currently the most advanced models for organic complexation are the (a) Non-Ideal-Competitive-Adsorption (NICA-Donnan) (e.g. Kinniburgh et al., 1996; Koopal et al., 2005; van Riemsdijk et al., 2006), (b) Humic Ion Binding Model (latest version Model VI; earlier versions Model V and WHAM) (e.g. Tipping, 1994; Christensen et al., 1998; Tipping, 1998; van Riemsdijk et al., 2006), and (c) Stockholm Humic Model (SHM) (e.g. Gustafsson et al., 2003; Linde et al., 2007). They can be combined with other speciation models to calculate metal speciation in complex natural systems like soils (e.g. Weng et al., 2001; Dijkstra et al., 2004; Khai et al., 2008). The NICA-Donnan model is a continuous site-distribution, electrostatic model, which does not use defined stability constants for specific sites. Even though a good compilation of generic FA and HA values exists (e.g. Milne et al., 2001; Milne et al., 2003), translation of these continuous site-distribution values into PHREEQC is therefore difficult (Crawford, 1996). Model VI and SHM are both very similar discrete-site electrostatic models, which account for the heterogeneities of organic matter by describing protonation/deprotonation in terms of two median affinity distribution (pK_A and pK_B) values and an associated range (ΔpK_A and ΔpK_B) on two different surface sites, which can be interpreted as carboxylic and phenolic functional group sites. Metal complexation is described for 8 monodentate (4 at site A, 4 at site B) and 12 bidentate sites, which is specified by complexation constants for site A and B and via a proximity factor, correlation of proton binding to metal binding strengths and addition of monodentate log_k values to represent bidentate log_k values (Tipping, 1994; Tipping, 2002; Gustafsson et al., 2003). The Tipping and Hurley (1992) values have been translated into PHREEQC (Crawford, 1996),

while the SHM is integrated into VisualMINTEQ (Gustafsson et al., 2003). To the best of my knowledge, none of these models have been combined with 3D-solute transport models in groundwater. This is most likely due to the large number of species generated and therefore a simplified version was created.

As the mobile organic species in this study were plant derived fulvic acids, the Suwannee River Fulvic Acid (Srfa) was used as main species, which has been found to be similar to terrestrial NOM (Cabaniss et al., 2007). Other authors have used pyromellitic acid (benzene-1,2,4,5-carboxylic acid) as low molecular weight analogue for FA (Evanko and Dzombak 1999; Buerge-Weirich et al., 2003; Johnson et al., 2005). Both have been described with 4 proton binding sites (Leenheer et al., 1995; Evanko and Dzombak 1999; Lu and Allen, 2002), while Tipping (1994) uses diprotic generic fulvate and humate species. PHREEQC speciation calculation showed that the unprotonated $Srfa^{4-}$ is the main species (>99%) in stormwater over pH 3.5-7.5. Molecular weight of the masterspecies was set to 12 g/mol, as it was measured as DOC, rather than as mol of FA.

A literature review showed that a range of different organic complexation values for Cu and Zn can be found (Table VI-4). A stochastic model showed that Cu complexation constants (log_k) ranged from 0-15 for Srfa, with usually a peak at lower log_k values and a peak at higher log_k values (Cabaniss et al., 2007). This corresponds to complexation constants for a weak site (e.g. carboxylic group) and a strong site (e.g. phenolic group), which are commonly given in the literature. Srfa is reported to have about 70% carboxylic groups and about 30% phenolic groups with 6.9-9.4 mmol/g-C of carboxylic groups (Ma et al., 2001; Lu and Allen, 2006). This is similar to the assumption in Model VI, where site B (phenolic) is assumed to be half the number of sites than site A (carboxylic) (Tipping and Hurley, 1992).

Two different complexes were therefore chosen to be possible for metal (Me) complexation with Srfa: $Me^{2+} + Srfa^{4-} = MeSrfa^{2-}$ (log_k_a) and $Me^{2+} + HSrfa^{3-} = MeHSrfa^{-}$ (log_k_b). Cu log_k_a (Table VI-6) was chosen following the wateq4f.dat (Tipping, 1994), Davis (1984), Leenheer et al. (1998) and Lu and Allan (2006) (see Table VI-4). A higher value for Cu log_k_b (Table VI-6) was chosen in analogue to (Buerge-Weirich et al., 2003) and Lu and Allen (2006) (see Table VI-4). Complexation constants for Zn are reported less in the literature, but were found to be about 1 log unit lower than Cu complexation constants in accordance with the hydrolysis constant (Tipping and Hurley, 1992). Tipping et al. (2002) found competition effects for Cu with Al and Fe and with Ca for Zn. Al and Fe concentration are low throughout the experiment and the effects of Ca complexation on Cu and Zn speciation were negligible

in the concentration range and conditions found in stormwater or groundwater, hence no further complexes were defined.

Table VI-4: Selected literature values for organic complexation constants of various metals with organic acids.

organic acid	ion	log_k$_1$	log_k$_2$	Reference
Fulvate/Humate	Cu	6.2		wateq4f.dat after Tipping, 1994
DOC from lake sediments	Cu	5.2		Davis, 1984
SrDOM	Cu	4.9		Christensen et al., 1999
generic FA	Cu	0.5	6.7	Gustafsson et al., 2003
generic HA	Cu	0	6.2	Gustafsson et al., 2003
Srfa, at pH 6	Cu	5.2		Leenheer et al., 1998
SrFA	Cu	7.45	9.13	Ma et al., 2001
SrHA	Cu	7.47	9.37	Ma et al., 2001
peat HA	Cu	0.5	3.26	Syrovetnik et al., 2008
peat HA	Cu	1.1	3.8	Tipping, 1993
soil HA	Cu	1.8	2	Tipping, 1993
soil HA	Cu	0.5	3.1	Tipping et al., 1995
generic FA	Cu	2.1	6	Tipping et al., 2002
generic HA	Cu	2	5.6	Tipping et al., 2002
river water DOM	Cu	6.5	8.27	Lu and Allen, 2006
pyromellitic acid	Cu	4.95	7.91	Buerge-Weirich et al., 2003
DOC from lake sediments	$CuOH^+$		9.8	Davis, 1984
generic FA	Zn	1.95	9.95	Gustafsson et al., 2003
generic HA	Zn	1.45	9.45	Gustafsson et al., 2003
SrFA, at pH 6	Zn	3.8		Leenheer et al., 1998
peat HA	Zn	1.5	4.64	Syrovetnik et al., 2008
generic FA	Zn	1.6	4.3	Tipping et al., 2002
generic HA	Zn	1.5	3.9	Tipping et al., 2002

log_k$_1$: weak site; log_k$_2$: strong site; Sr: Suwannee River, FA: fulvic acid, HA: humic acid, DOM: dissolved organic matter, DOC: dissolved organic carbon

In metal spiked stormwater these values result in a Zn speciation of about 50% free Zn^{+2} and 50% $ZnSrfa^{2-}$, while Cu is dominated by $CuSrfa^{2-}$ for pH 5-7 (Figure VI-12). These values are supported by other studies, as near complete Cu complexation (Davis, 1984; Christensen et al., 1999; Zhao et al., 2007b) and Zn complexation of 20-80% have been reported (Düker et al., 1995; Warwick et al., 1998; Delolme et al., 2004; Dries et al., 2005; Zhao et al., 2007b). The considerably lower complexation constants reported by Tipping et al., 2002 were also tested, but resulted in nearly no complexation of Cu and Zn and were therefore dismissed.

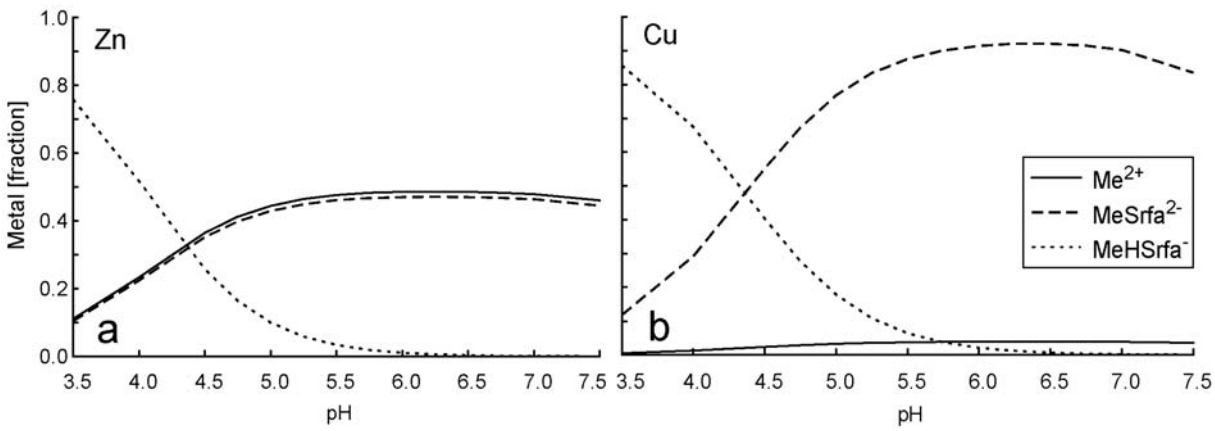

Figure VI-12: Aqueous speciation of metals (Me) vs. pH in 0.01 M Ca-HCO_3 solution with 10 mg/L Srfa: (a) Zn, total 1 mg/L and (b) Cu, total 1 mg/L.

VI.5.1.3 Surface complexation onto organic matter

A number of empirical and metal speciation studies have shown that solid organic matter is one of the most important factors for metal speciation of Cu and to a lesser extent for Zn (e.g. McBride et al., 1997; Lofts and Tipping, 1998; Weng et al., 2001; Khai et al., 2008) . For this model it is assumed that surface complexation onto organic matter can be represented by complexation with HA. Surface complexation onto organic matter basically combines the two above described concepts. Surface site type and stoichiometry have to be decided first. As carboxylic and phenolic surface groups are the most important functional groups, two separate surface sites (HawOH = weak site and HasOH = strong site) were created. Only monodentate binding was used to simplify coupling to the transport model. While Zn is mainly bound monodentate, bidentate binding for Cu, as well as Al and Fe, should be considered for an improved version of the model (Gustafsson and van Schaik 2003; Syrovetnik et al., 2008).

Complexation constants for HA and FA are often reported to be the same or very similar (Tipping and Hurley, 1992; Linde et al., 2007), even though other studies report stronger complexation by HA compared to FA (Milne et al., 2003; Weng et al., 2007). Often organic complexation models do not distinguish between mobile and immobile humic acids (Lofts and Tipping, 1998; Syrovetnik et al., 2008), while different complexation behaviour to adsorbed or dissolved organic acids has been reported (Davis, 1984; Gustafsson and Berggren Kleja, 2005; Saito et al., 2005). Paulson and Balistrieri (1999) reported increased adsorption to SOM compared to DOM by 0.6 log units. The selection of complexation constants was therefore the most challenging task. Comparable studies used either the NICA-Donnan approach (Weng et al., 2001) or a simplified Model V data set (Syrovetnik et al., 2008). Using the median complexation values from either approach will not readily translate the heterogeneities expressed in both models, as this option is not available in PHREEQC. As the NICA-Donnan model has the most complete and consistent dataset, median values for both sites on HA were adopted for Cu, Zn, Ca, Al and Fe (Milne et al., 2001; Milne et al., 2003). The importance of consistency in a dataset was emphasised by Dzombak and Morel (1990) and a systematic error can be accounted for by calibration of the site density. As with goethite the Donnan diffuse layer option was adopted to account for surface charge effects.

Site densities for both weak and strong sites on humic acids commonly range between 1.5-5 mmol/g (Lofts and Tipping, 1998, Filius et al., 2000; Weng et al., 2001; Gustafsson et al., 2003; Syrovetnik et al., 2008). While Model V uses a 2:1 ratio for carboxylic to phenolic sites, Buffle et al. (2007) estimate that 90% of sites are weak sites and only 10% strong sites. All

this information was taken into account to estimate a range for the total number of sites, but the actual values were subject to calibration.

Surface area values for SOM reported in the literature vary widely depending on the analysis method. Values are 0.6-18 m²/g by BET-N_2 (Chiou et al. 1990), 94-174 m²/g by BET-CO_2 (de Jonge and Mittelmeijer-Hazeleger, 1996) and 560-800 m²/g by ethylene glycol (EG) (Bower and Gschwend, 1952). De Jonge et al. (2000) concluded that organic matter has a high surface area with micropores <0.5 nm that cannot be penetrated by N_2. These subnanometres pores might also rate-limit sorption of other components and explain why specific sorption equilibrium is commonly obtained after prolonged time. A mean value of 135 m²/g was assumed in this study after the BET-CO_2 values, which seem the most reliable technique (de Jonge and Mittelmeijer-Hazeleger, 1996).

The mass of organic carbon was calculated using the loss of ignition (Table III-10) and assuming that 50% of the organic matter was organic carbon (Rowell, 1994; Lofts and Tipping, 1998), also including sediment mass and bulk density for each experiment.

Using the adopted values with the three surface sites showed that Cu sorption is dominated by Has sites for pH >5 (Figure VI-13) and agrees with findings from Lu and Allen (2002) that phenolic sites account for the majority of Cu binding in natural waters. Zn sorption shifted from Haw (weak site) to Has (strong site) to goethite sites with increasing pH (Figure VI-13). A significant shift for Zn from non-specific binding (weak sites) to specific binding (strong sites) with increase in pH has also been shown in other studies (Tiller et al., 1984b; Mesquita and Vieira e Silva, 1996; Weng et al., 2001). While it is recognised that the importance of each binding site is also obviously dependent on their proportion, this example (Figure VI-13) showed that the principal distribution pattern is reflected correctly within the model.

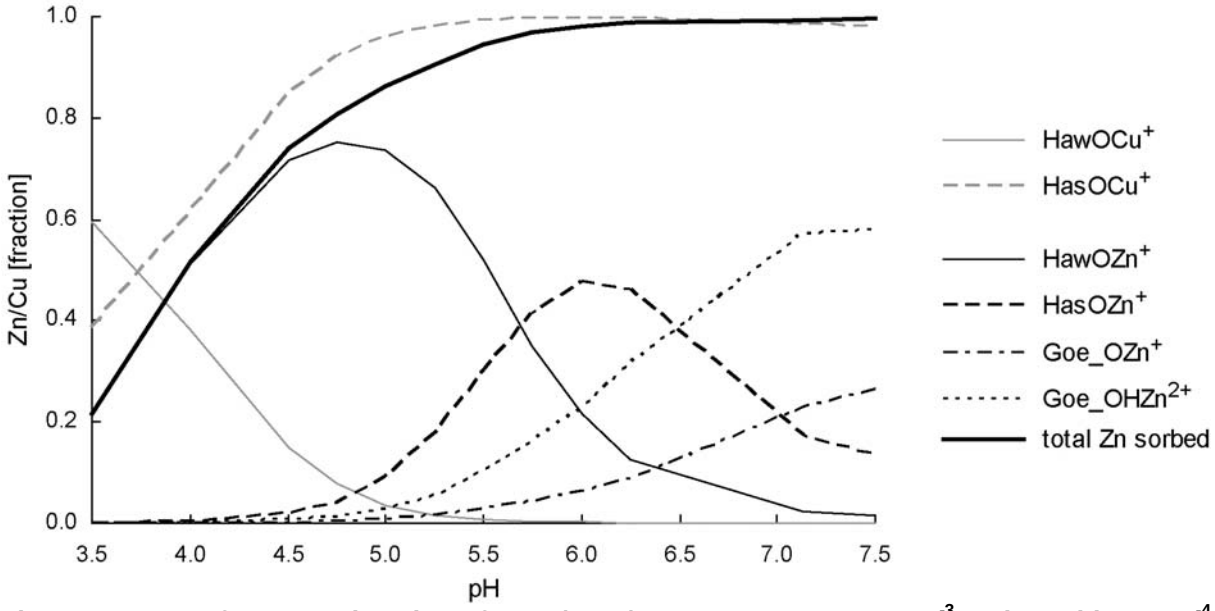

Figure VI-13: Surface complexation of 1 mg/L Zn/Cu versus pH onto 5*10^{-3} mol goethite, 5*10^{-4} mol Haw, 5*10^{-6} mol Has sites in 0.01 M Ca-HCO_3 solution.

VI.5.1.4 Sorption of organic matter onto minerals

The adsorption of organic acids onto mineral surfaces has been found in numerous experiments (e.g. Dunnivant et al., 1992; Gu et al., 1994; Gu et al., 1996a; Kaiser, 2003) and suspended particles in the field are often dominated by organic matter coatings (e.g. Day et al., 1994; Buffle and Leppard, 1995a; Tessier et al., 1996). These organic coatings change the surface properties of minerals significantly and are therefore important in metal speciation (Murphy and Zachara, 1995; Merdy et al., 2006). As sorption of NOM onto mineral surfaces is dependent on pH, ionic strength and NOM concentrations, description of sorption of NOM onto mineral surfaces is often empirical using conditional adsorption isotherms (Davis, 1982; Dunnivant et al., 1992; Gu et al., 1994; Paulson and Balistrieri, 1999; Schmitt, 2002).

At the other end of the spectrum are studies that describe the sorption mechanism in great detail (e.g. Filius et al., 2003; Weng et al. 2006; Buffle et al., 2007). Simplified, adsorption can be described analogous to binding of Fe^{3+} to organic acids and is largely due to ligand exchange and hydrogen bonding (Gu et al., 1994; Filius et al., 2000). Apart from hydrophobic fractions of NOM, carboxylic groups play a significant role in complexation with iron oxides surfaces (Kaiser, 2003), as they form dominantly monodentate inner-sphere complexes (Fu and Quan, 2006; Weng et al. 2006; Křepelová et al., 2008). The observed stronger sorption of HA compared to FA can be explained with the larger number of reactive ligands on the larger HA molecule (Weng et al., 2007). It has also been shown that the coverage is maximally a monolayer (Jardine et al., 1989; Day et al., 1994) and there might still be patches that are not covered with NOM on the mineral surface due to electrostatic repulsion and steric blocking effects (Davis, 1982; Weng et al., 2006; Křepelová et al., 2008).

Compared to oxide surfaces, sorption of organic ligand onto kaolinite has been shown to be limited (Dalang et al., 1984; Křepelová et al., 2008).

For this study an intermediate approach was chosen. After comparing stability constants for pyromellitic acid and Srfa found in the literature (Evanko and Dzombak, 1999; Buerge-Weirich et al., 2003; Johnson et al., 2005) values from Evanko and Dzombak (1999) for Srfa with three inner-sphere and one outer-sphere complexes were adopted for this study (see Table VI-6). Filius et al. (2000) also found that sorption of FA to goethite can be described with four surface species. Depending on the amount of available mineral surface sites the distribution of Srfa between non-specific sorption, specific sorption and dissolved Srfa species change (Figure VI-14). While non-specific sorption occurs over the whole pH range, specific sorption is limited to lower pH (<5.5), which is supported by findings from Filius et al., (2000).

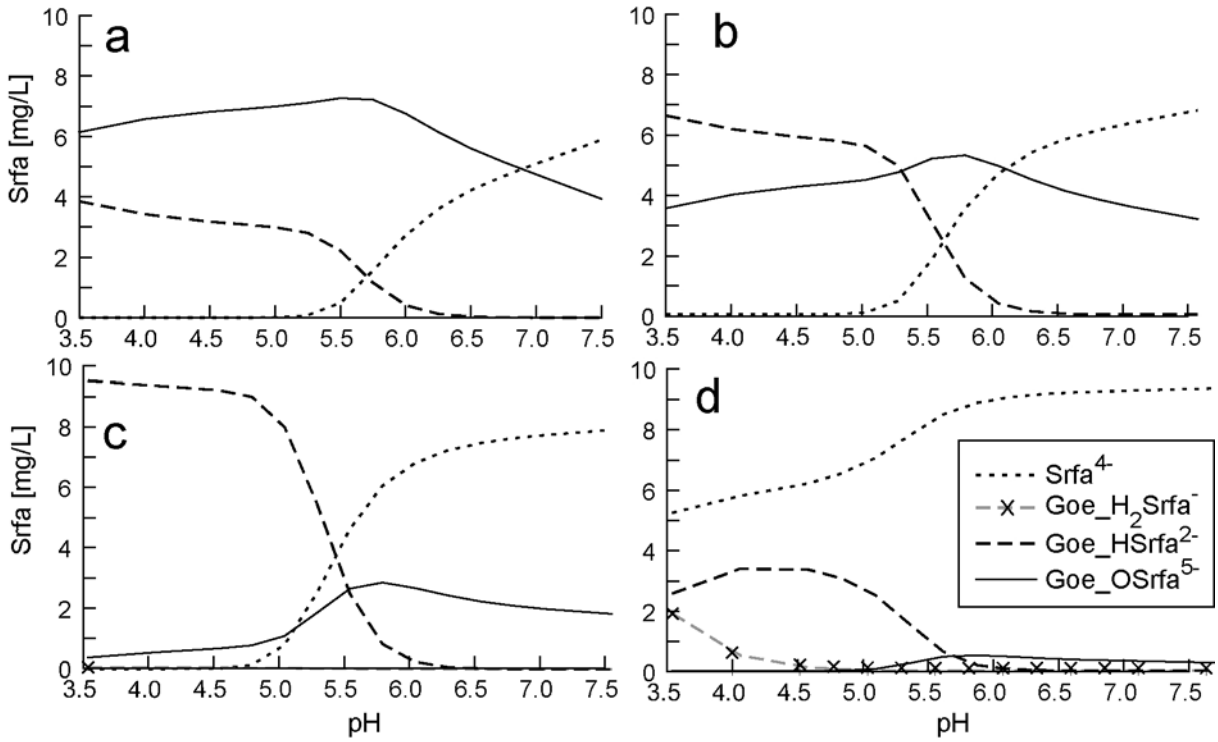

Figure VI-14: Speciation of Srfa (total 10 mg/L) vs. pH in 0.01M Ca-HCO_3 solution onto (a) 0.01, (b) 0.007, (c) 0.004, (d) 0.001 mol goethite surface site.

VI.5.1.5 Ternary complexes

In a natural system metals (Me), mineral surfaces (>SOH) and organic ligands (L) are often present together and interactions between minerals and organic ligands change the surface properties of either participant. Hence the sorption of metals onto organic-mineral complexes or sorption of metal-organic complexes onto minerals is different from binary systems (Honeyman and Santschi, 1988; Merdy et al., 2006). Often, the addition of organic acids to the binary metal-oxide system tends to enhance metal sorption at acidic to neutral pH and depresses metal sorption at alkaline pH (Murphy and Zachara, 1995). The effect is due to the

sorption of organic acids to mineral surfaces at lower pH, offering additional sorption sites to metal, while they keep metals in solution at higher pH. However, the overall effect is dependent on the relationship of the stability constant between the three binary systems (i.e. the participating components) (Murphy and Zachara 1995).

A number of empirical studies have investigated binary systems and compared the effect to the ternary system. Some studies found that the ternary system could be described well by addition of the binary system constants (e.g. Dalang et al., 1984; Davies-Colley et al., 1984; Zachara et al., 1994; Heidmann et al., 2005), while other studies found discrepancies when using the additivity approach (e.g. Schroth and Sposito, 1998; Vermeer et al., 1999; Christl and Kretzschmar, 2001). Metal stability constants often seem to be lower for organic ligands in solution than for sorbed organic ligands (Davis, 1984; Paulson and Balistrieri, 1999; Gustafsson and Berggren Kleja, 2005; Saito et al., 2005). The additivity approach might also overestimate the number of reactive mineral surface sites, as they will be masked by the sorbed organic ligand (Benyahya and Garnier, 1999)

While the actual ternary complex formation is not well studied, it can be envisaged as either metal-like (>SO(H)-Me-L) or ligand-like (>S-L-Me) (Nowack and Sigg, 1996), where either the metal ion or the ligand is the bridge between the other two components. The existence of both ligand- and metal-bridged ternary surface complexes has been supported spectroscopically in ternary metal ligand- adsorbent systems (von Zelewsky and Bemtgen, 1982; McBride, 1985; Hizal and Apak, 2006) and both forms were used by Schroth and Sposito (1998). Under acidic to neutral conditions as in this study ligand like sorption would be expected to be more important (Benyahya and Garnier, 1999; Hizal and Apak, 2006). In the ligand-like case, the metal binding to the complex is different from the sum of the binding to the individual components due to the surfaces interaction between the negatively charged humic acid and the positive metal oxide and resulting charge adaptations (Vermeer et al. 1999; Saito et al., 2005; Weng et al., 2006). The overall metal adsorption in a ternary system will be smaller than the additive value when the metal ion has a higher affinity to the organic ligand and will be larger when it has a higher affinity to the mineral surface (Vermeer et al. 1999). The affinity to either will change depending on pH and ionic strength (Weng et al., 2006; Weng et al., 2007).

Due to complex and still largely unknown effects, the formation of ternary complexes is often not invoked in models and a combination of two models for sorption to mineral and organic surfaces are used (e.g. Christl and Kretzschmar, 2001; Heidmann et al., 2005; MacDonald and Hendershot, 2006). If ternary complexes are included, it is often assumed that the

binding of the metal-ligand complex would be the same as binding of an uncomplexed ligand, as humic acid molecules would have enough sites available for binding both or ternary complexation constants are fitted to the results (Davis, 1984; Schroth and Sposito, 1998; Benyahya and Garnier, 1999). Stability constants for humic substances are also estimated from constants found for low molecular weight organic acids (Ali and Dzombak, 1996).

The literature review for ternary stability constants using the diffuse double layer model (Table VI-5) did not yield results for ligand like sorption of FA onto goethite. It showed though that log_k_1 values were commonly greater than 10 (reaction 1). EDTA (Nowack and Sigg, 1996) is a much stronger complexant than FA (Schmitt, 2002) and values are considerably higher. Following the additivity approach the complexation constants for the metal-ligand complex onto the mineral surface (reaction 2) could be derived by subtracting the aqueous complexation constant (reaction 3) from the reaction 1 constant (Nowack and Sigg, 1996), i.e.:

reaction 1: >SOH + Me + L + H^+ = >S-L-Me + H_2O (log_k_1)

reaction 2: >SOH + MeL + H^+ = >S-L-Me + H_2O (log_k_2)

reaction 3: Me + L = MeL (log_k_3)

with log_k_2 = log_k_1 – log_k_3

Table VI-5: Selected stability constants for the formation of ternary complexes from reaction 1.

metal (Me)	organic acid (L)	surface (>SOH)	ternary species	log_k_1	ref
Cu	phthalic acid (Phth); chelidamic acid (Chel)	goethite	>SOH-Cu-Phth >SOH-Cu-HChel >SO-Cu-Chel^{2-} >SOH-Cu-HChel$_2^{3-}$	10.91 13.06 -0.74 10.24	Ali and Dzombak, 1996
Cd Co	Salicyclic acid (Sal)	alumina	>SO-Cd-Sal$^-$ >S-Sal-CdOH >S-Sal-Co$^+$ >S-Sal-CoOH	10.86 16.9 21.7 15	Benyahya and Garnier, 1999
Cd Cu	Salicyclic acid Pyromellitic acid (Pyr)	goethite	>SO-Cd-Sal >S-Pyr-Cd >S-Pyr-Cu	8 16 17.5	Buerge-Weirich et al., 2003
Zn Cu Pb Ni	EDTA	goethite	>S-EDTA-Zn$^-$ >S-EDTA-Cu$^-$ >S-EDTA-Pb$^-$ >S-EDTA-Ni$^-$	28.1 31.0 30.0 30.7	Nowack and Sigg, 1996

Applying this approach as a first estimate for this study to the two surface complexes for Cu and Zn (using Buerge-Weirich et al. (2003) values for log_k_1) results in the values shown in Table VI-6. Speciation modelling showed that all Zn and Cu would be sorbed as Goe_SrfaMe$^-$ complex over the whole pH range (Figure VI-15a). As sorption of organic acids onto goethite have been found to occur mainly under acidic conditions (Buerge-Weirich et al., 2003), log_k_2 values were decreased to allow for metal complexation onto goethite at higher

pH (Table VI-6) (Figure VI-15c). A better definition of ternary complexes would be desirable for an improved model.

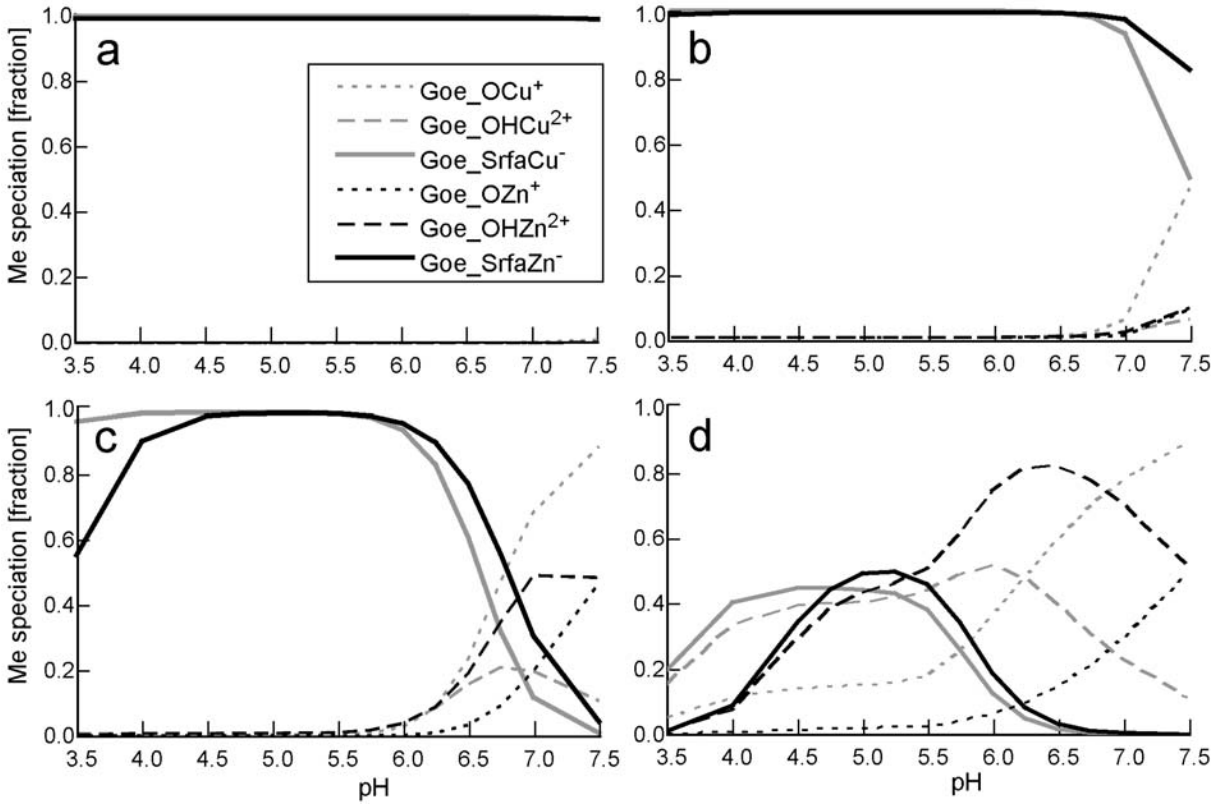

Figure VI-15: Sorbed metal speciation vs. pH with 1 mg/L Zn/Cu in 0.01 M Ca-HCO_3 solution and 10 mg/L Srfa onto 0.01 mol goethite surface site with decreasing affinity constants for ternary complexes Goe_SrfaMe$^-$ (a) log k 12.7, (b) log k 10.7, (c) log k 8.7 and (d) log k 6.7.

In summary, the following mass action equation and stability constants (Table VI-6) were added to the standard PHREEQC database for the surface complexation model used in VI.5.2 and VI.5.3.

Table VI-6: Added mass action equations and stability constants (log_k). Srfa (Suwannee River Fulvic Acid); Goe_OH: goethite surface site; HasOH: strong humic acid surface site; HawOH: weak humic acid surface site.

Cation surface complexation on goethite	log_k	ref.	log_k this study
Goe_OH + H^+ = Goe_OH_2^+	6.93	a	nc
Goe_OH = Goe_O^- + H^+	-9.65	a	nc
Goe_OH + Cu^{2+} = Goe_OCu^+ + H^+	1.39	a	nc
Goe_OH + Cu^{2+} = Goe_$OHCu^{2+}$	8.92	a	nc
Goe_OH + Zn^{2+} = Goe_OZn^+ + H^+	-0.96	a	nc
Goe_OH + Zn^{2+} = Goe_$OHZn^{2+}$	7.5	a	nc
Goe_OH + Ca^{2+} = Goe_OCa^+ + H^+	-6.48	a	nc
Goe_OH + Ca^{2+} = Goe_$OHCa^{2+}$	4.53	a	nc
Goe_OH + Mg^{2+} = Goe_OMg^+ + H^+	-3.02	a	nc
Goe_OH + Mg^{2+} = Goe_$OHMg^{2+}$	5.35	a	nc
Aqueous speciation of FA			
$Srfa^{4-}$ + H^+ = $HSrfa^{3-}$	1.7	b	nc
$Srfa^{4-}$ + 2 H^+ = H_2Srfa^{2-}	3.3	b	nc
$Srfa^{4-}$ + 3 H^+ = H_3Srfa^- (master species)	-4.3	b	nc
$Srfa^{4-}$ + 4 H^+ = H_4Srfa	5.6	b	nc
Cu^{2+} + $Srfa^{4-}$ = $CuSrfa^{2-}$	5.2	c	nc
Cu^{2+} + $HSrfa^{3-}$ = $CuHSrfa^-$	-	after e	8.0
Zn^{2+} + $Srfa^{4-}$ = $ZnSrfa^{2-}$	3.8	c	nc
Zn^{2+} + $HSrfa^{3-}$ = $ZnHSrfa^-$	-	after e	6.6
Surface complexation on humic acid			
HawOH + H^+ = $HawOH_2^+$	2.93	d	nc
HawOH + Cu^{2+} = $HawOCu^+$ + H^+	2.23	d	nc
HawOH + Zn^{2+} = $HawOZn^+$ + H^+	0.11	d	nc
HawOH + Ca^{2+} = $HawOCa^+$ + H^+	-1.37	d	nc
HawOH + Al^{3+} = $HawOAl^{2+}$ + H^+	-1.05	d	nc
HawOH + Fe^{3+} = $HawOFe^{2+}$ + H^+	5.0	d	nc
HasOH + H^+ = $HasOH_2^+$	8.0	d	nc
HasOH + Cu^{2+} = $HasOCu^+$ + H^+	6.85	d	nc
HasOH + Zn^{2+} = $HasOZn^+$ + H^+	2.39	d	nc
HasOH + Ca^{2+} = $HasOCa^+$ + H^+	-0.43	d	nc
HasOH + Al^{3+} = $HasOAl^{2+}$ + H^+	8.89	d	nc
HasOH + Fe^{3+} = $HasOFe^{2+}$ + H^+	17.5	d	nc
Sorption of FA onto goethite			
Goe_OH + H_3Srfa^- + H^+ = Goe_H_3Srfa + H_2O	13.4	b	nc
Goe_OH + H_3Srfa^- = Goe_H_2Srfa^- + H_2O	11.2	b	nc
Goe_OH + H_3Srfa^- = Goe_$HSrfa^{2-}$ + H^+ + H_2O	6.9	b	nc
Goe_OH + H_3Srfa^- = Goe_$OSrfa^{5-}$ + 4 H^+	-14	b	nc
Ternary complexes on goethite			
Goe_OH + $CuHSrfa^-$ + H^+ = Goe_HSrfaCu + H_2O	12.3	after e + f	8.7
Goe_OH + $CuHSrfa^-$ = Goe_$SrfaCu^-$ + H_2O	9.5	after e + f	6.7
Goe_OH + $ZnHSrfa^-$ + H^+ = Goe_HSrfaZn + H_2O	12.2	after e + f	8.7
Goe_OH + $ZnHSrfa^-$ = Goe_$SrfaZn^-$ + H_2O	9.4	after e + f	6.7

a: Mathur and Dzombak, 2006; b: Evanko and Dzombak, 1999; c: Leenheer et al., 1998; d: Weng et al., 2001;e: Buerge-Weirich et al., 2003; f: Nowack and Sigg, 1996; nc: no change

VI.5.1.6 Dual Domain

Dual domain (DD) was implemented for BR2 for a number of runs. The dual domain option in MT3DMS assigns a stagnant cell to each mobile cell, of which porosities are user defined. The mass transfer coefficient of a first order rate expression then calculates the diffusive exchange between the mobile and immobile cell. As DD is not a currently available option for PHT3D in PMWINpro, both parameters (i.e. porosity of immobile layer and transfer coefficient) were added directly in the input file (pht3drct.dat) and reactions were added in the name file (pht3d.in). Both parameters were varied within limits (see VI.5.3.5). Other sediment related values (e.g. exchange sites, surface sites) were assumed to be the same in the mobile and immobile domain.

VI.5.1.7 Kinetic biodegradation

As outlined in II.2.3.4 degradation of organic matter is an important process during ASR especially near the injection well and during storage and the effect of redox reaction on pH and alkalinity (see Table VI-7) in turn influence other inorganic processes (see II.4.5). The mineralisation of organic matter is generally mediated by microorganisms and can be described by two sequential steps: (1) fermentation, which transforms larger organic molecules into smaller organic molecules (e.g. formate, acetate, volatile fatty acids, hydrogen) and (2) respiration, which consumes these smaller organic molecules by different terminal electron acceptors (TEAs), e.g. oxygen, nitrate, ferric iron or sulphate (McMahon and Chapelle, 1991; Chapelle et al, 1995; Hunter et al., 1998). The partial equilibrium approach (PEA) assumes that the second step is fast and can be modelled as equilibrium reaction, while the first step is rate limiting (Postma and Jakobsen, 1996; Brun and Engesgaard, 2002). This approach has been applied successfully to a number of studies (Postma and Jakobsen, 1996; Brun et al., 2002; Prommer et al., 2002) and was also used for this study. Many studies also incorporate microbial growth and decay that can inhibit or stimulate biodegradation (Lensing et al., 1994; Prommer et al., 1999; Brun et al., 2002; Greskowiak et al., 2005), however, in this spatially defined column study microbial mass was assumed to be constant to simplify the model and due to the fact that no information about the bacterial nature and distribution in the column material was available. While chemolithotrophic redox processes using H_2 as an electron donor can occur in the subsurface (Lovley and Goodwin, 1988; Lovley and Phillips, 1988; Chapelle and Lovley, 1992), these reactions are not included. Secondary chemical redox reactions driven by the release of dissolved oxidised or reduced species are included as equilibrium processes in the general database though.

For each molecule Srfa removed a simple model organic compound formaldehyde (CH_2O) was added (e.g. Matsunaga et al., 1993; Barry, D. A. et al., 2002; Prommer and Stuyfzand,

2005). The kinetic reactions were defined for free dissolved Srfa, meaning that all sorbed and metal-complexed Srfa in solution cannot be degraded, which does not necessarily reflect real circumstances. Including dissolution of organic surface sites in an improved model (Figure VI-10) would therefore free more organic matter for biodegradation. The current use of a limited number of dissolved metal-Srfa complexes facilitates degradation.

The kinetic half reactions for each TEA were formulated as Monod expressions (Monod, 1949), which is applicable when the organic compound acts as primary energy source (Hunter et al., 1998), e.g. for oxygen as TEA:

$$\text{rate } O_2 = r_{O2} * C_{O2} / (K_{O2} + C_{O2})$$

with r_{o2}: maximum degradation rate using O_2 [mol/L/s], C_{O2}: concentration of O_2 [mol/L], and K: half saturation constant for O_2 [mol/L]. The total mineralisation rate was then calculated by adding up rates for oxygen, nitrate, goethite and sulfate (see Table VI-7). Manganese minerals were not included as their concentration was minimal and has been included into goethite equivalents. Hydrogeochemical conditions in the cell will decide which TEA is available and will be preferentially used. In the subsurface different redox zone may coexist close to each other due to heterogeneity in permeability (Lindberg and Runnells, 1984), or some redox zone might not exist at all, if the TEA is not available (Hunter et al., 1998). In the model this can only occur when dual domain is used.

Table VI-7: Kinetically modelled redox reactions with half saturation constants (after Parkhurst and Appelo, 1999) and various maximum degradation rates reported in the literature.

			max degradation rate (r) [mol/L/s]			
process	primary reaction (after Lensing et al., 1994)	half saturation constant (K) [mol/L]	Parkhurst and Appelo, 1999	Greskowiak et al. 2006 for $CH_2O(NH_3)_{0.15}$	Haerens (2004) for phenol	Matsunaga et al. 1993 for CH_2O
aerobic respiration	$CH_2O + O_2 = CO_2 + H_2O$	$2.94*10^{-4}$	$1.57*10^{-9}$	$1.53*10^{-10}$	$2.2*10^{-10}$	$3.5*10^{-11}$
denitrification	$5\ CH_2O + 4\ NO_3^- + 4\ H^+ = 5\ CO_2 + 2\ N_2 + 7\ H_2O$	$1.55*10^{-4}$	1.67*10-^{11}	$3.83*10^{-11}$	$4.7*10^{-11}$	$3.5*10^{-11}$
Fe(III) reduction	$CH_2O + 4\ FeOOH + 8\ H^+ = CO_2 + 4\ Fe^{2+} + 7\ H_2O$	$1*10^{-4}$	$5.0*10^{-11}$		$4.7*10^{-11}$	$3*10^{-11}$
Sulfate reduction	$2\ CH_2O + SO_4^{2-} + 2\ H^+ = CO_2 + HS^- + H_2O$	$1*10^{-4}$	$1*10^{-13}$ or $5.0*10^{-11}$		$3.8*10^{-11}$	$2.8*10^{-11}$

While degradation rates have been defined for a number of smaller organic contaminants (e.g. MacQuarrie et al., 1990; Essaid et al., 1995; Barry, D. A. et al., 2002), the degradation rate of DOC is obviously dependent on the composition and lability of the organic matter and hence no generic values have been defined. While labile fractions can be degraded in a few days and might therefore not even be injected, strongly humified material has half-life times of a few years (Kalbitz et al., 2003). The content of easily biodegradable material varies from 75% in fresh leaf litter derived DOM to 10-44% in soil derived DOM (Kalbitz et al., 2000;

Kalbitz et al., 2003). Horner et al. (2007) therefore used two DOC fractions with individual rate constants. In addition, the crystal structure, surface area and mineralogy of iron minerals have an affect on the reactivity of Fe oxides (Stumm and Sulzberger, 1992; Postma, 1993). Further information on the redox zonation and the nature of the organic matter would therefore be needed to calibrate the model properly. As a first estimation the reactions rates from Parkhurst and Appelo (1999) were used, which are implemented in PHT3D for a number of runs of BR2 (see VI.5.3.6) adding kinetics and rate inputs in the postfix.phrq file.

VI.5.2 Sensitivity analysis of conceptual model features

The following models all contain no mineral phases and one exchanger site with dataset b (Table VI-1). As outlined above (VI.5.1) the model is comprised of three surface sites and additional organic interactions, which were investigated separately exemplified by BR2 (VI.5.2) The three different sites showed different effects on Zn, Cu and pH behaviour and will be looked at separately to assess sensitivity of metals to each site and show some general emerging pattern. The effect of adding organic complexes (VI.5.2.5) in solution, sorption of organic matter onto goethite (VI.5.2.6) and ternary complexes (VI.5.2.7) were assessed as well. Then a combination of newly added parameters is presented (VI.5.3) for other experiments as well. Addition of dual domain (VI.5.3.5) and kinetic biodegradation (VI.5.3.6) to the best fit surface complexation model (SCM) is presented using BR2 as example again.

For comparison, Figure VI-16 shows the simulated curve if only the ion exchange site is present with no surface sites or organic complexes added. Both metals showed a snow plow effect at a very early, nearly non-retarded breakthrough during stormwater injection, which was due to competition with major cations for the exchange site. The metals were then completely expelled from the exchanger sites during recovery with increasing ionic strength and outflow values are equal to inflow values after day 30 (see Figure V-6 for inflow values). The pH outflow curve (Figure VI-16c) was basically equivalent to the inflow values (see Figure V-5a for inflow values) with only minimal delays.

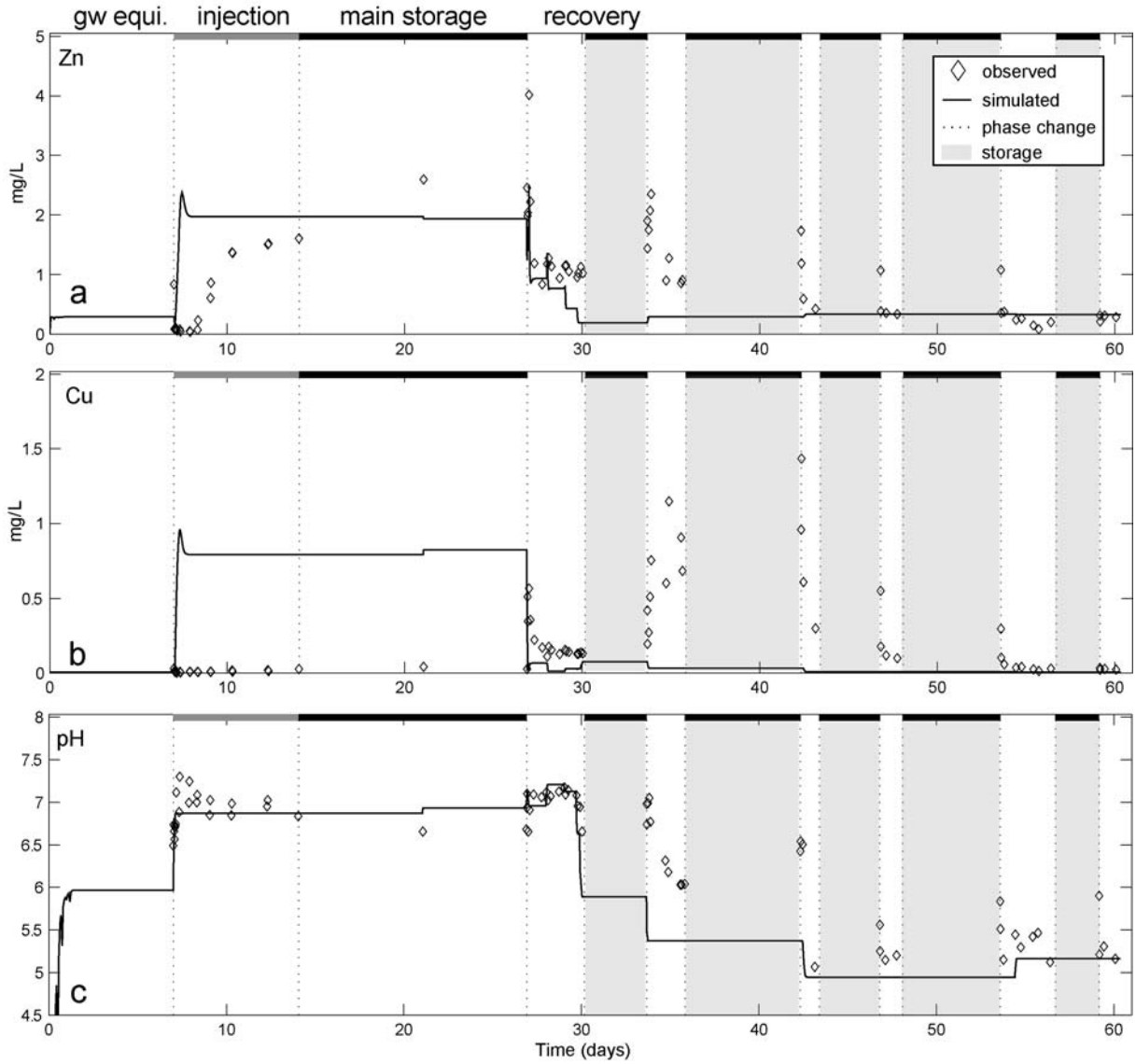

Figure VI-16: Simulated and observed concentrations for BR2 of (a) Zn, (b) Cu and (c) pH with 0.054 mol/kgw exchanger site, no surface sites and no organic complexation.

VI.5.2.1 Goethite surface sites

A goethite surface site was added as described in VI.5.1.1 and the number of sites was increased from 0.01 to 0.07 mol to asses the effect on Zn concentration (Figure VI-17), Cu concentration (Figure VI-18) and pH (Figure VI-20).

With increasing number of sites Zn breakthrough (Figure VI-17) was progressively more retarded and the snow plow effect reduced during stormwater injection, once Cu breakthrough was incomplete. With increasing amounts of Zn adsorbed during injection the release during the first stages of recovery accordingly increased. In addition, a small spike in Zn concentration between days 34-36 developed. Only for the highest number of sites did Zn desorption continue until the end of the experiment (Figure VI-17b). Zn was mainly adsorbed (about 65%) as outer-sphere complex at the outflow end of the aquifer material during

injection and was nearly completely released from the goethite surface site by day 34 (Figure VI-19a+b).

Cu breakthrough concentrations during stormwater injection decreased much more significantly than Zn concentrations (Figure VI-18). In contrast to Zn, Cu release during recovery was retarded and decreased with increasing number of sites. At low numbers of sites Cu release was observed due to lowering of the pH (day 34-36). This was greatly diminished with more sites. Cu was mainly adsorbed (about 85%) as inner-sphere complex at the inflow end of the material during stormwater injection. Distribution shifted towards outer-sphere complexes (about 75%) during recovery after Zn was released (Figure VI-19c+d) and was likely due to competition with major ions.

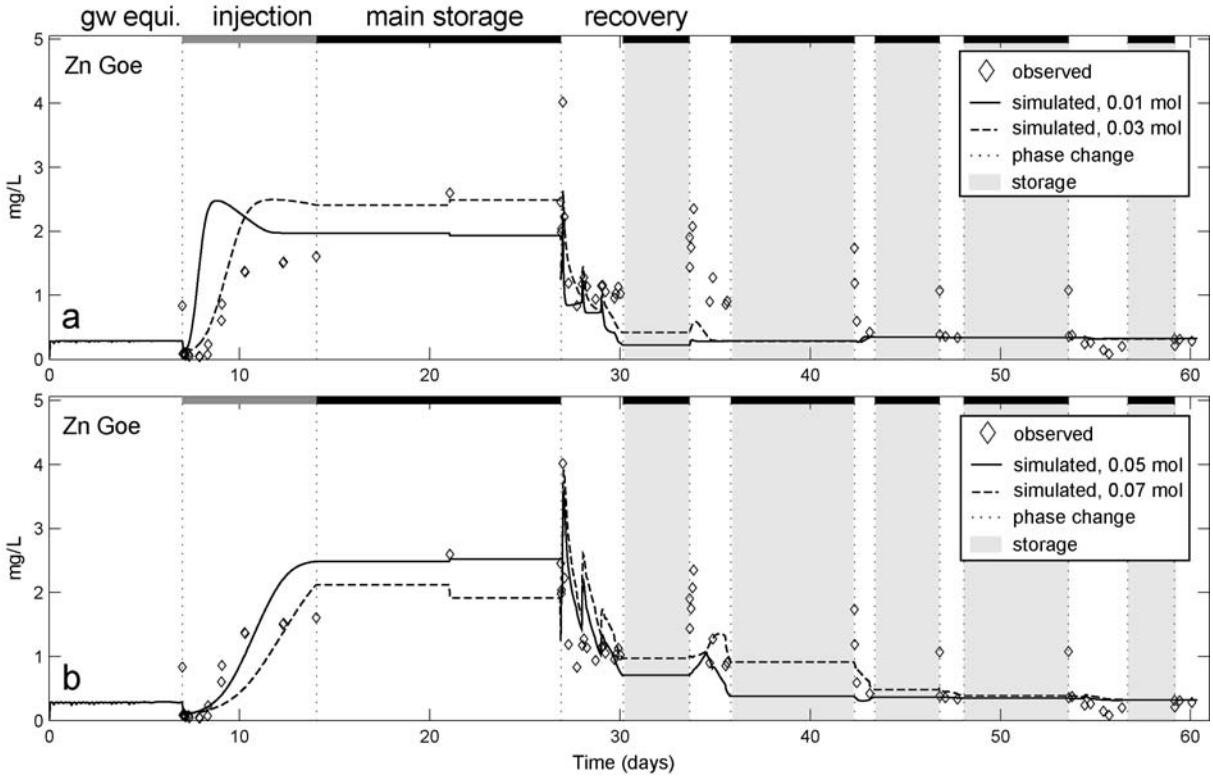

Figure VI-17: Simulated and observed Zn concentrations when adding the goethite surface site with (a) 0.01 mol (solid line) and 0.03 mol (dashed line) and (b) 0.05 mol (solid line) and 0.07 mol (dashed line).

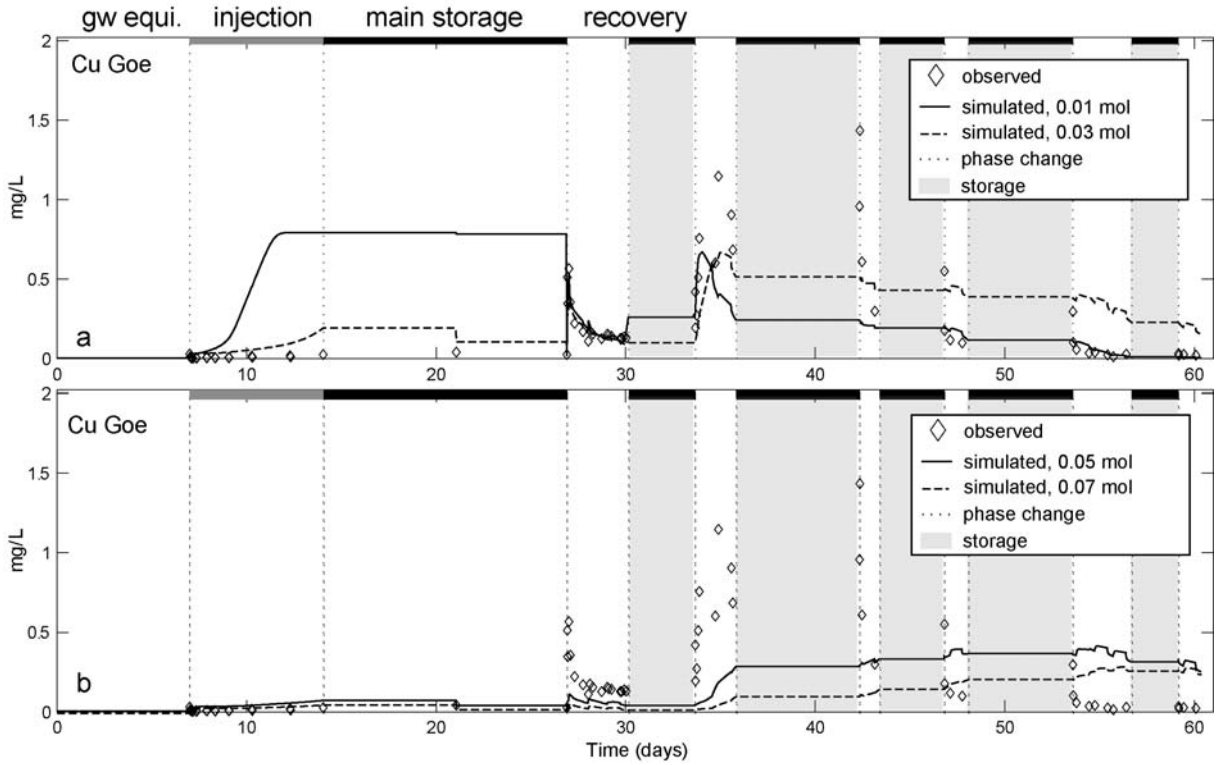

Figure VI-18: Simulated and observed Cu concentrations when adding the goethite surface site with (a) 0.01 mol (solid line) and 0.03 mol (dashed line) and (b) 0.05 mol (solid line) and 0.07 mol (dashed line).

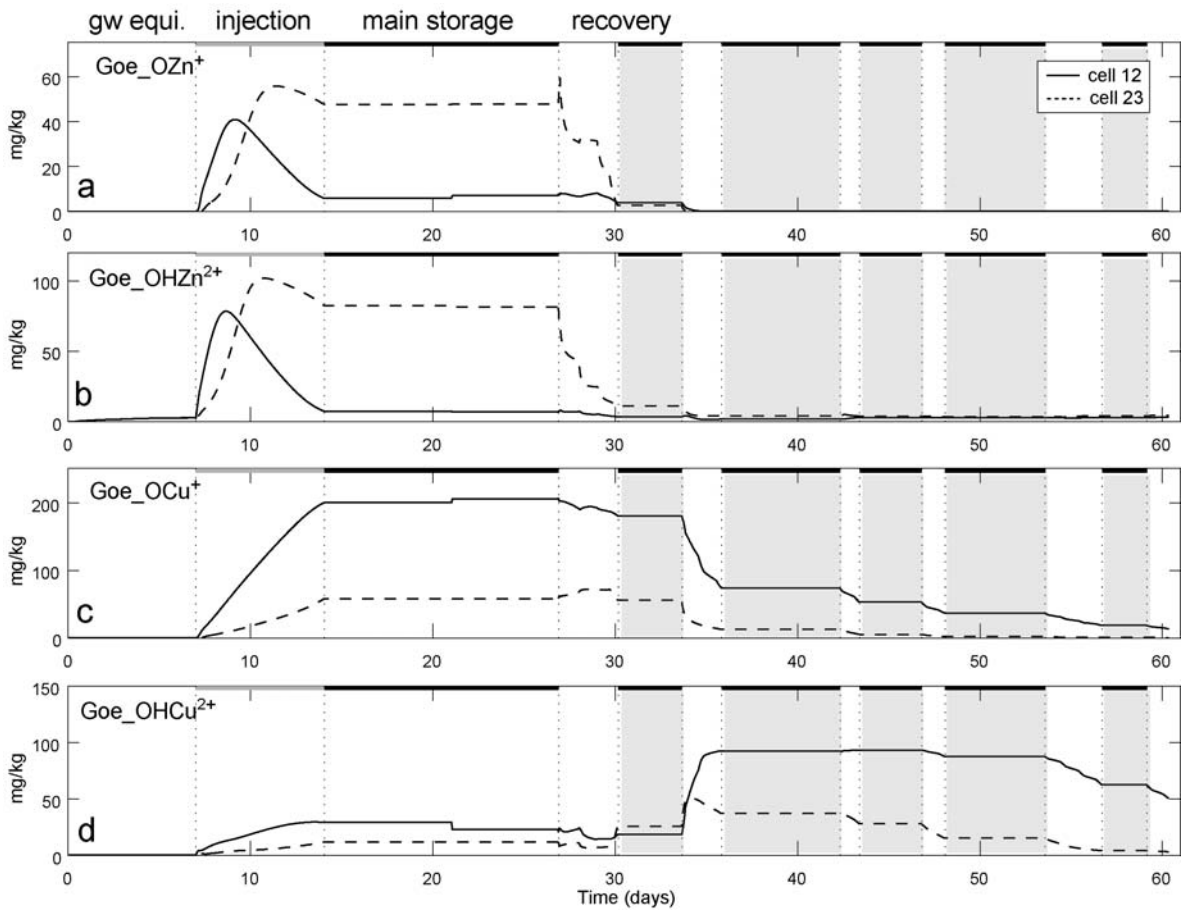

Figure VI-19: Simulated adsorbed species of Zn and Cu to 0.03 mol goethite surface site as (a) inner-sphere sorbed Zn, (b) outer-sphere sorbed Zn, (c) inner-sphere sorbed Cu and (d) outer-sphere sorbed Cu.

pH breakthrough at the start of stormwater injection was delayed with an increasing number of sites (see insets Figure VI-20) due to increased adsorption of metals which released increasing amounts of protons from the goethite surface site. In return, pH increased during recovery with increasing number of sites when higher amounts of released metals were exchanged with protons (Figure VI-20).

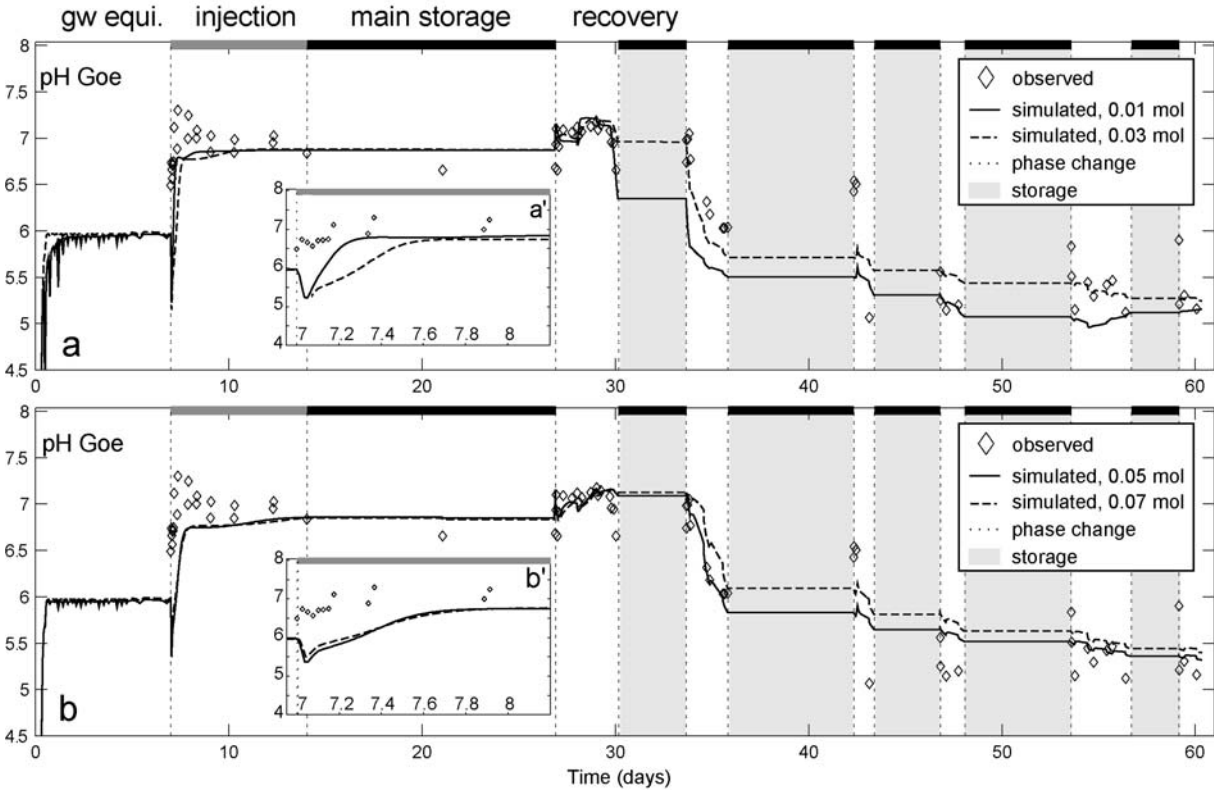

Figure VI-20: Simulated and observed pH when adding the goethite surface site with (a) 0.01 mol (solid line) and 0.03 mol (dashed line) and (b) 0.05 mol (solid line) and 0.07 mol (dashed line). Insets (') show pH at start of stormwater injection in detail.

VI.5.2.2 Strong HA surface sites

A strong humic acids surface site (Has) was added as described in VI.5.1.3 and the number of sites was increased from 0.01 to 0.04 mol to asses the effect on Zn concentration (Figure VI-21), Cu concentration (Figure VI-22) and pH (Figure VI-24).

The increase in sites of the strong humic acid site showed less pronounced effects on simulated Zn concentrations (Figure VI-21) compared to the goethite site. As with goethite the snow plow effect during injection was decreasing with the decreasing breakthrough of Cu, but the overall position of the simulated Zn breakthrough curve was only retarded slightly with increasing number of sites. The main effect of increasing sites during recovery was decreased concentration during stages 3 recovery (day 28-29) and increased concentration at the start of stage 4 (day 29-34). During injection Zn was sorbed first on Has sites at the start of the aquifer material but was then continuously displaced to the sites further down the flow path and was completely expelled during the first days of recovery (Figure VI-23a).

In contrast to Zn, Cu breakthrough was extremely influenced by an increase in number of sites of the Has site with Cu breakthrough completely suppressed at more than 0.028 mol sites (Figure VI-22). Increasing Has sites also continuously delayed Cu release during recovery and overall diminished Cu release. Most Cu was adsorbed on the aquifer material close to the inflow during injection and remained there during the main part of the recovery (Figure VI-23b). Cu was adsorbed in more than three times higher amounts than Zn due to the higher site affinity.

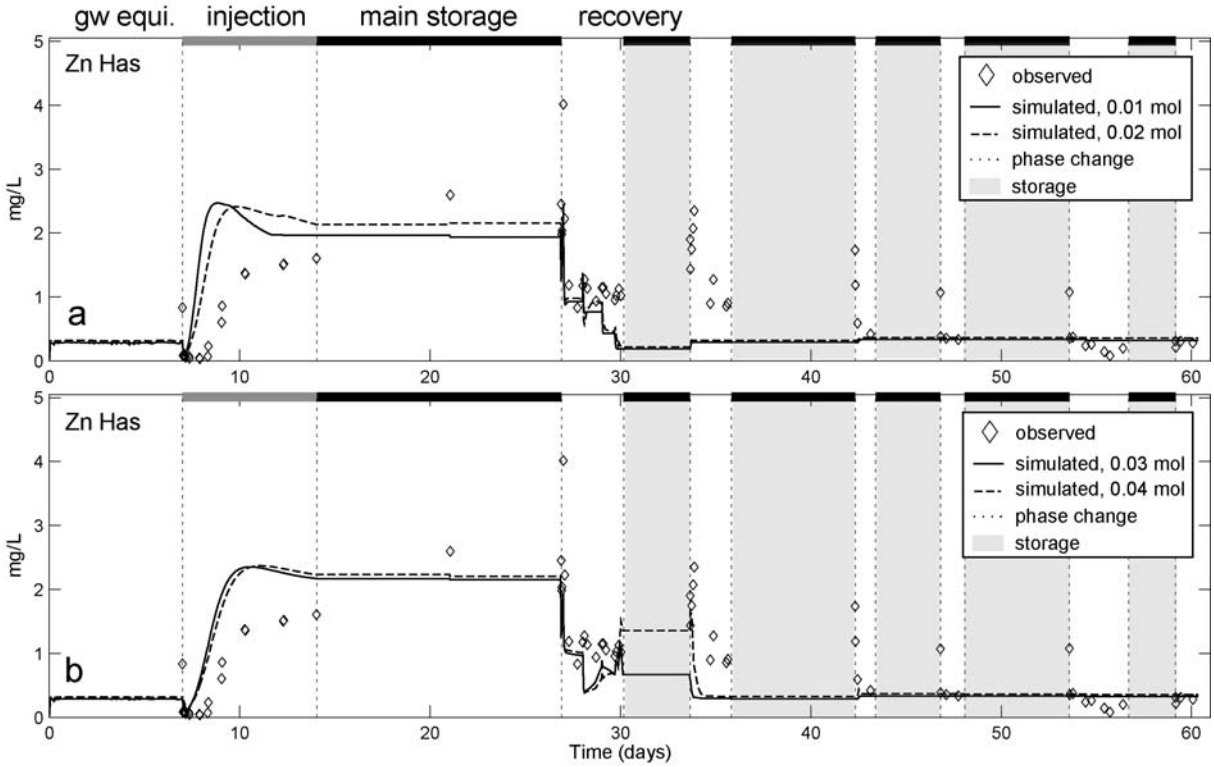

Figure VI-21: Simulated and observed Zn concentrations when adding the strong humic acid (Has) surface site with (a) 0.01 mol (solid line) and 0.02 mol (dashed line) and (b) 0.03 mol (solid line) and 0.04 mol (dashed line).

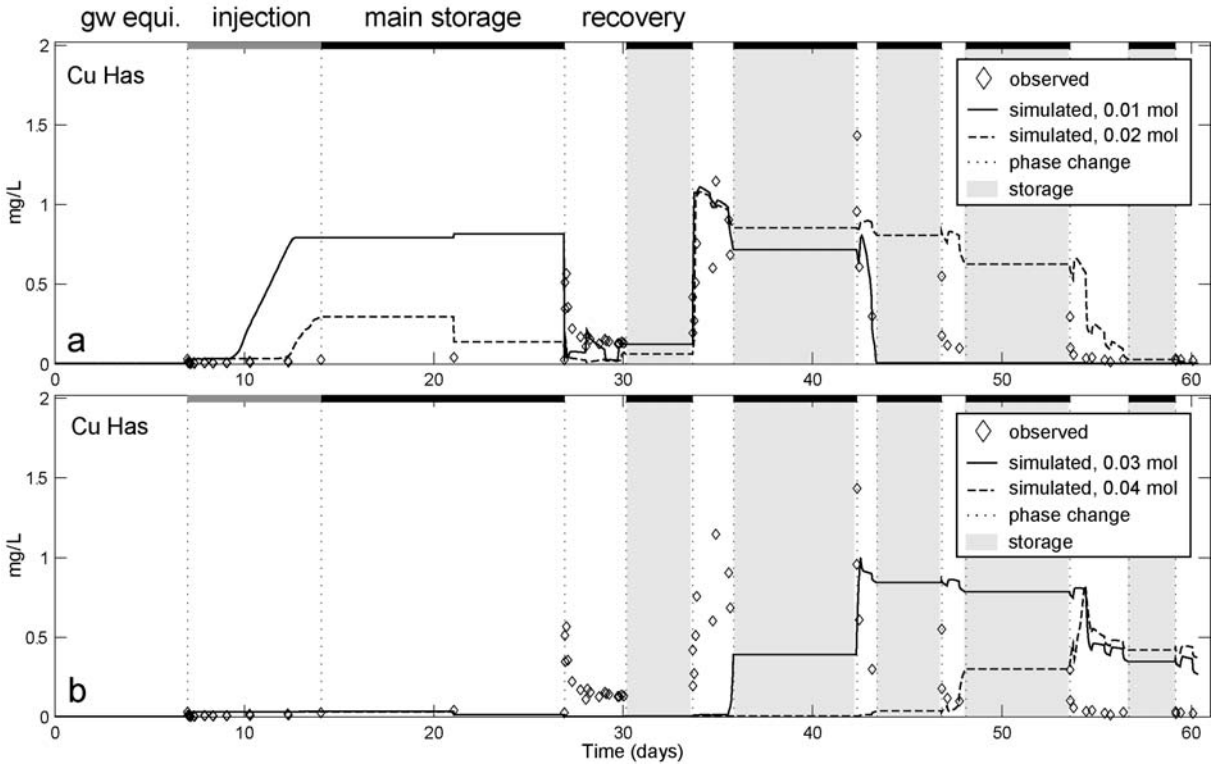

Figure VI-22: Simulated and observed Cu concentrations when adding the strong humic acid (Has) surface site with (a) 0.01 mol (solid line) and 0.02 mol (dashed line) and (b) 0.03 mol (solid line) and 0.04 mol (dashed line).

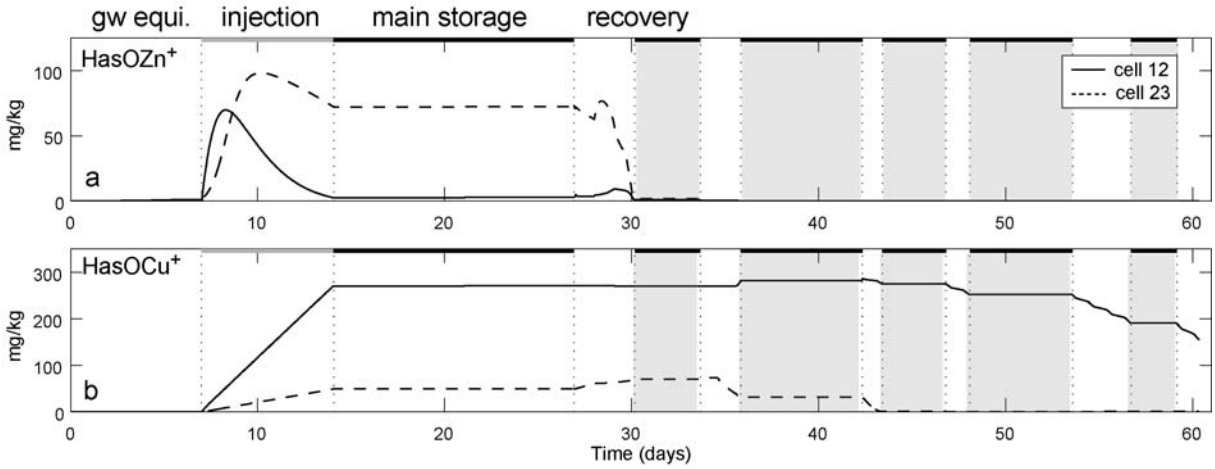

Figure VI-23: Simulated adsorbed species of Zn and Cu to 0.03 mol Has as (a) inner-sphere sorbed Zn and (b) inner-sphere sorbed Cu.

Similar to the goethite site, pH breakthrough at the start of stormwater injection was delayed with increasing number of sites on the Has site. In contrast to the goethite site, simulated pH values also dropped considerately (see insets Figure VI-24). Overall, pH values were also less buffered during recovery compared to the goethite site (Figure VI-24).

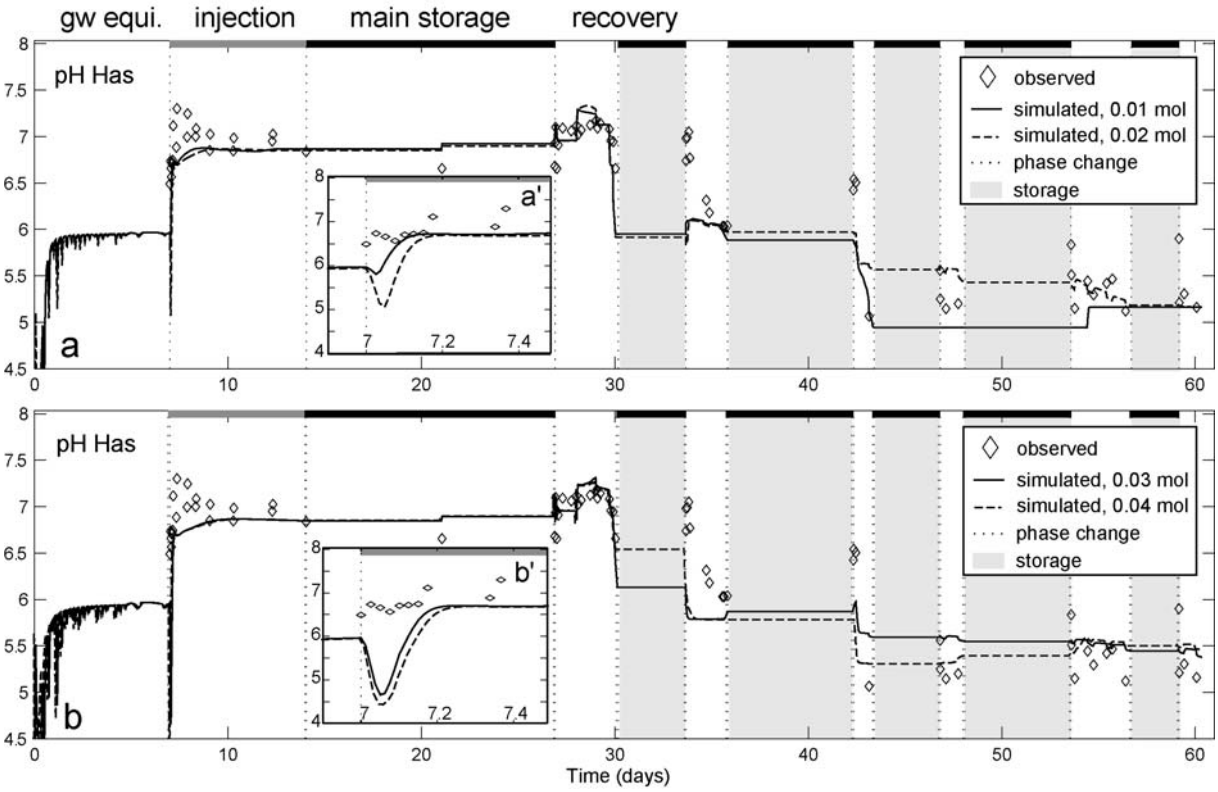

Figure VI-24: Simulated and observed pH when adding the strong humic acid (Has) surface site with (a) 0.01 mol (solid line) and 0.02 mol (dashed line) and (b) 0.03 mol (solid line) and 0.04 mol (dashed line). Insets (') show pH at start of stormwater injection in detail.

VI.5.2.3 Weak HA surface sites

A weak humic acids surface site (Haw) was added as described in VI.5.1.3 and the number of sites was increased from 0.05 to 0.4 mol to asses the effect on Zn and Cu concentration and pH (Figure VI-25). Compared to the goethite and Has surface sites, simulated Zn and Cu concentrations were rather insensitive to an increase in Haw sites, even when numbers exceeded values for goethite and Has by an order of magnitude.

Zn breakthrough at the start of stormwater injection was only retarded slightly and release pattern did not change extensively (Figure VI-25a), as only limited amounts of Zn were available for desorption. In contrast to the other two surface sites, Zn was nearly equally distributed throughout the column sediments (Figure VI-26a).

Cu breakthrough at the start of the stormwater injection was retarded more than Zn and Cu breakthrough was not complete anymore for sites greater than 0.35 mol. The increased amount of Cu sorbed during injection resulted in increased release of Cu during recovery after the pH was lowered (after day 34) (Figure VI-25b). Cu was sorbed in comparatively low amounts on Haw though with a slow but steady release during recovery starting from the then inflow end (cell 23) (Figure VI-26b).

In accordance with only limited changes in simulated Zn and Cu concentration with increasing number of Haw sites, simulated pH values also changed only slightly (Figure VI-25c). The main difference of Haw to the other two surface sites was an increase in pH at the start of stormwater injection (see insets Figure VI-25c). While this trend moves into the right direction, the observed increase was not matched by either surface site.

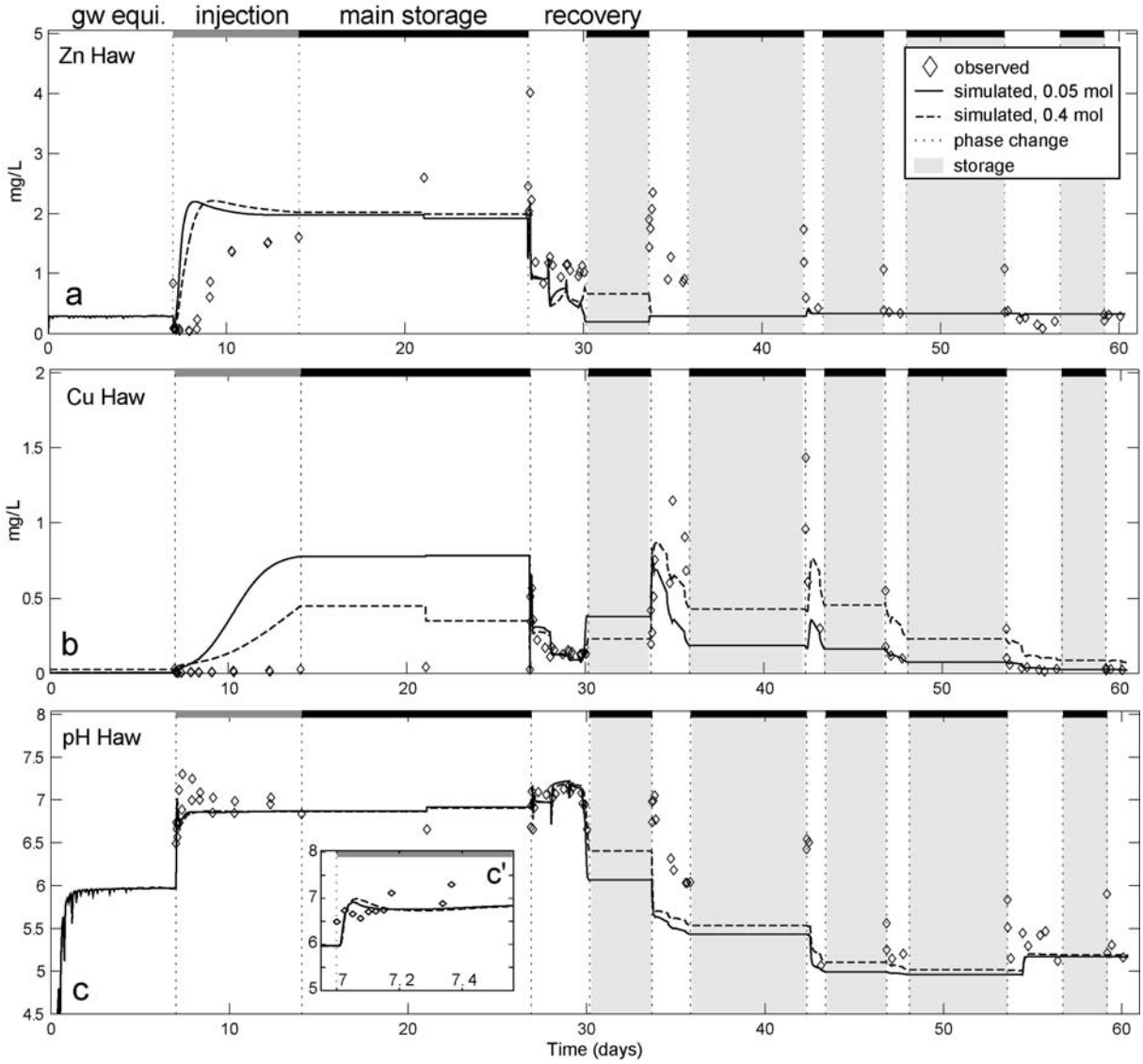

Figure VI-25: Simulated and observed (a) Zn concentrations, (b) Cu concentration and (c) pH when adding increasing numbers of weak humic acid (Haw) surface site. Solid line: 0.05 mol, dashed line: 0.4 mol of weak humic acid (Haw) site. Inset (c‘) shows pH at start of stormwater injection in detail.

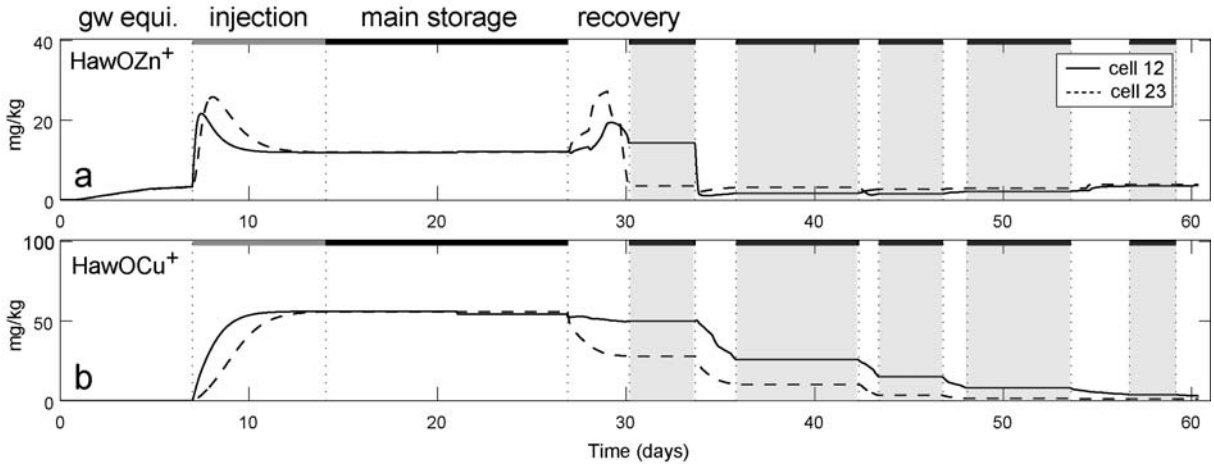

Figure VI-26: Simulated adsorbed species of Zn and Cu onto 0.02 mol Haw surface site as (a) inner-sphere sorbed Zn and (b) inner-sphere sorbed Cu.

VI.5.2.4 Combination of surface sites

The addition of only one of the three postulated surface sites was afflicted with the same problems as seen in the GC approach, i.e. no single site can accommodate the breakthrough and recovery behaviour of both Zn and Cu simultaneously. The use of combination of surface sites was therefore investigated.

The combination of the goethite site (0.02 mol) with the Has site (0.02 mol) resulted in an improved breakthrough behaviour of Zn and Cu, both now matching the retardation factor (Figure VI-27). The release of Zn during recovery was also improved, while Cu release was worsened due to delayed release. For pH the combination of both sites resulted in an overall improvement for the recovery phase, but worsened values for the start of the injection (Figure VI-27c'). The mismatch for pH at the start of the injection and for the extensive tailing of Zn breakthrough after day 10 were recurring themes, which could not be solved with either combination of surface sites.

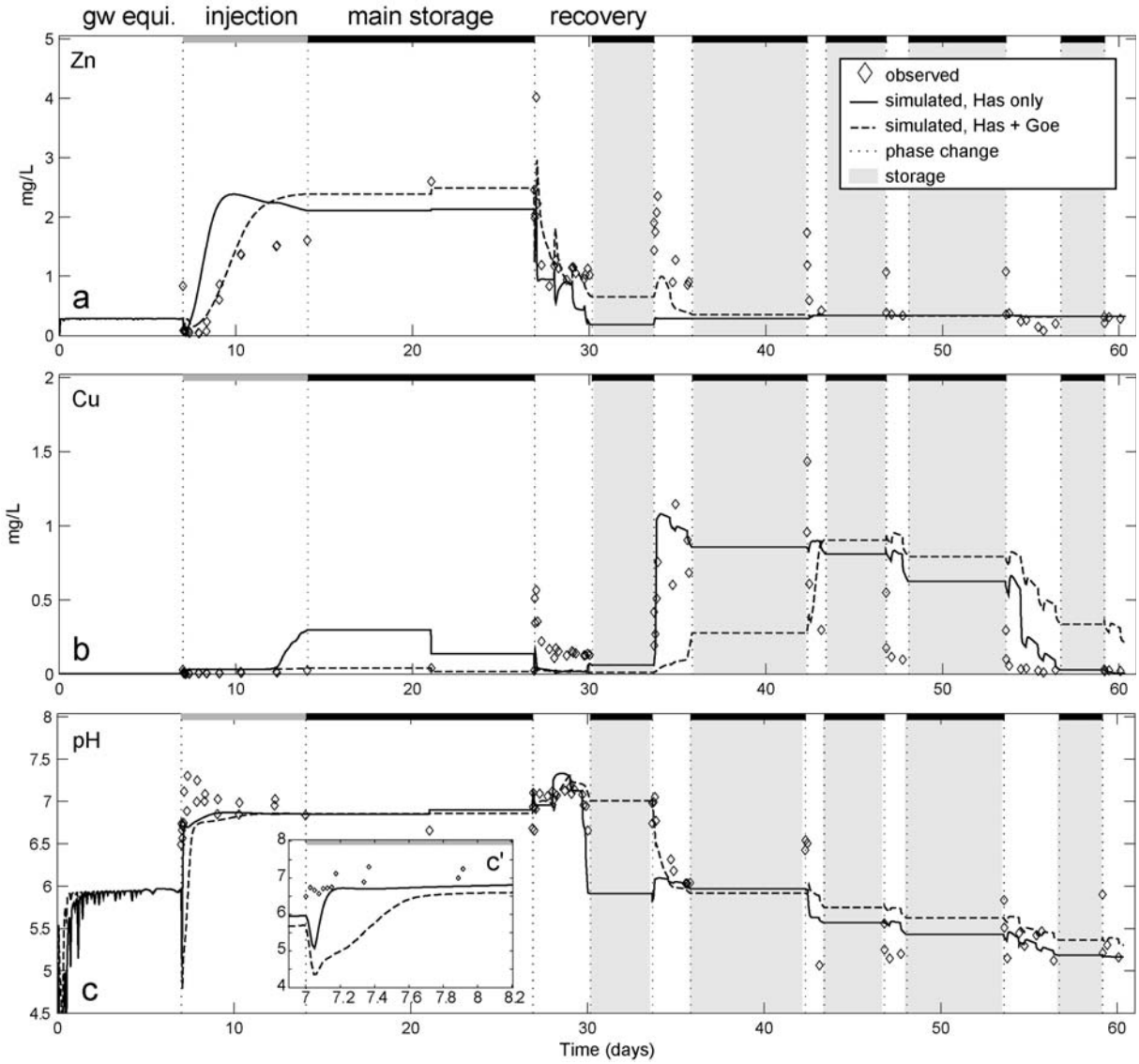

Figure VI-27: Simulated and observed (a) Zn concentrations, (b) Cu concentration and (c) pH when adding 0.02 mol goethite surface sites to 0.02 mol Has surface sites. Inset (c') shows pH at start of stormwater injection in detail.

The addition of the Haw site (0.1 mol) to the Has site (0.02 mol) resulted in only slight improvement for the simulated Zn concentration, but significantly improved Cu breakthrough during injection (Figure VI-28). It also delayed Cu release during recovery changing it for the worse. pH simulations were only slightly altered.

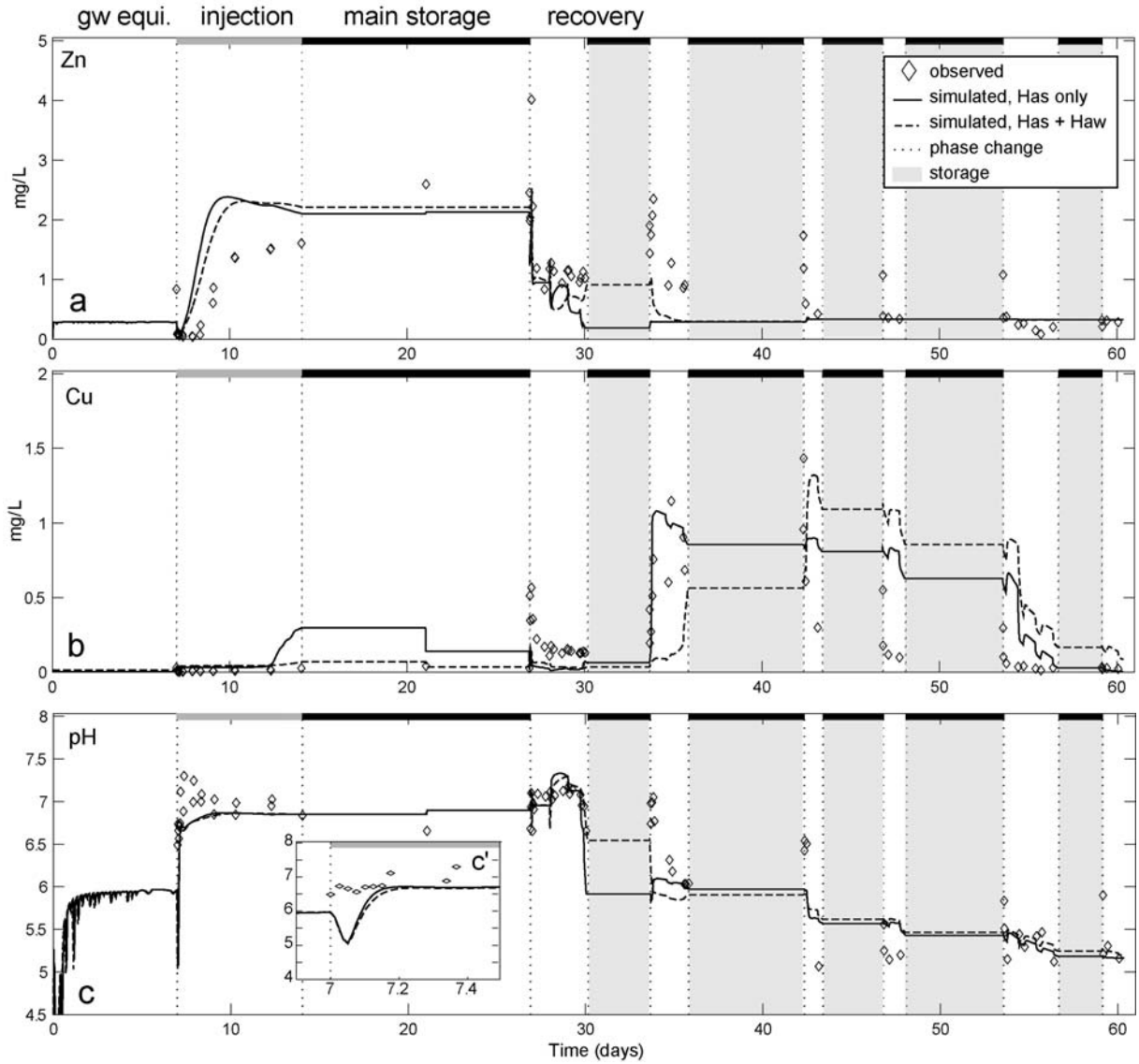

Figure VI-28: Simulated and observed (a) Zn concentrations, (b) Cu concentration and (c) pH when adding 0.1 mol Haw surface site to 0.02 mol Has surface site. Inset (c') shows pH at start of stormwater injection in detail.

Similarly to the above, the addition of the Haw site (0.1 mol) to the goethite site (0.02 mol) resulted only in a slightly alteration of the Zn breakthrough curve during injection and slightly more release of Zn during at the start of recovery, while Cu breakthrough during injection was significantly reduced (Figure VI-29). The shift in Cu release during recovery was less severe than in the above example though and changes to pH were also minor.

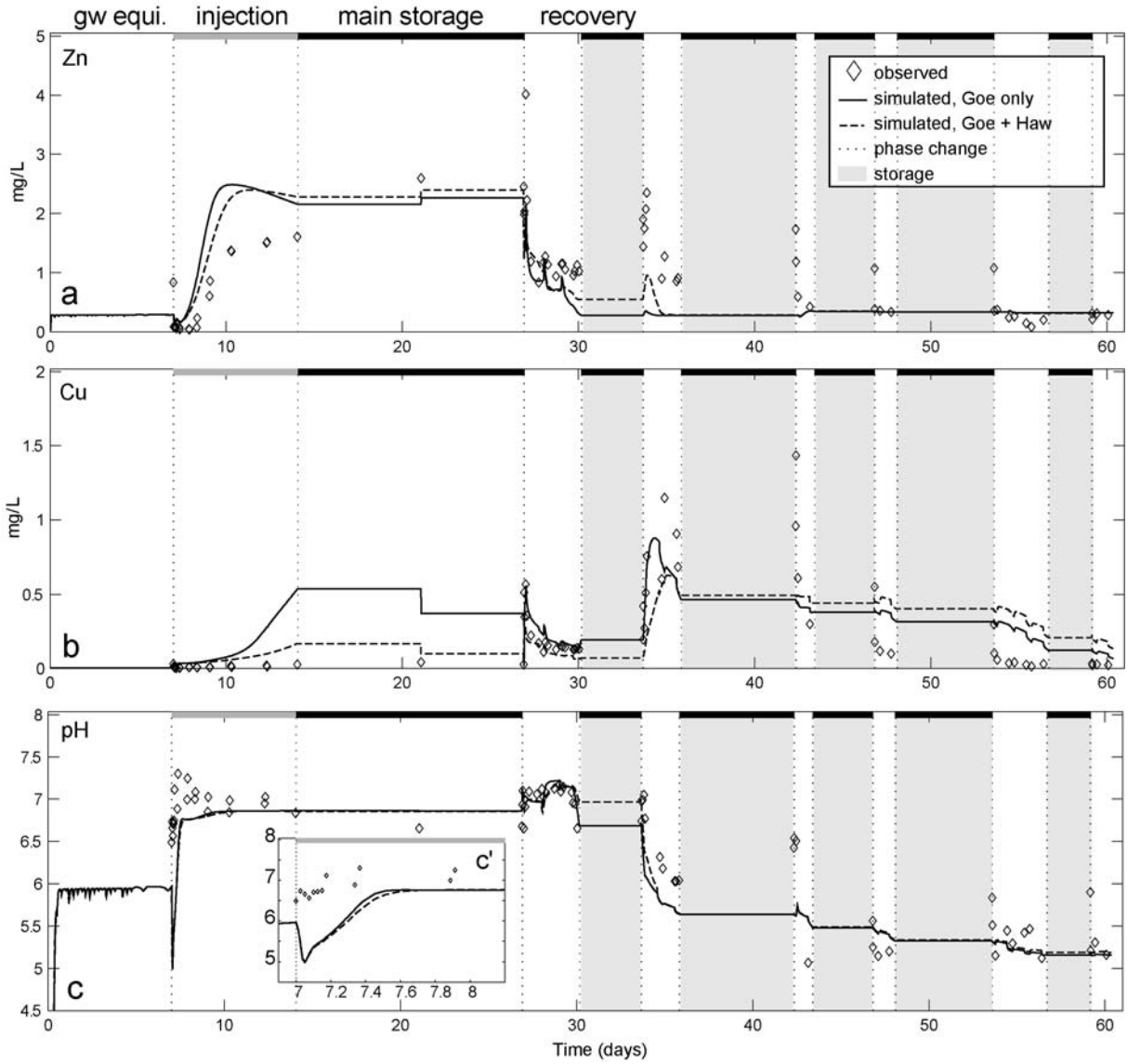

Figure VI-29: Simulated and observed (a) Zn concentrations, (b) Cu concentration and (c) pH when adding 0.1 mol Haw surface site to 0.02 mol goethite surface site. Inset (c') shows pH at start of stormwater injection in detail.

The addition of the Haw site (0.1 mol) to the goethite (0.02 mol) and Has site (0.02 mol) therefore showed the same minor changes as discussed above (Figure VI-30). To simplify the model and speed up processing time the Haw site might not be necessary.

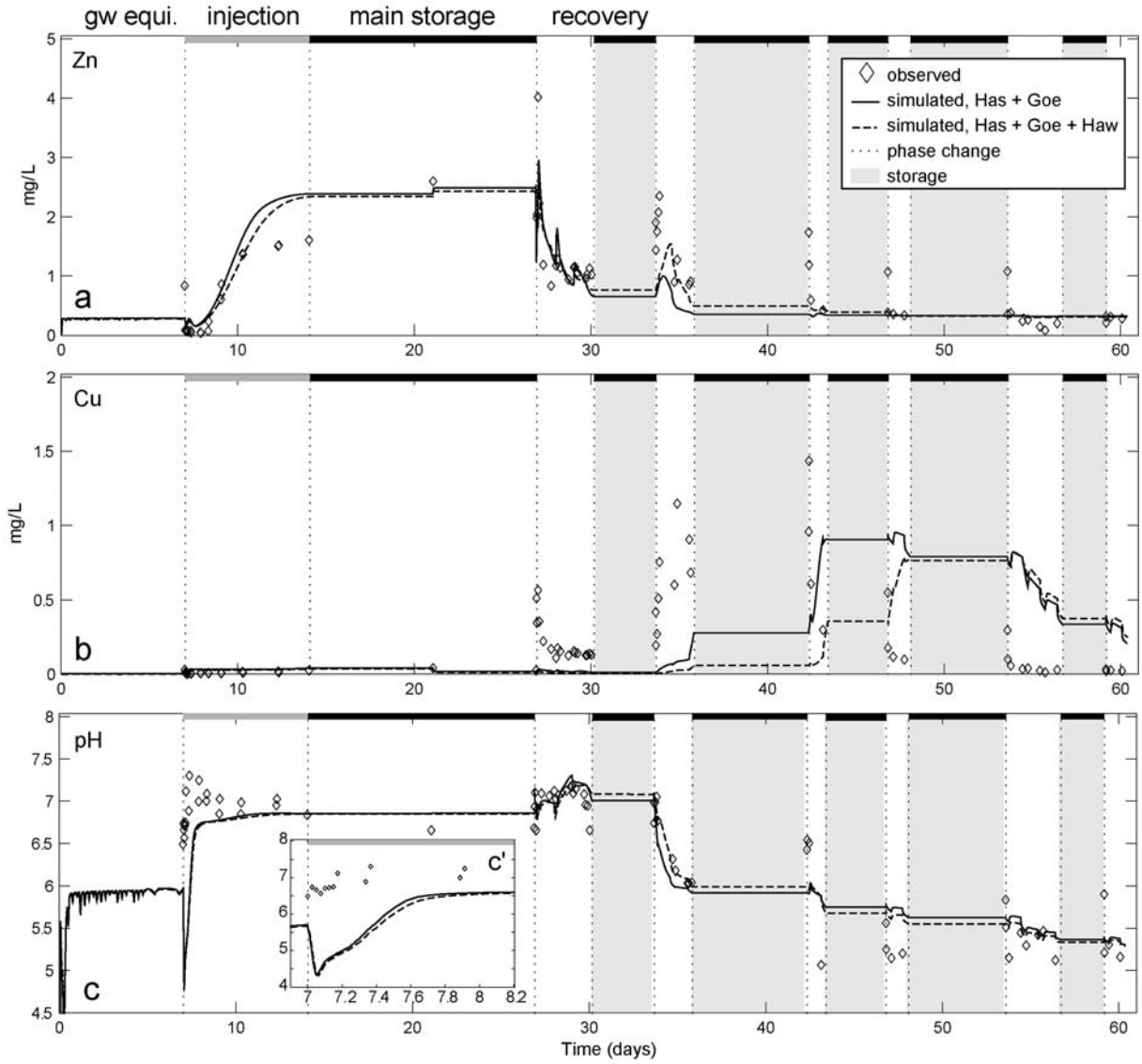

Figure VI-30: Simulated and observed (a) Zn concentrations, (b) Cu concentration and (c) pH when adding 0.1 mol Haw surface site to 0.02 mol goethite and Has surface sites. Inset (c') shows pH at start of stormwater injection in detail.

VI.5.2.5 Organic complexes

Organic complexation of Zn and Cu in solution as defined in VI.5.1.2 resulted in Cu being nearly completely complexed with DOC (90%), while Zn was complexed only to about 40% with DOC (Figure VI-31). In accordance with preliminary PHREEQC speciation calculations (see Figure VI-12) both metals were present as $MeSrfa^{-2}$ complex, while $MeHSrfa^{-}$ complexes were below 0.3%. The amount of complexed metals decreased with the increase in salinity during the recovery phase to <80% and <20% for Cu and Zn, respectively, due to competition with major ions (Figure VI-31). While organic complexation changed the speciation of metals in solution, it is still defined as equilibrium reaction and the Le Châtelier's principle is working, meaning that free metals taken out of solution by adsorption will be counter-acted by releasing metals out of the complex. This explains why no effects where seen for Zn and pH simulations when organic complexation was added to the model in the presence of any of the three surface sites (not shown). The addition of organic

complexation therefore seems of minor importance, but it is necessary for the formation of ternary complexes (see VI.5.2.7).

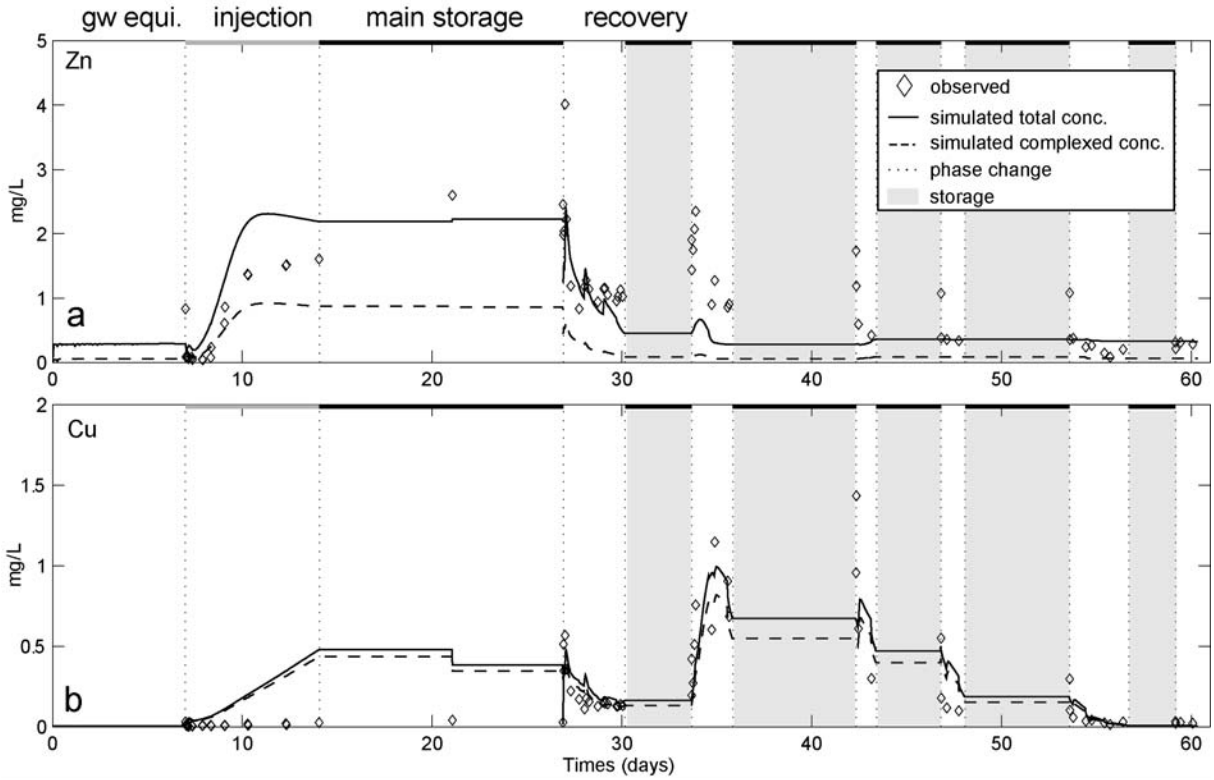

Figure VI-31: Simulated and observed concentrations of (a) total (solid line) and organically complexed (dashed line) Zn and (b) total (solid line) and organically complexed (dashed line) Cu when adding organic complexation to 0.03 mol goethite surface site.

The only noteworthy influence of the addition of organic complexes was found for simulated Cu concentrations in the presence of the goethite surface site (Figure VI-32). The addition of organic complexation resulted in less adsorption during injection and also increased desorption of Cu during large parts of the recovery phase. This behaviour has been observed in experiments (see IV.3.1.2; Brümmer et al., 1983; Lehman and Harter, 1984; He et al., 2006) and can be explained with the fact that Cu is nearly completely complexed and these complexes are not available for sorption. It is not clear though why the model would create this outcome, as the equilibrium reactions would generate new free Cu (~5%).

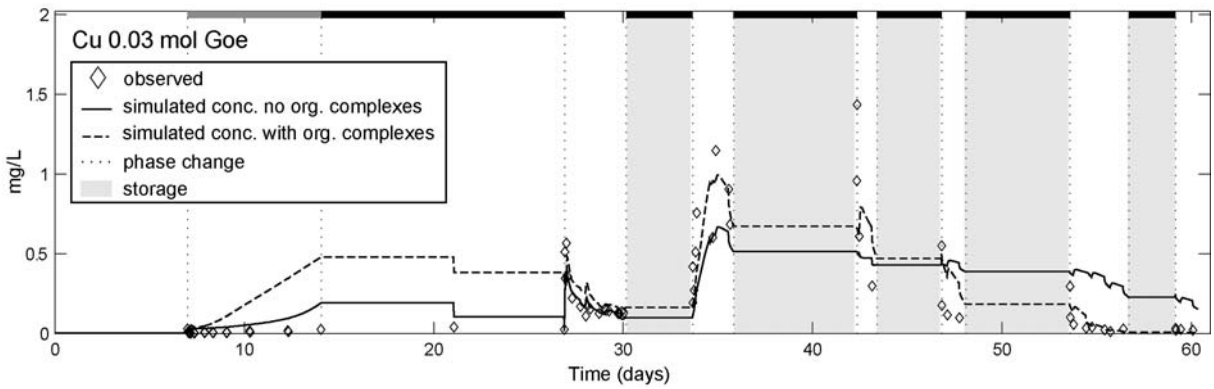

Figure VI-32: Simulated and observed concentrations of Cu when adding organic complexation to 0.03 mol goethite surface site.

VI.5.2.6 Sorption of organic matter onto goethite

The addition of sorption of uncomplexed fulvic acids onto goethite surface sites as defined in VI.5.1.4 was mainly added to match observed TOC concentrations. It could also be used to define ternary complexes, which lead to the same results (not shown) as discussed below (VI.5.2.7) using complexed metals and goethite sites.

As expected from the PHREEQC simulation (see Figure VI-14) the main sorbed species was the outer-sphere complex Goe_OSrfa^{5-}, which was only exceeded by the Goe_HSrfa^{2-} complex when the pH was lower than about 7 (Figure VI-33). However, the amounts sorbed were low and the simulated TOC concentration was hardly affected by it. The small increase of TOC at the start of injection (Figure VI-34a') was due to desorption of more Goe_HSrfa^{2-} than was compensated for by sorption of Goe_OSrfa^{5-}. The observed adsorption of TOC at the start of injection and the TOC release at the start of recovery could not be matched (Figure VI-34). As these effects were most likely due to particulate organic matter deposition and release (see V.3.2.2), which was not incorporated in the model, a misfit was not unreasonable. An increase in affinity constants (log k) of Srfa sorption onto goethite surface sites by up to four magnitudes only slightly increased adsorption at the start of injection (not shown). Once ternary complexation was added all sorbed Srfa species dropped to negligible values and no further improvement on simulated TOC concentration was observed (not shown), as surface sites on goethite were dominated by ternary complexes and free metals (see Figure VI-38).

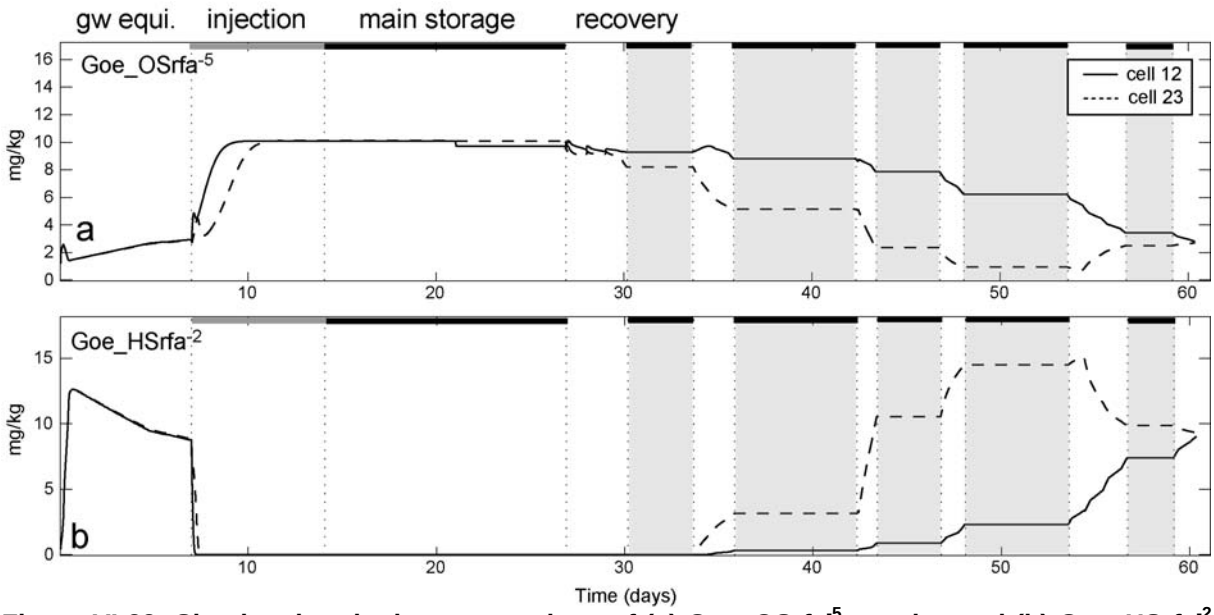

Figure VI-33: Simulated sorbed concentrations of (a) Goe_OSrfa^{-5} species and (b) Goe_HSrfa^{-2} species onto 0.03 mol goethite surface site.

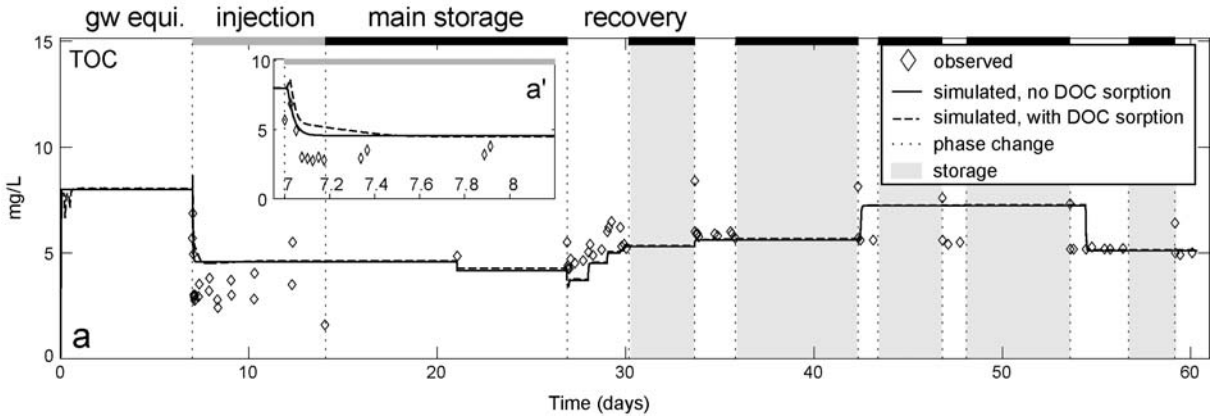

Figure VI-34: Simulated and observed concentrations of TOC without DOC sorption (solid line) and with DOC sorption (dashed line) onto 0.03 mol goethite surface site. Inset (a‘) shows TOC at start of stormwater injection in detail.

However, the addition of DOC sorption had effects on pH and on metal concentrations. The sorption of DOC onto goethite reduced the pH at the start of stormwater injection (Figure VI-35c’) and resulted in more buffering during the later part of recovery (Figure VI-35c). The latter resulted in a prolonged release of Cu rather than the otherwise observed narrow spike between day 34-35 (Figure VI-35b). It was also observed that adsorption of Zn and Cu during injection was increased due to DOC sorption, which was not expected as sorption of DOC would reduce the available sorption sites on goethite. The species distribution on goethite showed that the increased adsorption was due to increased amounts in both inner- and outer-sphere complexes for both Zn and Cu (Figure VI-36). While the explanation for this phenomenon is missing at this point and this new feature of the model might need further investigation, once ternary complexes were added there was no significant change in Zn and Cu concentrations anymore. The only noteworthy effect then was a drop in pH at the start of injection (not shown).

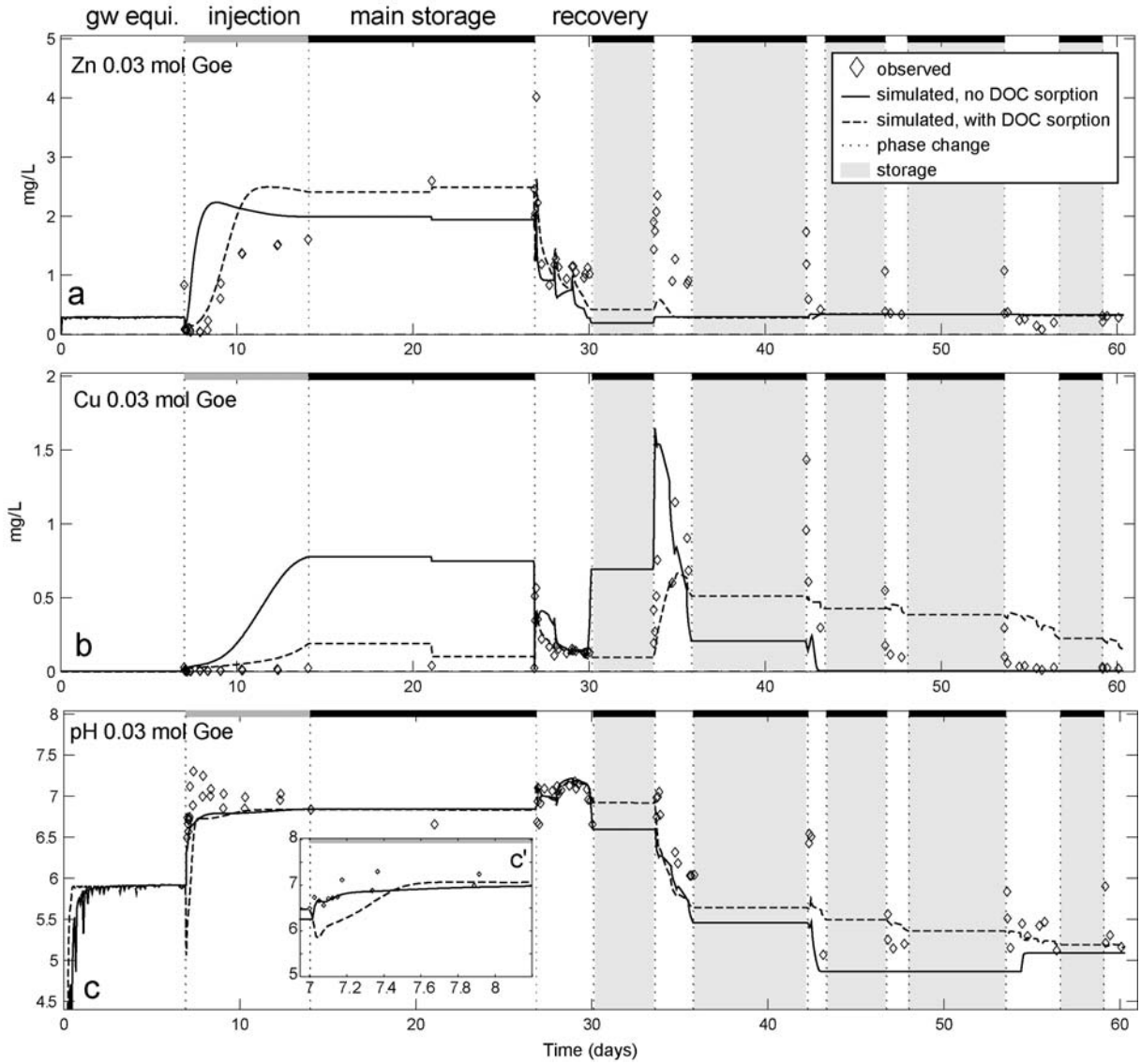

Figure VI-35: Simulated and observed (a) Zn concentration, (b) Cu concentration and (c) pH when adding DOC sorption to 0.03 mol goethite surface site. Inset (c') shows pH at start of stormwater injection in detail.

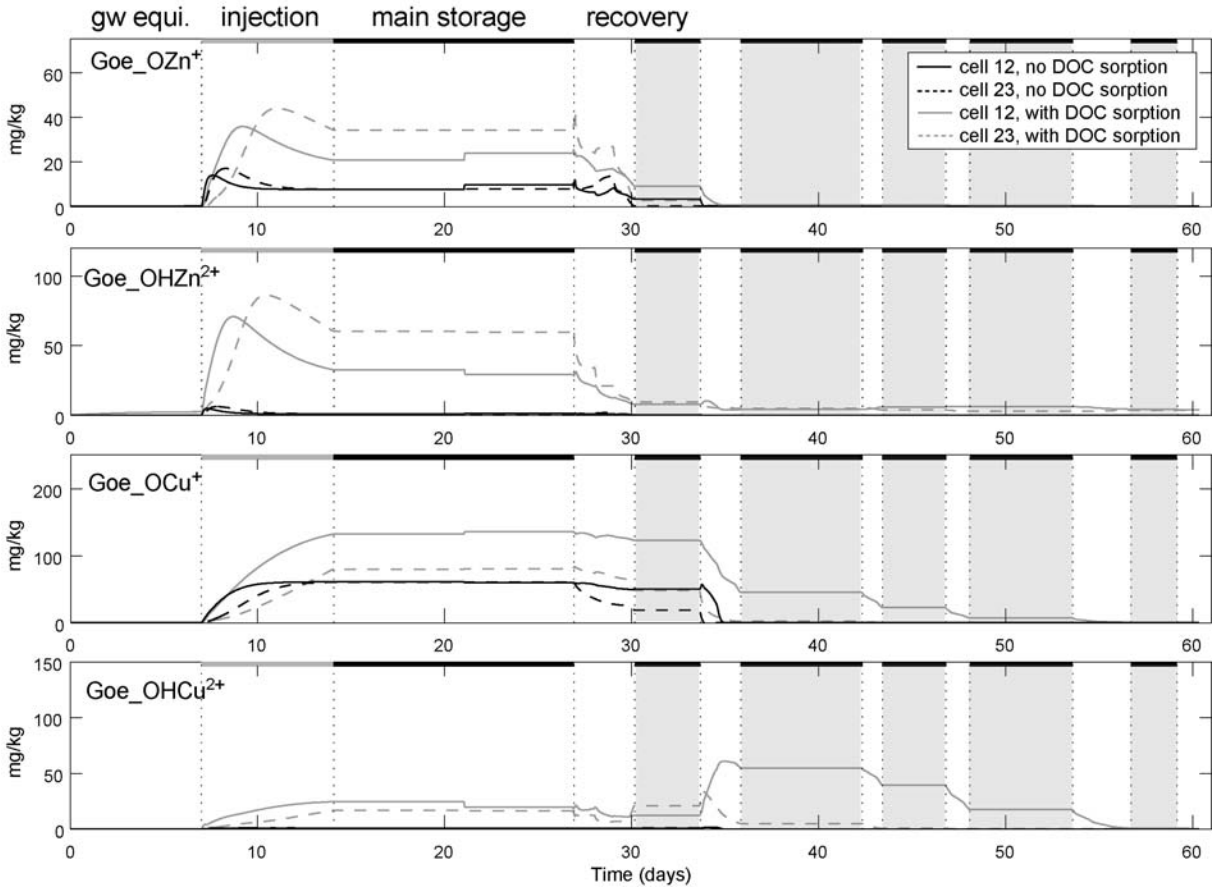

Figure VI-36: Simulated adsorbed species of Zn and Cu onto 0.03 mol goethite surface site without DOC sorption (black line) and with DOC sorption (grey lines) as (a) inner-sphere sorbed Zn, (b) outer-sphere sorbed Zn (c) inner-sphere sorbed Cu and (d) outer-sphere sorbed Cu.

VI.5.2.7 Ternary complexes

The addition of ternary complexes as complexed metals sorbing onto goethite surface sites defined in VI.5.1.5 was investigated.

One effect of the addition of ternary complexes with increasing affinity constants (log k) was a change in breakthrough curve shape from a gently to a more abrupt change in slope for both Zn and Cu (Figure VI-37a+b). In addition, Cu release during recovery after day 34 was nearly completely suppressed as the associated simulated decrease in pH favours ternary complexation. The distribution on the goethite surface shifted significantly from inner-sphere to outer-sphere for both Zn and Cu as ternary complexes occupy the inner-sphere surface sites (Figure VI-38). The second ternary species (Goe_HSrfaMe) was of negligible value as nearly no $MeHSrfa^-$ was present in solution. The sorption of DOC onto goethite was also reduced to negligible values (not shown) as ternary complexes had a higher affinity to the goethite surface sites.

Another effect was an increase in pH at the start of injection (Figure VI-37c'), which was a significant improvement. Unfortunately, it resulted also in a decrease in pH buffering during

recovery (Figure VI-37c) deteriorating the fit to observed values. Once all three surface sites were added though the changes in pH, Zn and Cu concentrations due to the addition of ternary complexes were generally less pronounced (not shown).

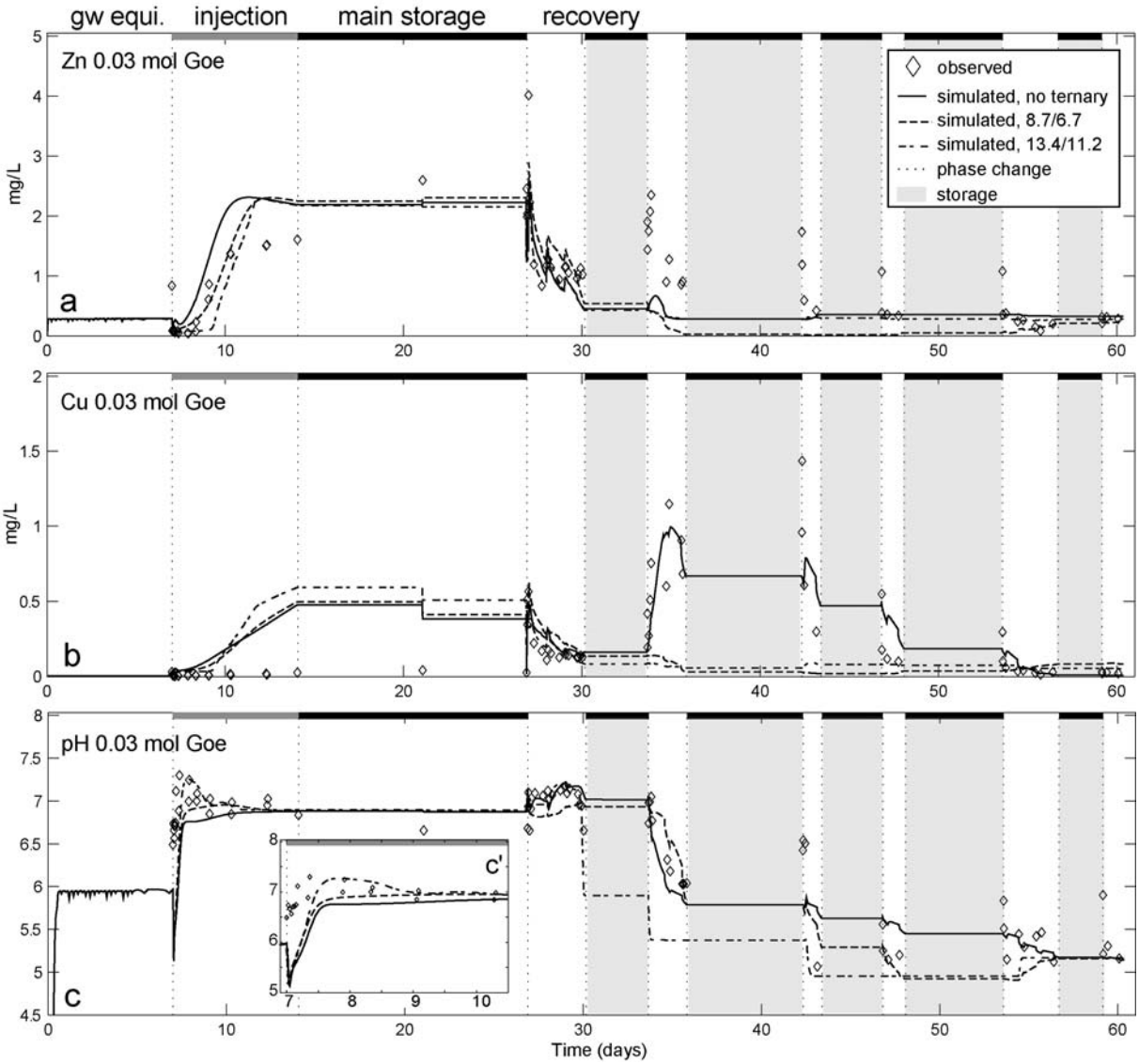

Figure VI-37: Simulated and observed concentrations of (a) Zn concentration, (b) cu concentration and (c) pH with no ternary complexes (solid line), ternary complexes with lower log_k values (dashed line) and ternary complexes with higher log_k values (dash-dotted line) onto 0.03 mol goethite surface sites. See Table VI-6 for log_k values. Inset (c') shows pH at start of stormwater injection in detail.

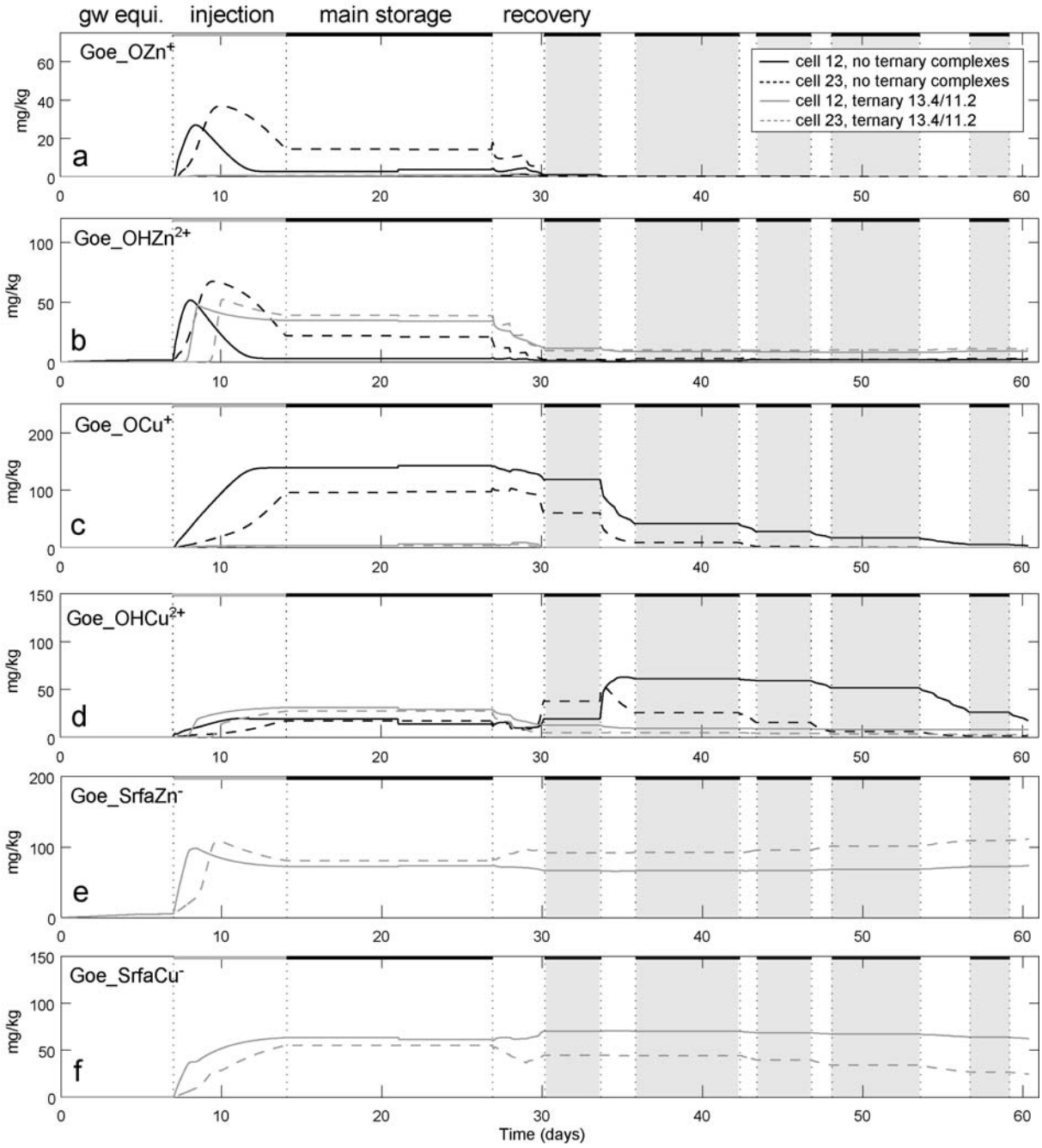

Figure VI-38: Simulated adsorbed species of Zn and Cu onto 0.03 mol goethite surface site without ternary complexation (black line) and with ternary complexation (grey lines) as (a) inner-sphere sorbed Zn, (b) outer-sphere sorbed Zn (c) inner-sphere sorbed Cu, (d) outer-sphere sorbed Cu, (e) ternary Zn complex and (f) ternary Cu complex.

VI.5.2.8 Summary of conceptual CA model

With all components of the conceptual model added the following conclusions could be drawn:

- A single surface site would not be able to simulate the observed Zn and Cu concentration and at least two surface sites would be needed (as indicated in batch and column tests)

- Cu concentrations were predominantly controlled by the strong humic acid surface site and by formation of ternary complexes on goethite the later stage of recovery (Figure VI-39).
- Zn concentrations were largely controlled by the goethite surface site, where Zn was sorbed as outer-sphere and ternary complex (Figure VI-39).
- Simulations were relatively insensitive to the weak humic acid site, when using number of sites in a similar range to Has and goethite and even at much higher numbers sorption of Cu and Zn were limited (Figure VI-39).
- Dissolved Cu was primarily present as organic complex.
- Sorption of DOC onto goethite was of minor importance once ternary complexes were added and might be omitted from the model.
- The observed increase of pH at the start of the injection could not be simulated with any combination of parameters trialled. The addition of ternary complexes showed the most promising improvement for this problem so far. Kinetic biodegradation showed some improvement for this mismatch (see VI.5.3.6).
- The observed prolonged tailing of Zn at the end of the injection phase could not be simulated with the conceptual model as this would be due to non-equilibrium conditions (see V.3.3.1.6)
- The observed spike in pH, Zn and Cu concentration after the shorter storages during the recovery phase were not simulated with the conceptual model. These are most likely due to non-equilibrium in the column, which could be due to a combination of dual domain, kinetic biodegradation or kinetic mineral dissolution. All three mechanisms should be investigated for an improved conceptual model. Release of particulate metals due to the change in flow velocity after storage should also be considered (see V.3.3.1.4).

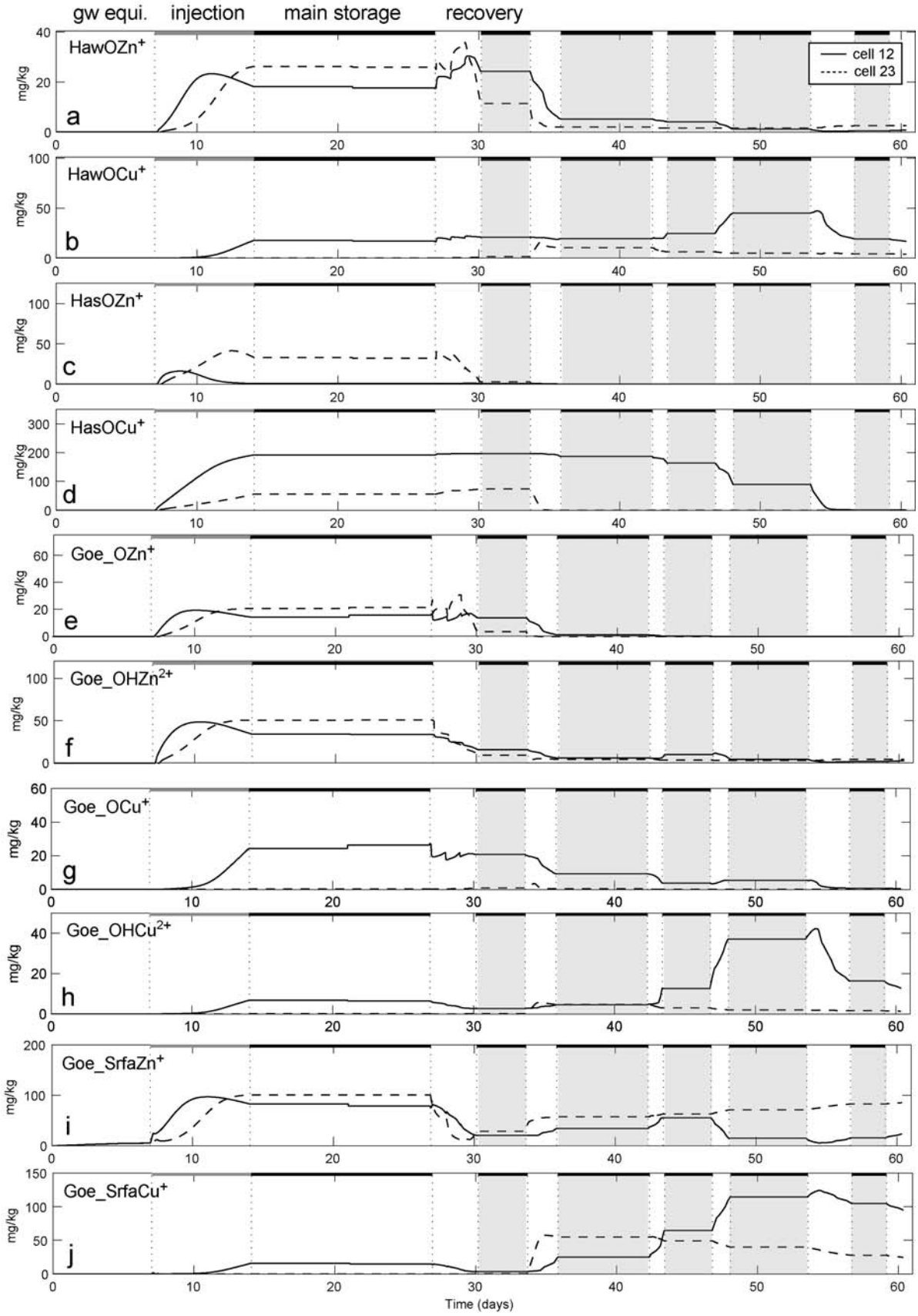

Figure VI-39: Simulated adsorbed species of Zn and Cu to 0.02 mol Has, 0.1 mol Haw and 0.02 mol goethite surface sites with ternary complexation (8.7/6.7) as (a) Zn sorbed on Haw, (b) Cu sorbed to Haw, (c) Zn sorbed to Has, (d) Cu sorbed to Has, (e) inner-sphere sorbed Zn on goethite, (f) outer-sphere sorbed Zn on goethite, (g) inner-sphere sorbed Cu, (h) outer-sphere sorbed Cu on goethite, (i) ternary Zn complex and (j) ternary Cu complex.

VI.5.3 CA model performance for column experiments

After the different features of the conceptual model were investigated as described above (VI.5.2), the model was applied to the other aquifer materials and experiment 3 (see chapter V). The mass of the surface minerals were adjusted to Al-, Fe oxide and solid organic carbon content of the sediments. The total number of surface sites was then manually adjusted to find the best fit. It could be shown above (VI.5.2) that nearly all observed feature could be modelled with the conceptual model. The difficulty was to fit all measured features for pH, Cu and Zn at the same time.

VI.5.3.1 BR experiment 2

Using all features of the conceptual model Figure VI-40 (solid lines) shows the best compromise for Zn, Cu and pH. While much better fits could be achieved for individual components, this resulted in a deterioration of fit for other components. As observed before the tailing of Zn breakthrough and the peaks in concentration after the storages could not be modelled. In this compromise (Figure VI-40a, solid line) the release of Zn during day 34-36 was also not fitted. Cu breakthrough was slightly too high towards the end of the injection phase. While the peak heights for Cu release were fitted, they were about 3 days of flow too late. pH values were in reasonable agreement except for the start of stormwater injection.

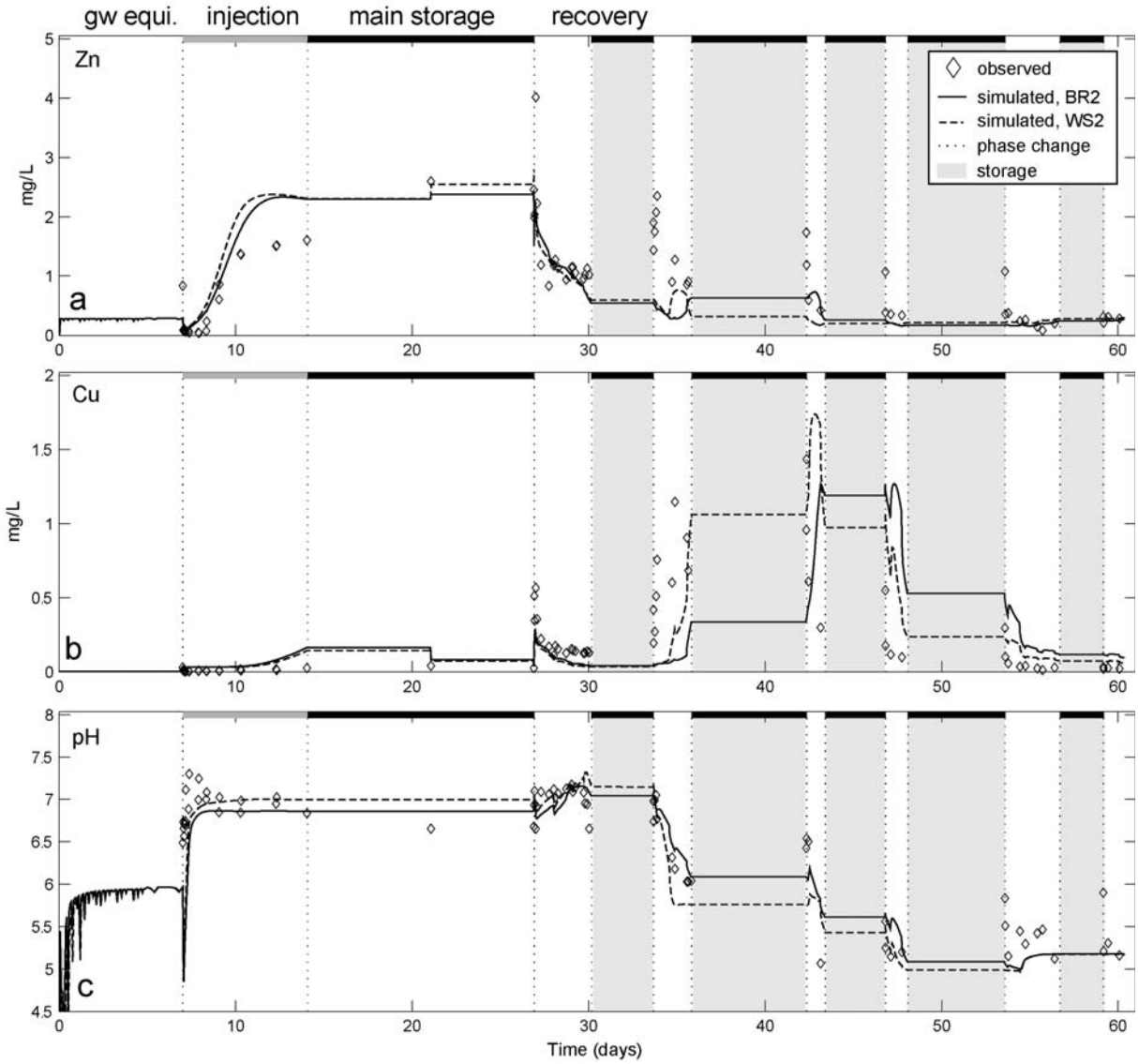

Figure VI-40: Simulated and observed concentrations of (a) Zn concentration, (b) Cu concentration and (c) pH for BR2 (solid line) and WS2 (dashed line). See TableVII-8 for used amounts of surface sites.

VI.5.3.2 WS experiment 2

The sediments BR and WS had similar concentration of organic matter and CEC (Table III-10). The difference in sediment pH was dampened by the groundwater equilibration and hence BR and WS showed very similar results during the column experiment. Accordingly, simulation results showed very similar outcome and the same misfits as observed for BR2 (Figure VI-40, dashed lines).

VI.5.3.3 BL experiment 2

BL showed a much higher sorption capacity during column experiments with only limited breakthrough of Zn. From the column experiments a value of about four times more specific sites for BL compared to BR/WS were deduced (see V.3.3.1), which were attributed to higher organic matter content (see Table III-10). Nevertheless, an increase in organic surface sites by about 4 times did not decrease Zn breakthrough sufficiently and resulted in no Cu release

during recovery (Figure VI-41, dashed lines). In contrast, an increase in goethite surface sites decreased Zn breakthrough significantly and even allowed for a limited release of Cu (Figure VI-41, solid lines). It was achieved by a significant deterioration in pH fit though. This indicates that affinity constants for Zn and Cu should be readjusted to represent the observed stronger affinity of Zn to organic surfaces.

The mismatch in pH at the start of injection was even more pronounced due to the increase in surface sites. This indicates that a significant process that reduces proton concentrations was not incorporated in the model or reactions that produce protons were overemphasized. One possible explanation might also be that surface sites and DOC added to the model are assumed to be occupied by protons to start with, in reality though these sites could be occupied by other cations or metals present in the groundwater and stormwater. Their release would therefore not result in a drop in pH. Further models should equilibrate surface sites and DOC with the appropriate solution to exclude this possibility.

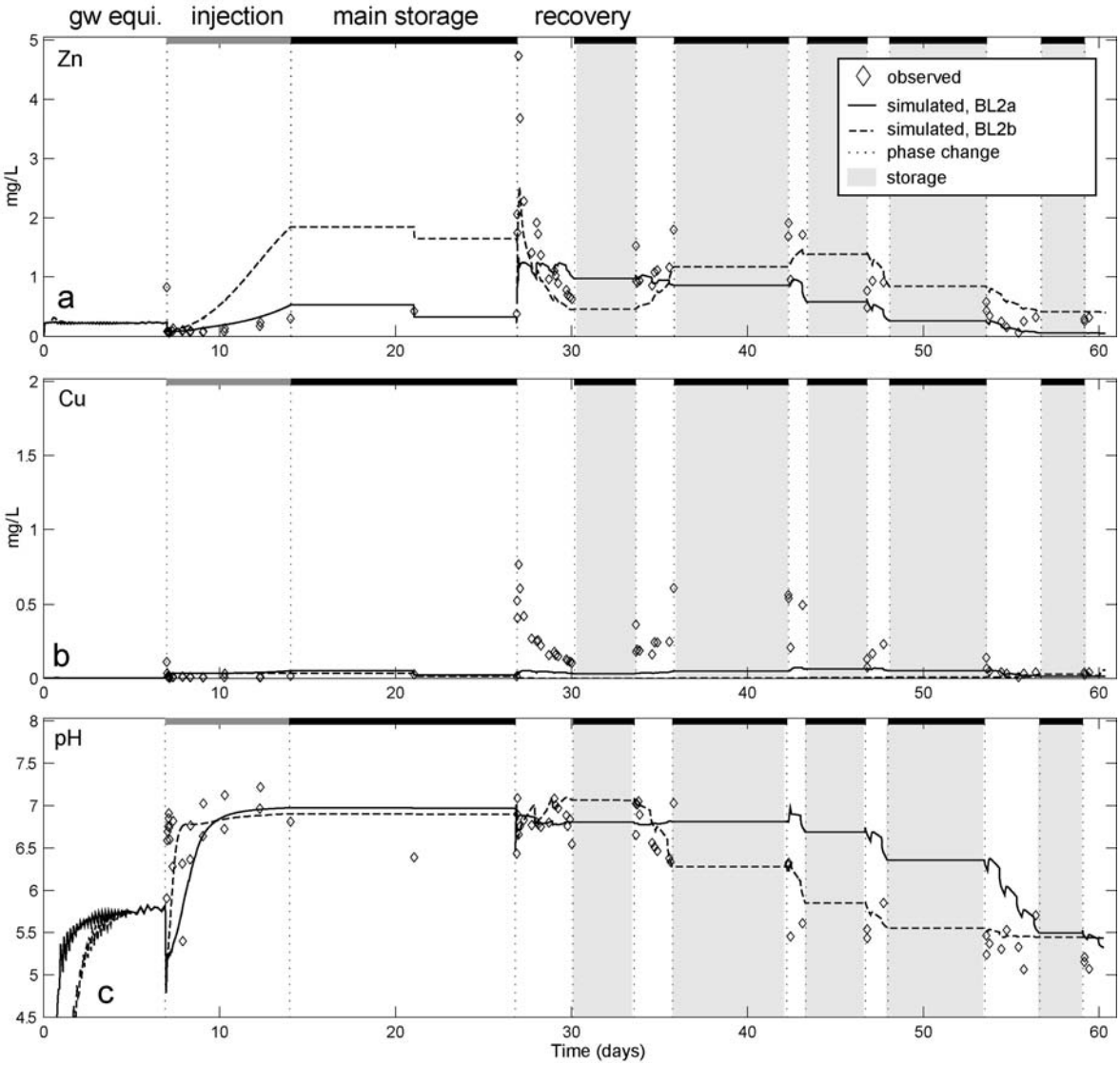

Figure VI-41: Simulated and observed concentrations of (a) Zn concentration, (b) Cu concentration and (c) pH for BL2. See TableVII-8 for used amounts of surface sites.

VI.5.3.4 Experiment 3

The main difference of exp.3 compared to exp.2 was the spiking of stormwater with DOC. This lead to two effects for all three sediments: (a) Cu was transported as organic colloidal complex through the column and (b) deposited organic matter increased specific surface sites and limited release of Zn and Cu (see V.3.3). Both of these processes, i.e. colloidal transport and deposition of organic matter, were not incorporated in the current model. Hence, the model could not represent Cu behaviour, esp. the breakthrough during injection. Simulations that came closest to the observed breakthrough were only achieved if the affinity constants for Cu onto both organic surface sites were decreased to nearly zero, mimicking a bypassing of Cu and are shown exemplary for WS3 (Figure VI-42).

As noticed for simulation of exp 2, no increase in values after storage phases was modelled, which would also be due to missing kinetic degradation and mineral dissolution. Also pH values were too low at the start of injection as observed for simulations for exp. 2 (see above). In addition, simulated pH values were too low after 32.5 days, indicating that some buffering mechanism was missing in the model. This would most likely be buffering from the intercepted organic carbon.

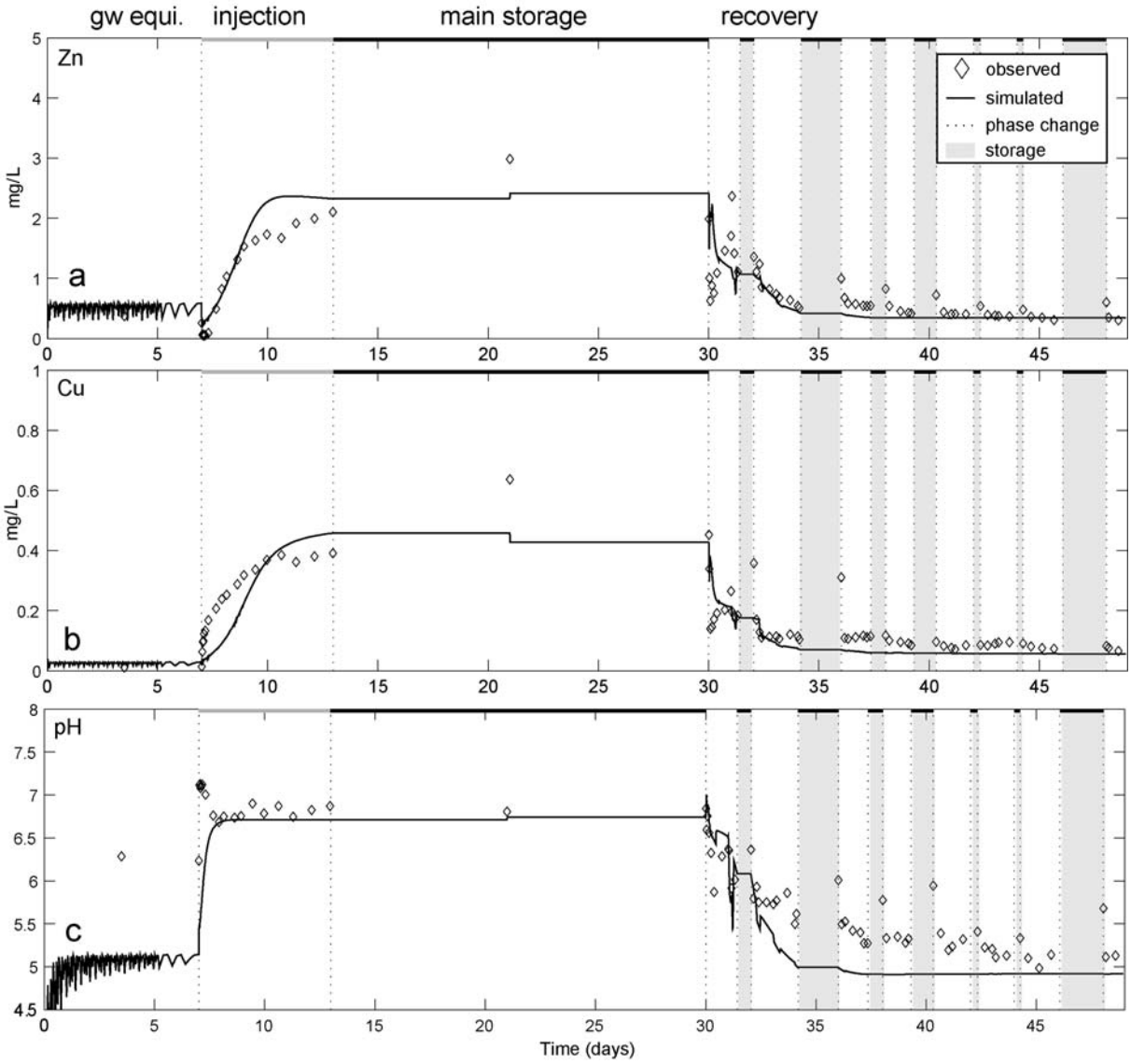

Figure VI-42: Simulated and observed concentrations of (a) Zn concentration, (b) Cu concentration and (c) pH for WS3. See TableVII-8 for used amounts of surface sites.

VI.5.3.5 Dual domain

While the transport of sorbing solutes is generally modelled as ideal instantaneous equilibrium reaction, this is a simplification of the naturally occurring reactions. Heterogeneities in the natural medium result in hydraulic non-equilibrium due to the formation of immobile pockets and preferential flow paths (Bouchard et al., 1988; Brusseau and Rao, 1989). Hydraulic non-equilibrium behaviour will manifest itself in prolonged tailing of a breakthrough curve and spikes of concentration changes after flow interruption for all components (Reedy et al., 1996). As both phenomenons were detected during column studies an immobile region was implemented for a number of runs for BR2 (see VI.5.1.6).

The results showed no change in simulated concentrations for Zn, Cu and pH for all trialled combinations of immobile porosity (0.1-0.5) and first-order exchange coefficient/mass

transfer coefficient (0.0005-0.5 1/d). This was an unexpected outcome, which might be due to the fact
that simulations are very sensitive to the fraction of immobile porosity and mass transfer coefficient and therefore the optimal combination was not found (Reedy et al., 1996; Maraqa, 2001; Worch, 2004). It has also to be taken into account, that simulated spikes after storage phases would be very short and concentrations would drop back to previous values very fast, while observed values from samples would represent a mean values over a longer time. The spikes might have been missed in model runs, when output times did not cover this short event.

However, field studies (Haggerty and Gorelick, 1995; Feehley et al., 2000, Flach et al., 2004) have shown that dual domain behaviour is an important process, considerably effecting transport of reactive components. It would therefore be desirable to implement dual domain behaviour for upscaling of this model even if effects were too small to be detected during column experiments.

VI.5.3.6 Kinetic biodegradation

Degradation of organic matter has been found to be an important process during ASR and river bank filtration and has been investigated frequently (e.g. Greskowiak et al., 2005; Horner et al., 2007; Kedziorek et al., 2008). Due to its indirect influences on redox conditions and pH, it has potential implications for metal behaviour. The addition of a simple kinetic biodegradation reaction (see VI.5.1.7) mainly resulted in short increased values of pH during each storage in accordance with measured values (Figure VI-43c dashed line) (note: no changes in simulated values during storage are visible on the graphs as they depict values in the EC meter, where no kinetic degradation was assigned to take place). These had only minor effects on metal concentrations though (Figure VI-43a+b dashed line), apart from a spike in Zn concentration after the main storage. When the maximum degradation rate was increased by one magnitude (Figure VI-43 dash-dotted line) pH values were raised over the whole experiment. This was an improvement for simulated pH values during the injection phase but a degradation during the recovery phase. The effect of higher pH resulted in less sorption of Cu onto organic surface sites and less sorption of Cu ternary complexes and the subsequent increased breakthrough of Cu during injection triggered the snow plow effect of Zn breakthrough. Oxygen concentration were only lowered to about 4-4.5 mg/L during storage (not shown), meaning that no denitrification of iron reduction was taking place.

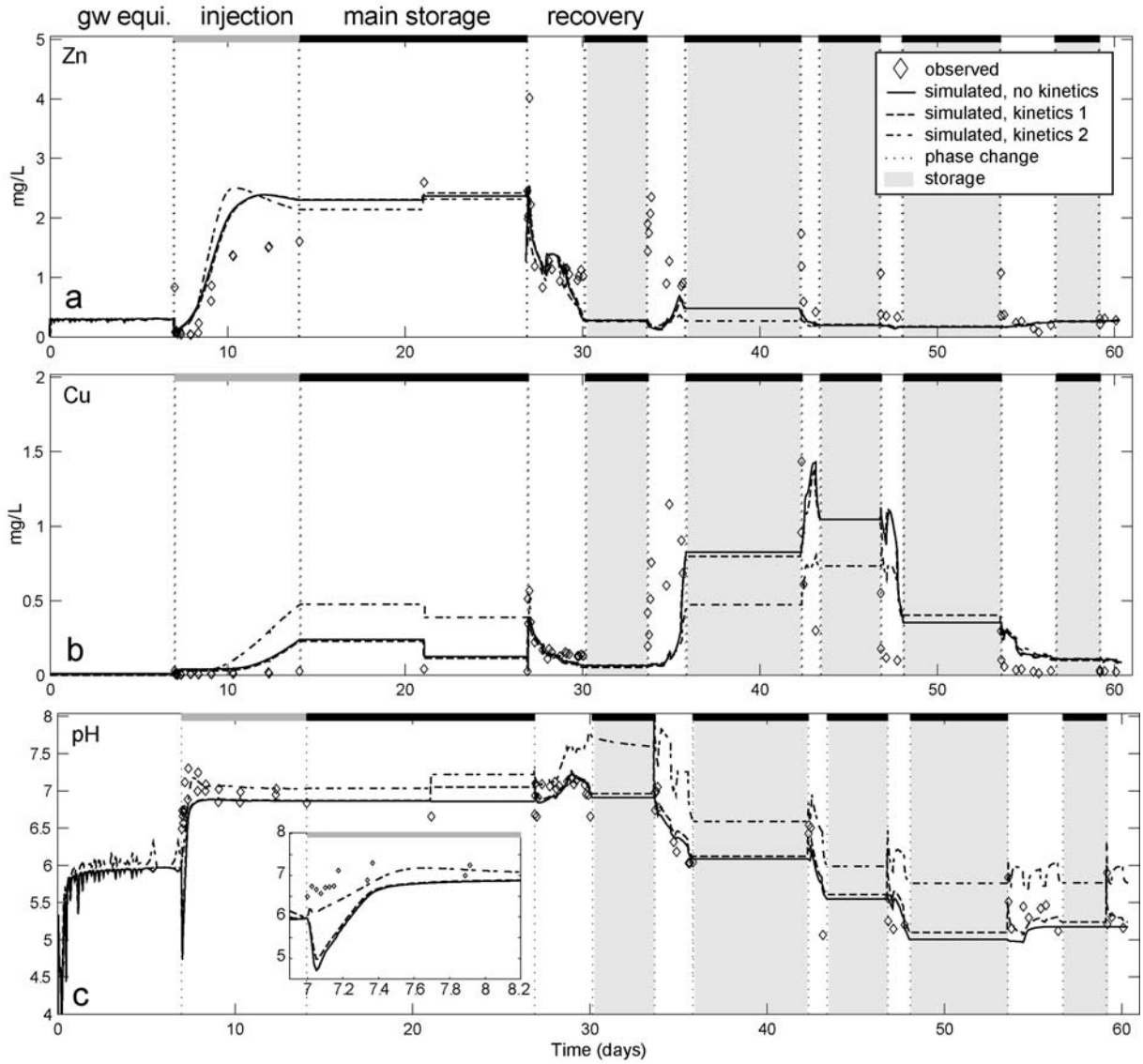

Figure VI-43: Simulated and observed concentrations of (a) Zn concentration, (b) Cu concentration and (c) pH onto 0.012 mol goethite and 0.016 mol Has with kinetic biodegradation (dashed line) using values after Parkhurst and Appelo (1999), see Table VI-7, and increased maximum degradation rate for aerobic degradation of 1.57*10^{-8} mol/L/s (dash-dotted line).

The addition of kinetic biodegradation to simulations of experiment 3 on the other hand, where oxygen concentrations were zero during the recovery phase, showed an increase in pH during minor storage phases that matched the trend of the measured pH (not shown).

While the improvement for model simulations of the column experiments were visible but limited, kinetic biodegradation is an important process and additional improvements could be expected, if this feature would be developed further. To fully appreciate the effect of organic biodegradation it would be necessary to include:

- filtration/release of particulate organic carbon to adjust the amount of organic carbon source
- simulation of growth and decay of biomass to adjust degradation rates

- change in amounts of organic surface sites with changes in both POC and biomass, as microorganisms also offer sorption sites for metals (Muris et al, 2005; Guine et al., 2006)
- dissolution/precipitation of minerals due to changes in redox conditions and pH
- coupling of surface sorption sites to mineral phases reflecting changes in mineral amounts due to dissolution/precipitation

VI.6 Model evaluation

VI.6.1 Objective functions

So far evaluation of the model performance was qualitative, based on visual judgements. As outlined in VI.2.4 quantitative performance evaluation can be undertaken with objectives functions.

It was observed that all five different objective functions(see equation VI-2 to VI-6) showed the same trends for all three parameters, i.e. decreasing MAE coincided with decreasing RMSE and increasing E, E' and R^2 towards unity (Figure VI-44). The highest scatter was observed for R^2, which would be the least favoured function, as it does not contain a direct evaluation of observed to simulated data (see equation VI-3). E' values are exactly correlated to MAE as they both use the sum of absolute errors between observed and simulated values. MAE and RMSE are absolute values that have to be related to the value of the evaluated parameter, meaning that an evaluation across parameters is less intuitive. E is more sensitive to extreme values compared to E' due to the squared errors. This sensitivity is beneficial when judging how well the model would simulate loads, where peaks would account for the bulk of load while errors in low background levels do not influence the overall load significantly. Therefore E was used as main objective function.

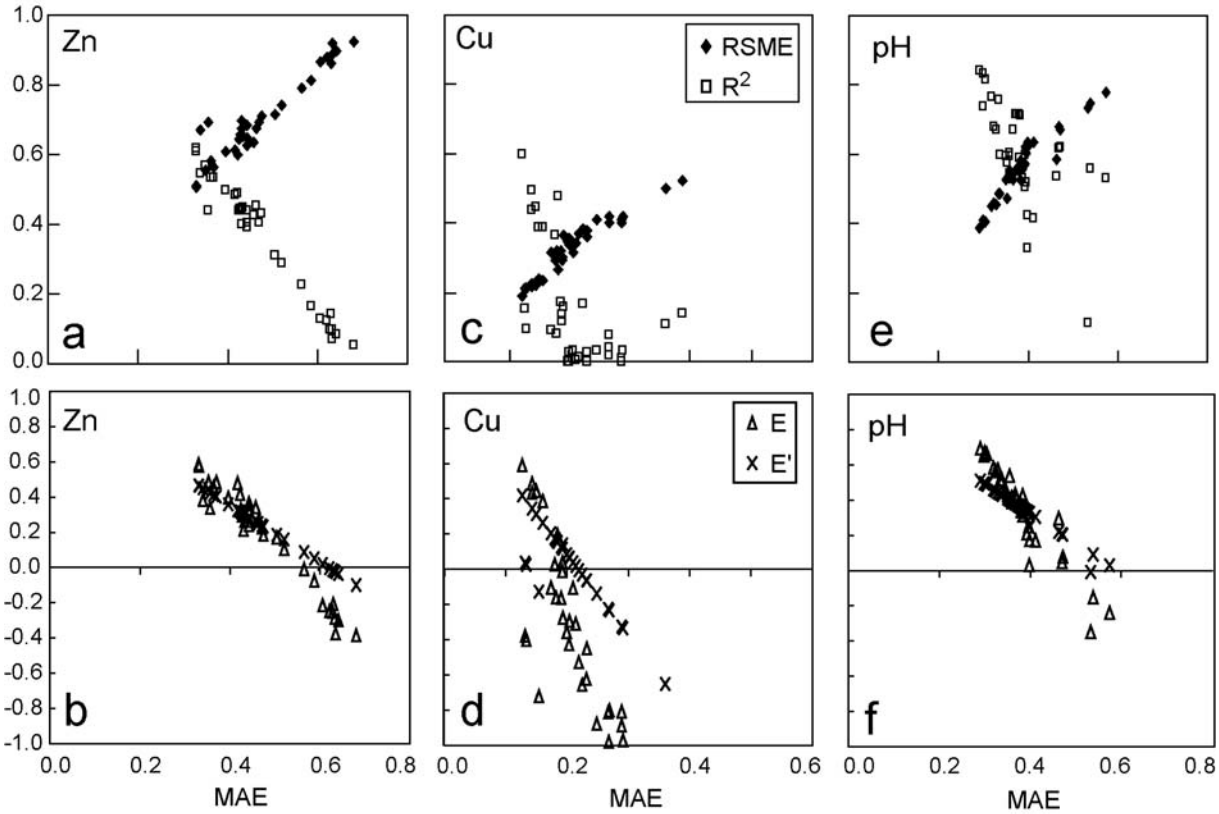

Figure VI-44: Correlation between different objective functions for model runs listed in Table VI-8 (except K_d approach) for (a+b) Zn, (c+d) Cu and (e+f) pH. MAE: mean absolute error, RMSE: root mean squared error, R^2: coefficient of determination, E: coefficient of efficiency; E': modified coefficient of efficiency, see VI.2.4 for equations.

The K_d approach had by far the worst E value (Table VI-8), underlining the inappropriateness of this approach. The GC approach also showed rather low values. The relative high values for the adjusted ion exchange approach come at the cost of a significantly compromised fit for calcium. None of the CA simulations had values above 0.4 for all three parameters at the same time and overall Cu had the worst fit. The simulations for BR2 with the highest E values for all three parameters were simulation with only or mainly goethite surface sites, which is in agreement with the sediment analysis. The model was most sensitive to the amount of goethite and Has surface sites and to the affinity constants for formation of various surface complexes (Tebes-Stevens et al., 2001).

Table VI-8: Coefficient of efficiency (E) (see equation VI-5) values for Zn, Cu and pH for simulations shown in graphs. All simulations are for BR2 if not indicated otherwise.

graph VI-	simple approaches						Zn	Cu	pH	Sum
4	K_d						-3.81	-17.6	-0.24	-21.65
5	ion exchange, dataset a						-0.21	-1.79	0.37	-1.63
7	ion exchange, dataset c						0.24	0.04	0.67	0.95
9 S	GC, original set						-0.37	-0.88	0.37	-0.88
9 D	GC, optimised set						0.18	-0.43	-0.15	-0.40
16	control = ion exchange, dataset b						-0.39	-2.06	0.37	-2.07
	CA surface complexation modelling									
	Goe [mol]	**Haw [mol]**	**Has [mol]**	**OC**	**DOC**	**TC**				
17a, 18a, 20a S	0.01			no	yes	no	-0.21	-0.10	0.43	0.11
17a, 18a, 20a D	0.03			no	yes	no	0.33	0.44	0.42	**1.19**
17b, 18b, 20b S	0.05			no	yes	no	0.40	-0.11	0.51	0.80
17b, 18b, 20b D	0.07			no	yes	no	0.31	-0.31	0.54	0.54
21a, 22a, 24a S		0.01		no	yes	no	-0.25	0.03	0.66	0.44
21a, 22a, 24a D		0.02		no	yes	no	-0.01	0.19	0.56	0.75
21b, 22b, 24b S		0.03		no	yes	no	0.17	-0.81	0.36	-0.27
21b, 22b, 24b D		0.04		no	yes	no	0.37	-0.80	0.25	-0.18
25 S			0.05	no	yes	no	-0.30	-0.16	0.52	0.06
25 D			0.4	no	yes	no	-0.08	0.43	0.58	0.94
27 D	0.02	0.02		yes	yes	no	0.49	-0.89	0.17	-0.23
28 D		0.02	0.1	no	yes	no	0.34	-0.81	0.57	0.10
29 S	0.02			no	yes	no	0.11	0.49	0.33	0.92
29 D	0.02		0.1	no	yes	no	0.42	0.39	0.34	**1.14**
30 D	0.02	0.02	0.1	no	yes	no	0.59	-0.97	0.17	-0.21
35 S	0.03			no	no	no	-0.25	-0.66	0.69	-0.22
32 D	0.03			yes	no	no	-0.28	-0.98	0.66	-0.61
35 D	0.03			no	yes	no	0.11	0.49	0.33	0.92
37 S	0.03			yes	yes	no	0.32	0.59	0.43	**1.34**
37 D	0.03			yes	yes	8.7	0.26	-0.30	0.43	0.40
37 DD	0.03			yes	yes	13.4	0.26	-0.36	0.08	-0.02
39	0.02	0.02	0.1	yes	yes	13.4	0.57	-0.45	0.21	0.33
40 S	0.012	0.1	0.016	yes	yes	8.7	0.30	-0.16	0.40	0.53
40 D (WS2)	0.007	0.05	0.014	yes	yes	8.7	0.23	-0.01	0.30	0.51
41 S (BL2)	0.09	0.1	0.015	yes	yes	8.7	0.45	-0.62	0.31	0.14
41 D (BL2)	0.01	0.2	0.05	yes	yes	8.7	0.49	-0.28	0.39	0.60
42 (WS3)	0.012	0.05	0.005	yes	yes	8.7	0.48	-0.72	0.03	-0.21
43 S	0.012		0.016	yes	yes	8.7	0.34	-0.38	-0.35	-0.39
43 D	0.012		0.016	yes	yes	8.7	0.54	0.61	0.23	**1.38**

S: solid line, D: dashed line, DD: dash-dotted line; Goe: Goethite surface site; Haw: weak humic acid surface site; Has: strong humic acid site; OC: organic complexation in solution, DOC: sorption of DOC onto goethite, TC: ternary complexes with log k value for Goe_SrfaMe$^-$ complexes.

Objectives functions are not a good criterion for judging the success of time-series model predictions (Larsson and Jarvis, 1999) like this model with a number of different phases, as they do not depict any consistent shift in values or give temporal information on the goodness of fit. For example, E values are decreasing for pH with the addition of ternary complexes (see Figure VI-37c), while the graphs showed that pH during injection was improving, while pH during recovery was worsening. Similarly E values for Cu are decreasing with the addition of Haw sites (see Figure VI-29b), while the graphs clearly showed a

significant improvement in simulated Cu values during injection. Therefore, objectives functions should not be used without visual confirmation of an overall improvement in fit.

VI.6.2 Uncertainties

As mentioned in VI.2.4 uncertainties in models can be classified into three different categories related to:

(1) model structure

This is the category with the highest potential for error and contains the highest uncertainty. Apart from minor error introduced as numerical errors during calculations (e.g. numerical dispersion, truncation errors), models will always be a simplification of the natural processes. For example small scale heterogeneities are not accounted for and hydrodynamic dispersion is modelled with Ficks law. Commonly, models use the equilibrium approach for calculating component speciation. This is appropriate for simple components, but does not hold up once larger molecules like fulvic acids are introduced as these molecules not only change their speciation, but also their shape. For example, their position on surfaces can be hindered by steric considerations (Amirbahman and Olson, 1995). Complexation studies with a range of low molecular weight organic acids showed that not only the type of functional group, but also the spatial coordination to other functional groups influences the affinity to metals (Ali and Dzombak, 1996; Evanko and Dzombak, 1999). Also, the complexity of natural processes is immense and knowledge gaps limit the processes that can be incorporated into a model. Even if the exact composition and arrangement of functional groups of fulvic acids would be known, the number of possible reactions and values needed to describe them would overburden any current model capacity. In addition, the three dimensional arrangement of FA change with changes in solution composition or once they attach to surfacess. Hence, fulvic acids have to be described with a limited number of average parameters. For this model there are also a number of possible processes that are currently not incorporated (see VI.6.3).

(2) measured data and lack thereof

Simulations are evaluated against observed data, which themselves contain a number of uncertainties. Minor errors are due to uncertainties based in the analytical method, but the main errors occur during sampling. Firstly, the number of samples is always limited and short changes in parameter values could therefore be missed. Secondly, due to volumes needed for analysis, samples covered a longer time span than simulated values and represent an averaged concentration. It is therefore a reasonable assumption that actual concentration spikes would have been higher than measured values. In addition the calculation of PV has an uncertainty of about 10%, so measured peaks might in reality be slightly earlier or later. Thirdly, sample preparation and storage will alter the samples. While the uncertainties in all

these errors can be decreased with increasing number of samples or improvement of the sampling and analytical method, most evaluations are limited by the lack of measured data. For example, redox potential was not measured in this study as handling of samples in nitrogen atmosphere was not possible. Speciation of metals was also not measured as the equipment was not available. A more detailed characterisation of the sediments would have also been desirable. All studies are inherently limited in the amount of samples that can be obtained and small scale heterogeneities cannot be captured.

(3) model parameters

This category of errors is the only one that can be measured with objective functions. Uncertainties arise from the use of a less than optimal set of parameter values. Commonly parameter values are interdependent, meaning that improvements in one parameter results in a deterioration in other parameters. While automatic calibration tools like PEST, Monte-Carlo or NULL-space evaluation exist (Nocedal and Wright, 2006) and can calibrate for a number of parameters simultaneously, the results are still limited by problems like non-uniqueness of a set of parameters, local optima, spatial and temporal heterogeneities of parameters, database inaccuracy and uncertainties of the first two categories. Their use is also often impractical due to time constraints, e.g. a single run of the current model in this study took about three hours, as multi-component calibration algorithm would need to run at least 1000 times for a statistically confirmed minimum. Also, the nature of the coupled software does not necessarily allow the use of optimisation tools (Horner et al., 2007).

In conclusion, every model is limited by the amount of available data and the number of processes that can be simulated correctly. While there are various processes that were not included (see below) the used component additivity surface site model showed a vast improvement over K_d models that are still commonly applied in risk assessment evaluations.

VI.6.3 Further improvements

It is clearly recognised that the current model is not the final version and further improvements on the model fit are likely to be achieved with the addition of other processes. Some of these processes are already included in the software options, others would need further development and testing, while still others would mainly need more analysis to limit uncertainty or establish additional parameter values.

The most important processes that should be incorporated are:

(a) kinetic mineral and organic matter dissolution/precipitation

As discussed before (VI.3.2.3 and VI.4.3) kinetic dissolution and precipitation of minerals can be incorporated in PHREEQC. Of special interest would be pyrite dissolution due to the

release of incorporated trace ions like As, Ni and Zn, and the dissolution/precipitation of hydr-/oxides of Al, Mn and Fe, as these would change the sorptive capacities of the sediment. Similarly, the filtration and precipitation of organic carbon injected into the aquifer as well as the dissolution of injected and existing sedimentary organic carbon are important for the sorptive capacity. Results from experiment 3 could not be simulated without it. Dissolution of humic acids is sensitive to solution composition, e.g. can be enhanced with low molecular weight organic acids (Brigante et al., 2008) and high pH (Schnitzer and Kodama, 1966; Kuo and Baker, 1980). The challenge would be to formulate the appropriate kinetic reaction rates that vary with sediment and solution composition/properties (e.g. McBride, 1989; Cornell and Schwertman, 1996; Reichard et al., 2007).

(b) variable amounts of surface sites

Once dissolution/precipitation reactions of minerals and organic matter are included, the amount of surface sites can be coupled to these phases in PHREEQC. This feature has not been tested for PHT3D, but investigations are currently undertaken (H. Prommer, personal communication). Unsuccessful attempts to couple surface sites with mineral phase were also undertaken during this study, which resulted in convergence problems.

(c) colloidal transport

The results from experiment 3 and the mobilisation of particles at the start of stormwater injection and after storage phases clearly showed that colloids are present and contribute to metal transport. PHREEQC v.2.13 can accommodate surfaces that are mobile. For this feature to work, mobile surfaces need to have a diffuse double layer for charge neutrality and surface sites cannot be coupled to mineral phases or kinetic reactions. This feature will need more testing and questions remain on how to simulate the change from mobile to immobile surface and vice versa, i.e. deposition/mobilisation and aggregation/break up in a porous medium.

(d) improved kinetic biodegradation

As introduced in VI.3.5 and VI.5.4 kinetic biodegradation is an important process during ASR where oxygen, nitrate and organic carbon enriched stormwater is introduced into anaerobic and nutrient poor groundwater. Biodegradation simulations are closely linked with the above described processes: Filtration/release of organic carbon (process a) allows for the adjustment of available carbon source, biodegradation of organic material and growth/decay of biomass change the amount of available sorption sites (process b) and organic carbon is a possible colloidal carrier of metals further into the aquifer (process c). The induced changes in solution pH/Eh then bring about mineral dissolution/precipitation (process a), which further

changes the amount of surface sites (process b) and might even release inorganic colloids (process c). All of these changes influence metal sorption behaviour. While filtration and dissolution of organic carbon and growth and decay of biomass has been tested with PHT3D (Greskowiak et al., 2005), surface complexation and coupling of surfaces sites to phases have not been tested.

(e) kinetic sorption and complexation

In this model all sorption and complexation reactions were equilibrium reactions. In reality most biogeochemical processes are dynamic and involve rate-limiting steps, e.g. diffusive reactions. For example the complexation of metals with fulvic acids is influenced by the diffusion of the metal and FA towards each other, the elimination of a water molecule from the FA to form inner-sphere complexes and the dissociation of protons from the negatively-charged electric field of the FA to form outer-sphere complexes (Buffle et al., 2007). Slow sorption kinetics have also been shown to exist for sorption of metals onto mineral surfaces as metals have to overcome film diffusion, interparticle and intraparticle diffusion (Sparks, 2003). The combination of chemical kinetics and diffusive transport therefore result in a rate-limited sorption and complexation of metals, but parameter values required to simulate such calculations are not readily available.

(f) improved sorption and complexation reactions

In this model only monodentate binding to three different surface sites and monodentate complexation to FA in solution was implemented. In reality, a vast number of possible mono-, bi- and multidentate binding and complexation reactions to a large number of different functional groups are possible (e.g. Papini et al., 1999; Robertson and Leckie, 1999; Ponthieu et al., 2006). For organic acids not only the type of functional group, but also the spatial arrangement to other functional groups influences affinity of metals (Ali and Dzombak, 1996; Evanko and Dzombak, 1999). Affinity constants are also different if the FA is adsorbed or in solution (Dunnivant et al., 1992). Metal sorption onto minerals can also involve different geometries and affinity depends on the position of the functional group (e.g. edge, corner) and the crystal structure of the mineral (Ponthieu et al., 2006) and can change with ripening of the mineral (Thompson et al., 2006). Adjustments to affinity constants and the addition of multidentate binding might help to solve the problem experienced with simulations of Zn during stormwater injection in BL2 and the mismatch in pH at the start of stormwater injection for all cases. Even with extended analysis the determination of affinity constants for all possible positions is not likely to be possible though.

(g) upscaling to field scale

The final aim for this model is the use as predictive tool for potential new ASR sites in sandy aquifers. Significant differences between the laboratory conditions and the field are temperature, solid composition/structure and transport conditions as well as longer time scales. Temperature has been shown to influence chemical reaction rates like biodegradation rates and dissolution rates (von Gunten et al., 1991; Bourg and Bertin, 1993; Prommer and Stuyfzand, 2005). Large and small scale heterogeneities in aquifer hydraulic properties and mineral composition will be much higher in the field (Koretsky, 2000). Hence dual domain transport, diffusively limited processes and non-equilibrium conditions will be of much higher significance. In addition, clogging processes due to injection of particulate matter and biomass growth and dissolution/precipitation of minerals will change aquifer properties significantly.

Overall, accounting for all possible processes that could determine the solubility of metals during stormwater ASR seems to be beyond the capacity of any single model.

VI.7 Conclusions

An attempt to model the results from previous column experiments with the reactive geochemical transport model PHT3D was undertaken. This was the first time that surface complexation was used with PHT3D. The component additivity approach for one mineral surface site and two organic surface sites was used. In addition the standard database was enlarged by organic complexation in solution, sorption of FA and metal-organic complexes onto the mineral surface.

This model is a step in the right direction to understand metal behaviour during stormwater ASR in sandy aquifers. Different aspects of the result were simulated sufficiently and magnitudes of metal concentrations were achieved. Nevertheless, the overall performance of the model was moderate. As with other models, this model included only a subset of biogeochemical relevant processes and further improvements are needed. The main discrepancies could be attributed to colloidal transport of metals, the complex nature and interaction potential of organic acids, kinetic processes and a lack of geochemical equilibrium in the column. In addition, there are uncertainties connected to the used reactions and affinity constants.

Chapter VII: Conclusions and assessment

"The most alarming of all man's assaults upon the environment is the contamination of air, earth, rivers, and sea with dangerous and even lethal materials."
Rachel Carson, Silent Spring, 1962

The risk associated with water recycling to augment drinking water supplies is currently under review and stormwater reuse and managed aquifer recharge are part of the Australian guidelines for water recycling (NWQMS, 2007). As elevated levels of metals are ubiquitous in urban stormwater (e.g. Makepeace et al., 1995; Duncan, 2006) and metals cannot be degraded, their behaviour during stormwater ASR was investigated. In contrast to South Australia where stormwater ASR has been practiced for a number of years in limestone (see II.2.4.2 and II.2.4.3), Melbourne's potentially viable aquifers are mainly silicious (Dudding et al., 2006). As no field site was available for this study, laboratory experiments with local aquifer sediments, groundwater and stormwater were undertaken instead to evaluate the risk to the environment posed by injected metals during stormwater ASR.

In the following the main results of stormwater, groundwater and aquifer material sampling, batch and column experiments and the geochemical modelling will be summarised (VII.1). The implications for field sites (VII.2) and a critical evaluation of the study (VII.3) are given.

VII.1 Summary of results

VII.1.1 Characterisation of solutions and sediments

The analysis of about 50 stormwater samples from different catchments around Melbourne showed high variability between events and catchments. The roof catchment had significantly lower values for all parameters. Roof runoff is unlikely to be the single source for stormwater ASR though, as rain tanks are commonly employed for roof runoff storage and reuse (e.g. Coombes et al., 2000; Hatt et al., 2006). Relative to overseas studies other catchments in Melbourne showed elevated concentrations of Zn (~1.1 mg/L) and comparable concentrations of Cu (~50 µg/L). Compared to other metals Zn and Cu were predominantly found in the dissolved and fine particulate fraction. Hence their concentrations were still considerably above freshwater ecosystem guideline values after sedimentation. Without further pretreatment noteworthy amounts of Zn and Cu are therefore likely to be injected into the aquifer in dissolved and colloidal form.

Groundwater was extracted from one bore in the Tertiary Fyansford Formation-Brighton Group aquifer, SE Melbourne, after a small scale investigation. As ASR schemes are commonly implemented in brackish aquifers to limit the impact on beneficial use and interference with other users, groundwater with a salinity of about 3000 µS/cm and pH 5 was selected.

Three different aquifer materials were used in this study. The brown (BR) and black (BL) sediments from the Tertiary Brighton Group were both highly weathered sands with only minor amounts of Al and Fe and were therefore quite acidic, pH 4.3 and 2.8, respectively. The black colour derived under anoxic swampy conditions and was due to coating with humic acids. This gave BL a significantly higher organic carbon content and cation exchange capacity. Minor amounts of pyrite were responsible for the extremely low pH. The third sediment was a less weathered Quaternary alluvial sand from the Werribee Delta (WS). It contained slightly higher amounts of Al, Fe, Mn and K and was of neutral pH. Geogenic amounts of metals were low in all three sediments. Even though clay was ≤0.2% for all sediments they showed measurable release of inorganic and organic colloids (~200 nm) when mixed with neutral low ionic strength stormwater.

VII.1.2 Influence of single factors during batch experiments

The different adsorption series with Zn, Cu and partially DOC spiked stormwater and desorption series with groundwater for the three different sediments had the following results:

- At the low concentration range used most adsorption isotherms were linear and adsorption was higher for Cu compared to Zn for all sediments. Langmuir graphs were curved indicating the existence of more than one type of adsorption site. Adsorption isotherms were very steep for pH > 5 pointing to surface complexation.
- Zn adsorption was strongly pH dependent for BR and BL with pH_{50} values of 5.5 and 4.5, respectively, typical for metal like sorption. Cu adsorption was maximal between pH 6-6.5 and decreased either side of this pH range indicating ligand like sorption. pH dependence was less strong for WS with overall higher adsorption. The corresponding opposite behaviour was found for desorption.
- The addition of dissolved FA showed mixed results: (a) significantly decreased adsorption of Zn and Cu to WS, (b) slightly decreased adsorption of Cu to BR, (c) increased adsorption of Cu to BL, (d) increased release of Cu during desorption experiments and (e) adsorption of DOC to the sediments at lower pH especially, BR and WS. Neutral pH values on the other hand triggered the dissolution of HA from the sediment matrix, especially from BL. It is therefore important to understand the

different effects of dissolved FA and sedimentary HA, especially for Cu which forms stabile organic complexes.

- A slight solid-solution effect on adsorption was observed for WS, once concentration were normalised and the change in pH was accounted for, and could be due to sorption sites with different metal affinities or non-equilibrium conditions.
- Salinity effects on adsorption and desorption were limited, probably due to the low metal loading.
- Overall desorption was limited as specifically sorbed metals are not desorbed by ion exchange. In analogy to adsorption results, Zn desorption was considerably greater compared to Cu with the metal release decreasing from BR > BL > WS.
- Cu desorption was decreased under anoxic conditions, but no clear effect was visible for Zn.

Overall Cu was strongly bound to all sediments, and formed organic complexes leading to ligand like sorption. Zn was sorbed less specifically and was highly affected by changes in pH showing metal like sorption. Sorption capacities of all sediments were not exceeded leading to limited desorption.

VII.1.3 Influence of multiple factors during column experiments

The column experiments consisted of four stages mimicking one stormwater ASR cycle. First columns were equilibrated with brackish groundwater, then stormwater was injected. After two weeks of storage, the flow was reversed and the previously collected stormwater outflow was fed back through the column. Salinity of inflow solutions were then stepwise increased and pH was decreased to mimic mixing with groundwater. Shorter storages were also incorporated as recovery would not take place as one continuous extraction.

The stormwater used for the first experiment was unspiked and Zn and Cu concentrations were unusually low in stormwater while they were unusually high in the groundwater. Conclusions from this experiment were therefore limited. The second experiment was undertaken with stormwater spiked with Cu and Zn and neutral oxic groundwater and the pH was only decreased later in the recovery phase. The third experiment used anoxic groundwater of pH 5 throughout and stormwater was additionally spiked with DOC. The main results of these two experiments are:

- During stormwater injection Zn showed complete breakthrough for BR and WS and starting breakthrough for BL. Solubility was slightly increased due to the addition of DOC. The breakthrough for BR and WS resembled an H-isotherm pointing to a high and a low affinity surface site, while the BL isotherm was much more gradual pointing

to a more gradual change in surface site metal affinity exhibited by different organic functional groups.

- Cu was completely adsorbed during stormwater injection of the second experiment, while solubility was significantly increased with the addition of DOC, with BL again showing the highest retardation of all sediments. The shape of the Cu breakthrough curve suggested transport as organic colloids and complexes and ligand influenced sorption for all three sediments.
- Particle mobilisation from the aquifer was observed at the start of stormwater injection due to the lowered ionic strength and during storages related to organic biodegradation and probably mineral dissolution. In conjunction, increased concentrations of Zn and Cu after storages were observed due to colloidal transport and release from matrix induced by changes in solution parameters during storage.
- During recovery Zn was released continuously due to dilution and competition with major ions and protons resulting in high recovery efficiency. Cu release was triggered by a decrease in pH during the second experiment. Both metals showed decreased desorption during the third experiment resulting in very limited release of Cu. The retained fraction of added DOC had significantly increased specific sorption sites and anoxic conditions were less favourable for metal release.
- During batch experiments BR and BL had shown lower affinity for metals than WS. During column experiments though BR and WS showed lower metal affinity compared to BL, reflecting the higher amount of organic carbon in BL. The acidic sediments BR and BL needed extensive flushing with groundwater to release the pool of reserve acidity, significantly altering the character of the surface sites.
- Hydraulic non-equilibrium conditions due to small scale heterogeneities in hydraulic properties and diffusion limited flow was observed. Chemical non-equilibrium was due to rate limited sorption visible in extensive tailing. Kinetic biodegradation resulted in sharp metal concentrations and pH increases after storage.
- Elevated concentration of arsenic were observed after the introduction of oxic stormwater to the anoxic pyritic sediment BL. The rate of oxidation was increased with the addition of organic carbon.

In conclusion, injected amounts of Zn are mobile and will mainly be recovered. Cu can be mobile in the presence of mobile organic carbon, but will mainly accumulate in the aquifer until the sorption capacity is exceeded. The release of metals was triggered by reduction in pH, increase in ionic strength and particle mobilisation. Metal concentrations were high after storage phases. Minor sediment constituents, especially organic matter, significantly reduce metal mobility.

VII.1.4 Implementation of results into reactive geochemical transport modelling

From the column experiments it is clear, that the distinction between mobile and immobile organic carbon is crucial, as mobile organic carbon increases solubility of metals and facilitates their transport, while immobile organic carbon enhances the accumulation of metals in the subsurface. Organic carbon in stormwater consists of a conglomerate of organic molecules with different molecular weights and functional groups. Accordingly a fraction will be mobile in the subsurface, while other fractions will either be strained, precipitate or sorb to the matrix becoming immobile. In low ionic strength solution remobilisation of organic carbon can occur by biodegradation, increase in pH or dissolved small organic acids.

In this modelling study mobile and immobile organic carbon, sorption of DOC onto the matrix and the formation of ternary complexes was implemented into a reactive geochemical transport model. Still missing is mainly the remobilisation of organic carbon and changes in surface site amounts that are induced by the transformation of organic carbon between mobile and immobile phase or by mineral precipitation and dissolution.

Accordingly, simulated results of experiment 2 are significantly better than simulations of experiment 3. While the presented model is a significant improvement to simpler approaches further processes have to be included to simulate non-equilibrium effects and the complex behaviour of organic matter that is one of the main drivers for metal behaviour.

VII.2 Implications for stormwater ASR in sandy aquifers

While the results gained during the laboratory experiments are only representative for short term behaviour the lessons learned could be translated into long term behaviour in sandy aquifers. It should be remembered that spiked metal concentrations during the experiments were considerably higher than expected injected stormwater concentrations, i.e. about four times higher for Zn and about 50 times higher for Cu. One also has to consider that other metals would be present in stormwater and especially Al and Fe would strongly be competing for sorption sites.

The prognosis for injected Zn would be that it would be relatively mobile within the aquifer and would be present throughout the injected freshwater zone. It would be partially adsorbed onto surface sites especially during the first number of ASR cycles, but largely be recovered in similar amounts as injected. If we assume a mean injected stormwater concentration of about 500 µg/L (see Table III-5) and assume that Zn is on average recovered in similar concentrations, then this concentration would be well below the drinking water guideline of 3

mg/L (NHMRC, 2004) and below the irrigation water guideline of 2 mg/L (ANZECC and ARMCANZ, 2000) and should be fit for these purposes. In contrast, these concentrations would be drastically exceeding freshwater ecosystem guidelines of 8 µg/L (ANZECC and ARMCANZ, 2000) and should not be used for environmental flows.

The prognosis for injected Cu would need to be differentiated into different scenarios.

Scenario A: low concentrations of organic carbon

For scenario A, injected Cu would be largely adsorbed to the aquifer matrix slowly filling up sorption sites from the injection well outwards to the edge of the freshwater zone, expelling less strongly sorbed metals like Zn in its wake. Desorption due to dilution would be highest close to the injection well, where high volumes of recovered water are flowing past. Unless pH values of streaming in recovery water are not significantly lower than pH 6, release of Cu would be limited though and Cu would accumulate in the aquifer over the long-term. If the surrounding groundwater has lower pH values, the creation of a larger buffer zone and recovery volumes less than injected volumes would drastically reduce the impact of the original groundwater. Nevertheless, a breakthrough of low pH groundwater in zones of higher transmissivity could result in a surge of desorbed Cu in the recovered water, which could be many times higher than injected concentrations depending on the sorption capacity of the aquifer. Hence, special attention should be paid to recovered Cu values in low pH groundwater ASR settings. In these settings, continuous monitoring of pH would be recommendable, as pH would be a good surrogate indicator for elevated metal concentrations. If we assume a mean injected stormwater concentration of about 15 µg/L (see Table III-5) and assume that Cu is largely retained in the sediment, Cu concentrations in recovered water would be well below drinking water guidelines of 2 mg/L (NHMRC, 2004) and irrigation water values of 0.2 mg/L (ANZECC and ARMCANZ, 2000). Use would only be compromised by low pH release of previously accumulated Cu. As freshwater ecosystem guidelines are set as low as 1.4 µg/L (ANZECC and ARMCANZ, 2000), recovered water would most likely be still not fit for environmental flows, especially in the later years of operation of the ASR scheme, when the sorption capacity has been exceeded.

Scenario B: elevated amounts of injected organic carbon

As discussed above injected organic carbon can be mobile or immobile in the subsurface. The formation of mobile Cu-ligand complexes would increase Cu solubility and transport, spreading Cu faster throughout the freshwater zone than in the previous scenario and would result in higher recovery of Cu. However, significant portions of the previously mobile organic complexes would presumably be deposited with an increase of ionic strength during recovery, and hence increase Cu accumulation throughout the subsurface. The immobile

carbon would accumulate close to the injections well and fuel redox reactions. As not all organic carbon will be degraded quickly, retained amounts of organic carbon would significantly increase the sorption capacity of the aquifer allowing for a longer and higher accumulation of Cu. On the other hand release of Cu after storage phases would likely be increased due to the biochemical changes and dissolution and degradation of part of the immobile organic carbon during storage. Backflushed solutions and initially recovered volumes could therefore be unsuitable for reuse.

Scenario C: elevated amounts of colloids

Relevant concentrations of colloids could result from injected particles, be due to mobilisation of aquifer fines or be produced during mineral dissolution and precipitation. They have the potential to transport adsorbed metals that would usually be classified as immobile. In general, colloids will be transported along preferential flow path, e.g. zones of higher permeability, and will aggregate and be deposited once ionic strength reaches the critical limit at the outer edge of the freshwater zone. Over a number of ASR cycles this could lead to a localised accumulation of fines, potentially lowering permeability and leading to a localised higher metal concentration at the fringe of the storage zone. Overall this would lead to lower recovered metal concentrations.

For a first estimate on possible accumulated Cu concentrations a rough calculation could be as follows: With an injected Cu concentration of 15 µg/L it would add up to an injected amount of 15 kg of Cu per year and GL and amount to 300 kg/GL in a live span of 20 years. If we further assume a mean porosity of 0.33 an average Cu concentration of 67 mg/kg would result over 20 years. The experiments showed that even sediments consisting to >98 wt% of sand exhibited considerable sorption capacity with more than 200 mg/kg for Cu (see Figure V-7) and hence Cu concentrations could easily be accommodated within the sediment. Comparing the potentially accumulated concentration with the sediment quality guideline target value of 34 mg/kg (ANZECC and ARMCANZ, 2000) shows that the accumulation of Cu would be well above the threshold effect level. Similar calculations for an injected Zn concentration of 500 µg/L would result in 2200 mg/kg Zn compared to a sediment quality guideline value of 150 mg/kg. This would mean that more than 90% of Zn would have to be recovered to stay below the sediment target value, which could be achievable in low sorption capacity sediments.

Prospects for decommissioned ASR schemes

It is clear that ASR schemes would be decommissioned once they are no longer viable, e.g. due to clogging of the aquifer or decreasing volumes of stormwater available for injection. Once the injections have stopped the previous groundwater flow and original groundwater

conditions re-establish themselves over time. In the long term this would result in desorption of accumulated metals due to dilution effects. Desorption would be accelerated if groundwater was of low pH, which could result in an increased release of metals into groundwater fed surface water ecosystems, which would be potentially problematic. Desorption would be limited if groundwater was highly reducing and metals would be precipitated as sulfides.

Aquifer selection recommendations

The choice of the aquifer would be restricted by the available aquifer in the location of source and demand of water, and the storage capacity needed for the ASR scheme. From the point of view of this study, the recommendations for an aquifer selection are divided by the question: (a) Do metal concentrations in the recovered water need to be very low (e.g. use for environmental flows) or (b) would long term metal accumulation that might later pose a risk to downstream systems be of concern and hence recovery of injected metals would be preferred? In the first case high sorptive capacities are a bonus, while in the latter case low sorptive capacities are needed.

Accordingly, a local aquifer with limited recharge to surface water and adjacent aquifers would be the most suitable situation. In this case the aquifer could be used for water purification and high sorptive capacity would be appreciated to lower metal concentrations of the recovered water to a minimum. The accumulated metals in the aquifer would pose very limited risk to surrounding ecosystems. If on the other hand the aquifer is highly connected to other aquifers and discharges into adjacent surface waters, then low sorptive capacity and a high recovery efficiency of injected metals would be more appropriate. Given that irrigation and drinking water guidelines allow for much higher metal concentrations than are tolerated by freshwater organisms, high metal recovery would seem to be the most preferred option. It should be taken into account that the sorptive capacity of the aquifer will generally be increased with the injection of colloids and organic carbon as well.

Analysis of aquifer sediments before the implementation of an ASR scheme should include:

- fine clay, to assess potential mobilisation of colloids from the matrix
- organic carbon, which offers high amounts of specific sorption sites
- pyrite, which is generally an undesirable mineral due to release of arsenic and other trace metals
- cation exchange capacity and possibly specific sorption capacity to assess the accumulation potential of metals

The evaluation of sediment analysis should take into account that surface coatings consisting of oxides and organic matter do not contribute a great deal of mass but offer a large amount

of reactive surface area. Low values of Fe^{2+} in the native groundwater would also be favourable as this would prevent the precipitation of amorphous iron hydroxides, which would also increase the sorption potential.

Monitoring recommendations

If accumulation of metals in the aquifers constitutes a concern, the ASR project should regularly be monitoring metal concentrations of injected and recovered (including backflushed) waters to be able to calculate the retained amount of metals in the subsurface. Currently no ASR project has undertaken this mass balance for metals. As no stormwater ASR project in sandy aquifers has been established yet, field data to validate the current laboratory experiments would be desirable. Additionally, the monitoring of backflushed waters is of special importance as these would potentially contain the highest metal concentrations and should include analysis for As. These volumes should not be discharged into streams without the knowledge of metal concentrations and have to be disposed of correctly or treated before discharge. The continuous monitoring of pH would be highly recommended, as pH would be a good surrogate indicator for elevated metal concentrations. Low pH readings could then trigger additional sampling and analysis for metals before reuse.

Pretreatment recommendations

The remediation of aquifers from heavy metal contamination is a difficult and expensive task and it would therefore be advisable to limit the potential for metal accumulation in the aquifer regardless of the specific situation. Recommendations for pretreatment would therefore include the lowering of injected metal concentrations (including Al and Fe) as well as organic carbon and colloid concentrations, as the latter increase the retention potential of the aquifer. This kind of pretreatment would also be beneficial in other respects as the potential for biological and mechanical clogging would be reduced.

Pretreatment for metals could be achieved with biofiltration, exchangers or reactive filters, while organic matter and colloids would best be reduced via coagulation and precipitation (Kurniawan et al., 2006). While this kind of pretreatment would be desirable, the benefits have to be weighed against the disadvantages of use of chemicals, disposal of waste sludge and associated carbon emissions. Pretreatment with natural or recycled substances and low carbon imprint should be investigated. For particulates and organic carbon slow sand filtration or roughing filtration would be possible (Page et al., 2006). Metal removal could be achieved with oxide-coated sands (Sansalone, 1999; Genç-Fuhrman et al., 2007), biosorbens like tree fern (Ho, 2003), agricultural waste products like hulls (Marshall and Champagne, 1995) or wetlands (Walker and Hurl, 2002; Maine et al., 2007). The

assessment of the most appropriate pretreatment method is beyond the scope of this study though.

VII.3 Critical evaluation and outlook

This study combined a number of different laboratory methods and computer simulations to investigate the factors that would potentially influence the behaviour of injected Zn and Cu during stormwater ASR in sandy aquifers. While release of metals from geogenic minerals during ASR has attracted considerable attention, injected metals have previously been mainly overlooked. This could be attributed to the fact that fully monitored stormwater ASR sites are located in limestone areas where injected stormwater and recovered water metal concentrations are low. The interest in using stormwater ASR to augment the urban water supply has also dramatically increased during the last few years and new legislation and guidelines to incorporate this technique into the urban water cycle are underway, prompting further risk assessment.

Apart from addressing this new question concerning stormwater ASR, a number of other contributions were made:

- Stormwater analyses in Melbourne were extended to accommodate pH, major ions and TOC/DOC, which are parameters affecting metal speciation.
- Groundwater analyses in the Fyansford Formation-Brighton Group aquifer added water quality data to very limited exiting monitoring.
- A critical analysis of the solid-solution effect in batch and column tests was presented.
- A new design of column experiment to mimic an ASR cycle was able to show different processes occurring during injection, storage and recovery. Especially the reversal in flow has not been practiced in many column experiments, but is central to ASR.
- The column tests extended over a large number of pore volumes and used low flow velocities, which is crucial in assessing long-term behaviour.
- This study used actual stormwater and groundwater thereby including interactions between solution components.
- PHT3D was tested with the new feature of surface complexation.
- PHT3D was enlarged to incorporate organic complexation.

Obviously, this study was not without weaknesses and hindsight revelations. In general, a higher number of replicates for batch and column experiments would be needed to get a statistically rigorous result, but the duplicate column results showed a reasonable agreement.

It would also have been desirable to conduct more and longer column experiments, so only one parameter would have been varied at a time rather than a combination of parameters and Cu breakthrough could have been completed, but the number of samples that can be analysed in one study will always be limited by funding and time constraints. It was also unfortunate that the ICP-OES analysis was not undertaken on campus, so samples had to be collected and were analysed after the experiments. This resulted in the first column experiment being less useful due to the unknowingly extremely low metal concentrations in the stormwater. The improvements that could have been undertaken during the geochemical modelling have been discussed in detail (see VI.6.3) and could be the aim of another PhD study.

Judging from the column experiments, batch experiments could be improved by a prolonged pre-washing of the sediments and by increasing the metal concentration range to match metal loads to facilitate the comparison between these two techniques. The use of in-line EC meters with a higher volume than the porevolume should also be avoided in further column experiments as the induced mixing significantly increases measurement uncertainty. The use of dried sediment samples should also be discouraged as this significantly changes the redox status of minerals, the microbial community and organic matter (Schulte, 1995; Kaiser et al., 2001).

Further study regarding the long term effect of stormwater ASR in sandy aquifer would be welcomed and should include field investigations, which were anticipated for this study but did not eventuate. Investigations into sustainable and cost effective ways of stormwater pretreatment for a range of parameters would be of highest priority. Further evaluation of the effects of colloidal transport and the various reactions and interactions of organic matter should be carried out and incorporated into PHT3D, so it could be used as a valuable predictive tool for risk assessment.

The final verdict from this study would be that water recycling and reuse is a necessity in the current situation of many cities in the world with dwindling surface and groundwater resources and stormwater ASR is a valuable tool in fulfilling this task. Additional pretreatment that might be necessary to bring recycled water up to acceptable standards for humans should in reality be undertaken anyway to meet acceptable standards for other organisms before these waters are discarded into waterways.

Bibliography

Agbenin, J.O. and Felix-Henningsen, P., 2004. Dynamics of copper fractions and solubility in a savanna soil under continuous cultivation. Nutrient Cycling in Agroecosystems 68 (2), 117-125.

Agbenin, J.O. and Olojo, L.A., 2004. Competitive adsorption of copper and zinc by a Bt horizon of a savanna Alfisol as affected by pH and selective removal of hydrous oxides and organic matter. Geoderma 119 (1-2), 85-95.

AGT (Australian Groundwater Technologies), CSIRO Land and Water, Sinclair Knight Merz (SKM) and United Water International, 2002. Assessment of the potential of reclaimed water ASR in metropolitan Melbourne. 2002/12, Australian Groundwater Technologies, Adelaide.

Ahnstrom, Z.S. and Parker, D.R., 1999. Development and Assessment of a Sequential Extraction Procedure for the Fractionation of Soil Cadmium. Soil Sci. Soc. Am. J. 63 (6), 1650-1658.

Ahyerre, M., Chebbo, G., Tassin, B. and Gaume, E., 1998. Storm water quality modelling, an ambitious objective? Water Sci. Technol. 37 (1), 205-213.

Ainsworth, C.C., Gassman, P.L., Pilon, J.L. and van der Sluys, W.G., 1994. Cobalt, cadmium, and lead sorption to hydrous iron oxide: Residence time effect. Soil Sci. Soc. Am. J. 58 (6), 1615-1623.

Akagi, J., Zsolnay, A. and Bastida, F., 2007. Quantity and spectroscopic properties of soil dissolved organic matter (DOM) as a function of soil sample treatments: Air-drying and pre-incubation. Chemosphere 69 (7), 1040-1046.

Akratanakul, S., Boersma, L. and Klock, G.O., 1983. Sorption Processes in Soils as Influenced by Pore Water Velocity: 2. Experimental Result. Soil Sci. 135 (6), 331-341.

Ali, M.A. and Dzombak, D.A., 1996. Interactions of copper, organic acids, and sulfate in goethite suspensions. Geochim. Cosmochim. Ac. 60 (24), 5045-5053.

Allison, J.D., Brown, D.S. and Novo-Gradac, K.J., 1990. MINTEQA2/PRODEFA2, a geochemical assessment model for environmental systems: version 3.0 user's manual, Report EPA/600/3-91/021. United States Environmental Protection Agency. Athens, Georgia, USA.

Alloway, B.J., 1990. Heavy metals in soils. Halsted Press, Glasgow, New York.

Almulla, A., Hamad, A. and Gadalla, M., 2005. Aquifer storage and recovery (ASR): A strategic cost-effective facility to balance water production and demand for Sharjah. Desalination 174 (2), 193-204.

Amirbahman, A., Kent, D.B., Curtis, G.P. and Davis, J.A., 2006. Kinetics of sorption and abiotic oxidation of arsenic(III) by aquifer materials. Geochim. Cosmochim. Ac. 70 (3), 533-547.

Amirbahman, A. and Olson, T.M., 1995. The role of surface conformations in the deposition kinetics of humic matter-coated colloids in porous media. Colloids Surf., A 95 (2-3), 249-259.

Anderson, D.M., Gilbert, P.M. and Burkholder, J.M., 2002. Harmful Algal Blooms and Eutrophication: Nutrient Sources, Composition, and Consequences. Estuaries 25 (4b), 704-726.

Anderson, P.R. and Benjamin, M.M., 1990. Modeling adsorption in aluminum-iron binary oxide suspensions. Environ. Sci. Technol. 24 (10), 1586-1592.

Antoniadis, V., McKinley, J.D. and Zuhairi, W.Y.W., 2007. Single-element and competitive metal mobility measured with column infiltration and batch tests. J. Environ. Qual. 36 (1), 53-60.

ANZECC and ARMCANZ, 2000. Australian and New Zealand Guidelines for Fresh and Marine Water Quality - Volume 1: The Guidelines (Chapters 1-7). 4, Australian and New Zealand Environment and Conservation Council (ANZECC); Agriculture and Resource Management Council of Australia and New Zealand (ARMCANZ), Canberra.

APHA, 1998. Standard methods for the examination of water and wastewater. Standard methods. American Public Health Association, American Water Works Association and Water Pollution Control Federation, (APHA-AWWA-WPCF), Washington, D.C.

Appelo, C.A.J., 1994. Some Calculations on Multicomponent Transport with Cation Exchange in Aquifers. Ground Water 32 (6), 968-975.

Appelo, C.A.J., Hendriks, J.A. and van Veldhuizen, M., 1993. Flushing factors and a sharp front solution for solute transport with multicomponent ion exchange. J. Hydrol. 146, 89-113.

Appelo, C.A.J. and Postma, D., 1999b. A consistent model for surface complexation on birnessite (-MnO2) and its application to a column experiment. Geochim. Cosmochim. Ac. 63 (19-20), 3039-3048.

Appelo, C.A.J. and Postma, D., 1999a. Geochemistry, groundwater and pollution. Balkema, Rotterdam.

Appelo, C.A.J., Willemsen, A., Beekman, H.E. and Griffioen, J., 1990. Geochemical calculations and observations on salt water intrusions. II. Validation of a geochemical model with laboratory experiments. J. Hydrol. 120 (1-4), 225-250.

Arias, M., Perez-Novo, C., Lopez, E. and Soto, B., 2006. Competitive adsorption and desorption of copper and zinc in acid soils. Geoderma 133 (3-4), 151-159.

Arias, M., Perez-Novo, C., Osorio, F., Lopez, E. and Soto, B., 2005. Adsorption and desorption of copper and zinc in the surface layer of acid soils. J. Colloid Interface Sci. 288 (1), 21-29.

Arnaut, L.G., Formosinho, S.J. and Burrows, H., 2006. Chemical kinetics : from molecular structure to chemical reactivity. Elsevier, Amsterdam; Oxford.

Arthur, J.D., Dabous, A.A. and Cowart, J.B., 2002. Mobilization of arsenic and other trace elements during aquifer storage and recovery, Southwest Florida. In: G.R. Aiken and E.L. Kuniansky (Eds.), U.S. Geological Survey Artificial Recharge Workshop April 2-4. USGS Open-File Report 02-89, Sacramento, California, pp. 47-50.

Asano, T. (Ed.), 1985. Artificial recharge to groundwater. Butterworth, Boston.

ASCE, 2001. Standard Guidelines for Artificial Recharge, EWRI/ASCE 34-01, American Society of Civil Engineers (ASCE), New York.

ASTM, 1968. D 2434: Standard Test Method for Permeability of Granular Soils (Constant Head). American Society for Testing and Materials

ASTM, 2001. D 4316 - 93 (2001) Standard test method for distribution ratios by the short-term batch method. American Society for Testing and Materials (ASTM).

Aualiitia, T.U. and Pickering, W.F., 1988. Sediment analysis--lability of selectively extracted fractions. Talanta 35 (7), 559-566.

Avena, M.J. and Koopal, L.K., 1998. Desorption of Humic Acids from an Iron Oxide Surface. Environ. Sci. Technol. 32 (17), 2572-2577.

Backhus, D.A., Ryan, J.N., Groher, D.M., MacFarlane, J.K. and Gschwend, P.M., 1993. Sampling Colloids and Colloid-Associated Contaminants in Ground Water. Ground Water 31 (3), 466-479.

Baeyens, B. and Bradbury, M.H., 1997. A mechanistic description of Ni and Zn sorption on Na-montmorillonite Part I: Titration and sorption measurements. J. Contam. Hydrol. 27 (3-4), 199-222.

Bahr, J., Grundl, T., Harrington, G., Krohelski, J. and Werner, M., 2002. A Review of Aquifer Storage Recovery Techniques, Wisconsin Department of Natural Resources.

Bahr, J.M. and Rubin, J., 1987. Direct Comparison of Kinetic and Local Equilibrium Formulations for Solute Transport Affected by Surface Reactions. Water Resour. Res. 23 (3), 438-452.

Bajracharya, K., Tran, Y.T. and Barry, D.A., 1996. Cadmium adsorption at different pore water velocities. Geoderma 73 (3-4), 197-216.

Baker, M.A., Valett, H.M. and Dahm, C.N., 2000. Organic carbon supply and metabolism in a shallow groundwater ecosystem. Ecology 81 (11), 3133-3148.

Ball, J.W. and Nordstrom, D.K., 1991. User's manual for WATEQ4F, with revised thermodynamic data base and test cases for calculating speciation of major, trace and redox elements in natural waters, U.S. Geol. Surv. Open-File Report 91-183.

Barbosa, A.E. and Hvitved-Jacobsen, T., 1999. Highway runoff and potential for removal of heavy metals in an infiltration pond in Portugal. Sci. Total Environ. 235 (1-3), 151-159.

Barna, R., Fernandez, A. and Hlavackova, P., 2007. Assessment methodologies for copper and zinc mobility in a neutral synthetic soil: The influence of pH. Colloids Surf., A 306 (1-3), 56-67.

Barraud, S., Gautier, A., Bardin, J.P. and Riou, V., 1999. The impact of intentional stormwater infiltration on soil and groundwater. Water Sci. Technol. 39 (2), 185-192.

Barrodale, I. and Roberts, F.D.K., 1980. Algorithm 552: Solution of the Constrained l_1 Linear Approximation Problem [F4]. ACM Trans. Math. Softw. 6 (2), 231-235.

Barrow, N.J., 1986a. Testing a mechanistic model. II. The effects of time and temperature on the reaction of zinc with a soil. J. Soil Sci. 37, 277-286.

Barrow, N.J., 1986b. Testing a mechanistic model. VI. Describing the effects of pH on Zinc retention by soils. J. Soil Sci. 37, 295-302.

Barrow, N.J., Bowden, J.W., Posner, A.M. and Quirk, J.P., 1981. Describing the Adsorption of Copper, Zinc and Lead on a Variable Charge Mineral Surface. Aust. J. Soil Res. 19, 309-321.

Barry, D.A., Bajracharya, K., Crapper, M., Prommer, H. and Cunningham, C.J., 2000. Comparison of split-operator methods for solving coupled chemical non-equilibrium reaction/groundwater transport models. Mathematics and Computers in Simulation 53 (1-2), 113-127.

Barry, D.A., Prommer, H., Miller, C.T., Engesgaard, P., Brun, A. and Zheng, C., 2002. Modelling the fate of oxidisable organic contaminants in groundwater. Adv. Water Res. 25 (8-12), 945-983.

Barry, K., Pavelic, P., Dillon, P., Rattray, K., Dennis, K. and Gerges, N., 2002. Aquifer storage and recovery of stormwater Andrew Farm, South Australia: compilation of data from the 1993-98 trial. 17/02, CSIRO Land and Water, Adelaide.

Bartlett, R. and James, B., 1980. Studying dried, stored soil samples-some pitfalls. Soil Sci. Soc. Am. J. 44, 721-724.

Bauer, M. and Blodau, C., 2006. Mobilization of arsenic by dissolved organic matter from iron oxides, soils and sediments. Sci. Total Environ. 354 (2-3), 179-190.

Baumann, T., Fruhstorfer, P. and Nießner, R., 1998. Sickerwassertransport von Kolloiden und Schwermetallen in Bergbaufolgelandschaften – Felduntersuchungen und Laborversuche. Grundwasser 1, 3-13.

Baun, D.L. and Christensen, T.H., 2004. Speciation of Heavy Metals in Landfill Leachate: A Review. Waste Manage. Res. 22 (1), 3-23.

Béchet, B., Durin, B. and Legret, M., 2004. Mobilisation of solute and colloidal heavy metals from a retention pond sediment. In: M. Desbordes and B. Chocat (Eds.), Novatech 2004: 5th International Conference on Sustainable techniques and strategies in urban water management, Lyon, France, pp. 1277-1284.

Béchet, B., Durin, B., Legret, M. and Le Cloirec, P., 2006. Colloidal speciation of heavy metals in runoff and interstitial waters of a retention/infiltration pond. Water Sci. Technol. 54 (6-7), 307-314.

Beckett, P.H.T., 1989. The use of extractants in studies on trace metals in soils, sewage sludges, and sludge-treated soils. Adv. Soil Sci. 9, 143-176.

Beckett, R. and Le, N.P., 1990. The role or organic matter and ionic composition in determining the surface charge of suspended particles in natural waters. Colloids Surf. 44, 35-49.

Beckie, R., 1996. Measurement Scale, Network Sampling Scale, and Groundwater Model Parameters. Water Resour. Res. 32 (1), 65-76.

Beddek, R., ElMahdi, A., Barnett, B. and Kennedy, T., 2005. Integration of Groundwater Models within an Economical Decision Support System Framework. In: A. Zerger and R.M. Argent (Eds.), MODSIM 2005 International Congress on Modelling and Simulation, Modelling and Simulation Society of Australia and New Zealand, December 2005, pp. 608-614.

Beekman, H.E., Anthony, C. and Appelo, J., 1990. Ion chromatography of fresh- and salt-water displacement: Laboratory experiments and multicomponent transport modelling. J. Contam. Hydrol. 7 (1-2), 21-37.

Benedetti, M.F., Milne, C.J., Kinniburgh, D.G., van Riemsdijk, W.H. and Koopal, L.K., 1995. Metal Ion Binding to Humic Substances: Application of the Non-Ideal Competitive Adsorption Model. Environ. Sci. Technol. 29 (2), 446-457.

Benedetti, M.F., van Riemsdijk, W.H., Koopal, L.K., Kinniburgh, D.G., Gooddy, D.C. and Milne, C.J., 1996. Metal ion binding by natural organic matter: From the model to the field. Geochim. Cosmochim. Ac. 60 (14), 2503-2513.

Benjamin, M.M. and Leckie, J.O., 1981b. Conceptual Model for Metal-Ligand-Surface Interactions during Adsorption. Environ. Sci. Technol. 15 (9), 1050-1057.

Benjamin, M.M. and Leckie, J.O., 1981a. Multiple-site adsorption of Cd, Cu, Zn, and Pb on amorphous iron oxyhydroxide. J. Colloid Interface Sci. 79 (1), 209-221.

Benyahya, L. and Garnier, J.M., 1999. Effect of Salicylic Acid upon Trace-Metal Sorption (CdII, ZnII, CoII, and MnII) onto Alumina, Silica, and Kaolinite as a Function of pH. Environ. Sci. Technol. 33 (9), 1398-1407.

Bertrand-Krajewski, J.-L. and Bradin, J.P., 2002. Uncertainties and representativity of measurements in stormwater storage tanks. In: E.W. Strecker and W.C. Huber (Eds.), 9th International Conference on Urban Drainage. American Society of Civil Engineers, Portland, Oregon, USA, pp. 16.

Bethke, C.M. and Brady, P.V., 2000. How the Kd Approach Undermines Ground Water Cleanup. Ground Water 38 (3), 435-443.

Bjerg, P.L., Ammentorp, H.C. and Christensen, T.H., 1993. Model simulations of a field experiment on cation exchange-affected multicomponent solute transport in a sandy aquifer. J. Contam. Hydrol. 12 (4), 291-311.

Boethling, R.S., Howard, P.H., Meylan, W., Stiteler, W., Beauman, J. and Tirado, N., 1994. Group contribution method for predicting probability and rate of aerobic biodegradation. Environ. Sci. Technol. 28 (3), 459-465.

Boethling, R.S. and Mackay, D., 2000. Handbook of property estimation methods for environmental chemicals environmental and health sciences. Lewis Publishers, Boca Raton.

Bolton, E.W., Lasaga, A.C. and Rye, D.M., 1999. Long-term flow/chemistry feedback in a porous medium with heterogenous permeability; kinetic control of dissolution and precipitation. Am. J. Sci. 299 (1), 1-68.

BOM, 2008. Climate Data online, Bureau of Meteorology (BOM), Australia.
Borkovec, M., Bürgisser, C.S., Černík, M., Glättli, U. and Sticher, H., 1996. Quantitative Description of Multi-Component Reactive Transport in Porous Media: An Empirical Approach. Transport in Porous Media 25, 193-204.
Borkovec, M. and Westall, J., 1983. Solution of the Poisson-Boltzmann equation for surface excesses of ions in the diffuse layer at the oxide-electrolyte interface. J. Electroanal. Chem. 150 (1-2), 325-337.
Bouchard, D.C., Wood, A.L., Campbell, M.L., Nkedi-Kizza, P. and Rao, P.S.C., 1988. Sorption nonequilibrium during solute transport. J. Contam. Hydrol. 2 (3), 209-223.
Bourg, A.C.M. and Bertin, C., 1993. Biogeochemical processes during the infiltration of river water into an alluvial aquifer. Environ. Sci. Technol. 27 (4), 661-666.
Bouwer, E.J., McCarty, P.L., Bouwer, H. and Rice, R.C., 1984. Organic contaminant behavior during rapid infiltration of secondary wastewater at the Phoenix 23rd avenue project. Water Res. 18 (4), 463-472.
Bouwer, H., 1996. Issues in artificial recharge. Water Sci. Technol. 33 (10-11), 381-390.
Bouwer, H., 2002. Artificial recharge of groundwater: hydrogeology and engineering. Hydrogeol. J. 10 (1), 121-142.
Bower, C.A. and Gschwend, F.B., 1952. Ethylene glycol retention by soils as a measure of surface area and interlayer swelling. Soil Sci. Soc. Am. J. 16, 342-345.
Boyle, D.P., Gupta, H.V. and Sorooshian, S., 2000. Toward Improved Calibration of Hydrologic Models: Combining the Strengths of Manual and Automatic Methods. Water Resour. Res. 36 (12), 3663-3674.
Bradl, H.B., 2004. Adsorption of heavy metal ions on soils and soils constituents. J. Colloid Interface Sci. 277 (1), 1-18.
Braskerud, B.C., Lundekvam, H. and Krogstad, T., 2000. The impact of hydraulic load and aggregation on sedimentation of soil particles in small constructed wetlands. J. Environ. Qual. 29 (6), 2013-2020.
Brendler, V., Richter, J., Nebelung, C. and Vahle, A., 2004. Development of a Mineral-Specific Sorption Database for Surface Complexation Modeling. Part I: Final Report. Project PtWt+E 02E9471, Dresden.
Brigante, M., Zanini, G. and Avena, M., 2008. On the dissolution kinetics of humic acid particles. Effect of monocarboxylic acids. Chemosphere 71 (11), 2076-2081.
Brown, C.J., Hatfield, K. and Newman, M., 2006. Lessons learned from a review of 50 ASR projects from the United States, England, Australia, India, and Africa, Increasing Freshwater Supplies, Proceedings of the 2006 UCOWR/NIWR Annual Conference, Santa Fe, New Mexico, USA July 18-20, 2006.
Brümmer, G., Tiller, K.G., Herms, U. and Clayton, P.M., 1983. Adsorption-desorption and/or precipitation-dissolution processes of zinc in soils. Geoderma 31 (4), 337-354.
Brümmer, G.W., Gerth, J. and Herms, U., 1986. Heavy Metal Species, Mobility and Availability in Soils. J. Plant Nutr. Soil Sci. 149, 382-398.
Brun, A., Christensen, F.D. and Christiansen, J.S., 1998. Water quality modelling at the Langerak deep-well recharge site. In: J.H. Peters and et al. (Eds.), Artificial Recharge of Groundwater; Proceedings of the Third International Symposium on Artificial Recharge of Groundwater - Tisar 98. Balkema, Amsterdam, Netherlands, pp. 305-310.
Brun, A. and Engesgaard, P., 2002. Modelling of transport and biogeochemical processes in pollution plumes: literature review and model development. J. Hydrol. 256 (3-4), 211-227.
Brun, A., Engesgaard, P., Christensen, T.H. and Rosbjerg, D., 2002. Modelling of transport and biogeochemical processes in pollution plumes: Vejen landfill, Denmark. J. Hydrol. 256 (3-4), 228-247.
Brusseau, M.L., 1995. The effect of nonlinear sorption on transformation of contaminants during transport in porous media. J. Contam. Hydrol. 17 (4), 277-291.
Brusseau, M.L., Hu, Q. and Srivastava, R., 1997. Using flow interruption to identify factors causing nonideal contaminant transport. J. Contam. Hydrol. 24 (3-4), 205-219.
Brusseau, M.L. and Rao, P.S.C., 1989. The influence of sorbate-organic matter interactions on sorption nonequilibrium. Chemosphere 18 (9-10), 1691-1706.
Brusseau, M.L., Rao, P.S.C., Jessup, R.E. and Davidson, J.M., 1989. Flow interruption: A method for investigating sorption nonequilibrium. J. Contam. Hydrol. 4 (3), 223-240.
Bucheli, T.D., Müller, S.R., Herbele, S. and Schwarzenbach, R.P., 1998. Occurrence and behaviour of pesticides in rainwater, roof runoff, and artificial stormwater infiltration. Environ. Sci. Technol. 32 (22), 3457-3464.

Buchter, B., Davidoff, B., Amacher, M.C., Hinz, C., Iskandar, I.K. and Selim, H.M., 1989. Correlation of Freundlich Kd and n Retention Parameters with Soils and Elements. Soil Sci. 148 (5), 370-379.

Buddemeier, R.W. and Hunt, J.R., 1988. Transport of colloidal contaminants in groundwater: radionuclide migration at the Nevada test site. Appl. Geochem. 3 (5), 535-548.

Buerge-Weirich, D., Behra, P. and Sigg, L., 2003. Adsorption of Copper, Nickel, and Cadmium on Goethite in the Presence of Organic Ligands. Aquat. Geochem. 9 (2), 65-85.

Buffle, J., Altmann, R.S., Filella, M. and Tessier, A., 1990. Complexation by natural heterogeneous compounds: Site occupation distribution functions, a normalized description of metal complexation. Geochim. Cosmochim. Ac. 54 (6), 1535-1553.

Buffle, J. and Leppard, G.G., 1995a. Characterization of Aquatic Colloids and Macromolecules. 1. Structure and Behavior of Colloidal Material. Environ. Sci. Technol. 29 (9), 2169-2175.

Buffle, J. and Leppard, G.G., 1995b. Characterization of Aquatic Colloids and Macromolecules. 2. Key Role of Physical Structures on Analytical Results. Environ. Sci. Technol. 29 (9), 2176-2184.

Buffle, J., Zhang, Z. and Startchev, K., 2007. Metal Flux and Dynamic Speciation at (Bio)interfaces. Part I: Critical Evaluation and Compilation of Physicochemical Parameters for Complexes with Simple Ligands and Fulvic/Humic Substances. Environ. Sci. Technol. 41 (22), 7609-7620.

Bunn, R.A., Magelky, R.D., Ryan, J.N. and Elimelech, M., 2002. Mobilization of Natural Colloids from an Iron Oxide-Coated Sand Aquifer: Effect of pH and Ionic Strength. Environ. Sci. Technol. 36 (3), 314-322.

Bürgisser, C.S., Cerník, M., Borkovec, M. and Sticher, H., 1993. Determination of Nonlinear Adsorption Isotherms from Column Experiments: An Alternative to Batch Studies. Environ. Sci. Technol. 27 (5), 943-948.

Butler, T.W., 2006. Geochemical and biological controls on trace metal transport in an acid mine impacted watershed. Environ. Geochem. Health 28 (3), 231-241.

Cabaniss, S.E., Maurice, P.A. and Madey, G., 2007. A stochastic model for the synthesis and degradation of natural organic matter. Part III: Modeling Cu(II) complexation. Appl. Geochem. 22 (8), 1646-1658.

Cabaniss, S.E. and Shuman, M.S., 1988a. Copper binding by dissolved organic matter: I. Suwannee River fulvic acid equilibria. Geochim. Cosmochim. Ac. 52 (1), 185-193.

Cabaniss, S.E. and Shuman, M.S., 1988b. Copper binding by dissolved organic matter: II. Variation in type and source of organic matter. Geochim. Cosmochim. Ac. 52 (1), 195-200.

Calmano, W., Hong, J. and Förstner, U., 1993. Binding and mobilization of heavy metals in contaminated sediments affected by pH and redox potential. Water Sci. Technol. 28 (8-9), 223-235.

Cances, B., Ponthieu, M., Castrec-Rouelle, M., Aubry, E. and Benedetti, M.F., 2003. Metal ions speciation in a soil and its solution: experimental data and model results. Geoderma 113 (3-4), 341.

Cappuyns, V. and Swennen, R., 2005. Kinetics of element release during combined oxidation and pHstat leaching of anoxic river sediments. Appl. Geochem. 20 (6), 1169-1179.

Carbonaro, R.F. and Di Toro, D.M., 2007. Linear free energy relationships for metal-ligand complexation: Monodentate binding to negatively-charged oxygen donor atoms. Geochim. Cosmochim. Ac. 71 (16), 3958-3968.

Carrera, J., 1993. An overview of uncertainties in modelling groundwater solute transport. J. Contam. Hydrol. 13 (1-4), 23-48.

Carrera, J., Alcolea, A., Medina, A., Hidalgo, J. and Slooten, L.J., 2005. Inverse problem in hydrogeology. Hydrogeol. J. 13 (1), 206-222.

Cash, J.R. and Karp, A.H., 1990. A variable order Runge-Kutta method for initial value problems with rapidly varying right-hand sides. ACM Trans. Math. Softw. 16 (3), 201-222.

Cavallaro, N. and McBride, M.B., 1984. Zinc and copper Sorption and Fixation by an Acid Soil Clay: Effect of Selective Dissolutions. Soil Sci. Soc. Am. J. 48 (5), 1050-1054.

Černík, M., Barmettler, K., Grolimund, D., Rohr, W., Borkovec, M. and Sticher, H., 1994. Cation transport in natural porous media on laboratory scale: multicomponent effects. J. Contam. Hydrol. 16 (4), 319-337.

Champ, D.R., Gulens, J. and Jackson, R.E., 1979. Oxidation-reduction sequences in ground water flow systems. Can. J. Earth Sci. 16, 12-23.

Chapelle, F.H. and Lovley, D.R., 1992. Competitive-exclusion of sulfate reduction by Fe(III)-reducing bacteria - a mechanism for producing discrete zones of high-iron ground-water. Ground Water 30 (1), 29-36.

Chapelle, F.H., McMahon, P.B., Dubrovsky, N.M., Fujii, R.F., Oaksford, E.T. and Vroblesky, D.A., 1995. Deducing the distribution of terminal electron-accepting processes in hydrologically diverse groundwater systems. Water Resour. Res. 31 (2), 359-371.

Characklis, G.W., Dilts, M.J., Simmons Iii, O.D., Likirdopulos, C.A., Krometis, L.-A.H. and Sobsey, M.D., 2005. Microbial partitioning to settleable particles in stormwater. Water Res. 39 (9), 1773-1782.

Charlatchka, R. and Cambier, P., 2000. Influence of reducing conditions on solubility of trace metals in contaminated soils. Water Air Soil Pollut. 118, 143-167.

Cheremisinoff, N.P., 2002. Handbook of water and wastewater treatment technologies. Butterworth-Heinemann, Boston.

Chernick, M.R., 2007. Bootstrap Methods : A Guide for Practitioners and Researchers. John Wiley & Sons.

Chiang, W.H. and Kinzelbach, W., 2001. 3D-Groundwater modeling with PMWIN. Springer Berlin, Heidelberg, New York.

Chiang, W.-H. and Kinzelbach, W., 2005. 3D-groundwater modeling with PMWIN : a simulation system for modeling groundwater flow and transport processes. Springer, Berlin, New York.

Chiou, C.T., Lee, J.F. and Boyd, S.A., 1990. The surface area of soil organic matter. Environ. Sci. Technol. 24 (8), 1164-1166.

Christensen, J.B., Botma, J.J. and Christensen, T.H., 1999. Complexation of Cu and Pb by DOC in polluted groundwater: a comparison of experimental data and predictions by computer speciation models (WHAM and MINTEQA2). Water Res. 33 (15), 3231-3238.

Christensen, J.B. and Christensen, T.H., 2000. The effect of pH on the complexation of Cd, Ni and Zn by dissolved organic carbon from leachate-polluted groundwater. Water Res. 34 (15), 3743-3754.

Christensen, J.B., Jensen, D.L. and Christensen, T.H., 1996. Effect of dissolved organic carbon on the mobility of cadmium, nickel and zinc in leachate polluted groundwater. Water Res. 30 (12), 3037-3049.

Christensen, J.B., Tipping, E., Kinniburgh, D.G., Gron, C. and Christensen, T.H., 1998. Proton Binding by Groundwater Fulvic Acids of Different Age, Origins, and Structure Modeled with the Model V and NICA-Donnan Model. Environ. Sci. Technol. 32 (21), 3346-3355.

Christl, I. and Kretzschmar, R., 2001. Interaction of copper and fulvic acid at the hematite-water interface. Geochim. Cosmochim. Ac. 65 (20), 3435-3442.

Christl, I., Milne, C.J., Kinniburgh, D.G. and Kretzschmar, R., 2001. Relating Ion Binding by Fulvic and Humic Acids to Chemical Composition and Molecular Size. 2. Metal Binding. Environ. Sci. Technol. 35 (12), 2512-2517.

Chuan, M.C., Shu, G.Y. and Liu, J.C., 1996. Solubility of heavy metals in a contaminated soil: effects of redox potential and pH. Water Air Soil Pollut. 90, 543-556.

Cohen, S.D. and Hindmarsh, A.C., 1996. CVODE, as stiff/nonstiff ODE solver in C. Computers in Physics 10 (2), 138-143.

Cole, R.H., Frederick, R.E., Healy, R.P. and Rolan, R.G., 1984. Preliminary findings of the Priority Pollutant Monitoring Project of the Nationwide Urban Runoff Program. Journal Water Pollut. Control Fed. 56 (7), 898-908.

Contin, M., Mondini, C., Leita, L. and Nobili, M.D., 2007. Enhanced soil toxic metal fixation in iron (hydr)oxides by redox cycles. Geoderma 140 (1-2), 164-175.

Coombes, P. and Kuczera, G., 2001. BDP environment design guide: Strategic use of stormwater, Department of Civil, Surveying and Environmental Engineering, Newcastle.

Coombes, P.J., Argue, J.R. and Kuczera, G., 2000. Figtree Place: a case study in water sensitive urban development (WSUD). Urban Water 1 (4), 335-343.

Cornell, R.M. and Schwertmann, U., 1996. The Iron Oxides. VCH Publishers, Weinheim.

Covelo, E.F., Vega, F.A. and Andrade, M.L., 2007. Competitive sorption and desorption of heavy metals by individual soil components. J. Hazard. Mater. 140 (1-2), 308-315.

Cowan, C.E., Zachara, J.M., Smith, S.C. and Resch, C.T., 1992. Individual Sorbent Contributions to Cadmium Sorption on Ultisols of Mixed Mineralogy. Soil Sci. Soc. Am. J. 56 (4), 1084-1094.

Crawford, M.B., 1996. PHREEQEV: The incorporation of a version of Model V for organic complexation in aqueous solutions into the speciation code phreeqe. Computers and Geosciences 22 (2), 109-116.

CSIRO and BOM, 2008. Climate change in Australia. CSIRO and Bureau of Meteorology http://www.climatechangeinaustralia.gov.au

Csuros, M., 1994. Environmental sampling and analysis for technicians. Lewis Publishers, Boca Raton.

Cullen, W.R. and Reimer, K.J., 1989. Arsenic speciation in the environment. Chem. Rev. 89 (4), 713-764.

Dagan, G., 1989. Flow and transport in porous formations. Springer-Verlag, Berlin, New York.

Dalang, F., Buffle, J. and Haerdl, W., 1984. Study of the Influence of Fulvic Substances on the Adsorption of Copper(II) Ions at the Kaolinite Surface. Environ. Sci. Technol. 18 (3), 135-141.

Datry, T., Malard, F. and Gibert, J., 2004. Dynamics of solutes and dissolved oxygen in shallow urban groundwater below a stormwater infiltration basin. Sci. Total Environ. 329 (1-3), 215-229.

Davidson, C.M., Ferreira, P.C.S. and Ure, A.M., 1999. Some sources of variability in application of the three-stage sequential extraction procedure recommended by BCR to industrially-contaminated soil. Fresenius J. Anal. Chem. 363 (5), 446-451.

Davies-Colley, R.J., Nelson, P.O. and Williamson, K.J., 1984. Copper and cadmium uptake by estuarine sedimentary phases. Environ. Sci. Technol. 18 (7), 491-499.

Davis, A.C., Patterson, B.M., Grassi, M.E., Robertson, B.S., Prommer, H. and McKinley, A.J., 2007. Effects of Increasing Acidity on Metal(loid) Bioprecipitation in Groundwater: Column Studies. Environ. Sci. Technol. 41 (20), 7131-7137.

Davis, A.P., Shokouhian, M. and Ni, S., 2001b. Loading estimates of lead, copper, cadmium, and zinc in urban runoff from specific sources. Chemosphere 44 (5), 997-1009.

Davis, A.P., Shokouhian, M., Sharma, H. and Minami, C., 2001a. Laboratory Study of Biological Retention for Urban Stormwater Management. Water Environ. Res. 73 (5), 5-14.

Davis, J.A., 1982. Adsorption of natural dissolved organic matter at the oxide/water interface. Geochim. Cosmochim. Ac. 46 (11), 2381-2393.

Davis, J.A., 1984. Complexation of trace metals by adsorbed natural organic matter. Geochim. Cosmochim. Ac. 48 (4), 679-691.

Davis, J.A., Coston, J.A., Kent, D.B. and Fuller, C.C., 1998. Application of the Surface Complexation Concept to Complex Mineral Assemblages. Environ. Sci. Technol. 32 (19), 2820-2828.

Davis, J.A., Coston, J.A., Kent, D.B., Hess, K.M., Joye, J.L., Brienen, P. and Campo, K.W., 2001. Multispecies Reactive Tracer Test in a Sand and Gravel Aquifer, Cape Cod, Massachusetts. Part 2: Transport of Chromium (VI) and Lead-, Copper-, and Zinc-EDTA Tracers. EPA/600/R-01/007b, National Risk Management Research Laboratory, U.S. Environmental Protection Agency, Cincinnati.

Davis, J.A., James, R.O. and Leckie, J.O., 1978. Surface Ionization and Complexation at the Oxide/Water Interface. J. Colloid Interface Sci. 63 (3), 480-499.

Davis, J.A. and Kent, D.B., 1990. Surface complexation modelling in aqueous geochemistry. In: M.F. Hochella, A.F. White and G.M. Bancroft (Eds.), Mineral-water interface geochemistry. Reviews in mineralogy. Mineralogical Society of America, Washington, D.C., 177-260.

Davis, J.A. and Leckie, J.O., 1978. Effect of adsorbed complexing ligands on trace metal uptake by hydrous oxides. Environ. Sci. Technol. 12, 1309-1315.

Davranche, M. and Bollinger, J.-C., 2000. Release of Metals from Iron Oxyhydroxides under Reductive Conditions: Effect of Metal/Solid Interactions. J. Colloid Interface Sci. 232 (1), 165-173.

Davranche, M. and Bollinger, J.-C., 2001. A desorption-dissolution model for metal release from polluted soil under reductive conditions. J. Environ. Qual. 30 (5), 1581-1586.

Day, D.M., Hart, B.T., McKelvie, I.D. and Beckett, R., 1994. Adsorption of natural organic matter onto goethite. Colloids Surf., A 89, 1-13.

de Jonge, H., de Jonge, L.W. and Mittelmeijer-Hazeleger, M.C., 2000. The microporous structure of organic and mineral soil materials. Soil Sci. 165 (2), 99-108.

de Jonge, H. and Mittelmeijer-Hazeleger, M.C., 1996. Adsorption of CO2 and N2 on Soil Organic Matter: Nature of Porosity, Surface Area, and Diffusion Mechanisms. Environ. Sci. Technol. 30 (2), 408-413.

de Ruiter, H. and Stuyfzand, P.J., 1998. An experiment on well recharge of oxic water into an anoxic aquifer. In: J.H. Peters and et al. (Eds.), Artificial Recharge of Groundwater; Proceedings of the Third International Symposium on Artificial Recharge of Groundwater - Tisar 98. Balkema, Amsterdam, Netherlands, pp. 299-304.

Dechesne, M., Barraud, S. and Bardin, J.-P., 2004. Spatial distribution of pollution in an urban stormwater infiltration basin. J. Contam. Hydrol. I72 (1-4), 189-205.

Deletic, A. and Orr, D., 2005. Pollution Buildup on Road Surfaces. J. Environ. Eng. 131 (1), 49-59.

Delolme, C., Hebrard-Labit, C., Spadini, L. and Gaudet, J.-P., 2004. Experimental study and modeling of the transfer of zinc in a low reactive sand column in the presence of acetate. J. Contam. Hydrol. 70 (3-4), 205-224.

Dempsey, B.A., Tai, Y.L. and Harrison, S.G., 1993. Mobilization and removal of contaminants associated with urban dust and dirt. Water Sci. Technol. 28 (3-5), 225-230.

Department of Infrastructure, 2002. Melbourne 2030: Planning for sustainable growth, State of Victoria, Dept. of Infrastructure, Melbourne.

Deshmukh, A.P., Pacheco, C., Hay, M.B. and Myneni, S.C.B., 2007. Structural environments of carboxyl groups in natural organic molecules from terrestrial systems. part 2: 2D NMR spectroscopy. Geochim. Cosmochim. Ac. 71, 3533-3544.

Di Chio, D., Potenz, D. and Righetti, E., 1999. Degradation of organic substances in the soil: proposal for a mathematical model. Bioresour. Technol. 67 (3), 267-278.

Di Toro, D.M., Mahony, J.D., Kirchgraber, P.R., O'Byrne, A.L., Pasquale, L.R. and Piccirilli, D.C., 1986. Effects of Nonreversibility, Particle Concentration, and Ionic Strength on Heavy Metal Sorption. Environ. Sci. Technol. 20, 55-61.

Dijkstra, J.J., Meeussen, J.C.L. and Comans, R.N.J., 2004. Leaching of Heavy Metals from Contaminated Soils: An Experimental and Modeling Study. Environ. Sci. Technol. 38 (16), 4390-4395.

Dijkstra, J.J., van der Sloot, H.A. and Comans, R.N.J., 2002. Process identification and model development of contaminant transport in MSWI bottom ash. Waste Manage. 22 (5), 531-541.

Dillon, P., 2004. Draft code of practice for aquifer storage and recovery, Victorian Smart Water Fund.

Dillon, P., 2005. Future management of aquifer recharge. Hydrogeol. J. 13 (1), 313-316.

Dillon, P. and Ellis, D., 2004. Australian water conservation and reuse research program. Water 40 (1), 27-28.

Dillon, P. and Molloy, R., 2006. Technical Guidance for ASR CSIRO Land and Water Client Report.

Dillon, P., Page, D., Pavelic, P., Taylor, R., Laube, S., Cierpka, A., Barry, K., Levett, K., Vanderzalm, J. and Molloy, R., 2007. Commissioning of the ASR Trial at the Rossdale Golf Club, Smart Water Fund, Melbourne.

Dillon, P., Pavelic, P., Massmann, G., Barry, K. and Correll, R., 2001. Enhancement of the membrane filtration index (MFI) method for determining the clogging potential of turbid urban stormwater and reclaimed water used for aquifer storage and recovery. Desalination 140 (2), 153-165.

Dillon, P., Pavelic, P., Sibenaler, X., Gerges, N. and Clark, R., 1997. Aquifer storage and recovery of stormwater runoff. Water 24 (4), 7-11.

Dillon, P., Pavelic, P., Toze, S., Rinck-Pfeiffer, S., Martin, R., Knapton, A. and Pidsley, D., 2006. Role of aquifer storage in water reuse. Desalination 188 (1-3), 123-134.

Dillon, P., Toze, S., Pavelic, P., Skjemstad, J., Davis, G., Miller, R., Correll, R., Kookana, R., Ying, G.-G., Filderbrandt, S., Banning, N., Gordon, C., Wall, K., Nicholson, B., Vanderzalm, J., Le Gal La Salle, C., Giber, M., Ingrand, V., Guinamant, J.-L., Stuyfzand, P., Prommer, H., Greskowiak, J., Swift, R., Hayes, M., OcHara, G., Mee, B. and Johnson, I., 2005. Water quality improvements during aquifer storage and recovery, Vol. 1, Subsurface Processes for Water Quality Improvement, AWWARF.

Dillon, P.J., Hickinbotham, M.R. and Pavelic, P., 1994. Review of International Experience in Injecting Water into Aquifer for Storage and Reuse. In: Institution of Engineers Australia and International Association of Hydrogeologists (Eds.), Water down under 94: Adelaide, South Australia, 21-25 November 1994. Institution of Engineers Australia, Barton, A.C.T., pp. 13-19.

Dillon, P.J. and Pavelic, P., 1996. Guidelines on the quality of stormwater and treated wastewater for injection into aquifers for storage and reuse. Research report no 109, Centre for Groundwater Studies, Adelaide.

DIN ISO 13536, 1997. Soil quality - Determination of the potential cation exchange capacity and exchangeable cations using barium chloride solution buffered at pH = 8,1 (ISO 13536:1995). Beuth.

Doherty, J., 2000. PEST - Model-Independent Parameter Estimation. User's manual. Watermark Numerical Computing, Brisbane, Australia.

Dolničar, S. and Schäfer, A.I., 2006. Public perception of desalinated versus recycled water in Australia, AWWA Desalination Symposium.

DPI, 2008d. Explore Victoria online – GeoVic, Department of Primary Industries, Victoria, Australia.

DPI, 2008a. Minerals and Petroleum, Geoscience Victoria, Borehole Database, Department of Primary Industries, Victoria, Australia.

DPI, 2008b. Minerals and Petroleum, Geoscience Victoria, Geological Survey Reports, Department of Primary Industries, Victoria, Australia.

DPI, 2008c. Minerals and Petroleum, Geoscience Victoria, Victorian Geoscientific Database, Department of Primary Industries, Victoria, Australia.

Dries, J., Bastiaens, L., Springael, D., Kuypers, S., Agathos, S.N. and Diels, L., 2005. Effect of humic acids on heavy metal removal by zero-valent iron in batch and continuous flow column systems. Water Res. 39 (15), 3531-3540.

Droppo, I.G., 2001. Rethinking what constitutes suspended sediment. Hydrological Processes 15, 1551-1564.

DSE, 2008a. Groundwater Database, Department of Sustainability and Environment, Victoria, Australia.

DSE, 2004. Securing our water future together, Victorian Government, Department of Sustainability and Environment (DSE), Melbourne.

DSE, 2008b. Victorian Water Resources Data Warehouse, Department of Sustainability and Environment, Victoria, Australia.

Dudal, Y. and Gerard, F., 2004. Accounting for natural organic matter in aqueous chemical equilibrium models: a review of the theories and applications. Earth-Science Reviews 66 (3-4), 199.

Dudding, M., Evans, R., Dillon, P. and Molloy, R., 2006. Report on Broad Scale Map of ASR Potential for Melbourne, SKM and CSIRO Land and Water, Melbourne.

Düker, A., Ledin, A., Karlsson, S. and Allard, B., 1995. Adsorption of zinc on colloidal (hydr)oxides of Si, Al and Fe in the presence of a fulvic acid. Appl. Geochem. 10 (2), 197-205.

Duncan, H.P., 2006. Chapter 3: Urban stormwater pollutant characteristics. In: T.H.F. Wong (Ed.), Australian Runoff Quality - A guide to Water Sensitive Urban Design. Engineers Australia.

Dunnivant, F.M., Jardine, P.M., Taylor, D.L. and McCarthy, J.F., 1992. Cotransport of cadmium and hexachlorobiphenyl by dissolved organic carbon through columns containing aquifer material. Environ. Sci. Technol. 26, 360-368.

Dzombak, D.A. and Morel, F.M.M., 1990. Surface complexation modeling - Hydrous ferric oxide. Wiley and Sons, New York.

Egirani, D.E., Baker, A.R. and Andrews, J.E., 2005. Copper and zinc removal from aqueous solution by mixed mineral systems I. Reactivity and removal kinetics. J. Colloid Interface Sci. 291, 319-325.

Elimelech, M., Nagai, M., Ko, C.H. and Ryan, J.N., 2000. Relative Insignificance of Mineral Grain Zeta Potential to Colloid Transport in Geochemically Heterogeneous Porous Media. Environ. Sci. Technol. 34 (11), 2143-2148.

Elimelech, M. and O'Melia, C.R., 1990. Kinetics of deposition of colloidal particles in porous media. Environ. Sci. Technol. 24 (10), 1528-1536.

Elliott, H.A. and Huang, C.P., 1979. The adsorption characteristics of Cu(II) in the presence of chelating agents. J. Colloid Interface Sci. 70 (1), 29-45.

Elliott, H.A., Liberati, M.R. and Huang, C.P., 1986. Competitive Adsorption of Heavy Metals by Soils. J. Environ. Qual 15 (3), 214-219.

Ellis, J.B., 2000. Infiltration systems: a sustainable source-control option for urban stormwater quality management? J.CIWEM 14 (1), 27-34.

Elrashidi, M.A. and O'Connor, G.A., 1982. Influence of solution composition on sorption of zinc by soils. Soil Sci. Soc. Am. J. 46, 1153-1158.

Elzinga, E.J., Rouff, A.A. and Reeder, R.J., 2006. The long-term fate of Cu2+, Zn2+, and Pb2+ adsorption complexes at the calcite surface: An X-ray absorption spectroscopy study. Geochim. Cosmochim. Ac. 70 (11), 2715-2725.

Elzinga, E.J., van Grinsven, J.J.M. and Swartjes, F.A., 1999. General purpose Freundlich isotherms for cadmium, copper and zinc in soils. Eur. J. Soil Sci. 50 (1), 139-149.

Emmett, A.J., Clarke, S. and Howles, S., 1996. Conjunctive wetland treatment/aquifer storage and recovery at Regent Gardens residential development, Northfield, South Australia. Desalination 106 (1-3), 407-410.

Enfield, C.G., Bengtsson, G. and Lindqvist, R., 1989. Influence of macromolecules on chemical transport. Environ. Sci. Technol. 23 (10), 1278-1286.

EPA SA, 2004. Code of Practice for Aquifer Storage and Recovery. ISBN 1 876562 55 2, EPA South Australia (EPA SA), Adelaide.

EPA Victoria, 2003. State Environment Protection Policy (Waters of Victoria). Publication 905, Victorian Environmental Protection Agency, Melbourne.

Eriksson, E., Baun, A., Scholes, L., Ledin, A., Ahlman, S., Revitt, M., Noutsopoulos, C. and Mikkelsen, P.S., 2007. Selected stormwater priority pollutants — a European perspective. Sci. Total Environ. 383, 41-51.

Essaid, H.I., Bekins, B.A., Godsy, E.M., Warren, E., Baedecker, M.J. and Cozzarelli, I.M., 1995. Simulation of aerobic and anaerobic biodegradation processes at a crude oil spill site. Water Resour. Res. 31 (12), 3309-3327.

Evanko, C.R. and Dzombak, D.A., 1999. Surface Complexation Modeling of Organic Acid Sorption to Goethite. J. Colloid Interface Sci. 214 (2), 189-206.

Fasfous, I.I., Yapici, T., Murimboh, J., Hassan, N.M., Chakrabarti, C.L., Back, M.H., Lean, D.R.S. and Grégoire, D.C., 2004. Kinetics of Trace Metal Competition in the Freshwater Environment: Some Fundamental Characteristics. Environ. Sci. Technol. 38 (19), 4979-4986.

Fedotov, P.S., Savonina, E.Y., Wennrich, R. and Ladonin, D.V., 2007. Studies on trace and major elements association in soils using continuous-flow leaching in rotating coiled columns. Geoderma 142 (1-2), 58-68.

Feehley, C.E., Zheng, C. and Molz, F.J., 2000. A Dual-Domain Mass Transfer Approach for Modeling Solute Transport in Heterogeneous Aquifers: Application to the Macrodispersion Experiment (MADE) Site Water Resour. Res. 36 (9), 2501-2515.

Fehlberg, E., 1969. Klassische Runge-Kutta-Formeln fünfter und siebenter Ordnung mit Schrittweiten-Kontrolle. Computing 4 (2), 93-106.

Fehse, K.-U., 2004. Zur Sorption von Zink-Ionen an natürliche und technische Sorbentien unter Berücksichtigung des Feststoff:Lösung-Verhältnisses, Institut für Agrartechnik und Landeskultur der Landwirtschaftlichen Fakultät, Martin-Luther-Universität Halle-Wittenberg, Halle/Saale.

Fetter, C.W., 1993. Contaminant Hydrogeology. Macmillan Publishing Company, New York, USA.

Filius, J.D., Lumsdon, D.G., Meeussen, J.C.L., Hiemstra, T. and van Riemsdijk, W.H., 2000. Adsorption of fulvic acid on goethite. Geochim. Cosmochim. Ac. 64 (1), 51-60.

Filius, J.D., Meeussen, J.C.L., Lumsdon, D.G., Hiemstra, T. and van Riemsdijk, W.H., 2003. Modeling the binding of fulvic acid by goethite: the speciation of adsorbed FA molecules. Geochim. Cosmochim. Ac. 67 (8), 1463.

Fischer, D., Charles, E.G. and Baehr, A.L., 2003. Effects of stormwater infiltration on quality of groundwater beneath retention and detention basins. J. Environ. Eng. 129 (5), 464-471.

Fitz-Simons, T., Wayland, M., Mintz, D. and Schneider, T., 1998. U.S. status of particulates -- Monitoring, modeling, background, trends, and standards, Studies in Environmental Science. Elsevier Science B.V., 125-129.

Flach, G.P., Crisman, S.A. and Molz, F.J., 2004. Comparison of Single-Domain and Dual-Domain Subsurface Transport Models. Ground Water 42 (6), 815-828.

Fletcher, T.D., Poelsma, P., Li, Y. and Deletic, A., 2004. Wet and Dry Weather Performance of Constructed Stormwater Wetlands. In: T. Daniell (Ed.), Int. Conference on Water Sensitive Urban Design: cities as catchments, WSUD 2004, Adelaide, Australia, pp. 461-470.

Foppen, J.W.A. and Schijven, J.F., 2006. Evaluation of data from the literature on the transport and survival of Escherichia coli and thermotolerant coliforms in aquifers under saturated conditions. Water Res. 40 (3), 401-426.

Forbes, E.A., Posner, A.M. and Quirk, J.P., 1976. The specific adsorption of divalent Cd, Co, Cu, Pb, and Zn on goethite. J. Soil Sci. 27 (2), 154-166.

Förstner, U., 1993. Dispersion of contaminants from landfill operations. In: D. Petruzzelli and F.G. Helfferich (Eds.), Migration and Fate of Pollutants in Soils and Subsoils. Springer-Verlag, Berlin, Heidelberg, 435-454.

Fotovat, A., Naidu, R. and Sumner, M.E., 1997. Water : soil ratio influences aqueous phase chemistry of indigenous copper and zinc in soils. Aust. J. Soil Res. 35, 687-709.

Francey, M., Fletcher, T.D., Deletic, A. and Duncan, H., submitted. New Insights into the Quality of Urban Stormwater in South Eastern Australia. J. Water Res. PL-ASCE

Fu, H. and Quan, X., 2006. Complexes of fulvic acid on the surface of hematite, goethite, and akaganeite: FTIR observation. Chemosphere 63 (3), 403-410.

Fuchs, S., Brombach, H. and Weiß, G., 2004. New database on urban runoff pollution. In: M. Desbordes and B. Chocat (Eds.), Novatech 2004: 5th International Conference on Sustainable techniques and strategies in urban water management, Lyon, France, pp. 145-152.

Fuller, C.C., Davis, J.A., Coston, J.A. and Dixon, E., 1996. Characterization of metal adsorption variability in a sand and gravel aquifer, Cape Cod, Massachusetts, U.S.A. J. Contam. Hydrol. 22 (3-4), 165-187.

Furrer, G., von Gunten, U. and Zobrist, J., 1996. Steady-state modelling of biogeochemical processes in columns with aquifer material 1. Speciation and mass balances. Chem. Geol. 133 (1-4), 15-28.

Gaganis, P. and Smith, L., 2006. Evaluation of the uncertainty of groundwater model predictions associated with conceptual errors: A per-datum approach to model calibration. Adv. Water Res. 29 (4), 503-514.

Gaines, G.L. and Thomas, H.C., 1953. Adsorption studies on clay minerals. II. A formulation of the thermodynamics of exchange adsorption. J. Chem. Phys. 21 (4), 714-718.

Gapon, E.N., 1933. Theory of exchange adsorption. J. Gen. Chem. 3, 667-669.

Garrels, R.M. and Christ, C.L., 1965. Solutions, Minerals and Equilibria. Harper and Row, New York.

Genç-Fuhrman, H., Mikkelsen, P.S. and Ledin, A., 2007. Simultaneous removal of As, Cd, Cr, Cu, Ni and Zn from stormwater: Experimental comparison of 11 different sorbents. Water Res. 41 (3), 591-602.

Gerges, N.Z., Dillon, P.J., Sibenaler, X.P., Martin, R.R., Pavelic, P., Howles, S.R. and Dennis, K., 2002b. South Australian experience in aquifer storage and recovery. In: P. Dillon (Ed.), Management of Aquifer Recharge for Sustainability, Proceedings of the International Symposium on Artificial Recharge of Groundwater, 4th, Adelaide, Australia, Sept. 22-26, 2002, pp. 453-458.

Gerges, N.Z., Howles, S.R., Dennis, K., Dillon, P.J. and Barry, K.E., 2002a. Town water supply purification using aquifer storage and recovery in a saline aquifer. In: P. Dillon (Ed.), Management of Aquifer Recharge for Sustainability, Proceedings of the 4th Int. Symposium on Artificial Recharge of Groundwater, Sept. 22-26, Adelaide, Australia, pp. 459-464.

GHD, 1981. Characterisation of pollution in urban stormwater runoff. 60, Gutteridge Haskins & Davey (GHD), Environment Protection Authority of Victoria (Vic EPA), Canberra.

Ghosh, S.K. and Schnitzer, M., 1980. Macromolecular structures of humic substances. Soil Sci. 129 (5), 266-276.

Giles, C.H., D'Silva, A.P. and Easton, I.A., 1974b. A general treatment and classification of the solute adsorption isotherm part. II. Experimental interpretation. J. Colloid Interface Sci. 47 (3), 766-778.

Giles, C.H., Smith, D. and Huitson, A., 1974a. A general treatment and classification of the solute adsorption isotherm. I. Theoretical. J. Colloid Interface Sci. 47 (3), 755-765.

Gillman, G.P., 1981. Effects of pH and Ionic Strength on the Cation Exchange Capacity of Soils with Variable Charge. Aust. J. Soil Res. 19, 93-96.

Göbel, P., Dierkes, C. and Coldewey, W.G., 2007. Storm water runoff concentration matrix for urban areas. J. Contam. Hydrol. 91, 26-42.

Gödde, M., David, M.B., Christ, M.J., Kaupenjohann, M. and Vance, G.F., 1996. Carbon mobilization from the forest floor under red spruce in the Northeastern U.S.A. Soil Biol. Biochem. 28 (9), 1181-1189.

Goh, K.-H. and Lim, T.-T., 2005. Arsenic fractionation in a fine soil fraction and influence of various anions on its mobility in the subsurface environment. Appl. Geochem. 20 (2), 229-239.

Goldberg, S., 1991. Sensitivity of surface complexation modeling to the surface site density parameter. J. Colloid Interface Sci. 145 (1), 1-9.

Goldberg, S., 2005. Surface Complexation Modeling. In: D. Hillel and J.L. Hatfield (Eds.), Encyclopedia of soils in the environment. Elsevier, London, 97-108.

Goldberg, S., Criscenti, L.J., Turner, D.R., Davis, J.A. and Cantrell, K.J., 2007. Adsorption Desorption Processes in Subsurface Reactive Transport Modeling. Vadose Zone J. 6 (3), 407-435.

Gomes, P.C., Fontes, M.P.F., Silva, A.G.d., Mendonca, E.d.S. and Netto, A.R., 2001. Selectivity sequence and competitive adsorption of heavy metals by Brazilian soils. Soil Sci. Soc. Am. J. 65 (4), 1115-1121.

Gómez-Ariza, J.L., Giráldez, I., Sánchez-Rodas, D. and Morales, E., 1999. Metal readsorption and redistribution during the analytical fractionation of trace elements in oxic estuarine sediments. Anal. Chim. Ac. 399 (3), 295-307.

Goodman, B.A., 1986. Adsorption of Metal Ions and Complexes on Aluminosilicate Minerals. In: J.A. Davis and K.F. Hayes (Eds.), Geochemical processes at mineral surfaces. ACS symposium series. American Chemical Society, Washington, DC, 342-361.

Greenland, D.J., 1971. Interactions between humic and fulvic acids and clays. Soil Sci. 111 (1), 34-41.

Greskowiak, J., Prommer, H., Massmann, G. and Nützmann, G., 2006. Modeling Seasonal Redox Dynamics and the Corresponding Fate of the Pharmaceutical Residue Phenazone During Artificial Recharge of Groundwater. Environ. Sci. Technol. 40 (21), 6615-6621.

Greskowiak, J., Prommer, H., Vanderzalm, J., Pavelic, P. and Dillon, P., 2005. Modeling of carbon cycling and biogeochemical changes during injection and recovery of reclaimed water at Bolivar, South Australia. Water Resour. Res. 41, W10418, doi:10.1029/2005WR004095.

Griffiths, R.A., 2004. Sorption and desorption by ideal two-compartment systems: unusual behavior and data interpretation problems. Chemosphere 55, 443-454.

Grolimund, D., Borkovec, M., Barmettler, K. and Sticher, H., 1996. Colloid-facilitated transport of strongly sorbing contaminants in natural porous media: a laboratory column study. Environ. Sci. Technol. 30, 3118-3123.

Grolimund, D., Borkovec, M., Federer, P. and Sticher, H., 1995. Measurement of Sorption Isotherms with Flow-Through Reactors. Environ. Sci. Technol. 29 (8), 2317-2321.

Grolimund, D., Elimelech, M., Borkovec, M., Barmettler, K., Kretzschmar, R. and Sticher, H., 1998. Transport of in Situ Mobilized Colloidal Particles in Packed Soil Columns. Environ. Sci. Technol. 32 (22), 3562-3569.

Gromaire-Mertz, M.-C., Garnaud, S., Gonzalez, A. and Chebbo, G., 1999. Characterisation of urban runoff pollution in Paris. Water Sci. Technol. 39 (2), 1-8.

Gronvall, G.S., 1992. The Fyansford Formation. In: W.A. Peck, J.L. Neilson, R.J. Olds and K.D. Seddon (Eds.), Engineering geology of Melbourne : proceedings of the Seminar on Engineering Geology of Melbourne, Melbourne, Victoria, Australia, 16 September 1992. A.A. Balkema, Rotterdam, 175-183.

Grove, D.B. and Stollenwerk, K.G., 1987. Chemical reactions simulated by groundwater-quality models. J. Am. Water Resour. Assoc. 23 (4), 601-615.

Grünheid, S., Amy, G. and Jekel, M., 2005. Removal of bulk dissolved organic carbon (DOC) and trace organic compounds by bank filtration and artificial recharge. Water Res. 39 (14), 3219-3228.

Grybos, M., Davranche, M., Gruau, G. and Petitjean, P., 2007. Is trace metal release in wetland soils controlled by organic matter mobility or Fe-oxyhydroxides reduction? J. Colloid Interface Sci. 314 (2), 490-501.

Gu, B., Mehlhorn, T.L., Liang, L. and McCarthy, J.F., 1996a. Competitive adsorption, displacement, and transport of organic matter on iron oxide: I. Competitive adsorption. Geochim. Cosmochim. Ac. 60 (11), 1943-1950.

Gu, B., Mehlhorn, T.L., Liang, L. and McCarthy, J.F., 1996b. Competitive adsorption, displacement, and transport of organic matter on iron oxide: II. Displacement and transport. Geochim. Cosmochim. Ac. 60 (16), 2977-2992.

Gu, B., Schmitt, J., Chen, Z., Liang, L. and McCarthy, J.F., 1994. Adsorption and Desorption of Natural Organic Matter on Iron Oxide: Mechanisms and Models. Environ. Sci. Technol. 28 (1), 38-46.

Guine, V., Spadini, L., Sarret, G., Muris, M., Delolme, C., Gaudet, J.P. and Martins, J.M.F., 2006. Zinc Sorption to Three Gram-Negative Bacteria: Combined Titration, Modeling, and EXAFS Study. Environ. Sci. Technol. 40 (6), 1806-1813.

Gupta, H.V., Sorooshian, S. and Yapo, P.O., 1998. Toward Improved Calibration of Hydrologic Models: Multiple and Noncommensurable Measures of Information. Water Resour. Res. 34 (4), 751-763.

Gustafsson, J.P. and Berggren Kleja, D., 2005. Modeling Salt-Dependent Proton Binding by Organic Soils with the NICA-Donnan and Stockholm Humic Models. Environ. Sci. Technol. 39 (14), 5372-5377.

Gustafsson, J.P., Pechova, P. and Berggren, D., 2003. Modeling Metal Binding to Soils: The Role of Natural Organic Matter. Environ. Sci. Technol. 37 (12), 2767-2774.

Gustafsson, J.P. and van Schaik, J.W.J., 2003. Cation binding in a mor layer: batch experiments and modelling. Eur. J. Soil Sci. 54 (2), 295-310.

Haerens, B., 2004. Reactive transport modelling of a groundwater contamination from a former coking plant. PhD Thesis, Dep. of Geography and Geology, KU Leuven, Leuven.

Haggerty, R. and Gorelick, S.M., 1995. Multiple-Rate Mass Transfer for Modeling Diffusion and Surface Reactions in Media with Pore-Scale Heterogeneity. Water Resour. Res. 31 (10), 2383-2400.

Haldar, M. and Mandal, L.N., 1979. Influence of soil moisture regimes and organic matter application on the extractable Zn and Cu content in rice soils. Plant and Soil 153, 203-213.

Hallberg, M., Renman, G. and Lundbom, T., 2007. Seasonal Variations of Ten Metals in Highway Runoff and their Partition between Dissolved and Particulate Matter. Water Air Soil Pollut. 181, 183-191.

Hammer, M.J., 2008. Water and wastewater technology. Pearson/Prentice Hall, Upper Saddle River, N.J.

Han, Y.H., Lau, S.L., Kayhanian, M. and Stenstrom, M.K., 2006. Correlation analysis among highway stormwater pollutants and characteristics. Water Sci. Technol. 53 (2), 235-243.

Hancock, S., 1992. Groundwater and corrosivity. In: W.A. Peck, J.L. Neilson, R.J. Olds and K.D. Seddon (Eds.), Engineering geology of Melbourne : proceedings of the Seminar on Engineering Geology of Melbourne, Melbourne, Victoria, Australia, 16 September 1992. A.A. Balkema, Rotterdam, 51-57.

Hanna, K., 2007. Sorption of two aromatic acids onto iron oxides: Experimental study and modeling. J. Colloid Interface Sci. 309 (2), 419-428.

Harbaugh, A.W., Banta, E.R., Hill, M.C. and McDonald, M.G., 2000. MODFLOW-2000, the U.S. Geological Survey Modular Ground-Water Model - User Guide to Modularization Concepts and the Ground-Water Flow Process. Open-File Report 00-92, U.S. Geological Survey, Reston, Virginia.

Harmel, R.D. and Smith, P.K., 2007. Consideration of measurement uncertainty in the evaluation of goodness-of-fit in hydrologic and water quality modeling. J. Hydrol. 337 (3-4), 326-336.

Harris, G., Batley, G., Fox, D., Hall, D., Jernakoff, P., Molloy, R., Murray, A.G., Newell, B., Parslow, J.S., Skyring, G.W. and Walker, S., 1996. Port Phillip Bay Environmental Study Final Report. 064305927X, CSIRO, Canberra, Australia.

Harrison, R.M. and Wilson, S.J., 1985. The chemical composition of highway drainage waters I. Major ions and selected trace metals. Sci. Total Environ. 43 (1-2), 63-77.

Harter, R.D., 1983. Effect of Soil pH on Adsorption of Lead, Copper, Zinc, and Nickel. Soil Sci. Soc. Am. J. 47, 47-51.

Harter, R.D. and Naidu, R., 2001. Review and analysis: An assessment of environmental and solution parameter impact on trace-metal sorption by soils. Soil Sci. Soc. Am. J. 65 (3), 597-612.

Hatt, B., Fletcher, T.D. and Deletic, A., in press. Hydrologic and pollutant removal performance of stormwater biofiltration systems at the field scale. J. Hydrol.

Hatt, B.E., Deletic, A. and Fletcher, T.D., 2006. Integrated treatment and recycling of stormwater: a review of Australian practice. J. Environ. Manage. 79 (1), 102-113.
Hatt, B.E., Fletcher, T.D. and Deletic, A., 2007. Treatment performance of gravel filter media: Implications for design and application of stormwater infiltration systems. Water Res. 41 (12), 2513-2524.
Hay, M.B. and Myneni, S.C.B., 2007. Structural environments of carboxyl groups in natural organic molecules from terrestrial systems. Part 1: Infrared spectroscopy. Geochim. Cosmochim. Ac. 71, 3518-3532.
Haydon, S. and Deletic, A., 2006. Development of a coupled pathogen-hydrologic catchment model. J. Hydrol. 328, 467-480.
Hayes, K.F., Redden, G., Ela, W. and Leckie, J.O., 1991. Surface complexation models: An evaluation of model parameter estimation using FITEQL and oxide mineral titration data. J. Colloid Interface Sci. 142 (2), 448-469.
He, Z.L., Zhang, M., Yang, X.E. and Stoffella, P.J., 2006. Release Behavior of Copper and Zinc from Sandy Soils. Soil Sci. Soc. Am. J. 70, 1699-1707.
Heberer, T., 2002. Occurrence, fate, and removal of pharmaceutical residues in the aquatic environment: a review of recent research data. Toxicol. Lett. 131 (1-2), 5-17.
Heidmann, I., Christl, I. and Kretzschmar, R., 2005. Aggregation Kinetics of Kaolinite-Fulvic Acid Colloids as Affected by the Sorption of Cu and Pb. Environ. Sci. Technol. 39 (3), 807-813.
Hem, J.D., 1961. Stability field diagrams as aids in iron chemistry studies. American Water Works Association (AWWA) 53, 211-232.
Hem, J.D., 1972. Chemistry and occurrence of cadmium and zinc in surface water and ground water. Water Resour. Res. 8, 661-679.
Herczeg, A.L., Rattray, K.J., Dillon, P.J., Pavelic, P. and Barry, K.E., 2004. Geochemical processes during five years of aquifer storage recovery. Ground Water 42 (3), 438-445.
Hering, J.G. and Morel, F.M.M., 1988. Humic acid complexation of calcium and copper. Environ. Sci. Technol. 22 (10), 1234-1237.
Hering, J.G. and Stumm, W., 1990. Oxidation adn reductive dissolution of minerals. In: M.F. Hochella and A.F. White (Eds.), Mineral-water interface geochemistry. Reviews in mineralogy. Mineralogical Society of America, Washington, D.C., 427-465.
Herms, U. and Brümmer, G.W., 1984. Solubility and retention of heavy metals in soils. J. Plant Nutr. Soil Sci. 147, 400-424.
Herngren, L., Goonetilleke, A. and Ayoko, G.A., 2005. Understanding heavy metal and suspended solids relationships in urban stormwater using simulated rainfall. J. Environ. Manage. 76 (2), 149-158.
Hiemstra, T., Venema, P. and van Riemsdijk, W.H., 1996. Intrinsic Proton Affinity of Reactive Surface Groups of Metal (Hydr)oxides: The Bond Valence Principle. J. Colloid Interface Sci. 184 (2), 680-692.
Hinz, C., 2001. Description of sorption data with isotherm equations. Geoderma 99 (3-4), 225-243.
Hinz, C. and Selim, H.M., 1994. Transport of zinc and cadmium in soils: Experimental evidence and modeling approaches. Soil Sci. Soc. Am. J. 58 (5), 1316-1327.
Hiromatsu, K., Yakabe, Y., Katagiri, K. and Nishihara, T., 2000. Prediction for biodegradability of chemicals by an empirical flowchart. Chemosphere 41 (11), 1749-1754.
Hizal, J. and Apak, R., 2006. Modeling of copper(II) and lead(II) adsorption on kaolinite-based clay minerals individually and in the presence of humic acid. J. Colloid Interface Sci. 295 (1), 1-13.
Ho, Y.-S., 2003. Removal of copper ions from aqueous solution by tree fern. Water Res. 37 (10), 2323-2330.
Hogan, P., Ball, J., Batley, G. and Brockbank, C., 1995. The impact of urban stormwater runoff from impervious road surfaces. In: Australian Water and Wastewater Association (AWWA) (Ed.), 16th Federal Convention proceedings. Australian Water & Wastewater Association, Sydney, NSW, pp. 907-914.
Hogg, D.S., McLaren, R.G. and Swift, R.S., 1993. Desorption of copper from some New Zealand soils. Soil Sci. Soc. Am. J. 57, 361-366.
Honeyman, B.D. and Santschi, P.H., 1988. Metals in aquatic systems. Environ. Sci. Technol. 22 (8), 862-871.
Horneman, A., van Geen, A., Kent, D.V., Mathe, P.E., Zheng, Y., Dhar, R.K., O'Connell, S., Hoque, M.A., Aziz, Z. and Shamsudduha, M., 2004. Decoupling of As and Fe release to Bangladesh groundwater under reducing conditions. Part I: Evidence from sediment profiles. Geochim. Cosmochim. Ac. 68 (17), 3459-3473.
Horner, C., Holzbecher, E. and Nützmann, G., 2007. A coupled transport and reaction model for long column experiments simulating bank filtration. Hydrological Processes 21 (8), 1015-1025.

Horner, R., Skupien, J., Livingston, E. and Shaver, E., 1994. Fundamentals of urban runoff management, Terrene Institute in Cooperation with US EPA

Horner, R.M.W., Jarvis, R.J. and Mackie, R.I., 1986. Deep bed filtration: A new look at the basic equations. Water Res. 20 (2), 215-220.

Howard, P.H., 2000. Chapter 12: Biodegradation. In: R.S. Boethling and D. Mackay (Eds.), Handbook of property estimation methods for environmental chemicals environmental and health sciences. Lewis Publishers, Boca Raton.

Howe, C., Jones, R.N., Maheepala, S. and Rhodes, B., 2005. Melbourne Water Climate Change Study: Implications of potential climate change for Melbourne's water resources. CMIT-2005-106, Melbourne Water, CSIRO Urban Water, CSIRO Atmospheric Research.

Hubbs, S.A., 2006. Riverbank Filtration Hydrology. Springer Netherlands.

Hunter, K.S., Wang, Y. and van Cappellen, P., 1998. Kinetic modeling of microbially-driven redox chemistry of subsurface environments: coupling transport, microbial metabolism and geochemistry. J. Hydrol. 209, 53-80.

Hunter, R.J., 2001. Foundations of colloid science. Oxford University Press, Oxford.

Hutchins, C.M., Teasdale, P.R., Lee, J. and Simpson, S.L., 2007. The effect of manipulating sediment pH on the porewater chemistry of copper- and zinc-spiked sediments. Chemosphere 69 (7), 1089-1099.

Irving, H. and Williams, R.J.P., 1948. Order of stability of metal complexes. Nature 162, 746-747.

Iu, K.L., Pulford, I.D. and Duncan, H.J., 1981a. Influence Of Waterlogging And Lime Or Organic-Matter Additions On The Distribution Of Trace-Metals In An Acid Soil. 1. Manganese and Iron. Plant and Soil 59 (2), 317-326.

Iu, K.L., Pulford, I.D. and Duncan, H.J., 1981b. Influence Of Waterlogging And Lime Or Organic-Matter Additions On The Distribution Of Trace-Metals In An Acid Soil. 2. Zinc And Copper. Plant and Soil 59 (2), 327-333.

Jacobs, L.A., von Gunten, H.R., Keil, R. and Kuslys, M., 1988. Geochemical changes along a river-groundwater infiltration flow path: Glattfelden, Switzerland. Geochim. Cosmochim. Ac. 52 (11), 2693-2706.

James, R.O. and Healy, T.W., 1972. Adsorption of Hydrolyzable Metal Ions at the Oxide-Water Interface III. A Thermodynamic Model of Adsorption. J. Colloid Interface Sci. 40 (1), 65-81.

James, R.V. and Rubin, J., 1979. Applicability of the local equilibrium assumption to transport through soil of solutes affected by ion exchange. In: E.A. Jenne (Ed.), Chemical Modeling of Aqueous Systems. Am. Chem. Soc. Syrup. Ser., 225-235.

Jardine, P.M., Weber, N.L. and McCarthy, J.F., 1989. Mechanisms of dissolved organic carbon adsorption on soil. Soil Sci. Soc. Am. J. 53 (5), 1378-1385.

Jenne, E.A., 1968. Controls on Mn, Fe, Co, Ni, Cu, and Zn Concentrations in Soils and Water: the Significant Role of Hydrous Mn and Fe Oxides. In: American Chemical Society. Division of Water Air and Waste Chemistry. (Ed.), Trace inorganics in water : a symposium. Advances in chemistry series ; 73. American Chemical Society, Washington, 337-387.

Jenne, E.A., 1995. Metal Adsorption onto and Desorption from Sediments. II. Artifact Effects. Mar. Freshwater Res. 46, 1-18.

John, D.E. and Rose, J.B., 2005. Review of Factors Affecting Microbial Survival in Groundwater. Environ. Sci. Technol. 39 (19), 7345-7356.

Johnson, G.R., Gupta, K., Putz, D.K., Hu, Q. and Brusseau, M.L., 2003. The effect of local-scale physical heterogeneity and nonlinear, rate-limited sorption/desorption on contaminant transport in porous media. J. Contam. Hydrol. 64 (1-2), 35-58.

Johnson, J.S., Baker, L.A. and Fox, P., 1999. Geochemical transformations during artificial groundwater recharge: soil-water interactions of inorganic constituents. Water Res. 33 (1), 196-206.

Johnson, P.R., Sun, N. and Elimelech, M., 1996. Colloid Transport in Geochemically Heterogeneous Porous Media: Modeling and Measurements. Environ. Sci. Technol. 30 (11), 3284-3293.

Johnson, S.B., Yoon, T.H. and Brown, G.E., 2005. Adsorption of Organic Matter at Mineral/Water Interfaces: 5. Effects of Adsorbed Natural Organic Matter Analogues on Mineral Dissolution. Langmuir 21 (7), 2811-2821.

Johnson, W.P. and Amy, G.L., 1995. Facilitated Transport and Enhanced Desorption of Polycyclic Aromatic Hydrocarbons by Natural Organic Matter in Aquifer Sediments. Environ. Sci. Technol. 29, 807-817.

Jones, G.W. and Pichler, T., 2007. Relationship between Pyrite Stability and Arsenic Mobility During Aquifer Storage and Recovery in Southwest Central Florida. Environ. Sci. Technol. 41 (3), 723-730.

Kaiser, K., 2003. Sorption of natural organic matter fractions to goethite ([alpha]-FeOOH): effect of chemical composition as revealed by liquid-state 13C NMR and wet-chemical analysis. Org. Geochem. 34 (11), 1569-1579.

Kaiser, K., Kaupenjohann, M. and Zech, W., 2001. Sorption of dissolved organic carbon in soils: effects of soil sample storage, soil-to-solution ratio, and temperature. Geoderma 99, 317-328.

Kalbitz, K., Schmerwitz, J., Schwesig, D. and Matzner, E., 2003. Biodegradation of soil-derived dissolved organic matter as related to its properties. Geoderma 113 (3-4), 273-291.

Kalbitz, K., Solinger, S., Park, J.-H., Michalzik, B. and Matzner, E., 2000. Controls on the dynamics of dissolved organic matter in soils: a review. Soil Sci. 165 (4), 277-304.

Kalbitz, K. and Wennrich, R., 1998. Mobilization of heavy metals and arsenic in polluted wetland soils and its dependence on dissolved organic matter. Sci. Total Environ. 209 (1), 27-39.

Kanso, A., Gromaire, M.-C., Gaume, E., Tassin, B. and Chebbo, G., 2003. Bayesian approach for the calibration of models: application to an urban stormwater pollution model. Water Sci. Technol. 47 (4), 77-84.

Kaplan, D.I., Bertsch, P.M. and Adriano, D.C., 1995. Facilitated Transport of Contaminant Metals Through an Acidified Aquifer. Ground Water 33 (5), 708-717.

Kaplan, D.I., Bertsch, P.M., Adriano, D.C. and Miller, W.P., 1993. Soil-born mobile colloids as influenced by water flow and organic carbon. Environ. Sci. Technol. 27, 1193-1200.

Karathanasis, A.D., 1999. Subsurface Migration of Copper and Zinc Mediated by Soil Colloids. Soil Sci. Soc. Am. J. 63, 830-838.

Karathanasis, A.D. and Johnson, D.M.C., 2006. Subsurface transport of Cd, Cr, and Mo mediated by biosolid colloids. Sci. Total Environ. 354 (2-3), 157.

Karlsson, T., 2005. Complexation of Cadmium, Copper and Methyl Mercury to Functional Groups in Natural Organic Matter: Studied by X-ray Absorption Spectroscopy and Binding Affinity Experiments. Doctoral thesis Thesis, Faculty of Forest Sciences, Department of Forest Ecology, Swedish University of Agricultural Sciences, Umeå.

Karthikeyan, K.G. and Elliott, H.A., 1999. Surface Complexation Modeling of Copper Sorption by Hydrous Oxides of Iron and Aluminum. J. Colloid Interface Sci. 220 (1), 88-95.

Kashem, M.A. and Singh, B.R., 2001. Metal availability in contaminated soils: I. Effects of flooding and organic matter on changes in Eh, pH and solubility of Cd, Ni and Zn. Nutrient Cycling in Agroecosystems 61, 247-255.

Kayhanian, M., Stransky, C., Bay, S., Lau, S.L. and Stenstrom, M.K., 2008. Toxicity of urban highway runoff with respect to storm duration. Sci. Total Environ. 389 (2-3), 386-406.

Kedziorek, M.A.M., Geoffriau, S. and Bourg, A.C.M., 2008. Organic Matter and Modeling Redox Reactions during River Bank Filtration in an Alluvial Aquifer of the Lot River, France. Environ. Sci. Technol. 42 (8), 2793-2798.

Kenley, P.R., 1992. Brighton Group - Geology. In: W.A. Peck, J.L. Neilson, R.J. Olds and K.D. Seddon (Eds.), Engineering geology of Melbourne : proceedings of the Seminar on Engineering Geology of Melbourne, Melbourne, Victoria, Australia, 16 September 1992. A.A. Balkema, Rotterdam, 191-196.

Kent, D.B., Abrams, R.H., Davis, J.A., Coston, J.A. and LeBlanc, D.R., 2000. Modeling the influence of variable pH on the transport of zinc in a contaminated aquifer using semiempirical surface complexation models. Water Resour. Res. 36 (12), 3411-3425.

Kent, D.B., Davis, J.A., Anderson, L.C.D., Rea, B.A. and Coston, J.A., 2002. Effect of adsorbed metal ions on the transport of Zn- and Ni-EDTA complexes in a sand and gravel aquifer. Geochim. Cosmochim. Ac. 66 (17), 3017-3036.

Kent, D.B., Wilkie, J.A. and Davis, J.A., 2007. Modeling the movement of a pH perturbation and its impact on adsorbed zinc and phosphate in a wastewater-contaminated aquifer. Water Resour. Res. 43 (W07440), doi:10.1029/2005WR004841.

Kerndorff, H. and Schnitzer, M., 1980. Sorption of metals on humic acid. Geochim. Cosmochim. Ac. 44 (11), 1701-1708.

Kersten, M. and Förstner, U., 1987. Effect of sample pretreatment on the reliability of solid speciation data of heavy metals -- implications for the study of early diagenetic processes. Mar. Chem. 22 (2-4), 299-312.

Khai, N.M., Öborn, I., Hillier, S. and Gustafsson, J.P., 2008. Modeling of metal binding in tropical Fluvisols and Acrisols treated with biosolids and wastewater. Chemosphere 70, 1338-1346.

Kheboian, C. and Bauer, C.F., 1987. Accuracy of selective extraction procedures for metal speciation in model aquatic sediments. Anal. Chem. 59 (10), 1417-1423.

Khilar, K.C. and Fogler, H.S., 1984. The existence of a critical salt concentration for particle release. J. Colloid Interface Sci. 101 (1), 214-224.

Kim, N.D. and Fergusson, J.E., 1991. Effectiveness of a commonly used sequential extraction technique in determining the speciation of cadmium in soils. Sci. Total Environ. 105, 191-209.

Kim, S.-B. and Corapcioglu, M.Y., 2002. Contaminant transport in dual-porosity media with dissolved organic matter and bacteria present as mobile colloids. J. Contam. Hydrol. 59 (3-4), 267-289.

King, K.S., 2005. Hydrogeological Assessment Tools for Modelling Transport of Metals in Groundwater, The Science Advisory Board for Contaminated Sites in British Columbia, Buffalo NY 14207.

Kinniburgh, D.G., 1986. General Purpose Adsorption Isotherms. Environ. Sci. Technol. 20 (9), 895-904.

Kinniburgh, D.G., Milne, C.J., Benedetti, M.F., Pinheiro, J.P., Filius, J., Koopal, L.K. and van Riemsdijk, W.H., 1996. Metal Ion Binding by Humic Acid: Application of the NICA-Donnan Model. Environ. Sci. Technol. 30 (5), 1687-1698.

Knabner, P., Totsche, K.U. and Kögel-Knabner, I., 1996. The modeling of reactive solute transport with sorption to mobile and immobile sorbents 1. Experimental evidence and model development. Water Resour. Res. 32 (6), 1611-1622.

Ko, C.-H. and Elimelech, M., 2000. The "Shadow Effect" in Colloid Transport and Deposition Dynamics in Granular Porous Media: Measurements and Mechanisms. Environ. Sci. Technol. 34 (17), 3681-3689.

Konikow, L.F., 1986. Predictive accuracy of a groundwater model – lessons from a postaudit. Ground Water 24, 173-184.

Konikow, L.F., August, L.L. and Voss, C.I., 2001. Effects of clay dispersion on aquifer storage and recovery in coastal aquifers. Transport in Porous Media 43 (1), 45-64.

Kookana, R.S., Naidu, R. and Tiller, K.G., 1994. Sorption non-equilibrium during cadmium transport through soils. Aust. J. Soil Res. 32, 635-651.

Koopal, L.K., Saito, T., Pinheiro, J.P. and van Riemsdijk, W.H., 2005. Ion binding to natural organic matter: General considerations and the NICA-Donnan model. Colloids Surf., A 265 (1-3), 40-54.

Kopchynski, T., Fox, P., Alsmadi, B. and Berner, M., 1996. The effects of soil type and effluent pre-treatment on soil aquifer treatment. Water Sci. Technol. 34 (11), 235-242.

Koretsky, C., 2000. The significance of surface complexation reactions in hydrologic systems: a geochemist's perspective. J. Hydrol. 230 (3-4), 127-171.

Krause, C., Fisch, E. and Rohrbach, G., 1993. Cation Exchange Capacity - A contribution to the standardization of methods for the estimation of the suitability of clays for the basis layer in waste disposal sites. Keramische Zeitschrift 45 (7), 385-389.

Křepelová, A., Reich, T., Sachs, S., Drebert, J. and Bernhard, G., 2008. Structural characterization of U(VI) surface complexes on kaolinite in the presence of humic acid using EXAFS spectroscopy. J. Colloid Interface Sci. 319 (1), 40-47.

Kretzschmar, R., Borkovec, M., Grolimund, D. and Elimelech, M., 1999. Mobile subsurface Colloids and Their Role in Contaminant Transport. Adv. Agron. 66, 121-193.

Kretzschmar, R. and Sticher, H., 1997. Transport of humic-coated iron oxide colloids in a sandy aquifer: influence of Ca2+ and trace metals. Environ. Sci. Technol. 31, 3497-3504.

Kuo, S. and Baker, A.S., 1980. Sorption of Copper, Zinc, and Cadmium by Some Acid Soils. Soil Sci. Soc. Am. J. 44, 969-974.

Kurniawan, T.A., Chan, G.Y.S., Lo, W.-H. and Babel, S., 2006. Physico-chemical treatment techniques for wastewater laden with heavy metals. Chem. Eng. J. 118 (1-2), 83-98.

Lane, A.P., Lakey, R.C. and Leonard, J.G., 1992. The hydrogeology of the Melbourne region. In: W.A. Peck, J.L. Neilson, R.J. Olds and K.D. Seddon (Eds.), Engineering geology of Melbourne : proceedings of the Seminar on Engineering Geology of Melbourne, Melbourne, Victoria, Australia, 16 September 1992. A.A. Balkema, Rotterdam, 13-19.

Langmuir, D., 1997. Aqueous environmental geochemistry. Prentice Hall, Upper Saddle River, N.J.

Larsson, M.H. and Jarvis, N.J., 1999. Evaluation of a dual-porosity model to predict field-scale solute transport in a macroporous soil. J. Hydrol. 215 (1-4), 153-171.

Lasaga, A.C. and Kirkpatrick, R.J., 1981. Kinetics of geochemical processes. Reviews in mineralogy; v. 8. Mineralogical Society of America, Washington, D.C.

Lattemann, S. and Höpner, T., 2008. Environmental impact and impact assessment of seawater desalination. Desalination 220 (1-3), 1-15.

Lawrence, I. and Breen, P., 2006. Chapter 2: Stormwater contaminant processes and pathways. In: T.H.F. Wong (Ed.), Australian Runoff Quality - A guide to Water Sensitive Urban Design. Engineers Australia.

Laxen, D.P.H., 1985. Trace metal adsorption/coprecipitation on hydrous ferric oxide under realistic conditions : The role of humic substances. Water Res. 19 (10), 1229-1236.

Le Gal La Salle, C., Vanderzalm, J., Hutson, J., Dillon, P., Pavelic, P. and Martin, R., 2002. Isotope contribution to geochemical investigations for aquifer storage and recovery. In: P. Dillon (Ed.), Management of Aquifer Recharge for Sustainability, Proceedings of the International Symposium on Artificial Recharge of Groundwater, 4th, Adelaide, Australia, Sept. 22-26, 2002, pp. 265-268.

Lee, H., Lau, S.-L., Kayhanian, M. and Stenstrom, M.K., 2004. Seasonal first flush phenomenon of urban stormwater discharges. Water Res. 38 (19), 4153-4163.

Lee, M.-K. and Saunders, J.A., 2003. Effects of pH on Metals Precipitation and Sorption: Field Bioremediation and Geochemical Modeling Approaches. Vadose Zone J. 2, 177-185.

Leenheer, J.A., Brown, G.K., MacCarthy, P. and Cabaniss, S.E., 1998. Models of Metal Binding Structures in Fulvic Acid from the Suwannee River, Georgia. Environ. Sci. Technol. 32 (16), 2410-2416.

Leenheer, J.A., Wershaw, R.L. and Reddy, M.M., 1995. Strong-Acid, Carboxyl-Group Structures in Fulvic Acid from the Suwannee River, Georgia. 2. Major Structures. Environ. Sci. Technol. 29 (2), 399-405.

Legates, D.R. and McCabe Jr., G.J., 1999. Evaluating the use of "goodness-of-fit" measures in hydrologic and hydroclimatic model validation. Water Resour. Res. 35 (1), 233-241.

Legret, M. and Pagotto, C., 1999. Evaluation of pollutant loadings in the runoff waters from a major rural highway. Sci. Total Environ. 235 (1-3), 143-150.

Lehmann, R.G. and Harter, R.D., 1984. Assessment of copper-soil bond strength by desorption kinetics. Soil Sci. Soc. Am. J. 48, 769-772.

Lensing, H.J., Vogt, M. and Herrling, B., 1994. Modeling of biologically mediated redox processes in the subsurface. J. Hydrol. 159 (1-4), 125-143.

Leonard, J., 1992. Port Phillip Region groundwater resources - future use and management. Department of Water Resources Victoria, Melbourne.

Leonard, J.G., 1979. Preliminary assessment of the groundwater resources in the Port Phillip region. No 66, Geological Survey Victoria

Department of Minerals and Energy, Melbourne.

Leonard, J.G., 1983. Hydrogeology and hydrochemistry of an unconsolidated Tertiary aquifer system in the southeastern suburbs of Melbourne, Victoria. In: M.J. Knight, E.J. Minty, R.B. Smith and Geological Society of Australia. Engineering Geology Specialist Group. (Eds.), Collected case studies in engineering geology, hydrogeology and environmental geology, Special publication / Geological Society Australia no. 11. Engineering Geology Specialist Group Geological Society of Australia, Sydney, 181-208.

Li, A. and Dai, J., 2006. Effects of fulvic fractions on the pH-dependent sorption of Cu(II) to kaolinite. Water Res. 40 (10), 1951-1956.

Liang, L., McCarthy, J.F., Jolley, L.W., McNabb, J.A. and Mehlhorn, T.L., 1993. Iron dynamics: Transformation of Fe(II)/Fe(III) during injection of natural organic matter in a sandy aquifer. Geochim. Cosmochim. Ac. 57 (9), 1987-1999.

Liang, L. and Morgan, J.J., 1990. Chemical aspects of iron oxide coagulation in water: Laboratory studies and implications for natural systems. Aquatic Sciences - Research Across Boundaries 52 (1), 32-55.

Liebens, J., 2001. Heavy metal contamination of sediments in stormwater management systems: the effect of land use, particle size, and age. Environ. Geol. 41 (3-4), 341-351.

Limousin, G., Gaudet, J.P., Charlet, L., Szenknect, S., Barthes, V. and Krimissa, M., 2007. Sorption isotherms: A review on physical bases, modeling and measurement. Appl. Geochem. 22 (2), 249-275.

Lin, E., Page, D. and Pavelic, P., 2008. A new method to evaluate polydisperse kaolinite clay particle removal in roughing filtration using colloid filtration theory. Water Res. 42 (3), 669-676.

Lindberg, R.D. and Runnels, D.D., 1984. Ground Water Redox Reactions: An Analysis of Equilibrium State Applied to Eh Measurements and Geochemical Modeling. Science 225 (4665), 925-927.

Linde, M., Öborn, I. and Gustafsson, J., 2007. Effects of Changed Soil Conditions on the Mobility of Trace Metals in Moderately Contaminated Urban Soils. Water Air Soil Pollut. 183 (1), 69-83.

Liu, C.-L., Chang, T.-W., Wang, M.-K. and Huang, C.-H., 2006. Transport of cadmium, nickel, and zinc in Taoyuan red soil using one-dimensional convective-dispersive model. Geoderma 131 (1-2), 181-189.

Liu, D., Johnson, P.R. and Elimelech, M., 1995. Colloid Deposition Dynamics in Flow-Through Porous Media: Role of Electrolyte Concentration. Environ. Sci. Technol. 29 (12), 2963-2973.

Lofts, S. and Tipping, E., 1998. An assemblage model for cation binding by natural particulate matter. Geochim. Cosmochim. Ac. 62 (15), 2609-2625.

Lovley, D.R., Coates, J.D., Blunt-Harris, E.L., Phillips, E.J.P. and Woodward, J.C., 1996. Humic substances as electron acceptors for microbial respiration. Nature 382 (August), 445-448.

Lovley, D.R. and Goodwin, S., 1988. Hydrogen concentrations as an indicator of the predominant terminal electron-accepting reactions in aquatic sediments. Geochim. Cosmochim. Ac. 52 (12), 2993-3003.

Lovley, D.R. and Phillips, E.J.P., 1988. Novel Mode of Microbial Energy Metabolism: Organic Carbon Oxidation Coupled to Dissimilatory Reduction of Iron or Manganese. Appl. Environ. Microbiol. 54 (6), 1472-1480.

Lu, Y. and Allen, H.E., 2002. Characterization of copper complexation with natural dissolved organic matter (DOM)—link to acidic moieties of DOM and competition by Ca and Mg. Water Res. 36, 5083-5101.

Lu, Y. and Allen, H.E., 2006. A predictive model for copper partitioning to suspended particulate matter in river waters. Environ. Pollut. 143 (1), 60-72.

Luoma, S.N. and Jenne, E.A., 1976. Estimating Bioavailability of Sediment-Bound Trace Metals with Chemical Extractants. Trace Substances in Environmental Health X, 343-351.

Lyklema, J., 1991. Fundamentals of interface and colloid science. Academic Press, London ; Sydney.

Ma, H., Allen, H.E. and Yin, Y., 2001. Characterization of isolated fractions of dissolved organic matter from natural waters and a wastewater effluent. Water Res. 35 (4), 985-996.

Ma, L.Q. and Dong, Y., 2004. Effects of incubation on solubility and mobility of trace metals in two contaminated soils. Environ. Pollut. 130 (3), 301-307.

MacDonald, J.D. and Hendershot, W.H., 2006. Modelling trace metal partitioning in forest floors of northern soils near metal smelters. Environ. Pollut. 143 (2), 228-240.

MacQuarrie, K.T.B., Sudicky, E.A. and Frind, E.O., 1990. Simulation of Biodegradable Organic Contaminants in Groundwater 1. Numerical Formulation in Principal Directions. Water Resour. Res. 26 (2), 207-222.

Maine, M.A., Sune, N., Hadad, H., Sanchez, G. and Bonetto, C., 2007. Removal efficiency of a constructed wetland for wastewater treatment according to vegetation dominance. Chemosphere 68 (6), 1105-1113.

Makepeace, D.K., Smith, D.W. and Stanley, S.J., 1995. Urban stormwater quality: summary of contaminant data. Crit. Rev. Environ. Sci. Technol. 25 (2), 93-139.

Malandrino, M., Abollino, O., Giacomino, A., Aceto, M. and Mentasti, E., 2006. Adsorption of heavy metals on vermiculite: Influence of pH and organic ligands. J. Colloid Interface Sci. 299 (2), 537-546.

Malard, F. and Hervant, F., 1999. Oxygen supply and the adaptations of animals in groundwater. Freshwater Biol. 41 (1), 1-30.

Maliva, R.G., Guo, W. and Missimer, T.M., 2006. Aquifer Storage and Recovery: Recent Hydrogeological Advances and System Performance. Water Environ. Res. 78 (13), 2428-2435.

Manning, B.A. and Goldberg, S., 1996. Modeling Competitive Adsorption of Arsenate with Phosphate and Molybdate on Oxide Minerals. Soil Sci. Soc. Am. J. 60, 121-131.

Manning, P.G. and Ramamoorthy, S., 1973. Equilibrium studies of metal-ion complexes of interest to natural waters-VII. Mixed-ligand complexes of Cu(II) involving fulvic acid as primary ligand. J. Inorg. Nucl. Chem. 35, 1577-1581.

Maraqa, M.A., 2001. Prediction of mass-transfer coefficient for solute transport in porous media. J. Contam. Hydrol. 53 (1-2), 153-171.

Marguí, E., Salvado, V., Queralt, I. and Hidalgo, M., 2004. Comparison of three-stage sequential extraction and toxicity characteristic leaching tests to evaluate metal mobility in mining wastes. Anal. Chim. Ac. 524 (1-2), 151-159.

Marks, R., Chapman, F., Lane, S. and Purdie, M., 2005. Parafield urban stormwater harvesting facility. Water 32 (5), 42-45.

Marshall, W.E. and Champagne, E.T., 1995. Agricultural byproducts as adsorbents for metal ions in laboratory prepared solutions and in manufacturing wastewater. J. Environ. Sci. Health Part A A 30 (2), 241-261.

Martin, J.M., Nirel, P. and Thomas, A.J., 1987. Sequential extraction techniques: Promises and problems. Mar. Chem. 22 (2-4), 313-341.

Martínez-Villegas, N. and Martínez, C.E., 2008. Solid- and Solution-Phase Organics Dictate Copper Distribution and Speciation in Multicomponent Systems Containing Ferrihydrite, Organic Matter, and Montmorillonite. Environ. Sci. Technol. 42 (8), 2833-2838.

Mason, Y., Ammann, A.A., Ulrich, A. and Sigg, L., 1999. Behavior of Heavy Metals, Nutrients, and Major Components during Roof Runoff Infiltration. Environ. Sci. Technol. 33 (10), 1588-1597.

Mathur, S.S. and Dzombak, D.A., 2006. Surface complexation modeling: goethite. In: J. Lützenkirchen (Ed.), Surface complexation modelling. Interface Science and Technology. Elsevier, 443-468.

Matocha, C.J., Karathanasis, A.D., Rakshit, S. and Wagner, K.M., 2005. Reduction of Copper(II) by Iron(II). J. Environ. Qual. 34 (5), 1539-1546.

Matsunaga, T., Karametaxas, G., von Gunten, H.R. and Lichtner, P.C., 1993. Redox chemistry of iron and manganese minerals in river-recharged aquifers: A model interpretation of a column experiment. Geochim. Cosmochim. Ac. 57 (8), 1691-1704.
McBride, M.B., 1978. Copper(II) interactions with kaolinite: Factors controlling adsorption. Clays Clay Miner. 26, 101-106.
McBride, M.B., 1982. Cu2+-adsorption characteristics of aluminum hydroxide and oxyhydroxides. Clays Clay Miner. 30 (1), 21-28.
McBride, M.B., 1985. Influence of glycine on Cu2+ adsorption by microcrystalline gibbsite and boehmite. Clays Clay Miner. 33, 397-402.
McBride, M.B., 1989. Reactions controlling heavy metal solubility in soils. Adv. Soil Sci. 10, 1-56.
McBride, M.B., 1994. Environmental chemistry of soils. Oxford University Press, New York.
McBride, M.B. and Blasiak, J.J., 1979. Zinc and copper solubility as a function of pH in an acid soil. Soil Sci. Soc. Am. J. 43, 866-870.
McBride, M.B., Sauvé, S. and Hendershot, W., 1997. Solubility control of Cu, Zn, Cd and Pb in contaminated soils. Eur. J. Soil Sci. 48, 337-346.
McCarthy, D.T., Deletic, A., Mitchell, V.G., Fletcher, T.D. and Diaper, C., 2008. Uncertainties in stormwater E. coli levels. Water Res. 42 (6-7), 1812-1824.
McCarthy, J.F. and Degueldre, C., 1993. Sampling and characterization of colloids and particles in groundwater for studying their role in contaminant transport. In: J. Buffle and H.P. Van Leeuwen (Eds.), Environmental Particles. Environmental Analytical and Physical Chemistry Series. Lewis Publisher, Boca Raton, 247-315.
McCarthy, J.F. and McKay, L.D., 2004. Colloid Transport in the Subsurface: Past, Present, and Future Challenges. Vadose Zone J. 3 (2), 326-337.
McCarthy, J.F., Williams, T.M., Liang, L.Y., Jardine, P.M., Jolley, L.W., Taylor, D.L., Palumbo, A.V. and Cooper, L.W., 1993. Mobility of Natural Organic Matter in a Sandy Aquifer. Environ. Sci. Technol. 27 (4), 667-676.
McCarthy, J.F. and Zachara, J.M., 1989. Subsurface transport of contaminants. Environ. Sci. Technol. 23 (5), 496-502.
McDowell-Boyer, L.M., 1992. Chemical mobilization of micron-sized particles in saturated porous media under steady flow conditions. Environ. Sci. Technol. 26 (3), 586-593.
McKenzie, R.M., 1980. The Adsorption of Lead and Other Heavy Metals on Oxides of Manganese and Iron. Aust. J. Soil Res. 18, 61-73.
McKinley, J.P. and Jenne, E.A., 1991. Experimental Investigation and Review of the “Solids Concentration” Effect in Adsorption Studies. Environ. Sci. Technol. 25 (12), 2082-2087.
McLaren, R.G., Lawson, D.M. and Swift, R.S., 1986. Sorption and desorption of cobalt by soils and soil components. J. Soil Sci. 37, 413-426.
McLaren, R.G., Williams, J.G. and Swift, R.S., 1983. The adsorption of copper by soil samples from Scotland at low equilibrium solution concentrations. Geoderma 31 (2), 97-106.
McLean, J., 2004. Aurora – Delivering a Sustainable Urban Water System for a New Suburb. In: T. Daniell (Ed.), Int. Conference on Water Sensitive Urban Design: cities as catchments, WSUD 2004, Adelaide, Australia, pp. 22-32.
McMahon, P.B. and Chapelle, F.H., 1991. Microbial production of organic acids in aquitard sediments and its role in aquifer geochemistry. Nature 349 (6306), 233-235.
McQuarrie, J.P. and Carlson, K., 2003. Secondary Benefits of Aquifer Storage and Recovery: Disinfection By-Product Control. J. Environ. Eng. 129 (5), 412-418.
Medina, D.A.B., 2006. Zinc mobility in groundwater: reactive transport modeling of acid drainage and contaminant behaviour at a galvanization site. Master of Science Thesis, Environmental Geochemistry, Universiteit Utrecht, Utrecht.
Mehlich, A., 1948. Determination of Cation and Anion-Exchange Properties of Soils. Soil Sci. 66, 429-445.
Meima, J.A. and Comans, R.N.J., 1998. Application of Surface Complexation/Precipitation Modeling to Contaminant Leaching from Weathered Municipal Solid Waste Incinerator Bottom Ash. Environ. Sci. Technol. 32 (5), 688-693.
Melbourne Water, 2004. MUSIC input parameters, Melbourne Water, Melbourne.
Melbourne Water, 2008. Water Storages. Melbourne Water. http://www.melbournewater.com.au/content/water/water_storages
Merdy, P., Huclier, S. and Koopal, L.K., 2006. Modeling metal-particle interaction with an Emphasis on Natural Organic Matter. Environ. Sci. Technol. 40 (24), 7459-7466.
Mesquita, M.E. and Vieira e Silva, J.M., 1996. Zinc adsorption by a calcareous soil. Copper interaction. Geoderma 69 (1-2), 137-146.
Middlemis, H., 2000. Groundwater flow modelling guideline. project 125, Murray-Darling basin commission, Perth.

Mikkelsen, P.S., Hafliger, M., Ochs, M., Jacobsen, P., Tjell, J.C. and Boller, M., 1997. Pollution of soil and groundwater from infiltration of highly contaminated stormwater - a case study. Water Sci. Technol. 36 (8-9), 325-330.

Mikkelsen, P.S., Weyer, G., Berry, C., Walden, Y., Colandini, V., Poulsen, S., Grotehusmann, D. and Rohlfing, R., 1994. Pollution from urban stormwater infiltration. Water Sci. Technol. 29 (1/2), 293–302.

Miller, G.T., 2005. Living in the environment : principles, connections, and solutions. Thomson Brooks/Cole, Pacific Grove, CA.

Miller, R., Correll, R., Dillon, P. and Kookana, R., 2002. ASRRI: a predictive index of contaminant attenuation during aquifer storage and recovery. In: P. Dillon (Ed.), Management of Aquifer Recharge for Sustainability, Proceedings of the 4th International Symposium on Artificial Recharge of Groundwater. Balkema, Adelaide, Australia, pp. 68-74.

Miller, W.P., Martens, D.C. and Zelazny, L.W., 1986a. Effect of sequence in extraction of trace metals from soils. Soil Sci. Soc. Am. J. 50 (3), 598-601.

Miller, W.P., Martens, D.C., Zelazny, L.W. and Kornegay, E.T., 1986b. Forms of solid phase copper in copper-enriched swine manure. J. Environ. Qual 15 (1), 69-72.

Mills, W.B., Liu, S. and Fong, F.K., 1991. Literature review and model (COMET) for colloid/metals transport in porous media. Ground Water 29 (2), 199-208.

Milne, C.J., Kinniburgh, D.G. and Tipping, E., 2001. Generic NICA-Donnan Model Parameters for Proton Binding by Humic Substances. Environ. Sci. Technol. 35 (10), 2049-2059.

Milne, C.J., Kinniburgh, D.G., van Riemsdijk, W.H. and Tipping, E., 2003. Generic NICA-Donnan Model Parameters for Metal-Ion Binding by Humic Substances. Environ. Sci. Technol. 37 (5), 958-971.

Mirecki, J.E., 2004. Water-Quality Changes During Cycle Tests at Aquifer Storage Recovery (ASR) Systems of South Florida. ERDC/EL TR-04-8, US Army Corps of Engineers.

Miretzky, P., Munoz, C. and Carrillo-Chavez, A., 2006. Experimental Zn(II) retention in a sandy loam soil by very small columns. Chemosphere 65 (11), 2082-2089.

Mitchell, G., 2004. Integrated Urban Water Management: A review of current Australian practice, CSIRO.

Mitchell, G.V., Mein, R.G. and McMahon, T., 2002. Utilising Stormwater and Wastewater Resources in Urban Areas. Aust. J. Water Resour. 6 (1), 31-43.

Monod, J., 1949. The growth of bacterial cultures. Annu. Rev. Microbiol. 3, 371- 394.

Morabito, R., 1995. Extraction techniques in speciation analysis of environmental samples. Fresenius J. Anal. Chem. 351 (4), 378-385.

Mosley, L.M., Hunter, K.A. and Ducker, W.A., 2003. Forces between Colloid Particles in Natural Waters. Environ. Sci. Technol. 37 (15), 3303-3308.

Msaky, J.J. and Calvet, R., 1990. Adsorption behavior of copper and zinc in soils: influence of pH on adsorption characteristics. Soil Sci. 150 (2), 513-522.

Mulligan, C.N. and Yong, R.N., 2004. Natural attenuation of contaminated soils. Environ. Int. 30 (4), 587-601.

Muris, M., Delolme, C., Gaudet, J.P. and Spadini, L., 2005. Assessment of biofilm destabilisation and consequent facilitated zinc transport. Water Sci. Technol. 51 (2), 21-28.

Murphy, E.M. and Zachara, J.M., 1995. The role of sorbed humic substances on the distribution of organic and inorganic contaminants in groundwater. Geoderma 67 (1-2), 103-124.

Murphy, E.M., Zachara, J.M., Smith, S.C. and Phillips, J.L., 1992. The sorption of humic acids to mineral surfaces and their role in contaminant binding. Sci. Total Environ. 117-118, 413-423.

Murray, A.G. and Parslow, J.S., 1999. Modelling of nutrient impacts in Port Phillip Bay .. a semi-enclosed marine Australian ecosystem. Mar. Freshwater Res. 50, 597-611.

Murray, D.J., Healy, T.W. and Fuerstenau, D.W., 1968. The adsorption of aqueous metal on colloidal hydrous manganese oxide. Adv. Chem. Ser. 79, 74-81.

Muthukaruppan, M., Chiew, F. and Wong, T., 2002. Size Distribution and Partitioning of Urban Pollutants, 9th International Conference on Urban Drainage. American Society of Civil Engineers, Portland, Oregon, USA.

Naidu, R. and Harter, R.D., 1998. Effect of different organic ligands on cadmium sorption by and extractability from soils. Soil Sci. Soc. Am. J. 62, 644-650.

Nash, J.E. and Sutcliffe, J.V., 1970. River flow forecasting through conceptual models part I -- A discussion of principles. J. Hydrol. 10 (3), 282-290.

Nesbitt, H.W. and Young, G.M., 1982. Early Proterozoic climates and plate motions inferred from major element chemistry of lutites. Nature 299 (5885), 715-717.

NHMRC (National Health and Medical Research Council), 2004. Australian Drinking Water Guidelines, National Water Quality Management Strategy. Commonwealth of Australia.

Nicholson, B.C., Dillon, P.J. and Pavelic, P., 2002. Fate of disinfection by-products during aquifer storage and recovery. In: P. Dillon (Ed.), Management of Aquifer Recharge for Sustainability, Proceedings of the International Symposium on Artificial Recharge of Groundwater, 4th, Adelaide, Australia, Sept. 22-26, 2002, pp. 155-160.

Nicholson, R.V., Cherry, J.A. and Reardon, E.J., 1983. Migration of contaminants in groundwater at a landfill: A case study 6. Hydrogeochemistry. J. Hydrol. 63 (1-2), 131-176.

Nightingale, H.I. and Bianchi, W.C., 1977. Ground-water turbidity resulting from artificial recharge. Ground Water 15 (2), 146-152.

Nirel, P.M.V. and Morel, F.M.M., 1990. Pitfalls of sequential extractions. Water Res. 24 (8), 1055-1056.

Nocedal, J. and Wright, S.J., 2006. Numerical Optimization. Springer, New York, NY.

Norrström, A.C., 2005. Metal mobility by de-icing salt from an infiltration trench for highway runoff. Appl. Geochem. 20 (10), 1907-1919.

Nowack, B. and Sigg, L., 1996. Adsorption of EDTA and Metal–EDTA Complexes onto Goethite. J. Colloid Interface Sci. 177, 106-121.

Nowack, B. and Sigg, L., 1997. Dissolution of Fe(III) (hydr) oxides by metal-EDTA complexes. Geochim. Cosmochim. Ac. 61 (5), 951-963.

NRC (National Research Council), 2007. Prospects for Managed Underground Storage of Recoverable Water, The National Academy of Sciences, Washington, D.C., USA.

NWQMS, 2006. Australian Guidelines for Water Recycling: Managing Health and Environmental Risks. In: N.W.Q.M.S. (NWQMS) (Ed.). Natural Resource Management Ministerial Council, Environment Protection and Heritage Council, Australian Health Ministers Conference.

NWQMS, 2007. Australian Guidelines for Water Recycling: Managing Health and Environmental Risks (Phase 2): Augmentation of Drinking Water Supplies. In: N.W.Q.M.S. (NWQMS) (Ed.). Natural Resource Management Ministerial Council, Environment Protection and Heritage Council, Australian Health Ministers Conference.

Obropta, C.C. and Kardos, J.S., 2007. Review of Urban Stormwater Quality Models: Deterministic, Stochastic, and Hybrid Approaches1. J. Am. Water Resour. Assoc. 43 (6), 1508-1523.

O'Connor, D.J. and Connolly, J.P., 1980. The effect of concentration of adsorbing solids on the partition coefficient. Water Res. 14 (10), 1517-1523.

OECD/OCDE, 2000. OECD guideline for the testing of chemicals: adsorption - desorption using a batch equilibrium method. 106, OECD.

Oliver, Y.M., Gerritse, R.G., Dillon, P.J. and J., S.K.R., 1996. Fate and Mobility of Stormwater and Wastewater Contaminants in Aquifers - 2. Adsorption Studies in Carbonate Aquifers. 68, Centre for Groundwater Studies, Adelaide.

Olivie-Lauquet, G., Gruau, G., Dia, A., Riou, C., Jaffrezic, A. and Henin, O., 2001. Release of Trace Elements in Wetlands: Role of Seasonal Variability. Water Res. 35 (4), 943-952.

Oliviera, I.B., Demond, A.H. and Salehzadeh, A., 1996. Packing of sands for the production of homogeneous porous media. Soil Sci. Soc. Am. J. 60 (1), 49-53.

Oppel, J., Broll, G., Löffler, D., Meller, M., Römbke, J. and Ternes, T., 2004. Leaching behaviour of pharmaceuticals in soil-testing-systems: a part of an environmental risk assessment for groundwater protection. Sci. Total Environ. 328 (1-3), 265-273.

O'Rourke, M. and Shugg, A., 1998. Impacts of groundwater discharges in the catchments and streams of the Port Phillip Region. In: T.R. Weaver and C.R. Lawrence (Eds.), Groundwater: sustainable solutions. International Association of Hydrogeologists (Australian National Chapter), University of Melbourne, Melbourne, Australia, pp. 527-532.

Pabich, W., Valiela, I. and Hemond, H., 2001. Relationship between DOC concentration and vadose zone thickness and depth below water table in groundwater of Cape Cod, U.S.A. Biogeochemistry 55 (3), 247-268.

Padmanabham, M., 1983. Comparative Study of the Adsorption-Desorption Behaviour of Copper(II), Zinc(II), Cobalt(II) and Lead(II) at the Goethite-Solution Interface. Aust. J. Soil Res. 21, 515-525.

Page, D., Wakelin, S., van Leeuwen, J. and Dillon, P., 2006. Review of biofiltration processes relevant to water reclamation via aquifers, CSIRO Land and Water Science, Report 47/06.

Pan, G. and Liss, P.S., 1998. Metastable-Equilibrium Adsorption Theory I. Theoretical. J. Colloid Interface Sci. 201, 71-76.

Pan, G., Liss, P.S. and Krom, M.D., 1999. Particle concentration effect and adsorption reversibility. Colloids Surf., A 151, 127-133.

Papini, M.P., Kahie, Y.D., Troia, B. and Majone, M., 1999. Adsorption of Lead at Variable pH onto a Natural Porous Medium: Modeling of Batch and Column Experiments. Environ. Sci. Technol. 33, 4457-4464.

Pardo, M.T. and Guadalix, M.E., 1996. Zinc sorption-desorption by two Andepts: effect of pH and support medium. Eur. J. Soil Sci. 47, 257-263.

Parkhurst, D.L. and Appelo, C.A.J., 1999. User's guide to PHREEQC (version 2). 99-4259, US Geological Survey Water-Resources Investigations.

Parkhurst, D.L. and Petkewich, M.D., 2002. Geochemical modeling of an aquifer storage recovery experiment Charleston, South Carolina, Proceedings of the Artificial Recharge Workshop, April 2002, pp. 38-41.

Parsons, S. and Evans, R., 2002. Epping North Aquifer Storage and Recovery Investigation: stage 2 - Initial field investigations and preliminary analysis, Sinclair Knight Merz, Melbourne.

Parsons, S. and Sibenaler, Z., 2004. Mernda Stormwater ASR Assessment -Report on Preliminary Field Investigations: Drilling and Aquifer Pumping Test, Sinclair Knight Merz (SKM); Australian Groundwater Technologies (AGT), Melbourne.

Paulson, A.J. and Balistrieri, L., 1999. Modeling Removal of Cd, Cu, Pb, and Zn in Acidic Groundwater during Neutralization by Ambient Surface Waters and Groundwaters. Environ. Sci. Technol. 33 (21), 3850-3856.

Pavelic, P., Dillon, P., Barry, K. and Gerges, N., 2006b. Hydraulic evaluation of aquifer storage and recovery (ASR) with urban stormwater in a brackish limestone aquifer. Hydrogeol. J. 14 (8), 1544-1555.

Pavelic, P., Dillon, P., Cook, P. and Barry, K., 2006c. Characterisation of the weathered bedrock aquifer at the Rossdale Golf Club ASR trial site, CSIRO Land and Water.

Pavelic, P., Dillon, P. and Simmons, C.T., 2006a. Multiscale Characterization of a Heterogeneous Aquifer Using an ASR Operation. Ground Water 44 (2), 155-164.

Pavelic, P., Dillon, P.J., Barry, K.E., Vanderzalm, J.L., Correll, R. and Rinck-Pfeiffer, S.M., 2007. Water quality effects on clogging rates during reclaimed water ASR in a carbonate aquifer. J. Hydrol. 334, 1-16.

Pavelic, P., Ragusa, S.R., Flower, R.L., Rinck-Pfeiffer, S.M. and Dillon, P.J., 1998. Diffusion chamber method for in situ measurement of pathogen inactivation in groundwater. Water Res. 32 (4), 1144-1150.

Peck, W.A., Neilson, J.L., Olds, R.J. and Seddon, K.D. (Eds.), 1992. Engineering geology of Melbourne : proceedings of the Seminar on Engineering Geology of Melbourne, Melbourne, Victoria, Australia, 16 September 1992. A.A. Balkema, Rotterdam.

Peitgen, H.-O., 1989. Newton's method and dynamical systems. Kluwer Academic, Dordrech; Boston.

Petrunic, B.M., MacQuarrie, K.T.B. and Al, T.A., 2005. Reductive dissolution of Mn oxides in river-recharged aquifers: a laboratory column study. J. Hydrol. 301, 163-181.

Pettigrove, V. and Hoffmann, A., 2003. Major sources of heavy metal pollution during base flows from sewered urban catchments in the city of Melbourne, Proceedings of the 3rd South Pacific Conference on Stormwater and Aquatic Resource Protection and the Annual Australasian Chapter of the International Erosion Control Association, Auckland, New Zealand, May 14-16 2003., pp. 10.

Pitcher, S.K., Slade, R.C.T. and Ward, N.I., 2004. Heavy metal removal from motorway stormwater using zeolites. Sci. Total Environ. 334-335, 161-166.

Pitt, R., Clark, S. and Field, R., 1999. Groundwater contamination potential from stormwater infiltration practices. Urban Water 1 (3), 217-236.

Plummer, L.N., Wigley, T.M.L. and Parkhurst, D.L., 1978. The kinetics of calcite dissolution in CO 2 - water systems at 5 degrees to 60 degrees C and 0.0 to 1.0 atm CO 2. Am. J. Sci. 278 (2), 179-216.

Po, M., Kaercher, J.D. and Nacncarrow, B.E., 2003. Literature review of factors influencing public perceptions of water reuse. Technical Report 54/03, CSIRO Land and Water.

Ponthieu, M., Juillot, F., Hiemstra, T., van Riemsdijk, W.H. and Benedetti, M.F., 2006. Metal ion binding to iron oxides. Geochim. Cosmochim. Ac. 70 (11), 2679-2698.

Postma, D., 1993. The reactivity of iron oxides in sediments: A kinetic approach. Geochim. Cosmochim. Ac. 57 (21-22), 5027-5034.

Postma, D. and Appelo, C.A.J., 2000. Reduction of Mn-oxides by ferrous iron in a flow system: column experiment and reactive transport modeling. Geochim. Cosmochim. Ac. 64 (7), 1237-1247.

Postma, D. and Jakobsen, R., 1996. Redox zonation: Equilibrium constraints on the Fe(III)/SO4-reduction interface. Geochim. Cosmochim. Ac. 60 (17), 3169-3175.

Powelson, D.K., Gerba, C.P. and Yahya, M.T., 1993. Virus transport and removal in wastewater during aquifer recharge. Water Res. 27 (4), 583-590.

Press, W.H., Teukolsky, S.A., Vetterling, W.T. and Flannery, B.P., 1992. Numerical Recipes in C - The Art of Scientific Computing. Cambridge University Press, Cambridge; New York.

Prommer, H., 2002. PHT3D: A reactive Multicomponent Transport Model for Saturated Porous Media. Contaminated Land Assessment and Remediation Research Centre, The University of Edinburgh, UK, pp. 132.

Prommer, H., Barry, D.A. and Davis, G.B., 2002. Modelling of physical and reactive processes during biodegradation of a hydrocarbon plume under transient groundwater flow conditions. J. Contam. Hydrol. 59 (1-2), 113-131.

Prommer, H., Barry, D.A. and Zheng, C., 2003. MODFLOW/MT3DMS-based reactive multicomponent transport modeling. Ground Water 41 (2), 247-257.

Prommer, H., Davis, G.B. and Barry, D.A., 1999. Geochemical changes during biodegradation of petroleum hydrocarbons: field investigations and biogeochemical modelling. Org. Geochem. 30 (6), 423-435.

Prommer, H., Grassi, M.E., Davis, A.C. and Patterson, B.M., 2007. Modeling of Microbial Dynamics and Geochemical Changes in a Metal Bioprecipitation Experiment. Environ. Sci. Technol. 41 (24), 8433-8438.

Prommer, H. and Stuyfzand, P.J., 2005. Identification of Temperature-Dependent Water Quality Changes during a Deep Well Injection Experiment in a Pyritic Aquifer. Environ. Sci. Technol. 39 (7), 2200-2209.

Pulford, I.D., 1986. Mechanisms controlling zinc solubility in soils. J. Soil Sci. 37, 427-438.

Puls, R.W. and Powell, R.M., 1992. Transport of inorganic colloids through natural aquifer material: implications for contaminant transport. Environ. Sci. Technol. 26 (3), 614-621.

Pyne, R.D.G., 1995. Groundwater recharge through wells: a guide to aquifer storage recovery. Lewis Publishers, Boca Raton.

Pyne, R.D.G., 2006. Attenuation of Disinfection Byproducts during ASR Storage. Southwest Hydrology (Nov/Dec), 26-34.

Qin, J.-J., Htun Oo, M., Nyunt Wai, M., Lee, H., Hong, S.P., Kim, J.E., Xing, Y. and Zhanga, M., 2005. Pilot study for reclamation of secondary treated sewage effluent. Desalination 171 (3), 299-305.

Quevauviller, P., Rauret, G., Muntau, H., Ure, A.M., Rubio, R., López-Sánchez, J.F., Fiedler, H.D. and Griepink, B., 1994. Evaluation of a sequential extraction procedure for the determination of extractable trace metal contents in sediments. Fresenius J. Anal. Chem. 349 (12), 808-814.

Radcliffe, J.C., 2004. Water recycling in Australia, Australian Academy of Technological Sciences and Engineering, Burwood, VIC.

Rangsivek, R. and Jekel, M.R., 2005. Removal of dissolved metals by zero-valent iron (ZVI): Kinetics, equilibria, processes and implications for stormwater runoff treatment. Water Res. 39 (17), 4153-4163.

Rattray, K.J., 1999. Geochemical reactions induced in carbonate bearing aquifers through artificial recharge. MSc Thesis, School of Earth Sciences, Flinders University of South Australia, Adelaide.

Raveh, A. and Avnimelech, Y., 1978. The effect of drying on the colloidal properties and stability of humic compounds. Plant and Soil 50, 545-552.

Raymond, J.W., Rogers, T.N., Shonnard, D.R. and Kline, A.A., 2001. A review of structure-based biodegradation estimation methods. J. Hazard. Mater. 84 (2-3), 189-215.

Read, J., Wevill, T., Fletcher, T. and Deletic, A., 2008. Variation among plant species in pollutant removal from stormwater in biofiltration systems. Water Res. 42 (4-5), 893-902.

Reardon, E.J., 1981. Kd's – Can they be used to describe reversible ion sorption reaction in contaminant migration? Ground Water 19, 279–286.

Reedy, O.C., Jardine, P.M., Wilson, G.V. and Selim, H.M., 1996. Quantifying the diffusive mass transfer of nonreactive solutes in columns of fractured saprolite using flow interruption. Soil Sci. Soc. Am. J. 60 (5), 1376-1384.

Rees, R.M. and Parker, J.P., 2005. Filtration increases the correlation between water extractable organic carbon and soil microbial activity. Soil Biol. Biochem. 37 (12), 2240-2248.

Reichard, P.U., Kretzschmar, R. and Kraemer, S.M., 2007. Rate laws of steady-state and non-steady-state ligand-controlled dissolution of goethite. Colloids Surf., A 306 (1-3), 22-28.

Rendell, P.S., Batley, G.E. and Cameron, A.J., 1980. Adsorption as a control of metal concentrations in sediment extracts. Environ. Sci. Technol. 14 (3), 314-318.

Rinck-Pfeiffer, S., 2000. Physical and biochemical clogging processes arising from aquifer storage and recovery (ASR) with treated wastewater. PhD Thesis, School of Chemistry, Physics and Earth Sciences, Flinders University of South Australia, Adelaide.

Rinck-Pfeiffer, S., Pitman, C. and Dillon, P., 2006. Stormwater ASR in practice and ASTR (Aquifer Storage Transfer and Recovery) under investigation in Salisbury, South Australia, Proceedings of the 5th International Symposium on Management of Aquifer Recharge ISMAR5, Berlin, Germany, 11–16 June 2005. Recharge systems for protecting and enhancing groundwater resources. IHP-VI, Series on Groundwater No. 13. UNESCO, pp. 151-159.

Robertson, A.P. and Leckie, J.O., 1998. Acid/Base, Copper Binding, and Cu2+/H+ Exchange Properties of Goethite, an Experimental and Modeling Study. Environ. Sci. Technol. 32 (17), 2519-2530.

Robertson, A.P. and Leckie, J.O., 1999. Acid/Base, Copper Binding, and Cu2+/H+ Exchange Properties of a Soil Humic Acid, an Experimental and Modeling Study. Environ. Sci. Technol. 33 (5), 786-795.

Rode, M., Suhr, U. and Wriedt, G., 2007. Multi-objective calibration of a river water quality model--Information content of calibration data. Ecol. Model. 204 (1-2), 129-142.

Rose, A.L. and Waite, D.T., 2007. Reconciling kinetic and equilibrium observations of iron(III) solubility in aqueous solutions with a polymer-based model. Geochim. Cosmochim. Ac. 71 (23), 5605-5619.

Rowell, D.L., 1994. Soil science: methods and applications. Longman Scientific & Technical; Wiley, Harlow, Essex; New York.

Roy, S.B. and Dzombak, D.A., 1996. Colloid release and transport processes in natural and model porous media. Colloids Surf., A 107, 245-262.

Rubin, J. and James, R.V., 1973. Dispersion-Affected Transport of Reacting Solutes in Saturated Porous Media: Galerkin Method Applied to Equilibrium-Controlled Exchange in Unidirectional Steady Water Flow. Water Resour. Res. 9 (5), 1332-1356.

Ryan, J.N. and Elimelech, M., 1996. Colloid mobilization and transport in groundwater. Colloids Surf., A 107, 1-56.

Ryan, J.N. and Gschwend, P.M., 1990. Colloid mobilization in two Atlantic coastal plain aquifers: field studies. Water Resour. Res. 26 (2), 307-322.

Ryan, J.N. and Gschwend, P.M., 1994. Effects of Ionic Strength and Flow Rate on Colloid Release: Relating Kinetics to Intersurface Potential Energy. J. Colloid Interface Sci. 164 (1), 21-34.

Saaltink, M.W., Ayora, C., Stuyfzand, P.J. and Timmer, H., 1998. Modelling the effects of deep artificial recharge on groundwater quality. In: J.H. Peters and et al. (Eds.), Artificial Recharge of Groundwater; Proceedings of the Third International Symposium on Artificial Recharge of Groundwater - Tisar 98. Balkema, Amsterdam, Netherlands, pp. 423-425.

Saaltink, M.W., Ayora, C., Stuyfzand, P.J. and Timmer, H., 2003. Analysis of a deep well recharge experiment by calibrating a reactive transport model with field data. J. Contam. Hydrol. 65 (1-2), 1-18.

Sahuquillo, A., Lopez-Sanchez, J.F., Rubio, R., Rauret, G., Thomas, R.P., Davidson, C.M. and Ure, A.M., 1999. Use of a certified reference material for extractable trace metals to assess sources of uncertainty in the BCR three-stage sequential extraction procedure. Anal. Chim. Ac. 382 (3), 317-327.

Saiers, J.E. and Hornberger, G.M., 1999. The influence of ionic strength on the facilitated transport of cesium by kaolinite colloids. Water Resour. Res. 35 (6), 1713-1727.

Saito, T., Koopal, L.K., Nagasaki, S. and Tanaka, S., 2005. Analysis of Copper Binding in the Ternary System Cu2+/Humic Acid/Goethite at Neutral to Acidic pH. Environ. Sci. Technol. 39 (13), 4886-4893.

Sansalone, J.J., 1999. Adsorptive infiltration of metals in urban drainage - media characteristics. Sci. Total Environ. 235 (1-3), 179-188.

Sansalone, J.J. and Buchberger, S.G., 1997. Partitioning and first flush of metals in urban roadway storm water. J. Environ. Eng. 123 (2), 134-143.

Sansalone, J.J., Buchberger, S.G. and Koechling, M.T., 1995. Correlations between heavy metals and suspended solids in highway runoff: implications for control strategies. Transportation Research Record 1483, 112-119.

Sastre, J., Rauret, G. and Vidal, M., 2007. Sorption-desorption tests to assess the risk derived from metal contamination in mineral and organic soils. Environ. Int. 33 (2), 246-256.

Sauvé, S., Hendershot, W. and Allen, H.E., 2000. Solid-Solution Partitioning of Metals in Contaminated Soils: Dependence on pH, Total Metal Burden, and Organic Matter. Environ. Sci. Technol. 34 (7), 1125-1131.

Scheidegger, A., Bürgisser, C.S., Borkovec, M., Sticher, H., Meeussen, H. and van Riemsdijk, W.H., 1994. Convective transport of acids and bases in porous media. Water Resour. Res. 30 (11), 2937–2944.

Scheidegger, A.M. and Sparks, D.L., 1996. A critical assessment of sorption-desorption mechanisms at the soil mineral/water interface. Soil Sci. 161 (12), 813-831.

Schijven, J.F., Medema, G., Vogelaar, A.J. and Hassanizadeh, S.M., 2000. Removal of microorganisms by deep well injection. J. Contam. Hydrol. 44 (3-4), 301-327.

Schindler, P.W., Fürst, B., Dick, R. and Wolf, P.U., 1976. Ligand properties of surface silanol groups. I. Surface complex formation with Fe3+, Cu2+,Cd2+ and Pb2+. J. Colloid Interface Sci. 55 (2), 469-475.

Schindler, P.W. and Stumm, W., 1987. The Surface Chemistry of Oxides, Hydroxides, and Oxide Minerals In: W. Stumm and J.J. Morgan (Eds.), Aquatic Surface Chemistry: Chemical Processes at the Particle-Water Interface, 83-110.

Schlieker, M., Schuring, J., Hencke, J. and Schulz, H.D., 2001. The influence of redox processes on trace element mobility in a sandy aquifer--an experimental approach. J. Geochem. Explor. 73 (3), 167-179.

Schmitt, D., 2002. Charakterisierung der Bindung von Metallionen an natürliche organische Substanzen und deren Auswirkungen auf Adsorption und Transport, Chemical Engineering, University Fridericiana Karlsruhe, Karlsruhe.

Schmitt, D., Saravia, F., Frimmel, F.H. and Schuessler, W., 2003. NOM-facilitated transport of metal ions in aquifers: importance of complex-dissociation kinetics and colloid formation. Water Res. 37 (15), 3541-3550.

Schnitzer, M., 1969. Reactions between Fulvic acid, a Soil Humic Compound and Inorganic Soil Constituents Soil Sci. Soc. Am. J. 33, 75-81.

Schnitzer, M. and Kodama, 1966. Montmorillonite: Effect of pH on Its Adsorption of a Soil Humic Compound. Science 153 (3731), 70-71.

Schnitzer, M. and Skinner, S.I.M., 1966. Organo-metallic interactions in soils: 5. Stability constants of Cu++, Fe++, and Zn++-Fulvic acid Complexes. Soil Sci. 102 (6), 361-365.

Scholze, R., Novotny, V. and Schonter, R., 1993. Efficiency of best management practices for controlling priority pollutants in runoff. Water Sci. Technol. 28 (3-5), 215-224.

Schroth, B.K. and Sposito, G., 1998. Effect of Landfill Leachate Organic Acids on Trace Metal Adsorption by Kaolinite. Environ. Sci. Technol. 32 (10), 1404-1408.

Schulte, A., 1995. Influence of Soil Sample Preparation on Cd and Cu Adsorption in Acid Forest Soils. J. Plant Nutr. Soil Sci. 158, 465-467.

Schulte, A. and Beese, F., 1994. Adsorption Density Isotherms for Heavy Metals and Their Ecological Signification. J. Plant Nutr. Soil Sci. 157, 295-303.

Schweich, D. and Sardin, M., 1981. Adsorption, partition, ion exchange and chemical reaction in batch reactors or in columns -- A review. J. Hydrol. 50, 1-33.

Seaman, J.C., Bertsch, P.M. and Miller, W.P., 1995. Chemical Controls on Colloid Generation and Transport in a Sandy Aquifer. Environ. Sci. Technol. 29 (7), 1808-1815.

Seidel-Morgenstern, A., 2004. Experimental determination of single solute and competitive adsorption isotherms. J. Chromatogr., A 1037 (1-2), 255-272.

Sekaly, A.L.R., Mandal, R., Hassan, N.M., Murimboh, J., Chakrabarti, C.L., Back, M.H., Grégoire, D.C. and Schroeder, W.H., 1999. Effect of metal/fulvic acid mole ratios on the binding of Ni(II), Pb(II), Cu(II), Cd(II), and Al(III) by two well-characterized fulvic acids in aqueous model solutions. Anal. Chim. Ac. 402 (1-2), 211-221.

Selim, H.M., Buchter, B., Hinz, C. and Ma, L., 1992. Modeling the Transport and Retention of Cadmium in Soils: Multireaction and Multicomponent Approaches. Soil Sci. Soc. Am. J. 56 (4), 1004-1015.

Selim, H.M.E. and Iskandar, I.K., 1999. Fate and transport of heavy metals in the vadose zone. Lewis Publishers, Boca Raton.

Sen, T.K. and Khilar, K.C., 2006. Review on subsurface colloids and colloid-associated contaminant transport in saturated porous media. Adv. Colloid Interface Sci. 119 (2-3), 71-96.

Sharpin, M.G. and Morison, A.J., 1995. Environmental impacts of stormwater treatment measures. In: Australian Water and Wastewater Association (AWWA) (Ed.), 16th Federal Convention proceedings. Australian Water & Wastewater Association, Sydney, NSW, pp. 427-433.

Shum, M. and Lavkulich, L., 1999. Speciation and solubility relationships of Al, Cu and Fe in solutions associated with sulfuric acid leached mine waste rock. Environ. Geol. 38 (1), 59-68.

Shuman, L.M., 1986. Effect of ionic strength and anions on zinc adsorption by two soils. Soil Sci. Soc. Am. J. 50, 1438-1442.

Silveira, M.L., Alleoni, L.R.F., O'Connor, G.A. and Chang, A.C., 2006. Heavy metal sequential extraction methods - A modification for tropical soils. Chemosphere 64 (11), 1929-1938.

Simpson, M.J. and Landman, K.A., 2008. Theoretical analysis and physical interpretation of temporal truncation errors in operator split algorithms. Mathematics and Computers in Simulation 77 (1), 9-21.

Singh, D., McLaren, R.G. and Cameron, K.C., 2006. Zinc sorption-desorption by soils: Effect of concentration and length of contact period. Geoderma 137 (1-2), 117-125.

Sinke, A.J.C., Dury, O. and Zobrist, J., 1998. Effects of a fluctuating water table: column study on redox dynamics and fate of some organic pollutants. J. Contam. Hydrol. 33 (1-2), 231-246.

Skaggs, T.H. and Barry, D.A., 1996. Assessing uncertainty in subsurface solute transport: efficient first-order reliability methods. Environmental Software 11 (1-3), 179-184.

Skjemstad, J.O., Hayes, M.H.B. and Swift, R.S., 2002. Changes in natural organic matter during aquifer storage. In: P. Dillon (Ed.), Management of Aquifer Recharge for Sustainability, Proceedings of the 4th International Symposium on Artificial Recharge of Groundwater, Adelaide, Australia, pp. 149-154.

SKM and CSIRO Land and Water, 2005. Preliminary Hydrogeological Assessment of ASR at Rossdale Golf Club, Smart Water Fund, Developing Aquifer Storage and Recovery (ASR) Opportunities in Melbourne.

Slavek, J., Wold, J. and Pickering, W.F., 1982. Selective extraction of metal ions associated with humic acids. Talanta 29 (9), 743-749.

Smedley, P.L. and Kinniburgh, D.G., 2002. A review of the source, behaviour and distribution of arsenic in natural waters. Appl. Geochem. 17 (5), 517-568.

Smith, A. and Dillon, P., 1997. Fluid flow and biogeochemical processes in porous media: a survey of laboratory column designs. 77, Centre for Groundwater Studies (CGS), Glen Osmond.

Smith, D.C., Senior, E. and Dicks, H.M., 1999. Irrigation of Soil with Synthetic Landfill Leachate – Breakthrough Behaviour of Selected Pollutants. Water Air Soil Pollut. 109 (1), 327-342.

Smullen, J.T., Shallcross, A.L. and Cave, K.A., 1999. Updating the U.S. nationwide urban runoff quality data base. Water Sci. Technol. 39 (12), 9-16.

Song, L., Johnson, P.R. and Elimelech, M., 1994. Kinetics of Colloid Deposition onto Heterogeneously Charged Surfaces in Porous Media. Environ. Sci. Technol. 28 (6), 1164-1171.

Sonnenberg, A., 2003. Simultane Sorption von Blei(II), Kupfer(II) und Chrom(III) in Säulenversuchen mit ungestörten, versauerten Waldböden, Fakultät für Naturwissenschaften Department Chemie, Universität Paderborn.

Sparks, D.L., 2003. Environmental soil chemistry. Academic Press, Amsterdam ; Sydney.

Sparks, D.L., 2005. Sorption - Metals. In: D. Hillel and J.L. Hatfield (Eds.), Encyclopedia of soils in the environment. Elsevier, London, 532-537.

Sposito, G., 1983. On the surface complexation model of the oxide-aqueous solution interface. J. Colloid Interface Sci. 91 (2), 329-340.

Sposito, G., 1984. The surface chemistry of soils. Oxford University Press, New York.

Sposito, G., 1998. On Points of Zero Charge. Environ. Sci. Technol. 32 (19), 2815-2819.

Starr, J.L. and Parlange, J.-Y., 1979. Dispersion in soil columns: the snow plow effect. Soil Sci. Soc. Am. J. 43, 448-450.

Steefel, C.I. and Lasaga, A.C., 1994. A coupled model for transport of multiple chemical species and kinetic precipitation/dissolution reactions with application to reactive flow in single phase hydrothermal systems. Am. J. Sci. 294 (5), 529-592.

Stevenson, F.J., 1977. Nature of divalent transition metal complexes of humic acids as revealed by a modified potentiometric titration method. Soil Sci. 123 (1), 10-17.

Stevenson, F.J., 1982. Humus chemistry : genesis, composition, reactions. Wiley, New York.

Stumm, W. and Morgan, J.J., 1996. Aquatic chemistry: chemical equilibria and rates in natural waters. Environ. Sci. Technol. Wiley, New York.

Stumm, W. and Sulzberger, B., 1992. The cycling of iron in natural environments: Considerations based on laboratory studies of heterogeneous redox processes. Geochim. Cosmochim. Ac. 56 (8), 3233-3257.

Stuyfzand, P.J., 1998a. Quality changes upon injection into anoxic aquifers in the Netherlands: Evaluation of 11 experiments. In: J.H.e.a. Peters (Ed.), Artificial Recharge of Groundwater; Proceedings of the Third International Symposium on Artificial Recharge of Groundwater - Tisar 98. Balkema, Amsterdam, Netherlands, pp. 283-291.

Stuyfzand, P.J., 1998b. Simple models for reactive transport of pollutants and main constituents during artificial recharge and bank filtration. In: J.H.e.a. Peters (Ed.), Artificial Recharge of Groundwater; Proceedings of the Third International Symposium on Artificial Recharge of Groundwater - Tisar 98. Balkema, Amsterdam, Netherlands, pp. 427-434.

Stuyfzand, P.J., Vogelaar, A.J. and Wakker, J., 2002. Hydrogeochemistry of prolonged deep well injection and subsequent aquifer storage in pyritiferous sands; DIZON pilot, Netherlands. In: P. Dillon (Ed.), Management of Aquifer Recharge for Sustainability, Proceedings of the International Symposium on Artificial Recharge of Groundwater, 4th, Adelaide, Australia, Sept. 22-26, 2002, pp. 107-110.

Stuyfzand, P.J., Wakker, J.C. and Putters, B., 2006. Water quality changes during Aquifer Storage and Recovery (ASR): results from pilot Herten (Netherlands), and their implications for modeling, Proceedings of the 5th International Symposium on Management of Aquifer Recharge ISMAR5, Berlin, Germany, 11–16 June 2005. Recharge systems for protecting and enhancing groundwater resources. IHP-VI, Series on Groundwater No. 13. UNESCO, pp. 164-173.

Sun, N.-Z., Yang, S.-L. and Yeh, W.W.-G., 1998. A proposed stepwise regression method for model structure identification. Water Resour. Res. 34, 2561-2572.

Sun, X. and Davis, A.P., 2007. Heavy metal fates in laboratory bioretention systems. Chemosphere 66 (9), 1601-1609.

Sutherland, R.A., 2002. Comparison between non-residual Al, Co, Cu, Fe, Mn, Ni, Pb and Zn released by a three-step sequential extraction procedure and a dilute hydrochloric acid leach for soil and road deposited sediment. Appl. Geochem. 17, 353-365.

Swartz, C.H., Blute, N.K., Badruzzman, B., Ali, A., Brabander, D., Jay, J., Besancon, J., Islam, S., Hemond, H.F. and Harvey, C.F., 2004. Mobility of arsenic in a Bangladesh aquifer: Inferences from geochemical profiles, leaching data, and mineralogical characterization. Geochim. Cosmochim. Ac. 68 (22), 4539-4557.

Syrovetnik, K., Malmstrom, M.E. and Neretnieks, I., 2008. Modelling retention of heavy metals in the Oostriku peat bog, Estonia: Comparison of predicted and observed results. Appl. Geochem. In Press, Corrected proof, doi:10.1016/j.apgeochem.2008.01.007.

Tebes-Stevens, C.L., Espinoza, F. and Valocchi, A.J., 2001. Evaluating the sensitivity of a subsurface multicomponent reactive transport model with respect to transport and reaction parameters. J. Contam. Hydrol. 52 (1-4), 3-27.

Tessier, A., Campbell, P.G.C. and Bisson, M., 1979. Sequential extraction procedure for the speciation of particulate trace metals. Anal. Chem. 51 (7), 844-851.

Tessier, A., Fortin, D., Belzile, N., DeVitre, R.R. and Leppard, G.G., 1996. Metal sorption to diagenetic iron and manganese oxyhydroxides and associated organic matter: Narrowing the gap between field and laboratory measurements. Geochim. Cosmochim. Ac. 60 (3), 387-404.

Thiele, S. and Leinweber, P., 2001. Parameterization of Freundlich adsorption isotherms for heavy metals in soils from an area with intensive livestock production. J. Plant Nutr. Soil Sci. 164, 623-629.

Thomas, J.M., McKay, W.A., Cole, E., Landmeyer, J.E. and Bradley, P.M., 2000. The fate of haloacetic acids and trihalomethanes in an aquifer storage and recovery program, Las Vegas, Nevada. Ground Water 38 (4), 605-614.

Thompson, A., Chadwick, O.A., Rancourt, D.G. and Chorover, J., 2006. Iron-oxide crystallinity increases during soil redox oscillations. Geochim. Cosmochim. Ac. 70 (7), 1710-1727.

Thomson, E.A., Luoma, S.N., Cain, D.J. and Johansson, C., 1980. The effect of sample storage on the extraction of Cu, Zn, Mn and organic material from oxidized estuarine sediment. Water Air Soil Pollut. 14, 215-233.

Thurman, E.M., 1985. Organic geochemistry of natural waters. Developments in Biogeochemistry; 2. M. Nijhoff; Distributors for the U.S. and Canada, Kluwer Academic, Dordrecht; Boston; Hingham, MA, USA.

Tiller, K.G., Gerth, J. and Brümmer, G., 1984b. The relative affinities of Cd, Ni and Zn for different soil clay fractions and goethite. Geoderma 34 (1), 17-35.

Tiller, K.G., Gerth, J. and Brümmer, G., 1984a. The sorption of Cd, Zn and Ni by soil clay fractions: Procedures for partition of bound forms and their interpretation. Geoderma 34 (1), 1-16.

Tiller, K.G., Nayyar, V.K. and Clayton, P.M., 1979. Specific and non-specific sorption of cadmium by soil clays as influenced by zinc and calcium. Aust. J. Soil Res. 17 (1), 17-28.

Timmer, H. and Stuyfzand, P.J., 1998. Deep well recharge in a polder area near the river Rhine. In: J.H. Peters and et al. (Eds.), Artificial Recharge of Groundwater; Proceedings of the Third International Symposium on Artificial Recharge of Groundwater - Tisar 98. Balkema, Amsterdam, Netherlands, pp. 181-185.

Tipping, E., 1993. Modelling ion binding by humic acids. Colloids Surf., A 73, 117-131.

Tipping, E., 1994. WHAMC--A chemical equilibrium model and computer code for waters, sediments, and soils incorporating a discrete site/electrostatic model of ion-binding by humic substances. Computers and Geosciences 20 (6), 973-1023.

Tipping, E., 1998. Humic Ion-Binding Model VI: An Improved Description of the Interactions of Protons and Metal Ions with Humic Substances. Aquat. Geochem. 4 (1), 3-48.

Tipping, E., 2005. Modelling Al competition for heavy metal binding by dissolved organic matter in soil and surface waters of acid and neutral pH. Geoderma 127 (3-4), 293-304.

Tipping, E., Fitch, A. and Stevenson, F.J., 1995. Proton and copper binding by humic acid: application of a discrete-site/electrostatic ion-binding model. Eur. J. Soil Sci. 46 (1), 95-101.

Tipping, E. and Hurley, M.A., 1988. A model of solid-solution interactions in acid organic soils, based on the complexation properties of humic substances. Eur. J. Soil Sci. 39 (4), 505-519.
Tipping, E. and Hurley, M.A., 1992. A unifying model of cation binding by humic substances. Geochim. Cosmochim. Ac. 56 (10), 3627-3641.
Tipping, E., Rey-Castro, C., Bryan, S.E. and Hamilton-Taylor, J., 2002. Al(III) and Fe(III) binding by humic substances in freshwaters, and implications for trace metal speciation. Geochim. Cosmochim. Ac. 66 (18), 3211-3224.
Toner, B., Manceau, a., Marcus, M.A., Millet, d.B. and Sposito, G., 2005. Zinc sorption by a bacterial biofilm. Environ. Sci. Technol. 39 (21), 8288-8294.
Torno, H.C., Marsalek, J. and Desbordes, M. (Eds.), 1986. Urban runoff pollution. NATO ASI series. Ecological sciences, G10. Springer-Verlag, Berlin; New York.
Tournassat, C., Greneche, J.-M., Tisserand, D. and Charlet, L., 2004. The titration of clay minerals: I. Discontinuous backtitration technique combined with CEC measurements. J. Colloid Interface Sci. 273 (1), 224-233.
Town, R.M. and Powell, H.K.J., 1993. Ion-selective electrode potentiometric studies on the complexation of copper(II) by soil-derived humic and fulvic acids. Anal. Chim. Ac. 279, 221-233.
Toze, S., 2004. Pathogen survival in groundwater during artificial recharge. In: J. Steenvoorden and T. Endreny (Eds.), Wastewater re-use and groundwater quality. IAHS, 70-84.
Toze, S., 2006. Water reuse and health risks -- real vs. perceived. Desalination 187 (1-3), 41-51.
Toze, S., Dillon, P., Pavelic, P., Nicholson, B. and Gibert, M., 2001. Aquifer storage and recovery: Removal of contaminants from stored waters. Water 28 (7), 41-44.
Tran, Y.T., Bajracharya, K. and Barry, D.A., 1998. Anomalous cadmium adsorption in flow interruption experiments. Geoderma 84 (1-3), 169-184.
Treweek, G.P. and Morgan, J.J., 1980. Prediction of Suspension Turbidities from Aggregate Size Distribution. In: M.C. Kavanaugh and J.O. Leckie (Eds.), Particulates in Water: Characterization, Fate, Effects, and Removal. Lewis, Michigan, 329-351.
Tsang, D.C.W. and Lo, I.M.C., 2006. Competitive Cu and Cd Sorption and Transport in Soils: A Combined Batch Kinetics, Column, and Sequential Extraction Study. Environ. Sci. Technol. 40 (21), 6655-6661.
Tuccillo, M.E., 2006. Size fractionation of metals in runoff from residential and highway storm sewers. Sci. Total Environ. 355 (1-3), 288-300.
Tufenkji, N. and Elimelech, M., 2004. Deviation from the Classical Colloid Filtration Theory in the Presence of Repulsive DLVO Interactions. Langmuir 20 (25), 10818-10828.
Tufenkji, N. and Elimelech, M., 2005. Breakdown of Colloid Filtration Theory: Role of the Secondary Energy Minimum and Surface Charge Heterogeneities. Langmuir 21 (3), 841-852.
Tufenkji, N., Ryan, J.N. and Elimelech, M., 2002. The promise of bank filtration: A simple technology may inexpensively clean up poor-quality raw surface water. Environ. Sci. Technol. 36 (21), 422A-428A.
US EPA, 1999. Preliminary Data Summary of Urban Storm Water Best Management Practices. EPA-821-R-99-012, US EPA, Washington DC.
Valocchi, A.J., 1985. Validity of the local equilibrium assumption for modelling sorbing solute transport through homogeneous soils. Water Resour. Res. 21, 808-820.
Valocchi, A.J., Street, R.L. and Roberts, P.V., 1981. Transport of ion-exchanging solutes in groundwater: chromatographic theory and field simulation. Water Resour. Res. 17 (5), 1517-1527.
van Cappellen, P. and Wang, Y., 1996. Cycling of iron and manganese in surface sediments; a general theory for the coupled transport and reaction of carbon, oxygen, nitrogen, sulfur, iron, and manganese. Am. J. Sci. 296 (3), 197-243.
van der Lee, J. and De Windt, L., 2001. Present state and future directions of modeling of geochemistry in hydrogeological systems. J. Contam. Hydrol. 47 (2-4), 265-282.
van Dijk, H., 1971. Cation binding of humic acids. Geoderma 5 (1), 53-67.
van Geen, A., Rose, J., Thoral, S., Garnier, J.M., Zheng, Y. and Bottero, J.Y., 2004. Decoupling of As and Fe release to Bangladesh groundwater under reducing conditions. Part II: Evidence from sediment incubations. Geochim. Cosmochim. Ac. 68 (17), 3475-3486.
van Genuchten, M.T. and Wierenga, P.J., 1986. Solute dispersion coefficients and retardation factors, Methods of Soil Analysis: Part 1. Physical and Mineralogical Methods. Agronomy Monograph, 1025-1053.
van Riemsdijk, W.H., Koopal, L.K., Kinniburgh, D.G., Benedetti, M.F. and Weng, L., 2006. Modeling the Interactions between Humics, Ions, and Mineral Surfaces. Environ. Sci. Technol. 40 (24), 7473-7480.

Vanderzalm, J., Le Gal La Salle, C. and Dillon, P., 2006a. Behaviour of trace metals and metalloids during Aquifer Storage and Recovery (ASR) of reclaimed water in a carbonate aquifer at Bolivar, South Australia, Proceedings of the 5th International Symposium on Management of Aquifer Recharge ISMAR5, Berlin, Germany, 11–16 June 2005. Recharge systems for protecting and enhancing groundwater resources. IHP-VI, Series on Groundwater No. 13. UNESCO, pp. 316-321.

Vanderzalm, J., Le Gal La Salle, C., Hutson, J. and Dillon, P., 2003. Behaviour of metals during reclaimed water aquifer storage and recovery. Geophys. Res. Abstr. 5 (07910).

Vanderzalm, J.L., Dillon, P.J. and Le Gal La Salle, C., 2007. Arsenic mobility under variable redox conditions induced during ASR. In: P. Fox (Ed.), Proceedings of the 6th International Symposium on Managed Artificial Recharge of Groundwater, ISMAR6, Phoenix, Arizona, USA Oct 28-Nov 2, 2007. Management of aquifer recharge for sustainability. Acacia Publishing, Inc., Phoenix, Arizona, pp. 209-219.

Vanderzalm, J.L., Le Gal La Salle, C. and Dillon, P.J., 2006b. Fate of organic matter during aquifer storage and recovery (ASR) of reclaimed water in a carbonate aquifer. Appl. Geochem. 21 (7), 1204-1215.

Vanderzalm, J.L., Le Gal La Salle, C., Hutson, J.L. and Dillon, P.J., 2002. Water quality changes during aquifer storage and recovery at Bolivar, South Australia. In: P. Dillon (Ed.), Management of Aquifer Recharge for Sustainability, Proceedings of the International Symposium on Artificial Recharge of Groundwater, 4th, Adelaide, Australia, Sept. 22-26, 2002, pp. 83-88.

Vanselow, A.P., 1932. Equilibria of the base-exchange reactions of bentonites, permutites, soil colloids and zeolites. Soil Sci. 33, 95-113.

Vaze, J. and Chiew, F.H.S., 2003a. Comparative evaluation of urban storm water quality models. Water Resour. Res. 39 (10), 1280, doi:10.1029/2002WR001788.

Vaze, J. and Chiew, F.H.S., 2003b. Study of pollutant washoff from small impervious experimental plots. Water Resour. Res. 39 (6), 1160, doi:10.1029/2002WR001786.

Vega, E., Lesikar, B. and Pillai, S.D., 2003. Transport and survival of bacterial and viral tracers through submerged-flow constructed wetland and sand-filter system. Bioresour. Technol. 89 (1), 49-56.

Vermeer, A.W.P., McCulloch, J.K., van Riemsdijk, W.H. and Koopal, L.K., 1999. Metal Ion Adsorption to Complexes of Humic Acid and Metal Oxides: Deviations from the Additivity Rule. Environ. Sci. Technol. 33 (21), 3892-3897.

Victoria Stormwater Committee, 1999. Urban Stormwater: Best Practice Environmental Management Guidelines.

Victorian Government, 2004. Water Act 1989. No. 80/1989, Version 072, incorporating amendments as at 1 July 2004.

Victorian Government, 2006. Alternative Urban Water Supplies Regulatory Review: Managed Aquifer Recharge (MAR).

Victorian Government, 2007. Environmental Protection Policy 1970. No. 8056 of 1970, Version 161, incorporating amendments as at 1 September 2007.

Voegelin, A., Barmettler, K. and Kretzschmar, R., 2003. Heavy metal release from contaminated soils: Comparison of column leaching and batch extraction results. J. Environ. Qual. 32 (3), 865-875.

Voegelin, A., Scheinost, A.C., Buhlmann, K., Barmettler, K. and Kretzschmar, R., 2002. Slow Formation and Dissolution of Zn Precipitates in Soil: A Combined Column-Transport and XAFS Study. Environ. Sci. Technol. 36 (17), 3749-3754.

Voegelin, A., Vulava, V.M. and Kretzschmar, R., 2001. Reaction-Based Model Describing Competitive Sorption and Transport of Cd, Zn, and Ni in an Acidic Soil. Environ. Sci. Technol. 35 (8), 1651-1657.

Voegelin, A., Vulava, V.M., Kuhnen, F. and Kretzschmar, R., 2000. Multicomponent transport of major cations predicted from binary adsorption experiments. J. Contam. Hydrol. 46 (3-4), 319-338.

von Gunten, H.R., Karametaxas, G., Krahenbuhl, U., Kuslys, M., Giovanoli, R., Hoehn, E. and Keil, R., 1991. Seasonal biogeochemical cycles in riverborne groundwater. Geochim. Cosmochim. Ac. 55 (12), 3597-3609.

von Gunten, U. and Zobrist, J., 1993. Biogeochemical changes in groundwater-infiltration systems: Column studies. Geochim. Cosmochim. Ac. 57 (16), 3895-3906.

von Zelewsky, A. and Bemtgen, J.M., 1982. Formation of ternary copper(II) complexes at the surface of silica gel as studied by ESR spectrometry. Inorg. Chem. 21 (5), 1771-1777.

Walker, D.J., 2001. Modelling sedimentation processes in a constructed stormwater wetland. Sci. Total Environ. 266 (1-3), 61-68.

Walker, D.J. and Hurl, S., 2002. The reduction of heavy metals in a stormwater wetland. Ecol. Eng. 18 (4), 407-414.
Walker, F.P., Schreiber, M.E. and Rimstidt, J.D., 2006. Kinetics of arsenopyrite oxidative dissolution by oxygen. Geochim. Cosmochim. Ac. 70 (7), 1668-1676.
Walker, T. and Wong, T.H.F., 1999. Effectiveness of Street Sweeping for Stormwater Pollution Control. Technical Report 99/8, Cooperative Reserach Centre for Catchment Hydrology.
Walling, D.E. and Moorehead, P.W., 1989. The particle size characteristics of fluvial suspended sediment: an overview. Hydrobiologia 176/177, 125-149.
Walsh, C.J., 2004. Protection of in-stream biota from urban impacts: minimise catchment imperviousness or improve drainage design? Mar. Freshwater Res. 55, 317-326.
Walsh, C.J., Roy, A.H., Feminella, J.W., Cottingham, P.D., Groffman, P.M. and Morgan II, R.P., 2005. The urban stream syndrome: current knowledge and the search for a cure. J. N. Am. Benthol. Soc. 24 (3), 706-723.
Walter, A.L., Frind, E.O., Blowes, D.W., Ptacek, C.J. and Molson, J.W., 1994. Modeling of multicomponent reactive transport in groundwater: 1. Model development and evaluation. Water Resour. Res. 30 (11), 3137-3148.
Wang, F., Chen, J. and Forsling, W., 1997. Modeling Sorption of Trace Metals on Natural Sediments by Surface Complexation Model. Environ. Sci. Technol. 31 (2), 448-453.
Warwick, P., Hall, A., Pashley, V., van der Lee, J. and Maes, A., 1998. Zinc and cadmium mobility in sand: effects of pH, speciation, Cation Exchange Capacity (CEC), humic acid and metal ions. Chemosphere 36 (10), 2283-2290.
Weerasooriya, R., Dharmasena, B. and Aluthpatabendi, D., 2000. Copper-gibbsite interactions: an application of 1-pK surface complexation model. Colloids Surf., A 170 (1), 65-77.
Welch, A.H. and Stollenwerk, K.G. (Eds.), 2003. Arsenic in ground water. Kluwer Academic Publishers, Boston/Dordrecht/London.
Welp, G. and Brümmer, G.W., 1998. Adsorption and solubility of ten metals in soil samples of different composition. J. Plant Nutr. Soil Sci. 162, 155-161.
Wen, X., Du, Q. and Tang, H., 1998. Surface Complexation Model for the Heavy Metal Adsorption on Natural Sediment. Environ. Sci. Technol. 32 (7), 870-875.
Weng, L., Fest, E.P.M.J., Fillius, J., Temminghoff, E.J.M. and van Riemsdijk, W.H., 2002a. Transport of Humic and Fulvic Acids in Relation to Metal Mobility in a Copper-Contaminated Acid Sandy Soil. Environ. Sci. Technol. 36 (8), 1699-1704.
Weng, L., Temminghoff, E.J.M., Lofts, S., Tipping, E. and van Riemsdijk, W.H., 2002b. Complexation with Dissolved Organic Matter and Solubility Control of Heavy Metals in a Sandy Soil. Environ. Sci. Technol. 36 (22), 4804-4810.
Weng, L., Temminghoff, E.J.M. and van Riemsdijk, W.H., 2001. Contribution of Individual Sorbents to the Control of Heavy Metal Activity in Sandy Soil. Environ. Sci. Technol. 35 (22), 4436-4443.
Weng, L., van Riemsdijk, W.H. and Hiemstra, T., 2007. Adsorption of humic acids onto goethite: Effects of molar mass, pH and ionic strength. J. Colloid Interface Sci. 314 (1), 107-118.
Weng, L., van Riemsdijk, W.H., Koopal, L.K. and Hiemstra, T., 2006. Ligand and Charge Distribution (LCD) model for the description of fulvic acid adsorption to goethite. J. Colloid Interface Sci. 302 (2), 442-457.
Western, A.W., Nolan, J.B., Hughes, R.L. and O'Neill, I.C., 1998. Mixing Behavior of Density-Stratified Pools. J. Hydraul. Eng. 124 (3), 280-287.
Williamson, M.A. and Rimstidt, J.D., 1994. The kinetics and electrochemical rate-determining step of aqueous pyrite oxidation. Geochim. Cosmochim. Ac. 58 (24), 5443-5454.
Wisotzky, F. and Cremer, N., 2003. Sequential extraction procedure in columns. Part 1: Development and description of a new method. Environ. Geol. 44, 799-804.
Wong, T. (Ed.), 2006. Australian runoff quality - A guide to Water Sensitive Urban Design. Institution of Engineers, Australia.
Wong, T., Coleman, J., Duncan, H.P., Fletcher, T.D., Jenkins, G., Siriwardena, L. and Wootton, R., 2003. MUSIC Version 2.0, MUSIC Development Team, CRC for Catchment Hydrology, Melbourne.
Worch, E., 2004. Modelling the solute transport under nonequilibrium conditions on the basis of mass transfer equations. J. Contam. Hydrol. 68 (1-2), 97-120.
Xu, N. and Gao, Y., 2008. Characterization of hematite dissolution affected by oxalate coating, kinetics and pH. Appl. Geochem. 23 (4), 783-793.
Yang, J.Y., Yang, X.E., He, Z.L., Li, T.Q., Shentu, J.L. and Stoffella, P.J., 2006. Effects of pH, organic acids, and inorganic ions on lead desorption from soils. Environ. Pollut. 143 (1), 9-15.
Yeh, G.T. and Tripathi, V.S., 1989. A Critical Evaluation of Recent Developments in Hydrogeochemical Transport Models of Reactive Multichemical Components. Water Resour. Res. 25 (1), 93-108.

Yeh, W.W.-G., 1986. Review of Parameter Identification Procedures in Groundwater Hydrology : The Inverse Problem. Water Resour. Res. 22 (2), 95-108.

Ying, G.-G., Kookana, R.S. and Dillon, P., 2003. Sorption and degradation of selected five endocrine disrupting chemicals in aquifer material. Water Res. 37 (15), 3785-3791.

Yousef, Y.A., Hvitved-Jacobsen, T., Harper, H.H. and Lin, L.Y., 1990. Heavy metal accumulation and transport through detention ponds receiving highway runoff. Sci. Total Environ. 93, 433-440.

Yuan, S., Xi, Z., Jiang, Y., Wan, J., Wu, C., Zheng, Z. and Lu, X., 2007. Desorption of copper and cadmium from soils enhanced by organic acids. Chemosphere 68 (7), 1289-1297.

Yuan, Y., Hall, K. and Oldham, C., 2001. A preliminary model for predicting heavy metal contaminant loading from an urban catchment. Sci. Total Environ. 266 (1-3), 299-307.

Zachara, J.M., Resch, C.T. and Smith, S.C., 1994. Influence of humic substances on Co2+ sorption by a subsurface mineral separate and its mineralogic components. Geochim. Cosmochim. Ac. 58 (2), 553-566.

Zachara, J.M., Smith, S.C. and Kuzel, L.S., 1995. Adsorption and dissociation of Co-EDTA complexes in iron oxide-containing subsurface sands. Geochim. Cosmochim. Ac. 59 (23), 4825-4844.

Zachara, J.M., Smith, S.C., Resch, C.T. and Cowan, C.E., 1992. Cadmium Sorption to Soil Separates Containing Layer Silicates and Iron and Aluminum Oxides. Soil Sci. Soc. Am. J. 56 (4), 1074-1084.

Zehetner, V.V., 2000. Nickel and copper sorption in acid forest soils. Soil Sci. 165 (6), 463-472.

Zhao, L.Y.L., Schulin, R. and Nowack, R., 2007a. The Effects of Plants on the Mobilization of Cu and Zn in Soil Columns. Environ. Sci. Technol. 41 (8), 2770-2775.

Zhao, L.Y.L., Schulin, R., Weng, L. and Nowack, B., 2007b. Coupled mobilization of dissolved organic matter and metals (Cu and Zn) in soil columns. Geochim. Cosmochim. Ac. 71 (14), 3407-3418.

Zheng, C. and Bennett, G.D., 1995. Applied contaminant transport modeling: theory and practice. Van Nostrand Reinhold, New York.

Zheng, C., Hill, M.C. and Hsieh, P.A., 2001. MODFLOW-2000, The U.S. Geological Survey Modular Ground-Water Model - User Guide to the LMT6 Package, the Linkage with MT3DMS for Multi-Species Mass Transport Modelling. Open File Report 01-82, U.S. Geological Survey, Denver, Colorado.

Zheng, C. and Wang, P.P., 1999. MT3DMS: A Modular Three-Dimensional Multispecies Transport Model for Simulation of Advection, Dispersion, and Chemical Reactions of Contaminants in Groundwater Systems; Documentation and User's Guide. Contract Report SERDP-99-1, US Army Corps of Engineers.

Zhou, W., Beck, B.F. and Green, T.S., 2003. Evaluation of a peat filtration system for treating highway runoff in a karst setting. Environ. Geol. 44, 187-202.

Zhu, C. and Anderson, G.M., 2002. Environmental applications of geochemical modeling. Cambridge University Press, Cambridge.

Zimmermann, J., Dierkes, C., Göbel, P., Klinger, C., Stubbe, H. and Coldewey, W.G., 2005. Metal concentrations in soil and seepage water due to infiltration of roof runoff by long term numerical modelling. Water Sci. Technol. 51 (2), 11-19.

Ziper, C., Komarneni, S. and Baker, D.E., 1988. Specific cadmium sorption in relation to the crystal chemistry of clay minerals. Soil Sci. Soc. Am. J. 52 (1), 49-53.

Zwar, J.R., 2004. Water Sensitive Urban Design: A Perspective from Outback South Australia. In: T. Daniell (Ed.), Int. Conference on Water Sensitive Urban Design: cities as catchments, WSUD 2004, Adelaide, Australia, pp. 647-659.

Appendix A: Publications and Conferences

- **Int. Conference on Water sensitive urban design: cities as catchments, WSUD 2004, Adelaide, 21-25th Nov 2004:**
  Participation and co-authorship:
  Mudd, G.M., Deletic, A., Fletcher, T.D. and Wendelborn, A., 2004. A Review of Urban Groundwater in Melbourne : Considerations for WSUD. In: T. Daniell (Ed.), Int. Conference on Water sensitive urban design: cities as catchments, WSUD 2004, Adelaide, pp. 428-438
- **Inaugural Australasian Hydrogeology Conference, Melbourne, 1st-3rd Dec 2004:**
  Poster presentation and extended abstract in conference proceedings:
  Wendelborn, A., Mudd, G. and Deletic, A., 2004: Water quality issues for injection aquifer recharge and recovery in Melbourne, pp. 3
- **ISMAR 05, 5th International Symposium on Management of Aquifer Recharge, Berlin/Germany, 11-16th June 2005:**
  Poster presentation and peer reviewed paper:
  Wendelborn, A., Mudd, G., Deletic, A. and Dillon, P., 2006. Research on metals in stormwater for aquifer storage and recovery in alluvial aquifers in Melbourne, Australia, Proceedings of the 5th International Symposium on Management of Aquifer Recharge ISMAR5, Berlin, Germany, 11–16 June 2005. Recharge systems for protecting and enhancing groundwater resources. IHP-VI, Series on Groundwater No. 13. UNESCO, pp. 322-328.

Submitted journal papers:

Wendelborn, A., Mudd, G. and Deletic, A., submitted. Sorption behaviour of zinc and copper from stormwater injected into siliceous aquifer materials for aquifer storage and recovery (ASR) – 1. Batch experiments. J. Contam. Hydrol.

Wendelborn, A., Mudd, G. and Deletic, A., submitted. Sorption behaviour of zinc and copper from stormwater injected into siliceous aquifer materials for aquifer storage and recovery (ASR) – 2. Column experiments. J. Contam. Hydrol.

Appendix B: Water sample analysis

Table A-1: Full analysis of all stormwater samples. See Table IV-1 for catchment parameters.

	event characteristics									major ions [mg/L]						
ID	event date	rainfall [mm]	intensity [mm/h]*	peak flow rate [L/s]	total flow volume [ML]	duration [h]	ADWP [d]	pH	EC [µS/cm]	Ca	Mg	Na	K	HCO_3	Cl	SO_4
MR1	6/01/05	2.0	2.0	2.3	$0.7*10^{-3}$	0.3	2	5.6	37	0.5	0.5	4.9	0.3	2.7	8.2	2.4
MR2	28/01/05	3.4	1.8	1.5	$1.1*10^{-3}$	1.0	11	5.7	29	1.7	0.5	1.7	0.4	2.1	3.4	3.6
MR3	29/01/05	4.8	0.6	0.5	$1.1*10^{-3}$	3.0	1	5.3	17	0.6	0.2	1.0	0.2	4.3	1.9	2.7
MR4	1/02/05	2.6	0.6	0.4	$0.5*10^{-3}$	1.8	2	5.9	61	1.0	0.8	7.4	0.4	1.6	14.0	3.4
MR5	3/02/05	6.0	2.4	2.1	$2.1*10^{-3}$	1.3	2	5.0	6	0.1	0.1	0.2	0.1	4.2	0.3	0.4
MR6	3/04/05	3.4	1.0	0.9	$0.8*10^{-3}$	2.8	6	6.9	48	3.8	0.6	2.4	0.5	12.6	2.8	1.7
MR7	9/06/05	9.8	0.6	0.4	$3.2*10^{-3}$	7.8	9	5.9	10	0.6	0.1	1.3	0.2	3.8	0.7	1.2
MR8	13/06/05	11.6	1.2	1.3	$4.1*10^{-3}$	4.5	4	5.7	4	0.2	0.0	1.1	0.1	4.2	0.2	1.1
MR9	24/07/05	7.6	1.6	1.4	$3.3*10^{-3}$	4.2	8	6.0	16	1.7	0.1	1.2	0.1	3.5	0.9	1.3
MR10	3/08/05	2.8	2.0	2.6	$0.8*10^{-3}$	2.5	8	6.1	6	0.4	0.0	0.8	0.1	1.0	0.2	0.9
MR11	9/08/05	4.6	1.4	2.2	$1.9*10^{-3}$	3.4	2	5.7	8	0.3	0.1	1.5	0.2	2.2	1.0	1.8
MR12	30/08/05	17.4	4.0	2.9	$3.8*10^{-3}$	9.2	7	5.2	7	0.4	0.1	0.9	0.1	6.7	0.6	0.9
MR13	28/09/05a	2.2	0.6	0.4	$0.8*10^{-3}$	1.5	11	5.9	4	0.3	0.1	1.1	0.1	2.1	1.0	0.5
MR14	28/09/05b	65.2	4.4	4.0	$3.8*10^{-3}$	3.5	0	5.2	6	0.2	0.0	1.1	0.1	4.6	0.7	0.6
MR15	11/10/05	4.8	0.8	0.6	$1.5*10^{-3}$	3.0	3	5.7	14	0.2	0.1	2.2	0.2	2.5	2.4	0.8
MR16	19/10/05	4.8	0.6	0.2	$1.3*10^{-3}$	4.0	8	6.0	12	1.0	0.2	1.7	0.3	1.3	1.8	1.3
MR17	25/10/05	4.2	2.0	2.2	$1.3*10^{-3}$	1.5	3	5.9	6	0.2	0.0	1.0	0.1	0.4	0.4	0.5
GR1	28/01/05	2.6	1.4	340	0.32	2.0	11	6.5	95	7.4	1.3	6.3	2.7	27.7	8.4	8.6
GR2	29/01/05	3.6	0.6	160	0.48	5.0	1	6.4	58	4.5	0.7	4.1	1.3	12.2	5.7	5.4
GR3	3/02/05	4.8	1.4	450	0.98	1.2	5	6.9	54	4.5	1.2	4.0	0.9	17.4	4.0	5.8
GR4	15/02/05	5.2	1.2	339	0.83	4.2	3	6.9	52	4.2	0.8	3.7	0.9	12.6	5.2	5.2
GR5	5/03/05	12.0	2.2	578	1.87	4.1	18	6.5	65	4.2	0.9	5.8	1.0	10.9	7.8	3.7
GR6	10/04/05	2.8	1.6	369	0.32	0.5	7	6.6	93	6.3	1.3	7.4	2.1	12.8	11.0	5.5
GR7	14/04/05	19.8	2.0	552	3.78	6.2	3	6.9	39	3.3	0.6	3.2	0.7	10.3	2.8	2.3
GR8	23/05/05	4.8	1.4	292	0.75	7.6	22	6.4	66	5.3	0.9	5.8	1.2	13.4	3.6	5.3
GR9	9/06/05	12.4	0.8	213	1.96	8.3	9	6.6	58	4.2	0.7	5.1	1.0	11.5	4.3	3.4
GR10	30/06/05	4.0	0.4	115	0.63	9.5	7	6.9	71	6.0	1.0	5.9	1.1	21.3	3.5	6.2
GR11	9/08/05	4.8	1.8	446	0.90	3.5	2	6.8	67	4.5	1.1	5.6	0.8	13.5	4.6	6.2
GR12	30/08/05	15.4	2.6	1136	3.38	8.3	7	6.3	38	3.9	0.8	3.3	0.8	10.0	2.5	3.6
GR13	31/08/05	2.4	1.6	396	0.44	0.3	1	6.6	60	4.7	1.5	6.3	0.9	11.4	7.3	6.0
GR14	28/09/05	14.6	4.8	1156	2.94	11.0	2	6.7	45	4.8	0.7	4.1	0.8	11.9	3.0	1.9
GR15	11/10/05	4.4	1.0	261	0.92	2.8	3	6.8	39	3.4	0.6	4.3	0.8	11.4	4.2	1.6
GR16	19/10/05	4.6	0.6	163	0.93	3.3	8	6.2	56	4.8	0.7	4.1	0.8	17.2	3.0	1.9
GR17	3/11/05	8.8	2.8	734	2.04	4.0	3	6.3	46	6.2	1.1	6.4	1.4	13.2	4.5	2.6
GR18	7/11/05	12.6	1.8	726	2.60	2.0	4	6.2	31	5.1	1.0	4.5	1.2	12.6	5.6	3.0
RI1	10/12/04	9.4	8.4	2850	3.46	2.0	1	6.6	52	6.3	0.7	3.8	1.2	21.7	2.0	3.4
RI2	16/01/05	3.0	1.4	185	0.58	3.0	12	6.4	128	8.8	2.0	12.0	3.4	30.0	16.0	9.0
RI3	29/01/05	4.2	0.8	190	0.88	4.0	1	6.5	114	8.8	1.6	7.0	3.2	27.7	9.3	8.6
RI4	5/03/05	0.6	0.6	11	1.89	0.1	18	6.7	120	8.8	1.6	10.0	2.4	28.5	14.0	7.7
RI5	10/04/05	3.8	2.8	573	0.73	0.4	7	6.8	150	12.0	2.1	11.0	4.4	46.9	16.0	9.0
RI6	14/04/05	19.8	1.4	567	4.59	6.6	4	6.9	73	4.8	1.0	4.5	2.0	15.3	4.5	3.8
RI7	23/05/05	4.4	1.4	257	0.85	1.8	22	6.5	123	11.0	2.0	8.4	3.7	30.4	7.9	9.9
RI8	9/06/05	12.6	0.8	253	3.23	8.8	9	7.1	125	8.0	1.7	8.3	2.5	33.7	9.0	6.0
RI9	9/08/05	4.4	1.8	298	0.86	3.4	2	7.1	78	8.9	1.0	5.7	1.4	26.1	4.7	6.4
RI10	30/08/05	13.2	3.2	939	3.01	8.6	7	6.6	70	7.1	0.9	4.3	1.5	22.5	3.4	4.5
RI11	28/09/05	11.8	4.2	1386	3.35	4.0	11	6.5	59	6.9	0.8	4.7	1.5	19.7	3.3	5.1
RI12	11/10/05	4.20	1.0	277	1.07	2.5	3	6.9	71	7.4	1.3	8.4	2.3	20.6	20.0	5.8
RI13	19/10/05	6.20	0.6	220	1.37	5.0	8	6.4	171	7.3	1.1	5.7	2.4	23.1	5.2	4.0
RI14	30/04/06	12.0	1.4	561	3.59	15.5	1	na	na	na	na	na	na	na	na	na
SR1	28/01/05	6.2	3.4	490	0.67	3.0	10	6.5	96	9.2	1.3	10.0	2.5	29.4	14.0	5.0
SR2	2/02/05	144	4.4	470	10.6	20.0	4	6.7	74	6.9	1.2	6.6	1.2	21.6	8.5	6.0
ER1	9/06/05	17.6	1.4	277	2.56	8.5	11	na	na	na	na	na	na	na	na	na
ER2	11/10/05	na	na	436	2.79	na	na	7.5	359	9.9	3.6	18.0	1.6	63.4	7.3	5.2
ER3	19/10/05	na	na	440	3.00	na	na	6.8	123	8.8	1.8	8.4	1.9	24.8	9.5	3.2

MR: Monash Roof; GR: Gilby Rd, RI: Richmond, SR: Shepherds Rd, ER: Eley Rd, * over 10 mins, ADWP: antecedent dry weather period

Table A-1: continued

						metal (total) [µg/L]										Sum
ID	TOC [mg-C/L]	DOC [mg-C/L]	TSS [mg/L]	TP [mg-P/L]	TN [mg-N/L]	Al	As	Cd	Cr	Cu	Fe	Mn	Ni	Pb	Zn	metals [mg/L]
MR1	2	3	11	0.05	0.82	1215	<d.l.	<d.l.	5	9	1192	14	3	6	101	2.54
MR2	5	4	91	0.13	2.70	4370	<d.l.	<d.l.	16	27	4897	60	10	21	343	9.74
MR3	2	2	8	0.03	1.30	503	<d.l.	<d.l.	0	4	390	10	0	2	127	1.04
MR4	2	2	7	0.02	0.99	na	na	<d.l.	2	3	106	10	na	0	142	0.26
MR5	2	2	3	0.01	0.51	na	na	<d.l.	0	2	55	4	na	0	40	0.10
MR6	7	3	198	0.22	1.88	na	na	<d.l.	13	14	7270	111	na	6	204	7.62
MR7	2	1	8	0.02	0.57	na	na	<d.l.	2	3	334	15	na	<d.l.	152	0.51
MR8	3	2	3	0.03	0.37	na	na	<d.l.	0	7	92	6	na	<d.l.	81	0.19
MR9	6	4	128	0.23	5.79	412	<d.l.	<d.l.	0	3	390	10	4	8	70	0.90
MR10	6	3	53	0.06	0.84	954	<d.l.	<d.l.	4	7	937	21	7	12	126	2.07
MR11	2	1	20	0.02	0.53	315	<d.l.	<d.l.	0	3	319	8	0	1	59	0.70
MR12	1	<1	25	0.03	0.39	1401	<d.l.	<d.l.	4	4	1252	30	1	3	77	2.77
MR13	2	2	2	0.05	0.60	16	<d.l.	<d.l.	0	3	85	5	4	2	85	0.20
MR14	2	<1	4	0.01	0.34	441	<d.l.	<d.l.	1	5	502	22	1	13	69	1.05
MR15	2	2	3	0.02	0.75	201	<d.l.	<d.l.	<d.l.	<d.l.	180	7	0	11	108	0.51
MR16	4	3	5	0.02	1.00	416	<d.l.	<d.l.	3	4	393	16	1	2	110	0.94
MR17	3	<1	14	0.02	0.73	534	<d.l.	<d.l.	1	5	592	10	5	2	64	1.21
GR1	17	9	138	0.67	4.44	4515	<d.l.	0	18	84	5936	103	15	42	1456	12.2
GR2	9	6	17	0.11	1.46	747	<d.l.	1	3	17	802	19	2	2	738	2.33
GR3	6	3	54	0.09	1.00	2453	<d.l.	<d.l.	5	11	3031	29	5	3	335	5.87
GR4	9	4	68	0.15	1.40	na	na	<d.l.	3	14	625	16	na	7	644	1.31
GR5	9	6	70	0.18	1.30	na	na	<d.l.	5	33	1239	32	na	17	675	2.00
GR6	15	11	197	0.66	4.70	na	na	<d.l.	16	49	5973	110	na	33	1264	7.44
GR7	3	3	43	0.19	1.06	na	na	<d.l.	4	14	1593	27	na	3	442	2.08
GR8	10	6	78	0.34	1.80	na	na	<d.l.	10	56	2912	47	na	28	1009	4.06
GR9	8	6	40	0.14	0.98	na	na	<d.l.	5	22	1457	28	na	15	800	2.33
GR10	15	9	74	0.22	1.30	na	na	<d.l.	13	35	4294	50	na	7	1005	5.40
GR11	5	4	82	0.20	1.20	2048	<d.l.	0	7	16	2501	55	9	19	428	5.08
GR12	5	3	98	0.24	0.97	4733	<d.l.	1	15	38	5348	81	12	32	654	10.9
GR13	4	3	69	0.12	1.10	3468	<d.l.	0	10	18	3686	53	8	25	523	7.79
GR14	5	3.18	136	na	na	9464	<d.l.	1	25	78	12871	143	26	53	685	23.3
GR15	6	6	30	na	na	2628	<d.l.	0	8	16	2886	50	7	106	656	6.36
GR16	5	3.2	24	na	na	3105	<d.l.	1	12	39	4148	94	13	25	1519	8.96
GR17	14	10	77	0.06	1.80	2690	<d.l.	0	8	19	3383	54	10	22	449	6.64
GR18	11	9	62	0.20	1.60	51961	<d.l.	9	144	273	70478	1052	156	342	3814	128
RI1	9	4	318	0.83	3.65	11034	5	1	25	90	13040	155	23	243	1826	26.4
RI2	12	10	196	0.72	4.70	6398	<d.l.	0	14	57	7941	126	17	84	1395	16.0
RI3	20	10	167	0.62	2.90	5495	<d.l.	0	14	64	7151	126	19	103	1664	14.6
RI4	21	10	247	0.82	3.70	na	na	<d.l.	8	48	3618	103	na	98	1113	4.99
RI5	21	na	525	1.82	7.43	na	na	<d.l.	16	75	8407	160	na	159	1416	10.2
RI6	6	3	46	0.29	1.66	na	na	<d.l.	3	20	1378	36	na	64	643	2.14
RI7	16	10.0	351	0.95	4.86	na	na	<d.l.	22	104	13238	228	na	193	2038	15.8
RI8	8	7.0	157	0.50	2.50	na	na	<d.l.	12	36	7121	99	na	50	1109	8.43
RI9	5	4.0	177	0.43	2.50	3519	<d.l.	0	10	41	4586	93	14	81	867	9.21
RI10	7	4.0	165	0.51	2.10	6035	<d.l.	1	16	64	6769	127	20	113	1151	14.3
RI11	8	5.0	202	0.59	2.68	6899	<d.l.	1	20	74	9784	169	26	160	1428	18.6
RI12	10	7.0	52	0.30	2.30	1922	<d.l.	0	6	26	2592	61	9	84	733	5.43
RI13	9	9.0	66	na	na	1125	<d.l.	0	5	30	1571	38	7	26	774	3.58
RI14	na	na	53	0.32	2.30	6802	<d.l.	4	23	119	10169	174	28	204	2835	20.4
SR1	17	9	432	1.15	6.24	9121	<d.l.	<d.l.	19	74	12004	197	13	83	897	22.4
SR2	6	4	220	0.29	1.81	3324	1	<d.l.	5	11	3658	30	6	3	175	7.21
ER1	na	na	79	na	na	na	na	<d.l.	4	16	1892	26	na	2	336	2.28
ER2	5	4.00	35	0.14	1.30	1587	<d.l.	0	1	27	1777	24	5	14	322	3.76
ER3	8	8.00	43	0.20	2.00	1446	<d.l.	0	2	46	1782	40	5	8	409	3.74

MR: Monash Roof; GR: Gilby Rd, RI: Richmond, SR: Shepherds Rd, ER: Eley Rd, TOC: total organic carbon, DOC: dissolved organic carbon, TSS: total suspended solids, TP: total phosphorus, TN: total nitrogen, na: not analysed, d.l.: detection limit

Table A-1: continued

	metals (>63 µm) [µg/L]										metals (0.45-63 µm) [µg/L]					
ID	Al	As	Cd	Cr	Cu	Fe	Mn	Ni	Pb	Zn	Al	As	Cd	Cr	Cu	Fe
MR1	560	<1.4	<0.1	3	4	634	6	2	6	16	482	<29	<1	2	2	527
MR2	2087	<1.4	<0.1	8	15	2638	24	5	21	75	2098	<29	<1	6	8	2229
MR3	61	<1.4	<0.1	0	0	58	1		2	3	267	<29	<1	<2.2	<0.8	306
MR4	na	na	<0.1	0	0	10	0	na	0	1	na	na	<0.7	2	2	90
MR5	na	na	<0.1	0	0	10	0	na	0	0	na	na	<0.7	<0.6	1	41
MR6	na	na	0	5	6	3454	45	na	6	76	na	na	<0.7	6	6	3801
MR7	na	na	<0.1	1	1	125	2	na	<0.1	2	na	na	<0.7	1	0	204
MR8	na	na	<0.1	<0.1	0	10	0	na	<0.1	2	na	na	<0.7	<0.6	2	74
MR9	56	<0.1	<0.1	0	0	64	2	0	1	1	356	<0.1	<0.7	<3	2	326
MR10	121	<0.1	<0.1	0	0	159	2	0	1	0	582	<0.1	<0.7	3	<1	692
MR11	42	<0.1	<0.1	0	1	48	1	0	1	1	273	<0.1	<0.7	<3	1	263
MR12	366	<0.1	0	1	2	387	7	1	3	9	1035	<0.1	<0.7	3	3	866
MR13	16	<0.1	<0.1	0	0	19	0	0	2	<0.2	<100	<0.1	<0.7	<3	<1	<70
MR14	255	<0.1	<0.1	1	1	328	3	1	2	3	186	<0.1	<0.7	<3	<1	174
MR15	12	<0.1	<0.1	<0.2	0	13	0	0	2	<0.2	188	<0.1	<0.7	<3	<1	89
MR16	277	<0.1	<0.1	1	2	270	4	1	2	15	140	<0.1	<0.7	2	<1	123
MR17	235	<0.1	<0.1	1	1	261	3	1	2	6	299	<0.1	<0.7	<3	2	332
GR1	988	<1.4	0	4	20	1435	24	3	16	378	3317	<29	<1	12	45	4309
GR2	127	<1.4	<0.1	1	1	175	3	0	2	24	447	<29	1	3	4	573
GR3	111	<1.4	<0.1	0	1	156	3	0	3	16	2142	<29	<1	5	5	2681
GR4	na	na	<0.1	0	1	109	2	na	1	12	na	na	<0.7	2	8	499
GR5	na	na	<0.1	0	2	70	2	na	1	11	na	na	<0.7	4	23	1126
GR6	na	na	0	10	25	3878	69	na	27	427	na	na	1	6	15	2076
GR7	na	na	0	1	4	695	11	na	3	79	na	na	<0.7	3	6	886
GR8	na	na	0	1	7	400	8	na	5	81	na	na	<0.7	7	34	2430
GR9	na	na	0	1	4	315	7	na	3	66	na	na	<0.7	3	9	1099
GR10	na	na	<0.1	0	1	51	1	na	0	12	na	na	1	10	20	3992
GR11	1022	<0.1	0	4	9	1306	28	3	11	141	1026	<0.1	<0.7	4	4	1195
GR12	3418	<0.1	1	11	27	3883	59	8	24	292	1315	<0.1	<0.7	4	6	1465
GR13	2005	<0.1	0	6	10	2208	31	5	13	160	1463	<0.1	<0.7	4	5	1478
GR14	2464	<0.1	0	8	30	4297	49	8	20	200	6683	<0.1	1	17	44	8353
GR15	974	<0.1	0	2	5	1105	25	2	95	117	1654	<0.1	<0.7	6	6	1709
GR16	2820	<0.1	1	9	24	3677	73	8	18	503	285	<0.1	<0.7	3	4	471
GR17	1592	<0.1	0	5	10	2026	36	5	11	139	1098	<0.1	<0.7	4	5	1357
GR18	51	<0.1	<0.1	0	0	58	1	0	0	11	51910	<0.1	9	144	268	70353
RI1	9320	5	1	21	77	11439	133	17	227	1626	1543	<29	<1	4	7	1552
RI2	2107	<1.4	0	5	23	3074	52	5	41	497	4138	<29	<1	8	24	4786
RI3	1594	<1.4	0	5	21	2389	47	5	57	604	3680	<29	<1	7	29	4615
RI4	na	na	0	1	5	358	9	na	12	89	na	na	1	6	39	3223
RI5	na	na	1	8	38	3924	67	na	99	668	na	na	1	7	32	4450
RI6	na	na	0	1	6	710	10	na	60	72	na	na	<0.7	2	5	619
RI7	na	na	1	8	38	5500	106	na	93	940	na	na	1	13	48	7607
RI8	na	na	0	2	8	1748	41	na	20	356	na	na	<0.7	9	17	5257
RI9	2186	<0.1	0	6	26	2945	63	8	56	498	1333	<0.1	<0.7	5	9	1612
RI10	4750	<0.1	1	13	48	5285	102	14	89	816	1233	<0.1	<0.7	4	9	1484
RI11	2975	<0.1	1	10	39	4597	89	13	91	724	3924	<0.1	<0.7	10	29	5118
RI12	451	<0.1	0	2	7	747	29	3	54	150	1471	<0.1	<0.7	5	10	1760
RI13	815	<0.1	0	2	12	1156	24	3	17	203	310	<0.1	<0.7	<3	5	415
RI14	5710	<0.1	4	20	92	8753	149	18	183	1588	1063	<0.1	1	3	19	1387
SR1	3293	<1.4	<0.1	7	27	4658	81	5	44	505	5546	<29	<1	12	41	6954
SR2	159	1	0	1	1	272	4	1	3	15	2542	<29	<1	5	6	2918
ER1	na	na	<0.1	0	1	174	5	na	2	18	na	na	<0.7	3	7	1516
ER2	301	0	0	1	8	408	9	1	3	49	1175	<0.1	<0.7	<3	12	1248
ER3	1061	0	0	2	27	1357	28	2	8	134	385	<0.1	<0.7	<3	5	425

MR: Monash Roof; GR: Gilby Rd, RI: Richmond, SR: Shepherds Rd, ER: Eley Rd, na: not analysed, d.l.: detection limit

Table A-1: continued

	metals (0.45-63 um) [ug/L]				metals (<0.45 um) [ug/L]									
ID	Mn	Ni	Pb	Zn	Al	As	Cd	Cr	Cu	Fe	Mn	Ni	Pb	Zn
MR1	5	1	<30	<3	174	<29	<1	<2.2	4	31	3	<2	<30	84
MR2	21	6	<30	<3	185	<29	<1	2	5	30	15	<2	<30	267
MR3	3	<2	<30	<3	175	<29	<1	<2.2	3	26	7	<2	<30	124
MR4	5	na	<0.6	25	na	na	<0.7	<0.6	2	5	5	na	<0.6	117
MR5	2	na	<0.6	<0.5	na	na	<0.7	<0.6	1	4	1	na	<0.6	39
MR6	51	na	<0.6	71	na	na	<0.7	1	2	15	15	na	<0.6	56
MR7	4	na	<0.6	<0.5	na	na	<0.7	<0.6	2	5	10	na	<0.6	150
MR8	1	na	<0.6	<0.5	na	na	<0.7	<0.6	6	9	4	na	<0.6	80
MR9	7	<4	7	<3	<100	<0.1	<0.7	<3	1	<70	2	<4	<7	69
MR10	7	<4	<7	<3	252	<0.1	<0.7	<3	6	86	13	5	7	126
MR11	3	<4	<7	<3	<100	<0.1	<0.7	<3	1	8	3	<4	<7	58
MR12	12	<4	<7	<3	<100	<0.1	<0.7	<3	<1	<70	12	<4	<7	68
MR13	<1	<4	<7	<3	<100	<0.1	<0.7	<3	3	<70	5	<4	<7	85
MR14	<1	<4	10	<3	<100	<0.1	<0.7	<3	4	<70	18	<4	<7	66
MR15	2	<4	9	<3	<100	<0.1	<0.7	<3	1	78	5	<4	<7	108
MR16	2	<4	<7	<3	<100	<0.1	<0.7	<3	2	<70	10	<4	<7	95
MR17	3	5	<7	<3	<100	<0.1	<0.7	<3	2	<70	3	<4	<7	58
GR1	38	7	26	229	210	<29	<1	2	19	192	41	5	<30	849
GR2	7	1	<30	19	173	<29	<1	<2.2	12	54	9	<2	<30	695
GR3	23	2	<30	98	200	<29	<1	<2.2	5	194	4	2	<30	221
GR4	12	na	6	365	na	na	1	1	5	18	2	na	<0.6	267
GR5	24	na	16	336	na	na	<0.7	1	9	42	7	na	<0.6	329
GR6	23	na	5	185	na	na	<0.7	<0.6	10	19	18	na	<0.6	652
GR7	11	na	<0.6	89	na	na	<0.7	<0.6	4	13	5	na	<0.6	274
GR8	26	na	22	264	na	na	<0.7	2	15	82	13	na	1	664
GR9	14	na	10	110	na	na	<0.7	1	9	43	7	na	1	624
GR10	37	na	7	332	na	na	<0.7	2	14	250	11	na	<0.6	661
GR11	14	<4	8	32	<100	<0.1	<0.7	<3	3	<70	12	4	<7	255
GR12	17	<4	8	54	<100	<0.1	<0.7	<3	4	<70	5	4	<7	308
GR13	16	<4	11	81	<100	<0.1	<0.7	<3	3	<70	6	<4	1	282
GR14	92	15	33	269	317	<0.1	<0.7	<3	5	222	2	4	1	216
GR15	20	5	11	114	<100	<0.1	<0.7	<3	5	72	5	<4	<7	425
GR16	4	<4	<7	111	<100	<0.1	<0.7	<3	11	<70	17	6	<7	905
GR17	16	6	11	47	<100	<0.1	<0.7	<3	4	<70	2	<4	<7	263
GR18	1047	156	341	3630	<100	<0.1	<0.7	<3	5	67	4	<4	<7	173
RI1	18	4	16	116	171	<29	<1	<2.2	5	49	5	2	<30	84
RI2	49	8	43	221	153	<29	<1	<2.2	10	81	25	4	<30	676
RI3	53	13	46	316	221	<29	<1	2	14	147	26	<2	<30	744
RI4	78	na	86	748	na	na	<0.7	1	4	37	16	na	<0.6	276
RI5	51	na	60	506	na	na	<0.7	1	6	33	42	na	<0.6	242
RI6	5	na	4	8	na	na	<0.7	<0.6	9	49	21	na	<0.6	562
RI7	90	na	92	654	na	na	<0.7	1	18	131	32	na	8	444
RI8	48	na	25	296	na	na	<0.7	1	10	115	10	na	5	457
RI9	22	<4	25	127	<100	<0.1	<0.7	<3	6	29	7	5	<7	243
RI10	19	6	18	97	52	<0.1	<0.7	<3	7	<70	5	<4	6	238
RI11	76	10	63	394	<100	<0.1	<0.7	<3	5	69	5	3	6	311
RI12	22	7	24	149	<100	<0.1	<0.7	<3	9	86	10	<4	6	434
RI13	5	<4	10	58	<100	<0.1	<0.7	<3	13	<70	9	4	<7	513
RI14	21	5	22	696	28	na	<0.7	<0.6	8	29	4	5	<0.6	551
SR1	71	7	39	250	281	<29	<1	<2.2	7	392	46	<2	<30	142
SR2	21	<2	<30	24	624	<29	<1	<2.2	5	468	6	5	<30	136
ER1	14	na	<0.6	10	na	na	<0.7	1	8	202	7	na	<0.6	308
ER2	14	<4	11	86	111	<0.1	<0.7	<3	7	121	2	3	<7	187
ER3	5	<4	<7	<3	<100	<0.1	<0.7	<3	14	<70	7	<4	<7	275

MR: Monash Roof; GR: Gilby Rd, RI: Richmond, SR: Shepherds Rd, ER: Eley Rd, na: not analysed, d.l.: detection limit

Table A-2: Analysis of mean values for column samples of experiment 2: flow parameters, physico-chemical parameters and anions.

BR – exp. 2	flow parameters				physico-chemical parameters					anions [mg/L]				
sample ID	runtime [d]	mean PV*	total outflow [mL]	flow velocity [mL/min]	pH	EC [µS/cm]	turbidity [NTU]	TOC [mg-C/L]	DOC [mg-C/L]	HCO_3	Cl	Br	NO_3	SO_4
BR2 gw equi	6.90	na	na	1.2	6.5	3053	0.4	6	na	10.6	827	4.7	8.5	17.1
BR2 stw 01	7.03	3	46	1.3	6.7	363	286	7	na	14.0	88.4	0.6	1.6	2.2
BR2 stw 02	7.05	9	95	1.4	6.7	384	70	5	3	14.5	80.9	0.5	1.5	2.0
BR2 stw 03	7.08	15	146	1.4	6.6	322	18	3	na	15.0	66.2	0.4	1.3	1.9
BR2 stw 04	7.10	21	191	1.4	6.7	273	13	3	3	15.5	51.5	0.3	1.2	1.8
BR2 stw 05	7.12	27	241	1.4	6.7	214	10	3	na	15.8	41.5	0.3	1.1	1.6
BR2 stw 06	7.15	33	289	1.3	6.7	168	8.3	3	3	16.0	31.4	0.2	1.1	1.4
BR2 stw 07	7.17	56	615	1.4	7.1	113	7.1	3	1	16.2	8.4	0.1	1.0	1.8
BR2 stw 08	7.34	79	671	1.4	6.9	91	6.1	3	na	18.8	4.4	0.0	0.9	1.0
BR2 stw 09	7.37	143	1655	1.3	7.3	73	3.5	4	na	21.9	2.6	0.0	0.8	0.6
BR2 stw 10	7.89	207	1708	1.4	7.0	66	3.6	3	3	22.3	2.6	0.0	0.8	0.6
BR2 stw 11	7.91	256	2458	1.3	7.2	63	2.5	4	4	23.2	1.7	0.0	0.8	0.4
BR2 stw 12	8.33	306	2510	1.3	7.0	62	2.5	3	na	24.1	2.1	0.0	0.8	0.5
BR2 stw 13	8.36	391	3836	1.3	7.1	63	1.7	2	na	25.1	1.7	0.0	0.8	0.5
BR2 stw 14	9.06	475	3883	1.2	6.9	64	1.6	4	3	25.2	2.1	0.0	0.8	0.6
BR2 stw 15	9.08	616	6118	1.3	7.0	64	0.9	3	2	25.3	2.2	0.0	0.7	0.6
BR2 stw 16	10.28	756	6166	1.3	6.8	63	0.8	3	na	24.9	2.2	0.0	0.8	0.6
BR2 stw 17	10.31	985	9839	1.3	7.0	55	0.6	4	na	24.5	2.2	0.0	0.8	0.6
BR2 stw 18	12.29	1215	9893	1.3	7.0	66	0.4	4	3	25.2	2.2	0.0	0.8	0.6
BR2 stw 19	12.32	1410	13015	1.3	7.0	66	0.4	6	5	25.9	2.2	0.0	0.8	0.6
BR2 stw 20	14.04	1606	13064	1.3	6.8	56	0.5	2	na	25.9	2.2	0.0	0.8	0.6
BR2 main st 1	21.07	1612	13114	1.4	6.7	77	2.2	5	na	27.0	2.2	0.0	1.2	2.7
BR2 main st 2	26.89	1618	13162	1.3	6.7	74	3.3	6	5	27.5	2.2	0.0	1.2	2.7
BR2 gw rev 1	26.92	1624	13210	1.7	6.9	67	1.1	4	na	22.0	2.2	0.0	1.0	1.6
BR2 gw rev 2	26.94	1638	13397	2.0	7.1	61	0.8	4	4	21.2	2.2	0.0	1.0	1.6
BR2 gw 01-20	27.00	1665	13642	2.0	6.7	461	0.4	4	na	19.7	102	0.5	2.1	7.9
BR2 gw 02-20	27.09	1710	14139	1.6	6.9	694	0.2	5	5	20.1	161	0.8	3.3	12.5
BR2 gw 03-20	27.31	1790	14932	1.2	7.1	689	0.3	5	na	20.8	163	0.8	3.5	12.6
BR2 gw 04-20	27.75	1892	15796	2.2	7.1	701	0.4	5	3	21.5	165	0.8	3.8	12.7
BR2 gw 05-50	28.03	1961	16053	2.1	7.1	1305	0.5	5	na	18.6	321	1.3	5.6	22.5
BR2 gw 06-50	28.11	2006	16522	2.1	7.0	1575	0.5	5	5	16.2	418	1.7	7.3	29.3
BR2 gw 07-50	28.27	2084	17322	1.2	7.1	1595	0.5	5	na	16.3	416	1.7	7.3	29.2
BR2 gw 08-50	28.73	2188	18228	2.0	7.1	1610	0.6	5	na	16.3	413	1.7	7.4	29.0
BR2 gw 09-80	29.04	2260	18485	2.6	7.2	2200	0.4	6	na	17.4	574	2.9	8.9	40.5
BR2 gw 10-80	29.11	2306	18969	2.3	7.1	2440	0.3	6	6	16.8	633	3.3	9.8	44.7
BR2 gw 11-80	29.25	2393	19899	1.4	7.1	2438	0.3	6	na	16.5	633	3.3	9.8	44.7
BR2 gw 12 pH6	29.72	2466	20153	2.5	7.1	2460	0.3	6	na	13.5	643	3.3	10.0	44.9
BR2 gw 13 pH6	29.79	2510	20629	2.5	7.0	2505	0.4	5	na	8.6	652	3.3	10.3	45.2
BR2 gw 14 pH6	29.92	2565	21034	2.5	6.9	2450	0.4	5	na	7.7	652	3.3	10.3	45.2
BR2 gw 15 pH6	30.03	2619	21514	2.5	6.7	2435	0.3	5	na	6.8	652	3.3	10.3	45.2
BR2 gw 16 st	33.67	2652	21568	2.6	7.0	2425	0.3	8	na	na	na	na	na	na
BR2 gw 17 pH5	33.68	2671	21826	2.6	6.7	2430	0.3	6	na	3.9	na	na	na	na
BR2 gw 18	33.75	2704	22093	2.6	7.0	2440	0.3	6	na	10.9	658	3.3	10.7	45.5
BR2 gw 19	33.82	2732	22330	2.6	7.1	2420	0.3	6	na	na	na	na	na	na
BR2 gw 20	33.89	2792	23255	0.9	6.8	2420	0.3	6	na	7.6	na	na	na	na
BR2 gw 21	34.59	2850	23735	2.5	na	na	na	na	na	na	na	na	na	na
BR2 gw 22	34.73	2923	24235	2.1	6.3	2440	0.3	6	na	na	na	na	na	na
BR2 gw 23	34.89	3038	25113	0.9	6.2	2405	0.3	6	na	na	na	na	na	na
BR2 gw 24	35.57	3111	25419	2.6	6.0	2430	0.3	6	na	na	na	na	na	na
BR2 gw 25	35.65	3167	26025	2.5	6.0	2525	0.3	6	na	1.9	na	na	na	na
BR2 gw 26	35.82	3173	26074	2.4	6.0	2555	0.3	6	na	na	na	na	na	na
BR2 gw 27 st	42.34	3210	26113	2.6	6.4	2500	0.3	8	na	23.2	na	na	na	na
BR2 gw 28	42.35	3242	26545	2.7	6.5	2490	0.3	6	na	17.8	na	na	na	na
BR2 gw 29	42.46	3328	27522	1.0	6.5	2380	0.3	6	na	na	na	na	na	na
BR2 gw 30	43.14	3449	28499	2.5	5.1	2330	0.3	6	na	4.8	na	na	na	na

PV*: pore volume from start of stormwater injection, TOC: total organic carbon, DOC: dissolved organic carbon; gw equi: phase 1 groundwater equilibration, stw: phase 2 stormwater injection; main st: phase 3 main storage; gw: phase 4 recovery with increasing amounts of groundwater. st: shorter storage. See Table VI-2 for details.

Table A-2: continued

BR – exp. 2	flow parameters				physico-chemical parameters					anions [mg/L]				
sample ID	runtime [d]	mean PV*	total outflow [mL]	flow velocity [mL/min]	pH	EC [µS/cm]	turbidity [NTU]	TOC [mg-C/L]	DOC [mg-C/L]	HCO_3	Cl	Br	NO_3	SO_4
BR2 gw 31 st	46.81	3512	28555	2.6	5.6	2445	0.3	8	na	0.1	499	4.7	9.6	60.1
BR2 gw 32	46.82	3583	29625	2.5	5.3	2495	0.3	6	na	na	na	na	na	na
BR2 gw 33	47.12	3705	30504	1.0	5.1	2490	0.3	5	na	0.8	511	4.8	10.7	63.4
BR2 gw 34	47.75	3820	31485	2.0	5.2	2490	0.3	6	na	na	na	na	na	na
BR2 gw 35 st	53.59	3883	31533	2.3	5.8	2505	0.3	7	na	na	na	na	na	na
BR2 gw 36	53.60	3923	32141	2.5	5.5	2580	0.3	5	na	na	na	na	na	na
BR2 gw 37	53.77	4014	33001	0.9	5.2	2455	0.3	5	na	na	na	na	na	na
BR2 gw 38	54.44	4127	33974	2.2	5.4	2510	0.3	5	na	na	na	na	na	na
BR2 gw 39	54.75	4240	34834	0.9	5.3	2530	0.3	5	na	0.8	503	2.9	0.3	38.1
BR2 gw 40	55.43	4351	35792	2.2	5.4	2515	0.3	5	na	na	na	na	na	na
BR2 gw 41	55.72	4459	36583	0.8	5.5	2455	0.3	5	na	na	na	na	na	na
BR2 gw 42	56.40	4568	37566	2.3	5.1	2510	0.3	5	na	na	na	na	na	na
BR2 gw 43 st	59.16	4631	37604	1.3	5.9	2525	0.3	6	na	na	na	na	na	na
BR2 gw 44	59.18	4691	38544	2.6	5.2	2505	0.3	5	na	na	na	na	na	na
BR2 gw 45	59.44	4807	39486	1.0	5.3	2480	0.3	5	na	0.9	481	2.8	0.3	38.3
BR2 gw 46	60.08	4926	40467	2.3	5.2	2510	0.3	5	na	na	na	na	na	na
BL - exp. 2														
BL2 gw equi	6.90	na	na	1.2	5.9	3050	0.6	6	na	0.4	1322	6.9	8.3	49.1
BL2 stw 01	7.03	3	43	1.2	6.6	401	282	10	na	2.0	84.9	0.5	1.4	2.0
BL2 stw 02	7.05	10	89	1.3	6.7	401	116	8	5	4.5	84.0	0.5	1.4	2.0
BL2 stw 03	7.08	17	136	1.3	6.8	341	62	5	na	5.1	70.7	0.5	1.4	1.9
BL2 stw 04	7.10	23	177	1.3	6.9	302	40	5	3	5.3	57.3	0.4	1.4	1.7
BL2 stw 05	7.12	29	224	1.3	6.9	238	25	5	na	5.5	47.9	0.3	1.3	1.6
BL2 stw 06	7.15	36	269	1.3	6.7	212	17	5	na	5.9	38.4	0.3	1.1	1.5
BL2 stw 07	7.17	62	573	1.3	6.6	119	5.5	4	na	5.9	18.4	0.1	0.5	0.7
BL2 stw 08	7.34	88	624	1.3	6.3	80	5.5	4	na	8.1	9.7	0.1	0.3	0.4
BL2 stw 09	7.37	159	1537	1.2	6.8	43	2.1	4	na	8.9	4.3	0.0	0.1	0.2
BL2 stw 10	7.89	229	1585	1.2	6.3	49	4.7	4	na	10.2	2.6	0.0	0.9	0.7
BL2 stw 11	7.91	288	2335	1.3	5.4	46	2.3	3	na	10.0	2.6	0.0	0.8	0.6
BL2 stw 12	8.33	346	2383	1.2	6.4	49	2.6	3	na	12.9	2.3	0.0	1.0	0.8
BL2 stw 13	8.36	436	3558	1.2	6.8	50	1.6	3	na	15.8	2.3	0.0	0.8	0.6
BL2 stw 14	9.06	525	3600	1.1	6.6	53	1.8	3	na	15.2	2.3	0.0	0.8	0.7
BL2 stw 15	9.08	670	5530	1.1	7.0	54	1.2	3	na	14.5	2.2	0.0	0.7	0.7
BL2 stw 16	10.28	815	5571	1.1	6.7	56	0.8	3	na	17.5	2.1	0.0	0.7	0.7
BL2 stw 17	10.31	1031	8479	1.0	7.1	59	1.0	3	na	20.5	2.2	0.0	0.7	0.7
BL2 stw 18	12.29	1248	8516	0.9	7.0	61	0.8	3	na	20.8	2.3	0.0	0.8	0.7
BL2 stw 19	12.32	1403	10591	0.8	7.2	59	0.6	5	5	21.8	2.3	0.0	0.8	0.7
BL2 stw 20	14.04	1559	10623	0.9	6.8	60	0.9	3	na	21.0	2.3	0.0	0.8	0.7
BL2 main st 1	21.07	1566	10672	1.4	6.4	92	2.6	8	na	18.0	2.3	0.0	0.7	3.2
BL2 main st 2	26.89	1573	10725	1.4	6.4	80	3.7	7	7	20.0	2.3	0.0	0.7	3.2
BL2 gw rev 1	26.92	1581	10773	1.8	6.9	67	1.3	3	na	17.0	2.0	0.0	0.6	2.7
BL2 gw rev 2	26.94	1598	10966	2.1	7.1	56	0.9	5	4	16.2	1.9	0.0	0.6	2.6
BL2 gw 01-20	27.00	1631	11219	2.1	6.7	479	0.9	4	na	14.7	98	0.5	2.2	7.9
BL2 gw 02-20	27.09	1687	11724	1.6	6.8	684	0.3	4	4	14.7	163	0.8	3.6	13.1
BL2 gw 03-20	27.31	1782	12516	1.2	6.8	686	0.5	4	na	15.0	164	0.8	3.6	13.2
BL2 gw 04-20	27.75	1903	13374	2.1	6.8	696	0.6	5	4	14.3	165	0.8	3.6	13.2
BL2 gw 05-50	28.03	1985	13627	2.0	6.8	1289	0.8	5	na	14.2	322	1.3	5.9	22.7
BL2 gw 06-50	28.11	2037	14093	2.1	6.8	1545	0.9	5	5	12.1	412	1.7	7.6	29.1
BL2 gw 07-50	28.27	2130	14894	1.2	6.8	1590	0.9	5	na	12.7	415	1.7	7.5	29.2
BL2 gw 08-50	28.73	2255	15797	2.0	6.8	1575	0.9	5	na	13.2	417	1.7	7.5	29.4
BL2 gw 09-80	29.04	2340	16051	2.6	7.1	2170	0.7	6	na	14.4	559	2.9	9.1	38.8
BL2 gw 10-80	29.11	2394	16530	2.3	7.0	2450	0.3	7	7	14.3	634	3.3	10.4	44.0
BL2 gw 11-80	29.25	2497	17445	1.4	7.0	2435	0.4	7	na	14.6	634	3.3	10.4	44.0
BL2 gw 12 pH6	29.72	2582	17691	2.4	6.9	2485	0.4	7	na	10.5	634	3.3	10.0	43.9
BL2 gw 13 pH6	29.79	2635	18165	2.5	6.8	2540	0.4	7	na	7.5	634	3.3	9.7	43.8

PV*: pore volume from start of stormwater injection, TOC: total organic carbon, DOC: dissolved organic carbon; gw equi: phase 1 groundwater equilibration, stw: phase 2 stormwater injection; main st: phase 3 main storage; gw: phase 4 recovery with increasing amounts of groundwater. st: shorter storage. See Table VI-2 for details.

Table A-2: continued

BL – exp. 2	flow parameters				physico-chemical parameters					anions [mg/L]				
sample ID	runtime [d]	mean PV*	total outflow [mL]	flow velocity [mL/min]	pH	EC [µS/cm]	turbidity [NTU]	TOC [mg-C/L]	DOC [mg-C/L]	HCO_3	Cl	Br	NO_3	SO_4
BL2 gw 14 pH6	29.92	2699	18564	2.5	6.8	2470	0.4	7	na	6.2	647	3.3	9.5	44.7
BL2 gw 15 pH6	30.03	2763	19042	2.4	6.5	2435	0.4	7	na	4.8	659	3.3	9.3	45.6
BL2 gw 16 st	33.67	2802	19091	2.3	7.0	2425	0.3	9	na	na	na	na	na	na
BL2 gw 17 pH5	33.68	2822	19323	2.4	6.7	2435	0.3	7	na	4.6	na	na	na	na
BL2 gw 18	33.75	2857	19562	2.3	7.0	2440	0.3	6	na	11.0	637	3.3	10.6	44.2
BL2 gw 19	33.82	2883	19776	2.3	7.1	2430	0.3	6	na	na	na	na	na	na
BL2 gw 20	33.89	2954	20642	0.8	6.9	2420	0.3	6	na	9.9	na	na	na	na
BL2 gw 21	34.59	3012	21122	2.5	na	na	na	na	na	na	na	na	na	na
BL2 gw 22	34.73	3105	21622	2.1	6.6	2435	0.3	6	na	na	na	na	na	na
BL2 gw 23	34.89	3239	22465	0.9	6.5	2410	0.3	6	na	na	na	na	na	na
BL2 gw 24	35.57	3322	22751	2.4	6.5	2440	0.3	6	na	na	na	na	na	na
BL2 gw 25	35.65	3383	23307	2.3	6.4	2520	0.3	6	na	3.7	na	na	na	na
BL2 gw 26	35.82	3389	23354	2.3	6.3	2555	0.3	6	na	na	na	na	na	na
BL2 gw 27 st	42.34	3430	23391	2.5	7.0	2615	0.3	9	na	50.2	na	na	na	na
BL2 gw 28	42.35	3468	23823	2.7	6.3	2470	0.3	7	na	50.4	na	na	na	na
BL2 gw 29	42.46	3571	24789	1.0	6.3	2370	0.3	6	na	na	na	na	na	na
BL2 gw 30	43.14	3713	25759	2.5	5.5	2305	0.3	6	na	13.1	na	na	na	na
BL2 gw 31 st	46.81	3788	25813	2.4	5.6	2460	0.3	9	na	13.3	502	4.6	8.8	65.5
BL2 gw 32	46.82	3873	26883	2.5	5.5	2510	0.3	6	na	na	na	na	na	na
BL2 gw 33	47.12	4019	27771	1.0	5.4	na	0.3	6	na	3.5	508	4.8	10.3	44.0
BL2 gw 34	47.75	4157	28759	2.0	na	na	0.3	6	na	na	na	na	na	na
BL2 gw 35 st	53.59	4233	28809	2.4	5.9	2555	0.3	11	na	na	na	na	na	na
BL2 gw 36	53.60	4282	29432	2.5	5.5	2580	0.3	7	na	na	na	na	na	na
BL2 gw 37	53.77	4391	30293	0.9	5.2	2470	0.3	6	na	na	na	na	na	na
BL2 gw 38	54.44	4526	31269	2.2	5.4	2505	0.3	6	na	na	na	na	na	na
BL2 gw 39	54.75	4661	32130	0.9	5.3	2555	0.3	5	na	na	498	2.8	0.3	39.7
BL2 gw 40	55.43	4794	33082	2.2	5.5	2510	0.3	5	na	na	na	na	na	na
BL2 gw 41	55.72	4923	33887	0.8	5.3	2475	0.3	5	na	na	na	na	na	na
BL2 gw 42	56.40	5054	34866	2.3	5.1	2505	0.3	5	na	na	na	na	na	na
BL2 gw 43 st	59.16	5128	34903	1.2	5.7	2535	0.3	9	na	na	na	na	na	na
BL2 gw 44	59.18	5197	35804	2.4	5.2	2515	0.3	5	na	na	na	na	na	na
BL2 gw 45	59.44	5329	36699	1.0	5.2	2485	0.3	5	5	0.2	488	2.8	0.3	38.4
BL2 gw 46	60.08	5463	37636	2.2	5.1	2515	0.3	5	na	na	na	na	na	na
WS - exp. 2														
WS2 gw equi	6.90	na	na	1.2	6.6	3100	0.3	6	na	11.5	815	4.6	8.9	16.7
WS2 stw 01	7.03	3	42	1.2	6.9	373	25	3	na	14.0	83.5	0.5	1.4	1.9
WS2 stw 02	7.05	11	91	1.4	6.8	378	29	4	3	14.6	77.8	0.5	1.3	1.8
WS2 stw 03	7.08	18	140	1.3	6.8	329	25	3	na	15.2	66.1	0.4	1.2	1.7
WS2 stw 04	7.10	26	183	1.3	6.9	280	16	3	2	15.7	54.4	0.4	1.1	1.6
WS2 stw 05	7.12	33	233	1.3	6.9	245	9.0	3	na	16.3	46.2	0.3	1.7	1.5
WS2 stw 06	7.15	41	279	1.3	6.9	213	5.6	2	na	16.9	38.0	0.3	2.4	1.4
WS2 stw 07	7.17	70	594	1.3	7.1	135	0.9	2	na	19.1	21.2	0.1	1.3	0.8
WS2 stw 08	7.34	99	647	1.3	7.0	110	0.7	2	na	20.4	13.3	0.1	0.8	0.5
WS2 stw 09	7.37	181	1613	1.3	7.2	71	0.5	2	na	22.4	5.88	0.0	0.4	0.2
WS2 stw 10	7.89	262	1663	1.3	7.1	67	0.5	2	na	21.9	2.58	0.0	0.7	0.5
WS2 stw 11	7.91	326	2413	1.3	7.2	63	0.5	2	na	22.1	2.58	0.0	0.7	0.5
WS2 stw 12	8.33	390	2463	1.3	7.0	63	0.6	2	na	23.4	2.40	0.0	0.7	0.5
WS2 stw 13	8.36	496	3735	1.3	7.0	63	0.3	2	na	24.8	2.50	0.0	0.7	0.5
WS2 stw 14	9.06	602	3781	1.2	6.9	65	0.3	2	na	25.0	2.21	0.0	0.7	0.5
WS2 stw 15	9.08	779	5946	1.3	7.0	62	0.3	2	na	25.2	2.19	0.0	0.8	0.5
WS2 stw 16	10.28	956	5993	1.3	6.9	63	0.3	2	na	25.3	2.19	0.0	0.8	0.5
WS2 stw 17	10.31	1243	9538	1.2	6.9	66	0.5	2	na	25.5	2.19	0.0	0.8	0.5
WS2 stw 18	12.29	1531	9593	1.3	7.0	67	0.3	2	na	25.3	2.25	0.0	0.8	0.5
WS2 stw 19	12.32	1775	12577	1.2	7.0	66	0.3	5	5	24.9	2.25	0.0	0.8	0.5
WS2 stw 20	14.04	2018	12626	1.3	6.9	67	0.4	2	na	25.0	2.25	0.0	0.8	0.5

PV*: pore volume from start of stormwater injection, TOC: total organic carbon, DOC: dissolved organic carbon; gw equi: phase 1 groundwater equilibration, stw: phase 2 stormwater injection; main st: phase 3 main storage; gw: phase 4 recovery with increasing amounts of groundwater. st: shorter storage. See Table VI-2 for details.

Table A-2: continued

WS – exp. 2	flow parameters				physico-chemical parameters					anions [mg/L]				
sample ID	runtime [d]	mean PV*	total outflow [mL]	flow velocity [mL/min]	pH	EC [µS/cm]	turbidity [NTU]	TOC [mg-C/L]	DOC [mg-C/L]	HCO_3	Cl	Br	NO_3	SO_4
WS2 main st 1	21.07	2025	12673	1.3	6.8	85	1.5	6	na	24.0	2.55	0.0	1.2	2.1
WS2 main st 2	26.89	2033	12728	1.5	6.8	81	2.0	7	6	24.0	2.55	0.0	1.2	2.1
WS2 gw rev 1	26.92	2041	12777	1.8	7.0	68	0.9	4	na	23.8	1.91	0.0	0.9	1.5
WS2 gw rev 2	26.94	2061	12971	2.1	7.2	63	0.4	3	2	23.8	1.99	0.0	1.0	1.6
WS2 gw 01-20	27.00	2097	13226	2.1	6.9	460	0.2	5	na	22.1	91.8	0.4	1.9	7.0
WS2 gw 02-20	27.09	2158	13734	1.6	6.9	666	0.3	3	3	21.6	161	0.8	3.3	12.4
WS2 gw 03-20	27.31	2261	14522	1.2	7.1	691	0.4	3	na	21.8	163	0.8	3.4	12.5
WS2 gw 04-20	27.75	2393	15379	2.1	7.1	693	0.4	5	4	22.1	164	0.8	3.6	12.6
WS2 gw 05-50	28.03	2482	15631	2.0	7.1	1215	0.4	5	na	19.7	304	1.3	5.4	20.5
WS2 gw 06-50	28.11	2539	16098	2.1	7.1	1565	0.4	6	5	18.1	394	1.7	7.0	26.6
WS2 gw 07-50	28.27	2642	16915	1.2	7.1	1585	0.3	6	na	18.2	397	1.7	7.0	27.4
WS2 gw 08-50	28.73	2781	17833	2.1	7.2	1595	0.4	6	na	18.3	401	1.7	7.0	28.1
WS2 gw 09-80	29.04	2875	18093	2.7	7.2	2180	0.8	6	na	15.8	546	2.8	10.8	37.6
WS2 gw 10-80	29.11	2935	18577	2.3	7.0	2505	1.0	6	na	13.4	647	3.3	12.8	44.5
WS2 gw 11-80	29.25	3048	19501	1.4	7.1	2485	0.8	6	na	12.1	647	3.3	12.8	44.5
WS2 gw 12 pH6	29.72	3142	19754	2.5	7.0	2515	0.4	6	na	10.4	651	3.3	11.9	44.7
WS2 gw 13 pH6	29.79	3200	20230	2.5	6.9	2460	0.4	6	na	7.9	655	3.3	11.1	45.0
WS2 gw 14 pH6	29.92	3271	20633	2.5	6.9	2480	0.3	6	na	6.5	650	3.3	10.3	44.7
WS2 gw 15 pH6	30.03	3342	21118	2.5	6.6	2465	0.5	6	na	5.1	645	3.3	9.4	44.5
WS2 gw 16 st	33.67	3385	21171	2.5	7.0	2420	0.4	8	na	na	na	na	na	na
WS2 gw 17 pH5	33.68	3409	21418	2.5	6.8	2430	0.4	6	na	3.3	na	na	na	na
WS2 gw 18	33.75	3449	21676	2.5	6.9	2440	0.4	6	na	8.8	656	3.3	10.4	45.2
WS2 gw 19	33.82	3477	21906	2.5	6.9	2430	0.4	6	na	na	na	na	na	na
WS2 gw 20	33.89	3560	22796	0.9	6.8	2420	0.4	6	na	7.7	na	na	na	na
WS2 gw 21	34.59	3618	23276	2.5	na	na	na	na	na	na	na	na	na	na
WS2 gw 22	34.73	3728	23776	2.1	6.4	2430	0.4	6	na	na	na	na	na	na
WS2 gw 23	34.89	3873	24614	0.9	6.3	2405	0.4	6	na	na	na	na	na	na
WS2 gw 24	35.57	3964	24907	2.5	6.2	2435	0.4	6	na	na	na	na	na	na
WS2 gw 25	35.65	4034	25491	2.4	6.1	2525	0.4	6	na	1.2	na	na	na	na
WS2 gw 26	35.82	4040	25539	2.4	5.9	2540	0.4	6	na	na	na	na	na	na
WS2 gw 27 st	42.34	4088	25578	2.6	6.8	2580	0.4	8	na	16.3	na	na	na	na
WS2 gw 28	42.35	4129	26004	2.7	5.9	2455	0.4	7	na	15.8	na	na	na	na
WS2 gw 29	42.46	4238	26938	0.9	5.3	2370	0.4	5	na	na	na	na	na	na
WS2 gw 30	43.14	4388	27884	2.5	5.1	2390	0.4	5	na	3.6	na	na	na	na
WS2 gw 31 st	46.81	4468	27940	2.5	5.6	2460	0.4	8	na	14.1	503	4.7	8.5	58.8
WS2 gw 32	46.82	4561	29010	2.5	5.3	2505	0.4	7	na	na	na	na	na	na
WS2 gw 33	47.12	4716	29844	0.9	5.1	na	0.4	5	na	0.8	507	4.9	10.4	57.1
WS2 gw 34	47.75	4857	30778	1.9	na	na	0.4	5	na	na	na	na	na	na
WS2 gw 35 st	53.59	4936	30823	2.1	5.9	2525	0.4	10	na	na	na	na	na	na
WS2 gw 36	53.60	4985	31391	2.3	5.5	2590	0.4	5	na	na	na	na	na	na
WS2 gw 37	53.77	5093	32182	0.8	5.1	2470	0.4	5	na	na	na	na	na	na
WS2 gw 38	54.44	5229	33085	2.0	5.3	2530	0.4	5	na	na	na	na	na	na
WS2 gw 39	54.75	5365	33876	0.8	5.3	2555	0.4	5	na	0.7	500	2.9	0.3	38.1
WS2 gw 40	55.43	5498	34757	2.1	5.5	2515	0.4	5	na	na	na	na	na	na
WS2 gw 41	55.72	5628	35497	0.8	5.4	2490	0.4	5	na	na	na	na	na	na
WS2 gw 42	56.40	5760	36401	2.1	5.3	2505	0.4	5	na	na	na	na	na	na
WS2 gw 43 st	59.16	5835	36438	1.2	5.9	2280	0.4	7	na	na	na	na	na	na
WS2 gw 44	59.18	5910	37338	2.4	5.2	2510	0.4	7	na	na	na	na	na	na
WS2 gw 45	59.44	6053	38225	1.0	5.3	2490	0.4	6	6	0.6	481	2.7	0.3	36.2
WS2 gw 46	60.08	6198	39152	2.2	5.2	2520	0.4	6	na	na	na	na	na	na

PV*: pore volume from start of stormwater injection, TOC: total organic carbon, DOC: dissolved organic carbon; gw equi: phase 1 groundwater equilibration, stw: phase 2 stormwater injection; main st: phase 3 main storage; gw: phase 4 recovery with increasing amounts of groundwater. st: shorter storage. See Table VI-2 for details.

Table A-2a: K_d values for adsorption experiments (series A4) with varying salinity of adsorption solution (BR- brown Tertiary Brighton Group sediment, BL – black Tertiary Brighton Group sediment, WS – Quaternary Werribee Delta sediment with no and 30 mg-C/L addition of fulvic acid.

	Zn				Cu			
% of added groundwater	0%	20%	50%	80%	0%	20%	50%	80%
0BR	2.6	2.7	2.7	2.0	59	64	69	31
30BR	2.6	2.2	2.1	2.1	41	68	34	31
0BL	2.5	1.5	1.5	1.7	79	59	127	72
30BL	2.7				75	65	74	69
0WS	~440	270	113	92	~800	~1290	~1250	~1510
30WS	~200				63	64	65	67

Table A-2b: % metal sorbed for adsorption experiments (series A5) with varying pre-equilibration condition (BR- brown Tertiary Brighton Group sediment, BL – black Tertiary Brighton Group sediment, WS – Quaternary Werribee Delta sediment with no and 30 mg-C/L addition of fulvic acid.

	Zn			Cu		
pre-equilibration	none	oxic groundwater	anoxic groundwater	none	oxic groundwater	anoxic groundwater
0BR	25.7	44.7	33.2	92.1	89.3	92.9
30BR	37.0	53.4	42.1	83.3	93.7	91.5
0BL	31.7	42.9	56.7	94.8	93.9	96.5
30BL	35.1	42.3	32.4	95.6	93.6	91.3
0WS	44.1	64.2	48.4	89.5	99.4	99.3
30WS	38.6	37.2	26.8	93.8	87.3	83.6

Table A-2c: % metal desorbed for desorption experiments of series D3 with varying salinity of desorption solution (BR- brown Tertiary Brighton Group sediment, BL – black Tertiary Brighton Group sediment, WS – Quaternary Werribee Delta sediment with no and 30 mg-C/L addition of fulvic acid. Negative values indicate adsorption.

	Zn				Cu			
% of added groundwater	0%	20%	50%	80%	0%	20%	50%	80%
0BR	7.4	-21.2	10.7	10.1	-0.2	-1.0	2.8	2.2
30BR	2.7	6.4	23.1	-0.7	-0.6	0.7	1.4	0.9
0BL	-3.1	2.7	23.4	-50.2	-0.2	0.2	1.5	0.5
0WS	4.7	10.2	23.6	8.3				
30WS					1.5	0.0	0.2	-0.4

Table A-3: Analysis of mean values for column samples of experiment 2, cations and metals.

BR – exp.2	major cations (total) [mg/L]				metals (total) [µg/L]						
sample ID	Na	K	Mg	Ca	Al	As	Cu	Fe	Mn	Ni	Zn
BR2 gw equi	429	1.7	69.5	14.4	na	na	30	51	86	17	835
BR2 stw 01	53.8	2.0	6.5	1.2	19004	35	12	9047	14	11	84
BR2 stw 02	53.3	0.6	8.1	1.7	4700	na	8	2230	9	na	92
BR2 stw 03	41.0	0.5	9.8	1.8	1282	na	6	817	12	na	107
BR2 stw 04	31.2	0.6	9.2	1.7	897	na	10	578	10	na	103
BR2 stw 05	24.5	0.4	9.0	1.5	639	na	na	436	9	na	85
BR2 stw 06	18.8	0.6	8.0	1.4	390	na	3	268	8	na	83
BR2 stw 07	9.6	0.5	7.3	1.4	239	7	2	176	7	na	59
BR2 stw 08	6.0	0.6	6.3	2.5	748	na	6	506	7	na	78
BR2 stw 09	3.9	0.5	2.6	8.8	177	na	4	149	6	na	45
BR2 stw 10	2.7	0.9	0.7	10.8	223	na	8	160	3	na	46
BR2 stw 11	2.3	0.5	0.7	11.8	152	na	7	107	3	na	40
BR2 stw 12	2.5	0.6	0.6	12.2	79	na	8	90	na	na	73
BR2 stw 13	2.2	0.5	0.5	12.4	124	na	5	93	2	na	233
BR2 stw 14	2.4	0.6	0.5	11.5	119	na	7	89	na	na	606
BR2 stw 15	2.3	0.5	0.5	11.9	64	na	7	74	na	na	861
BR2 stw 16	2.1	0.6	0.5	11.5	na	8	17	21	na	na	1373
BR2 stw 17	2.3	0.5	0.5	12.1	na	na	9	na	na	na	1360
BR2 stw 18	2.9	0.6	0.5	11.3	208	na	19	12	na	na	1505
BR2 stw 19	2.2	0.5	0.5	11.8	na	9	12	na	na	na	1518
BR2 stw 20	2.2	0.8	0.5	12.0	na	na	26	32	na	na	1607
BR2 main st 1	2.7	0.8	0.7	15.4	77	na	41	47	na	na	2598
BR2 main st 2	2.3	1.1	0.6	13.7	164	na	26	59	na	na	2456
BR2 gw rev 1	2.3	0.6	0.5	11.2	na	na	512	45	3	na	1983
BR2 gw rev 2	2.0	0.5	0.4	9.6	na	na	347	33	5	na	2038
BR2 gw 01-20	53.5	1.1	2.8	24.5	na	na	567	46	6	na	4016
BR2 gw 02-20	84.7	1.0	14.2	14.9	na	na	356	27	6	na	2228
BR2 gw 03-20	83.0	1.0	16.5	11.8	na	na	221	na	14	na	1188
BR2 gw 04-20	84.1	0.9	16.7	11.8	na	na	170	na	17	na	833
BR2 gw 05-50	167	1.1	29.2	17.7	na	na	110	15	28	5	1177
BR2 gw 06-50	213	1.0	38.1	13.0	na	na	175	15	35	4	1276
BR2 gw 07-50	214	1.0	38.9	12.2	na	na	155	23	40	5	1139
BR2 gw 08-50	212	1.0	38.5	12.1	na	na	126	18	40	na	941
BR2 gw 09-80	294	1.3	51.0	15.2	na	na	154	14	54	na	1145
BR2 gw 10-80	326	1.4	56.5	14.1	na	na	145	na	63	5	1154
BR2 gw 11-80	326	1.4	56.6	13.8	na	na	142	12	66	na	1053
BR2 gw 12 pH6	330	1.4	57.3	14.1	na	na	128	na	69	na	954
BR2 gw 13 pH6	328	1.4	56.9	13.9	na	na	128	11	73	5	1026
BR2 gw 14 pH6	328	1.5	56.4	13.7	na	na	137	18	68	6	1127
BR2 gw 15 pH6	327	1.5	56.8	13.7	na	na	131	27	70	6	1024
BR2 gw 16 st	332	2.6	58.2	14.6	na	na	420	36	85	24	1904
BR2 gw 17 pH5	330	1.6	56.8	13.8	na	na	195	19	75	5	1436
BR2 gw 18	332	1.6	58.0	14.4	na	na	271	27	78	7	1749
BR2 gw 19	na	na	na	na	na	na	511	41	86	12	2074
BR2 gw 20	328	1.6	57.3	14.9	na	6	756	36	84	15	2351
BR2 gw 21	na	na	na	na	na	na	na	na	na	na	na
BR2 gw 22	329	2.4	57.5	14.5	na	na	602	26	71	10	899
BR2 gw 23	323	2.3	56.9	16.4	na	na	1147	52	70	15	1275
BR2 gw 24	325	2.8	57.0	16.3	na	na	905	25	68	10	856
BR2 gw 25	337	2.2	58.3	15.7	na	na	684	29	68	14	908
BR2 gw 26	na	na	na	na	na	na	na	na	na	na	na
BR2 gw 27 st	213	1.7	40.4	11.6	122	na	957	175	73	26	1736
BR2 gw 28	269	2.0	49.4	12.7	55	6	1434	301	69	13	1189
BR2 gw 29	293	1.8	57.2	14.2	148	7	610	166	73	10	594
BR2 gw 30	270	1.4	51.4	13.3	206	na	299	444	67	6	422
BR2 gw 31 st	210	1.1	38.3	10.9	256	na	550	309	56	29	1073
BR2 gw 32	253	1.4	48.4	12.1	214	na	177	206	62	6	383
BR2 gw 33	254	1.5	46.1	12.1	187	na	117	122	63	6	356
BR2 gw 34	292	1.5	55.9	13.7	170	na	99	105	71	8	337
BR2 gw 35 st	299	1.9	57.6	15.4	128	na	296	806	80	38	1080

gw equi: phase 1 groundwater equilibration, stw: phase 2 stormwater injection; main st: phase 3 main storage; gw: phase 4 recovery with increasing amounts of groundwater. st: shorter storage. See Table VI-2 for details.

Table A-3: continued

BR – exp.2	major cations (total) [mg/L]				metals (total) [µg/L]						
sample ID	Na	K	Mg	Ca	Al	As	Cu	Fe	Mn	Ni	Zn
BR2 gw 36	279	1.6	54.8	13.3	173	na	102	463	70	6	356
BR2 gw 37	296	1.9	57.4	14.3	107	na	57	107	74	8	373
BR2 gw 38	230	1.3	42.7	10.7	179	na	35	252	57	na	241
BR2 gw 39	250	1.5	46.6	11.8	169	na	40	114	63	7	262
BR2 gw 40	153	1.0	26.7	7.1	505	na	24	233	38	12	146
BR2 gw 41	68	0.5	12.3	3.2	652	na	13	281	19	na	81
BR2 gw 42	193	1.1	36.0	8.6	306	7	29	147	47	6	202
BR2 gw 43 st	155	0.9	28.0	7.2	372	na	33	208	41	16	312
BR2 gw 44	181	1.1	32.2	8.1	327	5	21	193	44	na	212
BR2 gw 45	274	1.6	48.6	12.5	152	3	27	100	68	7	311
BR2 gw 46	258	1.3	43.9	11.7	157	na	22	98	64	9	282
BL - exp. 2											
BL2 gw equi	430	1.6	68.9	13.5	na	6	110	113	77	19	826
BL2 stw 01	60.4	0.8	7.4	1.5	18851	48	34	4362	12	10	80
BL2 stw 02	57.1	0.8	7.2	1.4	7778	34	12	1800	7	na	76
BL2 stw 03	49.1	0.3	6.7	1.2	3832	36	12	1077	8	na	71
BL2 stw 04	42.9	0.7	5.7	1.1	2480	24	10	696	6	na	70
BL2 stw 05	34.9	0.4	4.7	0.8	1417	19	10	529	5	na	70
BL2 stw 06	29.4	0.4	4.0	0.7	948	18	5	357	4	na	63
BL2 stw 07	15.1	0.4	3.5	0.6	278	12	3	96	3	na	64
BL2 stw 08	7.7	0.9	3.7	0.6	479	16	9	378	4	na	82
BL2 stw 09	3.4	0.5	3.8	0.5	77	9	8	49	3	7	132
BL2 stw 10	2.2	0.7	4.0	0.7	181	11	10	102	3	na	86
BL2 stw 11	2.0	0.5	4.3	0.9	82	na	11	52	4	5	104
BL2 stw 12	2.5	0.7	4.2	1.4	192	na	8	78	4	na	70
BL2 stw 13	2.0	0.5	3.9	3.0	112	8	9	35	4	4	91
BL2 stw 14	2.4	0.6	2.9	4.6	205	5	6	39	5	na	70
BL2 stw 15	2.0	0.5	2.0	7.1	108	8	8	66	6	na	79
BL2 stw 16	2.1	0.6	1.3	8.4	49	na	7	85	5	na	78
BL2 stw 17	2.2	0.5	0.9	10.1	na	na	31	42	5	na	131
BL2 stw 18	2.1	0.6	0.7	10.3	na	na	7	29	4	na	172
BL2 stw 19	2.2	0.5	0.6	11.0	na	na	9	38	4	na	232
BL2 stw 20	2.2	0.7	0.7	11.2	32	na	16	128	4	na	297
BL2 main st 1	2.9	0.7	1.1	16.9	94	na	27	43	7	na	422
BL2 main st 2	2.4	0.7	0.9	13.7	143	na	13	47	6	na	377
BL2 gw rev 1	2.0	0.5	0.5	11.0	na	na	524	34	4	na	2061
BL2 gw rev 2	2.0	0.4	0.4	8.2	na	5	406	29	3	4	1744
BL2 gw 01-20	51.3	1.1	1.5	28.0	12	na	769	16	4	na	4734
BL2 gw 02-20	86.4	1.0	6.0	25.9	na	na	606	na	4	na	3682
BL2 gw 03-20	86.0	1.0	12.3	16.1	na	na	420	na	4	na	2279
BL2 gw 04-20	85.4	1.0	15.2	11.7	na	5	267	na	6	na	1409
BL2 gw 05-50	165	1.2	28.7	19.2	na	na	252	32	11	na	1918
BL2 gw 06-50	211	1.0	33.7	19.0	na	na	256	30	15	na	1726
BL2 gw 07-50	215	1.0	36.8	14.5	na	na	222	38	18	6	1368
BL2 gw 08-50	211	1.0	37.7	12.3	na	na	157	33	24	na	963
BL2 gw 09-80	287	1.2	50.5	16.2	na	na	178	22	36	na	1102
BL2 gw 10-80	328	1.4	55.1	16.6	na	na	158	na	43	na	1023
BL2 gw 11-80	332	1.5	56.1	14.7	na	na	150	12	47	na	894
BL2 gw 12 pH6	329	1.4	56.5	14.1	na	na	128	14	53	na	779
BL2 gw 13 pH6	330	1.4	56.5	14.1	na	na	118	19	55	5	697
BL2 gw 14 pH6	334	1.4	57.0	14.1	na	na	112	20	59	na	660
BL2 gw 15 pH6	330	1.4	57.3	14.0	na	6	105	21	62	5	628
BL2 gw 16 st	332	4.0	59.7	15.1	16	na	363	106	82	8	1526
BL2 gw 17 pH5	331	1.7	57.3	14.5	na	na	180	23	69	na	933
BL2 gw 18	331	1.6	58.2	14.7	na	na	192	102	71	na	909
BL2 gw 19	327	1.6	57.9	14.9	na	na	na	na	na	na	na
BL2 gw 20	326	1.6	58.2	15.5	na	na	188	61	84	15	937
BL2 gw 21	na	na	na	na	na	na	na	na	na	na	na
BL2 gw 22	330	2.0	58.0	15.0	na	na	162	21	81	6	856

gw equi: phase 1 groundwater equilibration, stw: phase 2 stormwater injection; main st: phase 3 main storage; gw: phase 4 recovery with increasing amounts of groundwater. st: shorter storage. See Table VI-2 for details.

Table A-3: continued

BL – exp.2	major cations (total) [mg/L]				metals (total) [µg/L]						
sample ID	Na	K	Mg	Ca	Al	As	Cu	Fe	Mn	Ni	Zn
BL2 gw 23	323	2.3	58.2	16.3	na	na	243	32	87	15	1079
BL2 gw 24	321	2.4	56.8	16.9	na	na	242	23	84	6	1113
BL2 gw 25	335	2.3	57.9	17.1	na	na	247	23	82	7	1163
BL2 gw 26	335	2.3	57.9	17.1	na	na	na	na	na	na	na
BL2 gw 27 st	249	2.5	47.6	14.7	110	na	610	152	96	13	1799
BL2 gw 28	264	1.4	52.0	16.3	47	na	563	98	90	7	1684
BL2 gw 29	308	1.9	61.0	17.6	61	8	540	96	100	15	1913
BL2 gw 30	222	1.1	41.3	11.8	190	na	207	155	64	12	954
BL2 gw 31 st	284	1.3	54.4	14.3	188	na	495	251	124	18	1715
BL2 gw 32	244	1.4	46.7	12.1	177	8	129	221	63	13	766
BL2 gw 33	268	1.5	50.7	13.0	150	na	74	151	69	11	481
BL2 gw 34	288	1.6	56.2	14.3	131	na	166	526	76	15	934
BL2 gw 35 st	274	1.5	53.6	13.5	160	8	231	747	73	14	911
BL2 gw 36	309	1.9	59.3	14.8	98	8	140	513	77	12	577
BL2 gw 37	295	1.9	56.7	14.1	97	na	65	136	73	9	427
BL2 gw 38	263	1.4	51.6	12.4	145	na	48	129	66	9	344
BL2 gw 39	202	1.2	36.7	9.5	235	na	41	148	52	7	245
BL2 gw 40	139	0.8	27.3	6.3	412	na	32	206	36	na	151
BL2 gw 41	54.9	0.3	10.4	2.5	633	na	8	291	15	na	60
BL2 gw 42	147	1.0	25.2	6.8	389	na	32	239	38	7	249
BL2 gw 43 st	172	1.0	31.2	7.9	299	8	40	248	44	7	322
BL2 gw 44	241	1.2	41.3	10.9	196	6	39	178	59	6	293
BL2 gw 45	219	1.1	37.5	9.9	250	1	24	140	54	6	252
BL2 gw 46	291	1.5	50.1	13.3	133	na	40	94	71	6	317
WS - exp. 2											
WS2 gw equi	430	1.8	69.6	14.5	170	na	31	50	94	13	666
WS2 stw 01	56.5	0.5	5.8	1.1	2223	na	17	2945	13	na	65
WS2 stw 02	53.6	0.6	6.8	1.4	2543	na	8	3372	9	na	74
WS2 stw 03	46.6	0.5	8.4	1.5	1430	na	6	2349	16	na	89
WS2 stw 04	34.9	0.4	8.3	1.5	913	na	6	1500	10	na	78
WS2 stw 05	22.1	0.2	6.9	1.2	232	na	2	556	10	na	55
WS2 stw 06	23.4	0.4	8.9	1.6	148	na	6	355	10	na	79
WS2 stw 07	12.6	0.5	8.0	1.6	182	na	4	25	8	na	51
WS2 stw 08	8.1	0.9	7.4	2.2	215	na	7	20	7	na	56
WS2 stw 09	3.4	0.5	4.0	7.1	na	na	4	27	6	na	38
WS2 stw 10	2.2	0.7	1.6	10.0	na	na	8	33	5	na	49
WS2 stw 11	2.1	0.5	1.2	11.3	na	na	10	27	4	na	113
WS2 stw 12	2.2	0.5	0.9	11.2	na	na	6	15	4	na	233
WS2 stw 13	2.3	0.5	0.7	12.1	na	na	5	11	3	na	577
WS2 stw 14	2.4	0.5	0.6	11.5	188	na	10	24	3	na	920
WS2 stw 15	2.1	0.4	0.5	11.9	na	na	6	40	2	na	1193
WS2 stw 16	2.2	0.9	0.5	11.5	na	na	10	37	na	na	1416
WS2 stw 17	2.1	0.5	0.5	12.1	na	na	10	na	na	na	1620
WS2 stw 18	2.0	0.6	0.5	11.3	na	na	16	na	na	na	1679
WS2 stw 19	2.2	0.4	0.5	11.9	na	na	13	na	na	na	1739
WS2 stw 20	2.1	0.6	0.5	12.0	na	na	25	21	na	na	1800
WS2 main st 1	2.8	0.6	0.7	14.6	na	na	50	11	9	na	2745
WS2 main st 2	2.5	0.7	0.6	13.3	na	na	26	38	5	na	2370
WS2 gw rev 1	2.1	0.6	0.5	11.1	na	na	457	27	4	na	1913
WS2 gw rev 2	2.0	0.5	0.5	10.0	na	na	241	na	12	na	1875
WS2 gw 01-20	49.6	1.2	2.2	26.0	na	na	415	na	14	na	3505
WS2 gw 02-20	85.1	1.0	12.8	17.6	na	na	258	na	13	na	1994
WS2 gw 03-20	82.7	0.9	16.3	12.1	na	na	168	na	16	na	1072
WS2 gw 04-20	84.8	0.9	16.9	12.0	na	na	142	11	17	na	893
WS2 gw 05-50	157	1.3	28.1	17.6	na	na	111	na	28	na	1372
WS2 gw 06-50	206	1.2	37.1	13.5	na	na	145	na	36	na	1355
WS2 gw 07-50	207	1.2	38.2	12.6	na	na	124	11	39	na	1120
WS2 gw 08-50	206	1.2	37.8	12.6	na	na	100	na	41	na	990
WS2 gw 09-80	291	1.3	50.6	15.1	na	na	121	23	55	na	1255

gw equi: phase 1 groundwater equilibration, stw: phase 2 stormwater injection; main st: phase 3 main storage; gw: phase 4 recovery with increasing amounts of groundwater. st: shorter storage. See Table VI-2 for details.

Table A-3: continued

WS – exp.2	major cations (total) [mg/L]				metals (total) [µg/L]						
sample ID	Na	K	Mg	Ca	Al	As	Cu	Fe	Mn	Ni	Zn
WS2 gw 10-80	342	1.1	58.0	13.1	na	na	108	15	60	5	1245
WS2 gw 11-80	339	1.1	57.5	12.7	na	na	104	37	62	5	1002
WS2 gw 12 pH6	334	1.1	57.5	12.9	na	na	97	12	65	4	899
WS2 gw 13 pH6	330	1.4	57.2	13.4	na	na	111	11	71	5	1068
WS2 gw 14 pH6	333	1.4	57.2	13.5	na	na	116	16	67	5	1012
WS2 gw 15 pH6	328	1.4	57.1	13.6	na	na	110	16	73	6	989
WS2 gw 16 st	328	1.7	58.0	14.2	na	na	377	23	89	11	2123
WS2 gw 17 pH5	333	1.6	57.2	13.7	na	na	212	27	85	6	1570
WS2 gw 18	326	1.6	57.3	14.1	na	na	342	na	79	7	1943
WS2 gw 19	325	1.6	57.1	14.2	na	na	549	na	77	9	2008
WS2 gw 20	328	1.5	57.0	14.5	na	na	1223	14	73	10	2126
WS2 gw 21	na	na	na	na	na	na	na	na	na	na	na
WS2 gw 22	328	2.0	57.2	14.2	na	na	847	17	71	9	751
WS2 gw 23	321	2.3	56.6	16.1	na	na	1382	36	71	11	1131
WS2 gw 24	324	2.4	56.9	16.1	na	na	934	13	68	9	752
WS2 gw 25	337	2.1	58.2	15.6	na	na	670	na	71	9	816
WS2 gw 26	339	2.1	58.6	15.7	na	na	na	na	na	na	na
WS2 gw 27 st	245	2.0	44.9	12.4	58	na	888	100	153	10	2165
WS2 gw 28	296	1.8	55.8	14.4	76	na	1346	150	151	7	1067
WS2 gw 29	298	1.5	57.3	14.0	160	na	582	163	93	5	607
WS2 gw 30	207	0.9	38.2	10.1	241	na	152	586	59	5	316
WS2 gw 31 st	206	1.0	39.9	10.6	285	na	491	233	94	13	1352
WS2 gw 32	285	1.6	54.7	13.4	151	7	131	216	81	7	422
WS2 gw 33	263	1.4	49.3	12.6	205	na	120	179	68	8	499
WS2 gw 34	278	1.4	53.2	13.2	149	6	59	180	69	na	318
WS2 gw 35 st	297	1.8	58.0	14.6	98	5	211	100	107	12	1051
WS2 gw 36	295	1.8	57.8	14.2	134	13	71	95	82	7	350
WS2 gw 37	269	1.8	49.6	12.7	119	na	41	96	67	na	328
WS2 gw 38	267	1.5	51.8	12.5	125	na	31	85	66	8	269
WS2 gw 39	209	1.1	39.9	9.8	195	na	27	113	53	6	211
WS2 gw 40	64.7	0.3	13.9	3.0	616	6	10	280	18	1	62
WS2 gw 41	112	0.6	20.8	5.1	459	6	16	215	29	4	124
WS2 gw 42	170	0.9	30.9	7.8	368	na	17	169	43	11	176
WS2 gw 43 st	121	0.6	19.8	5.6	449	na	18	203	35	6	236
WS2 gw 44	199	1.1	36.3	9.1	217	7	19	120	50	5	228
WS2 gw 45	212	1.0	38.5	9.5	237	na	17	124	52	7	230
WS2 gw 46	208	1.0	37.6	9.4	241	na	14	122	52	5	221

gw equi: phase 1 groundwater equilibration, stw: phase 2 stormwater injection; main st: phase 3 main storage; gw: phase 4 recovery with increasing amounts of groundwater. st: shorter storage. See Table VI-2 for details.

Table A-4: Analysis of mean values for column samples of experiment 3: flow parameters, physico-chemical parameters and anions.

BR – exp. 3	flow parameters				physico-chemical parameters					anions [mg/L]				
sample ID	runtime [d]	mean PV	total outflow [mg/L]	velocity [mL/min]	pH	EC [µS/cm]	turbidity [NTU]	TOC [mg-C/L]	DOC [mg-C/L]	HCO_3	Cl	Br	NO_3	SO_4
BR3 gw equi	6.8	na	na	na	5.1	3095	0.6	8	7	0.0	745	3.0	10.1	69.7
BR3 stw 01	7.0	0.9	45	1.4	5.6	2260	2.7	12	8	3.7	397	1.6	6.0	45.2
BR3 stw 02	7.0	2.8	96	1.4	6.7	160	4.9	9	9	7.4	35.3	0.1	1.9	19.7
BR3 stw 03	7.1	4.8	145	1.4	6.6	88	4.0	18	na	11.3	23.0	0.1	1.8	14.0
BR3 stw 04	7.1	6.9	198	1.4	6.6	88	4.4	16	12	12.0	10.3	0.0	1.7	8.1
BR3 stw 05	7.1	8.9	249	1.4	6.6	90	4.6	14	na	12.7	10.1	0.0	1.6	7.5
BR3 stw 06	7.2	13	406	1.4	6.9	90	5.1	16	16	15.5	9.7	0.0	1.5	6.1
BR3 stw 07	7.3	25	823	1.4	7.0	98	5.8	17	15	18.1	9.6	0.0	1.0	5.7
BR3 stw 08	7.7	48	1591	1.1	6.8	100	7.3	20	17	26.8	9.2	0.0	0.1	4.9
BR3 stw 09	7.9	65	1638	1.3	6.6	105	7.9	18	na	27.1	9.3	0.0	0.1	4.9
BR3 stw 10	8.1	81	2428	1.3	6.7	105	8.2	21	20	28.0	9.3	0.0	0.1	5.0
BR3 stw 11	8.6	119	3525	1.3	7.0	105	6.4	19	19	29.8	9.4	0.0	0.1	5.2
BR3 stw 12	8.9	142	3573	1.3	6.9	110	5.1	19	na	30.2	9.6	0.0	0.1	5.1
BR3 stw 13	9.4	181	5486	1.3	7.0	110	4.5	19	17	30.8	9.9	0.0	0.1	5.0
BR3 stw 14	10.0	220	5532	1.3	6.9	110	4.3	19	na	31.3	10.2	0.0	0.1	4.9
BR3 stw 15	10.6	268	7859	1.2	6.8	113	3.0	19	17	32.1	10.6	0.0	0.1	4.8
BR3 stw 16	11.3	315	7908	1.1	6.6	115	2.2	19	na	31.1	10.5	0.0	0.5	4.2
BR3 stw 17	12.1	360	10109	0.9	6.7	110	2.0	18	17	30.3	10.3	0.0	0.8	3.7
BR3 stw 18	13.0	405	10157	0.8	6.8	118	19.4	25	22	32.1	10.7	0.0	0.7	3.8
BR3 main st 1	21.0	407	10208	1.3	6.6	160	13.8	44	37	46.5	8.5	0.6	0.1	16.4
BR3 main st 2	30.0	409	10256	1.3	6.4	163	14.0	40	36	42.8	8.9	0.6	0.1	14.9
BR3 gw rev 1	30.0	411	10305	2.3	6.5	115	8.4	26	na	28.0	8.9	0.4	0.1	6.7
BR3 gw rev 2	30.1	417	10534	2.3	6.8	90	1.5	20	15	18.8	7.8	0.4	0.1	4.5
BR3 gw 01-20	30.2	426	10786	2.3	6.2	698	1.3	13	na	4.9	197	0.4	0.2	16.8
BR3 gw 02-20	30.2	442	11312	3.4	5.8	795	0.7	13	13	4.0	225	0.5	0.2	18.3
BR3 gw 03-20	30.4	469	12114	3.5	5.3	798	0.7	12	na	3.0	226	0.5	0.2	19.3
BR3 gw 04-20	30.7	506	13180	1.3	6.3	798	0.7	12	11	2.9	227	0.5	0.2	19.3
BR3 gw 05-20	31.0	528	13220	2.4	6.3	810	0.9	12	na	2.5	228	0.5	0.2	19.4
BR3 gw 06-50	31.1	534	13483	2.6	6.2	1625	0.7	10	na	2.3	392	1.0	0.2	33.3
BR3 gw 07-50	31.2	550	14010	2.6	5.3	1740	0.6	10	11	2.0	426	1.1	0.2	36.3
BR3 gw 08-50	31.3	576	14810	3.0	6.0	1718	0.6	9	na	2.0	453	1.1	0.2	38.5
BR3 gw 09-50 st	32.0	593	14850	3.0	6.0	1745	3.8	15	na	2.0	453	1.1	0.2	38.5
BR3 gw 10-50	32.2	615	15881	3.2	5.8	1740	0.6	10	na	2.0	451	1.1	0.2	36.7
BR3 gw 11-80	32.3	641	16180	3.3	6.0	2540	0.6	8	na	1.8	644	1.0	0.5	54.8
BR3 gw 12-80	32.4	658	16737	3.3	5.9	2635	0.5	8	7	1.5	663	1.6	0.4	56.4
BR3 gw 13-80	32.8	692	17839	1.3	6.0	2650	0.7	8	8	1.5	655	1.6	0.3	63.8
BR3 gw 14-80	33.1	714	17882	2.7	5.9	2650	0.9	8	na	1.5	691	1.6	0.3	64.0
BR3 gw 15-80	33.2	732	18695	2.0	5.9	2600	0.5	8	na	1.5	685	1.6	0.3	64.5
BR3 gw 16	33.7	770	19803	1.1	6.0	2630	0.5	8	na	1.2	727	1.5	0.3	66.1
BR3 gw 17	34.0	793	19848	2.5	5.7	2603	0.9	8	na	1.2	725	1.5	0.3	65.9
BR3 gw 18	34.1	802	20260	2.3	5.7	2628	0.5	7	8	1.2	721	1.5	0.3	69.8
BR3 gw 19 st	36.0	811	20303	2.3	5.9	2630	3.9	15	13	1.4	747	1.6	0.3	64.9
BR3 gw 20	36.2	831	21256	2.3	5.3	2685	0.4	7	na	0.9	749	1.5	0.3	65.1
BR3 gw 21	36.3	851	21302	1.3	5.5	2710	1.0	7	na	1.1	744	1.3	0.3	64.7
BR3 gw 22	36.7	877	22539	1.3	5.5	2643	0.5	7	7	1.1	749	1.3	0.4	65.2
BR3 gw 23	37.0	902	22586	1.3	5.5	2650	0.6	7	na	1.1	746	1.3	0.4	64.5
BR3 gw 24	37.2	922	23532	2.2	5.4	2705	0.5	7	na	1.1	752	1.3	0.4	65.4
BR3 gw 25	37.3	942	23576	1.3	5.2	2665	0.8	7	na	1.1	744	1.3	0.4	64.7
BR3 gw 26 st	38.0	944	23616	1.3	5.9	2675	2.1	10	na	1.4	774	1.4	0.3	67.3
BR3 gw 27	38.2	961	24432	1.9	5.3	2640	0.6	7	na	1.2	742	1.3	0.4	64.5
BR3 gw 28	38.7	1000	25553	1.1	5.4	2650	0.6	6	6	1.1	742	1.3	0.4	64.3
BR3 gw 29	39.1	1023	25594	1.3	5.4	2680	0.7	7	na	0.5	735	1.3	0.4	63.9
BR3 gw 30	39.2	1034	26112	1.6	5.2	2665	0.6	7	na	0.4	734	1.3	0.4	63.9
BR3 gw 31 st	40.3	1045	26150	1.6	5.8	2575	2.1	10	na	1.2	749	1.4	0.3	65.1
BR3 gw 32	40.7	1067	27212	1.1	5.3	2605	0.4	7	na	0.2	752	1.3	0.4	65.4
BR3 gw 33	41.0	1089	27260	1.3	5.3	2650	0.7	7	na	0.2	744	1.3	0.4	64.7
BR3 gw 34	41.2	1102	27833	1.3	5.2	2665	0.5	7	na	0.2	731	1.3	0.4	63.5
BR3 gw 35	41.7	1134	28880	1.1	5.3	2640	0.5	7	7	0.2	780	1.3	0.4	64.9
BR3 gw 36 st	42.3	1156	28920	1.2	5.3	2605	1.8	8	na	1.0	712	1.3	0.4	61.9
BR3 gw 37	42.7	1177	29933	1.1	5.6	2610	0.6	8	na	1.5	716	1.2	0.5	62.3

PV*: pore volume from start of stormwater injection, TOC: total organic carbon, DOC: dissolved organic carbon; gw equi: phase 1 groundwater equilibration, stw: phase 2 stormwater injection; main st: phase 3 main storage; gw: phase 4 recovery with increasing amounts of groundwater. st: shorter storage. See Table VI-2 for details.

Table A-4: continued

BR – exp. 3	flow parameters				physico-chemical parameters					anions [mg/L]				
sample ID	runtime [d]	mean PV	total outflow [mg/L]	velocity [mL/min]	pH	EC [µS/cm]	turbidity [NTU]	TOC [mg-C/L]	DOC [mg-C/L]	HCO_3	Cl	Br	NO_3	SO_4
BR3 gw 38	43.0	1198	29974	1.2	5.2	2640	1.0	7	na	0.4	739	1.2	0.5	64.2
BR3 gw 39	43.2	1211	30594	1.4	5.1	2590	0.7	7	na	0.2	750	1.2	0.5	65.3
BR3 gw 40	43.6	1245	31641	1.1	5.2	2558	0.6	7	na	0.3	736	1.2	0.5	64.0
BR3 gw 41 st	44.3	1266	31680	1.1	5.2	2575	1.9	9	na	0.5	728	1.2	0.3	63.3
BR3 gw 42	44.6	1289	32758	1.1	5.2	2555	0.5	8	8	0.2	746	1.2	0.5	63.2
BR3 gw 43	45.1	1323	33388	1.4	5.0	2585	0.6	7	na	0.2	730	1.2	0.5	63.5
BR3 gw 44	45.7	1355	34375	0.9	5.1	2600	0.8	7	na	0.2	730	1.2	0.5	63.5
BR3 gw 45 st	48.0	1376	34417	1.3	5.6	2650	3.7	12	na	0.3	727	1.5	0.3	63.2
BR3 gw 46	48.1	1385	34815	1.4	5.2	2555	0.8	7	na	0.2	728	1.5	0.5	63.3
BR3 gw 47	48.6	1410	35689	0.9	5.2	2560	0.8	7	7	0.1	754	1.5	0.6	64.2
BL – exp. 3														
BL3 gw equ	7.0	na	na	na	4.4	3085	14.1	20	7	1.6	751	3.0	10.5	72.1
BL3 stw 01	7.0	0.9	45	1.4	4.4	2425	242.0	51	9	4.4	396	1.6	4.5	40.1
BL3 stw 02	7.0	2.6	96	1.4	6.1	125	490.0	56	16	7.3	25.3	0.1	0.1	6.9
BL3 stw 03	7.1	4.5	145	1.4	6.4	80	135.0	37	na	7.3	20.4	0.1	0.1	5.9
BL3 stw 04	7.1	6.3	199	1.4	6.1	75	65.5	30	15	6.5	10.2	0.0	0.1	4.0
BL3 stw 05	7.1	8.3	250	1.4	5.9	70	33.0	27	na	6.6	10.1	0.0	0.1	4.0
BL3 stw 06	7.2	12	406	1.4	5.9	65	26.5	21	17	5.7	10.0	0.0	0.1	3.8
BL3 stw 07	7.3	23	825	1.4	5.6	70	11.8	17	17	7.5	9.8	na	0.1	3.8
BL3 stw 08	7.7	44	1591	1.1	5.8	78	8.7	17	18	9.8	9.3	na	0.1	3.9
BL3 stw 09	7.9	59	1637	1.3	6.1	85	8.0	18	na	13.6	9.3	na	0.1	3.9
BL3 stw 10	8.1	75	2426	1.3	6.2	88	5.1	19	18	17.7	9.3	na	0.1	4.0
BL3 stw 11	8.6	109	3520	1.3	6.8	93	2.7	19	18	21.8	9.3	na	0.1	4.1
BL3 stw 12	8.9	130	3567	1.3	6.9	98	2.5	18	na	22.9	9.5	na	0.1	4.0
BL3 stw 13	9.4	166	5470	1.3	7.2	103	1.6	18	17	24.1	9.8	na	0.2	4.0
BL3 stw 14	10.0	202	5516	1.3	7.0	105	1.8	19	na	24.8	10.0	na	0.2	4.0
BL3 stw 15	10.6	245	7834	1.2	7.1	105	1.4	19	17	28.6	10.6	na	0.1	4.0
BL3 stw 16	11.3	289	7882	1.1	6.9	110	1.6	19	na	28.1	10.6	na	0.3	3.9
BL3 stw 17	12.1	333	10263	1.0	6.8	105	1.5	18	17	27.7	10.7	na	0.6	3.8
BL3 stw 18	13.0	378	10313	1.0	7.0	113	9.3	23	20	27.7	10.7	na	0.6	3.8
BL3 main st 1	17.0	380	10363	1.3	6.6	168	20.5	53	41	60.1	9.7	0.6	0.1	7.8
BL3 main st 2	25.5	381	10411	1.4	6.7	155	27.5	47	34	44.8	8.8	0.6	0.1	5.8
BL3 gw rev 1	30.5	383	10461	2.3	6.6	110	18.5	39	na	21.5	9.3	0.4	0.1	8.4
BL3 gw rev 2	31.0	388	10692	2.3	6.6	85	3.9	17	15	12.8	8.5	0.4	0.1	5.0
BL3 gw 01-20	31.1	397	10945	2.3	6.0	680	1.9	13	na	2.3	189	0.5	0.1	11.6
BL3 gw 02-20	31.2	411	11471	3.4	5.8	783	0.7	12	12	1.0	221	0.5	0.1	18.3
BL3 gw 03-20	31.3	436	12259	3.4	5.6	780	0.8	12	na	1.0	164	0.5	0.1	20.1
BL3 gw 04-20	31.7	470	13319	1.3	6.1	778	0.7	12	12	3.1	164	0.5	0.1	21.2
BL3 gw 05-20	31.9	490	13358	2.3	6.3	795	1.2	12	na	2.7	164	0.5	0.1	21.2
BL3 gw 06-50	32.0	495	13618	2.6	6.3	1605	0.7	10	na	2.3	364	1.1	0.2	30.0
BL3 gw 07-50	32.1	510	14140	2.6	5.7	1748	0.7	10	10	2.3	424	1.1	0.3	38.7
BL3 gw 08-50	32.3	534	14934	3.0	5.9	1700	0.8	10	na	2.3	430	1.1	0.3	39.7
BL3 gw 09-50 st	32.7	549	14975	3.1	6.3	1743	5.9	16	na	2.3	424	1.1	0.3	40.1
BL3 gw 10-50	33.1	568	15996	3.1	5.9	1720	0.7	10	na	2.3	424	1.1	0.3	38.7
BL3 gw 11-80	33.2	593	16293	3.3	6.2	2545	0.6	8	na	2.4	692	1.4	0.3	50.9
BL3 gw 12-80	33.3	608	16845	3.3	5.9	2630	0.6	8	7	2.5	701	1.4	0.4	63.2
BL3 gw 13-80	33.7	639	17943	1.3	5.8	2640	0.8	8	na	2.5	697	1.4	0.4	64.9
BL3 gw 14-80	34.0	659	17986	2.7	6.0	2635	1.0	8	na	1.5	685	1.4	0.4	70.7
BL3 gw 15-80	34.1	675	18792	2.0	6.0	2610	0.6	7	na	1.3	676	1.4	0.4	69.5
BL3 gw 16	34.6	710	19896	1.1	6.2	2630	0.6	7	na	0.9	720	1.5	0.3	70.9
BL3 gw 17	35.0	731	19941	2.4	5.8	2608	0.8	8	na	0.9	716	1.5	0.3	68.5
BL3 gw 18	35.0	739	20347	2.2	6.0	2615	0.6	8	8	0.9	719	1.5	0.3	68.6
BL3 gw 19 st	36.0	748	20390	2.4	6.2	2630	10.5	20	15	2.5	771	1.4	0.3	67.4
BL3 gw 20	37.1	766	21356	2.4	5.6	2675	0.5	7	na	1.8	769	1.2	0.3	66.9
BL3 gw 21	37.3	785	21402	1.3	5.9	2703	1.0	7	na	1.9	770	1.2	0.3	66.9
BL3 gw 22	37.6	808	22640	1.3	5.8	2635	0.5	7	10	1.9	773	1.2	0.3	67.4
BL3 gw 23	37.9	832	22686	1.3	5.8	2655	0.8	7	na	1.9	757	1.2	0.3	65.8
BL3 gw 24	38.1	850	23639	2.2	5.5	2700	0.4	7	na	1.9	761	1.2	0.3	66.2
BL3 gw 25	38.3	869	23681	1.2	5.7	2675	0.7	7	na	1.9	755	1.2	0.3	65.7
BL3 gw 26 st	38.6	870	23722	1.3	6.3	2685	2.2	12	na	2.8	786	1.3	0.3	68.3
BL3 gw 27	39.1	886	24552	1.9	5.7	2640	0.5	7	na	2.4	775	1.4	0.4	65.5
BL3 gw 28	39.6	922	25681	1.1	5.9	2655	0.6	7	7	2.0	776	1.4	0.4	65.5

PV*: pore volume from start of stormwater injection, TOC: total organic carbon, DOC: dissolved organic carbon; gw equi: phase 1 groundwater equilibration, stw: phase 2 stormwater injection; main st: phase 3 main storage; gw: phase 4 recovery with increasing amounts of groundwater. st: shorter storage. See Table VI-2 for details.

Table A-4: continued

BL – exp. 3	flow parameters				physico-chemical parameters						anions [mg/L]			
sample ID	runtime [d]	mean PV	total outflow [mg/L]	velocity [mL/min]	pH	EC [µS/cm]	turbidity [NTU]	TOC [mg-C/L]	DOC [mg-C/L]	HCO_3	Cl	Br	NO_3	SO_4
BL3 gw 29	40.0	943	25723	1.3	5.7	2680	0.6	7	na	2.0	798	1.4	0.4	65.5
BL3 gw 30	40.1	954	26247	1.6	5.6	2660	0.4	7	na	2.0	787	1.4	0.4	65.5
BL3 gw 31 st	40.7	964	26286	1.6	6.3	2580	3.0	12	na	2.2	796	1.4	0.4	69.2
BL3 gw 32	41.6	985	27374	1.1	5.7	2615	0.4	7	na	1.8	790	1.3	0.5	64.0
BL3 gw 33	41.9	1006	27422	1.3	5.3	2680	1.4	7	na	0.3	778	1.3	0.5	64.0
BL3 gw 34	42.1	1017	28008	1.3	5.7	2665	0.3	7	na	0.3	758	1.3	0.5	64.0
BL3 gw 35	42.6	1048	29078	1.1	5.7	2630	0.5	7	8	0.3	757	1.3	0.5	64.0
BL3 gw 36 st	43.1	1068	29118	1.2	5.9	2595	1.5	9	na	1.6	739	1.4	0.4	64.3
BL3 gw 37	43.6	1088	30153	1.1	5.5	2595	0.5	8	na	1.3	738	1.3	0.5	64.0
BL3 gw 38	43.9	1108	30194	1.2	5.7	2638	0.9	7	na	1.2	758	1.3	0.5	64.0
BL3 gw 39	44.1	1120	30826	1.4	5.6	2600	0.5	7	na	1.2	762	1.3	0.5	64.0
BL3 gw 40	44.6	1151	31888	1.1	5.6	2570	0.5	7	na	1.0	757	1.3	0.5	64.0
BL3 gw 41 st	45.1	1171	31928	1.1	5.8	2570	1.8	10	na	1.7	757	1.4	0.3	65.8
BL3 gw 42	45.6	1192	33024	1.1	5.6	2550	0.6	8	8	1.2	757	1.3	0.5	64.0
BL3 gw 43	46.1	1224	33664	1.4	5.4	2595	0.5	7	na	1.1	733	1.3	0.5	64.0
BL3 gw 44	46.6	1254	34669	0.9	5.6	2605	0.8	7	na	1.1	733	1.3	0.5	64.0
BL3 gw 45 st	48.0	1273	34712	1.3	5.9	2640	4.1	15	na	1.5	737	1.4	0.3	64.1
BL3 gw 46	49.1	1282	35116	1.4	5.5	2570	0.7	7	na	0.5	736	1.3	0.2	63.4
BL3 gw 47	49.5	1307	36075	1.0	5.5	2565	0.8	7	7	0.2	739	1.6	0.1	63.4
WS – exp. 3														
WS3 gw equ	7.0	na	na	na	6.3	3060	1.0	10	7	1.6	745	2.9	10.3	70.8
WS3 stw 01	7.0	0.8	45	1.3	6.2	2575	2.2	8	8	11.5	407	1.6	5.1	41.4
WS3 stw 02	7.0	2.5	95	1.4	7.1	283	30.0	33	13	21.8	56.0	0.2	0.7	10.7
WS3 stw 03	7.1	4.2	143	1.4	7.1	120	22.0	36	na	21.8	33.3	0.1	0.4	7.3
WS3 stw 04	7.1	6.0	196	1.4	7.1	110	13.0	30	16	25.8	10.6	0.0	0.1	3.9
WS3 stw 05	7.1	7.8	248	1.4	7.1	108	9.9	24	na	27.9	10.4	0.0	0.1	3.8
WS3 stw 06	7.2	11	401	1.4	7.1	108	7.6	23	16	29.9	10.3	na	0.1	3.8
WS3 stw 07	7.3	21	815	1.4	7.0	105	6.6	22	16	30.5	10.0	na	0.1	3.8
WS3 stw 08	7.7	42	1568	1.1	6.8	105	6.2	22	19	32.0	9.7	na	0.1	3.8
WS3 stw 09	7.9	56	1614	1.3	6.7	110	5.7	21	na	31.1	9.7	na	0.1	3.9
WS3 stw 10	8.1	70	2392	1.3	6.8	110	5.9	20	20	31.1	9.7	na	0.1	4.0
WS3 stw 11	8.6	103	3468	1.3	6.7	110	4.7	21	18	30.7	9.4	na	0.1	4.1
WS3 stw 12	8.9	123	3515	1.3	6.8	113	4.1	22	na	30.7	9.4	na	0.1	4.1
WS3 stw 13	9.4	156	5381	1.3	6.9	113	2.3	21	17	30.7	9.4	na	0.1	4.0
WS3 stw 14	10.0	190	5426	1.3	6.8	115	1.5	19	na	31.1	10.4	na	0.2	4.0
WS3 stw 15	10.6	230	7690	1.2	6.9	115	1.4	20	17	32.8	11.3	na	0.2	4.0
WS3 stw 16	11.3	271	7738	1.0	6.7	115	1.9	18	na	31.0	10.9	na	0.5	3.9
WS3 stw 17	12.1	312	10011	1.0	6.8	110	1.2	18	16	29.3	10.4	na	0.9	3.8
WS3 stw 18	13.0	353	10059	0.9	6.9	115	3.3	20	17	29.3	10.4	na	0.9	3.8
WS3 main st 1	17.0	354	10110	1.3	6.8	155	6.7	38	35	54.2	9.2	0.6	0.1	5.9
WS3 main st 2	25.5	356	10157	1.4	6.8	140	9.8	37	28	43.4	8.7	0.5	0.2	4.7
WS3 gw rev 1	30.5	358	10207	2.3	6.6	110	9.1	26	na	24.3	9.5	0.6	0.1	5.8
WS3 gw rev 2	31.0	363	10443	2.4	6.8	95	1.6	17	15	19.2	8.6	0.4	0.1	4.6
WS3 gw 01-20	31.1	372	10704	2.4	6.6	688	1.1	13	na	9.1	182	0.5	0.1	11.3
WS3 gw 02-20	31.2	386	11239	3.5	6.3	803	0.7	12	12	4.0	218	0.5	0.0	18.0
WS3 gw 03-20	31.3	409	12038	3.4	5.9	793	0.7	12	na	3.5	189	na	na	17.0
WS3 gw 04-20	31.7	442	13096	1.3	6.3	788	0.7	12	11	3.0	172	na	na	16.0
WS3 gw 05-20	31.9	461	13135	2.3	6.4	815	0.9	12	na	2.5	170	na	na	16.0
WS3 gw 06-50	32.0	466	13396	2.6	6.4	1593	0.6	10	na	2.0	361	na	na	27.5
WS3 gw 07-50	32.1	480	13919	2.6	5.9	1763	0.6	9	9	1.6	428	na	na	39.0
WS3 gw 08-50	32.3	503	14713	3.0	6.0	1720	0.7	9	na	1.5	430	na	na	40.6
WS3 gw 09-50 st	32.7	518	14753	3.0	6.4	1753	3.3	15	na	1.6	424	na	na	41.3
WS3 gw 10-50	33.1	537	15773	3.1	5.8	1748	0.6	10	na	1.5	429	1.1		40.4
WS3 gw 11-80	33.2	560	16071	3.3	5.9	2540	0.6	8	na	1.6	701	1.3	na	51.7
WS3 gw 12-80	33.3	575	16621	3.3	5.8	2625	0.6	7	7	1.6	705	1.3	na	63.0
WS3 gw 13-80	33.7	603	17703	1.3	5.8	2645	0.6	7	na	1.6	699	1.3		64.1
WS3 gw 14-80	34.0	623	17746	2.7	5.7	2650	1.0	8	na	1.2	684	1.3	na	64.1
WS3 gw 15-80	34.1	638	18544	2.0	5.8	2600	0.6	7	na	1.0	677	1.3	na	64.1
WS3 gw 16	34.6	671	19629	1.1	5.9	2625	0.6	7	na	0.5	720	1.4	0.4	64.3
WS3 gw 17	35.0	691	19673	2.4	5.5	2625	0.8	7	na	0.4	718	1.4	0.4	64.5
WS3 gw 18	35.0	699	20075	2.2	5.6	2620	0.5	8	7	0.3	718	1.5	0.4	64.6
WS3 gw 19 st	36.0	706	20116	2.2	6.0	2625	4.0	14	12	0.4	726	1.4	0.1	65.3

PV*: pore volume from start of stormwater injection, TOC: total organic carbon, DOC: dissolved organic carbon; gw equi: phase 1 groundwater equilibration, stw: phase 2 stormwater injection; main st: phase 3 main storage; gw: phase 4 recovery with increasing amounts of groundwater. st: shorter storage. See Table VI-2 for details.

Table A-4: continued

WS – exp. 3	flow parameters				physico-chemical parameters					anions [mg/L]				
sample ID	runtime [d]	mean PV*	total outflow [mg/L]	velocity [mL/min]	pH	EC [µS/cm]	turbidity [NTU]	TOC [mg-C/L]	DOC [mg-C/L]	HCO_3	Cl	Br	NO_3	SO_4
WS3 gw 20	37.1	723	21031	2.2	5.5	2670	0.7	8	na	0.5	721	1.3	0.1	64.0
WS3 gw 21	37.3	740	21074	1.2	5.5	2710	1.1	7	na	0.5	722	1.3	0.1	63.0
WS3 gw 22	37.6	762	22248	1.2	5.4	2625	0.5	7	12	0.5	728	1.3	0.1	62.6
WS3 gw 23	37.9	783	22294	1.2	5.4	2665	0.9	8	na	0.5	729	1.3	0.1	63.0
WS3 gw 24	38.1	801	23253	2.2	5.3	2705	0.5	7	na	0.5	731	1.3	0.1	63.3
WS3 gw 25	38.3	818	23297	1.3	5.3	2680	0.7	7	na	0.5	727	1.3	0.1	63.4
WS3 gw 26 st	38.6	820	23337	1.3	5.8	2690	1.8	10	na	0.6	753	1.3	0.1	64.4
WS3 gw 27	39.1	835	24166	1.9	5.3	2655	0.4	7	na	0.5	745	1.3	0.1	64.1
WS3 gw 28	39.6	870	25291	1.1	5.4	2655	0.4	7	7	0.5	750	1.3	0.1	64.0
WS3 gw 29	40.0	890	25332	1.3	5.3	2685	1.0	7	na	0.5	786	1.3	0.1	64.0
WS3 gw 30	40.1	900	25856	1.6	5.3	2660	0.5	7	na	0.5	773	1.3	0.1	64.0
WS3 gw 31 st	40.7	910	25894	1.6	5.9	2575	2.3	10	na	0.7	776	1.4	0.1	64.2
WS3 gw 32	41.6	930	26968	1.1	5.4	2610	0.6	7	na	0.5	761	1.3	0.1	63.9
WS3 gw 33	41.9	949	27015	1.3	5.2	2675	0.8	6	na	0.7	759	1.3	0.1	63.9
WS3 gw 34	42.1	960	27594	1.3	5.2	2650	0.4	7	na	0.7	742	1.3	0.1	63.9
WS3 gw 35	42.6	989	28644	1.1	5.3	2635	0.5	7	8	0.7	748	1.3	0.1	63.9
WS3 gw 36 st	43.1	1008	28683	1.2	5.4	2605	1.6	8	na	0.5	729	1.4	0.1	63.9
WS3 gw 37	43.6	1027	29702	1.1	5.2	2600	0.6	8	na	0.1	761	1.3	0.1	63.9
WS3 gw 38	43.9	1045	29743	1.2	5.2	2630	1.1	7	na	0.1	755	1.3	0.1	63.9
WS3 gw 39	44.1	1057	30368	1.4	5.1	2590	0.5	7	na	0.1	760	1.3	0.1	63.9
WS3 gw 40	44.6	1086	31412	1.1	5.1	2570	0.5	7	na	0.2	754	1.3	0.1	63.9
WS3 gw 41 st	45.1	1106	31451	1.1	5.3	2590	1.9	9	na	0.2	757	1.4	0.1	63.9
WS3 gw 42	45.6	1125	32528	1.1	5.1	2565	0.5	8	8	0.2	753	1.3	0.2	63.9
WS3 gw 43	46.1	1155	33157	1.4	5.0	2595	0.6	7	na	0.2	745	1.3	0.2	63.9
WS3 gw 44	46.6	1183	34135	0.9	5.1	2610	0.7	7	na	0.2	750	1.3	0.2	63.9
WS3 gw 45 st	48.0	1201	34177	1.3	5.7	2650	2.7	12	na	0.3	756	1.3	0.2	63.9
WS3 gw 46	49.1	1209	34569	1.4	5.1	2575	0.6	7	na	0.5	748	1.3	0.2	63.9
WS3 gw 47	49.5	1232	35497	1.0	5.1	2570	0.6	7	8	0.5	747	1.1	0.1	60.9

PV*: pore volume from start of stormwater injection, TOC: total organic carbon, DOC: dissolved organic carbon; gw equi: phase 1 groundwater equilibration, stw: phase 2 stormwater injection; main st: phase 3 main storage; gw: phase 4 recovery with increasing amounts of groundwater. st: shorter storage. See Table VI-2 for details.

Table A-5: Analysis of mean values for column samples of experiment 3, cations and metals.

BR – exp. 3	major cations (total) [mg/L]					metals (total) [µg/L]						
sample ID	Na	K	Mg	Ca	Si	Al	As	Cu	Fe	Mn	Ni	Zn
BR3 gw equi	500.6	3.1	61.9	9.9	8.0	na	na	20	528	102	12	557
BR3 stw 01	383.1	2.0	43.0	6.9	na	na	na	15	342	68	6	361
BR3 stw 02	25.2	0.9	2.4	0.1	na	29	na	17	129	na	na	84
BR3 stw 03	8.6	3.5	3.2	0.1	na	na	na	26	87	na	na	97
BR3 stw 04	6.2	4.1	4.1	0.1	na	20	na	31	93	na	na	61
BR3 stw 05	5.3	4.4	4.6	0.3	0.9	na	na	46	103	na	na	57
BR3 stw 06	4.9	4.3	4.2	2.4	na	59	na	61	125	5	2	45
BR3 stw 07	4.6	4.5	3.2	5.5	0.8	193	na	100	247	7	2	45
BR3 stw 08	4.6	4.6	2.4	8.1	0.8	304	na	144	231	8	2	112
BR3 stw 09	5.1	4.7	2.4	8.4	na	298	na	173	245	9	5	307
BR3 stw 10	4.6	4.7	2.3	8.6	na	324	na	182	250	9	3	485
BR3 stw 11	4.7	4.6	2.3	8.9	0.8	356	3	212	251	9	2	873
BR3 stw 12	4.7	4.6	2.2	8.9	na	269	na	244	216	9	4	1133
BR3 stw 13	4.6	4.6	2.2	9.0	na	257	na	256	201	9	3	1391
BR3 stw 14	4.8	4.7	2.2	9.0	na	244	na	286	197	9	4	1578
BR3 stw 15	4.9	5.3	2.3	9.1	0.9	151	5	311	171	9	3	1596
BR3 stw 16	4.8	5.1	2.2	9.3	na	85	6	304	148	9	4	2034
BR3 stw 17	4.7	5.0	2.2	9.0	na	83	3	316	123	8	4	2112
BR3 stw 18	4.8	5.2	2.5	10.2	na	1285	4	335	789	11	9	2413
BR3 main st 1	5.6	5.7	3.5	14.4	na	410	20	732	1990	27	12	3713
BR3 main st 2	6.0	5.2	3.1	13.0	na	199	42	455	5251	32	12	2974
BR3 gw rev 1	5.1	4.2	2.5	8.7	2.0	79	32	346	2521	53	8	1216
BR3 gw rev 2	4.5	3.9	1.5	5.8	1.2	39	14	134	2710	45	3	909
BR3 gw 01-20	94.8	6.5	8.4	16.6	2.2	11	6	131	3103	32	4	2007
BR3 gw 02-20	108	5.5	14.7	10.3	2.5	na	2	126	1100	22	6	1171
BR3 gw 03-20	109	5.5	15.6	9.4	na	na	na	122	339	27	4	1115
BR3 gw 04-20	109	5.5	15.7	9.2	na	na	na	176	131	29	7	1481

gw equi: phase 1 groundwater equilibration, stw: phase 2 stormwater injection; main st: phase 3 main storage; gw: phase 4 recovery with increasing amounts of groundwater. st: shorter storage. See Table VI-2 for details.

Table A-5: continued

BR – exp. 3	major cations (total) [mg/L]					metals (total) [µg/L]						
sample ID	Na	K	Mg	Ca	Si	Al	As	Cu	Fe	Mn	Ni	Zn
BR3 gw 05-20	109	5.6	15.8	9.2	na	10	na	218	71	29	5	1705
BR3 gw 06-50	241	5.5	30.8	13.1	na	na	na	164	79	47	7	2520
BR3 gw 07-50	264	4.8	34.7	10.5	na	na	na	137	130	51	6	1599
BR3 gw 08-50	280	4.9	36.0	9.9	na	na	na	135	133	57	5	1168
BR3 gw 09-50, st	280	4.9	36.6	10.0	na	46	6	276	911	63	7	1281
BR3 gw 10-50	279	5.0	36.1	9.9	4.5	17	14	127	123	59	6	1116
BR3 gw 11-80	416	3.7	51.6	12.5	na	183	4	88	98	81	7	1318
BR3 gw 12-80	430	3.0	53.7	11.5	5.5	na	na	76	34	83	6	978
BR3 gw 13-80	424	2.9	53.0	11.4	4.5	na	na	80	55	83	7	862
BR3 gw 14-80	421	2.9	52.8	11.3	na	na	na	79	53	83	7	771
BR3 gw 15-80	416	2.9	52.2	11.2	na	na	na	76	38	81	7	679
BR3 gw 16	443	3.2	56.8	11.3	6.0	na	na	88	41	82	6	603
BR3 gw 17	442	3.6	57.1	11.1	6.0	14	3	88	51	84	6	562
BR3 gw 18	440	3.5	57.0	11.1	6.0	na	na	82	41	84	6	514
BR3 gw 19, st	437	3.8	57.5	11.2	6.5	26	7	314	1327	94	7	929
BR3 gw 20	436	3.6	58.6	11.4	4.8	na	na	86	267	87	8	651
BR3 gw 21	433	3.6	58.4	11.3	5.5	na	na	87	78	86	7	533
BR3 gw 22	438	3.4	58.6	11.2	6.0	31	na	84	38	85	6	534
BR3 gw 23	437	3.4	58.3	11.2	na	36	na	89	70	84	7	506
BR3 gw 24	439	3.4	59.0	11.4	4.5	23	na	95	57	85	7	483
BR3 gw 25	435	3.4	58.4	11.2	6.0	31	16	105	69	84	6	485
BR3 gw 26, st	450	4.2	56.8	11.2	6.3	58	7	121	321	84	9	670
BR3 gw 27	451	3.9	56.0	11.0	6.5	na	3	96	161	81	9	487
BR3 gw 28	449	3.7	55.1	10.7	5.0	na	na	97	33	76	6	435
BR3 gw 29	446	3.6	54.2	10.6	6.5	29	na	96	46	75	5	410
BR3 gw 30	444	3.5	54.0	10.6	5.0	15	na	93	45	74	6	402
BR3 gw 31, st	438	3.7	52.7	10.3	4.8	17	3	113	418	75	11	645
BR3 gw 32	439	3.3	52.7	10.3	4.0	28	na	94	44	73	6	430
BR3 gw 33	434	3.3	52.3	10.2	6.0	na	na	89	39	72	5	378
BR3 gw 34	426	3.2	51.8	10.2	5.0	13	5	87	41	72	6	379
BR3 gw 35	423	3.1	51.7	10.1	4.5	na	na	94	36	68	5	381
BR3 gw 36, st	419	3.3	51.6	10.1	4.0	35	na	96	123	68	8	518
BR3 gw 37	419	3.2	51.7	9.9	6.0	na	na	71	39	68	5	320
BR3 gw 38	432	3.2	55.2	11.6	6.0	45	na	101	85	73	5	351
BR3 gw 39	436	3.4	55.7	11.7	3.5	38	4	114	87	73	6	350
BR3 gw 40	430	3.2	54.9	11.6	4.5	32	na	101	58	74	7	364
BR3 gw 41, st	428	3.8	54.0	11.6	4.0	36	na	100	126	74	10	478
BR3 gw 42	430	3.3	54.9	11.5	4.5	26	na	96	61	74	7	365
BR3 gw 43	425	3.3	54.4	11.5	4.0	27	9	89	85	73	7	353
BR3 gw 44	426	3.4	54.7	11.3	na	29	na	86	84	72	7	312
BR3 gw 45, st	426	3.9	54.2	11.3	7.0	55	2	114	1312	74	15	578
BR3 gw 46	425	3.8	54.1	11.2	na	24	na	84	252	72	7	341
BR3 gw 47	428	3.8	54.8	11.4	4.8	40	na	83	158	73	8	294
BL – exp. 3												
BL3 gw equ	504.5	2.5	63.6	10.6	8.0	1501	44	37	2938	100	15	539
BL3 stw 01	410.0	2.6	49.1	9.0	na	14582	41	50	5166	77	17	291
BL3 stw 02	22.2	0.8	1.6	0.4	na	28967	90	78	5896	9	15	66
BL3 stw 03	14.7	0.3	0.5	0.1	na	8683	76	60	2024	3	7	53
BL3 stw 04	19.8	0.4	0.4	0.0	na	5000	60	59	1350	na	na	55
BL3 stw 05	11.0	1.2	0.3	0.1	0.6	2453	47	62	779	1	6	59
BL3 stw 06	11.4	2.2	0.3	0.1	na	1000	28	64	450	3	na	58
BL3 stw 07	5.3	4.5	1.6	0.3	0.9	609	19	69	280	2	na	63
BL3 stw 08	4.7	4.6	3.1	0.6	0.9	564	12	84	273	2	3	59
BL3 stw 09	4.9	4.6	3.5	1.4	na	378	8	102	308	4	4	63
BL3 stw 10	4.7	4.6	3.2	3.0	na	233	9	104	156	4	na	48
BL3 stw 11	4.6	4.5	2.7	5.6	0.8	129	6	118	411	8	na	41
BL3 stw 12	4.7	4.6	2.6	6.6	na	103	5	132	145	7	3	52
BL3 stw 13	4.6	4.6	2.4	7.5	na	64	2	139	107	9	na	49
BL3 stw 14	4.8	4.7	2.4	8.1	na	52	na	156	116	11	4	87
BL3 stw 15	4.8	5.3	2.4	8.4	0.8	68	6	165	123	12	2	195
BL3 stw 16	4.8	5.1	2.4	9.0	na	42	7	153	227	14	3	331
BL3 stw 17	4.8	5.1	2.3	8.8	na	72	4	164	116	13	2	620
BL3 stw 18	5.0	5.5	2.4	9.3	na	618	4	202	255	14	3	1012
BL3 main st 1	5.9	6.1	4.2	15.8	na	951	72	536	2529	35	11	2099
BL3 main st 2	5.5	5.3	3.5	12.9	na	949	169	455	3760	28	10	1585
BL3 gw rev 1	4.9	4.3	2.3	7.9	1.5	748	77	426	2863	71	6	1111
BL3 gw rev 2	4.5	3.7	1.2	4.7	1.0	357	19	137	2225	45	3	924

gw equi: phase 1 groundwater equilibration, stw: phase 2 stormwater injection; main st: phase 3 main storage; gw: phase 4 recovery with increasing amounts of groundwater. st: shorter storage. See Table VI-2 for details.

Table A-5: continued

BL – exp. 3	major cations (total) [mg/L]					metals (total) [µg/L]						
sample ID	Na	K	Mg	Ca	Si	Al	As	Cu	Fe	Mn	Ni	Zn
BL3 gw 01-20	91.0	6.9	6.3	19.0	2.3	31	7	102	2666	67	5	3937
BL3 gw 02-20	107	5.4	11.0	13.0	2.5	10	na	90	1058	24	5	3095
BL3 gw 03-20	107	5.4	14.1	9.2	na	320	na	85	604	17	4	2000
BL3 gw 04-20	108	5.4	15.1	8.4	na	16	na	117	244	19	3	1611
BL3 gw 05-20	107	5.4	15.4	8.3	na	34	na	180	115	21	3	1535
BL3 gw 06-50	238	5.7	30.0	15.3	na	na	na	127	147	41	7	2505
BL3 gw 07-50	270	4.8	33.2	12.4	na	na	8	113	151	42	3	1870
BL3 gw 08-50	280	4.9	35.1	10.2	na	na	3	100	163	46	2	1383
BL3 gw 09-50 st	278	4.9	36.3	9.9	na	31	19	199	1083	53	2	1361
BL3 gw 10-50	278	4.9	35.5	9.6	4.5	na	6	90	141	52	2	1186
BL3 gw 11-80	419	3.7	51.1	14.0	6.5	na	5	60	77	78	2	1435
BL3 gw 12-80	425	2.9	52.3	12.2	6.5	na	2	56	70	77	3	1191
BL3 gw 13-80	422	2.8	52.5	11.4	3.5	na	na	56	47	78	3	1041
BL3 gw 14-80	419	2.8	52.5	11.4	na	16	na	57	74	80	3	944
BL3 gw 15-80	414	2.8	51.9	11.1	na	na	na	51	47	79	3	846
BL3 gw 16	443	3.2	56.7	11.4	6.0	10	na	59	41	81	3	767
BL3 gw 17	440	3.4	57.0	11.0	5.0	16	na	57	60	83	4	744
BL3 gw 18	440	3.4	56.7	11.0	6.5	na	na	52	36	82	3	685
BL3 gw 19 st	439	3.9	58.8	11.4	6.5	50	19	220	2290	94	3	971
BL3 gw 20	435	3.5	58.6	11.4	5.0	12	na	50	53	87	4	742
BL3 gw 21	435	3.6	58.4	11.3	5.5	na	na	55	65	85	4	641
BL3 gw 22	437	3.3	59.0	11.1	5.5	32	na	53	38	85	4	583
BL3 gw 23	437	3.3	58.5	11.0	na	23	na	53	39	85	4	512
BL3 gw 24	439	3.3	58.9	11.2	5.5	21	na	49	33	85	5	457
BL3 gw 25	437	3.3	58.5	11.1	4.0	16	3	52	53	85	5	425
BL3 gw 26 st	453	4.3	57.8	11.1	6.0	10	7	82	183	85	6	596
BL3 gw 27	450	3.8	55.6	10.8	5.5	na	3	44	33	81	5	422
BL3 gw 28	449	3.7	55.0	10.5	4.0	na	3	45	29	79	5	397
BL3 gw 29	448	3.6	54.1	10.4	6.0	na	na	48	57	76	5	368
BL3 gw 30	442	3.6	53.2	10.2	6.0	25	2	41	54	74	5	338
BL3 gw 31 st	446	3.9	54.3	10.3	5.0	14	5	80	318	77	6	498
BL3 gw 32	441	3.4	52.8	10.1	4.5	na	3	42	38	74	6	347
BL3 gw 33	436	3.4	52.6	9.9	6.5	na	na	40	33	73	5	307
BL3 gw 34	427	3.3	52.0	10.1	3.5	na	3	37	31	72	5	286
BL3 gw 35	424	3.1	52.2	10.0	5.0	na	3	39	36	70	5	269
BL3 gw 36 st	420	3.3	51.5	9.8	4.0	28	3	48	96	69	6	322
BL3 gw 37	420	3.2	52.0	9.9	4.0	12	na	59	58	68	7	301
BL3 gw 38	433	3.5	55.5	11.1	6.0	29	na	44	118	77	6	238
BL3 gw 39	433	3.5	55.4	11.5	6.0	na	na	40	42	73	6	220
BL3 gw 40	431	3.4	55.2	11.2	3.5	15	na	44	64	75	5	212
BL3 gw 41 st	429	3.9	53.7	11.2	4.5	28	na	56	141	74	6	262
BL3 gw 42	428	3.4	55.1	11.3	4.5	na	na	45	49	75	6	207
BL3 gw 43	426	3.4	54.8	11.3	4.5	14	4	45	69	74	7	192
BL3 gw 44	425	3.4	54.7	11.4	na	11	na	50	92	75	7	210
BL3 gw 45 st	428	3.9	55.2	11.5	7.0	30	5	88	1012	77	8	430
BL3 gw 46	427	3.8	54.0	11.5	na	14	na	53	108	75	8	282
BL3 gw 47	429	3.8	55.1	11.5	3.8	16	na	52	111	75	8	281
WS – exp. 3												
WS3 gw equ	505.3	2.5	63.1	10.2	7.0	na	na	11	13	175	9	371
WS3 stw 01	433.8	2.6	50.8	8.3	na	na	na	14	52	119	7	255
WS3 stw 02	47.4	0.7	4.3	0.9	na	1857	na	63	2646	20	5	58
WS3 stw 03	13.2	2.4	4.9	1.0	na	1509	na	96	2114	17	6	66
WS3 stw 04	9.6	3.7	5.4	0.5	na	1125	na	100	1500	11	na	55
WS3 stw 05	7.1	4.0	5.7	1.6	1.0	609	na	123	846	13	7	49
WS3 stw 06	6.1	4.3	5.0	3.2	na	400	na	133	450	8	3	55
WS3 stw 07	5.4	4.6	3.5	6.5	0.8	197	na	168	282	16	2	89
WS3 stw 08	5.0	4.6	2.9	8.0	0.9	156	na	207	251	20	3	494
WS3 stw 09	5.1	4.7	2.9	8.1	na	149	na	239	255	21	4	821
WS3 stw 10	4.8	4.8	2.6	8.4	na	136	na	253	245	20	2	1030
WS3 stw 11	4.7	4.8	2.5	8.8	0.9	158	na	288	259	23	3	1313
WS3 stw 12	4.9	4.8	2.5	8.9	na	114	na	318	219	24	4	1531
WS3 stw 13	4.8	4.9	2.4	9.0	na	65	na	337	147	24	3	1629
WS3 stw 14	5.0	5.3	2.3	9.0	na	40	6	369	121	22	3	1729
WS3 stw 15	5.0	5.5	2.3	9.1	0.9	38	2	385	125	20	3	1670
WS3 stw 16	4.9	5.3	2.3	9.0	na	42	3	362	114	21	3	1915
WS3 stw 17	4.8	5.2	2.2	8.9	na	21	na	381	86	19	4	1994
WS3 stw 18	5.0	5.5	2.4	9.6	na	68	na	391	213	20	4	2102

gw equi: phase 1 groundwater equilibration, stw: phase 2 stormwater injection; main st: phase 3 main storage; gw: phase 4 recovery with increasing amounts of groundwater. st: shorter storage. See Table VI-2 for details.

Table A-5: continued

WS – exp. 3	major cations (total) [mg/L]					metals (total) [µg/L]						
sample ID	Na	K	Mg	Ca	Si	Al	As	Cu	Fe	Mn	Ni	Zn
WS3 main st 1	5.7	5.7	3.5	13.2	na	45	na	637	600	288	9	2984
WS3 main st 2	5.4	5.0	3.0	10.8	na	45	4	453	1339	431	8	1985
WS3 gw rev 1	5.1	4.1	2.2	7.8	2.0	30	3	339	3043	76	5	1002
WS3 gw rev 2	4.7	4.0	1.8	6.1	1.1	18	na	140	1894	205	9	627
WS3 gw 01-20	91.0	7.0	9.3	17.4	2.0	18	na	146	621	583	4	879
WS3 gw 02-20	107	5.7	14.8	10.8	2.7	na	na	171	126	241	5	755
WS3 gw 03-20	108	5.6	15.5	9.6	na	na	na	191	72	123	5	1088
WS3 gw 04-20	108	5.5	15.7	9.4	na	na	na	203	71	93	6	1460
WS3 gw 05-20	108	5.6	15.7	9.3	na	na	na	265	209	88	24	1705
WS3 gw 06-50	237	6.0	30.6	12.9	na	31	na	197	61	124	8	2365
WS3 gw 07-50	282	5.2	35.8	10.5	na	na	na	184	68	116	6	1416
WS3 gw 08-50	283	5.1	36.1	10.1	na	na	na	184	88	99	6	1107
WS3 gw 09-50 st	280	5.1	36.5	10.2	na	11	na	358	361	109	5	1358
WS3 gw 10-50	282	5.1	36.3	10.1	4.5	na	na	170	77	93	6	1110
WS3 gw 11-80	421	3.9	51.3	12.3	na	na	na	129	43	110	7	1236
WS3 gw 12-80	426	3.0	53.1	11.5	6.0	na	na	111	35	105	6	852
WS3 gw 13-80	423	2.9	53.0	11.4	6.0	na	na	113	47	102	6	819
WS3 gw 14-80	419	2.9	52.7	11.4	na	13	na	115	60	99	7	737
WS3 gw 15-80	414	2.8	52.1	11.1	na	na	na	107	37	95	6	678
WS3 gw 16	441	3.5	57.2	11.2	6.0	11	4	122	44	96	6	637
WS3 gw 17	440	3.4	57.3	11.1	5.5	35	na	115	64	94	6	538
WS3 gw 18	439	3.5	57.0	11.0	6.5	11	na	104	32	93	5	505
WS3 gw 19 st	440	3.8	57.4	11.2	4.0	21	na	311	1028	119	6	994
WS3 gw 20	435	3.5	58.9	11.4	5.8	10	na	109	39	103	6	674
WS3 gw 21	436	3.6	58.7	11.4	5.5	na	na	107	58	97	6	581
WS3 gw 22	438	3.4	58.7	11.3	5.5	26	na	112	30	94	6	572
WS3 gw 23	439	3.5	58.9	11.3	na	53	na	117	49	93	6	544
WS3 gw 24	440	3.5	58.9	11.3	6.5	35	na	112	30	93	6	537
WS3 gw 25	438	3.4	58.7	11.3	6.0	22	na	115	43	92	6	544
WS3 gw 26 st	453	4.1	56.6	11.1	6.5	18	na	117	140	100	7	825
WS3 gw 27	449	4.0	55.2	10.9	6.0	na	na	101	22	88	6	539
WS3 gw 28	450	3.7	54.7	10.6	4.0	na	na	96	23	81	5	452
WS3 gw 29	447	3.7	53.9	10.5	5.5	84	na	91	75	79	5	427
WS3 gw 30	438	3.6	53.1	10.4	4.5	24	na	85	42	78	5	413
WS3 gw 31 st	442	3.7	53.3	10.5	4.5	15	na	97	46	87	7	719
WS3 gw 32	434	3.5	52.2	10.2	6.0	47	na	83	49	79	6	439
WS3 gw 33	432	3.5	52.4	10.3	6.5	14	na	77	34	76	5	404
WS3 gw 34	423	3.4	51.7	10.2	5.0	12	na	71	39	75	6	405
WS3 gw 35	423	3.2	52.1	10.1	4.0	14	na	85	28	73	5	404
WS3 gw 36 st	418	3.4	51.4	10.1	6.0	33	na	86	77	75	7	539
WS3 gw 37	427	3.3	53.7	10.8	6.0	16	na	84	36	75	5	391
WS3 gw 38	431	3.3	55.2	11.6	5.0	64	na	90	95	79	5	380
WS3 gw 39	434	3.4	55.4	11.6	6.0	35	na	95	59	77	5	371
WS3 gw 40	430	3.4	54.7	11.5	6.0	286	na	95	341	82	8	365
WS3 gw 41 st	431	3.9	54.5	11.6	6.0	55	na	91	259	79	8	478
WS3 gw 42	428	3.4	55.0	11.5	3.5	31	na	81	51	78	7	360
WS3 gw 43	424	3.4	54.5	11.4	4.0	26	na	76	47	76	7	345
WS3 gw 44	426	3.4	54.4	11.3	na	43	na	73	124	74	7	304
WS3 gw 45 st	429	3.9	54.5	11.3	7.0	30	na	83	200	83	9	598
WS3 gw 46	426	3.8	54.1	11.2	na	30	na	76	143	77	7	347
WS3 gw 47	427	3.8	54.8	11.5	4.0	29	na	66	115	75	9	300

gw equi: phase 1 groundwater equilibration, stw: phase 2 stormwater injection; main st: phase 3 main storage; gw: phase 4 recovery with increasing amounts of groundwater. st: shorter storage. See Table VI-2 for details.

Table A-6: Equations used by PHREEQC. For more details see Parkhurst and Appelo (1999)

a) for all aqueous species	$a_i = \gamma_I\, m_i$ and $n_i = m_i\, W_{aq}$
b) ionic strength of aqueous solution	$\mu = \frac{1}{2}\sum_i^{N_{sq}} z_i^2 \frac{n_i}{W_{aq}}$
c) general mass-action equation for aqueous species or exchanger species	$K_i = a_i \prod_m^{M_{aq}} a_m^{-c_{m,i}}$
d) Newton-Raphson method for total derivative of moles with respect to master unknowns	$dn_i = n_i \left[d\ln(W_{aq}) + \sum_m^{M_{aq}} c_{m,i}\, d\ln(a_m) - \frac{\partial}{\partial\mu}\ln(\gamma_i)\, d\mu \right]$
e) Davies equation for activity coefficients of aqueous species	$\log\gamma_i = -Az_i^2 \left(\frac{\sqrt{\mu}}{1+\sqrt{\mu}} - 0.3\mu \right)$
f) activity of exchanger species	$a_{i_e} = \gamma_{i_e} \frac{b_{e,i_e}\, n_{i_e}}{T_e}$
g) Gaines-Thomas convention for exchange species	$E^{z+} + z\,X^- = EX_z$
h) general mass-action equation for surface species i_{Sk} (with coulombic correction factor)	$K_{i_{Sk}}^{int} = \left(a_{iSk} \prod_m^{M} a_m^{-c_{m,iSk}} \right) e^{\frac{F\Psi_S}{RT}\Delta z_{iSk}}$
i) saturation index (SI) for minerals	$SI = \log \prod_m^{M_{aq}} a_m^{c_{m,p}}$
j) surface charge density	$\sigma_S = \frac{F}{A_{surf}} \sum_k^{K_S} \sum_{i_{Sk}}^{N_{Sk}} z_{i_{Sk}}\, n_{i_{Sk}}$

Annotation

μ	ionic strength
γ_I	molality of species i
Ψ_S	potential at surface (Volt)
σ_S	surface charge density
Δz_{iSk}	net change in surface charge due to the formation of the surface species
A	temperature dependent constant
a_i	activity coefficient of species i
A_{surf}	surface area of material (m²)
b_{eie}	number of equivalents of exchanger e occupied by the exchange species i_e
$c_{m,i}$	stoichiometric coefficent of master species m in species i
$c_{m,iS}$	stoichiometric coefficent of master species m in the association reaction for surface species i_{Sk}
E^{z+}	exchanging cation with charge z
F	Faraday constant (96493.5 J/V eq)
i_{Sk}	i^{th} surface species for surface-site type k in surface S
K_i	temperature –dependent equilibrium constant
K^{int}	intrinsic equilibrium constant
K_S	number of site types for surface S
m	master species
M_{aq}	total number of aqueous master species
m_i	moles in solution of species i
N_{aq}	number of aqueous species
R	gas constant (8.3147J/mol K)
T	temperature (Kelvin)
T_e	total number of exchanger sites for the exchanger in equivalents
W_{aq}	mass of solvent water
X-	exchange master species
z_i	ionic charge on species i

Table A-7: PHREEQC database used for PHT3D simulations in Chapter VI.

```
SOLUTION_MASTER_SPECIES
#######################################
#            essential definitions
#######################################
Alkalinity     CO3-2   1.0   61.0173  61.0173
E              e-      0      0              0
H              H+      -1.    1.008          1.008
H(0)           H2      0.0    1.008
H(1)           H+      -1.    1.008
O              H2O     0      16.00          16.00
O(-2)          H2O     0      16.00          16.00
O(0)           O2      0      16.00          16.00
#######################################
Al             Al+3    0      26.9815        26.9815
Br             Br-     0      79.904         79.904
C              CO3-2   2.0    61.0173   12.0111
C(+4)          CO3-2   2.0    61.0173
C(-4)          CH4     0.0    16.042
Ca             Ca+2    0      40.08          40.08
Cl             Cl-     0      35.453         35.453
Cr             CrO4-2  1      51.996         51.996
Cu             Cu+2    0      63.546         63.546
Cu(1)          Cu+     0      63.546
Cu(2)          Cu+2    0      63.546
Fe             Fe+3    0.0    55.847         55.847
Fe(+2)         Fe+2    0.0    55.847
Fe(+3)         Fe+3    -2.0   55.847
K              K+      0      39.102         39.102
Mg             Mg+2    0      24.312         24.312
Mn             Mn+3    0.0    54.938         54.938
Mn(2)          Mn+2    0.0    54.938
Mn(3)          Mn+3    0.0    54.938
Mn(6)          MnO4-2  0.0    54.938
Mn(7)          MnO4-   0.0    54.938
N              NO3-    0.0    14.0067        14.0067
N(0)           N2      0.0    14.0067
N(+3)          NO2-    0.0    14.0067
N(+5)          NO3-    0.0    14.0067
Na             Na+     0      22.9898        22.9898
S              SO4-2   0.0    96.0616        32.064
S(-2)          HS-     1.0    32.064
S(6)           SO4-2   0.0    96.0616
Si    H4SiO4      0.0       SiO2     28.0843
Zn             Zn+2    0      65.37          65.37
#### dummy species
D       D+            0.0    1.0        1.0
A       A-            0.0    1.0        1.0
# molar weight of species is set to 12 as
#measured as DO
#  Evanko and Dzombak 1999
Srfa      H3Srfa-0          12         12
###########################


SOLUTION_SPECIES
#######################################
#            essential definitions
#######################################
e- = e-
      log_k   0
      delta_h 0       kcal
H+ = H+
      log_k   0
      delta_h 0       kcal
      -gamma  9.0  0.0
H2O = H2O
      log_k   0
      delta_h 0       kcal
H2O + 0.01e- = H2O-0.01
      log_k -9
2H2O = O2 + 4H+ + 4e-
      log_k          -86.08
      delta_h 134.79 kcal
2 H+ + 2 e- = H2
      log_k          -3.15
      delta_h -1.759  kcal
CO3-2 = CO3-2
      log_k   0
      delta_h 0       kcal
      -gamma 5.4  0.0
#####################################
#D+ dummy cation
          D+ = D+
          log_k                0.0
#A- dummy anion
          A- = A-
          log_k                0.0
# Fulvic acid
          H3Srfa- = H3Srfa-
          log_k 0.0
#####################################
Al+3 = Al+3
      log_k   0
      delta_h 0       kcal
      -gamma  9.0  0.0
Br- = Br-
      log_k   0
      delta_h 0       kcal
      -gamma  4.0  0.0
Ca+2 = Ca+2
      log_k   0
      delta_h 0       kcal
      -gamma  6.0  .165
Cl- = Cl-
      log_k   0
      delta_h 0       kcal
      -gamma  3.0  .015
Cu+2 = Cu+2
      log_k   0
      delta_h 0       kcal
      -gamma  2.5  0.0
Cu+2 + e- = Cu+
      log_k   2.72
      delta_h 1.65    kcal
      -gamma  2.5  0.0
Fe+3 = Fe+3
      log_k   0
      delta_h 0       kcal
      -gamma  9.0  0.0
Fe+3 + e- = Fe+2
```

```
	log_k	13.032
	delta_h -10	kcal
	-gamma	6.0	0.0
K+ = K+
	log_k	0
	delta_h 0	kcal
	-gamma	3.0	.015
Mg+2 = Mg+2
	log_k	0
	delta_h 0	kcal
	-gamma	6.5	.20
Mn+2 + 4H2O = MnO4- + 8H+ + 5e-
	log_k	-127.824
	delta_h 176.62	kcal
	-gamma	3.0	0
Mn+2 + 4H2O = MnO4-2 + 8H+ + 4e-
	log_k	-118.44
	delta_h 150.02	kcal
	-gamma	5.0	0
Mn+3 = Mn+3
	log_k	0
	delta_h 0	kcal
	-gamma	9.0	0.0
Mn+3 + e- = Mn+2
	log_k	25.507
	delta_h 25.76	kcal
	-gamma	6.0	0.0
NO3- = NO3-
	log_k	0
	delta_h 0	kcal
	-gamma	3.0	0.0
NO3- + 2H+ + 2e- = NO2- + H2O
	log_k	28.57
	delta_h -43.76	kcal
2 NO3- + 12 H+ + 10 e- = N2 + 6 H2O
		log_k	207.08
		delta_h -312.130	kcal
Na+ = Na+
	log_k	0
	delta_h 0	kcal
	-gamma	4.0	.075
SO4-2 = SO4-2
	log_k	0
	delta_h 0	kcal
	-gamma	4.0	-.04
SO4-2 + 9H+ + 8e- = HS- + 4H2O
	log_k	33.66
	delta_h -60.14	kcal
	-gamma	3.5	0.0
Zn+2 = Zn+2
	log_k	0
	delta_h 0	kcal
	-gamma	6.0	0.0
H4SiO4 = H4SiO4
		log_k	0.0
#######################################
SOLUTION_SPECIES

CO3-2 + 10 H+ + 8 e- = CH4 + 3 H2O
	log_k	41.071
	delta_h -61.039 kcal
H2O = OH- + H+
	log_k	-13.998
	delta_h 13.345	kcal
	-gamma	3.5	0
Mg+2 + H2O = MgOH+ + H+
	log_k	-11.79
	delta_h 15.935	kcal
	-gamma	6.5	0
	-analytical -3.53	0.00513	-2917.1
Mg+2 + CO3-2 = MgCO3
	log_k	2.98
	delta_h 2.022	kcal
	-analytical 0.991	0.00667
Mg+2 + CO3-2 + H+ = MgHCO3+
	log_k	11.4
	delta_h -2.43	kcal
	-gamma	4	0
Mg+2 + SO4-2 = MgSO4
	log_k	2.25
	delta_h 1.399	kcal
Ca+2 + H2O = CaOH+ + H+
	log_k	-12.598
	delta_h 14.535	kcal
	-gamma	6	0
Ca+2 + CO3-2 + H+ = CaHCO3+
	log_k	11.33
	delta_h 1.79	kcal
	-gamma	6	0
	-analytical -9.448	0.03709	2902.39
Ca+2 + CO3-2 = CaCO3
	log_k	3.15
	delta_h 4.03	kcal
	-analytical -27.393	0.05617	4114.0
Ca+2 + SO4-2 = CaSO4
	log_k	2.309
	delta_h 1.47	kcal
Na+ + CO3-2 = NaCO3-
	log_k	1.268
	delta_h 8.911	kcal
	-gamma	5.4	0
Na+ + CO3-2 + H+ = NaHCO3
	log_k	10.08
	delta_h 0	kcal
Na+ + SO4-2 = NaSO4-
	log_k	0.7
	delta_h 1.12	kcal
	-gamma	5.4	0
K+ + SO4-2 = KSO4-
	log_k	0.85
	delta_h 2.25	kcal
	-gamma	5.4	0
	-analytical 3.106	0.00	-673.6
Al+3 + H2O = AlOH+2 + H+
	log_k	-4.99
	delta_h 11.899	kcal
	-gamma	5.4	0
Al+3 + 2H2O = Al(OH)2+ + 2H+
	log_k	-10.1
	delta_h 0	kcal
	-gamma	5.4	0
Al+3 + 4H2O = Al(OH)4- + 4H+
	log_k	-23
	delta_h 44.06	kcal
```

```
    -gamma  4.5     0
Al+3 + SO4-2 = AlSO4+
    log_k   3.02
    delta_h 2.15    kcal
    -gamma  4.5     0
Al+3 + 2SO4-2 = Al(SO4)2-
    log_k   4.92
    delta_h 2.84    kcal
    -gamma  4.5     0
Al+3 + 3H2O = Al(OH)3 + 3H+
    log_k   -16
    delta_h 0       kcal
Fe+2 + H2O = FeOH+ + H+
    log_k   -9.5
    delta_h 13.199  kcal
    -gamma  5       0
Fe+2 + 3H2O = Fe(OH)3- + 3H+
    log_k   -31
    delta_h 30.3    kcal
    -gamma  5       0
Fe+2 + SO4-2 = FeSO4
    log_k   2.25
    delta_h 3.23    kcal
Fe+2 + 2H2O = Fe(OH)2 + 2H+
    log_k   -20.57
    delta_h 28.565  kcal
Fe+2 + 2HS- = Fe(HS)2
    log_k   8.95
    delta_h 0       kcal
Fe+2 + 3HS- = Fe(HS)3-
    log_k   10.987
    delta_h 0       kcal
Fe+3 + H2O = FeOH+2 + H+
    log_k   -2.19
    delta_h 10.399  kcal
    -gamma  5       0
Fe+3 + SO4-2 = FeSO4+
    log_k   3.92
    delta_h 3.91    kcal
    -gamma  5       0
Fe+3 + Cl- = FeCl+2
    log_k   1.48
    delta_h 5.6     kcal
    -gamma  5       0
Fe+3 + 2Cl- = FeCl2+
    log_k   2.13
    delta_h 0       kcal
    -gamma  5       0
Fe+3 + 3Cl- = FeCl3
    log_k   1.13
    delta_h 0       kcal
Fe+3 + 2H2O = Fe(OH)2+ + 2H+
    log_k   -5.67
    delta_h 0       kcal
    -gamma  5.4     0
Fe+3 + 3H2O = Fe(OH)3 + 3H+
    log_k   -13.6
    delta_h 0       kcal
Fe+3 + 4H2O = Fe(OH)4- + 4H+
    log_k   -21.6
    delta_h 0       kcal
    -gamma  5.4     0
Fe+3 + 2SO4-2 = Fe(SO4)2-
    log_k   5.42
    delta_h 4.6     kcal
2Fe+3 + 2H2O = Fe2(OH)2+4 + 2H+
    log_k   -2.95
    delta_h 13.5    kcal
3Fe+3 + 4H2O = Fe3(OH)4+5 + 4H+
    log_k   -6.3
    delta_h 14.3    kcal
Mn+2 + Cl- = MnCl+
    log_k   0.607
    delta_h 0       kcal
    -gamma  5       0
Mn+2 + 2Cl- = MnCl2
    log_k   0.041
    delta_h 0       kcal
Mn+2 + 3Cl- = MnCl3-
    log_k   -0.305
    delta_h 0       kcal
    -gamma  5       0
Mn+2 + H2O = MnOH+ + H+
    log_k   -10.59
    delta_h 14.399  kcal
    -gamma  5       0
Mn+2 + 3H2O = Mn(OH)3- + 3H+
    log_k   -34.8
    delta_h 0       kcal
    -gamma  5       0
Mn+2 + SO4-2 = MnSO4
    log_k   2.26
    delta_h 2.17    kcal
Mn+2 + 2NO3- = Mn(NO3)2
    log_k   0.6
    delta_h -0.396  kcal
Mn+2 + CO3-2 + H+ = MnHCO3+
    log_k   11.6
    delta_h 0       kcal
    -gamma  5       0
H4SiO4 = H3SiO4- + H+
        log_k    -9.83
        delta_h 6.12      kcal
        -analytic         -302.3724
        -0.050698         15669.69
        108.18466         -1119669.0
H4SiO4 = H2SiO4-2 + 2 H+
        log_k    -23.0
        delta_h 17.6      kcal
        -analytic         -294.0184
        -0.072650         11204.49
        108.18466         -1119669.0
### Copper
Cu+ + 2Cl- = CuCl2-
    log_k   5.5
    delta_h -0.42   kcal
    -gamma  4       0
Cu+ + 3Cl- = CuCl3-2
    log_k   5.7
    delta_h 0.26    kcal
    -gamma  5       0
Cu+ + 2HS- = Cu(S4)2-3 + 2H+
    log_k   3.39
    delta_h 0       kcal
```

```
        -gamma  23      0
        -no_check
        -mass_balance Cu(S(-2)4)2
Cu+ + 2HS- = CuS4S5-3 + 2H+
        log_k   2.66
        delta_h 0       kcal
        -gamma  25      0
        -no_check
        -mass_balance CuS(-2)4S(-2)5
Cu+2 + CO3-2 = CuCO3
        log_k   6.73
        delta_h 0       kcal
Cu+2 + 2CO3-2 = Cu(CO3)2-2
        log_k   9.83
        delta_h 0       kcal
Cu+2 + Cl- = CuCl+
        log_k   0.43
        delta_h 8.65    kcal
        -gamma  4       0
Cu+2 + 2Cl- = CuCl2
        log_k   0.16
        delta_h 10.56   kcal
Cu+2 + 3Cl- = CuCl3-
        log_k   -2.29
        delta_h 13.69   kcal
        -gamma  4       0
Cu+2 + 4Cl- = CuCl4-2
        log_k   -4.59
        delta_h 7.78    kcal
        -gamma  5       0
Cu+2 + H2O = CuOH+ + H+
        log_k   -8
        delta_h 0       kcal
        -gamma  4       0
Cu+2 + 2H2O = Cu(OH)2 + 2H+
        log_k   -13.68
        delta_h 0       kcal
Cu+2 + OH- = CuOH+
        log_k 6.5
# Mathur and Dzombak 2006
Cu+2 + 2OH- = Cu(OH)2
        log_k 11.8
# Mathur and Dzombak 2006
Cu+2 + 4OH- = Cu(OH)4-2
        log_k 16.4
# Mathur and Dzombak 2006
Cu+2 + 3H2O = Cu(OH)3- + 3H+
        log_k   -26.899
        delta_h 0       kcal
Cu+2 + 4H2O = Cu(OH)4-2 + 4H+
        log_k   -39.6
        delta_h 0       kcal
2Cu+2 + 2H2O = Cu2(OH)2+2 + 2H+
        log_k   -10.359
        delta_h 17.539  kcal
        -analytical 2.497       0.0         -3833.0
Cu+2 + SO4-2 = CuSO4
        log_k   2.31
        delta_h 1.22    kcal
Cu+2 + 3HS- = Cu(HS)3-
        log_k   25.899
        delta_h 0       kcal
Cu+2 + CO3-2 + H+ = CuHCO3+
        log_k   13
        delta_h 0       kcal
## Zinc
Zn+2 + Cl- = ZnCl+
        log_k   0.43
        delta_h 7.79    kcal
        -gamma  4       0
Zn+2 + 2Cl- = ZnCl2
        log_k   0.45
        delta_h 8.5     kcal
Zn+2 + 3Cl- = ZnCl3-
        log_k   0.5
        delta_h 9.56    kcal
        -gamma  4       0
Zn+2 + 4Cl- = ZnCl4-2
        log_k   0.199
        delta_h 10.96   kcal
        -gamma  5       0
Zn+2 + H2O = ZnOH+ + H+
        log_k   -8.96
        delta_h 13.399  kcal
Zn+2 + 2H2O = Zn(OH)2 + 2H+
        log_k   -16.899
        delta_h 0       kcal
Zn+2 + 3H2O = Zn(OH)3- + 3H+
        log_k   -28.399
        delta_h 0       kcal
Zn+2 + 4H2O = Zn(OH)4-2 + 4H+
        log_k   -41.199
        delta_h 0       kcal
Zn+2 + OH- = ZnOH+
        log_k 5.0
# Mathur and Dzombak 2006
Zn+2 + 2OH- = Zn(OH)2
        log_k 11.1
# Mathur and Dzombak 2006
Zn+2 + 4OH- = Zn(OH)4-2
        log_k 13.6
# Mathur and Dzombak 2006
Zn+2 + H2O + Cl- = ZnOHCl + H+
        log_k   -7.48
        delta_h 0       kcal
Zn+2 + 2HS- = Zn(HS)2
        log_k   14.94
        delta_h 0       kcal
Zn+2 + 3HS- = Zn(HS)3-
        log_k   16.1
        delta_h 0       kcal
Zn+2 + SO4-2 = ZnSO4
        log_k   2.37
        delta_h 1.36    kcal
Zn+2 + 2SO4-2 = Zn(SO4)2-2
        log_k   3.28
        delta_h 0       kcal
Zn+2 + Br- = ZnBr+
        log_k   -0.58
        delta_h 0       kcal
Zn+2 + 2Br- = ZnBr2
        log_k   -0.98
        delta_h 0       kcal
Zn+2 + CO3-2 + H+ = ZnHCO3+
```

```
        log_k   12.4
        delta_h 0       kcal
Zn+2 + CO3-2 = ZnCO3
        log_k   5.3
        delta_h 0       kcal
Zn+2 + 2CO3-2 = Zn(CO3)2-2
        log_k   9.63
        delta_h 0       kcal
##### anions
CO3-2 + H+ = HCO3-
        log_k   10.33
        delta_h -3.617  kcal
        -gamma  5.4     0
        -analytical -6.498     0.02379    2902.39
CO3-2 + 2H+ = H2CO3
        log_k   16.681
        delta_h -2.247  kcal
SO4-2 + H+ = HSO4-
        log_k   1.987
        delta_h 4.91    kcal
        -gamma  4.5     0
        -analytical -5.3505    0.0183412
           557.2461
HS- + H+ = H2S
        log_k   6.994
        delta_h -5.3    kcal
        -analytical -11.17     0.02386    3279.0
HS- = S-2 + H+
        log_k   -12.918
        delta_h 12.1    kcal
        -gamma  5       0
HS- = S2-2 + H+
        log_k   -14.528
        delta_h 11.4    kcal
        -no_check
        -mass_balance S(-2)2
HS- = S3-2 + H+
        log_k   -13.282
        delta_h 10.4    kcal
        -no_check
        -mass_balance S(-2)3
HS- = S4-2 + H+
        log_k   -9.829
        delta_h 9.7     kcal
        -no_check
        -mass_balance S(-2)4
HS- = S5-2 + H+
        log_k   -9.595
        delta_h 9.3     kcal
        -no_check
        -mass_balance S(-2)5
HS- = S6-2 + H+
        log_k   -9.881
        delta_h 0       kcal
        -no_check
        -mass_balance S(-2)6

#####org complexes
# Evanko and Dzombak 1999,
# protonation constants after Leenheer et al.,
#1995
Srfa-4 + H+  = HSrfa-3
        log_k  1.7
Srfa-4 + 2H+ = H2Srfa-2
        log_k  3.3
H3Srfa- = Srfa-4 + 3H+
        log_k  -4.3
Srfa-4 + 4H+ = H4Srfa
        log_k  5.6
#metal-binding constants from Leenheer et al.,
#1998
Cu+2 + Srfa-4 = CuSrfa-2
        log_k 5.2
Cu+2 + HSrfa-3 = CuHSrfa-
        log_k  8.0
Zn+2 + Srfa-4 = ZnSrfa-2
        log_k 3.8
Zn+2 + HSrfa-3 = ZnHSrfa-
        log_k 6.6

#######################################
PHASES
Hfo
        Fe(OH)3 + 3H+ = Fe+3 + 3H2O
        log_k 42.02
Al(OH)3(a)
        Al(OH)3 + 3H+ = Al+3 + 3H2O
        log_k   10.38
        delta_h -27.045 kcal
Kaolinite                # from wateq4
        Al2Si2O5(OH)4 + 6H+ = 2Al+3 +
2H4SiO4 + H2O
        log_k           7.435
        delta_h -35.3 kcal
Gibbsite                 # from wateq4
        Al(OH)3 + 3H+ = Al+3 + 3H2O
        log_k           8.11
        delta_h -22.8 kcal
Boehmite                 # from wateq4
        AlOOH + 3H+ = Al+3 + 2H2O
        log_k           8.584
        delta_h -28.181 kcal
Goethite                 # from minteq.v4
        FeOOH + 3H+ = Fe+3 + 2H2O
        log_k    0.491
        delta_h -60.5843        kJ
Ferrihydrite     # from minteq.v4
        Fe(OH)3 + 3H+ = Fe+3 + 3H2O
        log_k    3.191
        delta_h -73.374 kJ
Fe(OH)3(a)       # from wateq4f.dat
        Fe(OH)3 + 3H+ = Fe+3 + 3H2O
        log_k           4.891
CupricFerrite    # from wateq4
CuFe2O4 + 8H+ = Cu+2 + 2Fe+3 + 4H2O
        log_k           5.880
        delta_h -38.690 kcal
Calcite
      CaCO3 = Ca+2 + CO3-2
      log_k   -8.475
      delta_h -2.585  kcal
      -analytical_expression 13.543    -0.0401
        -3000.0
Fe3(OH)8
```

```
	Fe3(OH)8 + 8H+ = 2Fe+3 + Fe+2 + 8H2O
	log_k	20.222
	delta_h -0	kcal
Fe(OH)2.7Cl0.3
	Fe(OH)2.7Cl0.3 + 2.7H+ = Fe+3 +
2.7H2O + 0.3Cl-
	log_k	-3.04
	delta_h -0	kcal
FeS(ppt)
	FeS + H+ = Fe+2 + HS-
	log_k	-3.915
	delta_h -0	kcal
Fe2(SO4)3
	Fe2(SO4)3 = 2Fe+3 + 3SO4-2
	log_k	3.58
	delta_h -59.12	kcal
Hematite
	Fe2O3 + 6H+ = 2Fe+3 + 3H2O
	log_k	-4.008
	delta_h -30.845 kcal
Mackinawite
	FeS + H+ = Fe+2 + HS-
	log_k	-4.648
	delta_h -0	kcal
Maghemite
	Fe2O3 + 6H+ = 2Fe+3 + 3H2O
	log_k	6.386
	delta_h -0	kcal
Magnetite
	Fe3O4 + 8H+ = 2Fe+3 + Fe+2 + 4H2O
	log_k	3.737
	delta_h -50.46	kcal
Pyrite
	FeS2 + 2H+ + 2e- = Fe+2 + 2HS-
	log_k	-18.479
	delta_h 11.3	kcal
Siderite
	FeCO3 = Fe+2 + CO3-2
	log_k	-10.55
	delta_h -5.328	kcal
Covellite
	CuS + H+ = Cu+2 + HS-
	log_k	-23.038
	delta_h 24.01	kcal
Chalcopyrite
	CuFeS2 + 2H+ = Cu+2 + Fe+2 + 2HS-
	log_k	-35.27
	delta_h 35.48	kcal
Sphalerite
	ZnS + H+ = Zn+2 + HS-
	log_k	-11.618
	delta_h 8.25	kcal
Quartz
		SiO2 + 2 H2O = H4SiO4
		log_k	-3.98
		delta_h	5.990 kcal
#######################################
EXCHANGE_MASTER_SPECIES
		X	X-
EXCHANGE_SPECIES
X- = X-
		log_k	0.0
Na+ + X- = NaX
		log_k	0.0
		-gamma		4.0	0.075
K+ + X- = KX
		log_k	0.7
		-gamma		3.5	0.015
		delta_h	-4.3
# Jardine & Sparks, 1984
H+ + X- = HX
		log_k	1
		-gamma		9.0	0.0
Ca+2 + 2X- = CaX2
		log_k	1.4	#original 0.8
		-gamma		5.0	0.165
		delta_h	7.2
# Van Bladel & Gheyl, 1980
Mg+2 + 2X- = MgX2
		log_k	0.6
		-gamma		5.5	0.2
		delta_h	7.4
# Laudelout et al., 1968
Fe+2 + 2X- = FeX2
		log_k	0.44
		-gamma		6.0	0.0
Cu+2 + 2X- = CuX2
		log_k	0.6
		-gamma		6.0	0.0
Zn+2 + 2X- = ZnX2
		log_k	0.8
		-gamma		5.0	0.0
Cd+2 + 2X- = CdX2
		log_k	0.8
Pb+2 + 2X- = PbX2
		log_k	1.05
Mn+2 + 2X- = MnX2
		log_k	0.52
		-gamma		6.0	0.0
Al+3 + 3X- = AlX3
		log_k	0.41
		-gamma		9.0	0.0

#######################################
# Goethite surface complexation
# Mathur, S. S. and Dzombak, D. A., 2006.
#Surface complexation modeling: goethite. In:
#Lützenkirchen, J. (Ed.), Surface
#complexation modelling. Elsevier.

SURFACE_MASTER_SPECIES
Goe_	Goe_OH
SURFACE_SPECIES
Goe_OH = Goe_OH
		log_k 0.0
#acid-base constants
Goe_OH + H+ = Goe_OH2+
		log_k	6.93
Goe_OH = Goe_O- + H+
		log_k -9.65
# Copper binding constants
Goe_OH + Cu+2 = Goe_OCu+ + H+
		log_k 1.39
Goe_OH + Cu+2 = Goe_OHCu+2
```

```
        log_k 8.92
# Zinc binding constants
Goe_OH + Zn+2 = Goe_OZn+ + H+
        log_k -0.96
Goe_OH + Zn+2 = Goe_OHZn+2
        log_k 7.5
# Calcium binding constants
Goe_OH + Ca+2 = Goe_OCa+ + H+
        log_k -6.48
Goe_OH + Ca+2 = Goe_OHCa+2
        log_k 4.53
# Magnesium binding constants
Goe_OH + Mg+2 = Goe_OMg+ + H+
        log_k -3.02
Goe_OH + Mg+2 = Goe_OHMg+2
        log_k 5.35
# ligand binding constants after Leenheer et al
1995
Goe_OH + H3Srfa- + H+ = Goe_H3Srfa + H2O
        log_k 13.4
Goe_OH + H3Srfa- = Goe_H2Srfa- + H2O
        log_k 11.2
Goe_OH + H3Srfa- = Goe_HSrfa-2 + H+ +
H2O
        log_k 6.9
Goe_OH + H3Srfa- = Goe_OSrfa-5 + 4H+
        log_k -14
# order of Cu and Srfa does not reflect any
#binding mechanism
# both reactions are ligand-like as OH is lost
#(inner-sphere) from surface not only H (outer-
#sphere)
Goe_OH + CuHSrfa- + H+ = Goe_CuHSrfa +
H2O
        log_k 8.7
Goe_OH + CuHSrfa- = Goe_CuSrfa- + H2O
        log_k 6.7
Goe_OH + ZnHSrfa- + H+ = Goe_ZnHSrfa +
H2O
        log_k 8.7
Goe_OH + ZnHSrfa- = Goe_ZnSrfa- + H2O
        log_k 6.7
#######################################
#humic acids sites after Weng et al., 2001

SURFACE_MASTER_SPECIES
Haco    HacoOH
Ha      HaOH

SURFACE_SPECIES
HacoOH = HacoOH
        log_k 0.0
HacoOH + H+ = HacoOH2+
        log_k 2.93
HacoOH + Ca+2 = HacoOCa+ + H+
        log_k -1.37
HacoOH + Al+3 = HacoOAl+2 + H+
        log_k -1.05
HacoOH + Fe+3 = HacoOFe+2 + H+
        log_k 5.0
HacoOH + Cu+2 = HacoOCu+ + H+
        log_k 2.23
HacoOH + Zn+2 = HacoOZn+ + H+
        log_k 0.11

HaOH = HaOH
        log_k 0.0
HaOH + H+ = HaOH2+
        log_k 8.0
HaOH + Ca+2 = HaOCa+ + H+
        log_k -0.43
HaOH + Al+3 = HaOAl+2 + H+
        log_k 8.89
HaOH + Fe+3 = HaOFe+2 + H+
        log_k 17.5
HaOH + Cu+2 = HaOCu+ + H+
        log_k 6.85
HaOH + Zn+2 = HaOZn+ + H+
        log_k 2.39

RATES
##########################
# biodegradation of fulvic acid
#Additive Monod kinetics
# Electron acceptors: O2, NO3, Fe and SO4
##########################
Srfa
-start
10 if (m <= 0) then goto 100
20  mO2 = mol("O2")
30  mNO3 = tot("N(5)")
31  mFe = EQUI("Goethite")
40  mSO4 = tot("S(6)")
50  rate = 1.57e-9*mO2/(2.94e-4 + mO2)
52  rate = rate + 1.67e-11*mNO3/(1.55e-4 +
        mNO3)
54  rate = rate + 5.0e-11*mFe/(1e-4 + mFe)
56  rate = rate + 1.e-13*mSO4/(1.e-4 + mSO4)
70  moles = rate * time
80 if (moles > m) then moles = m
100 save moles
-end

END
```